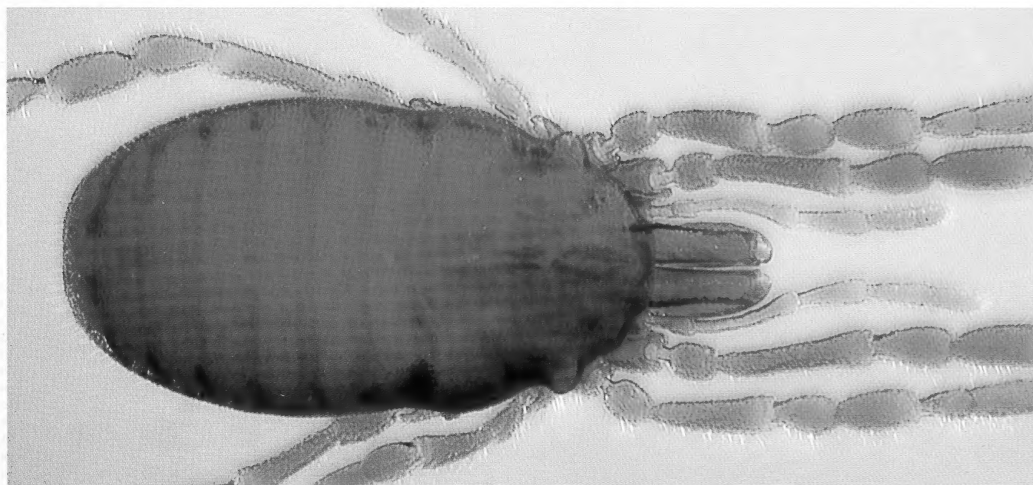# The genus *Siro* Latreille, 1796 (Opiliones, Cyphophthalmi, Sironidae) in North America with a phylogenetic analysis based on molecular data and the description of four new species

GONZALO GIRIBET AND WILLIAM A. SHEAR

THE GENUS *SIRO* LATREILLE, 1796 (OPILIONES, CYPHOPHTHALMI, SIRONIDAE), IN NORTH AMERICA WITH A PHYLOGENETIC ANALYSIS BASED ON MOLECULAR DATA AND THE DESCRIPTION OF FOUR NEW SPECIES

GONZALO GIRIBET[1] AND WILLIAM A. SHEAR[2]

ABSTRACT. The North American fauna of the Laurasian family Sironidae is examined phylogenetically and compared with species from Europe and Japan. The North American clade is not resolved as monophyletic. The phylogenetic analyses and detailed morphological study identified four cryptic species of sironids in the western United States, formerly considered within the geographical and morphological range of *Siro acaroides* (Ewing, 1923). These four species are described as *Siro boyerae* sp. nov., *Siro calaveras* sp. nov., *Siro clousi* sp. nov., and *Siro shasta* sp. nov. We also provide new localities for the previously known species in the western United States. *Siro boyerae* sp. nov. forms a clade with *Siro kamiakensis* (Newell, 1943) and with the East Coast species *Siro exilis* Hoffman, 1963, characterized by the presence of narrow coxae III that do not meet along the midline. The affinities of *S. calaveras* sp. nov., *S. clousi* sp. nov., and *S. shasta* sp. nov. remain largely unresolved, but *S. clousi* sp. nov., is not related to *S. acaroides* despite being found sympatrically.

INTRODUCTION

The cyphophthalmid genus *Siro* currently includes a series of species found in North America and continental Western Europe (Giribet, 2000; Juberthie, 1970; Novak and Giribet, 2006; Shear, 1980). The status of the European members of the genus *Siro* has been recently revised, and the radiation of species related to *Cyphophthalmus duricorius* Joseph, 1868, in the Balkans and adjacent geographic areas seems to be

unrelated to *Siro rubens* Latreille, 1804, and therefore considered a different genus (Boyer et al., 2005; Karaman, 2008; Murienne et al., 2010). In this article, we restrict the concept of *Siro* to a clade of recent Western European species composed of *S. rubens*; *Siro carpaticus* Rafalski, 1956; *Siro crassus* Novak & Giribet, 2006; and *Siro valleorum* Chemini, 1990, and to a clade of several North American species: *Siro acaroides* (Ewing, 1923); *Siro exilis* Hofman, 1963; *Siro kamiakensis* (Newell, 1943); and *Siro sonoma* Shear, 1980. The four previously known North American species were revised by Shear (1980) and profusely illustrated by de Bivort and Giribet (2004: figs. 10–39).

Siro acaroides was described in 1923 as the type of the new genus *Holosiro* Ewing, 1923, this species being the first cyphophthalmid discovered in the New World (Ewing, 1923). Later, it was recognized that the species could not be easily distinguished from the European *Siro* at the generic level, and *Holosiro* was considered a junior synonym of *Siro* (Newell, 1943). In the same article, Newell described a new species of American sironid in the new genus *Neosiro* Newell, 1943, for the species *Neosiro kamiakensis*. The new genus was based on the divided fourth tarsus of the male. Both species inhabit western North America, each originally described from single localities: *S. acaroides* from Benton County, southwestern Oregon, and *N. kamiakensis* from Whitman County in western Washington. An eastern North American species, *Siro*

[1] Museum of Comparative Zoology, Department of Organismic and Evolutionary Biology, Harvard University, 26 Oxford Street, Cambridge, Massachusetts 02138.
[2] Department of Biology, Hampden-Sydney College, Hampden-Sydney, Virginia 23943.

exilis, found in the Appalachian Mountains along the boundary between Virginia and West Virginia, was subsequently added to the list (Hoffman, 1963).

Meanwhile, Davis (1933) had described *Siro americanus* from northwestern Florida; after an unwarranted sojourn in the genus *Parasiro* Hansen and Sørensen, 1904 (Hinton, 1938), this species was made the type of the new genus *Metasiro* Juberthie, 1960 (Juberthie, 1960), within the family Sironidae (or Sironinae of Juberthie, 1970) (Giribet, 2000; Juberthie, 1970; Shear, 1980). Later on, Hoffman (1963) proposed the synonym genus *Floridogovea* Hoffman, 1963, for *Metasiro*. Based on ample morphological and molecular evidence, *Metasiro* is now considered a member of Neogoveidae (Boyer et al., 2007b; Giribet, 2007).

In 1980, Shear had access to a wide range of collections that had been assembled since 1947 (Shear, 1980). Contrary to the assertions of Ewing (1923) and Newell (1947), Shear (1980) proposed that *S. acaroides* was widely distributed in the Coast Ranges from northern California to Puget Sound and that *N. kamiakensis* occurred in at least one more locality in western Washington (Mt. Spokane) and at three places in Kootenai and Idaho Counties, in northern Idaho. Furthermore, Shear argued that the preponderance of characters of *N. kamiakensis* were consistent with a placement in the genus *Siro* and so synonymized Newell's genus *Neosiro*. Shear also added a distinctive fourth species of *Siro*, *S. sonoma* Shear, 1980, from Sonoma County in Northern California.

Some loose ends were mentioned in Shear's 1980 paper. In particular, a single female specimen from Calaveras County, California, in the Sierra Nevada Mountains, seemed clearly to be a new species, but Shear was reluctant to describe it from a single female example. Now additional material from that same collection has become available, and it is clear that this population represents a new, fifth species of American *Siro*. Additional material has also been recently collected by G. Giribet, S. Boyer, and R. M. Clouse in Calaveras Big Trees State Park, which was suitable for molecular work.

The map Shear published in 1980 did not correlate well with the list of localities given; a location for *S. acaroides* is shown significantly south of the California/Oregon border, but only Del Norte County records are listed in the text. This map symbol was added late in the preparation of the paper and referred to Shasta County specimens that were then considered *S. acaroides*. They are of a yet another new species.

A field trip through Idaho, Washington, Oregon, and Northern California by G. Giribet, S. Boyer, and R. M. Clouse in June 2005 yielded numerous collections of Cyphophthalmi, including all known species for the western United States, with the exception of the elusive *S. sonoma*. The aim of this trip was to obtain more specimens of the new species from Calaveras County and Shasta County, as well as to revisit other cyphophthalmid localities to obtain specimens suitable for molecular work for all the NW U.S. species. Two specimens of *S. sonoma* were collected by G. Giribet, T. Briggs, and D. Ubick in Monte Rio, December 2001. Phylogenetic analysis of the new specimens further revealed the presence of multiple cryptic lineages in the previously considered widespread species *S. acaroides*. Two of these species that could be characterized morphologically are described here. The new species double the number of known American sironids but also indicate that our knowledge of the American sironid fauna is still in its infancy.

California has not been intensively explored for cyphophthalmids. They are most easily collected from Berlese samples; the success of this method was demonstrated by the many specimens and new records of *S. acaroides* obtained by Ellen Benedict (Shear, 1980). We have also been successful collecting many live specimens by sifting with a 4-mm mesh size or via extraction with Winkler apparatus. But other than these

examples, most specimens have been obtained after occasional direct collecting. We predict that a thorough search of proper habitats in the Sierra Nevada, and both northern and southern Coast Ranges in California, will yield more new species of sironids. The distribution pattern of soil-dwelling organisms with species in the Appalachians in the east and the Coast Ranges and northern Idaho in the west often includes the central Rocky Mountains as well; *Siro* might be expected to turn up in Utah, Colorado, or New Mexico. With 43 extant species of sironids in Europe, it seems reasonable to expect that North America eventually could be shown to have more species than the 10 we know now.

MATERIALS AND METHODS

Abbreviations for Repository Institutions

AMNH	American Museum of Natural History, New York, New York, USA
BMNH	The Natural History Museum, London, United Kingdom
CAS	California Academy of Sciences, San Francisco, California, USA
CNHM	Field Museum of Natural History, Chicago, Illinois, USA (usually, FMNH for Field Museum of Natural History)
EME	Essig Museum of Entomology, U.C. Berkeley, Berkeley, California, USA
FMNH	Field Museum of Natural History, Chicago, Illinois, USA (in some labels, CNHM for Chicago Natural History Museum)
MCZ	Museum of Comparative Zoology, Harvard University, Cambridge, Massachusetts, USA
MHNG	Muséum d'histoire naturelle, Geneva, Switzerland
SMF	Senckenberg Museum, Frankfurt am Main, Frankfurt, Germany

Morphological Methods

For each species, the male holotype and a female paratype were photographed using a JVC KY-F70B digital camera mounted on a Leica MZ 12.5 stereomicroscope. A series of images (ca. 10) were taken at different focal planes and assembled with the dedicated software package Auto-Montage Pro Version 5.00.0271 (Syncroscopy, Frederick, Maryland, USA). Each specimen was photographed in dorsal, ventral, and lateral views, and when available, the holotype was always photographed. Full body measurements of the holotype and a female paratype were then taken from these photographs in Adobe Photoshop CS3 with the "Analysis" menu and were recorded in a spreadsheet. Total body length refers to the distance between midpoint of anterior and midpoint of posterior margin of the dorsal scutum. Body width refers to the maximum width, whether recorded in the prosomal or in the opisthosomal region.

One male and one female specimen of each species were examined with a FEI Quanta 200 SEM (Peabody, Massachusetts, USA). Appendage and body part measurements were taken from the digital micrographs in Adobe Photoshop CS3 with the "Analysis" menu and were recorded in a spreadsheet. Measurements of the chelicera, palp, and leg articles were mostly taken on their dorsal side, from the midpoint of the anterior margin to the midpoint of the posterior margin. Depths were measured on the lateral side at the widest portion, except for tarsus IV of the male, which was measured behind the adenostyle. Tarsal length does not include the claw. The position of the adenostyle on tarsus IV is given at the more clearly marked distal point, where it abruptly rises from the dorsal surface of the tarsus.

Finally, some body measurements were taken with an ocular micrometer on an Olympus SZH dissecting microscope, at 50×. Measurements of appendages temporarily mounted on microscope slides were
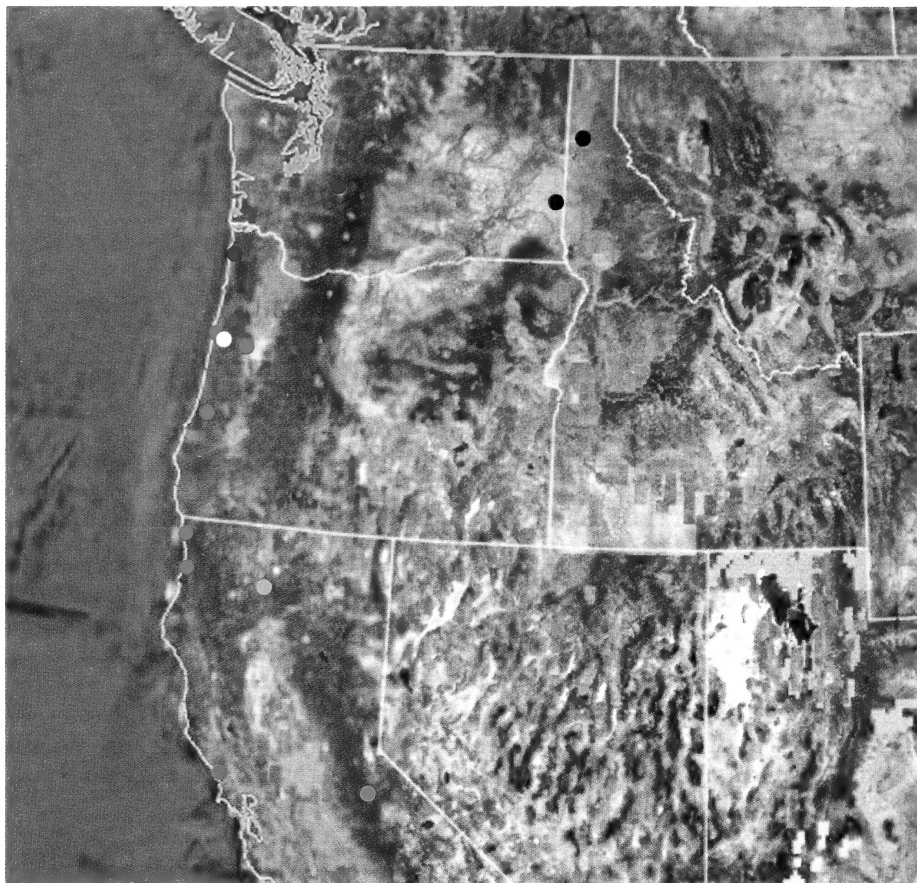
Figure 1.   Map of the NW United States with the sampled localities for *Siro acaroides* (red), *S. boyerae* sp. nov. (navy blue), *S. calaveras* sp. nov. (yellow), *S. clousi* sp. nov. (white), *S. kamiakensis* (black), *S. shasta* sp. nov. (orange), and *S. sonoma* (green). For details on the collecting localities, see Table 1 and Supplemental Appendix 1.

taken with an ocular micrometer on an Olympus BX50 compound microscope, at 100× with Nomarski differential interference contrast. Drawings were made using the latter microscope, equipped with a drawing tube; Nomarski contrast was used to clarify details of the spermatopositors.

Molecular Sampling

To evaluate the phylogenetic position of the new species and for testing the validity of the "widespread" species *S. acaroides*, we undertook phylogenetic analyses of molecular data from specimens of all American sironids (see distribution map in Fig. 1) and

multiple representatives of other sironid genera, including *Suzukielus* from Japan, *Paramiopsalis* and *Parasiro* from the Iberian Peninsula, *Siro* from France and Italy, and *Cyphophthalmus* from multiple localities in the Balkans (Table 1).

Molecular data were obtained from freshly collected specimens preserved in 96% EtOH at −80° C. DNA from preserved tissues was extracted with the use of the Qiagen DNeasy® Tissue Kit following standard protocols described, for example, by Boyer et al. (2005). Three different loci were chosen for this study. Ribosomal sequence data of complete 18S rRNA and a ca. 2.1-kb fragment of 28S rRNA were

TABLE 1. LIST OF TAXA, MCZ ACCESSION NUMBERS, LOCALITIES, AND GENBANK ACCESSION NUMBERS FOR EACH SEQUENCED LOCUS.

Species	MCZ Accession	Country, State	Coordinates	18S rRNA	28S rRNA	COI
Suzukielus sauteri	MCZ DNA101543	Japan	35°38′03″N, 139°14′28″E	DQ513138	DQ513116	DQ513108
Cyphophthalmus sp. nov.	MCZ DNA101342	Bulgaria	N/A	AY918870	DQ513117	AY918878
Cyphophthalmus cf. *teyrovskyi*	MCZ DNA100910	Montenegro	N/A	AY639482	DQ513118	AY639571
Cyphophthalmus trebinjanus	MCZ DNA101038	Bosnia & Herzegovina	N/A	AY639483	DQ513119	AY639572
Cyphophthalmus duricorius	MCZ DNA100487	Slovenia	N/A	AY639461	DQ513120*	AY639556
Paramiopsalis ramulosus	MCZ DNA100459	Spain	42°18′54″N, 008°29′12″W	AY639469	DQ513121	DQ513109
Parasiro coiffaiti	MCZ DNA101383	Spain	42°09′09″N, 001°55′49″E	AY918872	DQ513122	DQ513110
Siro rubens	MCZ DNA100457	France	44°05′00″N, 003°34′53″E	AY428818	AY859602	DQ513111
Siro valleorum	MCZ DNA100461	Italy	N/A	AY639492	DQ513123	AY639580
Siro acaroides	MCZ DNA100488	USA, Oregon	N/A	AY639490	DQ513128	AY639578
Siro acaroides	MCZ DNA101616	USA, Oregon	44°40′00″N, 123°55′58″W	DQ513142*	DQ513129*	DQ513113
Siro acaroides	MCZ DNA101619	USA, Oregon	43°58′58″N, 123°53′41″W	DQ513143	DQ513130	DQ513114
Siro acaroides	MCZ DNA101620	USA, California	41°50′17″N, 124°08′39″W	DQ513144	DQ513131*	-
Siro acaroides	MCZ DNA101621	USA, California	41°18′10″N, 124°01′03″W	DQ513145	DQ513132*	-
Siro boyerae sp. nov.	MCZ DNA101614	USA, Washington**	46°59′32″N, 121°50′47″W	DQ513139	DQ513125	DQ513112
Siro boyerae sp. nov.	MCZ DNA101617	USA, Oregon	45°54′56″N, 123°57′52″W	DQ513141	DQ513127	-
Siro calaveras sp. nov.	MCZ DNA101623	USA, California**	38°16′38″N, 120°18′19″W	DQ513146	DQ513133*	-
Siro clousi sp. nov.	MCZ DNA101871	USA, Oregon**	44°40′00″N, 123°55′58″W	DQ513140	DQ513126	-
Siro exilis	MCZ DNA100489	USA, Maryland	N/A	AY639491	DQ513124	AY639579
Siro kamiakensis	MCZ DNA101611	USA, Idaho	47°44′47″N, 116°42′07″W	DQ513147	DQ513134*	DQ513115
Siro kamiakensis	MCZ DNA101613	USA, Washington**	46°52′04″N, 117°09′28″W	DQ513148	DQ513135*	-
Siro shasta sp. nov.	MCZ DNA101622	USA, California**	41°03′49″N, 122°21′37″W	DQ513149	DQ513136*	-
Siro sonoma	MCZ DNA100507	USA, California**	38°26′37″N, 122°59′19″W	DQ513150*	DQ513137*	-

* Indicates partial sequences.
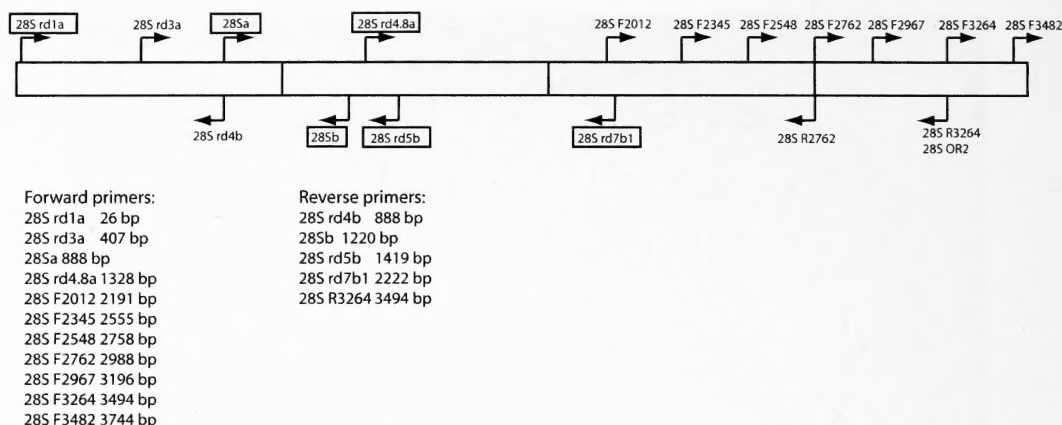** Denotes specimens from the type locality.

Figure 2. Schematic representation of a 28S rRNA locus with the primers listed in Supplemental Table 1 and used in this study. Primers used for amplification appear within a box. The position of each primer, in reference to the *Limulus polyphemus* 28S rRNA sequence AF212167 (Mallatt and Winchell, 2002), is provided. Information on primers not used in this study but included in the figure can be provided on request to G.G.

selected to resolve the deeper nodes in the trees, whereas the mitochondrial protein-coding gene cytochrome *c* oxidase subunit I (COI hereafter) was included to resolve more recent evolutionary events. The complete 18S rRNA loci were amplified in three overlapping fragments using the following primer pairs: 1F–4R, 3F–185sbi, and 18Sa2.0–9R. The 28S rRNA fragment was amplified in three overlapping fragments delimited by the following primer pairs: 28S rd1a–28Sb, 28Sa–28S rd5b, and 28S rd4.8a–28S rd7b1. COI was amplified with primer pair LCO1490–HCOoutout. Primer sequences, references, and annealing conditions are given in Supplemental Table 1. A map of the 28S rRNA primers used in this study is provided in Figure 2.

The amplified samples were purified using the QIAquick® PCR Purification Kit, labeled with BigDye® Terminator v3.0, and sequenced with an ABI 3730 genetic analyzer following manufacturer's protocols. Primers used in the sequencing reaction correspond to those used in the amplification step, with the addition of reverse primer 28S rd4b for the first fragment of 28S rRNA (see Table 1).

Chromatograms obtained from the automatic sequencer were read and "contig sequences" (assembled sequences) were assembled with the sequence editing software Sequencher™ 4.0 and further manipulated in MacGDE 2.4 (Linton, 2005). 18S rRNA measured between 1,762 and 1,763 bp and was divided into six fragments using defined primer regions. 28S rRNA was divided into 12 fragments defined by primer regions and conserved secondary structure motifs; two hypervariable fragments were deactivated from the analyses (but left in the raw data). The analyzed 28S rRNA segment (2,105–2,119 bp for the complete specimens) greatly expands previous cyphophthalmid datasets (e.g., Boyer et al., 2005; Giribet and Boyer, 2002; Schwendinger and Giribet, 2005). The protein-coding gene COI showed length variation. In addition, we combined published sequences with new sequences obtained with a primer located 3' of the old HCO2198 (Boyer et al., 2005; Folmer et al., 1994), yielding sequences between 654 and 663 bp for the old fragment and between 811 and 814 for the new fragment. COI was divided into five fragments to accommodate published sequences on the basis of the Folmer et al. (1994) primers, with the new sequences using a primer downstream of HCO2198. In total, the amount of genetic data per complete taxon is ca. 4.7 kb, although COI did not amplify for many of

the North American sironids despite good DNA yield. All new sequences have been deposited in GenBank under the accession numbers DQ513108–DQ513150 (Table 1).

Molecular Data Analysis

The molecular data were analyzed with POY version 3.0 (Wheeler et al., 2004) according to the direct optimization method with parsimony as the optimality criterion (Wheeler, 1996). The data for all genes were analyzed independently and in combination. Tree searches were conducted in parallel (with PVM [Parallel Virtual Machine]) on a cluster of 30 dual-processor nodes (between 1 and 2.4 GHz) assembled at Harvard University (darwin.oeb.harvard.edu). Commands for load balancing of spawned jobs were, in effect, to optimize parallelization procedures (*-parallel -dpm -jobspernode 2*). Trees were built through a random addition sequence procedure (100 replicates) followed by a combination of branch-swapping steps (SPR [subtree pruning and regrafting] and TBR [tree bisection and reconnection]), and continuing with tree fusing (Goloboff, 1999, 2002) to further improve tree length. Discrepancies between heuristic and actual tree length calculations were addressed by adjusting slop values (*-checkslop 10*). While doing tree refinements with *tbr*, *-checkslop n* accepts all trees that are within *n* tenths of a percent of the current minimum value. For example, *-checkslop 10* accepts all trees up to 1% above the current minimum length while doing TBR.

POY facilitates efficient sensitivity analysis (Giribet, 2003; Wheeler, 1995). All data sets (individual genes and combinations) were analyzed under 10 parameter sets, for a range of indel-to-transversion ratios and transversion-to-transition ratios. The indel-to-transversion ratio refers to the opening gap cost, in that the extension gap cost was always fixed to 1. One parameter set follows the proposal of De Laet (2005), in which gaps are assigned a cost of 3, nucleotide transformations are assigned a cost of 2, and the gap extension cost is set to 1. Implied

alignments—a topologically unique "alignment" or synapomorphy scheme (Giribet, 2005; Wheeler, 2003)—can be generated easily for each tree.

A character congruence technique, which is a modification of the ILD (Incongruence Length Difference) metric developed by Mickevich and Farris (1981; see also Farris et al., 1995), was used to select the most congruent parameter set, as proposed by Wheeler (1995; Table 2). The value is calculated for each parameter set by subtracting the sum of the scores of all partitions from the score of the combined analysis of all partitions, and normalizing it for the score of the combined length. This has been interpreted as a meta-optimality criterion for choosing the parameter set that best explains all partitions in combination, the one that maximizes overall congruence and minimizes character conflict among all the data (Giribet, 2003). This parameter set was given special consideration in the analysis of data from each individual gene and is referred to throughout this paper as the "optimal parameter set." Additionally, we discuss results from the strict consensus of all parameter sets explored, which has been interpreted as a measure of stability to model choice, as applied in statistical sensitivity analyses (Giribet, 2005; Wheeler, 2003), and the dependence on parameter set variation is shown graphically in the "Navajo rugs" at relevant nodes of our trees. Nodal support for all topologies was measured by parsimony jackknifing (Farris, 1997; Farris et al., 1996).

RESULTS

Sequence data were generated for all the known species of North American sironids, all of which have been recently collected by one of us (G.G.) and colleagues. However, *S. sonoma* has not been included in the analyses because it did not sequence well. After an initial collection of two specimens at the type locality in December 2001 (G.G., T. Briggs, D. Ubick), one male was used for SEM (de Bivort and Giribet, 2004), and a

TABLE 2. TREE LENGTHS FOR THE DIFFERENT PARTITIONS ANALYZED (18S = 18S rRNA; 28S = 28S rRNA; COI = CYTOCHROME *C* OXIDASE SUBUNIT I; MOL = THREE LOCI COMBINED) AND CONGRUENCE VALUE (ILD) FOR THE COMBINED ANALYSIS OF ALL THREE MOLECULAR LOCI COMBINED AT DIFFERENT PARAMETER SETS (LEFT COLUMN). THE FIRST NUMERAL USED IN THE PARAMETER SET COLUMN CORRESPONDS TO THE RATIO BETWEEN INDEL/TRANSVERSION, AND THE FOLLOWING TWO NUMBERS CORRESPOND TO THE RATIO BETWEEN TRANSVERSION/TRANSITION (E.G., 111 IS EQUAL WEIGHTS; 121 CORRESPONDS TO AN INDEL/ TRANSVERSION RATIO OF 1:1 AND A TRANSVERSION/TRANSITION RATIO OF 2:1, SO INDELS HAVE A COST OF 2, TRANSVERSIONS HAVE A COST OF 2, AND TRANSITIONS HAVE A COST OF 1); 3221 CORRESPONDS TO THE PARAMETER SET ADVOCATED BY DE LAET (2005). (FOR A LIST OF SPECIFIC STEP MATRICES SEE GIRIBET ET AL., 2002: APPENDIX 4). OPTIMAL ILD VALUE IS INDICATED IN ITALICS.

	18S	28S	COI	MOL	ILD
111	70	445	1605	2132	0.00563
121	94	654	2453	3227	0.00806
141	140	1035	3924	5139	0.00778
211	72	499	1647	2234	0.00716
221	96	752	2511	3373	0.00415
241	144	1224	4150	5543	0.00451
411	74	586	1664	2331	0.00300
421	100	907	2532	3572	0.00924
441	152	1521	4211	5966	0.01374
3221	*143*	*912*	*3259*	*4324*	*0.00231*

female specimen was used for molecular work. After several attempts at amplifying its DNA, we were only able to obtain short amplifications, some from exogenous sources. Although we obtained sironid sequences for a fragment of 18S rRNA and 28S rRNA, the amount of information in such fragments is small, causing the species to become a wildcard. Subsequent collecting trips to the same locality in June 2005 and January 2006 and to additional localities in Sonoma County in June 2005 yielded no additional specimens of *S. sonoma*. Therefore, the results presented and discussed here are without *S. sonoma*.

Amplification of 18S rRNA and 28S rRNA was successful for all the specimens included in our analyses, although we had some difficulties amplifying the three 28S rRNA fragments employed here for all the North American species (indicated with an asterisk in Table 1). Likewise, COI amplifications were problematic for many of the North American specimens, despite numerous attempts (more than 20 PCR conditions, including three primer sets in some cases), often yielding double bands or no amplifications at all. Band excision yielded sequence data of possible pseudogenes. Therefore, the COI data set lacks data on *Siro clousi*, *S. calaveras*, and *S. shasta*. Conclusions about the relationships of these three species are thus based entirely on the ribosomal data sets. It is known that COI evolution in Cyphophthalmi in general, and sironids in particular, is odd compared with other arthropods because it presents very high evolutionary changes, including several amino acid indel events (Boyer et al., 2005), and this could be the cause for the difficulties in amplifying this marker.

Molecular Data Analyses

After sensitivity analysis, the parameter set that showed the lowest incongruence according to our modified ILD metric was parameter set 3221, wherein gap openings receive a cost of 3, gap extensions cost 1, and all nucleotide transformations cost 2 (Table 2). Therefore, the results under this parameter set are discussed in more detail and are presented for each analyzed partition (Figs. 3, 4). Additionally, the strict consensus of all trees obtained under all parameter sets is also presented (Fig. 4B). Parameter variation is shown in the form of sensitivity plots ("Navajo rugs"; Fig. 4).

The analysis of the complete 18S rRNA data set for the optimal parameter set yielded 18 trees of 143 weighted steps and found trees of minimal length in 100% of the replicates performed. The strict consensus of these 18 trees (Fig. 3A) identifies five lineages of North American sironids, one including the species *S. kamiakensis*, *S. exilis*, and *S. boyerae* sp. nov. and supported with 100% jackknife frequency (JF hereafter), and four other lineages corresponding to *S. acaroides*, *S. clousi* sp. nov., *S. calaveras* sp. nov., and *S. shasta* sp. nov. Within the kamiakensis–exilis–boyerae clade, the analyses also find support for a clade including the East Coast species *S. exilis* and the West
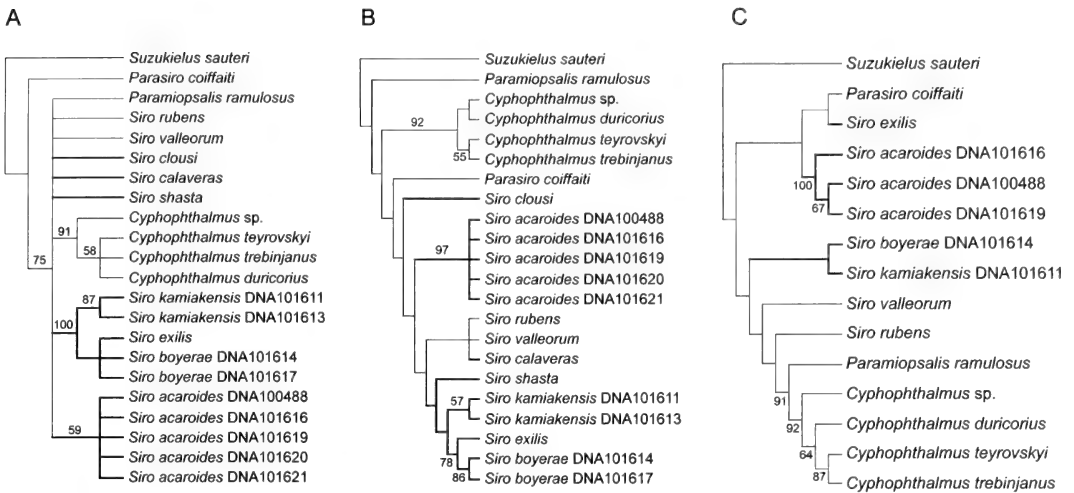
Figure 3.   Partitioned analyses for the optimal parameter set. (A) Strict consensus of 18 trees at 143 weighted steps for the analysis of the 18S rRNA data set. (B) Strict consensus of seven trees at 912 weighted steps for the analysis of the 28S rRNA data set. (C) Shortest tree at 3,259 weighted steps for the analysis of the COI data set. Numbers on branches indicate jackknife support values above 50%. Branches in bold refer to the North American species.

Coast species *S. boyerae* sp. nov. The analysis did not find support for the genus *Siro* or for the monophyly of the North American species.

The analysis of the 2.1-kb fragment of 28S rRNA data set for the optimal parameter set yielded seven trees of 912 weighted steps and found trees of minimal length in 37% of replicates; tree-fusing did not find additional trees. The strict consensus of these seven trees (Fig. 3B) shows monophyly of the genus *Siro* (JF < 50%), but not for the North American species. As in the 18S rRNA analysis, 28S rRNA supports monophyly of each species, as well as the exilis–boyerae (78% JF) and the kamiakensis–exilis–boyerae (JF < 50%) clades. In this tree, *S. shasta* sp. nov. is sister group to the latter clade, and *S. calaveras* sp. nov. appears in a clade with the two Western European species *S. rubens* and *S. valleorum*. As in the 18S rRNA analysis, the genus *Cyphophthalmus* finds ample jackknife support.

The analysis of the COI data set for the optimal parameter set (we remind the reader that COI shows length variation within Cyphophthalmi and therefore requires indel events) yielded a single tree of 3,259 weighted steps (Fig. 3C) and was obtained in 40% of the replicates performed. Support from the COI analysis is only found for *Cyphophthalmus* + *Paramiopsalis* (91% JF), *Cyphophthalmus* (92% JF), or the monophyly of *S. acaroides* (100% JF). The tree also shows monophyly of *S. kamiakensis* + *S. boyerae* sp. nov., but these do not form a clade with *S. exilis*. When compared with the other partitions, COI contributes 3.5 times more than 28S rRNA and almost 23 times more than 18S rRNA, in terms of their tree length.

The combined analysis of the three markers for the optimal parameter set yielded eight trees at 4,324 weighted steps, and these trees were found in 30% of the replicates performed, without improvement after tree fusing. The strict consensus of these eight trees is presented in Figure 4A, as opposed to the strict consensus obtained under all parameter sets (Fig. 4B). The tree shows nonmonophyly of *Siro* or of the North American members of the genus. As in some of the partitioned analyses, the combined analysis of all data identifies the exilis–boyerae (63% JF) and the kamiakensis–exilis–boyerae (JF < 50%) clades. The latter clade, despite its low jackknife sup-
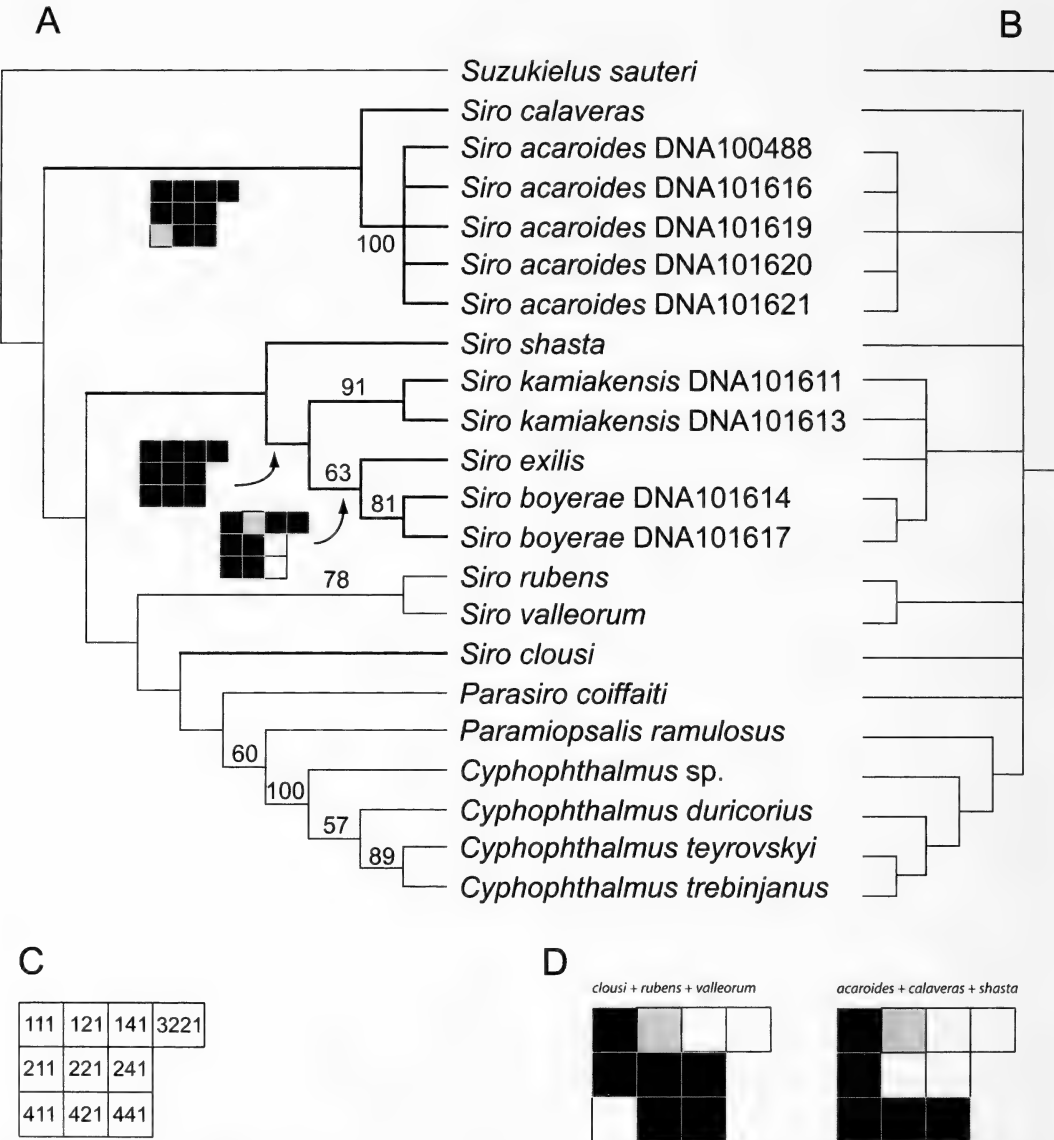
Figure 4.   Combined analysis of all loci. (A) Strict consensus of the eight shortest trees at 4,324 weighted steps obtained under the optimal parameter set. Numbers on nodes indicate jackknife support values above 50%. Branches in bold refer to the North American species. (B) Strict consensus of all trees obtained under all the explored parameter sets. (C) Legend for the Navajo rugs depicted in Figures 4A, D, indicating the parameter sets for each square. (D) Navajo rugs for two of the topologies not depicted in the trees obtained under the optimal parameter set. Legends for Navajo rugs: black square indicates monophyly; white square indicates non-monophyly; gray square indicates monophyly under some but not all of the shortest trees.

port, appears under all analytical parameter sets (Fig. 4B and corresponding Navajo rug), indicating its stability. Likewise, the exilis–boyerae clade appears under most analytical parameters. The combined anal-

ysis also suggests a relationship of *S. calaveras* sp. nov. to *S. acaroides*, again, with JF < 50%, but with enormous stability; only one parameter set suggests alternatives to the monophyly of the clade (see corre-

sponding Navajo rug in Fig. 4). A relationship of *S. shasta* sp. nov. to the kamiakensis–exilis–boyerae clade is obtained under the optimal parameter set only and shows JF < 50%. However, a number of parameter sets identifies *S. shasta* sp. nov. with the calaveras–acaroides clade (see corresponding Navajo rug, Fig. 4D). *Siro clousi* sp. nov. appears in alternative positions under the different parameter sets explored, but it mostly appears within a clade including the two Western European species *S. rubens* and *S. valleorum*.

Because of the lack of COI sequence data for some species and the enormous contribution by the COI locus, which has been shown to contain substantial homoplasy in previous analyses of cyphophthalmid relationships (Boyer et al., 2005; Schwendinger and Giribet, 2005), we undertook analysis of the two ribosomal genes alone. The combined analysis of the two ribosomal loci under the optimal parameter set yielded 14 trees of 1,066 weighted steps, and minimum tree length was found in 82% of replicates performed. The strict consensus of the 14 trees (Fig. 5) shows monophyly of *Siro*, but not monophyly of the North American species. As in the previous analyses, the data shows the kamiakensis–exilis–boyerae, exilis–boyerae, and calaveras–acaroides clades, but neither *S. shasta* sp. nov. nor *S. clousi* sp. nov. is unambiguously resolved. As in most previous analyses, the two European species of *Siro* and the four species of *Cyphophthalmus* form individual clades.

DISCUSSION

Phylogenetic analysis of the data analyzed in this study supports the presence of multiple lineages of North American sironids, although their relationships are not yet fully understood. One of the results of our analyses suggests that several specimens previously considered within the variation range of *S. acaroides* by Shear (1980) represent two independent lineages completely unrelated to *S. acaroides*. One of these, *S. clousi* sp. nov. is the largest
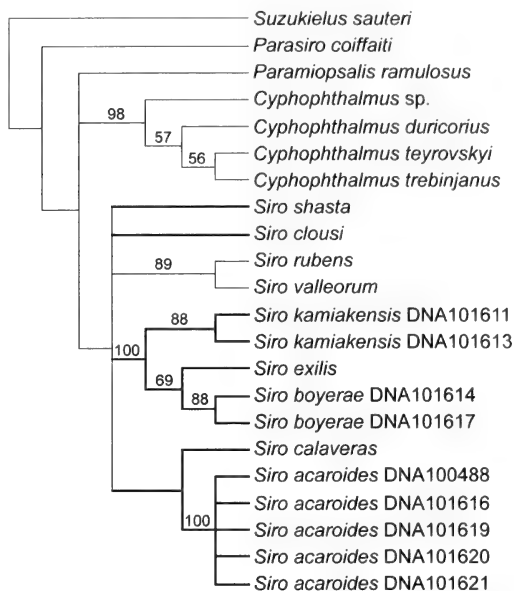

Figure 5. Strict consensus of the 14 trees at 1,066 weighted steps for the combined analysis of the two ribosomal loci. Numbers on branches indicate jackknife support values above 50%. Branches in bold refer to the North American species.

North American sironid and is found sympatrically with *S. acaroides*. However, under several parameter sets, *S. clousi* sp. nov. appears to be related to the Western European instead of the North American species. This result surely deserves further scrutiny by adding more species of Western European sironids, as well as more individuals of *S. clousi* sp. nov.

A second species formerly considered within the variation of *S. acaroides*, *S. boyerae* sp. nov., is more closely related to *S. kamiakensis* from Washington and Idaho than to *S. acaroides* from nearby localities and, in fact, appears as the sister group to the East Coast species *S. exilis*. The relationship of these three species, the designated kamiakensis–exilis–boyerae clade, is well supported by our data in terms of stability to parameter variation, and the three of them share a unique position of coxae III, which do not meet along the midline (see Fig. 21). The presence of a clade constituted by three species separated by distances of over 2,000 km on both sides of

the Rocky Mountains is, to say the least, surprising, especially because genetic differences in the ribosomal genes between *S. exilis* and *S. boyerae* sp. nov. are extremely low. And again, this could be explained by the great age of the group; North American sironids have been estimated to have diversified in the Jurassic, whereas they separated from their European counterparts in the Triassic (Giribet et al., 2010).

Siro acaroides, a broadly distributed species from the redwood forests of coastal Oregon and Northern California forms a distinct clade with other redwood species from the Central region of California, including *S. shasta* sp. nov. and *S. calaveras* sp. nov., and perhaps with *S. sonoma* (data not shown), all of them with much narrower ranges. This species complex parallels the toad *Anaxyrus boreas* species group (Goebel et al., 2009), although in the case of the species in the genus *Siro*, divergences could be much older than in *Anaxyrus*.

Concluding Remarks

The four new species elevate the number of described North American Cyphophthalmi to a total of 10, nine of which occur in the continental United States (Shear, 1980) and one in Mexico (Shear, 1977). This diversity is considerably lower than that recorded for Europe. However, the ranges of some of the North American species (e.g., *Metasiro americanus*) are quite large and could include cryptic species, given the patchy distribution and the low dispersal ability of Cyphophthalmi (see, e.g., Boyer et al., 2007a). The large geographic gap without cyphophthalmid specimens for the kamiakensis–exilis–boyerae clade furthermore suggests that more species could be expected from some elevated humid forests in the center of the continental United States, although climatic conditions in the present and in the past, as well as large episodes of flooding, could constrain the current distributions of Cyphophthalmi species, which are not found at higher latitudes. An interesting parallel is seen in another putatively ancient

arachnid group, the spider genus *Hypochilus*, with five species in the southern Appalachians, two in the southern Rocky Mountains, and three in California. But in this case, a morphological cladistic analysis showed that the three geographic areas also correspond to three clades (Catley, 1994). It remains clear that the North American cyphophthalmid fauna is still in serious need of further study, both at the faunistic and taxonomic levels, and indeed, single individuals, which could represent additional species, exist in museum collections.

TAXONOMY

Family Sironidae Simon, 1879
Genus *Siro* Latreille, 1796
Siro Latreille 1796: 185, Simon 1879: 144–145, Hansen and Sørensen 1904: 107–108, Juberthie 1970: 1383, Shear 1980: 3–5, Giribet 2000: 57 (complete references and previous synonymies).

***Siro boyerae* Giribet & Shear sp. nov.**
(Figs. 6–9)

Type Specimens

Holotype. Male (MCZ 92901 ex MCZ DNA101614) from Chenuis Fall (46°59′32″N, 121°50′47″W), Carbon River, Mount Rainier National Park, Pierce Co., WASHINGTON, collected 19.vi.2005 by S. L. Boyer, R. M. Clouse, & G. Giribet (Figs. 6A–C).

Paratypes. Three males (1 for DNA work) and 8 females (MCZ 92902, MCZ DNA101614; one in Figs. 6D–F), same collecting data as holotype; 2 males, 1 juvenile (FMNH; CNHM(HD)#57-42; B_26) from Carbon River, Mount Rainier National Park, Pierce Co., WASHINGTON, collected 16 June 1957 by H. S. Dybas; 5 males (1 used for DNA work), 2 females, 1 juvenile (MCZ DNA101617) from Ecola State Park (45°54′56″N, 123°57′52″W), Clatsop Co., OREGON, collected 20 June 2005 by S. L. Boyer, R. M. Clouse, & G. Giribet; 3 females, 9 juveniles (FMNH HD#68-149)
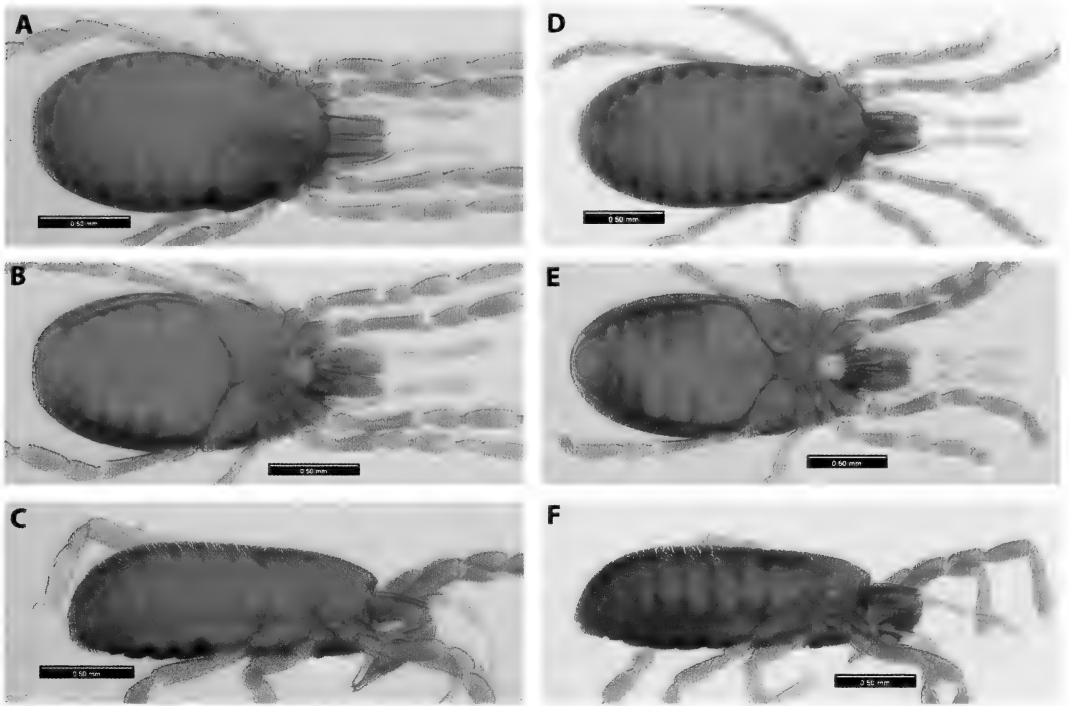
Figure 6.   *Siro boyerae* sp. nov. (A–C) Holotype male (MCZ 92901) in dorsal (A), ventral (B), and lateral (C) view. (D–F) Paratype female (MCZ 92902) in dorsal (D), ventral (E), and lateral (F) view. Scale bars 500 μm.

from Ecola State Park, Clastop Co., ORE-GON, collected 21 July 1968 by *J. Wagner*.

Additional Material

WASHINGTON: One male (MCZ DNA104929) from Lower Hendrickson Canyon (46°22′158″N, 123°39′950″W, 27 m), Wahkiakum Co., collected 23.i.2004 by *W. Leonard, M. Leonard, C. Richart, B. Dyle, & K. Norose*; 1 male (MCZ DNA104928) from Gregory Creek, 5.2 mi N of SR4 (46°15′552″N, 123°08′038″W, 125 m), Cowlitz Co., collected 21.iii.2004 by *W. Leonard & C. Richart*; 1 male, 1 female (EME) from Amanda Park, Quinault, Olympic Peninsula, collected 9.vii.1959 by *L. M. Smith*; 1 male, 3 females, 2 juveniles (FMNH; CNHM(HD)#57-73; B_306) from Fairfax, Pierce Co., collected 16.vi.1957 by *H. S. Dybas* in floor debris in mixed maple–alder; 1 female (FMNH; CMNH(HD)#57-41; B_297) from Chenuis Fall, Carbon River, Mount Rainier National Park, Pierce Co.,

collected 16.vi.1957 by *H. S. Dybas*; 2 males (FMNH) from Olympic Hot Springs, Olympic National Park, collected 18–19.vi.1957 by *H. S. Dybas*; 4 males, 2 females, 1 juvenile (CAS) from 2.5 mi due N Swift Reserve Dam, Skamania Co., collected by *T. Briggs, V. Lee, & K. Hom*; 4 males, 8 females, 5 juveniles (CAS) from 2.5 mi due N Swift Reserve Dam, Skamania Co., collected by *T. Briggs, V. Lee, & K. Hom*.

Etymology. The species is named after cyphophthalmid biologist Sarah L. Boyer, who assisted collecting the type material of the species, for her dedication to these animals.

Diagnosis. Siro boyerae is similar to *S. acaroides*, although the former is more slender (length/with ratio [L/W] = 1.84 in *S. boyerae* and 1.5 in *S. acaroides*). The two species differ in the open circle spiracles of *S. acaroides*, which are almost circular in *S. boyerae*. The spiracles also differ from those of *S. shasta* sp. nov. It can be distinguished from *S. kamiakensis*, *S. sonoma*, and *S.*

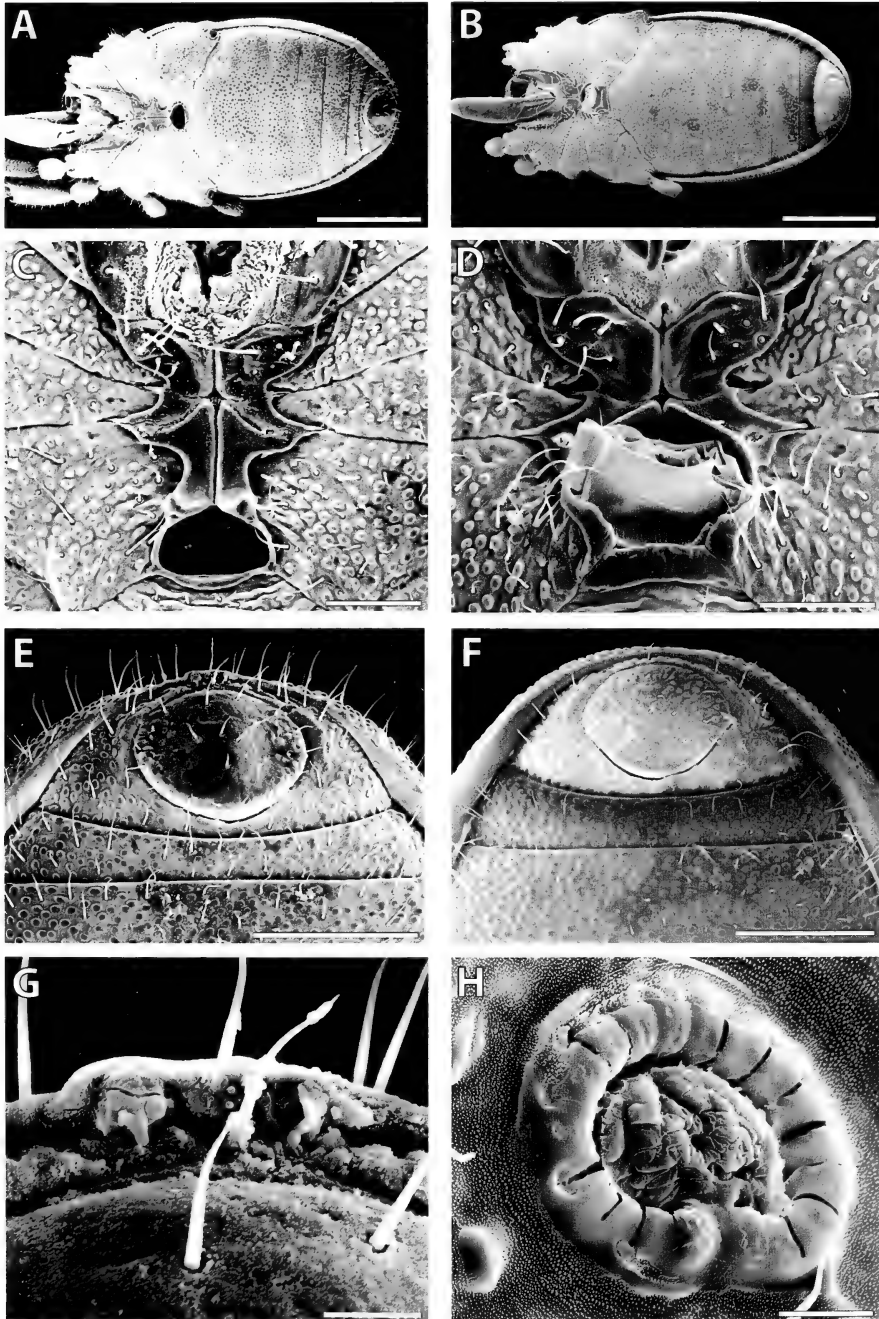Figure 7. *Siro boyerae* sp. nov. paratype male and female (MCZ 92902). (A) Paratype male in ventral position. (B) Paratype female in ventral position. (C) Male ventral thoracic complex. (D) Female ventral thoracic complex. (E) Male anal region. (F) Female anal region. (G) Detail of anal gland openings. (H) Female spiracle. (A, B, Scale bars 500 μm; C–D, scale bars 100 μm; E, F, scale bars 200 μm; G, H, scale bars 20 μm.)
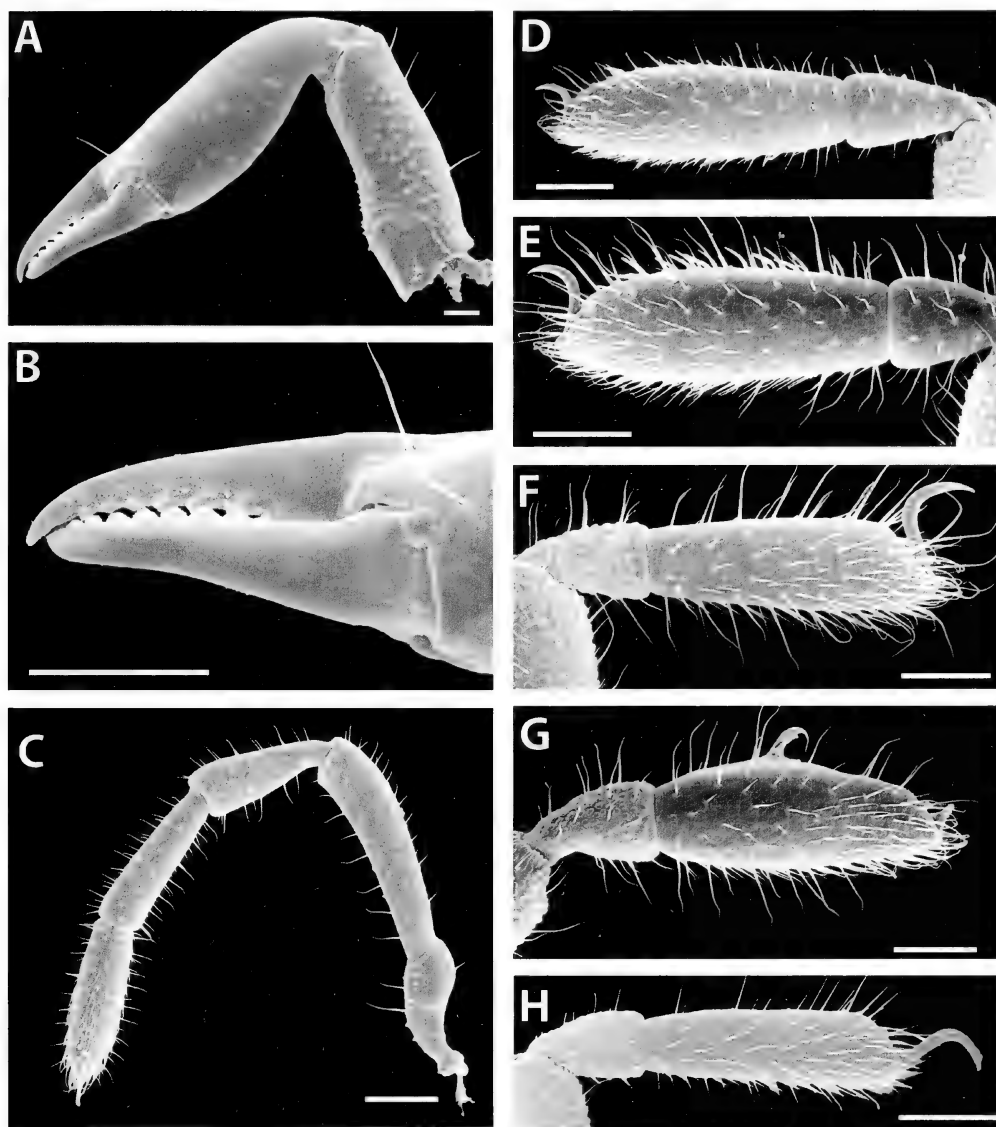
Figure 8. *Siro boyerae* sp. nov. paratype male and female (MCZ 92902). (A) Left chelicera of male. (B) Detail of the cheliceral pincer. (C) Left palp of male. (D) Metatarsus and tarsus I of male. (E) Metatarsus and tarsus II of male. (F) Metatarsus and tarsus III of male. (G) Metatarsus and tarsus IV of male. (H) Metatarsus and tarsus IV of female. (A, Scale bar 50 μm; B–H, scale bars 100 μm.)

clousi sp. nov. in lacking an anal keel in the male and from *S. shasta* sp. nov. because the latter has a depressed male anal plate (Fig. 7E). *Siro boyerae* shares with *S. exilis* (Fig. 21B), *S. kamiakensis* (Fig. 21C), and *S. sonoma* (Fig. 21D) endites of coxae III that do not meet along the midline (as opposed to *S. acaroides* [Fig. 21A], and the other three new species described herein), a character that might constitute a synapomorphy for them (see Figs. 3–5). However, the species can easily be separated from *S. sonoma* by the unmodified ventral surface of its male 4th tarsus and from *S. kamia-*

Figure 9.   *Siro boyerae* sp. nov. (A) Spermatopositor, ventral view. (B) Spermatopositor, dorsal view. (C) Ovipositor. (D) Ovipositor sensory organ. (C, Scale bar 200 µm; D, scale bar 50 µm.)

kensis by its undivided male 4th tarsus. Likewise, it can easily be separated from *S. shasta* because the latter lacks ornamentation in the legs.
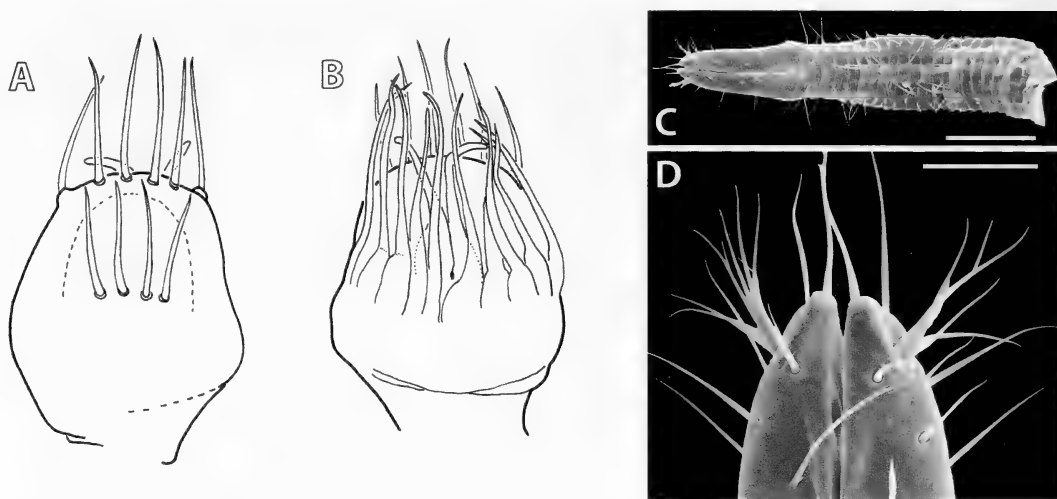
Description of Male. Small sironid of uniform chestnut brown color; total length of holotype 1.69 mm, maximum width at 3rd opisthosomal segment at 0.91 mm, body L/W = 1.84 (Fig. 6A). Anterior margin of dorsal scutum slightly convex; prosomal region almost semicircular. Ozophores conical, of type II (*sensu* Juberthie, 1970), with subterminal ozopore (*sensu* Novak and Giribet, 2006); maximum width across ozophores 0.75 mm. Eyes absent. Transverse prosomal sulcus little conspicuous; transverse opisthosomal sulci inconspicuous. Dorsal scutum with maximum height at around segments 4–5 (Fig. 6C).

Ventral prosomal complex (Figs. 6B, 7A, C) with coxae I–II free, coxae III–IV fused; coxae II and IV meeting along the midline, but not coxae III; coxae IV meeting along the midline for a distance greater than gonostome length; sternum absent; coxal pores clearly visible between coxae III and IV. Projections of coxae IV endites present in the anterior portion of gonostome wall (Fig. 7C). Male gonostome sub-semicircular, with slightly concave posterior margin,

wider than long (0.12 × 0.07 mm), and delimited laterally and anterolaterally by the elevated endites of coxae IV. Spiracles (Fig. 7H) of circular type (*sensu* Giribet and Boyer, 2002), circular to oval in shape in male, with a maximum diameter of 0.07 mm.

Ventral opisthosomal region (Fig. 7A) without conspicuous modifications other than in the anal plate. Opisthosomal tergite IX and sternites 8 and 9 fused into a broad corona analis (Fig. 7E); tergite VIII without modifications. Anal plate oval, 0.21 × 0.15 mm, only ornamented in the sides, with a rather inconspicuous longitudinal central ridge that leaves two depressions laterally. Three anal gland pores on tergite VIII of males (Fig. 7G). Cuticle with tuberculate-microgranular surface (*sensu* Murphree, 1988; this is referred to as "ornamented" hereafter), nearly uniform in dorsal areas and in ventral areas, including coxae.

Chelicerae (Fig. 8A) relatively short and robust; basal article in males 0.40 mm long, 0.14 mm wide, without a ventral process or a dorsal crest; 2nd article 0.59 mm long, 0.15 mm wide; movable finger 0.20 mm long; all articles with few setae, the proximal one almost entirely granulated but with sparse granulation; 8 uniform denticles on

TABLE 3. LEG MEASUREMENTS (LENGTH/WIDTH, MM) IN *SIRO BOYERAE* SP. NOV. MEASUREMENTS REFER TO MALE PARATYPE MOUNTED FOR SEM.

Leg	Trochanter	Femur	Patella	Tibia	Metatarsus	Tarsus	Total
I	0.14/0.11	0.43/0.12	0.22/0.12	0.28/0.12	0.18/0.10	0.38/0.13	1.65
II	0.11/0.10	0.33/0.11	0.19/0.11	0.22/0.12	0.15/0.09	0.33/0.11	1.35
III	0.14/0.09	0.23/0.11	0.16/0.10	0.19/0.11	0.09/0.07	0.29/0.08	1.14
IV	0.22/0.10	0.33/0.11	0.21/0.11	0.23/0.12	0.16/0.09	0.34/0.13	1.51

the cutting edge of each cheliceral finger (Fig. 8B). Second cheliceral segment not ornamented.

Palp (Fig. 8C) 1.11 mm long, smooth, slightly ornamented on trochanter. Measurements of palpal article length in SEM male paratype (mm): trochanter 0.165, femur 0.311, patella 0.205, tibia 0.212, tarsus 0.220; claw 0.037 mm long.

Legs relatively robust; leg formula I-IV-II-III (measurements in Table 3; Figs. 8D–G). Tarsus I with a concentration of setae, but not forming a distinct solea. Except for the tarsi I–IV and metatarsi I–II, all articles ornamented (Figs. 8D–G). Tarsus IV of male entire, with a narrow lamelliform adenostyle (Fig. 8G), subcylindrical at the base, with lateral pore; proximal margin at 40% of tarsal length. Claws hooked, smooth, without dentition or lateral pegs.

Spermatopositor (Figs. 9A, B) short, typical of sironids, smooth; with movable fingers, slightly curved outward, ending as hooks, longer than the membranous median lobe; microtrichial formula: 4, 6, 5+5 ($n = 1$). Gonopore complex not observed.

Description of Female. Total length 1.94 mm, maximum width 0.95 mm (L/W = 2.05; Fig. 6D). Ventral prosomal complex (Figs. 7B, D) only with coxae I–II meeting along the midline, coxae III delimiting the anterior part of gonostome. Female gonostome semicircular anteriorly, wider than long (Fig. 7D). Gonostome of female forming a tube. Corona analis not protruding or forming a tube (Fig. 7F). Female anal plate unmodified. Tarsus of leg IV (Fig. 8H) without modifications, narrower than that of males.

Ovipositor (Figs. 9C, D) 0.84 mm long, typical of *Siro* (see Juberthie, 1967), composed of two apical lobes and 20 circular

articles ($n = 1$), each with 8 short setae equal in length; these setae slightly longer toward the terminus; most basal article without setae. Apical lobes (Fig. 9D) each with a long terminal seta and ca. 12 setae slightly increasing in length toward the tip; sensitive processes with multibranching setae with 6 endings. Because of SEM examination, we have not studied the receptaculum seminis.

Siro calaveras Giribet & Shear sp. nov.
(Figs. 10–13)

Type Specimens

Holotype. Male (MCZ 92898, ex MCZ DNA101623) from North Grove (41°03′49″N, 122°21′37″W), Calaveras Big Trees State Park, Calaveras Co., CALIFORNIA, collected 23.vi.2005 by *S. L. Boyer, R. M. Clouse, & G. Giribet*; litter sifting (Figs. 10A–C).

Paratypes. Three males and 3 females (MCZ 92899, ex MCZ DNA101623); same collecting data as holotype; 1 male, 3 females, 1 juvenile (MCZ DNA101623), same collecting data as holotype (1 male and 1 female used for DNA extraction); 2 females, 2 juveniles (AMNH), from North Grove, Calaveras Big Trees State Park, Calaveras Co., CALIFORNIA, collected 5.iii.1958 by *L. M. Smith & R. O. Schuster*; 8 males, 11 females, 3 juveniles (AMNH), from North Grove, Calaveras Big Trees State Park, Calaveras Co., CALIFORNIA, collected 10.iii.1958 by *L. M. Smith & R. O. Schuster*, rotten log; 4 males (3 dissected for genitalia), 2 females (AMNH), from North Grove, Calaveras Big Trees State Park, Calaveras Co., CALIFORNIA, collected 5.iii.1958 by *L. M. Smith & R. O. Schuster*;
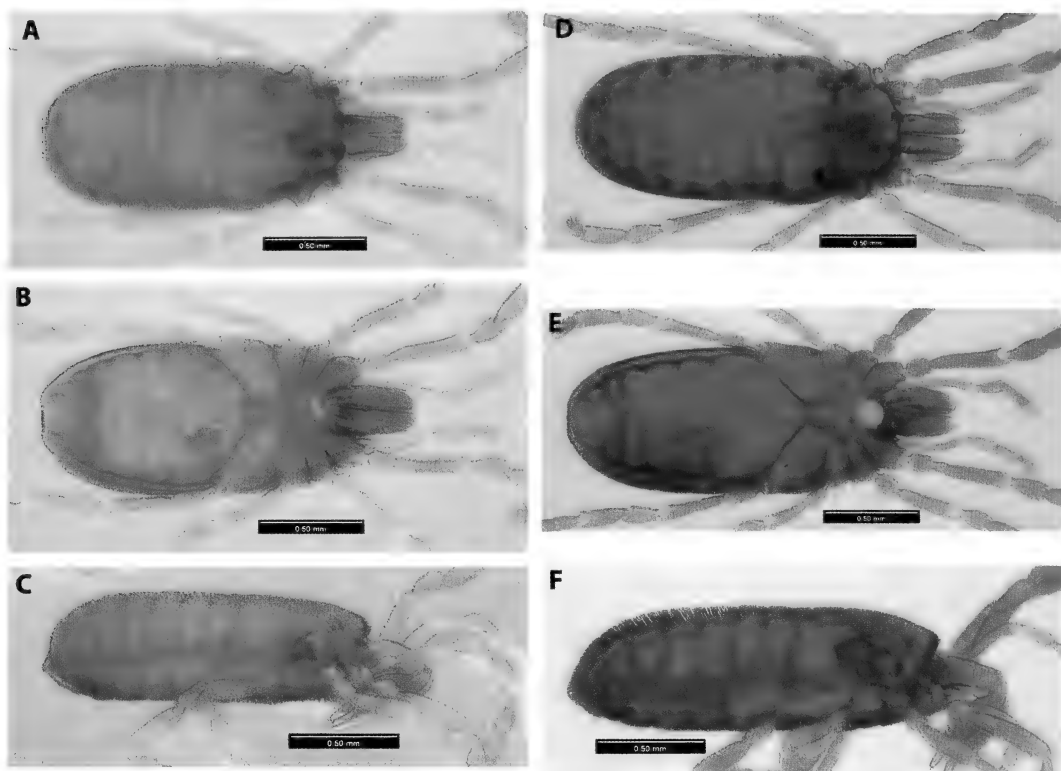
Figure 10.   *Siro calaveras* sp. nov. (A–C) Holotype male (MCZ 92898) in dorsal (A), ventral (B), and lateral (C) view. (D–F) Paratype female (MCZ 92899) in dorsal (D), ventral (E), and lateral (F) view. Scale bars 500 μm.

1 male, 1 female in SEM stubs (MCZ, ex AMNH), from North Grove, Calaveras Big Trees State Park, Calaveras Co., CALIFORNIA, collected 5.iii.1958 by *L. M. Smith & R. O. Schuster*; 1 female (CAS), from South Grove, Calaveras Big Trees State Park, Calaveras Co., CALIFORNIA, collected 13.vi.1956 by *B. J. Adelson*.

Etymology. The species epithet is a noun in apposition, after Calaveras Co., California.

Diagnosis. Siro calaveras (Fig. 10) is a more slender species (L/W = 1.99) than *S. acaroides* (L/W = 1.50), to which it is similar in body length, and the legs are also proportionally shorter, as is male tarsus IV (L/W = 2.0 as opposed to 2.9 in *S. acaroides*); *S. acaroides* has a rather smooth palpal trochanter, whereas that of *S. calaveras* is ornamented; the number of spermatopositor microtrichiae of both species is

the same. *Siro calaveras* is distinctly smaller than *S. shasta* (1.5 vs. 2.6 mm long), which lacks leg ornamentation and differs in spermatopositor microtrichiae. The species can easily be separated from *S. sonoma* by the unmodified ventral surface of its male tarsus IV and from *S. kamiakensis* by its undivided male tarsus IV. Unlike *S. exilis*, *S. calaveras* males have a concave 8th tergite. Finally, *S. calaveras* has a unique body profile (Fig. 10A) among North American species, with the body widest across the posterior opisthosomal part, rather than opisthosomal tergites 2 or 3.

Description of Male. Slender small sironid of uniform chestnut brown color; total length of holotype 1.53 mm, maximum width at prosoma at 0.77 mm, body L/W = 1.99 (Fig. 10A). Anterior margin of dorsal scutum slightly convex; prosomal region sub-semicircular. Ozophores conical, of
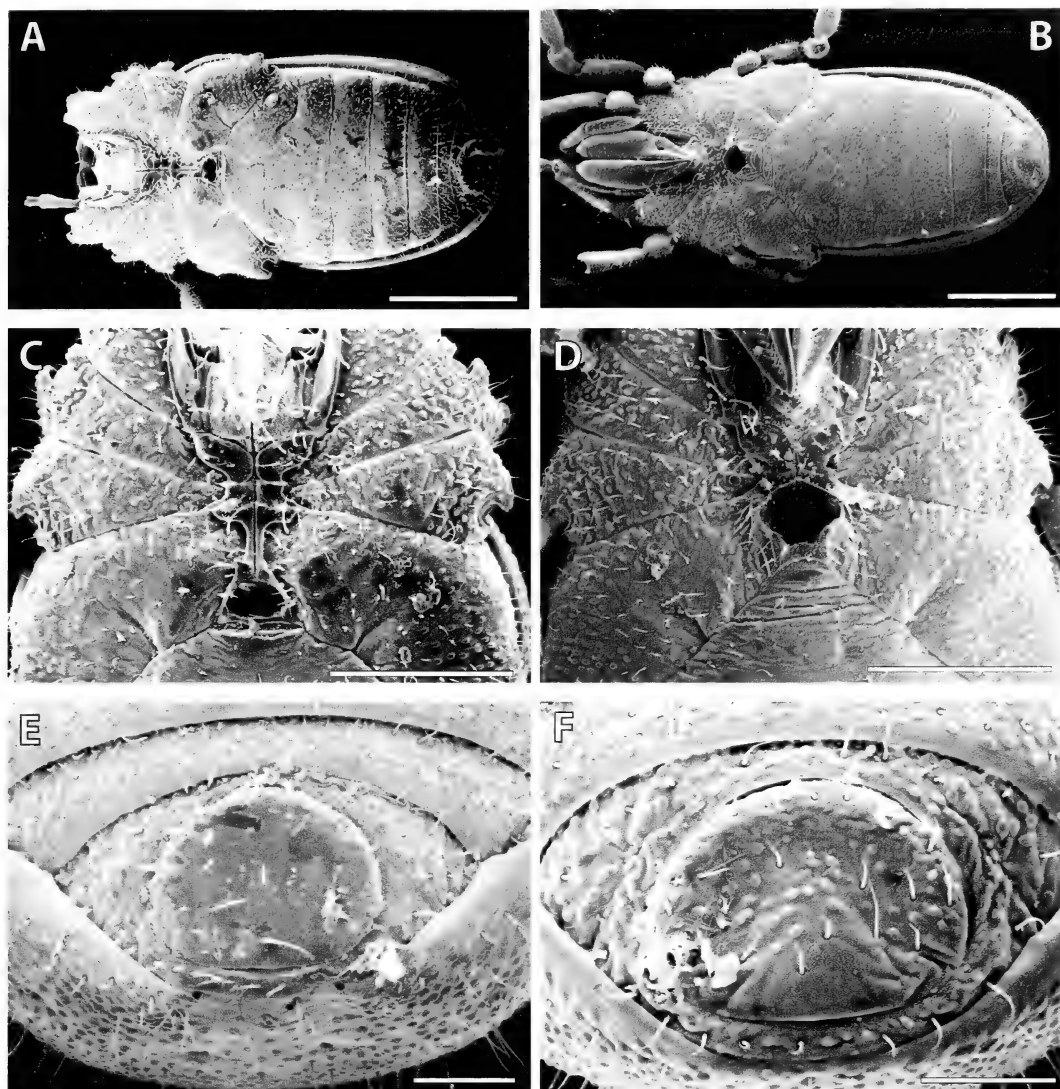
Figure 11.   *Siro calaveras* sp. nov. paratype male (MCZ 92899) and female (MCZ 92899). (A) Paratype male in ventral position. (B) Paratype female in ventral position. (C) Male ventral thoracic complex. (D) Female ventral thoracic complex. (E) Male anal region. (F) Female anal region. (A, B, Scale bars 500 μm; C, D, scale bars 300 μm; E, F, scale bars 100 μm.)

type II (*sensu* Juberthie, 1970), with sub-terminal ozopore (*sensu* Novak and Giribet, 2006), and entirely ornamented; maximum width across ozophores 0.72 mm. Eyes absent. Transverse prosomal sulcus incon-spicuous; transverse opisthosomal sulci in-conspicuous. Dorsal scutum with maximum height posterior end, but very similar along the length of the animal (Fig. 10C).

Ventral prosomal complex (Figs. 10B, 11A, E) with coxae I–II free, coxae III–IV fused; coxae II, III, and IV meeting along the midline; coxae IV meeting along the midline for a distance greater than gonos-tome length; sternum absent; coxal pores clearly visible between coxae III and IV. Projections of coxae IV endites present in the anterior portion of gonostome wall
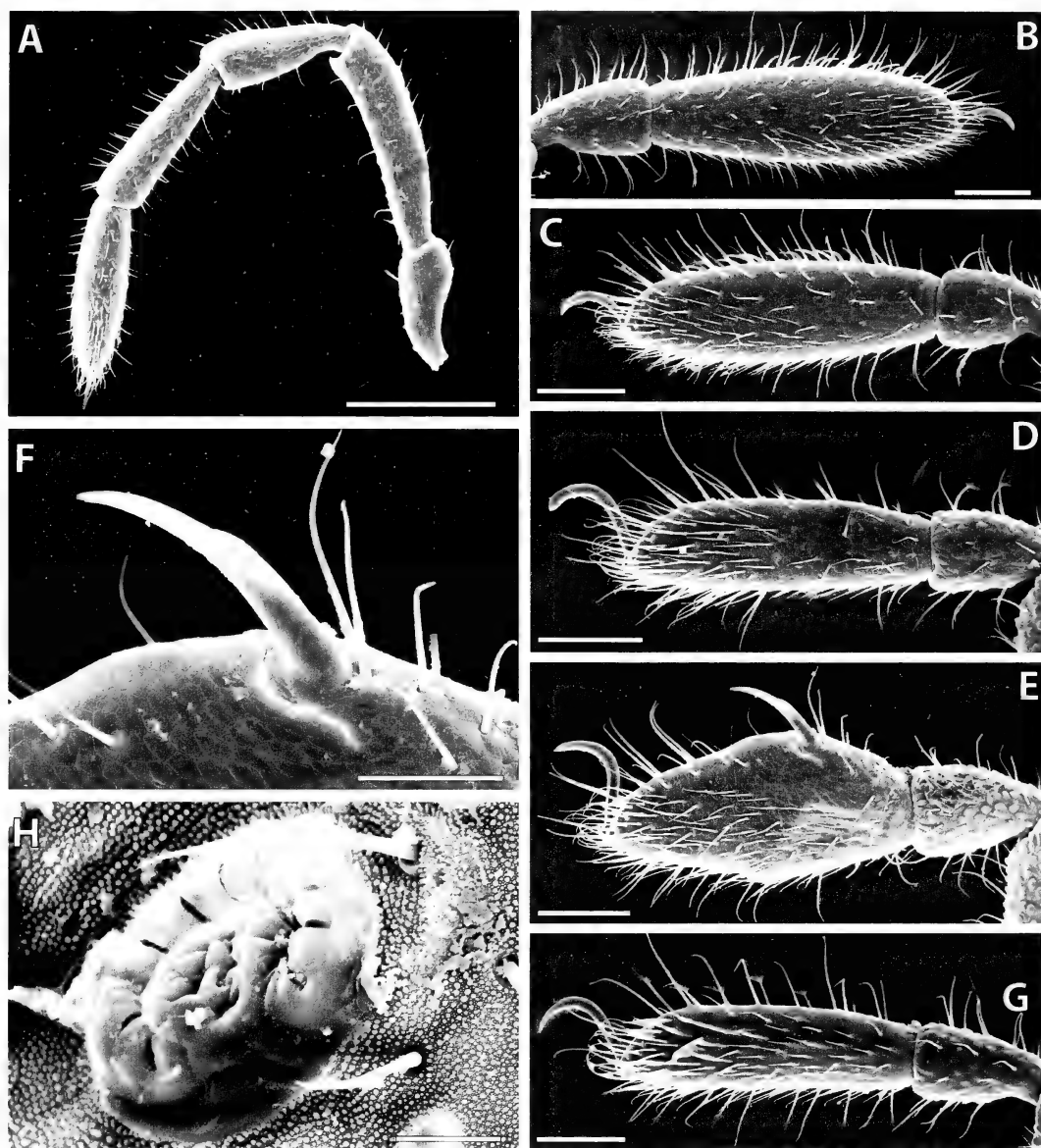
Figure 12.   *Siro calaveras* sp. nov. paratype male (MCZ 92899) and female (MCZ 92899). (A) Left palp of male. (B) Metatarsus and tarsus I of male. (C) Metatarsus and tarsus II of male. (D) Metatarsus and tarsus III of male. (E) Metatarsus and tarsus IV of male. (F) Detail of adenostyle. (G) Metatarsus and tarsus IV of female. (H) Spiracle. (A, Scale bar 200 μm; B–E, G, scale bars 100 μm; F, scale bar 50 μm; H, scale bar 20 μm.)

(Fig. 11C). Male gonostome semicircular, with straight posterior margin, wider than long (0.10 × 0.06 mm), and delimited laterally and anterolaterally by the elevated endites of coxae IV. Spiracles (Fig. 12H) of circular type (*sensu* Giribet and Boyer,

2002), circular to oval in shape in male, with a maximum diameter of 0.06 mm.

Ventral opisthosomal region (Fig. 11A) without conspicuous modifications other than in the anal plate. Opisthosomal tergite IX and sternites 8 and 9 fused into a broad
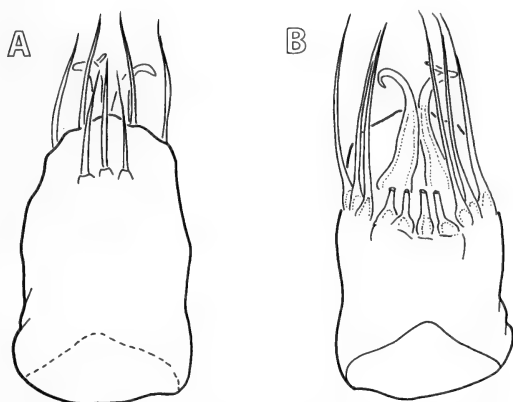
Figure 13. *Siro calaveras* sp. nov. (A) Spermatopositor, ventral view. (B) Spermatopositor, dorsal view.

corona analis (Fig. 11E); tergite VIII slightly bilobed. Anal plate oval, 0.22 × 0.17 mm, concave, mostly smooth, without ornamentation or a longitudinal carina. Three anal gland pores on tergite VIII of males (Fig. 11E). Cuticle with tuberculate–microgranular surface (*sensu* Murphree, 1988), nearly uniform in dorsal areas and in ventral areas including coxae.

Chelicerae robust; basal article in males 0.73 mm long, 0.17 mm wide, with a ventral process and a dorsal crest; 2nd article 0.60 mm long, 0.17 mm wide; movable finger 0.23 mm long; all articles with few setae, the proximal one almost entirely granulated with dense granulation; denticles on the cutting edge of each cheliceral finger uniform. Second cheliceral segment not ornamented.

Palp (Fig. 12A) 1.13 mm long, smooth, slightly ornamented on trochanter. Measurements of palpal article length in SEM male paratype (mm): trochanter 0.16, femur 0.31, patella 0.20, tibia 0.22, tarsus 0.24; claw 0.04 mm long.

Legs relatively robust; leg formula IV-I-II-III (measurements in Table 4; Figs. 12B–E). Tarsus I with a concentration of setae, but not forming a distinct solea. Except for tarsi I–IV and metatarsi I–II, all articles ornamented (Figs. 12B–E). Tarsus IV entire, globose, with a lamelliform adenostyle (Figs. 12E, F), subcylindrical at the base, with lateral pore (Fig. 12F); proximal margin at 31% of tarsal length. Claws hooked, smooth, without dentition or lateral pegs.

Spermatopositor (Figs. 13A, B) short, typical of sironids, smooth; with movable fingers, slightly curved outward, ending as hooks, longer than the membranous median lobe; microtrichial formula: 3, 4, 5+5 (n = 1). Gonopore complex not observed.

Description of Female. Total length 1.74 mm, maximum width 0.80 mm (L/W = 2.18; Fig. 10D). Ventral prosomal complex (Figs. 11B, F) only with coxae I–II meeting along the midline, coxae III delimiting the anterior part of gonostome. Female gonostome subtrapezoidal, wider than long. Gonostome of female forming a tube. Corona analis not protruding or forming a tube (Figs. 10D–F, 11B). Female anal plate (Fig. 11F) with modifications, slightly raised in the mid-posterior section, and forming two concave lateral areas; ornamentation is sparse. Tarsus of leg IV without modifications, narrower than that of males.

Ovipositor not studied.

Siro clousi Giribet & Shear sp. nov.
(Figs. 14–16)

Type Specimens

Holotype. Male (MCZ DNA101871 ex DNA101616large; used for DNA study)

Leg	Trochanter	Femur	Patella	Tibia	Metatarsus	Tarsus	Total
I	0.20/0.10	0.44/0.10	0.22/0.11	0.30/0.11	0.20/0.09	0.39/0.12	1.75
II	0.13/0.10	0.38/0.11	0.19/0.11	0.23/0.11	0.16/0.09	0.36/0.11	1.45
III	0.16/0.09	0.26/0.10	0.17/0.11	0.21/0.11	0.14/0.07	0.29/0.09	1.23
IV	0.25/0.10	0.40/0.11	0.24/0.12	0.28/0.11	0.28/0.10	0.33/0.16	1.78
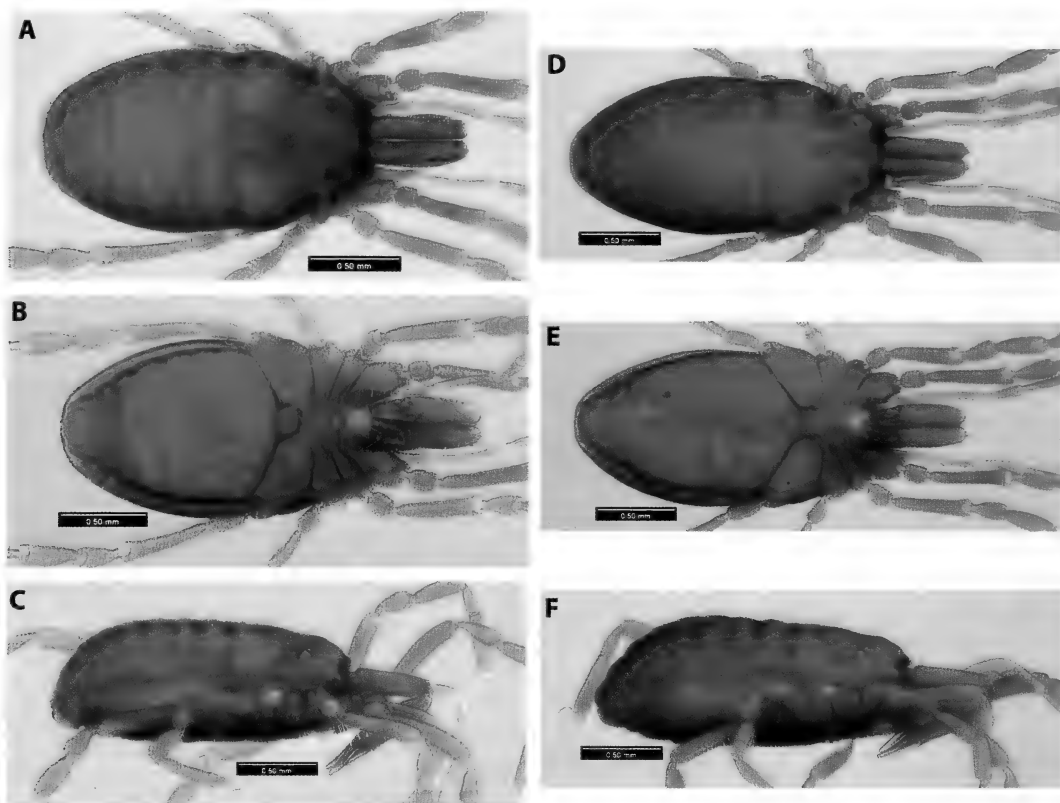
Figure 14.   *Siro clousi* sp. nov. (A–C) Holotype male (MCZ DNA101871) in dorsal (A), ventral (B), and lateral (C) view. (D–F) Paratype female (MCZ DNA101871) in dorsal (D), ventral (E), and lateral (F) view. Scale bars 500 µm.

from Olalla Road, Lincoln Co., OREGON, collected 20.vi.2005 by *S. L. Boyer, R. M. Clouse, & G. Giribet.*

Paratypes. Two females (1 female for DNA work; MCZ DNA101871 ex DNA 101616large).

Etymology. The species is named after cyphophthalmid biologist Ronald M. Clouse, who assisted collecting the type material of the species.

Diagnosis. Siro clousi sp. nov. is easily distinguished from *S. kamiakensis* in that the latter has a divided male tarsus IV, from *S. sonoma* in that the latter has a mesal modification in the male tarsus IV, and from *S. shasta* in that the latter lacks ornamentation on the legs. The species is larger than *S. acaroides*, which live sympatrically and can also be distinguished from it by the

spiracles, which are open in *S. acaroides*. The presence of the anal carina also distinguishes it from *S. acaroides, S. boyerae, S. calaveras,* and *S. shasta.* The presence of coxae III meeting along the midline also distinguishes it from *S. boyerae, S. exilis, S. kamiakensis,* and *S. sonoma.*

Description of Male. Medium-sized sironid of uniform chestnut brown color; total length of holotype 1.89 mm, maximum width at 3rd opisthosomal segment at 1.05 mm, body L/W = 1.80 (Fig. 6A). Anterior margin of dorsal scutum straight or slightly concave; prosomal region trapezoidal. Ozophores conical, of type II (*sensu* Juberthie, 1970), with subterminal ozopore (*sensu* Novak and Giribet, 2006), and entirely ornamented, with spiral ornamen-
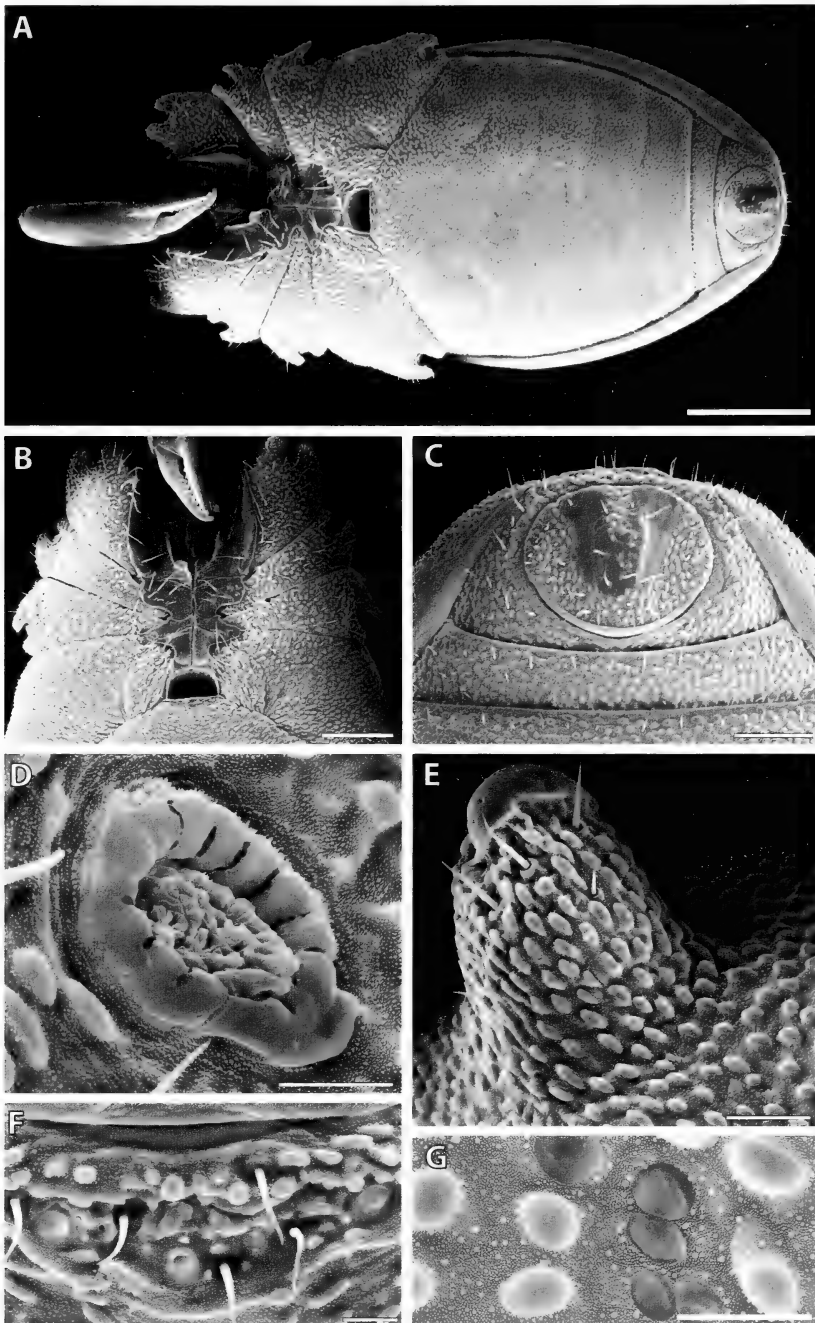
Figure 15. *Siro clousi* sp. nov. paratype male (MCZ DNA101871). (A) Paratype male in ventral position. (B) Male ventral thoracic complex. (C) Male anal region. (D) Spiracle. (E) Detail of the ozophore ornamentation. (F) Detail of the anal gland openings. (A, scale bar 400 μm; B, scale bar 200 μm, C, scale bar 100 μm; D, F, G, scale bars 20 μm; E, scale bar 40 μm.)
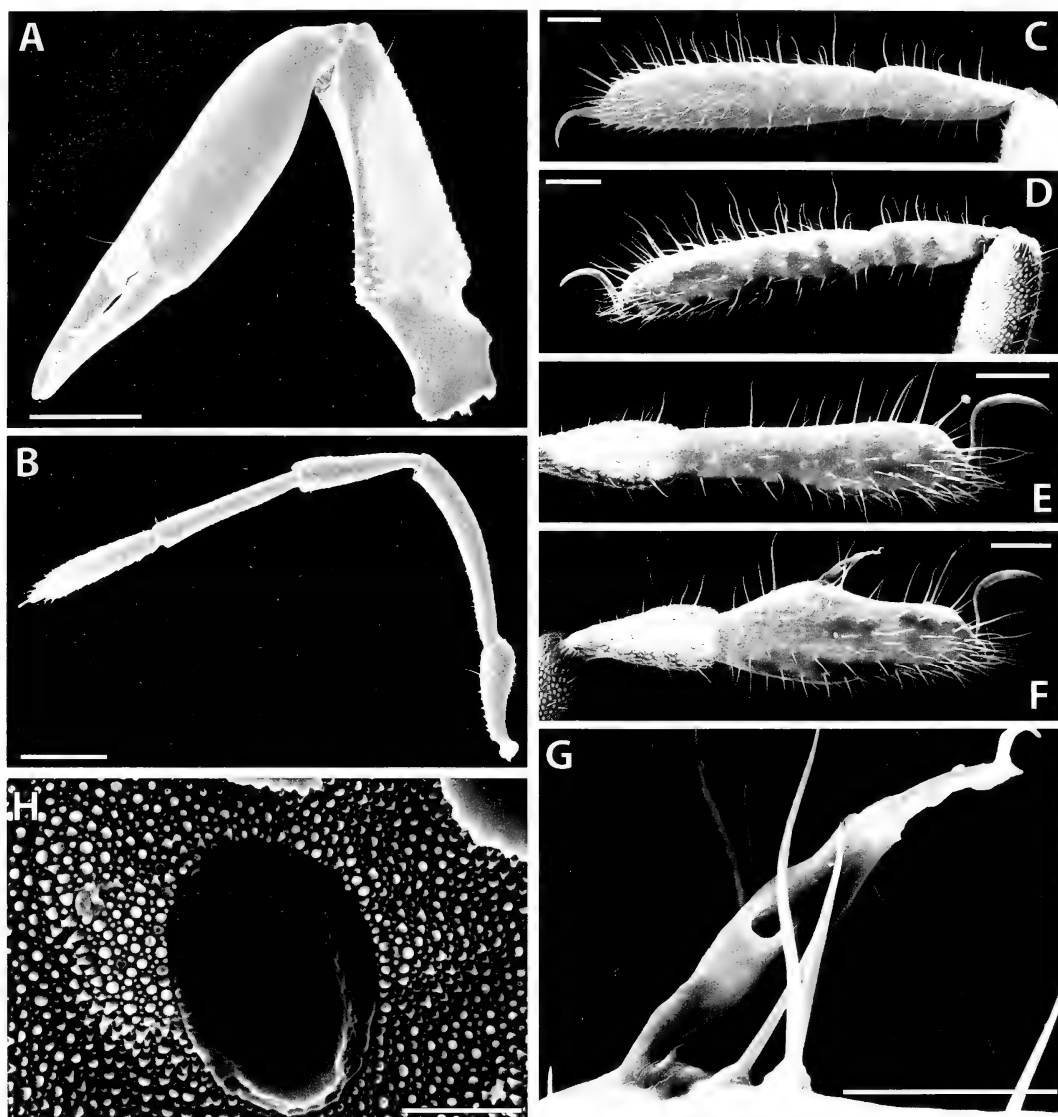
Figure 16.   *Siro clousi* sp. nov. paratype male (MCZ DNA101871). (A) Left chelicera. (B) Left palp. (C) Metatarsus and tarsus I. (D) Metatarsus and tarsus II. (E) Metatarsus and tarsus III. (F) Metatarsus and tarsus IV. (G) Detail of the adenostyle. (H) Detail of leg I cuticle ornamentation. (A, B, scale bars 200 m; C–F, scale bars 100 μm; G, scale bar 50 μm; H, scale bar 5 μm.)

tation (*sensu* de Bivort and Giribet, 2004); maximum width across ozophores 0.95 mm. Eyes absent. Transverse prosomal sulcus inconspicuous; transverse opisthosomal sulci inconspicuous. Dorsal scutum with maximum height at around segments 4–5 (Fig. 14C).

Ventral prosomal complex (Figs. 14B, 15A, B) with coxae I–II free, coxae III–IV fused; coxae II, III, and IV meeting along the midline; coxae IV meeting along the midline for a distance greater than gonostome length; sternum absent; coxal pores clearly visible between coxae III and IV.

TABLE 5.   LEG MEASUREMENTS (LENGTH/WIDTH, MM) IN *SIRO CLOUSI* SP. NOV. MEASUREMENTS REFER TO MALE PARATYPE MOUNTED FOR SEM.

Leg	Trochanter	Femur	Patella	Tibia	Metatarsus	Tarsus	Total
I	0.17/0.14	0.62/0.13	0.31/0.12	0.41/0.12	0.26/0.10	0.51/0.12	2.28
II	0.15/0.13	0.57/0.13	0.36/0.13	0.35/0.13	0.23/0.09	0.46/0.11	2.12
III	0.16/0.13	0.42/0.12	0.24/0.13	0.28/0.13	0.23/0.09	0.42/0.10	1.75
IV	0.25/0.13	0.54/0.13	0.29/0.14	0.32/0.14	0.25/0.11	0.46/0.17	2.11

Projections of coxae IV endites present in the anterior portion of gonostome wall (Fig. 15B). Male gonostome semicircular, with straight posterior margin, wider than long (0.13 × 0.07 mm), and delimited laterally and anterolaterally by the elevated endites of coxae IV. Spiracles (Fig. 15D) of circular type (*sensu* Giribet and Boyer, 2002), circular to oval in shape in male, with a maximum diameter of 0.05 mm.

Ventral opisthosomal region (Fig. 15A) without conspicuous modifications other than in the anal plate. Opisthosomal tergite IX and sternites 8 and 9 fused into a broad corona analis (Fig. 15C). Anal plate oval, 0.24 × 0.18 mm, mostly ornamented, with a conspicuous longitudinal central ridge that leaves two lateral depressions deprived of ornamentation. Three anal gland pores on tergite VIII of males (Fig. 15F). Cuticle with tuberculate-microgranular surface (*sensu* Murphree, 1988), nearly uniform in dorsal areas and in ventral areas including coxae.

Chelicerae (Fig. 16A) robust; basal article in males 0.69 mm long, 0.21 mm wide, with a ventral process and a dorsal crest; 2nd article 0.84 mm long, 0.18 mm wide; movable finger 0.30 mm long; all articles with few setae, the proximal one almost entirely granulated with dense granulation; denticles on the cutting edge of each cheliceral finger uniform. Second cheliceral segment not ornamented.

Palp (Fig. 16B) 1.65 mm long, smooth, slightly ornamented on trochanter. Measurements of palpal article length in SEM male paratype (mm): trochanter 0.23, femur 0.46, patella 0.30, tibia 0.35, tarsus 0.30; claw 0.05 mm long.

Legs relatively robust, leg formula I-II-IV-III (measurements in Table 5;

Figs. 16C–F). Tarsus I with a concentration of setae, but not forming a distinct solea. Except for the tarsi I–IV and metatarsi I–II, all articles ornamented (Figs. 16C–F). Tarsus IV of male entire, with a narrow lamelliform adenostyle (Fig. 16F), subcylindrical at the base, with lateral pore (Fig. 16G); proximal margin at 39% of tarsal length. Claws hooked, smooth, without dentition or lateral pegs.

Spermatopositor not studied.

Description of Female. Total length 2.04 mm, maximum width 1.02 mm (L/W = 1.99; Fig. 14D). Ventral prosomal complex (Fig. 14E) only with coxae I–II meeting along the midline, coxae III delimiting the anterior part of gonostome. Female gonostome semicircular anteriorly, wider than long. Gonostome of female forming a tube. Corona analis not protruding or forming a tube (Figs. 14D–F). Female anal plate unmodified. Tarsus of leg IV without modifications, narrower than that of males.

Ovipositor not studied.

Notes. *Siro clousi* sp. nov. is sympatric with the more widespread species *S. acaroides*, a considerably smaller species. Originally the specimens collected in the type locality, Olalla Road, were labeled as "large" and "small," but assigned the same MCZ DNA collection number, the vial containing the type material of the new species along with 4 males and 5 females of *S. acaroides*.

Siro shasta sp. nov.
(Figs. 17–20)

Type Specimens

Holotype. Male (AMNH) from 8 mi south of Dunsmuir, Shasta Co., CALIFORNIA,
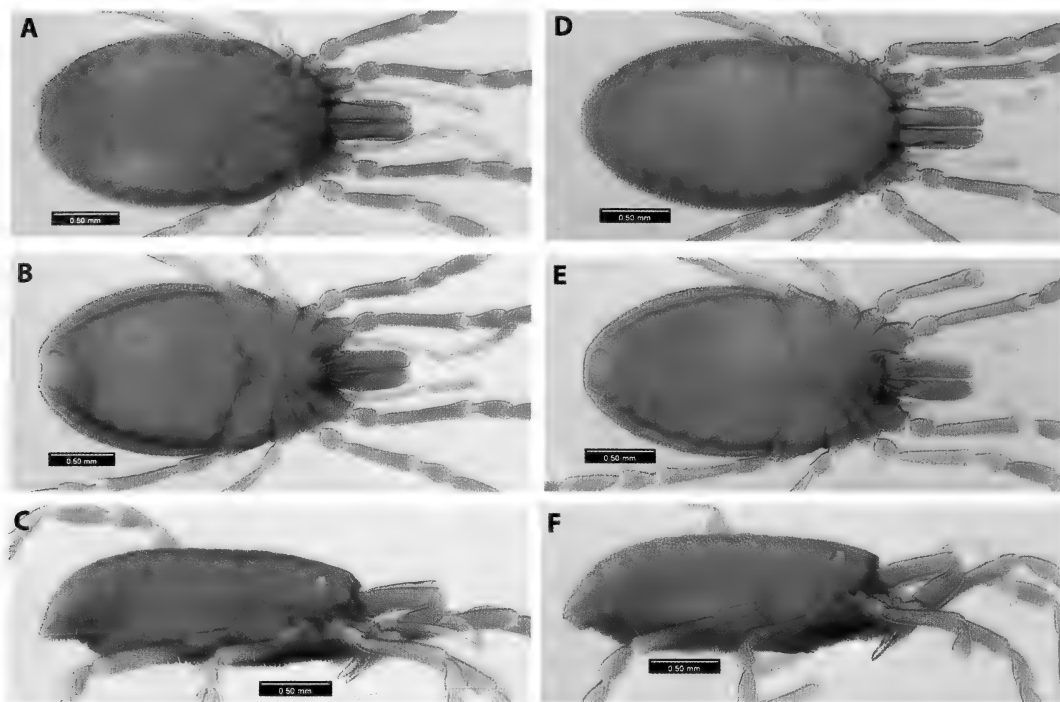
Figure 17.   *Siro shasta* sp. nov. (A–C) Holotype male (AMNH) in dorsal (A), ventral (B), and lateral (C) view. (D–F) Paratype female (AMNH) in dorsal (D), ventral (E), and lateral (F) view. Scale bars 500 μm.

collected 11.vii.1954 by *R. O. Schuster & E. E. Gilbert* (Figs. 6A–C).

Paratypes. Eight males, 6 females (AMNH), same collecting data as holotype; 1 male (MCZ 92985, ex AMNH, on SEM stub), 1 female (MCZ 92986, ex AMNH, on SEM stub), same collecting data as holotype; 3 males, 5 females (AMNH) from North of Hazel Creek, Shasta Co., CALIFORNIA, collected 26.vi.1954 by *R. O. Schuster & B. Adelson*; 1 female (MCZ DNA101622) from Sims bridge, Shasta National Forest, Shasta Co., CALIFORNIA, collected 22.vi.2005 by *S. L. Boyer, R. M. Clouse, & G. Giribet*.

Etymology. The species epithet is a noun in apposition, after Shasta Co., California.

Diagnosis. Siro shasta (Fig. 17) is notably larger, with longer, thinner legs, than any of the other western North American *Siro* species, being about one-third longer than *S. acaroides* (2.6 vs. 1.5 mm); the body is more robust (L/W = 1.7) than that of *S.*

calaveras, n. sp. (L/W = 1.9) and the 8th tergite of the male is noticeably more concave and bilobed than in any other North American species; in *S. exilis* the 8th tergite is convex. The entire 4th tarsus of the male differentiates the species from *S. kamiakensis*. The leg ornamentation differs considerably from all other North American species, being so sparse that it is barely noticeable elsewhere than on the trochanter and the dorsal part of the femur, whereas in all other species, legs I and II have a smooth tarsus and metatarsus only and legs III and IV have a smooth tarsus only. The ventral prosomal complex resembles mostly that of *S. acaroides, S. calaveras*, and *S. clousi*, in that the endites of coxae III meet along the midline, but not so in *S. boyerae, S. exilis*, or *S. kamiakensis*. The spiracles are similar to those of *S. acaroides*, in the form of an open circle, but differ from all other North American sironids, which have circular spiracles. The microtrichia of
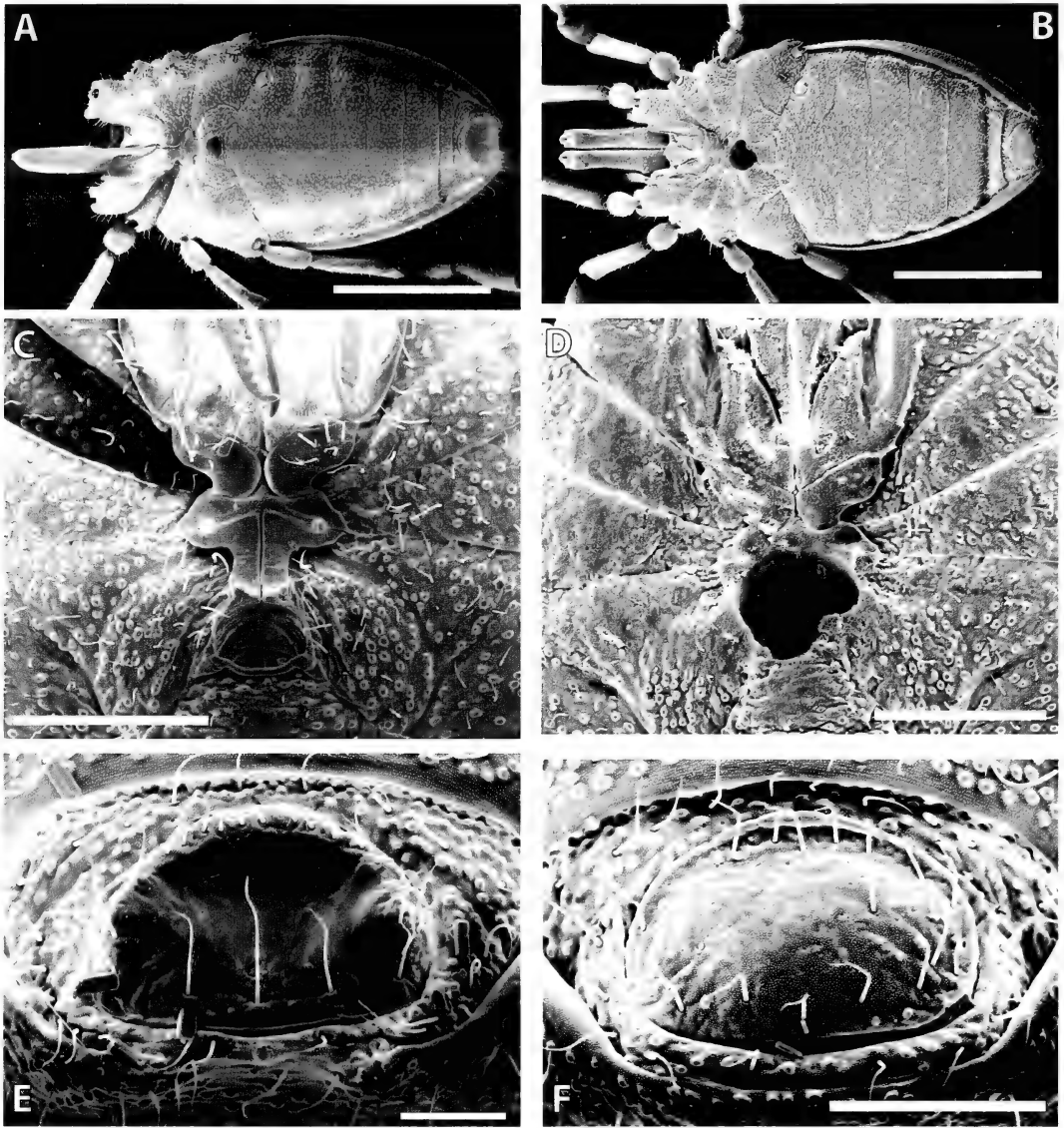
Figure 18.   *Siro shasta* sp. nov. paratype male (MCZ 92985) and female (MCZ 92986). (A) Paratype male in ventral position. (B) Paratype female in ventral position. (C) Male ventral thoracic complex. (D) Female ventral thoracic complex. (E) Male anal region. (F) Female anal region. (A, B, scale bars 1 mm; C, D, scale bars 300 μm; E, scale bar 100 μm; F, scale bar 200 μm.)

the penis is unique among North American *Siro*, with 4 apical, 6 ventral, and 10 dorsal microtrichiae, whereas the unusually large movable fingers of the penis are like those of the western species group.

Description of Male. Large sironid of uniform chestnut brown color; total length of holotype 2.33 mm, maximum width at 3rd opisthosomal segment at 1.38 mm, body L/W = 1.69 (Fig. 17A). Anterior margin of dorsal scutum bilobed; prosomal region sub-semicircular. Ozophores conical, of type II (*sensu* Juberthie, 1970), with subterminal ozopore (*sensu* Novak and Giribet, 2006), and entirely ornamented; maximum width across ozophores 1.02 mm.
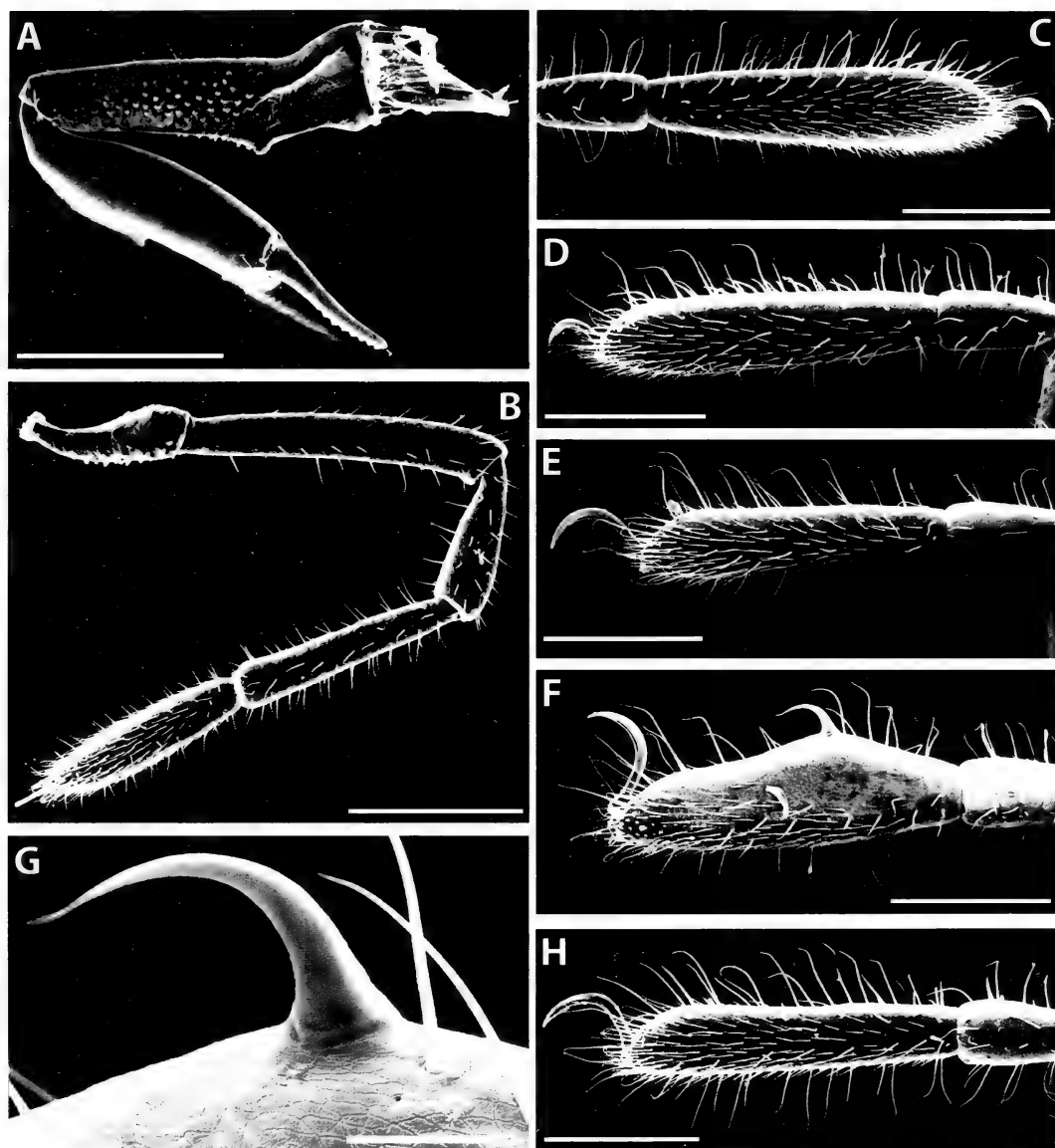
Figure 19.   *Siro shasta* sp. nov. paratype male (MCZ 92985) and female (MCZ 92986). (A) Left chelicera of male. (B) Left palp of male. (C) Metatarsus and tarsus I of male. (D) Metatarsus and tarsus II of male. (E) Metatarsus and tarsus III of male. (F) Metatarsus and tarsus IV of male. (G) Detail of adenostyle. (H) Metatarsus and tarsus IV of female. (A, scale bar 500 µm; B–F, H, scale bars 300 µm; G, scale bar 50 µm.)

Eyes absent. Transverse prosomal sulcus inconspicuous; transverse opisthosomal sulci inconspicuous. Dorsal scutum with maximum height at around segments 4–5 (Fig. 17C).

Ventral prosomal complex (Figs. 18A, E) with coxae I–II free, coxae III–IV fused; coxae II, III, and IV meeting along the midline; coxae IV meeting along the midline for a distance slightly greater than gonos-
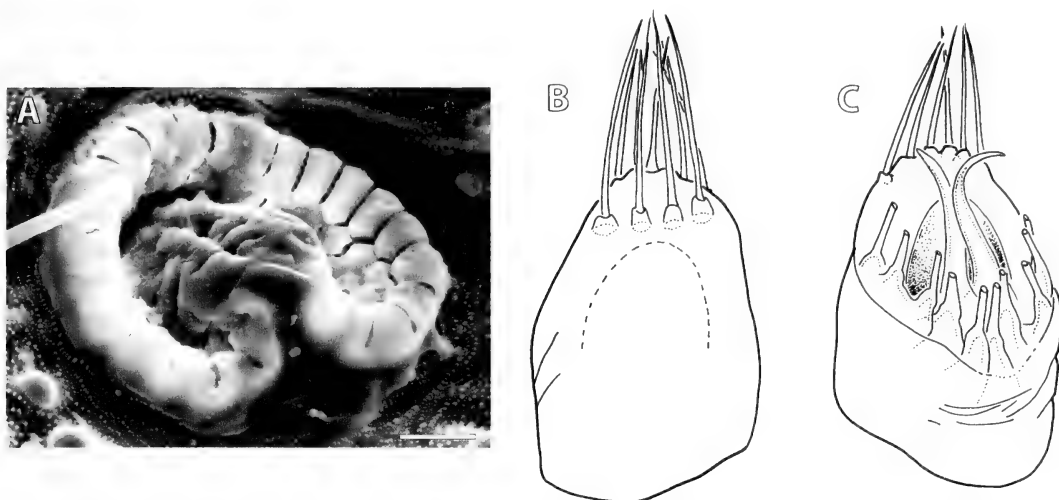
Figure 20. *Siro shasta* sp. nov. (A) Spiracle (scale bar 20 μm). (B) Spermatopositor, ventral view. (C) Spermatopositor, dorsal view.

tome length; sternum absent; coxal pores clearly visible between coxae III and IV. Projections of coxae IV endites present in the anterior portion of gonostome wall (Fig. 18C). Male gonostome almost oval in shape, with the posterior margin forming a concave lip, wider than long (0.14 × 0.10 mm), and delimited laterally and anterolaterally by the elevated endites of coxae IV. Spiracles (Fig. 20A) in the shape of an open circle (*sensu* Giribet and Boyer, 2002), with a maximum diameter of 0.10 mm.

Ventral opisthosomal region (Fig. 18A) without conspicuous modifications other than in the anal plate. Opisthosomal tergite IX and sternites 8 and 9 fused into a broad corona analis (Fig. 18E). Anal plate oval, 0.32 × 0.21 mm, completely depressed and smooth, except for the anterior and lateral rims. Three anal gland pores on tergite VIII of males. Tergite VIII depressed posteriorly, forming a bilobed posterior end. Cuticle with tuberculate-microgranular surface (*sensu* Murphree, 1988), nearly uniform in dorsal areas and in ventral areas including coxae.

Chelicerae (Fig. 19A) robust; basal article in males 0.85 mm long, 0.23 mm wide, with a ventral process but without a dorsal crest; 2nd article 1.07 mm long, 0.19 mm wide; movable

finger 0.35 mm long; all articles with few setae, the proximal one almost entirely granulated but with sparse granulation; denticles on the cutting edge of each cheliceral finger uniform, triangular, with 8 denticles in the moveable finger. Second cheliceral segment smooth, not ornamented.

Palp (Fig. 19B) 1.91 mm long, smooth, slightly ornamented on trochanter. Measurements of palpal article length in SEM male paratype (mm): trochanter 0.27, femur 0.55, patella 0.29, tibia 0.40, tarsus 0.40; claw 0.06 mm long.

Legs slender, leg formula I-IV-II-III (measurements in Table 6; Figs. 19C–F). Tarsus I with a concentration of setae, but not forming a distinct solea. Tarsi I–IV and metatarsi I–II smooth, all other articles presenting sparse ornamentation, to the point that metatarsi III–IV are almost smooth, but present a few tuberculate structures (Figs. 19E, F). Tarsus IV of male entire, swollen, with a small lamelliform adenostyle (Fig. 19F), subcylindrical at the base, with lateral pore (Fig. 19G); proximal margin at 35% of tarsal length. Claws hooked, smooth, without dentition or lateral pegs.

Spermatopositor (Figs. 20B, C) short, typical of sironids, smooth; with movable

fingers, slightly curved outward, ending as hooks, not much longer than the membranous median lobe; microtrichial formula: 4, 6, 5+5 (n = 1). Gonopore complex not observed.

Description of Female. Total length 2.40 mm, maximum width 1.29 mm (L/W = 1.85; Fig. 17D). Ventral prosomal complex (Figs. 18B, F) only with coxae I–II meeting along the midline, coxae III delimiting the anterior part of gonostome. Female gonostome near circular, wider than long. Gonostome of female forming a tube. Corona analis not protruding or forming a tube, with most of its surface deprived of macrotuberculate ornamentation, only presenting microtuberculate one (Fig. 18F). Tarsus of leg IV without modifications (Fig. 19H), narrower than that of males.

Ovipositor not studied.

Siro acaroides (Ewing, 1923)

Holosiro acaroides Ewing 1923: 338.
Siro acaroides: Newell 1947: 354; Shear 1980: 10.

The following new records establish a new southern limit for the distribution of *S. acaroides*, by about 50 mi. The records for the locality, "18 miles south of Klamath," were labeled as being from Del Norte Co., but that distance south of Klamath would be well into Humboldt Co., and the records are so given here. It is possible that *S. acaroides* occurs much farther south; there is a single juvenile (CAS) known from Mendocino Co., 2 mi south of Rockport, collected by *C. W. O'Brien*, 2.ii.1962. However, the possibility that this is another species cannot be dismissed.

We have also found that *S. acaroides* exhibits at least one unique character when compared with other North American *Siro*:

the palpal trochanter without tubercles (de Bivort and Giribet, 2002: fig. 16a).

CALIFORNIA: *Del Norte Co.*: One male (CAS) near Crescent City, Smith River, collected 9.xi.1956 by *J. Schuh*; 2 males, 1 female (CAS) 5 mi south of Crescent City, collected 9.ix.1958; 7 males (1 for DNA work) and 6 females (MCZ DNA101620) from Kings Valley, near Crescent City, collected 21.vi.2005 by *S. L. Boyer, R. M. Clouse, & G. Giribet. Humboldt Co.*: Thirteen males, 8 females (CAS) 18 mi south of Klamath, collected 13.viii.1953; 28 males, 28 females (CAS) collected 19.ix.1953; 5 males, 4 females (CAS) Big Lagoon, collected 13.viii.1953 by *G. A. Marsh & L. O. Schuster*; 3 males, 3 females (CAS) freshwater, collected 18.viii.1952 by *G. A. Marsh & L. O. Schuster*; 5 males (CAS) Prairie Creek Redwoods State Park, collected 8.ix.1958 by *L. M. Smith*; 7 males (1 for DNA work) and 9 females (1 for DNA work; MCZ DNA101621) from Lady Bird Johnson Grove, Redwood National and State Parks, collected 21.vi.2005 by *S. L. Boyer, R. M. Clouse, & G. Giribet.*

OREGON: *Benton Co.*: Thirteen males (1 for DNA work) and 19 females (MCZ DNA101618) from MacDonald State Forest, collected 20.vi.2005 by *S. L. Boyer, R. M. Clouse, & G. Giribet. Douglas Co.*: Eleven males (2 for DNA work) and 4 females (MCZ DNA101619) from Elliot State Forest, Umpqua State Scenic Corridor, collected 20.vi.2005 by *S. L. Boyer, R. M. Clouse, & G. Giribet.*

KEY TO MALES OF NORTH AMERICAN SIRONIDAE

1a. Male 4th tarsus divided ....*S. kamiakensis* (Newell, 1943)

TABLE 6.   LEG MEASUREMENTS (LENGTH/WIDTH, MM) IN *SIRO SHASTA* SP. NOV. MEASUREMENTS REFER TO MALE PARATYPE MOUNTED FOR SEM.

Leg	Trochanter	Femur	Patella	Tibia	Metatarsus	Tarsus	Total
I	0.27/0.18	0.83/0.14	0.38/0.16	0.58/0.16	0.31/0.12	0.70/0.16	3.07
II	0.18/0.15	0.68/0.16	0.28/0.16	0.45/0.16	0.26/0.11	0.62/0.13	2.47
III	0.25/0.16	0.51/0.15	0.26/0.17	0.41/0.16	0.25/0.11	0.57/0.13	2.25
IV	0.43/0.15	0.72/0.16	0.38/2.0	0.50/0.18	0.31/0.13	0.64/0.21	2.98
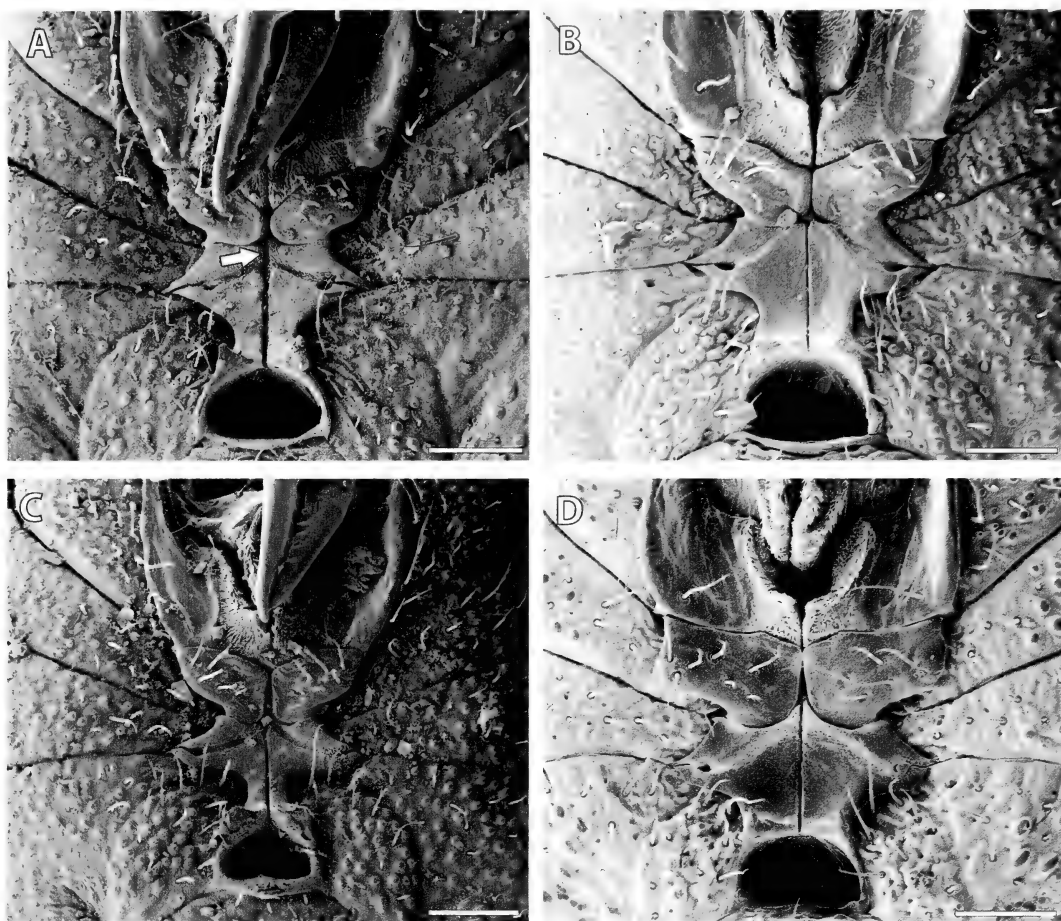
Figure 21.   Male ventral thoracic complex of described North American sironids. (A) *Siro acaroides* (arrowhead indicates the area of contact of the endites of cozae III). (B) *S. exilis.* (C) *S. kamiakensis.* (D) *S. sonoma.* (A–D, scale bars 100 µm.)

1b. Male 4th tarsus not divided 2

2a. Male 4th tarsus with a ventral lobe mesally excavated ....
.... *S. sonoma* Shear, 1980

2b. Male 4th tarsus without a ventral lobe 3

3a. Male tergite VIII convex, with small knob ....
..................*S. exilis* Hoffman, 1963.

3b. Male tergite VIII concave, without a knob 4

4a. Legs with very sparse ornamentation .... *S. shasta* sp. nov.

4b. Legs with basal articles ornamented until tibia I and II and until metatarsi III and IV 5

5a. Spiracles in the form of an open circle ... *S. acaroides* (Ewing, 1923).

5b. Spiracles circular 6

6a. Endites of coxae III not meeting along the midline ....
.... *S. boyerae* sp. nov.

6b. Endites of coxae III meeting along the midline 7

7a. Anal carina present ....
.... *S. clousi* sp. nov.

7b. Anal carina absent ....
.... *S. calaveras* sp. nov.

ACKNOWLEDGMENTS

LITERATURE CITED

BOYER, S. L., J. M. BAKER, and G. GIRIBET. 2007a. Deep genetic divergences in *Aoraki denticulata* (Arachnida, Opiliones, Cyphophthalmi): a widespread 'mite harvestman' defies DNA taxonomy. Molecular Ecology **16**: 4999–5016.

BOYER, S. L., R. M. CLOUSE, L. R. BENAVIDES, P. SHARMA, P. J. SCHWENDINGER, I. KARUNARATHNA, and G. GIRIBET. 2007b. Biogeography of the world: a case study from cyphophthalmid Opiliones, a globally distributed group of arachnids. Journal of Biogeography **34**: 2070–2085.

BOYER, S. L., I. KARAMAN, and G. GIRIBET. 2005. The genus *Cyphophthalmus* (Arachnida, Opiliones, Cyphophthalmi) in Europe: a phylogenetic approach to Balkan Peninsula biogeography. Molecular Phylogenetics and Evolution **36**: 554–567.

CATLEY, K. M. 1994. Descriptions of new *Hypochilus* species from New Mexico and California with a cladistic analysis of the Hypochilidae (Araneae). American Museum Novitates **3088**: 1–27.

DAVIS, N. W. 1933. A new opilionid from Florida (Arachnida, Cyphophthalmi). Journal of the New York Entomological Society **41**: 49–53.

DE BIVORT, B. L., and G. GIRIBET. 2004. A new genus of cyphophthalmid from the Iberian Peninsula with a phylogenetic analysis of the Sironidae (Arachnida : Opiliones : Cyphophthalmi) and a SEM database of external morphology. Invertebrate Systematics **18**: 7–52.

DE LAET, J. E. 2005. Parsimony and the problem of inapplicables in sequence data, pp. 81–116. *In* V. A. Albert (ed.), Parsimony, Phylogeny, and Genomics. Oxford: Oxford Univ. Press.

EWING, H. E. 1923. *Holosiro acaroides*, new genus and species—the only New World representative of the mite-like phalangids of the suborder Cyphophthalmi. Annals of the Entomological Society of America **16**: 387–390.

FARRIS, J. S. 1997. The future of phylogeny reconstruction. Zoologica Scripta **26**: 303–311.

FARRIS, J. S., V. A. ALBERT, M. KÄLLERSJÖ, D. LIPSCOMB, and A. G. KLUGE. 1996. Parsimony jackknifing outperforms neighbor-joining. Cladistics **12**: 99–124.

FARRIS, J. S., M. KÄLLERSJÖ, A. G. KLUGE, and C. BULT. 1995. Constructing a significance test for incongruence. Systematic Biology **44**: 570–572.

FOLMER, O., M. BLACK, W. HOEH, R. LUTZ, and R. C. VRIJENHOEK. 1994. DNA primers for amplification of mitochondrial cytochrome *c* oxidase subunit I from diverse metazoan invertebrates. Molecular Marine Biology and Biotechnology **3**: 294–299.

GIRIBET, G. 2000. Catalogue of the Cyphophthalmi of the world (Arachnida, Opiliones). Revista Ibérica de Aracnología **2**: 49–76.

———. 2003. Stability in phylogenetic formulations and its relationship to nodal support. Systematic Biology **52**: 554–564.

———. 2005. Generating implied alignments under direct optimization using POY. Cladistics **21**: 396–402.

———. 2007. Neogoveidae Shear, 1980, pp. 95–97. *In* R. Pinto-da-Rocha, G. Machado, and G. Giribet (eds.), Harvestmen: The Biology of Opiliones. Cambridge, Massachusetts: Harvard Univ. Press.

GIRIBET, G., and S. L. BOYER. 2002. A cladistic analysis of the cyphophthalmid genera (Opiliones, Cyphophthalmi). The Journal of Arachnology **30**: 110–128.

GIRIBET, G., G. D. EDGECOMBE, W. C. WHEELER, and C. BABBITT. 2002. Phylogeny and systematic position of Opiliones: a combined analysis of chelicerate relationships using morphological and molecular data. Cladistics **18**: 5–70.

GIRIBET, G., L. VOGT, A. PÉREZ GONZÁLEZ, P. SHARMA, and A. B. KURY. 2010. A multilocus approach to harvestman (Arachnida: Opiliones) phylogeny with

emphasis on biogeography and the systematics of Laniatores. Cladistics **26**. Available online only doi:10.1111/j1096-0031.2009.00296.x

Goebel, A. M., T. A. Ranker, P. S. Corn, and R. G. Olmstead. 2009. Mitochondrial DNA evolution in the *Anaxyrus* boreas species group. Molecular Phylogenetics and Evolution **50**: 209–225.

Goloboff, P. A. 1999. Analyzing large data sets in reasonable times: solutions for composite optima. Cladistics **15**: 415–428.

———. 2002. Techniques for analyzing large data sets, pp. 70–79. *In* R. DeSalle, G. Giribet, and W. Wheeler (eds.), Techniques in Molecular Systematics and Evolution. Basel: Brikhäuser Verlag.

Hinton, B. E. 1938. A key to the genera of the Suborder Cyphophthalmi with a description and figures of *Neogovea immsi*, gen. et sp.n. (Arachnida, Opiliones). Annals and Magazine of Natural History Ser.11 **2**: 331–338.

Hoffman, R. L. 1963. A new phalangid of the genus *Siro* from eastern United States, and taxonomic notes on other American sironids (Arach., Opiliones). Senckenbergiana Biologica **44**: 129–139.

Juberthie, C. 1960. Contribution a l'étude des opilions cyphophthalmes: description de *Metasiro* gen. n. Bulletin du Muséum National d'Histoire Naturelle **32**: 235–241.

———. 1967. *Siro rubens* (Opilion, Cyphophthalme). Revue d'Écologie et de Biologie du Sol **4**: 155–171.

———. 1970. Les genres d'opilions Sironinae (Cyphophthalmes). Bulletin du Muséum National d'Histoire Naturelle **41**: 1371–1390.

Karaman, I. M. 2008. Cyphophthalmi of Serbia (Arachnida, Opiliones), pp. 97–118. *In* D. Pavicevic and M. Perreau (eds.), Advances in the studies of the fauna of the Balkan Peninsula. Papers dedicated to the memory of Guido Nonveiller. Belgrade: Institute for Nature Conservation of Serbia.

Linton, E. W [Internet]. MacGDE: Genetic Data Environment for MacOS X. Mt. Pleasant (MI): Central Michigan University; c2005 [updated 2009 Jun 3; cited 2010 June 09]. Available from: http://macgde.bio.cmich.edu/.

Mallatt, J., and C. J. Winchell. 2002. Testing the new animal phylogeny: first use of combined large-subunit and small-subunit rRNA gene sequences to classify the protostomes. Molecular Biology and Evolution **19**: 289–301.

Mickevich, M. F., and J. S. Farris. 1981. The implications of congruence in *Menidia*. Systematic Zoology **30**: 351–370.

Murienne, J., I. Karaman, and G. Giribet. (2010). Explosive evolution of an ancient group of Cyphophthalmi (Arachnida: Opiliones) in the Balkan Peninsula. Journal of Biogeography **37**: 90–102.

Murphree, C. S. 1988. Morphology of the dorsal integument of ten opilionid species (Arachnida, Opiliones). The Journal of Arachnology **16**: 237–252.

Newell, I. M. 1943. A new sironid from North America (Opiliones, Cyphophthalmi, Sironidae). Transactions of the American Microscopical Society **62**: 416–422.

———. 1947. The rediscovery and clarification of *Siro acaroides* (Ewing) (Opiliones, Cyphophthalmi, Sironidae). Transactions of the American Microscopical Society **66**: 354–365.

Novak, T., and G. Giribet. 2006. A new species of Cyphophthalmi (Arachnida, Opiliones, Sironidae) from Eastern Slovenia. Zootaxa **1330**: 27–42.

Schwendinger, P. J., and G. Giribet. 2005. The systematics of the south-east Asian genus *Fangensis* Rambla (Opiliones : Cyphophthalmi : Stylocellidae). Invertebrate Systematics **19**: 297–323.

Shear, W. A. 1977. The opilionid genus *Neogovea* Hinton, with a description of the first troglobitic cyphophthalmid from the western hemisphere (Opiliones, Cyphophthalmi). The Journal of Arachnology **3**: 165–175.

———. 1980. A review of the Cyphophthalmi of the United States and Mexico, with a proposed reclassification of the suborder (Arachnida, Opiliones). American Museum Novitates **2705**: 1–34.

Wheeler, W. C. 1995. Sequence alignment, parameter sensitivity, and the phylogenetic analysis of molecular data. Systematic Biology **44**: 321–331.

———. 1996. Optimization alignment: the end of multiple sequence alignment in phylogenetics? Cladistics **12**: 1–9.

———. 2003. Implied alignment: a synapomorphy-based multiple-sequence alignment method and its use in cladogram search. Cladistics **19**: 261–268.

Wheeler, W. C., D. Gladstein, and J. De Laet. 2004. POY Version 3.0. New York: American Museum of Natural History.

Anolis chrysolepis Duméril & Bibron, 1837 (Squamata: Polychrotidae) revisited: Molecular phylogeny and taxonomy of the *Anolis chrysolepis* species group

ANNELISE B. D'ANGIOLELLA, TONY GAMBLE, TERESA C.S. AVILA-PIRES, GUARINO R. COLLI, BRICE P. NOONAN, AND LAURIE J. VITT

This publication has been printed on acid-free permanent paper stock.

ANOLIS CHRYSOLEPIS DUMÉRIL AND BIBRON, 1837 (SQUAMATA: IGUANIDAE), REVISITED: MOLECULAR PHYLOGENY AND TAXONOMY OF THE *ANOLIS CHRYSOLEPIS* SPECIES GROUP

ANNELISE B. D'ANGIOLELLA,[1] TONY GAMBLE,[2] TERESA C. S. AVILA-PIRES,[3] GUARINO R. COLLI,[4] BRICE P. NOONAN,[5] AND LAURIE J. VITT[6]

ABSTRACT. The *Anolis chrysolepis* species group is distributed across the entire Amazon basin and currently consists of *A. bombiceps* and five subspecies of *A. chrysolepis*. These lizards are characterized by moderate size, relatively narrow digital pads, and a small dewlap that does not reach the axilla. We used the mitochondrial gene *ND2* to estimate phylogenetic relationships among putative subspecies of *A. chrysolepis* and taxa previously hypothesized to be their close relatives. We also assessed the congruence between molecular and morphological datasets to evaluate the taxonomic status of group members. On the basis of the two datasets, we present a new taxonomy, elevating each putative subspecies of *A. chrysolepis* to species status. We provide new morphological diagnoses and new distributional data for each species.

Key words: *Anolis*, Amazon, Iguanidae, molecular phylogeny, taxonomy

RESUMO. O grupo de espécies *Anolis chrysolepis* atualmente consiste em *A. bombiceps* e cinco subespécies de *A. chrysolepis*, ocupando toda a Bacia Amazônica. Esses lagartos são caracterizados por tamanho moderado, lamelas digitais relativamente estreitas e um papo extensível que não chega às axilas. Nós utilizamos o gene mitocondrial *ND2* para estimar as relações filogenéticas entre as subespécies de *A. chrysolepis* e táxons previamente considerados parentes próximos. Nós também determinamos a congruência entre conjuntos de dados morfológicos e moleculares, para avaliar o status taxonômico dos membros desse grupo. Com base nos dois conjuntos de dados, apresentamos uma nova taxonomia, elevando cada subespécie de *A. chrysolepis* ao status de espécie. Fornecemos novas diagnoses morfológicas e novos dados de distribuição para cada espécie.

Palavras-chave: *Anolis*, Amazônia, Iguanidae, filogenia molecular, taxonomia

INTRODUCTION

The Pleistocene Refuge Hypothesis proposed almost simultaneously by Haffer (1969) and Vanzolini and Williams (1970) posits that patches of lowland tropical forest that existed during dry periods in the Pleistocene served as core areas for speciation in birds and in the lizard complex *Anolis chrysolepis*, respectively. Although the Pleistocene Refuge Hypothesis has been falsified for members of the *A. chrysolepis* species group because diversification occurred much earlier (15 mya) than the Pleistocene (Glor et al., 2001), relationships among all members of the group have not been worked out and related taxa (e.g., *A. meridionalis* and *A. bombiceps*) have not been properly placed with reference to the *A. chrysolepis* complex, and current names do not accurately reflect the evolutionary history of the group (Glor et al., 2001; Nicholson et al., 2005). Because the *A. chrysolepis* species group has been and continues to be a model for evolutionary (Nicholson et al., 2006, 2007; Schaad and Poe, 2010) and ecological (Vitt and Zani, 1996; Vitt et al., 2001, 2008) studies, it is critical that their relationships be properly understood. Here we present a phylogenetic hypothesis for the *A. chrysolepis* species

---

[1] Programa de Pós-Graduação em Zoologia UFPA-MPEG, Belém, PA, Brazil. Author for correspondence (annelise.dangiolella@gmail.com).

[2] University of Minnesota, Minneapolis, Minnesota.

[3] Museu Paraense Emílio Goeldi, Belém, PA, Brazil.

[4] Universidade de Brasília, Brasília, DF, Brazil.

[5] The University of Mississippi, University, Mississippi.

[6] University of Oklahoma, Norman, Oklahoma.

group using a much larger set of samples than was available previously and provide species names for taxa that can be identified as independent evolutionary lineages. Following de Queiroz (2007), we consider independent evolutionary lineages, here recognized on the basis of gene trees, analogous to species. Results of this study should be directly applicable to phylogeographic and phyloecological studies of the *A. chrysolepis* species group.

The *A. chrysolepis* group comprises two species: *A. chrysolepis* Duméril and Bibron, 1837, and *A. bombiceps* Cope, 1876. *Anolis chrysolepis* is currently composed of five subspecies: *A. chrysolepis chrysolepis*, in eastern Guiana (Brazil, French Guiana, Suriname, and southern Guyana); *A. chrysolepis planiceps* Troschel, 1848, in western Guiana (Brazil, Suriname, northwestern Guyana, Venezuela, and Trinidad); *A. chrysolepis scypheus* Cope, 1864, in western Amazonia (Colombia, Ecuador, Peru, and northwestern Brazil); *A. chrysolepis tandai* Avila-Pires, 1995, in southwestern Amazonia (Brazil and Peru); and *A. chrysolepis brasiliensis* Vanzolini and Williams, 1970, in Brazil, from Maranhão and enclaves of open vegetation in southern Pará south to São Paulo (Vanzolini and Williams, 1970; Avila-Pires, 1995; Icochea et al., 2001; Santos-Jr et al., 2007). *Anolis bombiceps* occurs in western Amazonia, in Peru, Colombia, and Brazil, at least in partial sympatry with *A. c. scypheus* and perhaps also with *A. c. tandai* (Avila-Pires, 1995). Members of the *A. chrysolepis* group are characterized by their moderate size (up to 83 mm snout–vent length); short heads; supraorbital semicircles usually forming a pronounced ridge; relatively narrow digital pads, with distal lamellae under phalanx ii forming a slightly prominent border; a dewlap that does not reach the axilla and is present in both sexes (but smaller in females); and keeled, imbricate ventral scales that are distinctly larger than dorsals.

The *A. chrysolepis* species group was examined morphologically by Vanzolini and Williams (1970), who recognized four sub-

species of *A. chrysolepis* and a distinct species, *A. bombiceps*. Vanzolini and Williams (1970: 13) believed the level of differentiation between the subspecies were "closest to species difference, and indicative, perhaps, of past and future potential species formation." *Anolis chrysolepis* was later examined by Avila-Pires (1995) under the name *A. nitens*. She described another subspecies, *A. n. tandai*, and observed that most specimens occurring in areas of intergradation according to Vanzolini and Williams (1970) could be assigned to one of the recognized subspecies.

Very little subsequent taxonomic research has been conducted on the species of the *A. chrysolepis* group. One molecular phylogenetic study included three of the described *A. chrysolepis* subspecies and found they formed a weakly supported clade (Glor et al., 2001). Glor et al. (2001: 2664) concluded that, "further study of geographical genetic interactions among these subspecies probably will reveal that they are distinct species." Additional molecular phylogenetic research, with broad outgroup sampling, recovered a well-supported clade consisting of *A. onca, A. annectans, A. lineatus, A. auratus, A. meridionalis,* and *A. chrysolepis,* although *A. chrysolepis* was represented by just a single individual from Roraima, Brazil (Nicholson et al., 2005). Members of this clade were included in another phylogenetic analysis (Nicholson et al., 2006), using the same three *A. chrysolepis* subspecies of Glor et al. (2001), which recovered a paraphyletic *A. chrysolepis*. Nicholson et al. (2006) found that *A. c. tandai* was more closely related to *A. meridionalis* and the *A. onca + A. annectans* clade, whereas *A. c. scypheus* and *A. c. planiceps* formed a clade that was the sister group to the remaining species + *A. auratus*. Like Glor et al. (2001), Nicholson et al. (2006) stressed the need for additional research into the systematics of *A. chrysolepis* and the possible existence of cryptic species. *Anolis bombiceps* has not been included in any molecular studies so far.

The name *A. chrysolepis* has a long and confusing history, with both *A. nitens* and *A.*

chrysolepis considered valid names for the species (Hoogmoed, 1973; Avila-Pires, 1995; Myers and Donnelly, 2008). Myers and Donnelly (2008) presented a detailed history of the use of these names, and Myers (2008) requested the International Commission of Zoological Nomenclature (ICZN) to give precedence of *A. chrysolepis* Duméril and Bibron, 1837, over *Draconura nitens* Wagler, 1830, which was accepted (ICZN, 2010).

In the present work, we analyzed mitochondrial DNA from the protein coding gene *ND2* and associated tRNA and morphological data from all five described subspecies of *A. chrysolepis* and related taxa to 1) recover the phylogenetic relationships among subspecies of *A. chrysolepis* and test previous phylogenetic hypotheses, 2) evaluate the taxonomic status of described subspecies of *A. chrysolepis*, and 3) present a revised taxonomy that incorporates this phylogenetic information.

MATERIALS AND METHODS

Taxon Sampling and DNA Sequencing

We sampled representatives of each of the five subspecies of *A. chrysolepis* (Table 1, Figure 1). Species previously shown to be closely related to *A. chrysolepis* were also included either from newly sequenced samples (e.g., *A. bombiceps*) or from previously published GenBank material (Glor et al., 2001; Nicholson, 2002; Nicholson et al., 2005, 2006). Genomic DNA was extracted from muscle, liver, or tail clips using DNeasy Blood and Tissue Kit (Qiagen, Valencia, California). Polymerase chain reaction was used to amplify portions of the mitochondrial protein-coding gene *ND2* (NADH dehydrogenase subunit 2) and adjacent tRNAs with primers LVT_Met-f.6_AnCr (AAGCTATTGGGCCCATACC) and LVT_5617_AnCr (AAAGTGYTTGAG-TTGCATTCA) (Rodriguez Robles et al., 2007). Polymerase chain reaction cleanup and DNA sequencing was performed by Agencourt Bioscience (Beverly, Massachusetts). Sequences were edited and aligned using SEQUENCHER ver. 4.2 (Gene Codes, Ann Arbor, Michigan). *ND2* sequences were translated into amino acids using MacClade ver. 4.08 (Maddison and Maddison, 1992) to confirm alignment and gap placement and ensure there were no premature stop codons.

Phylogenetic Analyses

We analyzed the *ND2* data using parsimony in PAUP ver. 4.0b10 (Swofford, 2001). Parsimony analysis was conducted using a heuristic search with 1,000 random taxon additions and tree bisection and reconnection (TBR) branch swapping and all characters equally weighted. We conducted 1,000 bootstrap replicates with 25 random additions per replicate to assess nodal support (Felsenstein, 1985).

Mitochondrial DNA (mtDNA) has been widely used to recover phylogenetic relationships among species and to delimit species (Avise et al., 1998; Grau et al., 2005; Gamble et al., 2008; Fenwick et al., 2009), and because of its shorter coalescent times, it is considered a good indicator of population history and species limits (Avise et al., 2000; Wiens and Hollingsworth, 2000; Wiens and Penkrot, 2002; Zink and Barrowclough, 2008; Barrowclough and Zink, 2009). However, the high substitution rate of mitochondrial DNA makes saturation, especially at third codon positions, a possible problem for accurate phylogenetic reconstruction (Jukes, 1987; Yoder et al., 1996, Glor et al., 2001, Hudson and Turelli, 2003). One way to minimize the effects of saturation is to use model-based phylogenetic methods like maximum likelihood (ML) and Bayesian analyses (Felsenstein, 1978; Jukes, 1987; Huelsenbeck et al., 2001, Lartillot et al., 2007). Additionally, the use of partitioned model–based analyses, with separate models of molecular evolution for each gene or codon, can minimize phylogenetic error (Bull et al., 1993; Lemmon and Moriarty, 2004; Nylander et al., 2004; Brandley et al., 2005). We conducted Bayesian analyses using MrBayes 3.1.2

TABLE 1.   MATERIAL EXAMINED FOR THE MOLECULAR PHYLOGENETIC ANALYSIS, INCLUDING TAXON NAME, MUSEUM NUMBERS, SPECIMEN LOCALITY, AND GENBANK NUMBERS.

Anolis Taxon	ID No.	Locality	GenBank
A. tandai	MPEG 22285	Itaituba, Pará, Brazil	JN191547
	MPEG 25029	Juruti, Pará, Brazil	JN191546
	LSUMZ H–14098	Rio Ituxi, Amazonas, Brazil	JN191542
	MPEG 25060	Coari, Amazonas, Brazil	JN191545
	LSUMZ H–16398	Rio Solimões, Amazonas, Brazil	JN191543
	LSUMZ H–16474	Rio Solimões, Amazonas, Brazil	JN191544
	LSUMZ H–13599	Rio Juruá, Acre, Brazil	JN191548
A. chrysolepis	MPEG 26590	Trombetas, Pará, Brazil	JN191532
	MPEG 26568	Faro, Pará, Brazil	JN191530
	MPEG 26563	Acari, Pará, Brazil	JN191531
	BPN780	Ralleighvallen, Suriname	JN191534
	MPEG 26584	Maicuru, Pará, Brazil	JN191533
	BPN 1587	Saul, French Guiana	JN191536
	BPN 1979	Saul, French Guiana	JN191541
	BPN 1874	Nouragues, French Guiana	JN191540
A. scypheus	LSUMZ H–12592	Reserva Faunistica Cuyabeno, Sucumbios Province, Ecuador	AF337804
	LSUMZ H–12543	Reserva Faunistica Cuyabeno, Sucumbios Province, Ecuador	AF337802
	LSUMZ H–12989	Reserva Faunistica Cuyabeno, Sucumbios Province, Ecuador	JN191568
A. planiceps	LSUMZ H–12300	Rio Ajarani, Roraima, Brazil	JN227867
	BPN 1080	Kartabo, Guyana	JN191550
	BPN 1082	Kartabo, Guyana	JN191549
	BPN 228	Imbaimadai, Guyana	JN191551
	BPN 96	Kartabo, Guyana	JN191552
A. brasiliensis	CHUNB 45077	Caseara, Tocantins, Brazil	JN191558
	CHUNB 45075	Minaçú, Goiás, Brazil	JN191559
	CHUNB 08842	Parauapebas, Pará, Brazil	JN191557
	CHUNB 43282	Brasilia, Distrito Federal, Brazil	JN191555
	CHUNB 34542	Novo Progresso, Pará, Brazil	JN191556
	CHUNB 27158	Mateiros, Tocantins, Brazil	JN227868
	CHUNB 11521	Palmas, Tocantins, Brazil	JN191565
	CHUNB 37528	São Domingos, Goiás, Brazil	JN191563
	CHUNB 37527	Paranã, Tocantins, Brazil	JN191562
	CHUNB 52471	Peixe, Tocantins, Brazil	JN191560
	GRC 16378	Alto Paraiso, Goiás, Brazil	JN191561
A. auratus	LSMUZ H–13928	Alter do Chão, Pará, Brasil.	JN191571
A. bombiceps	KU 222145	1.5 km N of Teniente Lopez, Loreto, Peru	JN191570
A. fuscoauratus	LSUMZ H–13566	Rio Juruá, Acre, Brazil	AF337786
A. meridionalis	LF166692	Reserva Mbaracayú, Canindeyu, Paraguay	AY909760
A. lineatus	LSUMZ H–5450	Netherlands Antilles	AF294287
A. onca	CIEZAH1156	Estado Falcón, Venezuela	DQ377357
A. annectens	CIEZAH1160	Estado Falcón, Venezuela	DQ377345
A. sericeus	LACM7069	Costa Rica	AY909778
A. isthmicus	MFO191	Mexico	AY909762
A. laeviventris	MVCFC12252	Guatemala	AY909756
A. sagrei	KdQ1797	La Habana, Cuba	AF337778
A. utilensis	LDW12480	Honduras	AY909785
A. grahami	JBL 250	Discovery Bay, Jamaica	AF055938
A. loveridgei	USNM10683	Honduras	AY909759
A. uniformis	n/a	Belize	AY909784
A. crassulus	MZFC6458	Mexico	AY909748
A. carolinensis	CCA 8051	Unknown	NC010972

(Huelsenbeck and Ronquist, 2001) on both the partitioned and unpartitioned datasets. Data were partitioned by codon with a fourth partition for tRNAs and the optimal partitioning strategy selected using Bayes Factors calculated from the harmonic mean likelihood values (Nylander et al., 2004; Brandley et al., 2005). We estimated the best fit model of sequence evolution for the data as a whole and for each partition separately using AIC scores in Modeltest (Posada, 2008). Bayesian analyses were initialized with a neighbor-joining tree and two separate analyses conducted for each partitioning strategy. Each analysis consisted of seven heated chains and one cold chain run for 2 million generations, with sampling every 1,000 generations. Post-burnin convergence was checked by visual inspection of likelihood values by generation using Tracer 1.5 (Rambaut and Drummond, 2009) and visual inspection of split frequencies using AWTY (Nylander et al., 2008). We also conducted partitioned Maximum Likelihood analysis, with data partitioned as above using RAXML ver. 7.0.4 (Stamatakis, 2006) using the GTR+GAMMA model for all partitions. We conducted 1,000 "fast bootstrap" replicates and 10 separate maximum likelihood searches. Bootstrap values ≥70 were considered as indicating strong support for both parsimony and ML analyses.

We calculated net among group distances (Nei and Li, 1979) between major lineages of the "A. chrysolepis species group" using MEGA 4 (Kumar et al., 2008). We calculated both uncorrected p-distances and corrected distances using the GTR model.

On the basis of our best ML tree, we compared alternative phylogenetic hypotheses using the Shimodaira-Hasegawa (SH) test (Shimodaira and Hasegawa, 1999) and the Approximately Unbiased (AU) test (Shimodaira, 2002). Three alternative hypotheses were considered: 1) monophyly of A. chrysolepis subspecies, excluding A. bombiceps and A. meridionalis; 2) monophyly of the A. chrysolepis subspecies + A. bombiceps, excluding only A. meridionalis;

and 3) monophyly of all A. c. tandai specimens, as identified by morphological data. We used RAxML7.0.4 (Stamatakis, 2006) to compute per-site log likelihoods that were input into CONSEL (Shimodaira and Hasegawa, 2001) to calculate P values. We also tested alternative phylogenetic hypotheses in a Bayesian framework and calculated the Posterior Probabilities of alternative hypotheses using the tree filter option in PAUP*.

Morphological Analyses

We collected morphological and morphometric data from 403 specimens (Appendix 1) from the following zoological collections: MZUSP, Museu de Zoologia da Universidade de São Paulo; CHUNB, Coleção Herpetológica da Universidade de Brasília; MPEG, Museu Paraense Emílio Goeldi; MCZ, Harvard Museum of Comparative Zoology; and KU, University of Kansas. Measurements were recorded with digital calipers to the nearest 0.1 mm on the right side of the body, except when specimens were damaged (in this case, the left side was used). Scale and measurement terminology follows Avila-Pires (1995).

We recorded the following morphometric data: snout–vent length (SVL), tail length (from posterior edge of precloacal plate), head width, head height, mouth length (from tip of snout to posterior margin of mouth), distance between orbits (minimum), ear-opening diameter, distance between nostrils (minimum), distance from mouth to ear (from anterior margin of ear-opening to posterior margin of mouth), snout length (from tip of snout to anterior margin of orbit), interparietal length, tibia length, foot length (from toe IV base to the heel), fourth toe length (from toe IV nail to toe base), and fourth toe maximum width. Additionally, we recorded the following meristic characters: scales around midbody, postrostrals, supralabials, infralabials, loreals (under second canthal), canthals, scales between second canthals, scales between supraorbital semicircles (minimum), scales

between interparietal and supraorbital semicircles (minimum), postmentals, fourth finger lamellae, and fourth toe lamellae.

A few measurements and scale counts could not be assessed for all specimens analyzed. In multivariate analysis, cases with missing observations will be dropped, weakening the analysis because of loss of information and degrees of freedom. To avoid simply deleting entire rows of data, missing observations can be estimated using a variety of methods, including mean substitution, regression, expectation maximization, maximum likelihood and multiple imputation (Tabachnick and Fidell, 2001; Quinn and Keough, 2002). Among these approaches for imputing values to missing observations, multiple imputation is the most robust and also makes fewer assumptions about the pattern of missing observations (Rubin, 1996; Van Buuren et al., 2006). Therefore, we imputed missing data using multivariate imputations by chained equations (Van Buuren et al., 2006), as implemented by package *mice* in R v. 2.12.0 (R Development Core Team, 2009).

To partition the total morphometric variation between size and shape variation, we defined body size as an isometric size variable (Rohlf and Bookstein, 1987) following Somers (1986): we calculated an isometric eigenvector, defined a priori with values equal to $p^{-0.5}$, where p is the number of variables (Jolicoeur, 1963), and obtained scores from this eigenvector, hereafter called body size, by postmultiplying the $n \times p$ matrix of log-transformed data, where n is the number of observations, by the $p \times 1$ isometric eigenvector. To remove the effects of body size from the log-transformed data, we used Burnaby's method (Burnaby, 1966): we postmultiplied the $n \times p$ matrix of the log-transformed data by a $p \times p$ symmetric matrix, $\mathbf{L}$, defined as:

$$\mathbf{L} = \mathbf{I}_p - \mathbf{V}(\mathbf{V}^T\mathbf{V})^{-1}\mathbf{V}^T$$

where $\mathbf{I}_p$ is a $p \times p$ identity matrix, $\mathbf{V}$ is the isometric size eigenvector defined above, and

$\mathbf{V}^T$ is the transpose of matrix $\mathbf{V}$ (Rohlf and Bookstein, 1987). Hereafter, we refer to the resulting size-adjusted variables as shape variables.

To identify morphometric and meristic variables that best discriminate among species, we used a stepwise discriminant analysis coupled with 100-fold cross-validation to measure classification performance (Quinn and Keough, 2002) using the package klaR in R v. 2.12.0 (R Development Core Team, 2009).

RESULTS

Phylogenetic Analyses

We sequenced 1,088 base pairs of the mitochondrial *ND2* gene and adjacent tRNAs, which contained 82 variable sites and 633 parsimony-informative characters. Thirty-nine new mtDNA sequences from 34 localities (Fig. 1) are reported and aligned with 14 previously published sequences.

A comparison of the partitioned Bayesian analyses to the unpartitioned analyses strongly favored the partitioned strategy (Bayes Factors > 860). We observed convergence among multiple Bayesian runs and utilized post-burnin samples (burnin = 1,000) to estimate model parameters and tree topology (Fig. 2). The partitioned ML analysis produced a single tree (Fig. 3, ln $L = -16,649.1489$) that had a similar topology to the partitioned Bayesian consensus tree at well-supported nodes. The Parsimony analysis produced 54 equally most parsimonious trees (TL = 3,832, CI = 0.337683, RI = 0.682552, RC = 0.230486, HI = 0.662317; Fig. 4). Subspecies formed strongly supported monophyletic groups in all analyses, with the exception of specimens of *A. c. tandai* from Acre. All analyses also recovered a paraphyletic *A. chrysolepis* with regard to *A. bombiceps* and *A. meridionalis* (Figs. 2–4). Sampled individuals of *A. chrysolepis*, *A. bombiceps*, and *A. meridionalis* were members of one of two clades; one (Clade A) composed of *A. c. chrysolepis*, *A. c. tandai*,
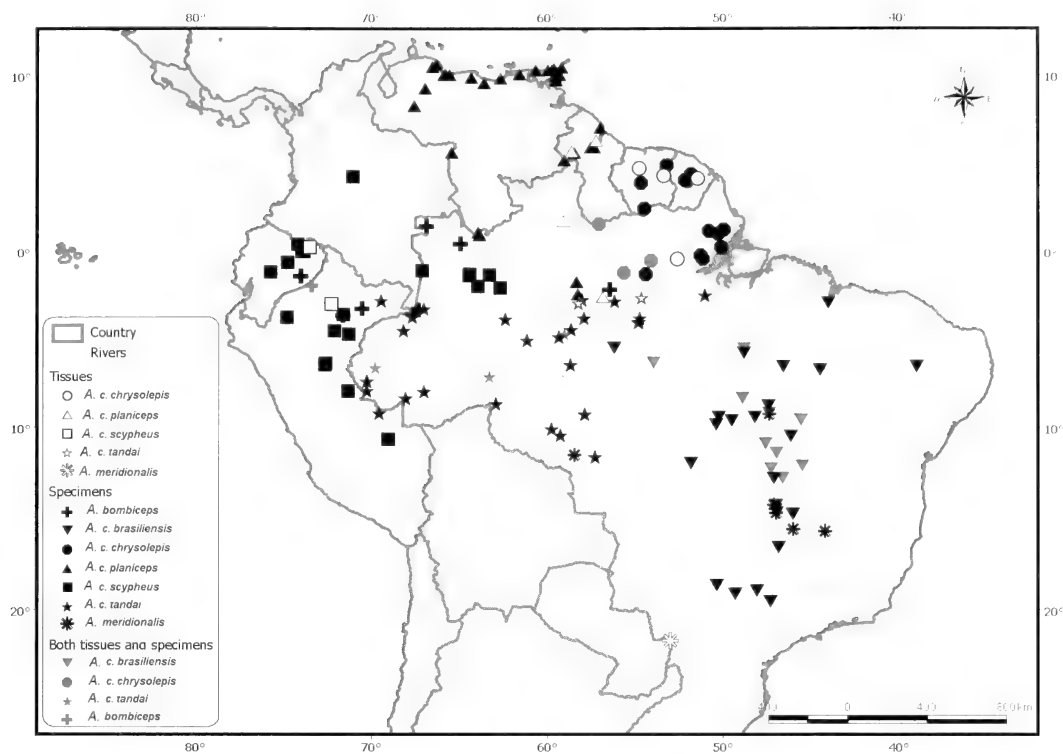
Figure 1.   Distribution of material examined of *A. c. chrysolepis, A. c. scypheus, A. c. tandai, A. c. brasiliensis, A. c. planiceps, A. bombiceps* and *A. meridionalis*. Symbols may represent more than one locality.

and *Anolis meridionalis* and another (Clade B) composed of *A. c. brasiliensis, A. c. planiceps, A. c. scypheus,* and *A. bombiceps.* Relationships among taxa in clade B were similar across all trees, with an *A. bombiceps* + *A. c. scypheus* clade and an *A. c. planiceps* + *A. c. brasiliensis* clade that are sister taxa. Relationships within Clade A varied depending on the analysis. Parsimony analysis recovered *A. c. tandai* from Acre (LSUMZ H13599) as the sister taxon of the *A. c. tandai* + *A. c. chrysolepis* clade. The ML and Bayesian trees, on the other hand, recovered the Acre *A. c. tandai* as the sister taxon of *A. c. chrysolepis,* but with low bootstrap support. The *A. c. chrysolepis* + *A. c. tandai* clade was well supported in all analyses, whereas the *A. c. chrysolepis* + *A. c. tandai* + *A. meridionalis* clade received poor nodal supported.

Uncorrected pairwise distances among lineages in the *A. chrysolepis* species group ranged from 5.0% between *A. c. tandai* and *A. c. chrysolepis* to 22.1% between *A. c. scypheus* and *A. meridionalis* (Table 2).

Both the SH and AU tests (Table 3) found that the alternative hypothesis of a monophyletic *A. chrysolepis,* excluding both *A. bombiceps* and *A. meridionalis,* resulted in a significantly worse tree than the ML tree. The ML tree constrained to exclude just *A. meridionalis* was not significantly worse than our best ML tree. Similarly, both tests found no significant difference between a tree constraining a monophyletic *A. c. tandai* and our best ML tree. Bayesian Posterior Probabilities of alternative hypotheses showed little to no support (e.g., Posterior Probabilities < 0.05) for a monophyletic *A. chrysolepis* excluding *A. bombiceps* and *A. meridionalis,* as well as a monophyletic *A. c. tandai.* The Bayesian Posterior Probability of a monophyletic *A. chrysolepis* + *A. bombiceps,* excluding *A. meridionalis,* received moderate support.
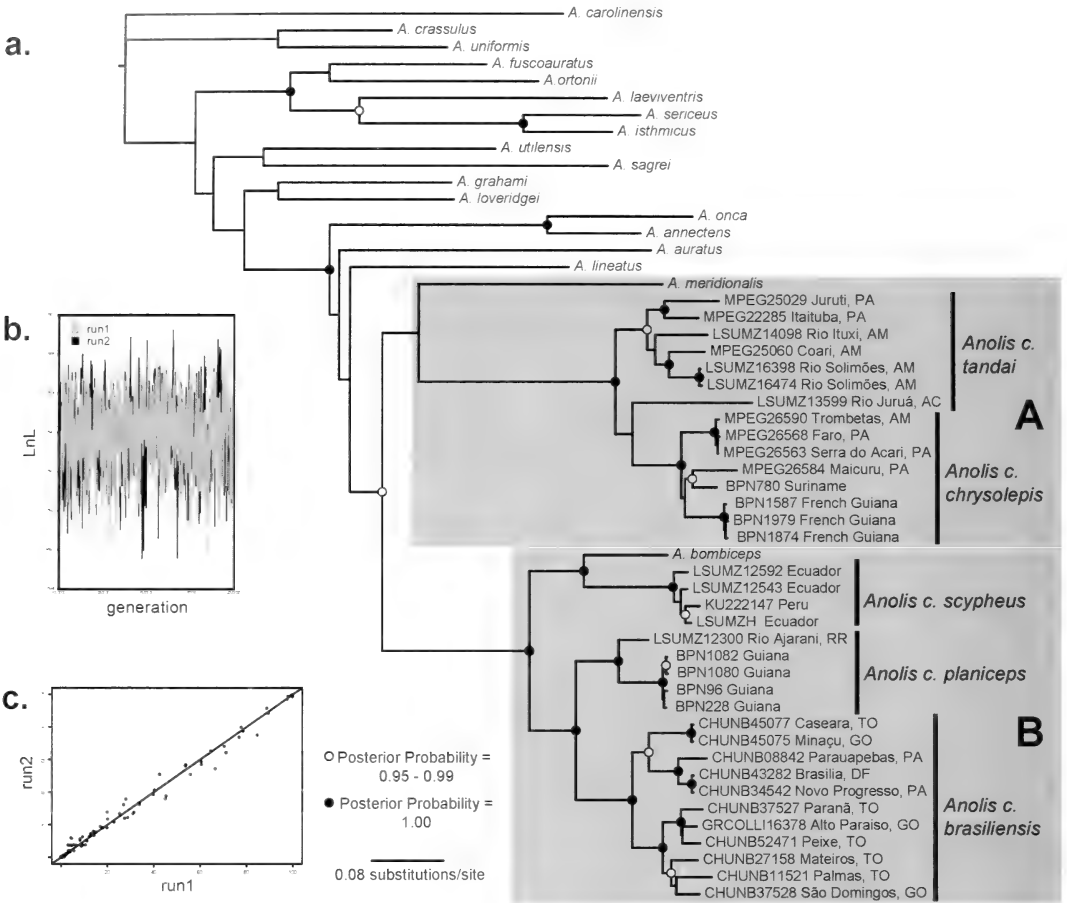
Figure 2. Results of the partitioned Bayesian analysis. a. Phylogeny of the *Anolis chrysolepis* species group and outgroups. Bayesian posterior probabilities >0.95 are indicated by circles at nodes. b. Trace plot of post-burnin log likelihood values for the two Bayesian runs. c. Bivariate plot of the split frequencies for the two Bayesian runs.

Morphological Analyses

The stepwise discriminant analysis applied on body size and all shape variables selected tibia length, interparietal length, and snout–vent length (all size-adjusted) as the most powerful discriminators of *A. chrysolepis* spp., *A. bombiceps*, and *A. meridionalis*, with a classification accuracy of 0.67 based on cross-validation. The first two linear discriminant functions based on these three variables explained about 99% of the total variation, the first function mainly representing a contrast between relative tibia length (−) versus relative SVL (+), and the second function repre-

senting primarily the variation in interparietal length (Table 4, Fig. 5). Results indicate that *A. meridionalis* and *A. c. brasiliensis* have short tibias and elongate bodies relative to total body size, whereas *A. c. tandai* and *A. c. chrysolepis* have long tibias and short bodies relative to total body size, and *A. bombiceps*, *A. c. planiceps*, and *A. c. scypheus* have intermediate values of these variables. Additionally, *A. c. planiceps* has the longest, and *A. c. chrysolepis* the shortest, interparietal relative to its body size. Morphologically, *A. c. chrysolepis* and *A. c. tandai* are very similar, whereas *A. meridionalis* is the most divergent species,
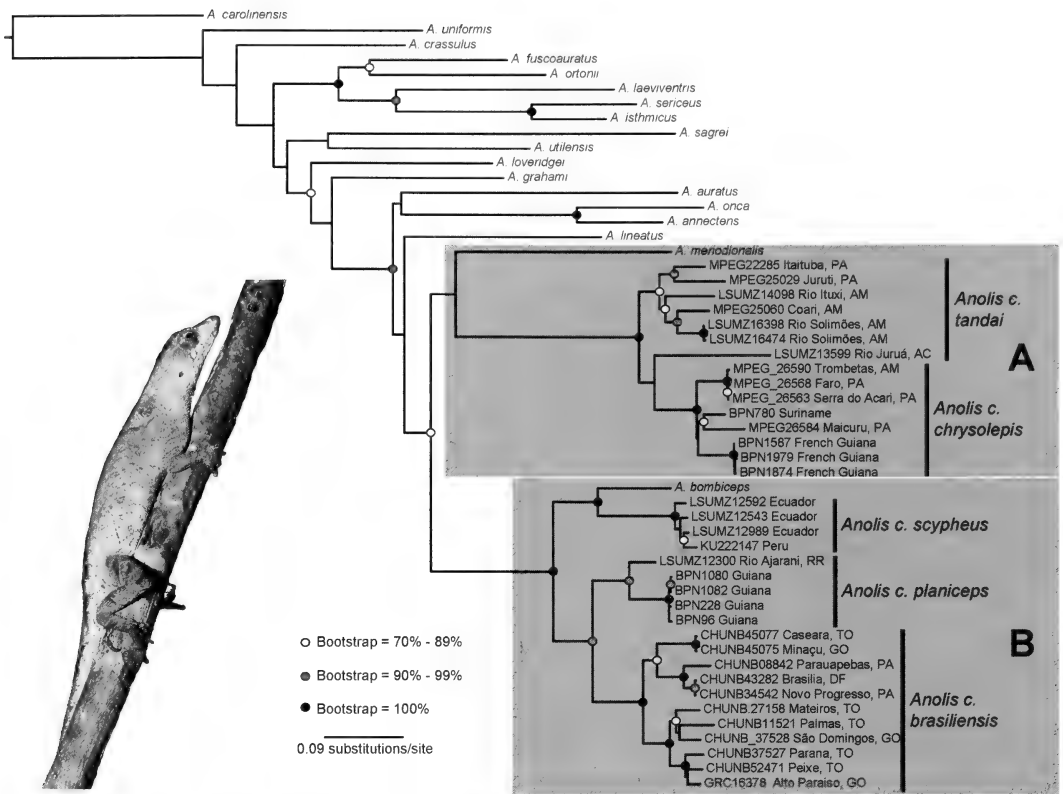
Figure 3.   Partitioned Maximum Likelihood phylogeny of the *Anolis chrysolepis* species group and outgroups. Bootstrap values >70% are indicated by circles at nodes. Photo: *Anolis brasiliensis* from São Domingos, Goiás, Brazil. Tony Gamble.

followed by *A. c. brasiliensis*. Nevertheless, classification accuracy based on morphology was moderate.

The stepwise discriminant analysis applied on meristic counts selected canthals, fourth toe lamellae, and scales between second canthals as the most powerful discriminators of the species, with a classification accuracy of 0.83 based on cross-validation (Fig. 6). The first two linear discriminant functions based on these three variables explained about 93% of the total variation. The first function mainly represented a contrast between canthals and scales between second canthals (−) versus fourth toe lamellae (+), whereas the second function primarily represented the variation in fourth toe lamellae and canthals (Table 5, Fig. 6).

Results indicate discrimination 1) in the number of canthals among *A. c. planiceps*

and *A. meridionalis* (small); *A. bombiceps*, *A. c. tandai*, and *A. c. chrysolepis* (large); and *A. c. brasiliensis* and *A. c. scypheus* (intermediate); 2) in the number of fourth toe lamellae among *A. c. chrysolepis* and *A. meridionalis* (small); *A. c. brasiliensis*, *A. c. planiceps*, and *A. c. scypheus* (large); and *A. bombiceps* and *A. c. tandai* (intermediate); and 3) in the number of scales between second canthals among *A. meridionalis* (few), *A. c. scypheus* and *A. tandai* (large), and the remaining species (intermediate). Overall, *A. c. chrysolepis*, *A. c. tandai*, and *A. bombiceps* are more similar, the same happening with *A. c. planiceps*, *A. brasiliensis*, and *A. c. scypheus*. *Anolis meridionalis* is the most divergent species. Classification accuracy based on meristic counts was relatively good.
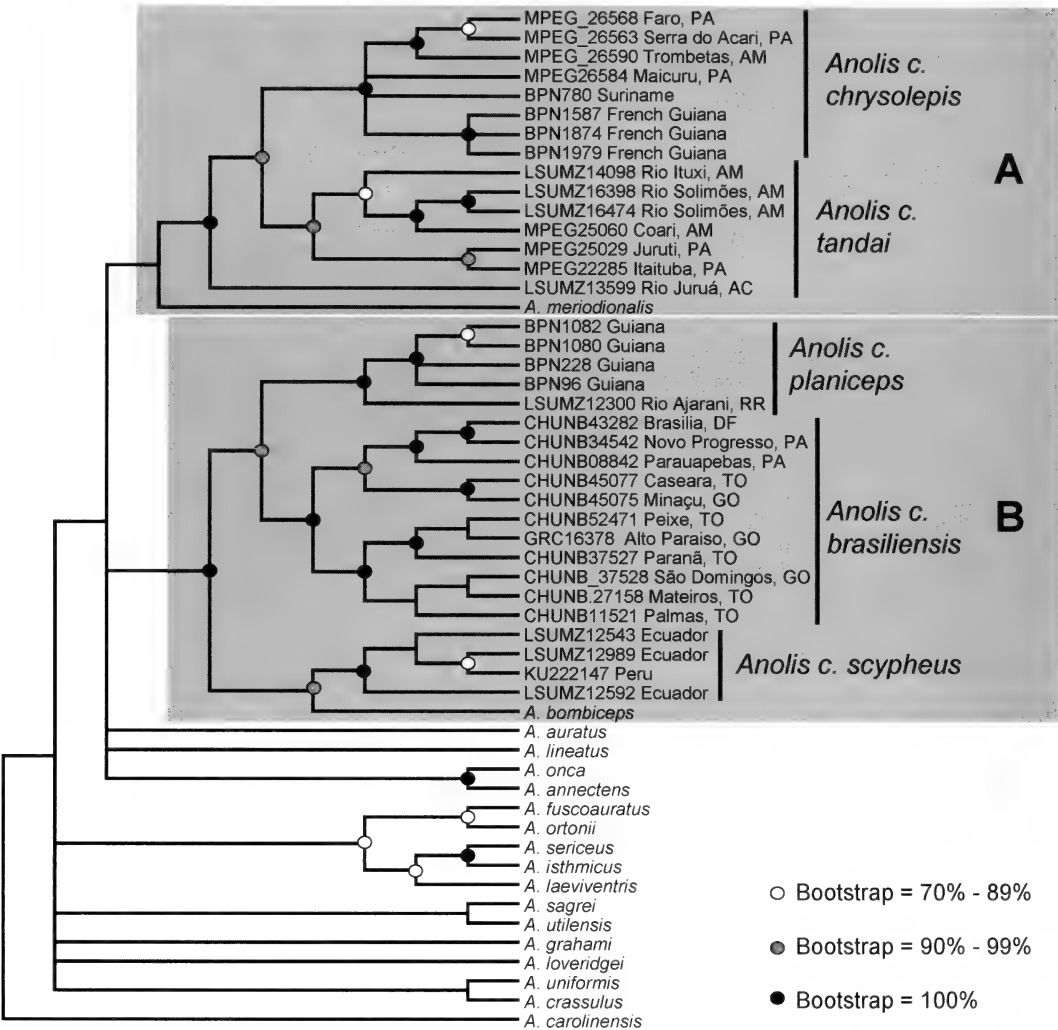
Figure 4.   Maximum Parsimony consensus phylogeny of the *Anolis chrysolepis* species group and outgroups.

TABLE 2.   NET BETWEEN GROUP DISTANCES FOR *ND2* AMONG THE *ANOLIS CHRYSOLEPIS* GROUP. DISTANCES ABOVE THE DIAGONAL ARE UNCORRECTED *P*-DISTANCES. DISTANCES BELOW THE DIAGONAL WERE MAXIMUM LIKELIHOOD–CORRECTED USING THE GTR MODEL.

	A. c. chrysolepis	A. c. tandai	A. c. planiceps	A. c. brasiliensis	A. c. scypheus	A. bombiceps	A. meridionalis
A. c. chrysolepis	—	0.050	0.195	0.173	0.192	0.189	0.201
A. c. tandai	0.059	—	0.169	0.149	0.167	0.170	0.171
A. c. planiceps	0.274	0.233	—	0.076	0.128	0.136	0.193
A. c. brasiliensis	0.249	0.209	0.093	—	0.114	0.121	0.193
A. c. scypheus	0.270	0.229	0.160	0.155	—	0.104	0.221
A. bombiceps	0.255	0.228	0.156	0.154	0.123	—	0.209
A. meridionalis	0.267	0.232	0.279	0.270	0.298	0.267	—

TABLE 3. COMPARISONS OF MAXIMUM LIKELIHOOD (ML) TREE SCORES (−LNL) AND *P* VALUES OF THE SH AND AU TESTS BETWEEN OUR BEST ML TREE AND THE CONSTRAINED TREES. BAYESIAN POSTERIOR PROBABILITIES OF ALTERNATIVE HYPOTHESES ARE ALSO SHOWN.

Hypothesis	$-\ln L$	Difference $-\ln L$	SH Test (*P*)	AU Test (*P*)	Bayesian Posterior Probability
Optimal tree	−16,900.3198	n/a	n/a	n/a	n/a
Monophyletic *A. chrysolepis* group	−16,963.9620	−63.6423	<0.001	<0.0001	0.000
Monophyletic *A. chrysolepis* group + *A. bombiceps*	−16,900.9392	−0.6194	0.867	0.571	0.219
Monophyletic *A. c. tandai*	−16,903.4524	−3.1326	0.726	0.420	0.020

DISCUSSION

The molecular phylogenetic analyses recovered six species-level taxa as part of the *A. chrysolepis* species group. These taxa can also be morphologically distinguished on the basis of morphometric and meristic characters. Even though we cannot infer relationships among these taxa on the basis of the meristic discriminant analysis, the results of this analysis are consistent with the existence of two clades: one containing *A. c. tandai*, *A. c. chrysolepis*, and *A. bombiceps* and another clade containing *A. c. brasiliensis* and *A. c. planiceps*. Meristic characters in *A. c. scypheus* appear to be intermediate between these two groups, which is also consistent with it being (together with *A. bombiceps*) the sister clade to *A. c. brasiliensis* + *A. c. planiceps*. *Anolis meridionalis* was quite distinct from other members of the *A. chrysolepis* species group on the basis of meristic characters.

We define the *A. chrysolepis* species group as the clade originating with the most recent common ancestor of *A. c. chrysolepis* and *A. c. brasiliensis*. *Anolis meridionalis* has not historically been allied with the *A. chrysolepis* species group because of its unique morphology. In particular, *A. meridionalis* differs from other members of the *A. chrysolepis* species group by having digital dilatations on phalanx ii and iii continuous with scales under phalanx i, instead of forming the prominent border observed in the *A. chrysolepis* subspecies and *A. bombiceps*. Although the node leading to the *A. chrysolepis* species group, including *A. meridionalis*, was well supported in the ML and Bayesian analyses, the presence of *A. meridionalis* in clade A received poor support in all phylogenetic analyses. For this reason, we could not reject the alternative hypothesis of a monophyletic *A. chrysolepis* group exclusive of *A. meridionalis*. This means that inclusion of *A. meridionalis* in the *A. chrysolepis* species group is still uncertain. Future phylogenetic analyses that include additional *A. meridio-*

TABLE 4. LINEAR DISCRIMINANT ANALYSIS OF THREE MORPHOMETRIC VARIABLES THAT BEST DISTINGUISH THE SPECIES AND SUBSPECIES OF *ANOLIS* STUDIED. VALUES REPRESENT MEANS OF SCALED, SIZE-ADJUSTED VARIABLES FOR EACH SPECIES AND COEFFICIENTS OF VARIABLES ON FIRST AND SECOND LINEAR DISCRIMINANT FUNCTIONS (LDF 1, LDF 2). PROPORTION OF TOTAL VARIATION EXPLAINED BY EACH LDF IN PARENTHESES.

Anolis Species	Tibia Length	Interparietal Length	Snout–Vent Length
A. bombiceps	0.57	−0.35	0.78
A. c. brasiliensis	−0.91	0.46	0.15
A. c. chrysolepis	0.67	−1.02	0.14
A. meridionalis	−1.67	0.58	1.46
A. c. planiceps	−0.02	0.79	−0.55
A. c. scypheus	−0.05	−0.32	−0.19
A. c. tandai	0.87	−0.60	0.11
LDF 1 (0.86)	−1.72	0.53	1.05
LDF 2 (0.13)	−0.60	−1.11	0.49
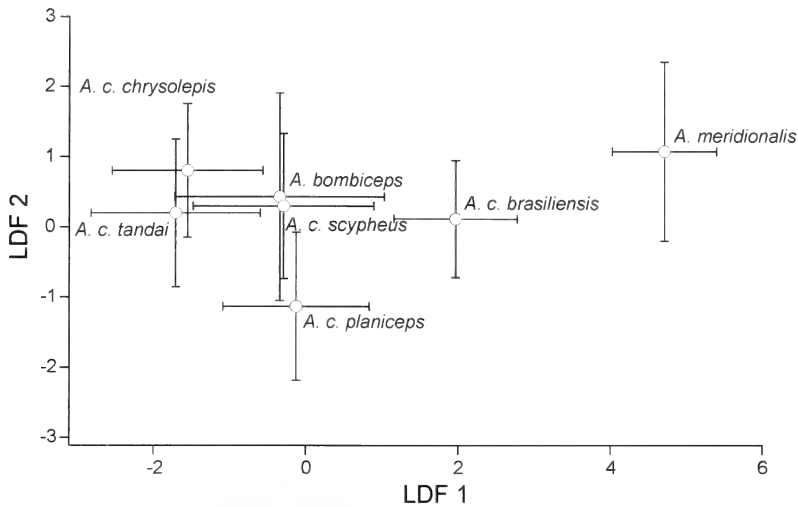
Figure 5.   Means (open circles) and standard deviations (error bars) of scores on first (LDF 1) and second (LDF 2) linear discriminant functions of tibia length, interparietal length, and snout–vent length (all size-adjusted; see text for details) for seven subspecies and two species of *Anolis*.

nalis samples and data from nuclear loci may help resolve this issue.

All described taxa in the molecular analyses formed well-supported, monophyletic groups, with the exception of *A. c. tandai*. The *A. c. tandai* individual from Acre fit the morphological diagnosis we present in this study but was either the sister taxon to *A. c. chrysolepis* (ML and Bayesian analyses) or the sister taxon to the

A. c. chrysolepis + *A. c. tandai* clade (parsimony analysis). The apparent paraphyly of *A. c. tandai* may be due to several phenomena, none of which are mutually exclusive. One possibility is phylogenetic error due to incomplete taxonomic sampling or lack of data (Graybeal, 1998; Mitchell et al., 2000). It is also possible that individuals from the Acre population represent an as yet undescribed, morphologically cryptic

Figure 6.   Means (open circles) and standard deviations (error bars) of scores on first (LDF 1) and second (LDF 2) linear discriminant functions of canthals, fourth toe lamellae, and scales between second canthals for seven species of *Anolis*.

Anolis Species	Canthals	Fourth Toe Lamellae	Scales Between Second Canthals
A. bombiceps	1.13	−0.63	−.022
A. c. brasiliensis	−0.09	0.72	−0.67
A. c. chrysolepis	0.41	−1.50	0.21
A. meridionalis	−0.77	−1.80	−1.05
A. c. planiceps	−1.48	0.42	−0.56
A. c. scypheus	0.09	0.56	0.99
A. c. tandai	0.96	−0.66	0.75
LDF 1 (0.74)	−1.38	0.92	−0.69
LDF 2 (0.18)	−0.92	−1.36	−0.20

species. Incomplete lineage sorting can also result in discordance between individual gene trees and the species tree because of the retention and/or sorting of ancestral polymorphisms, particularly when populations have diverged recently, have a large effective population size, or both (Maddison, 1997; Ballard and Whitlock, 2004; Maddison and Knowles, 2006). Additional phylogenetic analyses incorporating nuclear genes and additional taxa, as well as using methods that incorporate coalescent processes and incomplete lineage sorting, would be useful in clarifying relationships among *A. c. tandai* populations.

Our results show broad congruence among molecular and morphological data sets that are consistent with independent evolutionary lineages. Most importantly, each of these lineages is morphologically diagnosable. Genetic distances among sister taxa in the *A. chrysolepis* group were also comparable to *ND2* distances among sister species in other squamate taxa (Macey et al., 1998, 1999; Glor et al., 2001; Oliver et al., 2009). Therefore, we elevate each subspecies to species status under the general lineage species concept (de Queiroz, 1998, 1999, 2005, 2005a, 2005b, 2007). To facilitate future studies, each species, including *A. bombiceps* and *A. meridonalis*, is diagnosed below and an identification key is provided, considering morphological data collected for this study as well as data from the literature. Table 6 compares the main meristic and morphometric characters.

Taxonomy/Species Accounts

All descriptions of color pattern are based on literature, photographs of live animals, and preserved specimens.

Anolis chrysolepis Duméril and Bibron, 1837.

Anolis chrysolepis Duméril and Bibron, 1837:94 (lectotype MHNP 2456, type locality: La Mana, French Guiana); Cunha, 1961:60; Peters and Donoso-Barros, 1970:61; Avila Pires et al., 2010:94.

Anolis chrysolepis chrysolepis; Vanzolini and Williams, 1970:85; Hoogmoed, 1973:112; Hoogmoed and Avila-Pires, 1989:168.

Norops nitens chrysolepis; Savage and Guyer, 1991:366.

Anolis nitens chrysolepis; Avila-Pires, 1995:75.

Abbreviated Description. Maximum SVL 74 mm. Vertebral region with distinctly enlarged scales, middorsal row largest; number of rows of enlarged scales increases posteriorly. Scales on upper arms smaller than, to subequal to, vertebral scales. Supraorbital semicircles with scarcely enlarged scales. Supraocular scales keeled, slightly larger than or subequal to scales

TABLE 6. COMPARISONS OF MERISTIC CHARACTERS, BODY PROPORTIONS AND MEASUREMENTS (IN MILLIMETERS) AMONG THE SPECIES OF MEMBERS OF THE *ANOLIS CHRYSOLEPIS* GROUP.

Character*	*A. chrysolepis*	*A. tandai*	*A. scypheus*	*A. planiceps*	*A. brasiliensis*	*A. bombiceps*	*A. meridionalis*
No. of specimens	50	96	49	72	116	11	9
max. svl (mm)	74	70	80	76	69	74	56
midbody	101–156	91–150	110–174	110–149	112–155	125–137	79–106
midbody median and standard deviation values	123.18 ± 12.8	134.06 ± 7.43	145.94 ± 14.59	125.84 ± 9.46	129.12 ± 10.78	131.37 ± 3.08	92.22 ± 9.39
slabials	11–15	10–14	10–14	10–14	10–13	10–12	9–11
ilabials	11–15	10–14	10–13	9–11	8–12	10–13	8–11
prostrals	4–7	5–9	5–7	4–7	5–7	5–6	5
loreals	5–10	5–9	7–10	6–9	6–10	6–7	6–7
canthals	6–10	6–11	6–11	6–8	5–9	9–11	5–6
scales bet 2ᵃ canthals	9–14	10–15	9–15	8–14	8–14	9–12	8–10
scales bet semicirsorbits	1–4	1–4	1–5	1–3	0–3	1–3	0–1
interp–semicirsorbit	1–5	2–4	2–5	1–3	1–4	2–4	0–2
pmentals	4–8	4–8	4–8	4–8	4–8	6–8	5–8
lam-4fg	12–17	14–19	15–21	14–20	15–20	15–19	10–12
lam-4toe	18–26	20–28	26–35	19–34	25–32	21–29	18–24
tail/svl	1.15–2.17	1.48–2.42	1.66–2.53	1.33–3.27	1.22–2.54	1.69–2.18	1.97–2.38
mouth/svl	0.13–0.25	0.19–0.24	0.18–0.24	0.19–0.26	0.18–0.26	0.19–0.21	0.19–0.21
interp/head-w	0.07–0.19	0.08–0.24	0.11–0.25	0.16–0.32	0.11–0.30	0.10–0.28	0.16–0.30
tibia/svl	0.20–0.38	0.30–0.43	0.26–0.38	0.27–0.36	0.26–0.34	0.29–0.36	0.22–0.27
Interpatietal	0.64–1.65	0.84–2.22	0.81–2.37	0.98–2.79	0.92–2.65	1.1–2.9	1.28–2.07
head-w	5.93–10.5	5.31–11.41	5.67–13.08	4.95–12.14	7.25–11.75	8.96–10.73	6.95–8.07
head-alt	5.00–8.39	4.33–9.65	4.23–11.02	3.28–9.39	5.56–9.2	7.62–8.33	4.88–6.36
orbdist	4.01–6.39	3.4–7.19	3.04–8.31	3.31–8.41	4.39–7.26	6.09–6.65	4.02–4.86
eardiam	0.40–1.41	0.75–1.89	0.40–2.23	0.47–1.71	0.87–2.00	0.88–1.68	0.84–1.09
nostrilsdis	1.25–2.37	1.14–2.7	1.10–2.95	1.07–2.76	1.40–2.82	2.0–2.36	1.42–1.73
mouth to ear	1.13–3.03	1.6–2.92	1.09–3.09	1.06–3.52	0.96–2.72	1.47–2.18	1.28–1.53
snout	2.97–6.69	3.35–7.00	2.78–7.72	2.69–7.17	3.92–8.14	4.67–6.46	4.8–5.82
max. toe IV	20.94	24.42	26.91	28.31	21.63	25.51	14.12
max. foot	25.63	30.24	31.46	31.89	26.48	22.66	17.39
toe IV width	0.55–1.30	0.47–1.29	0.61–1.48	0.51–1.46	0.92–1.65	0.96–1.26	0.61–0.91

* Abbreviations: max. svl = maximun snout–vent length; midbody = number of scales around midbody; slabials = total number of supralabials; ilabials = total number of infralabials; prostrals = total number of postrostrals; scales bet 2ᵃ canthals = number of scales on the snout between the second canthals; scales bet semicirsorbits = minimum number of scales between supraorbital semicircles; interp–semicirsorbit = minimum number of scales between any of the supraorbital semicircles and interparietal; pmentals = number of postmentals; lam-4fg = number of expanded lamellae under the fourth finger; lam-4toe = number of expanded lamellae under fourth toe; tail/svl, mouth/svl, tibia/svl = respectively, the rates of the tail, mouth, and tibia length with the snout–vent length; interp/head-w = the rate of interparietal width with head width; interparietal = interparietal width; head-w = head width; head-alt = head height; orbdist = minimum distance between orbits; eardiam = ear diameter; nostrilsdis = minimum distance between nostrils; mouth to ear = minimum distance between mouth and ear; snout = from the tip of snout to anterior margin of orbit; max. toe IV = from toe IV base to the heel; max. foot = fourth toe length from toe nail to toe base; toe IV width = fourth toe width.

on snout, grading into granules laterally and posteriorly. Interparietal subequal to or slightly larger than adjacent scales (Fig. 7A, B).

Color in Preservative. Color pattern sexually dimorphic. Male dorsal color pale or grayish-brown with or without a wide light vertebral band bordered by a grayish-brown irregular band laterally. Paired triangular spots may be present along back; most specimens with paired triangular spots on sacral region. Female dorsal pattern less variable. A thin dark brown line begins at posterior corner of each eye at each side, converging toward neck and continuing along the body, where they delimit a lighter or plumbeous vertebral band that darkens and expands laterally on tail.

Dewlap Color in Life and Preservative. In preservative, male dewlap skin royal blue, dark blue, or blackish, with light scales or blue scales toward rim. Female dewlap cream, similar to surrounding area; scales may be darker at edge. In life, male dewlap skin usually royal blue or blackish blue with
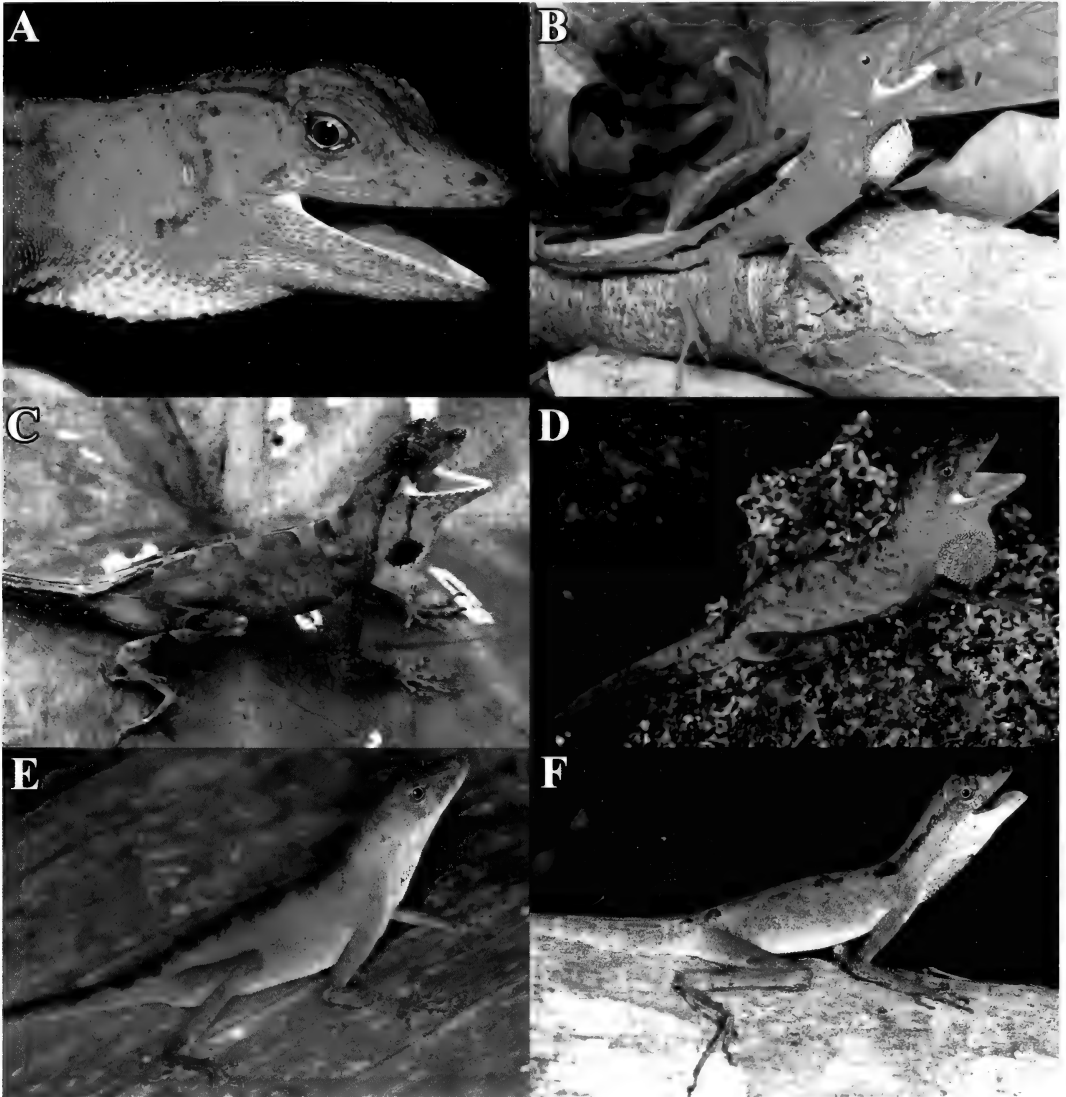
Figure 7. *Anolis chrysolepis* species group. A) *Anolis chrysolepis* female from Nassau Plateau, Suriname (Photo: Robert Langstroth), B) *Anolis chrysolepis* male from Faro, Pará, Brazil (Photo: Waldima Rocha), C) *Anolis tandai* female from Rio Juruá, Acre (Photo: Laurie J. Vitt), D) *Anolis tandai* male from Rio Juruá, Acre, Brazil (Photo: Laurie J. Vitt), E) *Anolis tandai* female from Rio Ituxi, Amazonas, Brazil (Photo: Laurie J. Vitt), F) *Anolis tandai* male from Amazonas, Brazil (Photo: Laurie J. Vitt).

light scales or blue scales along rim. Avila-Pires (1995) mentioned a cobalt-blue juvenile male dewlap (RMNH 24673) with white to orange scales, surrounded by a spectrum-orange area that extended through most of ventral surface of head. Female dewlap skin usually yellowish to orange with gray or cream scales; an orange lateral area extended through most of ventral surface of head may be present. Hoogmoed and Avila-Pires (1991) mentioned a female from French Guiana with yellow dewlap with orange scales, presenting a bluish area toward the rim.

Comparison with Other Species from the A. chrysolepis Species Group. This species

has proportionally the smallest interparietal length among the species of the group (Table 6). It differs from its sister taxon *A. tandai* mainly by a lower number of postrostral scales (4–7 in *A. chrysolepis* and 5–9 in *A. tandai*) and by female dewlap color, generally cream in *A. chrysolepis*; cream with a large central blue spot in *A. tandai*.

Distribution. Southern Guyana, Suriname, French Guiana and northern Brazil, in the states of Amapá and Pará.

Anolis tandai Avila-Pires, 1995.
Anolis chrysolepis; Vanzolini, 1986:18; Gascon and Pereira, 1993:181.
Anolis nitens tandai Avila-Pires, 1995:80 (holotype MPEG 15850, type locality: Rio Urucu, Amazonas state, Brazil); Icochea et al., 2001:140; Vitt et al., 2001:401; Santos-Jr et al., 2007:9; Avila-Pires et al., 2009:116.

Abbreviated Description. Maximum SVL 70 mm. Vertebral region with slightly enlarged scales; number of rows of enlarged scales increases posteriad. Scales on upper arms smaller than, or subequal to, vertebral scales. Supraorbital semicircles with scarcely enlarged scales. Supraocular scales weakly to distinctly keeled, approximately same size as scales on snout, laterally and posteriorly grading into granules, anteriorly surrounded by smaller scales. Interparietal moderately small, larger than adjacent scales (Fig. 7C–F).

Color in Preservative. Color pattern sexually dimorphic. In males, vertebral region usually distinct from flanks, with unclear limits between these areas. A pair of subtriangular dark spots present on sacral region. Some specimens may present sinuous lines, assuming subtriangular shapes along dorsum. Females usually with a well-delimited vertebral band, similar to *Anolis chrysolepis* females; occasionally dorsal pattern similar to males.

Dewlap Color in Life and Preservative. In preservative, male dewlap royal blue or blackish-blue with light scales. Female dewlap with central blue spot surrounded by a cream area; scales usually light colored. In life, male dewlap skin frequently blue or blackish, with light scales. Avila-Pires (1995) mentioned the dewlap in MPEG 15986 as "ultramarine with cream-color scales on rim." Dewlap in females, when extended, presents a large and central blue spot, surrounded by a cream area. Scales are frequently cream to orange. When not extended, dewlap presents a light rim and is blue laterally. Avila-Pires (1995) described the holotype MPEG 15850 female dewlap color as "sulphur-yellow with a large indigo-blue spot."

Comparison with Other Species from the A. chrysolepis Species Group. As already mentioned by Avila-Pires (1995), this species has the longest tibia in relation to SVL (0.30–0.43). For differences with *A. chrysolepis*, see above. Avila-Pires (1995) also mentioned the possible sympatry with *A. bombiceps*, which also has a blue or blackish blue dewlap (with no sexual dimorphism), but they can be distinguished by female dewlap color (a central blue spot, surrounded by a pale area in *A. tandai*), by the minimum number of scales between supraorbital semicircles (1–4 in *A. tandai* and 1–2 in *A. bombiceps*) and by the number of postmentals (4–8 in *A. tandai* and 6–8 in *A. bombiceps*).

Distribution. South of the Amazon River and west of the Tapajós River, in Brazil (states of Pará, Amazonas, Rondônia, Acre, and north of Mato Grosso), and in Peru.

Anolis planiceps Troschel, 1848.
Anolis planiceps Troschel, 1848:649 (holotype ZMB 529, type locality: Caracas, Venezuela).
Anolis chrysolepis planiceps; Vanzolini and Williams, 1970:85; Hoogmoed, 1973:125; Myers and Donnelly, 2008:100.
Anolis chrysolepis; Beebe, 1944:97; O'Shea, 1989:69; Zimmerman and Rodrigues, 1990:449; Martins, 1991:182.
Anolis eewi Roze, 1958:311 (holotype FMNH 74040, type locality: Chimantatepui, Bolívar, Venezuela).
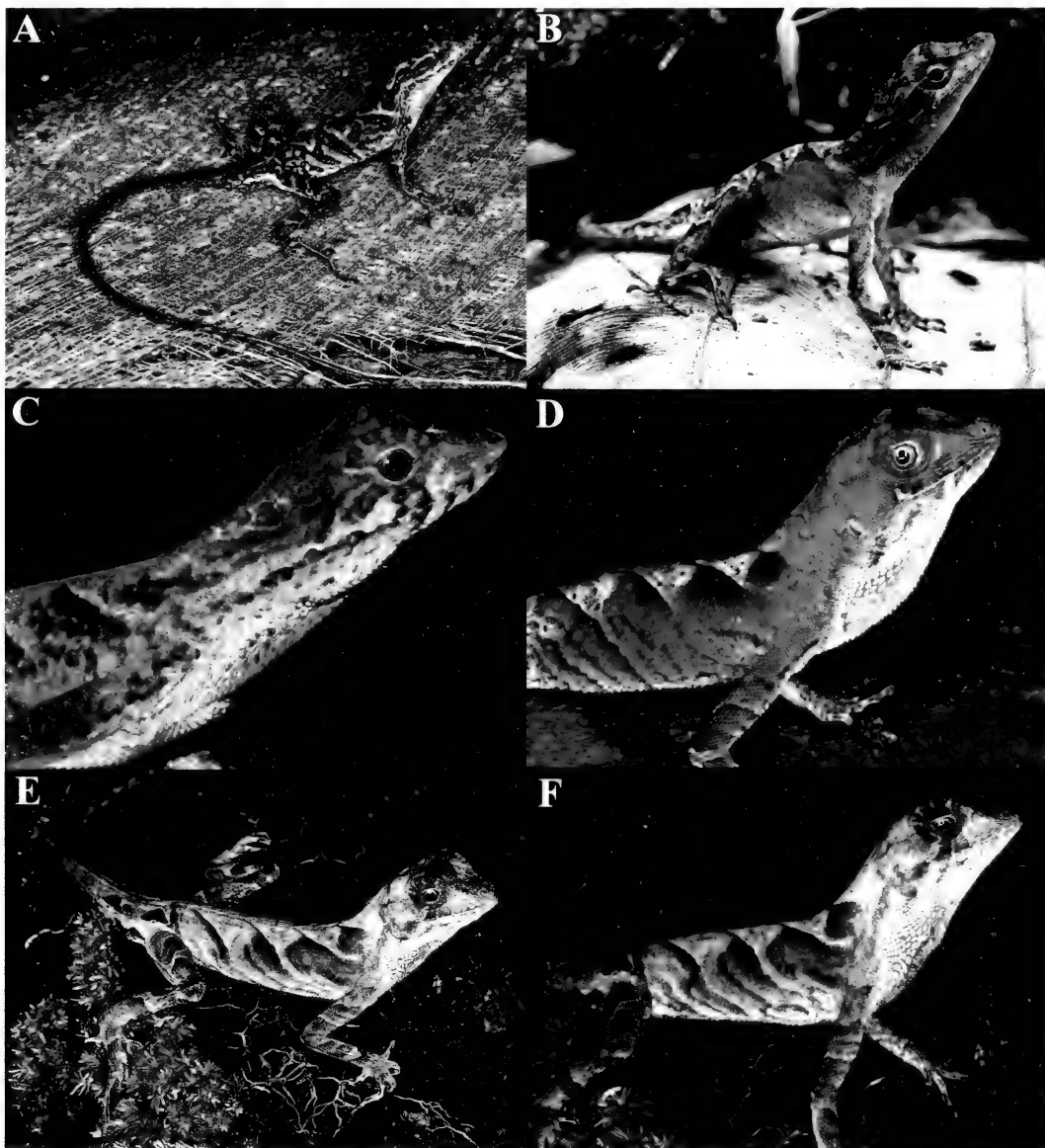
Figure 8.   *Anolis chrysolepis* species group. A) *Anolis planiceps* from Roraima, Brazil (Photo: Laurie J. Vitt), B) *Anolis planiceps* from Guatopo, Venezuela (Photo: Laurie J. Vitt), C) *Anolis planiceps* from Cuyuni-Mazaruni, Guyana (Photo: Robert Langstroth), D) *Anolis scypheus* from Ecuador (Photo: Laurie J. Vitt), E) *Anolis scypheus* from Ecuador (Photo: Laurie J. Vitt), F) *Anolis scypheus* from Ecuador (Photo: Laurie J. Vitt).

Anolis nitens: Boulenger, 1885:91; Beebe, 1944:200.

Norops nitens nitens; Savage and Guyer, 1991:366.

Anolis nitens nitens; Avila-Pires, 1995:70; Vitt et al., 2008:84.

Abbreviated Description. Maximum SVL 76 mm. Double row of enlarged vertebral scales extending from nape to base of tail; few to several rows of weakly keeled scales, increasing in number caudally, forming a gradual transition between double row of enlarged scales and

granules on flanks. Scales of upper arms markedly larger than vertebral scales. Supraorbital semicircles with enlarged scales, forming pronounced ridge in some specimens. Supraocular region with distinct group of enlarged, weakly keeled, scales surrounded by smaller scales. Interparietal distinctly larger than adjacent scales (Fig. 8A–C).

Color in Preservative. No sexual dimorphism in color pattern. Specimens usually have many chevrons along back, with tips directed posteriorly, sometimes forming the posterior border of rhomboid figures. A pair of triangular spots commonly present on sacral region. Myers and Donnelly (2008) described the color pattern of two adult males and one adult female as "orange with white or grayish white scales in basal rows, scales darker gray or blackish gray in distal rows."

Dewlap Color in Life and Preservative. Dewlap red, fading rapidly in preserved specimens, appearing cream-white, with light scales. A lateral lavender area may be present as mentioned by Avila-Pires (1995). In life, dewlap skin orange to reddish with grayish to cream scales. Myers and Donnelly (2008) found variation in the dewlap of four juveniles, including a female that had "a large bluish black basal spot on the dewlap, which had a bright orange periphery and mostly white scales (only a few dark scales)."

Comparison with the Other Species from the A. chrysolepis Species Group. This species has the proportionately largest interparietal scale. It differs from its sister taxon *A. brasiliensis* mainly by dewlap color (red in *A. planiceps* and blue or grayish/blackish blue in *A. brasiliensis*) and body size (*A. planiceps* reaches 76 mm, whereas *A. brasiliensis* reaches 69 mm).

Distribution. Venezuela, Trinidad, Guyana, and the states of Roraima and Amazonas on the northern part of Brazil.

Anolis brasiliensis Vanzolini and Williams, 1970.
Anolis chrysolepis; Amaral, 1937:1722.
Anolis chrysolepis brasiliensis; Vanzolini and Williams, 1970:85 (holotype MZUSP 10319, type locality Barra do Tapirapés, Mato Grosso, Brazil); Williams and Vanzolini, 1980:99; Vanzolini, 1981:253, 1986:3; Cunha et al., 1985:23.
Norops nitens brasiliensis; Savage and Guyer, 1991:366.
Anolis nitens brasiliensis; Avila-Pires, 1995:70; Werneck and Colli, 2006:1987.

Abbreviated Description. Maximum SVL 69 mm. Double row of enlarged vertebral scales from nape to base of tail; few to several rows of dorsal scales with weak keels, increasing in number caudally, gradually transitioning between double row of enlarged scales and granules on flanks. Scales of upper arms markedly larger than vertebral scales. Scales on snout from moderately keeled to smooth, heterogeneous in size, with no distinction between anterior and posterior scales. Supraorbital semicircles with enlarged, generally smooth scales. Supraocular region with most scales large and weakly keeled, surrounded by small scales. Interparietal distinctly larger than adjacent scales (Fig. 9A–D).

Color in Preservative. No sexual dimorphism in color pattern. Dorsal color grayish-brown or pale white, either uniform or not. A light vertebral band may be present, either narrow with undefined margins or wide; in both cases surrounded by darker area. A pair of triangular spots on sacral region commonly present, may be accompanied by second pair at the base of tail. Ventral region usually pale-white, may be marbled with brown spots.

Dewlap Color in Life and Preservative. Dewlap blue or grayish-blue, with light or grayish scales. In life, dewlap usually grayish blue or blackish blue, with dark scales varying from light-cream to dark gray. Some specimens from Tocantins state show the dewlap skin grayish-green tending to yellowish-beige along rim, with scales grayish-brown or pale-cream tending to brownish along rim. Some irregular light-blue lines may be present (Fig. 8D). Vanzolini and Williams (1970) do not describe the dewlap color but refer to the frontispiece plate
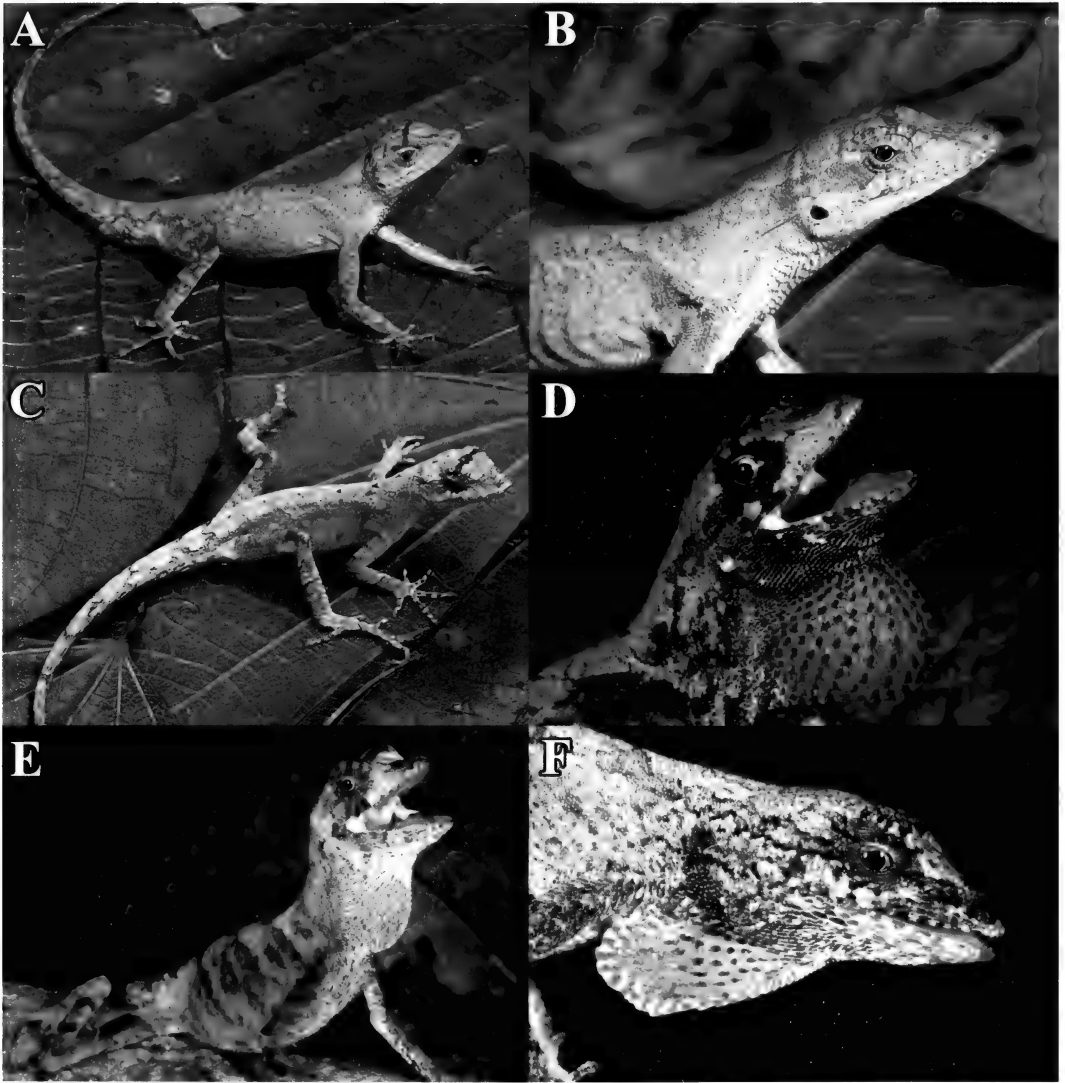
Figure 9.   *Anolis chrysolepis* species group. A) *Anolis brasiliensis* from Cantão, Tocantins, Brazil (Photo: Laurie J. Vitt), B) *Anolis brasiliensis* from Cantão, Tocantins, Brazil (Photo: Laurie J. Vitt), C) *Anolis brasiliensis* from Barra do Ouro, Tocantins, Brazil (Photo: Itamar Tonial), D) *Anolis brasiliensis* from Jalapão, Tocantins, Brazil (Photo: Laurie J. Vitt), E) *Anolis bombiceps* from Peru (Photo: Young Cage), F) Anolis meridionalis from Tocantins, Brazil (Photo: Itamar Tonial).

representing the dewlap color in life of a male as green with a brown edge along rim. Avila-Pires (1995) observed in specimens from Carajás, Southern Pará, "a blue dewlap, lighter in females, with scales varying from light to dark gray or cream and the surrounding area may be chrome-orange."

Comparison with the Other Species from the A. chrysolepis Species Group. Anolis

brasiliensis, along with *A. bombiceps*, has the largest toe IV among the other species of the *A. chrysolepis* group. *Anolis brasiliensis* differs from *A. planiceps*, mainly by dewlap color (red in *A. planiceps* and blue or grayish/blackish blue in *A. brasiliensis*) and body size (*A. planiceps* reaches 76 mm, whereas *A. brasiliensis* reaches 69 mm). *Anolis brasiliensis* is broadly sympatric with

A. meridionalis, although they occur in different habitats (see *A. meridionalis* description below) and they differ mainly by digital dilatations under phalanx ii and iii that form a prominent border in *A. brasiliensis*.

Distribution. Brazil, in southern Pará, Tocantins, Piauí, Maranhão, Ceará, Goiás, Mato Grosso, Minas Gerais, São Paulo, and Distrito Federal.

Two individuals housed in MCZ under the numbers R-60580 and R-60581 are labeled as paratypes of *A. c. brasiliensis* but have as localities Rio Juruá, Brazil, and Loreto, Peru, respectively. Vanzolini and Williams (1970) did not mention those individuals, which mean that they are not paratypes. Moreover, even though they have typical *A. brasiliensis* characteristics, it is extremely unlikely that the species occurs in these localities. Given their questionable data, we did not consider these individuals in the morphological analyses or elsewhere in this study.

Anolis scypheus Cope, 1864.
Anolis chrysolepis; Guichenot, 1855:15.
Anolis scypheus Cope, 1864:172 (holotype BM 1946.8.855, type locality: "Caracas" according to Boulenger, 1885, but considered an error by Vanzolini and Williams, 1970:85); Boulenger, 1885:90; Goeldi, 1902:16, 32; Cunha, 1961:67; Peters and Donoso-Barros, 1970:66.
Anolis incompertus incompertus Barbour, 1932:99 (holotype MCZ 32309, type locality: Villavicencio, Meta, Colombia).
Anolis chrysolepis scypheus: Vanzolini and Williams, 1970:85; Vanzolini, 1986:3.
Norops nitens scypheus; Savage and Guyer, 1991:366.
Anolis nitens scypheus; Avila-Pires, 1995:78.

Abbreviated Description. Maximum SVL 80 mm. Vertebral scales forming double row of enlarged dorsals along back. Scales of upper arms small relative to other species, larger than vertebral scales. Scales on snout relatively small, with raised surface. Supraorbital semicircles with enlarged scales, generally forming pronounced ridge. A small group of enlarged supraocular scales, grading into granules posteriorly and laterally, anteriorly surrounded by smaller scales. Interparietal distinctly larger than surrounded scales (Fig. 8D–F).

Color in Preservative. No sexual dimorphism in color pattern. Dorsum usually with caudally directed chevrons that may form the posterior border of rhomboid figures, similar to the pattern described for *A. planiceps*; or, it may show a broad band with lateral expansions (narrower at nape, extending caudally). A pair of subtriangular dark spots may be present on sacral region.

Dewlap Color in Life and Preservative. Dewlap color in preservative usually pale along rim with pale-cream or blackish scales, and blue with light scales in the center (Fig. 7). In life, dewlap skin red along rim (the red color vanishes very easily in preserved specimens) with red or blackish scales, and blue with pale-cream or light-brown scales laterally. Avila-Pires (1995) described the dewlap color of RMNH 24653 as "cobalt-blue with red rim, scales white with orange center."

Comparison with the Other Species from the A. chrysolepis Species Group. *Anolis c. scypheus* presents the proportionally maximum values of head width, head height, ear diameter, minimum distance between nostrils and SVL among all species of the *A. chrysolepis* species group. For differences with *A. bombiceps*, see *A. bombiceps* diagnosis below.

Distribution. Amazonian Colombia, Ecuador, Peru, and the northwestern part of Amazonas state in Brazil.

Anolis bombiceps Cope, 1876.
Anolis bombiceps Cope, 1876:168 (type apparently lost, type locality: Nauta, Peru); Goeldi, 1902:16, 32; Peters and Donoso-Barros, 1970:49; Vanzolini and Williams, 1970:86; 1986:28; Avila-Pires, 1995:54.

Norops bombiceps; Savage and Guyer, 1989:110.

Abbreviated Description. Maximum SVL 74 mm. Vertebral scales not or only slightly enlarged. Scales on upper arm subequal to, or slightly larger than, vertebral scales. Scales on snout anteriorly small, weakly to distinctly keeled, posteriorly larger, flat, usually uni- or multicarinated. Supraorbital semicircles with enlarged, keeled scales, forming pronounced ridge. Supraocular region with a group of distinctly enlarged scales surrounded posteriorly and laterally by granules. Interparietal scale distinctly larger than adjacent scales (Fig. 9E).

Color in Preservative. No sexual dimorphism in color pattern. Dorsal color usually brown, with irregular dark spots between hind limbs and irregular figures across limbs. V-shaped lines along back, with apex directed posteriorly, may be present.

Dewlap Color in Life and Preservative. Dewlap deep blue or blackish in preservative, with light or dark scales. In life, dewlap skin deep blue with light or dark scales.

Comparisons with the Other Species from the A. chrysolepis Species Group. Anolis *bombiceps* is sympatric with *A. scypheus* and may be sympatric with *A. tandai*, of which it can be distinguished by dewlap color (deep blue or blackish in *A. bombiceps*, blue on central region and red along rim in *A. scypheus*, and blue on central region and cream along rim on females of *A. tandai*; males of *A. tandai* and *A. bombiceps* have similar dewlap colors), number of loreals (6–7 in *A. bombiceps*, 5–9 in *A. tandai*, and 7–10 in *A. scypheus*), number of scales between the second canthals (9–12 in *A. bombiceps*, 10–15 in *A. tandai*, and 9–15 in *A. scypheus*), number of scales between supraorbital semicircles (1–2 in *A. bombiceps*, 1–4 in *A. tandai*, and 1–5 in *A. scypheus*) and postmentals (6–8 in *A. bombiceps* and 4–8 in *A. tandai* and *A. scypheus*).

Distribution. Amazonian Colombia, Ecuador, and Peru and in the State of Amazonas, Brazil. In this study, we reported *A. bombiceps* from two Brazilian localities, both in Amazonas state: Apuí, very close to the Colombian border and São Gabriel da Cachoeira.

Anolis meridionalis Boettger, 1885.
Anolis meridionalis Boettger, 1885a:437 (holotype lost, original type locality: Paraguay; neotype MNHN Paraguay 6608, type locality: Colonia Ybycui, Estancia Ybycui, Departamento Canindeyú, Paraguay, according to designation by Motte and Cacciali, 2009); Vanzolini and Williams, 1970:8; Peters and Donoso-Barros, 1970:60; Motte and Cacciali, 2009:19; Langstroth, 2006:154; Nicholson et al. 2006:2.
Anolis holotropis Boulenger, 1895:522 (holotype unknown, type locality: "Province Matto Grosso, Brazil").
Norops sladeniae Boulenger, 1903:69 (holotype unknown, type locality: "Chapadá, Matto Grosso" = Chapada dos Guimarães, Mato Grosso, Brasil, according to Vanzolini and Williams, 1970).
Anolis steinbachi Griffin, 1917:308 (holotype CM 988, type locality "Provincia del Sara, Bolívia").
Norops marmorata Amaral, 1932:63 (holotype MZUSP 737, type locality "Jaguará, Rio Grande, Minas Gerais, Brasil").
Anolis chrysolepis meridionalis; Hellmich, 1960:22 (partim, according to Vanzolini and Williams, 1970).
Norops meridionalis; Nicholson 2002:97.

Abbreviated Description. Maximum SVL 56 mm. Specimens analyzed presented vertebral scales anteriorly small, keeled, posteriorly increasing in size and forming a gradual transition toward the granules on flanks; they do not form rows of enlarged scales along dorsum. The neotype description provided by Motte and Cacciali (2009) states that vertebral scales form eight rows of enlarged scales along back that are distinctly larger than scales on the flanks. Scales on upper arm keeled, markedly larger than

vertebral scales. Scales on snout anteriorly weakly to distinctly keeled, uni- or multi-carinate and slightly larger than the flat posterior scales. Supraorbital semicircles with enlarged, weakly keeled scales. Supraocular region with a group of distinctly enlarged scales surrounded posteriorly and laterally by granules and anteriorly by smaller scales. Interparietal scale distinctly larger than adjacent scales. Loreals 6–7; canthals 5–6; 8–10 scales between second canthals; 0–1 scales between supraorbital semicircles; 0–2 scales between supraorbital semicircles and interparietal, postmentals 5–8 (Fig. 9F).

Color in Preservative. No sexual dimorphism in color pattern observed. Dorsal color usually grayish-brown, with a light cream, sometimes tending to reddish or light-orange, vertebral band. Dark brown V-shaped lines (apex directed posteriorly) may be present, as well as dark-brown irregular figures and spots across the limbs and in paravertebral region. A pair of subtriangular dark spots on sacral region frequently present.

Dewlap Color in Life and Preservative. When extended, dewlap skin in preservative blue or grayish-blue in center and pale or cream along rim, with light or dark scales. When not extended, grayish-blue laterally, with the center cream or beige. In life, dewlap skin deep blue in center and orange to pale yellow along rim. Scales may be darker on the center, tending to cream or beige on the border, changing to orange or pale yellow on anterior base of dewlap, along rim (Fig. 8F). Langstroth (2006) presented a dewlap photo of a male *A. meridionalis* from near the Zapocós Reservoir in Bolivia showing a deep blue skin with irregular grayish lines and light or dark scales, tending to grayish-green along rim.

Comparisons with the Other Species from the A. chrysolepis Species Group. Anolis meridionalis is sympatric with *A. brasiliensis*, of which it can be distinguished mainly by the digital dilatations on phalanx ii and iii, which are continuous with scales under phalanx i and do not form the prominent border observed in *A. brasiliensis*. *Anolis meridionalis* can also be distinguished from

A. brasiliensis by smaller body size (*A. meridionalis* reaches 56 mm, whereas *A. brasiliensis* reaches 69 mm), by the smaller number of scales between supraorbital semicircles (0–1 in *A. meridionalis* and 0–3 in *A. brasiliensis*), by the smaller number of scales between supraorbital semicircles and interparietal (1–4 in *A. brasiliensis* and 0–2 in *A. meridionalis*), and by the smaller number of fourth finger and toe lamellae (15–20 and 25–32, respectively, in *A. brasiliensis*, 10–12 and 18–24 in *A. meridionalis*). Besides these morphological differences, these species do not occur in the same habitat: *A. meridonalis* is commonly found in open areas densely covered by grass in Brazilian Cerrado (Vanzolini and Williams, 1970), whereas *A. brasiliensis* is a typical inhabitant of gallery forests in the same biome (Vitt et al., 2008). Vitt et al. (2008: 146) found "only two specimens of *A. brasiliensis* outside of forested habitat in typical Cerrado, and both were inside termite nests and inactive."

Distribution. Central Brazil, Paraguay, and Bolivia.

IDENTIFICATION KEY TO THE SPECIES OF THE *ANOLIS CHRYSOLEPIS* GROUP

1a. Digital dilatations under phalanx ii and iii are continuous with scales under phalanx i, not forming a prominent border; dewlap skin blue or grayish-blue in center and orange to yellowish-orange (it can be pale or cream in preserved specimens) along rim, with light or dark scales .... *A. meridionalis*

1b. Digital dilatations under phalanx ii form a prominent border over scales under phalanx I 2

2a. A weakly to distinctly double row of enlarged vertebral scales from nape to base of tail; scales on upper arm larger than vertebral scales 3

2b. Vertebral area with slightly or distinctly enlarged scales, of which the two vertebral rows may be larger than adjacent ones; scales on upper arm smaller than, to sub equal to, vertebral scales 5

3a. A double row of weakly enlarged vertebral scales; scales on upper arm slightly larger than vertebral scales; dewlap red along rim (it can be pale in some specimens), with red or blackish scales, and blue with light scales in the center .... *A. scypheus*

3b. A double row of distinctly enlarged vertebral scales from nape to base of tail; scales on upper arm distinctly larger than vertebral scales 4

4a. Supraorbital semicircles with enlarged, keeled scales, forming a pronounced ridge in some specimens; supraocular scales with a group of enlarged scales, surrounded in all their extension by distinctly smaller scales; dewlap skin red, but in preserved specimens it usually appear as pale, with light scales .... *A. planiceps*

4b. Supraorbital semicircles with enlarged and generally smooth scales; most supraocular scales large, grading laterally into smaller scales; dewlap skin in preserved specimens blue or grayish-blue with light or grayish scales .... *A. brasiliensis*

5a. Vertebral area with scales not or only slightly enlarged; interparietal scale distinctly larger than adjacent scales; dewlap skin deep blue or blackish-blue with light and grayish scales ...... *A. bombiceps*

5b. Vertebral area with scales slightly to distinctly enlarged; interparietal subequal to or slightly larger than adjacent scales 6

6a. Vertebral area with scales distinctly enlarged along back, numbers of enlarged rows increasing posteriorly; interparietal subequal to or slightly larger than adjacent scales; male dewlap royal blue, dark blue, or blackish, with light scales or blue scales toward the rim; female dewlap skin pale yellow to orange (it can be pale or cream in preserved specimens), and toward the rim scales may be darker .... *A. chrysolepis*

6b. Vertebral area with scales slightly enlarged along back, numbers of enlarged rows increasing posteriorly; interparietal larger than adjacent scales; male dewlap royal blue or blackish-blue, with light scales; female dewlap with a central blue spot, surrounded by a cream area; scales usually light .... *A. tandai*

ACKNOWLEDGMENTS

2010-9 and 302343/88–1) from CNPq. Fieldwork conducted by LJV and J. P. Caldwell was supported by NSF grants DEB 9200779, DEB 9505518, and DEB 0415430; those in Brazil were covered by Portaria MCT 170, de 28/09/94, and by IBAMA permit 073/94–DIFAS. Fieldwork conducted by GRC was covered by IBAMA permit 027/2003–CGFAU/LIC and supported by Programa Nacional de Diversidade Biológica PROBIO/MMA, project "Paisagens e biodiversidade: uma perspectiva integrada para o inventário e conservação da Serra do Cachimbo."

APPENDIX 1

Specimens examined (number of specimens of each species in parentheses).

Anolis chrysolepis (50). **SURINAM: Sipaliwini:** Tafelberg Nature Reserve (MCZ R-154861), **Nassau:** Nassau Plateau (MZUSP 29658), **Saramacca:** 1 km from Coppename River (MCZ R-155217). **FRENCH GUIANA:** Sophie trail S from St. Elie gold pits (MCZ R-77548), lower Matarony River, tributary of Approague River (MCZ R-118644, R-118641, R-110388), Saul (MCZ R-146767), **Sinnamary,** Petit Sant River (MPEG 15829, 15845). **GUIANA:** Onora (MCZ R-63350), Shudikar-won (MCZ R-65349). **BRAZIL: Amapá: Porto Platon** (MCZ 85010), **Serra do Navio** (MCZ R-79146, R-85009; MPEG 19676, 19678, 19679, 19680, 19681, 19682, 19683, 19685, 19686, 19687, 19688, 19690), **Mazagão:** Rio Maracá (MZUSP 8845, 8846; CHUNB 56761), **Laranjal do Jari** (CHUNB 56767; MZUSP 83222, 83224), **Pará:** Aldeia dos índios Tirió (MZUSP 13141), **Oriximiná:** FLONA Saracá-Taquera: Platô Aviso (MPEG 27114, 27217), Platô Almeidas (MPEG 26864), Estação Ecológica Grão-Pará, Serra do Acari (MPEG 26573, 27374, 27375, 27376, 27377, 26587, 26578, 26593), **Porto Trombetas:** Platô Bela Cruz (MPEG 24216), Platô Greig (MPEG 24218), **Faro:** Floresta Estadual de Faro (MPEG 26597).

Anolis planiceps (72). **VENEZUELA: Portuguesa** (MCZ R-176492, R-176491, R-176493, R-176494, R-176495, R-176496): Acarigua: Environs of Agua Blanca (MCZ R-123708), **Distrito Federal:** Puerto la Cruz (MCZ R-48782), **Amazonas:** Puerto Ayacucho (MCZ R-58328, R-84073), **Sucre:** Cunamacoa, San Rafael (MCZ R-48781), Peninsula of Paria, Yacua (MCZ R-43856, R-43860, R-43857, R-43858), **Aragua:** Palsamencho Parque, HPittier between Portochuelo and Ocumare (MCZ R-101817), **Carabobo:** Hacienda San Esteban, North of Puerto Cabello (MCZ R-107688), Goaiguaza: Miquija (MCZ R-121759, R-121758, R-121762, R-121760, R-121757), Salon: Las Quiguas (MCZ R-121753, R-81302), **Falcón:** Acosta, Pauji, (MCZ R-49035, R-48723, R-49037, R-48725,

R-48724, R-49036), Riecito (MCZ R-49050), **Miranda:** Guatapo (MCZ R-100438), **Bolivar:** Arabupu, Mt. Roraima (MCZ R-34868). **TRINIDAD:** Nariva Swamp, Cascadoux Trace (MCZ R-60800), Huevas Id. (MCZ R-100119), **Sangre Grande:** Toco (MCZ R-10746, R-10747), La Seiva (MCZ R-8998, R-8999, R-9000), **Trinidad:** Chacachacare (MCZ R-100118), Maruga (MCZ R-31495), Palmiste: 3 km S San Fernando (MCZ R-85011, R-85012, R-85013, R-85014, R-85015, R-85016, R-85017, R-85018, R-100120, R-100121, R-100122, R-81303, R-81304, R-81501, R-85474, R-85475, R-85473). **BRAZIL: Amazonas:** Serra da Neblina (MCZ R-86763), Manaus: Reserva Ducke (MCZ R-92682), Camp Gavião, approx. 100 km N of Manaus (MCZ R-168987). **GUYANA: Pomeroon-Supenaam:** Dawa (MCZ R-123745), **Cuyuni-Mazaruni:** Kaburi, 30 miles from Bartica (MCZ R-81306), Mazaruni River (MCZ R-39690), Kamakusa (MCZ R-65352).

Anolys scypheus (49). **PERU: Loreto:** (KU 222147), Rio Pacaya, Cahuana (MCZ R-160775), Galicia: west bank of Rio Tapiche (MCZ R-157245), Pampa Hermosa: near mouth Cushcbatey River (MCZ R-57369, R-57373, R-57372), **Amazonas:** Mouth of R.Santiago Maranon (MCZ R-57371), **Ucayali:** River Tamaya (MCZ R-57374), **Madre de Dios:** Cocha Cashu, NW of mouth of Rio Manu (MCZ R-178177). **ECUADOR: Napo:** Trail from Laguna Taracoa, S bank Rio Napo, 30 km downriver from Coca (MCZ R-154571), Hacienda 'Primavera' N bank Rio Napo 30 km from Coca (MCZ 92612, 154567, 154568), Prov. S side of Rio Napo, 6.5 km ESE of Puerto Misahualli, at La Cruz Blanca on ASuarez's land (MCZ R-171889), **Sucumbios:** Santa Cecilia (MCZ R-92601, R-92602, R-92603, R- 92604, R-92605, R-92608), Santa Cecilia, Rio Agvaratis (MCZ R-100010), Limon Cocha (MCZ R-156822, R-85098, R-85099, R-85100, R-85101, R-92610, R-92611, R-92612), **Chimborazo:** Riobamba (MCZ R-29290). **COLOMBIA: Meta:** Villavicencio: San Martin (MCZ R-32309, R-32310, R-32312, R-32313, R-32314, R-32315, R-32317), Bairro Povenir (MZUSP 36099, 36100). **BRAZIL: Amazonas:** Acanauí (MZUSP 47213, 47214), Rio Japurá: Serrinha (MZUSP 46793, 46794), Costa da Altamira (MZUSP 47301, 47302, 47303); Lago Amanã (MZUSP 60462).

Anolis tandai (96). **BRAZIL: Rondônia:** Espigão do Oeste (MPEG 21479, 21483, 21488, 21899), **Amazonas:** Estirão do Equador (MPEG 901), Rio Urucu (holotype: MPEG 15850), Benjamin Constant (paratypes: MPEG 15933, 15938, 15949, 15986, 15987, 15995; MZUSP 15898), Madeireira Sheffer, Rio Ituxi (MPEG 20372, 20473, 20474), Careiro da Várzea, estrada para Altazes (MPEG 18918, 18920, 18928, 18931, 18934, 18935), Tapauá (MZUSP 37763, 37764, 37765), Beruré (MZUSP 38101, 38102), Novo Aripuanã (MZUSP 42400), Borba (MZUSP 41077, 9145), Rio Juruá (MZUSP 700), Barreira do Matupiré, Rio Madeira, (MZUSP 42150), Maués, Bragança/São Tomé, Rio Paraconi (MPEG 27673, 27674, 27675, 27676), **Acre:** Rio Juruá, approx. 30 km North of Porto Walter of Walter (MPEG 20655, 20656, 20658, 20659,

20662, 20663, 20665, MZUSP 53270, 53271, 53272), Alto Purus (MZUSP 2413, 2514), Seringal Santo Antônio, próximo a Manoel Urbano (MZUSP 32097), Parque Nacional Serra do Divisor, Estirão do Panela (MZUSP 88656), Estirão do Equador (MZUSP 899), **Pará:** Parque Nacional da Amazônia, Itaituba (MPEG 21986, 21987, 21988, 21989, 21990, 21991), Parque Nacional da Amazônia, Uruá (MZUSP 52533, 52536, 52538, 52539), Cachoeira da Montanha (MZUSP 53657, 53658), Buburé (MZUSP 53692, 53693, 53695), Barreirinha, próximo a São Luis, Rio Tapajós (MZUSP 20679), **Mato Grosso:** Aripuanã (MZUSP 82590, 82585, 82589, 82587, 82591, 82593, 82586, 82592, 82588, 82594, 81502, 81512, 81501, 81520, 81505, 81497, 81508, 81514, 81494, 81491), Juruena (MZUSP 82402, 82404, 82397, 82403, 82400). **PERU: Loreto:** Rio Orosa (MZUSP 56658), Alto Curanja, Igarapé Champuia (MZUSP 3324, 3324).

Anolis brasiliensis (116). **BRAZIL: Mato Grosso:** Barra do Tapirapés (holotype: MZUSP 10319, paratypes: MCZ R-98284, R-98285, R-98286, R-98287, R-98288, R-98289), Porto Alegre do Norte (CHUNB 47842),Vila Rica (MZUSP 82874, 82884, 82882), **Tocantins:** Caseara (CHUNB 44989, 44992, 44499, 45000, 45009, 45036, 45028, 45026, 45022, 45030), Pium (CHUNB 24754, 24756), Palmas (CHUNB 25082, 24216, 11521, 11522, 24215, 16947, 25092, 11520, 24262, 15230, 16142, 16948), Peixe (CHUNB 52471, 52472, 52474), Porto Alegre do Tocantins (CHUNB 38918), Porto Nacional (CHUNB 47741, 47742, 47740), Mateiros (CHUNB 27161, 27158, 27162), Usina Hidroelétrica Luis Eduardo Magalhães (MZUSP 95466, 95467), **Goiás:** São Domingos (CHUNB 35282, 35257, 35288, 35319, 35285, 35314, 43823, 35315, 35311, 35258, 43824, 43832, 33020), Minaçu (CHUNB 11019, 11021, 10967, 10983, 49706, 48617, 10987, 49703, 10986, 10970, 10999, 08655, 29309), Colinas do Sul (CHUNB 50396, 50393, 50395, 44694), Valparaiso (CHUNB 08556, 08555), Luziânia (CHUNB 47427, 43408, 40865, 43407, 47426), Três Ranchos (CHUNB 44740), Goiânia (CHUNB 57318), **Minas Gerais:** Unaí (CHUNB 30888, 32873, 32867, 36287), **Distrito Federal:** Brasilia (CHUNB 49614), **Piauí:** Ribeiro Golçalves (CHUNB 57028), **Maranhão:** Carolina (CHUNB 51972, 51973, 51974, 51975), Gancho do Arari (MZUSP 60682), **Pará:** Novo Progresso (CHUNB 34542), Parauapebas (CHUNB 08855, 11132), Canaã dos Carajás (MPEG 25166), Itaituba, Jacareacanga (CHUNB 56398), **Ceará:** Arajara (MZUSP 51698, 51699, 51703, 51706), **São Paulo:** Bueno de Andrade (MZUSP 4384), Ibarra (MZUSP 4487), Itapura (MZUSP 551).

Anolis meridionalis (9). **BRAZIL: Minas Gerais:** Paracatu (CHUNB 26140, 26146), Buritizeiro (CHUNB 44522), **Rondônia:** Vilhena (CHUNB 11715), **Tocantins:** Palmas (CHUNB 12022, 12026), **Goiás:** Luziânia (CHUNB 43404, 43405), **Distrito Federal:** Brasilia (CHUNB 43282).

Anolis bombiceps (11). **PERU: Loreto** (MZUSP 13135, 131137, 13138), N.A. 1.5 km N of Teniente Lopez, 310 (KU 222145). **COLOMBIA: Amazonas:**

6 km NW of Leticia (MCZ R-112267). **ECUADOR: Pastaza:** Conambo (MZUSP 13140). **BRAZIL: Amazonas:** Apuí (CHUNB 38340); São Gabriel da Cachoeira: Missão Taraquá, Rio Uapés (MPEG 17819), Uatumã (MZUSP 17439), Igarapé Belém, Rio Solimões (MZUSP R-13026, 13027).

Anolis onca (1). **VENEZUELA: Falcón:** Rio Seco on Caribean Sea, between Urumaco and Coro (MCZ R-132736).

Anolis lineatus (1). **NETHERLANDS ANTILLES: Curaçao:** Cos Cora (MCZ R-83027).

Anolis sagrei sagrei (1). **JAMAICA: Westmoreland:** Savanna La Mar (MCZ R-161754).

Anolis auratus (1). **COLOMBIA: Magdalena:** Pozo Colorado, 11 km W of Santa Maria (MCZ R-104546).

LITERATURE CITED

AMARAL, A. 1932. Estudos sobre lacertílios neotropicais. I. Novos gêneros e espécies de lagartos do Brasil. *Memórias do Instituto Butantan* **7**: 51–74.

AMARAL, A. 1937. Herpetological collection from Central Brazil. Compte Rendus XIIe. *Congrès International de Zoologique. Lisbon* **1935**: 1720–1732.

AVILA-PIRES, T. C. S. 1995. Lizards of Brazilian Amazonia (Reptilia: Squamata). Zoologische Verhandelingen Leiden, **299**: 1–706.

AVILA PIRES, T. C. S., M. S. HOOGMOED, and W. A. ROCHA. 2010. Notes on the herpetofauna of northern Pará, Brazil: a forgotten part of the Guianan Region, I. Herpetofauna. Boletim Museu Paraense Emílio Goeldi. *Ciências Naturais* **5**: 13–112.

AVILA PIRES, T. C. S., L. J. VITT, S. S. SARTORIUS, and P. A. ZANI. 2009. Squamata (Reptilia) from four sites in southern Amazonia, with a biogeographic analysis of Amazonian lizards. Boletim Museu Paraense Emílio Goeldi. *Ciências Naturais* **4**: 99–118.

AVISE, J. C. 2000. *Phylogeography: The History and Formation of Species.* Cambridge: Harvard University Press.

AVISE, J. C., D. WALKER, and G. C. JOHNS. 1998. Speciation durations and Pleistocene: effects on vertebrate phylogeography. *Proceedings of the Royal Society of London. B* **265**: 1707–1712.

BALLARD, J. W., and M. C. WHITLOCK. 2004. The incomplete natural history of mitochondria. *Molecular Ecology* **13**: 729–744.

BARBOUR, T. 1932. New Anoles. *Proceedings of the New England Zoological Club* **12**: 97–102.

BARROWCLOUGH, G. F., and R. M. ZINK. 2009. Funds enough and time: mtDNA, nuDNA and the discovery of divergence. *Molecular Ecology* **18**: 2934–2936.

BEEBE, W. 1944 Field notes on the lizards of Kartabo, British Guiana, and Caripito, Venezuela. Part 2. Iguanidae. *Zoologica* **29**: 195–216.

BOETTGER, O. 1885a. Liste von Reptilien und Batrachiern aus Paraguay. *Zeitschrift für Naturwissenschaften, Halle* **58**: 213–248.

BOETTGER, O. 1885b. Berichtigung der Liste von Reptilien und Amphibien am Paraguay von Dr. O. Boettcher. *Zeitschrift für Naturwissenschaften, Halle* **58**: 436–437.

BOETTGER, O. 1895. Description of a new *Anolis* from Brazil. *Annals and Magazine of Natural History* **15**: 522–523.

BOETTGER, O. 1903. List of the batrachians and reptiles collected by M.A. Robert at Chapadá, Matto Grosso, and presented by Mrs. Percy Sladen to the British Museum. (Percy Sladen Expedition to Central Brazil). *Proceedings of the Zoological Society of London* **2**: 69–70.

BOULENGER, G. A. 1885. *Catalogue of the Lizards in the British Museum (Natural History).* Vol. 2. London: Taylor & Francis.

BRANDLEY, M. C., A. SCHMITZ, and T. W. REEDER. 2005. Partitioned Bayesian analysis, partition choice, and the phylogenetic relationships of scincid lizards. *Systematic Biology* **54**: 373–390.

BULL, J. J., J. P. HUELSENBECK, C. W. CUNNINGHAM, and D. L. SWOFFORD. 1993. Partitioning and combining data in phylogenetic analysis. *Systematic Zoology* **42**: 384–397.

BURNABY, T. P. 1966. Growth-invariant discriminant functions and generalized distances. *Biometrics* **22**: 96–110.

COPE, E. D. 1864. Contributions to the herpetology of tropical America. *Proceedings of the Academy of Natural Sciences of Philadelphia* **16**: 166–181.

COPE, E. D. 1876. Report on the reptiles brought by Professor James Orton from the middle and upper Amazon, and western Peru. *Journal of the Academy of Natural Sciences of Philadelphia* **8**: 159–183.

CUNHA, O. R. 1961. Lacertílios da Amazônia II. Os lagartos da Amazônia brasileira, com especial referência aos representados na coleção do Museu Goeldi. *Boletim do Museu Paraense Emílio Goeldi* **39**: 1–189.

CUNHA, O. R, F. P. NASCIMENTO, and T. C. S. AVILA-PIRES. 1985. Os Répteis da área de Carajás, Pará, Brasil (Testudines e Squamata). I. *Publicações Avulsas do Museu Paraense Emílio Goeldi* **40**: 9–92.

DE QUEIROZ, K. 1998. The general lineage concept of species, species criteria, and the process of speciation: a conceptual unification and terminological recommendation. *In* D. J. Howard and S. H. Berlocher (eds.), *Endless Forms: Species and Speciation.* New York: Oxford University Press.

DE QUEIROZ, K. 1999. The general lineage concept of species and the defining properties of the species category, pp. 49–89. *In* R. A. Wilson (ed.), *Species: New Interdisciplinary Essays.* Cambridge, Massachusetts: MIT Press.

DE QUEIROZ, K. 2005a. Ernst Mayr and the modern concept of species. *Proceedings of the National Academy of Science* **102**: 6600–6607.

DE QUEIROZ, K. 2005b. A unified concept of species and its consequences for the future of taxonomy. *Proceedings of the California Academy of Science* **18**: 196–215.

DE QUEIROZ, K. 2007. Species concept and species delimitation. *Systematic Biology* **56**: 879–886.

DIXON, J. R., and P. SOINI. 1986. The reptiles of the upper Amazon Basin, Iquitos Region, Peru. *Milwaukee: Milwaukee Public Museum Contributions in Biology and Geology* **4**: 1–58.

DUMÉRIL, A. M. C., and G. BIBRON. 1837. *Erpétologie Général ou Histoire Naturelle compléte des Reptiles.* Vol. 4. Paris: Librairie Encyclopédique de Roret.

FELSENSTEIN J. 1978. Cases in which parsimony or compatibility methods will be positively misleading. *Systematic Zoology* **27**: 401–410.

FELSENSTEIN, J. 1985. Confidence limits on phylogenies, an approach using the bootstrap. *Evolution* **39**: 783–791.

FENWICK, A. M., R. L. GUTBERLET, TB JR, J. A. EVANS, and C. L. PARKINSON. 2009. Morphological and molecular evidence for phylogeny and classification of South American pitvipers, genera *Bothrops, Bothriopsis,* and *Bothrocophias* (Serpentes: Viperidae). *Zoological Journal of the Linnean Society* **156**: 617–640.

FORBES, E. 1846. On the connection between the distribution of the existing fauna and flora of the British Isles, and the geological changes which have affected their area, especially during the epoch of the northern drift. *Memoirs of Geological Survey, Great Britain* **1**: 336–432.

GAMBLE, T., A. M. SIMONS, G. R. COLLI, and L. J. VITT. 2008. Tertiary climate change and the diversification of the Amazonian gecko genus *Gonatodes* (Sphaerodactylidae, Squamata). *Molecular Phylogenetics and Evolution* **46**: 269–277.

GASCON, C., and O. S. PEREIRA. 1993. Preliminary checklist of the herpetofauna of the upper Rio Urucu, Amazonas, Brazil. *Revista Brasileira de Zoologia* **10**: 179–183.

GLOR, R. E., L. J., VITT, and A. LARSON. 2001. A molecular phylogenetic analysis of diversification in Amazonian *Anolis* lizards. *Molecular Ecology* **10**: 2661–2668.

GOELDI, E. A. 1902. Lagartos do Brasil. *Boletim do Museu Paraense* **3**: 499–560.

GRAU, E. T., S. L. PEREIRA, L. F. SILVEIRA, E. HÖFLING, and A. WAJNTAL. 2005. Molecular phylogenetics and biogeography of Neotropical piping guans (Aves: Galliformes): *Pipile* Bonaparte, 1856 is synonym of *Aburria* Reichenbach, 1853. *Molecular Phylogenetics and Evolution* **35**: 637–645.

GRAYBEAL, A. 1998. Is it better to add taxa or characters to a difficult phylogenetic problem? *Systematic Biology* **47**: 9–17.

GRIFFIN, L. E. 1917. A list of the South American lizards in the Carnegie Museum, with descriptions of four new species. *Annals of the Carnegie Museum* **2**: 304–320.

GUICHENOT, A. 1855. Reptiles, pp. 1–95. *In* F. de Castelnau (ed.), *Animaux nouveaux ou rares recueillis pendant l'expédition dans les parties centrales de l'Amérique du Sud, de Rio de Janeiro a Lima, et de Lima au Para; exécutée par ordre du gouvernement français pendant les années 1843 a 1847, sous la direction du Comte Francis de Castelnau*. Paris: Chez P. Bertrand, Libraire Éditeur.

HAFFER, J. 1969. Speciation in Amazonian forest birds. *Science* **165**: 131–137.

HELLMICH, W. 1960. Die Sauria der Grand Chaco und seiner Randgebiete. *Abhandlungen Bayerische Akademie der Wissenschaften (N.F.)*, **101**: 1–131.

HOOGMOED, M. S. 1973. *Notes on the Herpetofauna of Surinam IV. The Lizards and Amphisbaenians of Surinam*. Biogeographica, 4. The Hague: Dr. W. Junk Publishers.

HOOGMOED, M. S., and T. C. S. AVILA-PIRES. 1989. Observations on the nocturnal activity of lizards on a marshy área in Serra do Navio, Brazil. *Tropical Zoology* **2**: 165–173.

HOOGMOED, M. S., and T. C. S. AVILA-PIRES. 1991. Annotated checklist of the herpetofauna of Petit Saut, Sinnamary River, French Guiana. *Zoologische Verhandelingen Leiden* **65**: 53–88.

HUDSON, R. R., and M. TURELLI. 2003. Stochasticity overrules the "three-times rule": genetic drift, genetic draft, and coalescence times for nuclear loci versus mitochondrial. *Evolution* **57**: 182–190.

HUELSENBECK, J. P., and F. RONQUIST. 2001. MRBAYES: Bayesian inference of phylogeny. *Bioinformatics* **17**: 754–755.

HUELSENBECK, J. P., F. RONQUIST, R. NIELSON, and J. P. BOLLBACK. 2001. Bayesian inference of phylogeny and its impact on evolutionary biology. *Science* **294**: 2310–2314.

ICOCHEA, J., E. QUISPITUPAC, A. PORTILLA, and E. PONCE. 2001. The amphibian and reptile fauna of the lower Urubamba region, Peru. *In* F. Dallmeier, A. Alonso, and P. Campbell (eds.), *Biodiversity of the Lower Urubamba Region, Peru*. SIMAB series 7. Washington, DC: Smithsonian Institution/MAB Biodiversity Program.

ICZN. 2010. OPINION 2256 (Case 3446) *Anolis chrysolepis* Duméril & Bibron, 1837 (Reptilia, Squamata): precedence given over *Draconura nitens* Wagler, 1830. *Bulletin of Zoological Nomenclature* **67**: 266–268.

JOLICOEUR, P. 1963. Multivariate generalization of allometry equation. *Biometrics* **19**: 497–499.

JUKES, T. H. 1987. Transitions, transversions, and the molecular evolutionary clock. *Journal of Molecular Evolution* **26**: 87–98.

KUMAR, S., M. NEI, J. DUDLEY, and K. TAMURA. 2008. MEGA: a biologist-centric software for evolutionary analysis of DNA and protein sequences. *Briefings in Bioinformatics* **9**: 299–306.

LANGSTROTH, R. 2006. Notas sobre *Anolis meridionalis* Boettger, 1885 (Squamata: Iguania: Polychrotidae) en Bolivia y comentarios sobre *Anolis steinbachi*. *Kempffiana* **2**: 154–172.

LARTILLOT, N., H. BRINKMANN, and H. PHILIPPE. 2007. Suppression of long-branch attraction artifacts in the animal phylogeny using a site-heterogeneous model. *BMC Evolutionary Biology* **7**: 1–14.

LEMMON, A. R., and E. C. MORIARTY. 2004. The importance of proper model assumption in Bayesian phylogenetics. *Systematic Biology* **53**: 265–277.

MACEY, J. R., J. A. SCHULTE, N. B. ANANJEVA, A. LARSON, N. RASTEGAR-POUYANI, S. M. SHAMMAKOV, and T. J. PAPENFUSS. 1998. Phylogenetic relationships among agamid lizards of the *Laudakia caucasia* species group: testing hypotheses of biogeographic fragmentation and an area cladogram for the Iranian Plateau. *Molecular Phylogenetics and Evolution* **10**: 118–131.

MACEY, J. R., Y. WANG, N. B. ANANJEVA, A. LARSON, and T. J. PAPENFUSS. 1999. Vicariant patterns of fragmentation among gekkonid lizards of the genus *Teratoscincus* produced by the Indian collision: a molecular phylogenetic perspective and an area cladogram for Central Asia. *Molecular Phylogenetics and Evolution* **12**: 320–332.

MADDISON, W. P. 1997. Gene trees in species trees. *Systematic Biology* **46**: 523–536.

MADDISON, W. P., and L. L. KNOWLES. 2006. Inferring phylogeny despite incomplete lineage sorting. *Systematic Biology* **55**: 21–30.

MADDISON, W. P., and D. R. MADDISON. 1992. *MacClade Version 3: Analysis of Phylogeny and Character Evolution*. Sunderland Massachusetts: Sinauer Associates.

MARTINS, M. 1991. The lizards of Balbina, central Amazonia, Brazil: a qualitative analysis of resource utilization. *Studies on Neotropical Fauna and Environment* **26**: 179–190.

MITCHELL, A., C. MITTER, and J. C. REGIER. 2000. More taxa or more characters revisited: combining data from nuclear protein-encoding genes for phylogenetic analyses of Noctuoidea (Insecta: Lepidoptera). *Systematic Biology* **49**: 202–224.

MOTTE, M. and P. CACCIALI. 2009. Descripción de un neotipo para *Anolis meridionalis* Boettger, 1885 (Sauria: Polychrotidae). *Cuadernos de Herpetología* **23**: 19–24.

MYERS, C. W. 2008. *Anolis chrysolepis* Duméril & Bibron, 1837 (Reptilia, Squamata): proposed precedence over Draconura nitens Wagler, 1830. *Bulletin of Zoological Nomenclature* **65**: 205–213.

MYERS, C. W., and M. A. DONNELLY. 2008. The summit herpetofauna of Auyantepui, Venezuela: report from the Robert G. Goelet American Museum—Terramar Expedition. *Bulletin of the American Museum of Natural History* **308**.

NEI, M., and W. H. LI. 1979. Mathematical model for studying genetic variation in terms of restriction endonucleases. *Proceedings of National Academy of Sciences* **76**: 5269–5273.

NICHOLSON, K. E. 2002. Phylogenetic analyzes and a test of the current infrageneric classification of *Norops* (Beta *Anolis*). *Herpetological Monographs* **16**: 93–120.

NICHOLSON, K. E., R. E. GLOR, J. J. KOLBE, A. LARSON, S. B. HEDGES, and J. B. LOSOS. 2005. Mainland colonization by island lizards. *Journal of Biogeography* **32**: 929–938.

NICHOLSON, K. E., L. J KOLBE, and J. B. LOSOS. 2007. Evolution of *Anolis* lizard dewlap diversity. *PLoS ONE* **2**: e274.

NICHOLSON, K. E., A. MIJARES-URRUTIA, and A. LARSON. 2006. Molecular phylogenetics of the *Anolis onca* series: a case history in retrograde evolution revisited. *Journal of Experimental Zoology (Molecular and Developmental Evolution)* **306**: 450–459.

NYLANDER, J. A. A., F. RONQUIST, J. P. HUELSENBECK, and J. L. NIEVES-ALDREY. 2004. Bayesian phylogenetic analysis of combined data. *Systematic Biology* **53**: 47–67.

NYLANDER, J. A. A., J. C. WILGENBUSCH, D. L. WARREN, and D. L. SWOFFORD. 2008. AWTY (are we there yet?): a system for graphical exploration of MCMC convergence in Bayesian phylogenetics. *Bioinformatics* **24**: 581–583.

OLIVER, P. M., M. ADAMS, M. S. LEE, M. N. HUTCHINSON, and P. DOUGHTY. 2009. Cryptic diversity in vertebrates: molecular data double estimates of species diversity in a radiation of Australian lizards (*Diplodactylus*, Gekkota). *Proceedings of Biological Sciences* **276**: 2001–2007.

O'SHEA, M. 1989. The herpetofauna of Ilha de Maracá State of Roraima, northern Brazil. *Proceedings of the 1988 U.K Herpetological Societies, Symposium on Captive Breeding* Reptiles: 51–72.

PETERS, J. A., and R. DONOSO-BARROS. 1970. Catalogue of the Neotropical squamata. Part II. Lizards and amphisbaenians. *United States National Museum Bulletin* **297**: 1–293.

POSADA, D. 2008. jModelTest: phylogenetic model averaging. *Molecular Biology and Evolution* **25**: 1253–1256.

QUINN, G. P., and M. J. KEOUGH, 2002. *Experimental Design and Data Analysis for Biologists*. Cambridge, UK: Cambridge University Press.

R DEVELOPMENT CORE TEAM. 2009. *R: A Language and Environment for Statistical Computing*. Vienna, Austria: R Foundation for Statistical Computing.

RAMBAUT, A., and A. J. DRUMMOND. 2009. *Tracer v1.5*. Available from http://beast.bio.ed.ac.uk.

RODRIGUEZ-ROBLES, J. A., T. JESKOVA, and M. A. GARCÍA. 2007. Evolutionary relationships and historical biogeography of *Anolis desechensis* and *Anolis monensis*, two lizards endemic to small islands in the Caribbean Sea. *Journal of Biogeography* **34**: 1546–1558.

ROHLF, F. J., and F. L. BOOKSTEIN. 1987. A comment on shearing as a method for "size correction." *Systematic Zoology* **36**: 356–367.

ROZE, J. A. 1958. Los reptiles del Chimantá Tepui (Estado Bolívar, Venezuela) colectados por la expedicion botanica del Chicago Natural History Museum. *Acta Biologica Venezuelica* **2**: 299–314.

RUBIN, D. B. 1996. Multiple imputation after 18+ years. *Journal of the American Statistical Association* **91**: 473–489.

SANTOS-JR, A. P., J. G. FROTA, and F. R. V. RIBEIRO. 2007. Reptilia, Squamata, Polychrotidae, *Anolis nitens tandai*: distribution extension, new State record, and geographic distribution map. *Check List* **3**: 9–10.

SAVAGE, J. M., and C. GUYER. 1989. Infrageneric classification and species composition of the anole genera, *Anolis, Ctenotus, Dactyloa, Norops* and *Semiurus* (Sauria: Iguanidae). *Amphibia-Reptilia* **10**: 105–116.

SAVAGE, J. M., and C. GUYER. 1991. Nomenclatural notes on anoles (Sauria: Polychridae): stability over priority. *Journal of Herpetology* **25**: 365–366.

SCHAAD, E. W., and S. POE. 2010. Patterns of ecomorphological convergence among mainland and island *Anolis* lizards. *Biological Journal of the Linnean Society* **101**: 852–859.

SHIMODAIRA, H. 2001. CONSEL: for assessing the confidence of phylogenetic tree selection. *Bioinformatics* **17**: 1246–1247.

SHIMODAIRA, H. 2002. An approximately unbiased test of phylogenetic tree selection. *Systematic Biology* **51**: 492–508.

SHIMODAIRA, H., and M. HASEGAWA. 1999. Multiple comparisons of log-likelihoods with applications to phylogenetic inference. *Molecular Biology and Evolution* **16**: 1114–1116.

SOMERS, K. M. 1986. Multivariate allometry and removal of size with principal components analysis. *Systematic Zoology* **35**: 359–368.

STAMATAKIS, A. 2006. RAxML-VI-HPC: maximum likelihood-based phylogenetic analyses with thousands of taxa and mixed models. *Bioinformatics* **22**: 2688–2690.

SWOFFORD, D. L. 2001. *PAUP. Phylogenetic Analysis Using Parsimony (and Other Methods)*. Version 4.0. Sunderland, Massachusetts: Sinauer Associates.

TABACHNICK, B. G., and L. S. FIDELL. 2001. *Using Multivariate Statistics*. Needham Heights, Massachusetts: Allyn and Bacon.

TROSCHEL, F. H. 1848. Amphibien. *In* R. Schomburgk (ed.), Reisen in British Guiana. *In* Den Jahren. Im Auftrag Sr. Majestat des Konigs von Preussen ausgefuhrt von Richard Schomburgk. **3**: 1840–1844. Versucheiner fauna und flora von British Guiana.

VAN BUUREN, S., J. P. L. BRAND, C. G. M. GROOTHUIS-OUDSHOORN, and D. B. RUBIN. 2006. Fully conditional specification in multivariate imputation. *Journal of Statistical Computation and Simulation* **76**: 1049–1064.

VANZOLINI, P. E., and E. E. WILLIAMS. 1970. South American anoles: the geographic differentiation and evolution of the *Anolis chrysolepis* species group (Sauria: Iguanidae). Part 1 and part 2. *Arquivos de Zoologia (São Paulo)* **19**: 1–124.

VANZOLINI, P. E. 1981. The vanishing refuge: a mechanism for ecogeographic speciation. *Papéis Avulsos de Zoologia (São Paulo)* **34**: 251–255.

VANZOLINI, P. E. 1986. *Levantamento herpetológico da área do estado de Rondônia sob a influência da rodovia BR 364*. Programa Polonoroeste, subprograma Ecologia Animal, Relatório de Pesquisa no. 1. Brasilia: Ministério de Ciência e Técnologia–CNPq.

VITT, L. J., W. E. MAGNUSSUM, T. C. S. AVILA-PIRES, and A. P. LIMA. 2008. *Guide to the Lizards of Reserva Adolpho Ducke, Central Amazônia*. Manaus: Áttena Design Editorial.

VITT, L. J., S. S. SARTORIUS, T. C. S. AVILA-PIRES, and M. C. ESPÓSITO. 2001. Life on the leaf litter: the ecology of *Anolis nitens tandai* in the brazilian Amazon. *Copeia* **2001**: 401–412.

VITT, L. J., D. B. SHEPARD, G. H. C. VIEIRA, J. P. CALDWELL, G. R. COLLI, and D. O. MESQUITA. 2008. Ecology of *Anolis nitens brasiliensis* in cerrado woodlands of Cantão. *Copeia* **2008**: 144–153.

VITT, L. J., and P. A. ZANI. 1996. Ecology of the South American Lizard *Norops chrysolepis* (Polychrotidae). *Copeia* **1996**: 56–68.

WAGLER, J. G. 1830. *Natürliches System der Amphibien, mit vorangehender Classification der Säugthiere und Vögel*. Munich: J.G. Cotta.

WERNECK, F. P., and G. R. COLLI. 2006. The lizard assemblage from seasonally dry tropical forest enclaves in the Cerrado biome and its association with the Pleistocenic Arc. *Journal of Biogeography* **33**: 1983–1992.

WIENS, J. J., and B. D. HOLLINGSWORTH. 2000. War of the iguanas: conflicting molecular and morphology phylogenies and long-branch attraction in iguanid lizards. *Systematic Biology* **49**: 143–149.

WIENS, J. J., and T. A. PENKROT. 2002. Delimiting species using DNA and morphological variation and discordant species limits in spiny lizards (*Sceloporus*). *Systematic Biology* **51**: 69–91.

WILLIAMS, E. E., and P. E. VANZOLINI. 1980. Notes and biogeographic comments on anoles from Brasil. *Papéis Avulsos de Zoologia, São Paulo* **34**: 99–108.

YODER, A. D., R. VILGALYS, and M. RUVOLO. 1996. Molecular evolutionary dynamics of cytochrome *b* in strepsirrhine primates: the phylogenetic significance of third-position transversions. *Molecular Biology and Evolution* **13**: 1339–1350.

ZIMMERMAN, B. L., and M. T. RODRIGUES. 1990. Frogs, snakes, and lizards of the INPA-WWF reserves near Manaus, Brazil, pp. 426–454. *In* A. H. Gentry (ed.), *Four Neotropical Rainforests*. London: Yale University Press.

ZINK, R. M., and G. F. BARROWCLOUGH. 2008. Mitochondrial DNA under siege in avian phylogeography. *Molecular Ecology* **17**: 2107–2121.

.

·

The power and utility of morphological characters in systematics: A fully resolved phylogeny of *Xenosaurus* and its fossil relatives (Squamata: Anguimorpha)

B.-A.S. BHULLAR

THE POWER AND UTILITY OF MORPHOLOGICAL CHARACTERS IN SYSTEMATICS: A FULLY RESOLVED PHYLOGENY OF *XENOSAURUS* AND ITS FOSSIL RELATIVES (SQUAMATA: ANGUIMORPHA)

B.-A. S. BHULLAR[1]

ABSTRACT. *Xenosaurus* is an enigmatic clade of Mexican and Central American lizards distinguished by knob-like scalation and flattening of the head and body associated with living in cracks within cliff faces. The position of *Xenosaurus* within the larger clade Anguimorpha is difficult to determine owing to a combination of primitive features and a unique, highly modified anatomy that obscures useful characters. Evidently, the phylogenetic stem of *Xenosaurus* represents a long independent history of evolution. Fortunately, several fossil taxa exist that can elucidate this history. These taxa include the extinct *Exostinus lancensis* (Cretaceous), *Exostinus serratus* (Oligocene), and *Restes rugosus* (Paleocene), the latter two known from substantial, cranial material (Bhullar, 2007; 2010). Using osteological and alcohol-preserved specimens, fossils, and high-resolution x-ray CT scans thereof, I attempted to reconstruct the relationships of the three fossil taxa and the six extant species of *Xenosaurus* that are available in U.S. collections.

Despite the considerable phylogenetic importance of *Xenosaurus* and its stem, this is the first phylogenetic analysis of the group. An exhaustive search of the skeleton, including osteoderms embedded in the skin visualized using CT scanning, yielded 274 new characters, substantially more than have been used previously in gross anatomy–based analyses of such a restricted group of reptiles. The great number of characters is largely the result of the availability of disarticulated skeletal material, CT scans showing internal bone structure and bones embedded in the skin, and attention to subtle anatomical differences whose validity could be assessed in terms of intraspecies variation because of the availability of large sample sizes for certain taxa.

My results suggested that *R. rugosus* is sister to the other xenosaurs, resolving a polytomy with other Anguimorpha recovered by previous work. *Exostinus lancensis* is problematic in that it may represent several distinct taxa, but it was recovered as sister to *E. serratus* + *Xenosaurus*, making *Exostinus* paraphyletic. *Exostinus serratus* emerged as sister to *Xenosaurus*. *Xenosaurus* comprises a northern clade consisting of *Xenosaurus newmanorum* and *Xenosaurus platyceps*; the remaining taxa are united as a southern clade. Within the southern clade, *Xenosaurus agrenon* and *Xenosaurus rectocollaris* are sister to *Xenosaurus grandis* and *Xenosaurus rackhami*. North–south splits within Xenosauridae mirror those of several other lizard clades and may be the legacy of the equatorial contraction of early Tertiary tropical forests. The fully resolved nature of the phylogeny and the congruence of the extant portion with molecular results indicates the continued relevance and efficacy of morphological systematics when an exhaustive anatomical analysis is performed to search for new characters.

Key words: Xenosaurs, Xenosauridae, squamates, lizards, extinct, paleontology, Anguimorpha, systematics, *Shinisaurus*

INTRODUCTION

Phylogenetic analysis using gross morphological characters, while once the standard approach to systematics, has in the last two decades been complemented by the huge number of characters (albeit with a very limited number of character states) available from the morphology of nucleic acids, or "molecular" data. Ancient fossil taxa, of course, can generally be included in phylogenetic analyses only when morphological data are in play, but for extant organisms the huge number of individual characters available from DNA sequences compared with the characters available from gross morphology has led to suggestions that morphological analyses are woefully inaccurate and obsolete (Scotland et al., 2003).

[1] Department of Geological Sciences, Jackson School of Geosciences, The University of Texas at Austin, Austin, Texas; and Department of Organismic and Evolutionary Biology, Harvard University, 16 Divinity Avenue, Bio Labs Room 4110, Cambridge, Massachusetts 02138 (bhartanjan.bhullar@gmail.com).

Indeed, early morphology-based analyses in particular often utilized only a few dozen characters—but still their resolving power could be considerable (Gauthier et al., 1988). However, far longer character lists and far better resolution can be achieved with the detailed consideration of the near-infinite aspects of organismal morphology at all scales. Here, I employ an exhaustive search for the characters most relevant to fossil taxa—those derived from skeletal anatomy—in an attempt to resolve the phylogeny of the enigmatic clade *Xenosaurus* and its fossil relatives.

Xenosaurus ("knob-scaled lizards") consists of unusual flat-bodied crevice-dwelling lizards distributed throughout Mexico and northern Central America. The relationships of the species within *Xenosaurus* and extinct taxa with affinities to the clade have not been treated in a published phylogenetic analysis. Two studies, by Gauthier (1982) and Conrad (2008; see also Conrad et al., 2011), presented hypotheses of relationships along the phylogenetic stem of *Xenosaurus*, although both dealt primarily with relationships within the larger clade Anguimorpha as a whole. In the first of these studies, Gauthier (1982) suggested that the Oligocene fossil taxon *Exostinus serratus* is sister to *Xenosaurus* to the exclusion of the Cretaceous *Exostinus lancensis* and the Paleocene *Restes rugosus* (*Exostinus rugosus* prior to reassignment in that work) but left the relationships of the latter two taxa unresolved. These taxa are described fully under Materials and Methods. A preferred hypothesis in which *R. rugosus* is sister to the remaining taxa and *E. lancensis* is sister to *E. serratus* was provided by Conrad (2008). Finally, an unpublished master's thesis (Canseco Márquez, 2005) included a hypothesis of relationships among the extant species of *Xenosaurus* based on squamation. That study included more species of *Xenosaurus* than were available to me, but for those which were included by Canseco Márquez (2005) and by me in this study, the phylogenetic hypotheses recovered for relationships within *Xenosaurus* is

identical. I did not include the characters from that study here in deference to the author of the work, who is preparing it for publication.

Hypotheses of the phylogeny of Anguimorpha as a whole were provided by McDowell and Bogert (1954) and Gauthier (1982). Those hypotheses were not explicitly tested by the authors, although Gauthier (1982) presented his hypothesis with an explicitly cladistic frame of reference. Anguimorpha was subjected to explicit phylogenetic analysis by several authors, some of whom used gross anatomical characters (Rieppel, 1980; Estes et al., 1988; Lee, 1998; Evans and Barbadillo, 1998; Gao and Norell, 1998; Conrad, 2005, 2008; Conrad et al., 2011) and others of whom used nucleic acid structure (Macey et al., 1999; Wiens and Slingluff, 2001; Townsend et al., 2004; Conrad et al., 2011).

In a cladistic framework, the phylogeny posited by McDowell and Bogert (1954) has an initial split between Varanoidea (here Platynota) and Diploglossa, the latter of which includes the remainder of Anguimorpha. The arrangement suggested that Varanoidea is split between *Heloderma* and *Lanthanotus borneensis* + *Varanus*, whereas Diploglossa is split between Diploglossinae and a trichotomy of Gerrhonotinae + Anguinae + Xenosauridae. Xenosauridae was used in the sense of *Shinisaurus crocodilurus* + *Xenosaurus*. A similar phylogeny was presented by Rieppel (1980), with Varanoidea sister to a clade whose first split is between Gerrhonotinae and all other taxa, with the latter then split into Xenosauridae and Diploglossinae + Anguinae. Xenosauridae was not nested within Anguidae in the topology presented by Gauthier (1982). Instead, he posited a trichotomy of Varanoidea, Xenosauridae, and Anguidae, the last consisting of Anguinae and Gerrhonotinae + Diploglossinae. The trichotomy was resolved by Estes et al. (1988) to Anguidae on one branch and Xenosauridae + Varanoidea on the other. The same topology was recovered by Lee (1998). According to Evans and Barbadillo (1998),

the initial split is between Xenosauridae and the remaining anguimorphs (in addition, Gekkota is nested within Anguimorpha, an unusual result that was not recovered in other studies). This topology, without the nested Gekkota, was also recovered by Gao and Norell (1998), as was the placement of the Mongolian taxon *Carusia intermedia* (Borsuk-Bialynicka, 1984) as the sister to Xenosauridae. Finally, a similar topology was recovered by Conrad (2005, 2008), save that *S. crocodilurus* and its extinct relative *Bahndwivici ammoskius* are sister to Varanoidea, leaving the initial split in Anguimorpha between *Xenosaurus* plus its allied extinct taxa and the remainder of Anguimorpha. *Carusia intermedia* emerged in the 2005 study as the sister taxon to Anguimorpha, and in the 2008 and 2011 studies as the sister to *Xenosaurus* and its extinct relatives. Within Anguidae, Anguinae and Diploglossinae are sister taxa to the exclusion of Gerrhonotinae.

Among the studies based on nucleic acid structure, the same data set was used by Macey et al. (1999) and Wiens and Slingluff (2001). Both groups recovered the same overall topology for Anguimorpha. The initial split according to those studies is a trichotomy among *Varanus, Heloderma*, and the remainder of Anguimorpha. The latter clade is split between *S. crocodilurus* and *Xenosaurus* + Anguidae. Within Anguidae, Anguinae and Gerrhonotinae are sister taxa to the exclusion of Diploglossinae. Several years after the publications of those focused studies on Anguimorpha, the first molecular structure–based phylogenies of all of Squamata appeared (Townsend et al., 2004; Vidal and Hedges, 2005). In general, most of the trees recovered in those analyses have the initial split in Anguimorpha between *S. crocodilurus* + Varanidae and Anguidae + *Heloderma* + *Xenosaurus* in some combination. An Anguidae + *Heloderma* clade appears more often than a *Heloderma* + *Xenosaurus* clade. The molecular structure–based phylogenies are thus broadly congruent with the newest gross anatomy–based phylogenies, save for the unprecedented

nonmonophyly of Varanoidea, a clade supported by numerous gross anatomical apomorphies (summarized by Gao and Norell, 1998; Conrad, 2005, 2008; Conrad et al., 2011).

Regarding outgroups to Anguimorpha, the gross anatomy–based and molecular structure–based phylogenies differ strikingly. All of the gross anatomy–based phylogenies have Anguimorpha as part of a monophyletic Scleroglossa (*sensu* Estes et al., 1988), with Iguania sister to that large clade. The appropriate outgroups to Anguimorpha would thus be found within "Scincomorpha" (whose monophyly is not universally supported), at least a part of which is, in most gross anatomy–based phylogenies, more closely related to Anguimorpha than is Gekkota. The molecular structure–based phylogenies, on the other hand, generally recover Iguania as more closely allied to Anguimorpha than any "scincomorph" clade, sometimes with Serpentes intervening.

Given the potential importance of *Xenosaurus* and its extinct relatives to resolving the phylogeny of Anguimorpha and thereby of Squamata as a whole, this study is directed at resolving the problematic relationships within the highly autapomorphic crown clade and its stem. The extinct taxa are particularly important to my analyses because they can break up the phylogenetic "long branch" leading to *Xenosaurus* (Gauthier et al., 1988). Two other factors were important to the viability of the study. First, museum collections in the United States have sufficient skeletal and wet-preserved specimens of extant *Xenosaurus* to allow a reasonable sampling of taxa and some assessment of intraspecific variation. Furthermore, some of the skeletal specimens I used were disarticulated. Many of the characters identified here would have been impossible to see in articulated skeletons. Finally, high-resolution CT scanning technology allowed the digital disarticulation of fossils in matrix and the visualization of osteoderms within the skin of extant specimens.

MATERIALS AND METHODS

Ingroup

The focus of the present study is *Xenosaurus* and its extinct relatives, also referred to herein as "xenosaurs" (*Shinisaurus* and its extinct relatives are likewise called "shinisaurs"). The term Xenosauridae is used exclusively to refer to the "traditional" clade, including xenosaurs and shinisaurs as sister taxa, a topology only supported by one of the two analyses performed here. The characters included are limited in large part to those pertinent to relationships within the xenosaur ingroup. Most of the 274 characters I describe and score (Table 1) are new or newly defined; derivation from previous literature is noted in the character descriptions. The extinct taxa are particularly important in light of the highly derived nature of the crown clade; they provide the opportunity to break up "long branches" and resolve problematic clades (Rowe, 1986; Gauthier et al., 1988).

Xenosaurus. Twelve extant species of *Xenosaurus* were included in the unpublished external anatomy–based phylogenetic analysis by Canseco Márquez (2005); two of those are undescribed, and I was unable to obtain four—*Xenosaurus arboreus, Xenosaurus sanmartinensis, Xenosaurus phalaroanthereon,* and *Xenosaurus penai*—from U.S. collections. Most species of *Xenosaurus* were once classified as subspecies of *Xenosaurus grandis* Gray 1856. Summaries of the taxonomic history of the group were provided by King and Thompson (1968), Ballinger et al. (2000), and Canseco Márquez (2005). The taxa used in my study (see Table 1) are *Xenosaurus newmanorum* Taylor 1949 (Fig. 1), *Xenosaurus platyceps* King and Thompson 1968 (Fig. 2), *Xenosaurus rackhami* King and Thompson 1968 (as *Xenosaurus grandis rackhami*) (Fig. 3), *X. grandis* (Fig. 4), *Xenosaurus agrenon* King and Thompson 1968 (as *Xenosaurus grandis agrenon*), and *Xenosaurus rectocollaris* Smith and Iverson 1993 (Fig. 5). Alcoholic specimens were available for all taxa, and skeletal material was available for all but *X. rectocollaris.* To supplement the skeletal material, I used high-resolution x-ray CT scans of the heads and bodies of all species save *X. agrenon,* for which the wet-preserved specimens were filled with metal shot that interfered with the scanning process. The scans were performed at the High-Resolution CT Scanning Facility at The University of Texas at Austin (UTCT) and allowed visualization of the articulated skeletons with the osteodermal armor in place.

Exostinus serratus. The included specimens, from the Oligocene of Colorado and Wyoming, were described by Bhullar (2008; 2010), as was the history of this taxon.

Exostinus lancensis. This is the most problematic taxon included in the study. It was described by Gilmore (1928) and Estes (1964) on the basis of fragmentary material from the Late Cretaceous of Wyoming and Montana. A summary of the history of the taxon until 1983 was provided by Estes (1983). Following that work, the only additional information on the anatomy of the taxon was provided by Gao and Fox (1996) on the basis of specimens from the western interior of Canada. Scoring here is based on those descriptions and on a number of undescribed specimens from the western United States in the collections of the American Museum of Natural History. For the purposes of this study, all of these disparate specimens are assumed to represent the same taxon. However, *E. lancensis* requires additional study. In particular, most of the American Museum specimens from the Lance Formation of Wyoming conform well to the descriptions of *E. lancensis* in the literature. However, frontals that are clearly associated with the characteristic parietals based on size, osteodermal sculpturing, and fit of the articular surfaces are large and unfused, whereas Gao and Fox (1996) described the anterior portion of a fused frontal that is nearly the same size. For the purposes of this study, frontal fusion is assumed to be ontogenetically variable in *E. lancensis,* but work on this taxon continues.

Restes rugosus. This taxon was described as *Exostinus rugosus* by Gilmore (1942) and further by Estes (1965). It was renamed *R. rugosus* by Gauthier (1982). It is known primarily from a single well-preserved but disarticulated specimen, YPM PU 14640 from the late Paleocene of Wyoming. Isolated frontals that Gauthier (1982) referred to the taxon were suggested to belong instead to a shinisaur or a platynotan by Smith (2006b). *Restes rugosus* was never fully described, nor has it been examined since the work of Gauthier (1982). The analysis here utilizes a low-resolution CT scan of the YPM PU 14640 block, which I found to contain a surprising amount of unexposed material. I had access to one additional specimen, an anterior section of a maxilla (UMMP 73565) from the Paleocene of Wyoming.

Outgroup

Anguimorpha. Because of the unresolved state of the larger clade Anguimorpha, it was necessary to use a variety of anguimorph taxa in the analysis. In general, the focus was upon extant taxa to minimize missing data, and because I was not attempting to resolve anguimorph relationships definitively. However, because *S. crocodilurus* was traditionally allied to *Xenosaurus* in Xenosauridae, the analysis includes two described fossil shinisaurs—*B. ammoskius* from the Eocene of Wyoming (Conrad, 2005, 2008) and *Merkurosaurus ornatus* from the Miocene of the Czech Republic (Klembara, 2008). These are the only included taxa that I scored entirely from the literature. I also included three anguids—the diploglossine *Celestus enneagrammus* (part of the clade sister to all other diploglossines; Macey et al., 1999), the anguine *Ophisaurus ventralis*, and the gerrhonotine *Elgaria multicarinata*. I excluded the problematic glyptosaurs (see Conrad, 2005, 2008) and *Anniella* (Wiens and Slingluff, 2001; Conrad, 2005, 2008). Within Varanidae, *L. borneensis* and the monitor lizard species *Varanus niloticus* and

Varanus exanthematicus were used (Fuller et al., 1998; Ast, 2001; Pianka and King, 2004). Helodermatidae is scored as a composite taxon. *Heloderma suspectum* suffices for scoring most characters of this clade. However, for two characters (96 and 97), the derived nature of *H. suspectum* affected the resolution of xenosaur phylogeny. The anterior (frontal and pre-orbital) skull roof osteoderms of extant *Heloderma* are highly domed, but those of *Primaderma nessovi* Nydam 2000, *Gobiderma pulchra* Borsuk-Białynicka 1984, and *Eurheloderma gallicum*, primitive taxa on the stem of *Heloderma*, are flat and plate-like (Hoffstetter, 1957; Gao and Norell, 2000; Nydam, 2000). The domed state of the extant taxa rendered ambiguous the nature of the flattened skull roof osteoderms of *R. rugosus*, whereas scoring the primitive state for the helodermatid lineage results in a most parsimonious hypothesis that *R. rugosus* is primitive relative to *Xenosaurus* + *E. lancensis* and pulls it out of a trichotomy with those taxa. In these cases, as noted, scoring was performed as though the ancestral states for the entire helodermatid lineage were being considered. When greater access to the skeletal material of these stem taxa is possible, they should be broken out and scored separately.

Outside of Anguimorpha. One non-anguimorph was used as an outgroup. A possible choice according to Conrad (2005) would be *C. intermedia* (Gao and Norell, 1998, 2000). However, *C. intermedia* is not universally agreed to lie outside of Anguimorpha and still cannot be as thoroughly scored as an extant taxon. Because of the overwhelming molecular scale support for an Anguimorpha + Iguania clade, I chose the iguanian *Pristidactylus torquatus* as my additional outgroup. No previous gross anatomical phylogenetic analysis has used this topology.

Variation

The assessment of intraspecies variation, including but not limited to ontogenetic

TABLE 1.   CHARACTER MATRIX FOR PHYLOGENETIC ANALYSIS OF *XENOSAURUS* AND ITS FOSSIL RELATIVE.

Xenosaurus spp.	1	2	3	4	5	6	7	8	9	10	11	12	13	14	15	16	17	18	19	20	21	22	23	24	25	26	27	28	29	30	31
serratus	2	0	1	1	0	1	2	3	1	0	1	0	0	1	0	0	0	?	1	1	2	1	0	1	2	0	0	0	1	?	?
rugosus	2	?	?	?	?	?	?	?	?	?	?	?	?	?	?	?	?	?	?	?	?	?	?	?	?	?	?	?	?	?	?
lancensis	1	?	?	?	?	?	?	?	?	?	?	?	?	?	?	?	?	?	?	?	?	?	?	?	?	?	?	?	?	?	?
newmanorum	2	1	1	1	0	1	2	4	2	1	1	0	1	1	0	1	1	?	1	0	4	2	1	1	2	1	1	1	2	2	1
platyceps	2	1	1	1	0	1	2	4	2	1	1	0	1	1	0	1	1	?	1	0	4	2	1	1	2	1	0	1	2	2	1
agrenon	2	1	1	1	0	1	2	4	2	1	2	1	0	1	0	0	1	0	1	1	3	1	1	1	2	1	1	0	1	1	1
rectocollaris	2	1	1	1	0	1	2	0	2	1	2	1	0	1	0	1	1	0	1	1	3	1	1	1	2	1	1	0	2	2	1
rackhami	2	1	1	1	1	1	2	4	2	1	2	1	0	1	1	0	1	0	1	1	3	1	1	1	2	1	1	1	1	2	1
grandis	2	1	1	1	1	1	2	4	2	1	2	1	0	1	1	0	1	0	1	2	3	1	1	1	2	1	0	1	1	2	1
ornatus	1	0	1	1	0	1	0	0	0	0	0	0	0	1	0	0	0	?	0	2	2	1	1	2	0	0	?	1	1	?	?
ammoskius	0	0	1	1	1	1	?	?	?	?	?	?	?	1	?	?	0	?	?	0	?	1	?	1	?	0	?	?	?	?	?
crocodilurus	0	0	0	1	1	1	1	0	0	0	0	0	0	0	0	0	0	0	0	0	2	0	0	0	2	0	0	0	0	?	0
multicarinata	0	0	0	0	0	1	0	0	0	0	0	0	0	0	0	1	0	0	0	1	1	0	0	1	2	0	0	0	1	?	0
ventralis	0	0	0	0	0	0	0	0	0	0	0	0	0	0	0	1	0	0	0	0	0	0	0	0	2	0	0	0	0	1	0
enneagrammus	0	0	0	0	0	0	0	0	0	0	0	0	0	0	0	0	0	0	0	0	0	0	0	0	3	0	0	0	1	1	0
suspectum	0	0	0	0	0	1	0	0	0	0	0	0	0	1	0	0	0	0	0	0	0	0	0	0	2	0	0	0	0	?	0
bornensis	0	0	0	0	0	1	1	0	0	0	0	0	0	1	0	0	0	0	0	0	1	0	0	0	3	1	0	0	0	?	0
niloticus	0	0	0	1	0	1	1	0	0	0	0	0	0	1	0	0	0	0	0	1	0	0	0	0	2	?	0	0	0	1	1
exanthematicus	0	0	0	1	0	1	1	0	0	0	0	0	0	1	0	0	0	0	0	0	1	0	0	0	0	0	0	0	0	0	0
torquatus	?	0	0	1	0	0	0	0	0	0	0	0	0	1	0	0	0	0	1	1	2	0	0	0	0	0	1	0	2	2	0

	32	33	34	35	36	37	38	39	40	41	42	43	44	45	46	47	48	49	50	51	52	53	54	55	56	57	58	59	60	61	62
serratus	?	?	?	?	?	?	?	?	?	?	?	2	1	0	1	1	0	1	1	1	1	1	1	2	4	0	0	1	2	3	4
rugosus	?	?	?	?	?	?	?	?	?	?	?	0	?	0	0	?	?	0	0	1	1	0	0	3	4	0	0	1	1	1	2
lancensis	?	?	?	?	?	?	?	?	?	?	?	?	?	0	0	?	?	0	0	1	?	?	0	?	?	?	?	?	?	?	3
newmanorum	1	1	1	1	0	1	0	1	0	1	1	3	1	1	1	1	0	1	0	1	2	0	0	2	5	1	1	1	0	1	4
platyceps	1	1	1	1	0	1	0	1	0	1	0	3	1	1	1	1	0	1	0	1	2	0	0	1	3	1	1	1	0	2	4
agrenon	1	1	1	1	1	2	0	0	1	1	0	1	1	1	2	1	0	1	0	1	2	1	1	2	1	1	1	1	1	1	4
rectocollaris	1	1	1	1	1	2	0	0	1	1	0	1	1	1	2	1	0	1	0	1	2	1	1	2	4	1	2	1	2	1	4
rackhami	1	1	1	1	1	2	0	0	1	1	0	1	1	1	1	1	0	1	0	1	2	0	0	1	3	1	3	1	1	1	4
grandis	1	1	1	1	1	2	0	0	1	1	0	1	1	1	1	1	0	1	0	1	2	1	1	2	2	1	0	1	1	1	4
ornatus	1	1	1	1	1	0	0	0	1	0	0	0	0	1	0	1	0	1	0	0	2	0	0	1	2	0	0	1	1	1	0
ammoskius	?	0	0	1	0	0	?	?	?	?	?	2	1	1	0	1	0	1	0	1	2	0	0	2	2	0	0	1	2	0	0
crocodilurus	0	0	0	0	0	0	0	0	?	0	0	0	1	1	0	1	0	0	0	1	2	0	0	2	2	0	0	1	0	0	0
multicarinata	1	0	0	0	0	0	0	0	?	0	0	2	1	1	2	1	0	1	0	0	2	0	0	2	4	0	0	1	1	1	1
ventralis	1	1	0	0	0	0	0	0	?	0	0	3	1	1	6	1	0	1	0	0	0	0	0	4	6	0	0	1	0	0	0
enneagrammus	1	0	0	0	0	0	0	0	?	0	0	3	1	1	2	1	0	0	0	0	0	0	0	3	2	0	0	1	0	0	0
suspectum	1	1	0	0	0	0	1	1	?	0	0	3	1	1	4	1	0	0	0	0	0	0	0	3	4	1	0	1	0	1	0
bornensis	1	0	0	0	0	0	0	0	?	0	0	3	1	1	6	1	0	0	0	0	0	0	0	5	6	1	0	0	0	0	0
niloticus	0	0	0	0	0	0	0	0	?	0	0	0	1	1	0	0	0	0	0	1	0	0	0	3	0	1	0	0	0	1	0
exanthematicus	0	0	0	0	0	0	0	0	?	0	0	0	0	1	0	0	0	0	0	0	0	0	0	2	0	0	0	0	1	0	0
torquatus	0	0	0	0	?	0	0	0	?	0	0	0	0	1	0	?	?	0	0	0	0	0	0	0	0	0	0	0	0	2	0

TABLE 1. CONTINUED.

Xenosaurus spp.	63	64	65	66	67	68	69	70	71	72	73	74	75	76	77	78	79	80	81	82	83	84	85	86	87	88	89	90	91	92	93
serratus	0	5	0	1	1	2	2	1	1	1	?	?	?	?	?	?	?	?	?	?	?	?	?	?	?	?	?	?	1	?	0
rugosus	1	7	0	1	1	?	1	0	0	1	?	?	?	?	?	?	?	?	1	?	?	?	?	?	?	?	?	?	1	?	?
lancensis	?	?	?	?	?	?	?	?	?	?	?	?	?	?	?	?	?	?	?	?	?	?	?	?	?	?	?	?	?	?	0
newmanorum	0	B	0	1	1	3	1	0	0	1	1	1	2	2	0	1	1	0	1	0	0	1	2	2	2	2	0	0	1	1	1
platyceps	0	B	0	1	3	3	1	0	0	1	1	1	2	2	0	1	1	1	?	0	1	1	2	1	1	1	0	0	1	1	1
agrenon	0	9	0	1	1	0	1	0	0	1	1	1	1	0	1	2	0	0	?	0	0	0	0	1	2	0	0	1	1	1	1
rectocollaris	0	B	0	1	1	0	1	0	0	1	0	1	1	1	0	2	0	0	?	0	1	0	0	0	1	4	0	1	1	1	1
rackhami	0	9	0	1	1	0	1	0	0	1	0	1	1	0	1	2	0	0	?	0	1	0	0	2	1	?	0	?	1	1	1
grandis	0	9	1	1	1	0	?	0	0	1	0	1	1	0	1	2	0	0	?	0	1	0	0	2	?	1	0	?	1	1	0
ornatus	1	?	1	?	1	1	1	0	0	?	0	1	?	1	0	?	1	1	1	0	1	?	1	?	?	1	1	0	1	0	0
amnoskius	1	8	0	1	0	0	1	0	0	0	1	1	1	1	0	0	0	?	?	0	0	1	0	0	0	0	0	0	0	0	0
crocodilurus	1	5	1	1	0	0	0	0	0	0	0	0	0	0	0	0	0	?	?	0	0	0	0	2	2	5	?	0	0	0	1
multicarinata	0	A	0	0	0	0	1	0	0	0	0	2	1	2	0	2	0	?	?	0	1	0	0	2	2	5	0	0	1	1	1
ventralis	0	9	1	0	0	0	1	0	0	0	0	0	0	0	0	0	0	?	?	0	0	0	0	0	0	5	0	0	0	?	1
enneagrammus	0	6	0	0	0	0	0	0	0	0	0	0	0	2	0	2	0	?	?	0	0	0	0	2	2	5	0	0	0	1	0
suspectum	1	?	?	?	1	0	0	1	0	0	0	1	0	1	0	0	0	?	?	0	0	1	0	0	0	0	1	0	0	0	0
borneensis	1	4	0	0	0	0	0	0	0	0	0	0	0	0	1	0	0	?	0	0	0	1	0	0	0	0	1	0	0	0	0
niloticus	1	4	0	0	0	0	?	0	0	0	0	0	0	0	0	0	0	?	0	0	0	0	0	2	2	1	0	?	?	1	0
exanthematicus	1	2	0	0	0	?	0	0	0	0	0	0	0	0	0	0	0	0	0	?	0	0	0	0	0	0	0	?	1	?	0
torquatus	0	9	0	0	0	1	0	0	?	?	0	0	0	0	?	0	0	?	?	0	1	0	0	0	0	5	0	0	1	1	1

	94	95	96	97	98	99	100	101	102	103	104	105	106	107	108	109	110	111	112	113	114	115	116	117	118	119	120	121	122	123	124
serratus	2	0	1	3	2	1	1	1	0	0	0	1	1	1	2	?	?	?	?	?	1	?	?	?	?	?	?	?	?	0	2
rugosus	?	0	0	2	0	1	0	0	0	?	0	0	0	0	0	0	0	?	?	1	1	?	?	1	?	?	?	?	?	0	1
lancensis	?	0	1	3	0	0	1	0	0	?	?	0	0	0	0	?	0	?	?	?	?	?	?	0	0	?	?	?	?	0	0
newmanorum	2	1	3	3	1	1	1	0	0	1	1	1	0	1	1	1	0	3	0	0	1	3	1	1	1	0	0	1	1	0	2
platyceps	2	1	3	3	1	1	0	0	1	0	1	1	0	0	1	2	0	3	0	1	1	3	0	1	0	0	1	0	0	0	2
agrenon	2	0	1	3	1	1	0	0	0	0	1	1	0	0	1	1	0	2	0	1	1	1	0	0	0	0	0	0	0	0	2
rectocollaris	2	0	3	3	1	1	0	0	0	0	1	1	0	0	0	1	0	2	0	0	1	2	0	0	0	0	1	0	0	0	2
rackhami	2	0	1	3	1	1	1	0	1	0	1	1	0	1	0	1	0	2	0	1	1	2	0	0	0	0	0	0	0	0	2
grandis	2	0	3	3	1	1	0	1	1	0	1	1	0	0	0	1	0	2	0	1	1	2	0	0	0	0	1	0	0	0	2
ornatus	2	0	1	1	1	1	1	0	1	0	1	1	?	0	1	0	0	2	1	1	1	2	0	0	0	0	1	1	1	0	2
amnoskius	1	0	3	0	1	0	0	0	0	0	1	1	1	0	0	0	0	0	0	1	1	1	1	1	0	0	0	0	0	0	0
crocodilurus	0	0	1	3	0	1	0	0	0	0	1	1	0	0	0	0	0	0	0	0	0	0	0	0	0	0	0	0	0	0	0
multicarinata	0	0	0	0	?	0	0	0	0	0	1	0	1	0	0	0	0	0	0	0	0	0	0	0	?	0	0	0	0	0	0
ventralis	0	0	0	0	?	0	0	0	0	0	1	0	1	0	0	0	0	0	0	0	0	0	0	0	?	0	0	0	0	0	0
enneagrammus	0	0	0	0	?	0	0	0	0	0	1	0	0	0	0	0	0	0	0	0	0	0	0	?	0	0	0	0	0	0	0
suspectum	0	0	0	0	?	0	1	0	0	0	1	0	0	1	1	0	0	0	0	0	0	0	0	0	0	0	0	1	0	0	0
borneensis	0	0	0	?	0	0	0	0	0	0	0	0	0	1	1	0	0	0	?	0	0	0	0	0	0	0	1	0	0	0	0
niloticus	0	0	0	?	0	0	1	1	1	0	0	1	1	2	2	0	0	0	0	?	0	0	0	0	0	0	1	0	0	0	0
exanthematicus	0	?	1	3	1	?	1	0	0	0	0	0	1	2	2	0	0	0	?	?	0	0	0	?	0	0	0	?	0	0	0
torquatus	1	0	1	3	0	1	0	0	1	1	0	0	0	0	0	?	0	?	0	0	0	0	0	?	0	0	0	0	0	0	0

TABLE 1. CONTINUED.

Xenosaurus spp.	125	126	127	128	129	130	131	132	133	134	135	136	137	138	139	140	141	142	143	144	145	146	147	148	149	150	151	152	153	154	155
serratus	1	0	0	0	1	1	0	1	0	?	?	0	?	?	?	?	?	?	0	?	?	?	?	?	?	?	?	?	?	?	?
rugosus	0	0	0	1	?	1	1	2	0	?	?	0	?	0	0	0	0	0	0	1	?	1	?	?	?	?	?	?	?	?	?
lancensis	1	?	?	?	?	?	?	?	?	?	?	?	?	?	?	?	?	?	?	?	2	?	C	?	?	?	?	?	?	?	?
newmanorum	1	0	1	1	1	1	0	2	0	0	2	1	1	0	0	0	1	1	1	0	2	1	4	0	1	0	0	1	0	3	1
platyceps	1	0	1	1	1	1	1	2	0	1	0	1	1	1	1	0	1	1	0	0	3	1	3	2	1	0	1	1	0	2	1
agrenon	1	1	0	1	1	1	0	2	0	1	0	1	1	1	0	1	0	0	0	0	0	1	0	3	1	0	1	0	0	1	1
rectocollaris	1	0	0	1	1	1	1	2	0	1	1	1	1	1	1	0	1	0	0	0	1	1	0	1	1	0	1	0	0	1	2
rackhami	1	0	1	1	1	1	0	2	1	0	2	1	1	1	1	1	0	0	0	0	1	1	2	3	1	0	1	1	0	1	2
grandis	1	1	1	1	1	1	1	2	1	1	1	1	1	1	2	1	1	1	1	1	1	1	5	2	0	0	2	0	0	0	0
ornatus	1	?	?	1	1	?	1	?	?	0	?	0	?	?	?	?	?	?	?	?	0	1	6	4	0	0	1	1	?	0	0
annoskius	0	1	0	0	0	1	0	1	0	1	2	1	1	0	0	0	1	0	0	0	0	0	9	3	0	0	?	1	?	?	0
crocodilurus	?	0	1	0	0	1	1	1	0	0	2	1	1	1	1	1	0	1	0	1	0	0	3	7	0	0	?	0	0	1	0
multicarinata	?	1	0	0	0	1	0	1	0	0	2	1	0	0	0	0	1	1	0	0	1	0	7	7	1	0	?	0	0	1	0
centralis	?	0	0	0	1	1	0	1	0	0	2	1	1	1	1	1	1	0	0	1	0	0	7	4	1	0	?	0	0	1	0
enneagrammus	?	1	0	0	0	1	0	1	0	0	2	0	0	0	0	0	0	0	0	0	0	0	4	7	0	0	?	0	?	2	0
suspectum	1	1	1	1	1	1	1	1	0	0	2	0	0	0	0	0	0	0	0	1	0	0	3	4	0	0	?	0	0	2	2
borneensis	?	0	0	0	0	0	0	0	0	0	2	0	0	0	0	0	0	0	0	0	0	0	8	7	0	0	2	0	0	1	0
niloticus	?	0	0	0	0	0	0	0	0	1	1	0	0	0	0	0	0	0	0	0	2	0	4	5	0	0	0	0	1	0	2
exanthematicus	?	0	0	0	0	0	0	1	1	2	0	1	0	0	0	0	0	0	0	0	0	0	5	0	0	2	?	0	0	1	1
torquatus	?	0	0	0	1	1	0	1	0	0	2	0	1	0	0	0	0	0	0	0	0	0	1	5	0	0	?	0	0	3	2

	156	157	158	159	160	161	162	163	164	165	166	167	168	169	170	171	172	173	174	175	176	177	178	179	180	181	182	183	184	185	186
serratus	?	?	?	?	?	?	?	?	?	?	?	?	?	?	?	?	?	?	?	?	?	?	?	?	?	?	?	?	1	1	1
rugosus	?	?	?	?	?	?	?	?	?	?	?	?	?	?	?	?	?	?	?	?	?	?	?	?	?	?	?	1	?	1	1
lancensis	0	1	0	?	0	?	?	?	?	?	0	?	?	?	?	?	?	?	?	?	?	?	?	?	?	0	?	1	1	0	1
newmanorum	0	1	1	1	0	1	1	1	1	1	0	2	1	3	0	0	0	2	0	0	0	0	0	1	0	1	0	0	0	0	1
platyceps	0	1	0	1	0	1	1	0	1	2	2	2	1	3	1	1	0	2	0	0	1	0	0	0	0	0	1	0	0	0	1
agrenon	2	0	0	0	1	1	0	1	2	2	2	2	1	3	1	0	0	1	1	0	0	0	0	0	0	1	2	0	0	0	1
rectocollaris	2	0	1	0	1	1	0	1	2	2	2	3	1	3	0	0	0	2	0	1	0	0	0	0	0	1	2	0	0	0	1
rackhami	1	1	0	1	1	1	2	2	3	3	3	3	1	1	0	0	0	1	2	0	0	1	0	0	0	1	1	1	0	1	1
grandis	0	0	0	0	2	2	2	1	2	2	3	3	2	2	0	0	0	1	2	0	0	0	0	1	0	0	2	0	0	1	1
ornatus	0	?	?	?	1	1	?	?	2	?	?	?	2	?	0	?	?	?	0	?	0	?	0	?	?	1	2	0	0	0	1
annoskius	0	0	0	0	0	0	0	0	0	?	0	0	0	0	0	0	0	0	0	0	0	0	0	1	0	0	?	0	0	0	0
crocodilurus	0	0	0	?	0	0	?	?	0	?	?	0	0	3	0	0	0	0	?	0	0	0	0	?	0	0	2	0	0	0	0
multicarinata	0	0	1	0	0	0	0	0	0	?	0	0	0	3	0	0	0	0	0	0	0	1	0	0	0	1	2	0	0	0	0
centralis	0	0	0	0	0	0	?	?	0	?	?	0	0	0	0	0	0	0	0	0	0	1	0	1	0	1	1	0	0	0	0
enneagrammus	1	0	0	0	0	0	?	?	0	?	?	0	0	0	0	?	0	0	0	?	0	0	0	0	0	0	0	1	0	1	1
suspectum	0	2	0	0	0	0	?	?	0	?	?	0	0	0	0	?	0	0	0	?	0	0	0	0	0	1	2	1	0	1	0
borneensis	1	2	0	1	0	?	?	?	0	?	?	0	0	0	0	0	0	0	0	0	0	0	0	0	0	0	1	1	0	1	0
niloticus	1	1	0	0	1	0	0	0	0	0	0	0	0	1	0	0	0	0	0	0	0	0	0	0	0	0	2	0	1	0	0
exanthematicus	0	0	1	1	0	0	?	0	0	?	0	0	0	0	1	0	2	2	0	0	0	0	0	2	2	0	2	0	1	0	0
torquatus	1	0	0	0	1	?	?	?	1	?	2	0	0	1	0	0	1	2	0	?	0	0	0	0	0	0	2	0	1	0	0

TABLE 1. CONTINUED.

Xenosaurus spp.	187	188	189	190	191	192	193	194	195	196	197	198	199	200	201	202	203	204	205	206	207	208	209	210	211	212	213	214	215	216	217
serratus	0	?	1	?	0	1	0	1	1	1	0	0	?	1	0	0	0	0	?	?	?	?	1	?	0	?	?	?	?	?	?
rugosus	0	?	1	?	1	0	1	0	1	1	0	0	?	1	?	?	1	1	?	?	0	?	0	1	?	?	?	1	?	?	?
laucensis	?	?	1	1	0	?	2	0	1	1	0	?	?	?	?	?	?	?	?	?	?	?	?	?	1	1	1	1	1	0	1
newmanorum	1	0	1	0	0	0	2	0	1	0	0	1	1	?	1	1	0	0	2	0	1	1	1	1	2	1	1	1	1	0	1
platyceps	1	0	1	1	0	0	3	0	0	0	0	1	0	?	1	0	1	0	2	1	1	1	1	0	2	1	1	2	2	0	1
agrenon	0	1	1	0	0	0	2	0	0	0	1	0	1	0	1	0	1	0	2	0	1	1	1	1	2	1	1	1	0	1	0
rectocollaris	0	1	1	1	0	0	2	0	2	0	1	1	0	0	1	0	1	0	2	0	0	1	0	1	2	1	2	2	0	0	0
rackhami	0	0	0	0	0	0	2	0	2	1	0	0	0	0	1	0	1	0	2	0	1	1	1	1	2	1	1	1	1	0	2
grandis	0	0	0	0	0	0	1	0	0	0	0	0	0	0	0	0	0	0	1	0	0	0	0	0	1	0	0	0	0	0	0
ornatus	0	?	0	?	0	?	1	0	2	1	1	0	0	0	0	0	0	0	0	0	1	0	0	0	1	0	0	0	0	0	0
ammoskius	?	?	?	0	0	?	1	2	1	1	0	?	0	0	1	1	0	0	2	?	1	1	0	1	1	1	1	0	0	0	2
crocodilurus	0	1	1	0	0	0	1	2	2	0	0	0	0	0	0	0	0	0	0	0	0	0	0	0	0	0	0	0	0	0	3
multicarinata	0	0	0	0	0	0	3	0	2	0	0	1	0	0	0	1	0	0	0	0	1	0	0	0	1	0	0	0	0	0	6
ventralis	0	0	0	0	0	0	0	0	1	0	0	0	0	0	0	0	0	0	0	0	0	0	0	0	1	0	0	0	0	0	0
enneagrammus	1	0	0	0	0	0	0	1	1	0	1	1	1	0	1	0	0	0	2	1	0	0	0	0	0	0	1	0	0	0	0
suspectum	0	1	0	0	0	0	0	2	2	0	0	0	0	0	0	1	0	0	1	0	1	0	0	0	0	0	0	0	1	0	0
borcensis	0	0	0	0	0	0	0	2	2	0	0	0	0	0	1	1	0	0	0	0	0	0	0	0	0	1	0	0	0	0	5
niloticus	0	0	0	0	0	0	0	2	0	0	0	0	0	0	1	0	0	0	0	0	0	0	0	1	0	0	0	1	1	0	0
exanthematicus	0	1	1	0	0	0	0	2	0	0	0	0	0	1	1	0	0	0	?	?	0	0	1	0	0	0	0	0	0	B	1
torquatus	?	1	0	?	0	0	0	0	0	1	0	?	0	1	0	0	0	0	0	?	0	0	0	1	0	0	0	0	1	0	?

Xenosaurus spp.	218	219	220	221	222	223	224	225	226	227	228	229	230	231	232	233	234	235	236	237	238	239	240	241	242	243	244	245	246	247	248
serratus	?	?	?	?	?	?	?	?	?	?	?	?	?	?	?	?	?	?	?	?	?	?	?	?	?	?	?	?	1	1	?
rugosus	?	?	?	?	?	?	?	?	?	?	?	?	?	?	?	?	?	?	?	?	?	?	?	?	?	?	?	?	1	1	?
laucensis	?	?	?	?	?	0	1	1	1	2	1	1	1	1	1	0	0	1	0	0	1	0	0	0	0	0	0	0	2	1	1
newmanorum	1	1	0	1	1	0	1	1	1	2	1	1	1	1	1	0	0	0	0	0	0	0	0	0	1	0	0	0	1	1	1
platyceps	1	1	0	0	2	1	1	1	2	2	1	0	1	1	0	0	0	1	0	0	0	0	0	0	0	0	0	0	3	1	3
agrenon	1	0	0	1	1	1	0	0	2	2	0	1	0	0	0	0	0	0	0	0	0	0	0	0	0	0	0	1	3	1	3
rectocollaris	0	0	0	1	1	1	0	0	2	2	1	1	1	1	0	2	1	0	1	0	0	0	2	0	0	0	0	0	3	1	2
rackhami	0	0	0	1	1	1	0	?	1	1	0	0	1	0	0	0	1	1	0	0	0	0	0	0	0	0	0	0	1	1	1
grandis	1	0	0	0	1	?	0	0	0	1	1	0	1	1	0	0	0	1	0	0	0	0	0	0	0	0	0	0	1	1	3
ornatus	1	0	?	0	1	0	0	0	0	1	0	0	0	0	0	0	0	0	0	0	0	2	0	0	0	0	0	0	0	0	2
ammoskius	0	0	0	0	0	0	0	0	0	0	0	0	0	0	0	0	0	0	0	0	0	0	0	0	0	0	0	0	3	0	3
crocodilurus	0	0	0	0	0	0	1	0	2	2	0	0	0	1	0	0	1	0	0	0	0	0	0	0	1	0	0	0	3	0	3
multicarinata	0	0	0	1	1	1	1	0	2	2	0	0	0	0	0	0	0	0	0	0	0	0	0	0	0	0	0	0	3	0	2
ventralis	0	0	0	0	0	0	0	?	2	2	0	1	0	0	0	0	1	0	0	0	0	0	0	0	0	0	0	0	1	0	1
enneagrammus	1	1	0	0	0	0	0	0	0	2	0	0	1	1	0	1	1	0	0	0	0	0	0	0	0	0	0	0	1	0	3
suspectum	1	0	0	0	1	0	0	0	2	2	0	0	0	0	0	0	0	0	0	0	0	0	0	0	0	0	0	0	0	0	1
borcensis	1	0	0	0	2	0	0	0	2	2	0	1	0	0	0	0	0	1	0	0	0	0	0	1	1	0	0	0	0	0	3
niloticus	1	0	0	1	0	1	0	0	2	1	1	1	0	0	0	1	1	0	0	1	1	0	1	0	0	0	0	0	0	0	1
exanthematicus	1	0	0	0	1	0	1	0	2	1	0	0	1	0	0	0	1	0	0	0	0	0	0	0	1	0	1	1	0	0	?
torquatus	0	0	0	0	1	0	0	0	1	1	0	0	1	0	0	0	0	1	0	0	0	2	0	0	0	0	1	0	1	?	?

TABLE 1. CONTINUED.

Varanus spp.	249	250	251	252	253	254	255	256	257	258	259	260	261	262	263	264	265	266	267	268	269	270	271	272	273	274
varidus	?	?	?	?	?	?	?	?	?	?	?	?	?	?	?	?	?	?	?	?	?	?	?	?	?	?
rugosus	?	?	?	?	?	?	?	?	?	?	?	?	?	?	?	?	?	?	?	?	?	?	?	?	?	?
laurensis	?	?	?	?	?	?	?	?	?	?	?	?	?	?	?	?	?	?	?	?	?	?	?	?	?	?
ueermanorum	0	0	1	0	0	0	1	0	0	3	0	0	1	0	0	2	1	1	1	0	0	1	0	1	0	0
platyceps	0	0	1	0	0	1	1	0	0	4	0	1	1	1	1	2	0	2	0	1	0	1	0	1	0	0
agrenon	3	?	0	?	?	?	0	?	?	?	?	?	?	?	?	?	?	?	2	2	1	2	0	2	2	0
rectocollaris	3	?	0	?	?	0	0	?	?	2	?	2	?	?	?	1	2	1	2	2	1	2	1	2	0	0
rackhami	6	?	0	3	2	?	0	3	?	2	?	3	?	?	?	3	3	?	2	2	1	2	0	2	2	0
grandis	3	?	?	2	2	?	?	2	?	2	?	3	?	?	?	3	3	?	2	2	1	2	0	2	2	0
ornatus	?	?	?	?	?	?	?	?	?	?	?	?	?	?	?	?	?	?	?	?	?	?	?	?	?	?
ammoskius	2	?	?	?	?	?	?	?	?	?	?	?	?	?	?	?	?	?	?	?	?	?	?	?	?	?
crocodilurus	4	0	0	0	2	0	0	2	0	—	?	2	0	?	1	—	2	0	2	1	1	2	0	0	0	0
multicarinata	3	0	0	0	0	0	0	0	0	3	—	0	0	?	0	0	0	—	0	0	0	0	0	2	0	—
ventralis	3	0	0	0	0	0	0	0	0	3	—	0	0	?	0	0	?	?	?	0	0	0	0	2	0	—
cuneagrammus	5	0	0	0	0	0	0	0	?	3	0	0	0	?	0	0	0	—	0	0	0	0	0	0	0	—
suspectum	6	0	1	0	0	—	—	0	0	—	—	0	0	?	0	0	0	—	0	0	0	0	0	0	0	—
bornensis	?	?	0	4	0	—	0	—	0	2	?	0	0	?	0	—	0	—	0	0	1	3	0	0	0	?
niloticus	?	?	?	4	?	?	?	?	?	?	?	?	?	?	?	?	?	?	?	?	?	?	?	?	?	?
exanthematicus	?	?	?	?	?	?	?	?	?	?	?	?	?	?	?	?	?	?	2	2	0	0	0	0	0	?
torquatus	?	?	?	?	?	?	?	4	?	0	?	3	?	?	?	4	3	?	2	2	0	0	0	0	0	0

variation, is an important but often overlooked aspect of character discovery for phylogenetic analysis (Barahona and Barbadillo, 1998; Wible, 2003; Bever, 2005, 2006, 2008). Large sample sizes representing a good sample of the populations of the species were not possible to obtain for all taxa here examined, but such samples were available for enough taxa to phylogenetically bracket several clades. Specifically, samples of 10 or more specimens, spanning most of postnatal ontogeny, were available for *V. exanthematicus*, *E. multicarinata*, *H. suspectum*, *X. platyceps*, and *X. grandis*. I also had a large sample of *X. rackhami* (see Supplementary Information), although very young individuals were lacking. When statements are made in the character descriptions regarding ontogenetic variation, they refer to the taxa listed above as being present as large samples or clades bracketed by them.

Observed variation is noted in the character descriptions. For most taxa scored, multiple specimens were available for examination (see specimen list in Supplementary Information). As might be expected, in general, sample sizes were low for the extinct taxa—one in the cases of *R. rugosus* (save for a small fragment of maxilla, UMMP 73565) and *B. ammoskius*. The weakest part of the extant ingroup in terms of variation assessment was the *X. agrenon* + *X. rectocollaris* clade. For each of these taxa, I had only a single skeletal specimen (but multiple wet specimens). However, I discovered multiple unique synapomorphies for the clade, and their position in my results is consistent, as mentioned above, with that recovered by other researchers using different sources of data from gross anatomy. In general, I was conservative in defining characters; most of the characters described in this work vary little within species for which multiple individuals were available. Any variation that was present is noted.

Another aspect of variation is the assessment of the relative ontogenetic age of the specimens examined, which affects the scoring of some characters. Within Squamata and more specifically Anguimorpha,
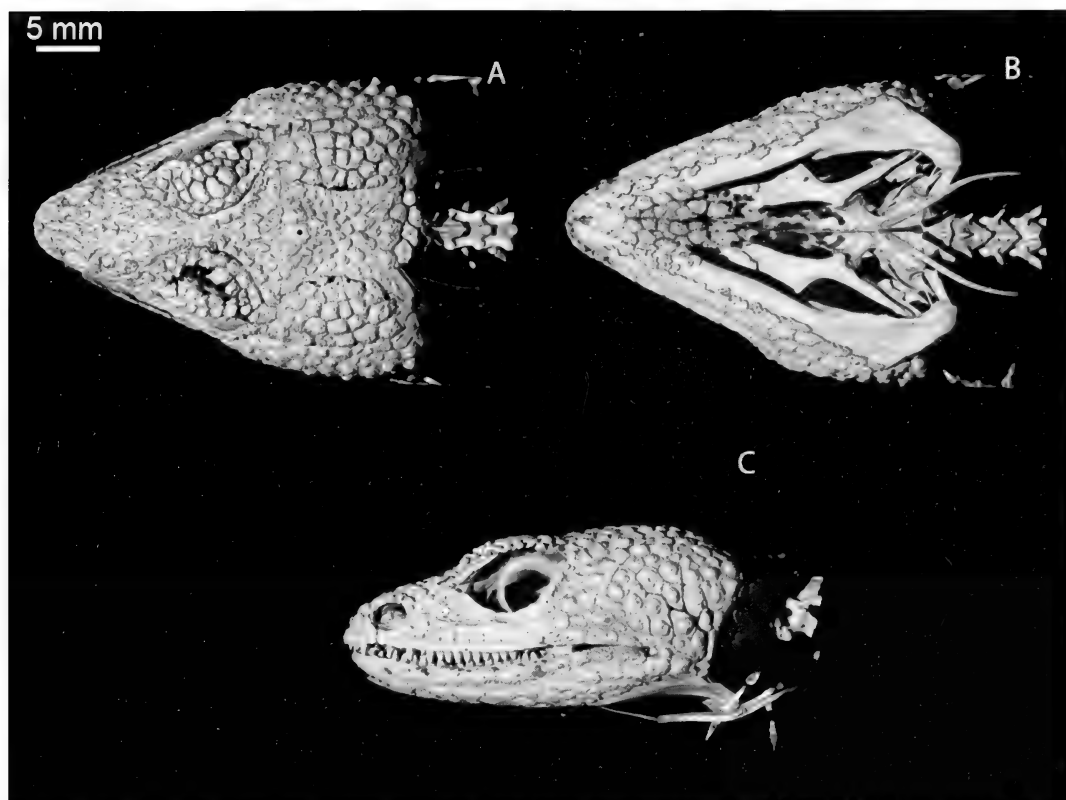
Figure 1.   Cranium of *Xenosaurus newmanorum*, CT scan of UMMZ 126056. A, Dorsal, anterior to the left. B, Ventral, anterior to the left. C, Left lateral, anterior to the left. Illustrates characters 114(1), 151(0), 184(0), 247(1), 248(1), 249(0), 251(0), 252(0), 255(1), 256(0), 257(0), 258(3), 259(0), 260(0), 261(1), 262(0), 263(0), 264(2).

several general ontogenetic trends can be bracketed as ancestral for the clade (Bever et al., 2005; Bhullar, 2006; Bhullar and Smith, 2008, for Anguimorpha). Ontogenetic age can thus be inferred for fossils and extant specimens without age data. *Merkurosaurus ornatus* specimens range from "subadults" with unfused frontals and proportionally shorter supratemporal processes of the parietal to large, mature adults with fused frontals, heavy osteodermal sculpturing, and long supratemporal processes (Klembara, 2008). The single known specimen of *B. ammoskius* appears to be a relatively mature adult based on the prominent osteodermal sculpturing on the skull roof and the proportionally great length of the supratemporal processes. The Yale *R.*

rugosus likewise has fully fused frontals and strong osteodermal sculpturing upon both the frontal and the maxillae, suggesting that it is a large, mature individual. Most specimens of *E. lancensis* have parietals that are heavily sculptured and rectangular in overall outline and are large compared with those of other xenosaurs, suggesting fairly advanced ontogenetic stages, but the frontals are unfused save in a few individuals, indicating immaturity (taking into account the cautionary notes regarding this taxon made earlier). Finally, the known specimens of *E. serratus* are approximately the same size as adults of other xenosaurs and bear heavy osteodermal sculpturing and generally "mature adult" proportions of the cranial elements.
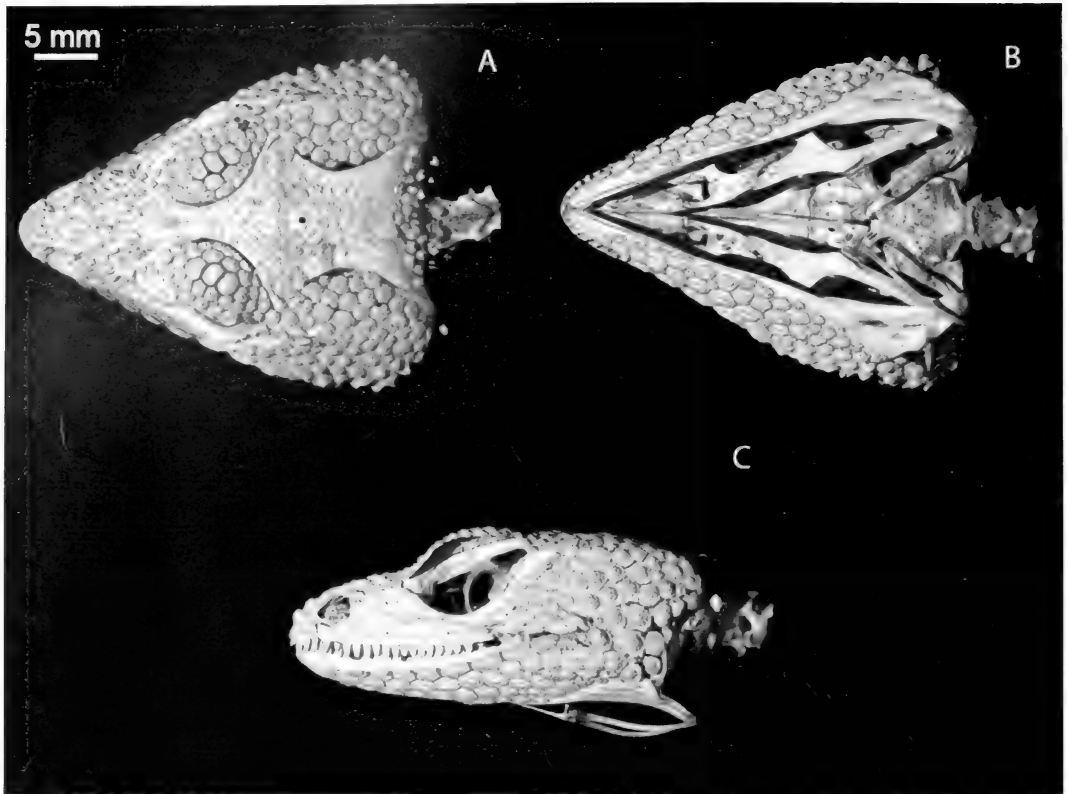
Figure 2.   Cranium of *Xenosaurus platyceps*, CT scan of UTA 23594, courtesy of Deep Scaly Project (2007; images from original data processing). A, Dorsal, anterior to the left. B, Ventral, anterior to the left. C, Left lateral, anterior to the left. Illustrates characters 26(1), 248(0), 250(0), 253(0), 254(1), 258(4), 260(1), 262(1), 263(1).

Analyses

Instead of a single preferred starting hypothesis, I use two, generating results referred to as Analysis 1 and Analysis 2 in the descriptions and discussions that follow. Starting conditions for Analysis 1 were inspired by phylogenies of Anguimorpha on the basis of nucleic acid structure, notably that of Townsend et al. (2004), which remains the most thorough and thoughtful analysis of these data. To generate Analysis 1, I used a constraint tree fixing extant taxa in the topology discussed previously for molecular studies (with an Anguidae + Helodermatidae clade instead of a Helodermatidae + *Xenosaurus* clade or a trichotomy) and leaving relationships among

xenosaurs, as well as among *Shinisaurus* and its extinct relatives, free to vary. To generate Analysis 2, I initially intended to constrain relationships based on a preferred gross anatomy–based phylogenetic hypothesis for Anguimorpha, but I found that my characters alone, with *P. torquatus* specified as the outgroup, generated a hypothesis identical to that of Conrad (2005, 2008), with one major difference: *Shinisaurus* and its extinct relatives are not sister to Varanoidea but are united with xenosaurs in the traditional Xenosauridae. This result obtained with overwhelming support even after the experimental addition of the characters uniting shinisaurs with varanoids in Conrad's analyses (2005, 2008; results not shown).
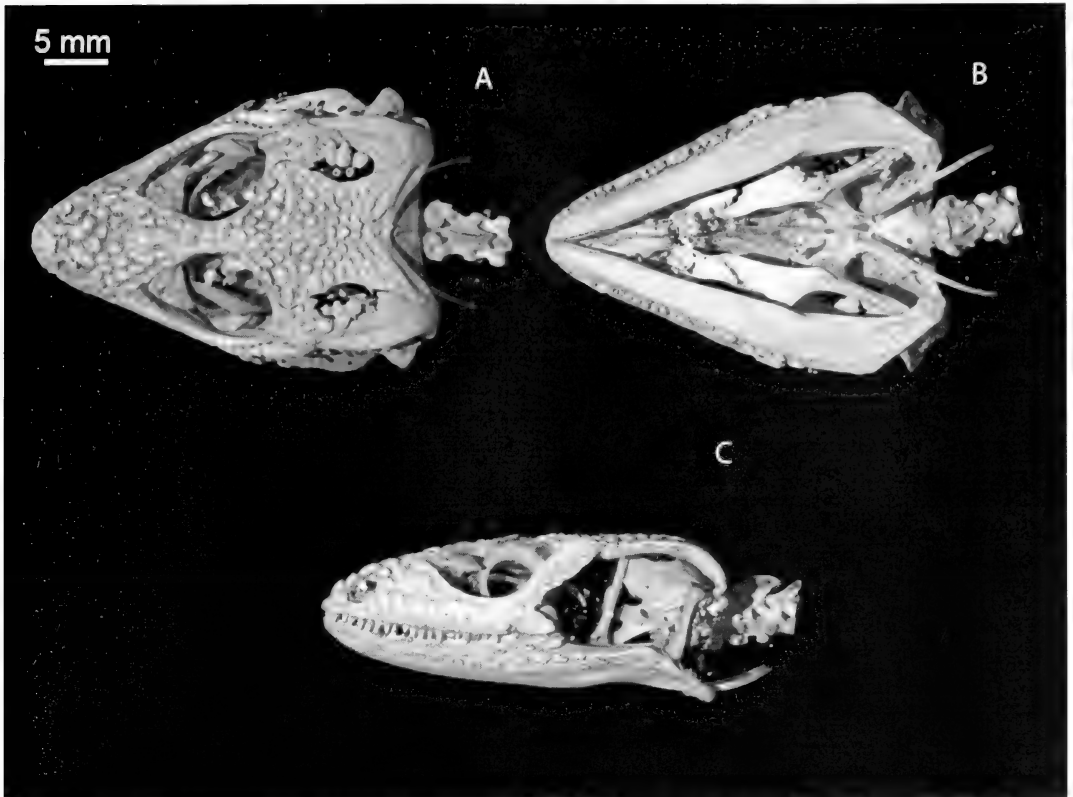
Figure 3.   Cranium of *Xenosaurus rackhami*, CT scan of UTEP 4555. A, Dorsal, anterior to the left. B, Ventral, anterior to the left. C, Left lateral, anterior to the left. Illustrates characters 28(0), 123(0), 133(1), 135(2), 249(6), 252(3), 256(3), 264(3).

Both analyses proceeded using the parsimony heuristic search option in PAUP* v. 4.0b10, with default options save that tree bisection and reconnection (TBR) branch swapping was enabled with 1,000 random addition sequences (Swofford, 2001). Bootstrap analyses were run with default settings save the parsimony settings noted above and the specification of 200 replicates. Each set of conditions yielded a single most parsimonious tree under all three character state optimization options, mercifully obviating calculations of consensus.

Ingroup relationships were identical in the results of Analysis 1 and Analysis 2. Because Analysis 2 was essentially unconstrained save for the specification of an uncontroversial outgroup, I was able to use a nonparametric Wilcoxon signed ranks test (Templeton test), automated through PAUP*, to assess whether the overall tree topologies (including the outgroups) were significantly different in terms of character support and evolution (Templeton, 1983; Larson, 1994).

Inapplicable and unknown data were both scored as ? under the default settings in PAUP* v. 4.0b10. Failing to distinguish between the two can be problematic because character states from applicable taxa can "bleed" to inapplicable taxa during optimization, but the alternative strategy of "absence coding" is also problematic (Strong and Lipscomb, 1999). Specifically, in such a case, inapplicability can be optimized as a synapomorphy when multiple taxa are scored as inapplicable for a single character. In several cases within this
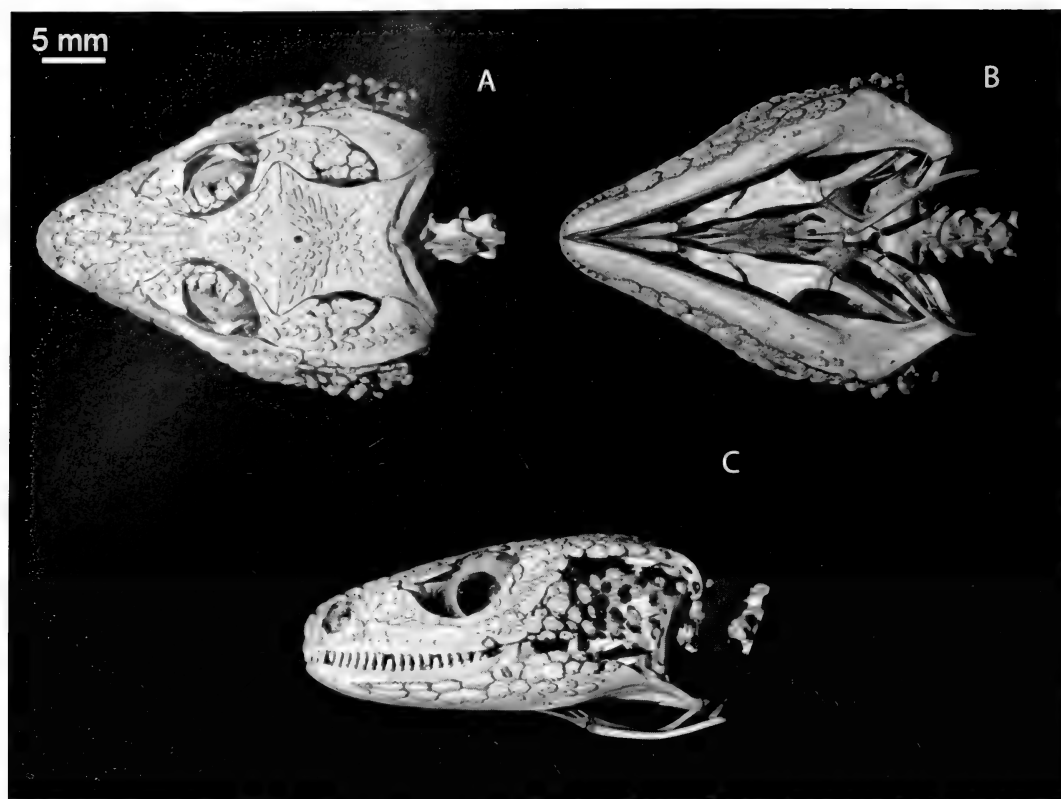
Figure 4.   Cranium of *Xenosaurus grandis*, CT scan of FMNH 123704, courtesy of Deep Scaly Project (2007; images from original data processing). A, Dorsal, anterior to the left. B, Ventral, anterior to the left. C, Left lateral, anterior to the left. Illustrates characters 135(1), 248(3), 250(1), 251(1), 252(2), 253(2), 256(2), 260(3).

analysis, this presence/absence scoring would be redundant with another character.

Multistate characters are discretizations of quantitative continua (counts or measurements) and were run as ordered, although the unordered setting was used to test the robusticity of the results. Mesquite v. 2.01 (Maddison and Maddison, 2008) was used to construct the character matrix and to trace character evolution. The process of discretizing continua necessarily leads to artificial bins, and the cutoffs for each character state are different to capture different levels of quantitative distinction among taxa. However, when more than two character states exist, the intervals are even. Even intervals prevent "cooking" of the data by selectively expanding some bins to

encompass extra taxa. I first described most of the characters expressed as numerical values in less precise or more "qualitative" terms (all valid "qualitative" characters can be expressed in quantitative terms; see Wiens, 2001). The numerical values serve to give additional precision to these differences; essentially, after describing the differences in the states of a character in comparative or "qualitative" terms, I searched for a numerical expression of these differences. This process explains why the cutoffs for different values are not always "standard" intervals of 5 or 10, for instance (though, as noted, they are always regular intervals). The logical next step would be to attempt quantification of all characters and to score them using more advanced numer-
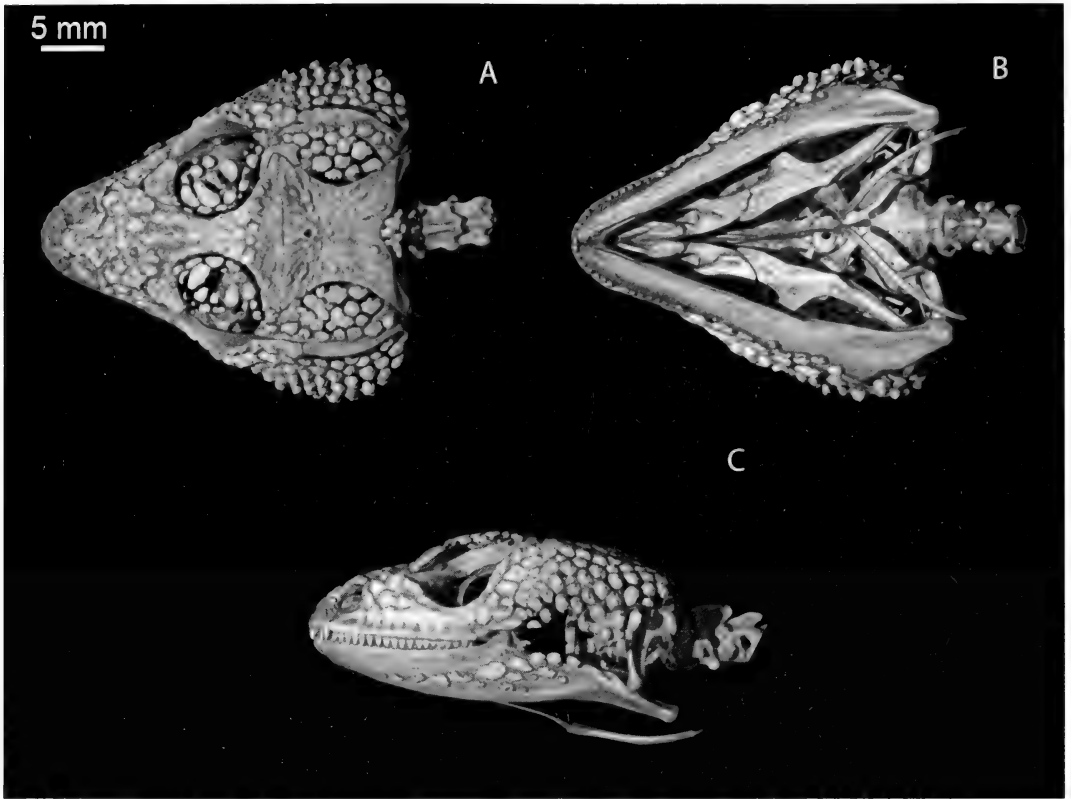
Figure 5. Cranium of *Xenosaurus rectocollaris*, CT scan of UF 51443. A, Dorsal, anterior to the left. B, Ventral, anterior to the left. C, Left lateral, anterior to the left. Illustrates characters 87(1), 123(1), 135(0), 165(2), 248(2), 249(3), 252(1), 253(1), 254(0), 255(0), 256(1), 257(1), 258(2), 259(1), 260(2), 264(4).

ical methods such as gap-weighting (Wiens, 2001). For the purposes of the present study, however, this analysis takes a middle ground.

Institutional Abbreviations

AMNH, American Museum of Natural History, New York; CAS, California Academy of Sciences, San Francisco; NAUQSP-JIM, Northern Arizona University Quaternary Sciences Program, Jim I. Mead collection (now housed at East Tennessee State University, Johnson City); FMNH, Field Museum of Natural History, Chicago; MCZ, Harvard Museum of Comparative Zoology, Cambridge; MVZ, Museum of Vertebrate Zoology, The University of California at Berkeley; TMM, Vertebrate Paleontology Laboratory, Texas Natural Science Center, The University of Texas at Austin; UF, Florida Museum of Natural History, Gainsville; TNHC, Texas Natural History Collections, The University of Texas at Austin; UMMZ, University of Michigan Museum of Zoology, Ann Arbor; USNM, National Museum of Natural History, Washington, DC; UTA, The University of Texas at Arlington Herpetological Collections, Arlington; UTEP, The University of Texas at El Paso Natural History Collections, El Paso; YPM, Yale Peabody Museum of Natural History, New Haven, Connecticut.

CHARACTER DESCRIPTIONS

Extended descriptions of characters and their distribution are contained in the electronic supplementary material. All char-
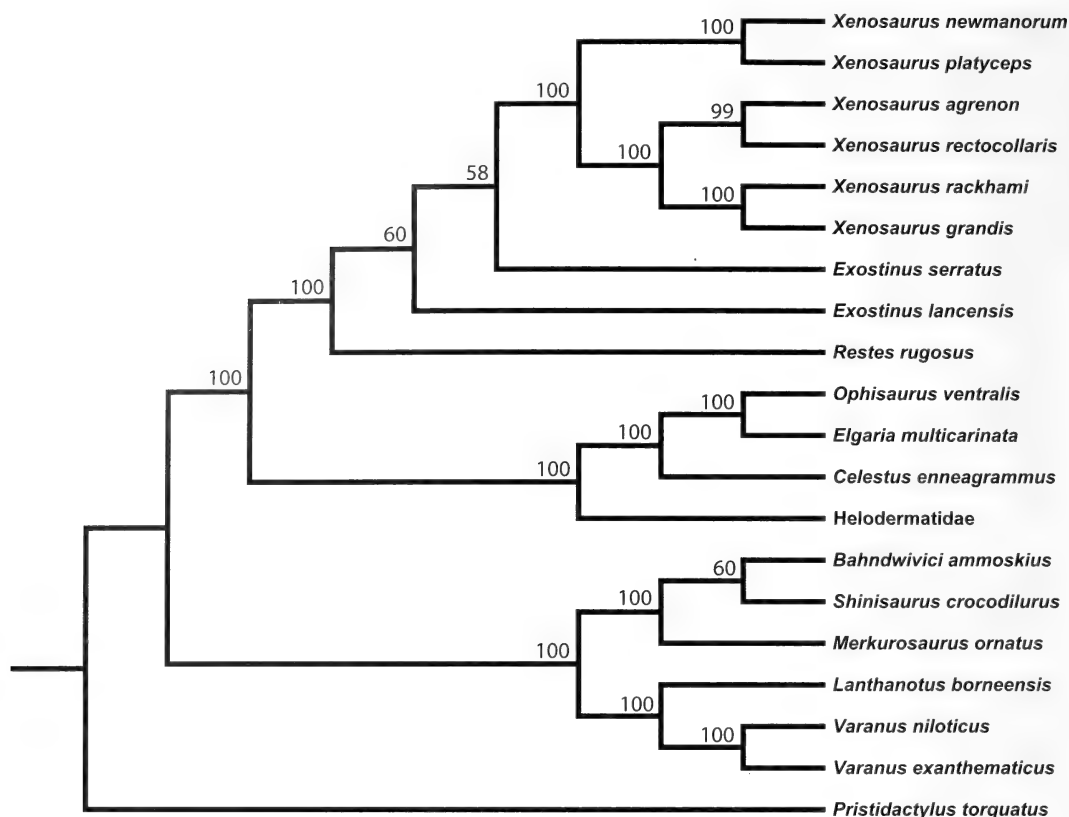
Figure 6.   Analysis 1 tree with bootstrap values greater than 50%.

acters refer to the condition in relatively large "adult" individuals, except where noted. Measurements are given to define some character states; most states, however, are illustrated, and the figures should be used as primary guides in scoring specimens. Intraspecific variation was accounted for by measurements of additional individuals and by simple visual comparison when possible. Where angles to a plane or an edge are given, the acute component is provided.

Comments on variation follow the character descriptions when variation that would affect scoring was evident. Given the low sample sizes of some of the taxa included in this study, the comments are certainly incomplete. An intensive study of variation in the characters used in this study is warranted but beyond the scope of the current work.

Description of the evolution of characters references both terminal taxa and clades that are supported by both resultant phylogenetic hypotheses (Figs. 6, 7), i.e., Anguimorpha, Anguidae, Varanidae, *S. crocodilurus* + *B. ammoskius* + *M. ornatus*, and all subclades within the clade *Xenosaurus* + *E. serratus*. *Varanus exanthematicus* + *Varanus niloticus* is referred to as *Varanus* where scorings do not differ in *Varanus salvator*, a taxon on the other branch from the basal split of *Varanus* (Fuller et al., 1998; Ast, 2001). *Bahndwivici ammoskius* was scored based on the description by Conrad (2006), and *M. ornatus* from that by Klembara (2008).

When character states are identified as synapomorphies of various clades, these statements are to be understood given the limitations of the taxon sampling for this study;
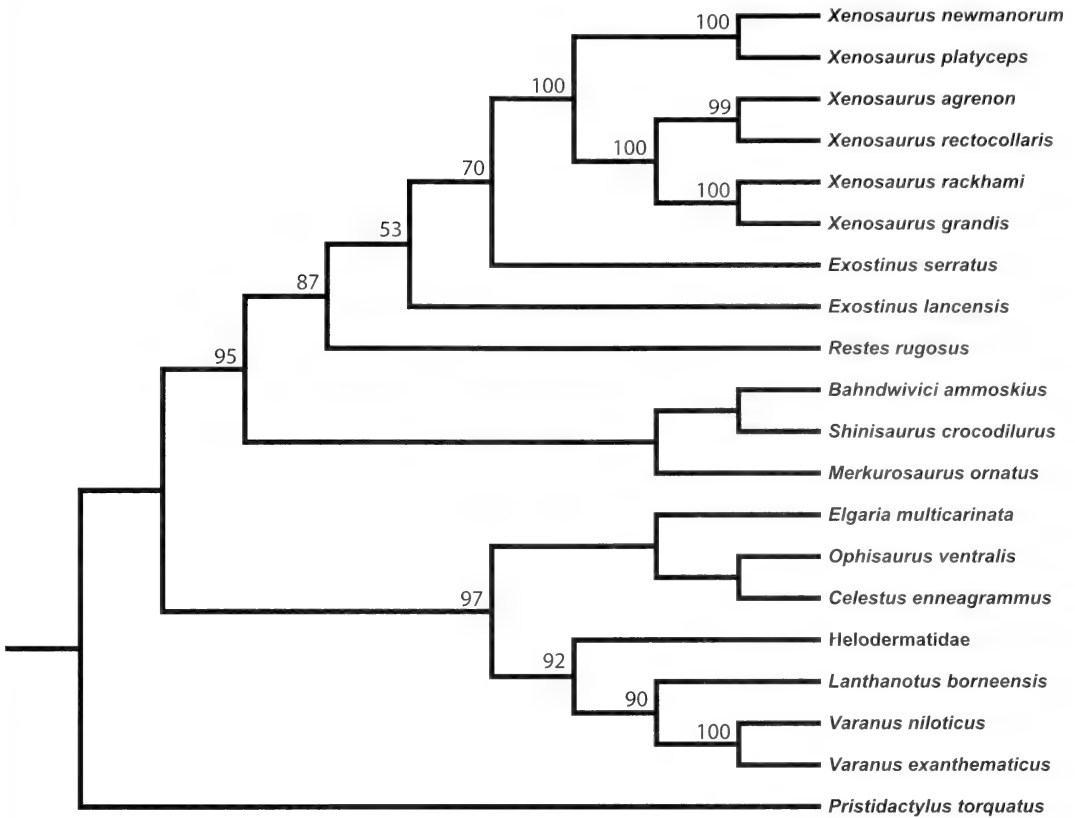
Figure 7.   Analysis 2 tree with bootstrap values greater than 50%.

thus, most stated synapomorphies of clades outside of *Xenosaurus* and its stem are likely to represent synapomorphies of more inclusive clades or may not be valid with the inclusion of the vast array of additional extant and extinct taxa within Anguimorpha (Conrad et al., 2011). Most characters are new; if a version of the character appeared in a previous analysis, the original analysis is cited parenthetically after the short description. The only characters that appeared in some form in previous analyses are 62, 91, 117, 124, 134, 145, 149, 189, 218, 224, 231, 246, and 272. Of those, only 91, 149, and 189 are essentially unmodified. The full taxon–character matrix is depicted in Table 1.

Dentition, General

1. Dentition: Tooth form (0) entirely uni-
cuspid with pointed apices (Fig. 8A); (1)

chisel-shaped (see Gao and Fox, 1996); (2) chisel-shaped, some bicuspidity (Fig. 8B).

Variation. Considerable ontogenetic variation occurs in tooth form. Bicuspidity develops during postnatal ontogeny in *Xenosaurus* and in Anguidae. However, whereas early (postnatal)-stage anguid teeth are nearly conical, in early-stage *Xenosaurus,* the chisel shape already obtains. The teeth of iguanians in general do not undergo a unicuspid-to-multicuspid transition during postnatal ontogeny, although the extremity of development of the cusps may increase with ontogenetic age. Moreover, in no observed taxon do the teeth progress during ontogeny from multicuspid to unicuspid. Thus, the fossils with bicuspid teeth *R. rugosus*
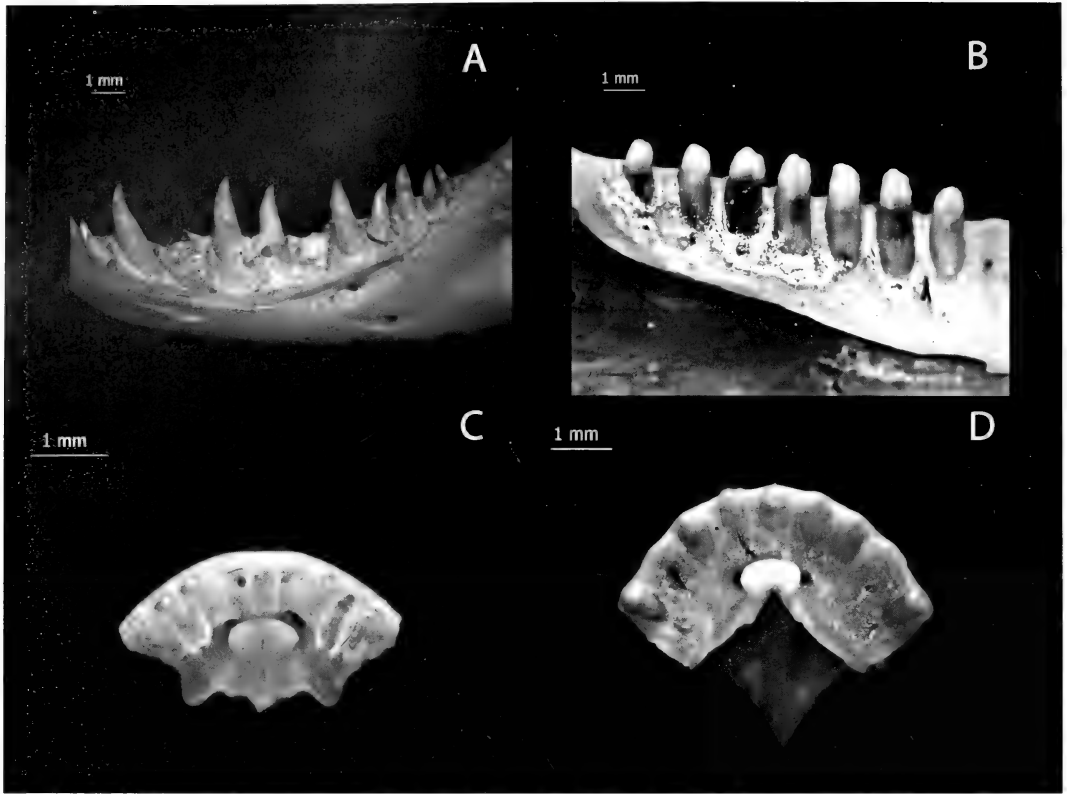
Figure 8.   A, Right dentary of *Shinisaurus crocodilurus* MVZ 204291, medial, anterior to the left. Illustrates character 1(0). B, Left dentary of *Xenosaurus newmanorum* uncatalogued NAUQSP-JIM specimen, medial, anterior to the right. Illustrates character 1(2). C, Premaxilla of *Elgaria multicarinata* TMM-M 8993, ventral, anterior to the top. Illustrates characters 2(0), 14(0). D, Premaxilla of *Xenosaurus newmanorum* uncatalogued NAUQSP-JIM specimen, ventral, anterior to the top. Illustrates characters 2(1), 14(1).

and *E. serratus* are scored as such and the inferred late ontogenetic stages of the fossil shinisaurs are beyond those at which the transition from unicuspid to multicuspid occurs in any observed extant specimen. Little variation occurs across broad ontogenetic stages in the general form of the teeth.

Evolution. Under both phylogenetic analyses, state (0), unicuspid teeth, is plesiomorphic within Anguimorpha as suggested by Gauthier (1982). Furthermore, under most hypotheses for the placement of Anguimorpha that have been suggested, having unicuspid teeth is a synapomorphy along the angui-

morph stem. If *C. intermedia* is on the anguimorph stem as suggested by Conrad (2005) and if the blunt, multicuspid state of the teeth of that taxon (Gao and Norell, 1998) is homologous to that of most other Scleroglossa, then this synapomorphy can be constrained to the internode between *C. intermedia* and Anguimorpha. However, various Mesozoic squamates with unicuspid teeth are placed by some phylogenetic analyses as a sister clade to all other Scleroglossa (Evans et al., 2005; but see Conrad, 2008), potentially complicating the optimization of unicuspidity. The chisel shape of the tooth crowns is a synapomorphy of

Xenosaurus and its fossil relatives. The presence of chisel-shaped teeth without bicuspidity in *E. lancensis* is either a primitive character of that taxon with bicuspidity a synapomorphy of *Xenosaurus* and an autapomorphy of *R. rugosus*, or the chisel-shaped state lacking bicuspidity is an autapomorphy of *E. lancensis* with the bicuspid chisel-shaped morphology as a synapomorphy of *Xenosaurus* + *Retes rugosus*.

Premaxilla

The premaxilla is unknown for *R. rugosus* and *E. lancensis*.

2. Premaxilla: Curvature of rostral arc in horizontal plane (0) relatively broad (Fig. 8C); (1) relatively acute (Fig. 8D).

    Variation. The premaxillae of most taxa become slightly less acute during ontogeny, but even early neonates of non-xenosaurs do not show the acute morphologies of adult *Xenosaurus*.

    Evolution. Acute curvature is a synapomorphy of *Xenosaurus* under both analyses.

3. Premaxilla: Height of dentigerous arc at suture of dermal surface to lateral (dermal) surface of maxilla: (0) dorsoventrally short, about one-fifth or less of mediolateral width between contralateral sutures (Fig. 9A); (1) tall, about one quarter or more of mediolateral width between contralateral sutures (Fig. 9B).

    Evolution. Under Analysis 1, two alternative hypotheses of character evolution each require three steps. In the first hypothesis of character evolution, the proportional tallness of the dentigerous arc is a synapomorphy of Anguimorpha. The shortness of the dentigerous arc is then a synapomorphy of Anguidae + Helodermatidae and of *Varanus*. In the second hypothesis of character evolution, relative tallness is independently a synapomorphy of *Xe-*

nosaurus + *E. serratus*, *S. crocodilurus* + *M. ornatus*, and *L. borneensis*. Under Analysis 2, relative tallness is a synapomorphy of Xenosauridae, independently of *L. borneensis*.

4. Premaxilla: Angle to the horizontal in transverse plane of lateral edges of rostral body connecting portion (0) low, 40° or lower (Fig. 9A); (1) high, greater than 40° (Fig. 9C).

    Evolution. Taking into account the relatively vertical condition in *P. torquatus* and the wide distribution of that condition in other non-anguimorph Squamata and sphenodontians (Evans, 1980; Fraser, 1982; Whiteside, 1986), a low angle to the horizontal of the lateral edges is a synapomorphy of Anguimorpha under both analyses. According to Analysis 1, a high angle to the horizontal within Aguimorpha is independently a synapomorphy of *E. serratus* + *Xenosaurus* and of *S. crocodilurus* + *M. ornatus*. According to Analysis 2, a high angle to the horizontal is a synapomorphy of Xenosauridae.

5. Premaxilla: Dorsolateral angle of dentigerous arc (0) formed by meeting of relatively straight edges, not produced into wedge (Fig. 9A); (1) produced into small wedge (Fig. 9B).

    Variation. The degree of development of the produced wedges varies within broad ontogenetic stages of *X. rackhami* and *X. grandis* but is always greater than that of the taxa scored as (0).

    Evolution. Under both analyses, production into wedges is a synapomorphy of *X. grandis* + *X. rackhami* and of *S. crocodilurus* + *M. ornatus*.

6. Premaxilla: Major premaxillary ethmoid canals (0) partially or completely bounded by connective tissue only, not fully surrounded by ossified premaxilla (Fig. 9D, left side); (1) bony, surrounded by ossified premaxilla (Fig. 9D, right side).
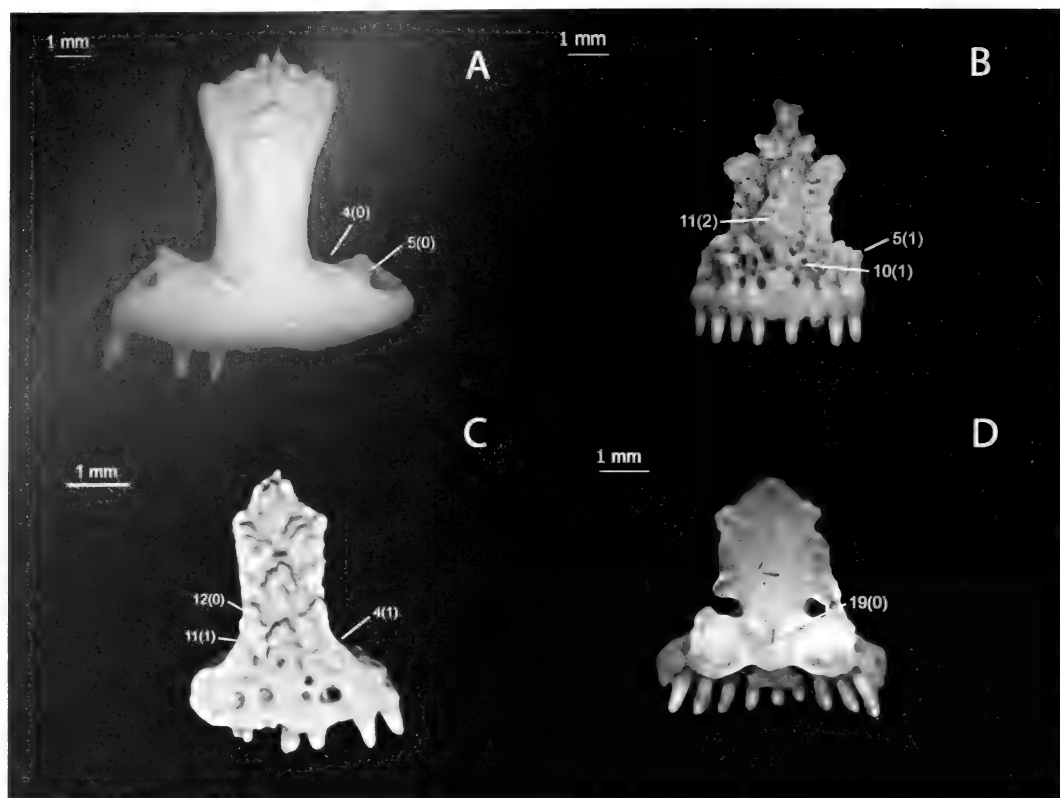
Figure 9.   A, Premaxilla of *Heloderma suspectum* TMM-M 9001, anterior. Illustrates characters 3(0), 4(0), 5(0), 7(0), 8(0), 9(0), 21(0). B, Premaxilla of *Xenosaurus grandis* NAUQSP-JIM 1460, anterior. Illustrates characters 3(1), 5(1), 7(2), 9(2), 10(1), 11(2), 12(1). C, Premaxilla of *Exostinus serratus*, CT scan of USNM v16565, anterior. Illustrates characters 4(1), 8(3), 9(1), 11(1), 12(0), 13(0). D, Premaxilla of *Elgaria multicarinata* TMM-M 8993, posterior. Illustrates characters 6(0), 6(1), 19(0).

Variation. The enclosure does not transform during postnatal ontogeny, but its does vary to some extent within taxa. Specifically, in one *S. crocodilurus* specimen examined, UF 71623, the enclosure is incomplete on one side. Enclosure is also present on one side in a single very large individual of *E. multicarinata*, TMM-M 8993 (Fig. 9D). In general, extremely large individuals, at least within anguimorphs, tend to develop extra flanges of bone that sometimes close previously open grooves for nerves and vasculature (personal observation).

Evolution. Under Analysis 1, enclosure of the medial ethmoidal canals is a synapomorphy of *Xenosaurus + E. serra-*

tus and of *S. crocodilurus* + Varanidae. Under Analysis 2, enclosure is a synapomorphy of Xenosauridae and an autapomorphy of *L. borneensis*. The hypothesis that Varanidae and its stem ancestrally showed enclosure of the canals is complicated by the existence of taxa along the stems of the two varanoid lineages (and perhaps Varanoidea as a whole) from the Cretaceous of Mongolia and the early Paleogene of Europe, including *Estesia mongoliensis*, *Aiolosaurus oriens*, *G. pulchra*, and *Necrosaurus* sp., that do not appear to show the morphology (Estes, 1983; Borsuk-Bialynicka, 1984; Norell et al., 1992; Norell and Gao, 1997; Gao and Norell, 1998,
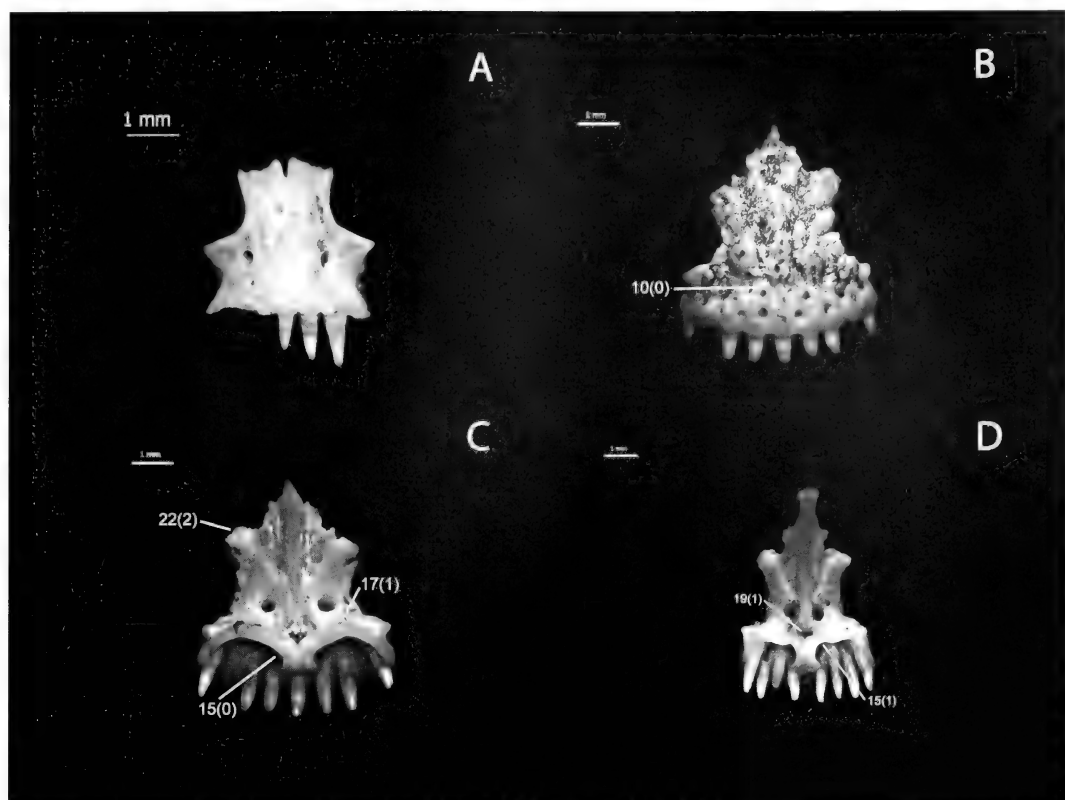
Figure 10. A, Premaxilla of *Shinisaurus crocodilurus* UF 72805, anterior. Illustrates characters 7(1), 9(0), 11(0). B, Premaxilla of *Xenosaurus newmanorum* uncatalogued NAUQSP-JIM specimen, anterior. Illustrates characters 8(4), 10(0), 13(1). C, Premaxilla of *Xenosaurus newmanorum* uncatalogued NAUQSP-JIM specimen, posterior. Illustrates characters 15(0), 16(1), 17(1), 18(1), 22(2), 23(1). D, Premaxilla of *Xenosaurus grandis* NAUQSP-JIM 1460, posterior. Illustrates characters 15(1), 16(0), 18(0), 19(1).

2000). However, the issue is resolved if Varanoidea is not monophyletic, as in Analysis 1, and most or all of these taxa lie along the helodermatid stem, as was suggested for *E. mongoliensis* and *G. pulchra* (Norell and Gao, 1997; Gao and Norell, 1998; Conrad, 2004, 2005, 2008).

7. Premaxilla: Number of anterior foramina collinear with main row of maxillary labial foramina (0) none (Fig. 9A); (1) two (Fig. 10A); (2) more than two (Fig. 9B).

Variation. Other than the variation in the degree of enclosure noted for Character 6, the number of lower foramina does not vary in observed specimens of those taxa scored as possessing two (but see variation in upper foramina noted under Character 8). Slight variation occurs in the number of foramina within the species of *Xenosaurus*—from three to five, for example, in *X. rackhami*. No variation that would affect scoring was evident.

Evolution. Under both analyses, the possession of several lower anterior foramina is a synapomorphy of *E. serratus* + *X. grandis*. Under Analysis 1, the ancestral state for the entire group, for *Xenosaurus* + Anguidae, and for *S. crocodilurus* + Varanidae is ambiguous between no foramina and two foramina. The ancestral state for Anguidae + Helodermatidae is no foramina. Under

Analysis 2, a lack of foramina is ancestral for the entire group and for Anguimorpha and two foramina is a synapomorphy of Varanidae; the ancestral state for Xenosauridae is ambiguous between no foramina and two foramina.

8. Premaxilla: Number of anterior foramina dorsal to main row of maxillary labial foramina (0) none (Fig. 9A); (1) one; (2) two; (3) three (Fig. 9C); (4) four or more (Fig. 10B).

    Evolution. Under both analyses, the presence of one to three dorsal foramina is a synapomorphy of *E. serratus* + *Xenosaurus* and an increased number of such foramina is a further synapomorphy of *Xenosaurus*. Absence of foramina is an autapomorphy of *X. rectocollaris.*

9. Premaxilla: Anterior surface of premaxilla just dorsal to teeth (0) flush with remainder of anterior surface (Fig. 9A); (1) raised into supradental thickening (Fig. 9C); (2) supradental thickening pronounced (Fig. 9B).

    Variation. Little noticeable variation was evident, save that very young individuals of *Xenosaurus* have a slightly less pronounced thickening.

    Evolution. Under both analyses, the presence of the premaxillary supradental thickening is a synapomorphy of *Xenosaurus* + *E. serratus.* The presence of a more pronounced thickening is a synapomorphy of *Xenosaurus.*

10. Premaxilla: Surface ventral to rostral osteoderm (0) rugose (Fig. 10B); (1) bearing discrete fused osteoderms (Fig. 9B).

    Variation. Osteoderms fuse to the premaxilla during postnatal ontogeny, but are present in mid-sized and large specimens within the species that possess them.

    Evolution. Under both analyses, rugosity of the surface ventral to the

rostral osteoderm is a possible synapomorphy of *E. serratus* + *Xenosaurus*; fusion of osteoderms in this region is a synapomorphy of the southern clade of *Xenosaurus.*

11. Premaxilla: Rostral osteoderm (0) absent (Fig. 10A); (1) oval and mediolaterally narrow (Fig. 9C); (2) rounded and mediolaterally wide (Fig. 9B).

    Variation. Other than the ontogenetic fusion of osteoderms to the premaxilla, I observed no intraspecific variation in this character.

    Evolution. Under both analyses, presence of a narrow rostral osteoderm is a synapomorphy of *E. serratus* + *Xenosaurus.* A rounded shape to the osteoderm is a synapomorphy of the southern clade of *Xenosaurus.*

12. Premaxilla: Distinct flanking osteoderms dorsolateral to rostral osteoderm (0) present (Fig. 9C); (1) absent (Fig. 9B).

    Evolution. Under both analyses, the presence of flanking osteoderms is a synapomorphy of *E. serratus* + *Xenosaurus.* Their absence is a synapomorphy of the southern clade of *Xenosaurus.*

13. Premaxilla: Rostral osteoderm and flanking osteoderms (when present) (0) smoothly domed or weakly keeled (Fig. 9C); (1) strongly keeled (Fig. 10B).

    Variation. The keel appears to form first during osteoderm development (unpublished observation), and as evidenced by juvenile *X. platyceps*, this character does not transform postnatally.

    Evolution. Under both analyses, a relatively smooth and rounded morphology is the primitive state for the rostral osteoderm, with strong keeling a synapomorphy of the northern clade of *Xenosaurus.*

14. Premaxilla: Medial edges of vomerine processes oriented in a horizontal plane

(0) more mediolaterally (Fig. 8C); (1) more anteroposteriorly (Fig. 8D).

Evolution. Under Analysis 1, mediolateral orientation is a synapomorphy of Anguidae and of *S. crocodilurus* (or a more inclusive shinisaur-related clade). Under Analysis 2, more ambiguity exists. With one possible hypothesis of character evolution, an anteroposterior orientation is ancestral, with a mediolateral orientation an autapomorphy of *S. crocodilurus*. A mediolateral orientation is then either a synapomorphy of Anguidae + Varanoidea with an anteroposterior orientation a synapomorphy of Varanidae, or a mediolateral orientation is a synapomorphy of Anguidae and an autapomorphy of Helodermatidae. The second hypothesis of character evolution is that a mediolateral orientation is ancestral. An anteroposterior orientation is thus an autapomorphy of *P. torquatus* and a synapomorphy of *E. serratus* + *Xenosaurus* on the one hand and Varanidae on the other.

15. Premaxilla: Medial edges of vomerine processes near midline convergence (0) straight, without dorsoventral bow (Fig. 10C); (1) with dorsoventral bow (Fig. 10D).

    Evolution. Under both analyses, the bowing or inflection is a synapomorphy of *X. rackhami* + *X. grandis*.

16. Premaxilla: Stalk of incisive process (0) relatively long, length similar to or greater than diameter (Fig. 10D); (1) relatively short, length shorter than diameter (Fig. 10C).

    Variation. Some variation does occur across ontogenetic stages within taxa; in particular, a few individuals of *X. rackhami* and *X. grandis* show shorter processes. However, the vast majority of specimens where adequate samples are available have incisive processes of approximately uniform relative length.

Evolution. Under both analyses, shortness of the stalk of the incisive process is a synapomorphy of the northern clade of *Xenosaurus* and an autapomorphy of *X. rectocollaris.* Under Analysis 1, shortness is a synapomorphy of Helodermatidae + Anguidae and an autapomorphy of *L. borneensis.* Under Analysis 2, shortness is a synapomorphy of Anguidae + Varanoidea. Within this clade, a longer morphology is a synapomorphy of *Varanus.*

17. Premaxilla: Accessory processes dorsal to vomerine processes (0) absent (Fig. 11A); (1) present (Fig. 10C).

    Evolution. Under both analyses, presence of the accessory dorsal processes is a synapomorphy of *Xenosaurus.*

18. Premaxilla: Accessory processes dorsal to vomerine processes (0) relatively short, nub-like (Fig. 10C); (1) relatively long and slender (Fig. 10D).

    Evolution. Under both analyses, relative length of the processes is a synapomorphy of the northern clade of *Xenosaurus.*

19. Premaxilla: Fossa for rostral process of nasal septum (0) relatively mediolaterally narrow (Fig. 9D); (1) relatively mediolaterally wide (Fig. 10D).

    Variation. Although the shape of the fossa varies somewhat among individuals, no variation so great as to affect the scoring of the character was evident.

    Evolution. Under both analyses, relatively great width of the fossa is a synapomorphy of *E. serratus* + *Xenosaurus.*

20. Premaxilla: Angle of rise of nasal process in sagittal plane (0) relatively low (Fig. 11B); (1) intermediate (Fig. 11C); (2) relatively great (Fig. 11D).

    Evolution. Under both analyses, a moderate angle is ancestral and a high angle is a synapomorphy of *S. crocodilurus* + *M. ornatus* and an autapomorphy of Helodermatidae. Also under both analyses, a low angle is a synapomorphy
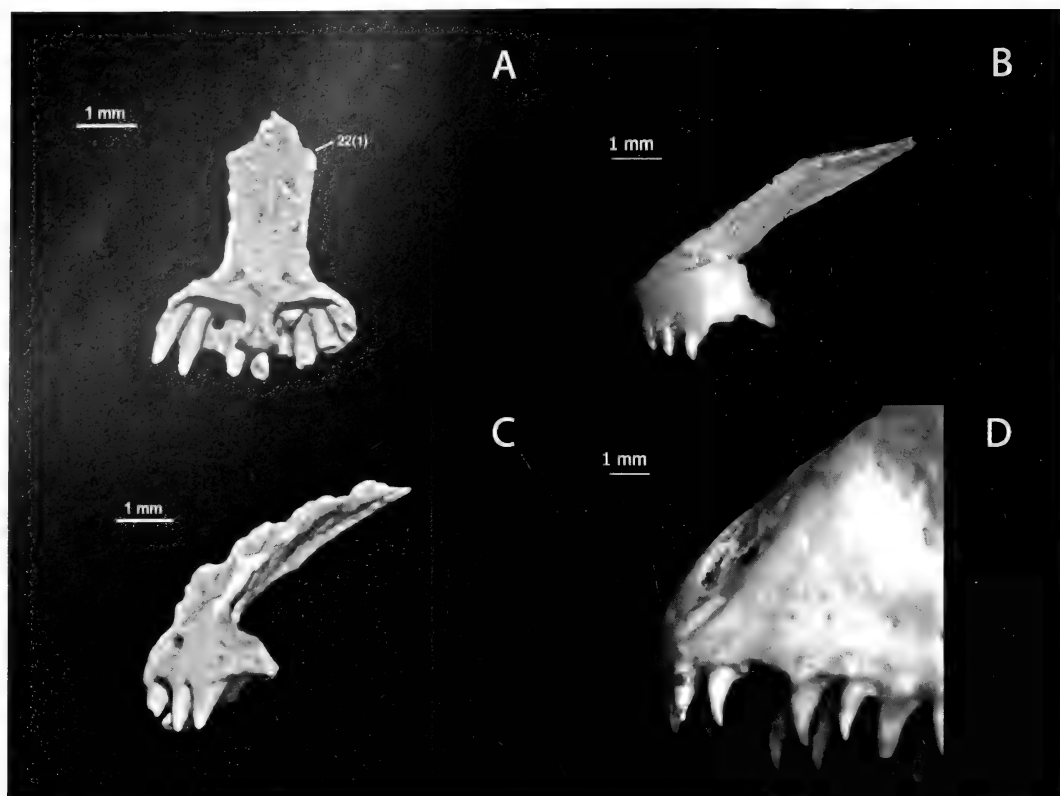
Figure 11.   A, Premaxilla of *Exostinus serratus*, CT scan of USNM v16565, posterior. Illustrates characters 17(0), 22(1), 23(0), 24(1). B, Premaxilla of *Elgaria multicarinata* TMM-M 8993, left lateral, anterior to the left. Illustrates character 20(0). C, Premaxilla of *Exostinus serratus*, CT scan of USNM v16565, left lateral, anterior to the left. Illustrates character 20(1). D, Rostrum of *Shinisaurus crocodilurus* MVZ 204291, left lateral, anterior to the left. Illustrates character 20(2).

of the northern clade of *Xenosaurus* and of *Varanus*. Under Analysis 1, a low angle is a synapomorphy of *E. multicarinata* + *O. ventralis*. Under Analysis 2, a low angle is either a synapomorphy of Anguidae with a moderate angle an autapomorphy of *C. enneagrammus* or an autapomorphy of *E. multicarinata* and of *O. ventralis*.

21. Premaxilla: Mediolateral width of nasal process at base (0) two to three tooth positions (Fig. 9A); (1) between four and five tooth positions (Fig. 12A); (2) five tooth positions (Fig. 11A); (3) between five and six tooth positions (Fig. 10D); (4) six or more tooth positions (Fig. 10C).

Variation. The values scored for this character are approximate; it can be difficult to determine precisely whether all or most of a tooth lies within the span of the nasal process. The character may need refining in the future. Nevertheless, at least comparatively, the scorings are sound.

Evolution. Under both analyses, a width of about five tooth positions is ancestral. This is largely a consequence of the state in *P. torquatus* and may seem unusual given the classical gross anatomy–based hypothesis of squamate phylogeny, in that many non-angui-morph scleroglossans have narrow nasal
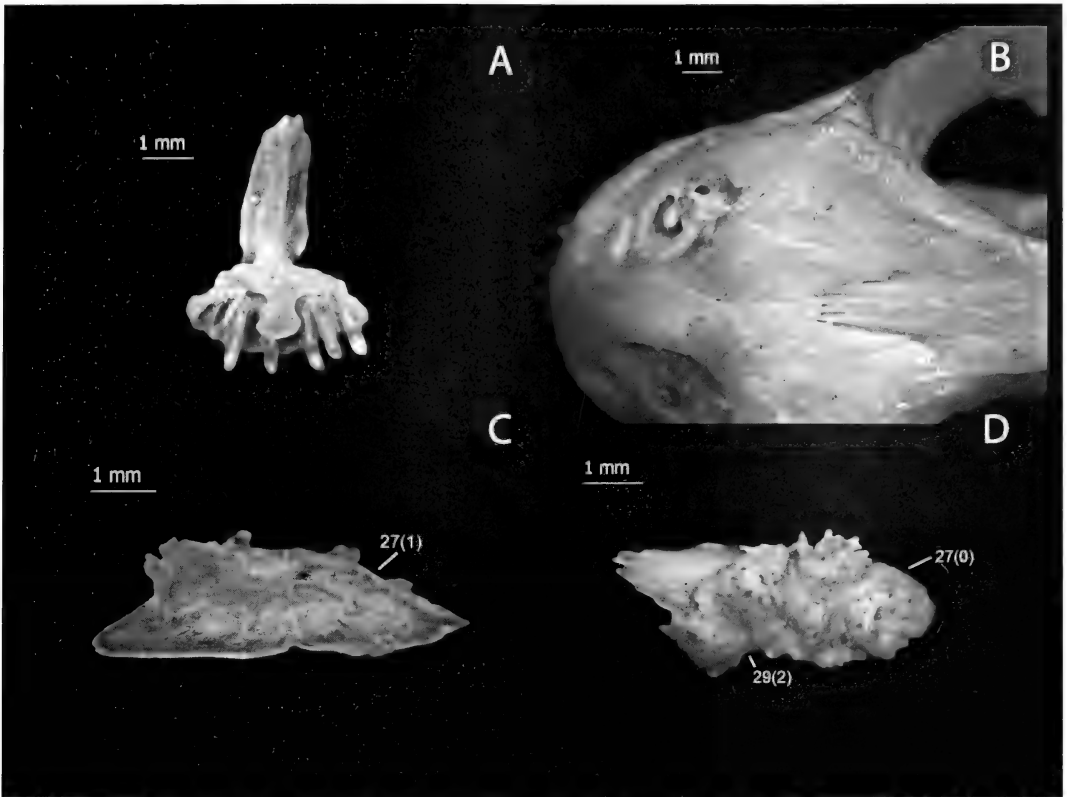
Figure 12.   A, Premaxilla of *Elgaria multicarinata* TMM-M 8958, posterior and slightly left lateral. Illustrates characters 21(1), 22(0), 24(0). B, Rostrum of *Shinisaurus crocodilurus* MVZ 204291, dorsal, anterior to the left. Illustrates characters 26(0), 67(0). C, Left nasal of *Xenosaurus grandis* NAUQSP-JIM 1460, ventral, anterior to the left. Illustrates character 27(0). D, Left nasal of *Xenosaurus platyceps* UF 45622, dorsal, anterior to the left. Illustrates characters 27(1), 28(1), 29(2).

processes. However, in support of the inference here presented, a relatively wide-based nasal process is shared by a host of primitive iguanians on the one hand (Polychrotinae, Corytophaninae, Hoplocercinae, *Leiolepis,* and *Uromastyx,* among others) and by *C. intermedia,* sometimes suggested to be the extinct sister taxon to Anguimorpha (Gao and Norell, 1998, 2000; Conrad, 2005, 2008). Under both analyses, a width of between five and six tooth positions is a synapomorphy of *Xenosaurus* and six or more is a synapomorphy of the northern clade of *Xenosaurus,* as well as an autapomorphy of *L. borneensis.* Under Analysis 1, a width of two to three tooth positions is a synapomorphy of Anguidae, and a width of between four and five tooth positions is an autapomorphy of *E. multicarinata.* A width of between four and five tooth positions is also a synapomorphy of *Varanus,* and a width of two to three an autapomorphy of *V. niloticus.* However, this result might be skewed by the unusual width of the snout of *V. exanthematicus.* Under Analysis 2, a width of between four and five tooth positions is a synapomorphy of Anguidae + Varanoidea; a width of two to three is a synapomorphy of *O. ventralis* + *C. enneagrammus* and an autapomorphy of both Helodermatidae and *V. niloticus.*

22. Premaxilla: Dorsolateral flare at contact with dermal surface of nasal (0) absent or minimal (Fig. 12A); (1) present with distinct dorsal wedge separated (Fig. 11A); (2) pronounced (Fig. 10C).

   Evolution. Under both analyses, a pronounced premaxillary flare is a synapomorphy of the northern clade of *Xenosaurus.* Under Analysis 1, the flaring morphology is a synapomorphy of *E. serratus* + *Xenosaurus.* Additionally, either the flare is a synapomorphy of *M. ornatus* + *S. crocodilurus* and no flare is an autapomorphy of *B. ammoskius,* or the flare is an autapomorphy of both *M. ornatus* and *S. crocodilurus.* Under Analysis 2, the flaring morphology is a synapomorphy of Xenosauridae, and the lack of a flare is an autapomorphy of *B. ammoskius.*

23. Premaxilla: Anterior portions of nasal facets (0) shallowly impressed (Fig. 11A); (1) deeply impressed (Fig. 10C).

   Evolution. Under both analyses, deep impression is a synapomorphy of *Xenosaurus* and an autapomorphy of *M. ornatus.*

24. Premaxilla: Keel between nasal facets (0) dorsoventrally extensive (Fig. 12A); (1) restricted to dorsal portion of nasal process (Fig. 11A).

   Evolution. Under Analysis 1, relatively great extent of the keel is unambiguously a synapomorphy of *E. multicarinata* + *O. ventralis.* At the initial split of the tree, the ancestral state is ambiguous. If the ancestral state is great extent, then restriction is either a synapomorphy of Anguimorpha with great extent an autapomorphy of Varanidae, or restriction is a synapomorphy of both Anguidae + *Xenosaurus* and *S. crocodilurus* + *M. ornatus.* If the ancestral state is restriction, then great extent is an autapomorphy of *P. torquatus* and a synapomorphy of Varanidae. Under Analysis 2, great extent is ancestral and restriction is a

synapomorphy of Xenosauridae and an autapomorphy of both *C. enneagrammus* and Helodermatidae.

25. Premaxilla: Tooth position count, average rounded to nearest integer, (0) 7; (1) 8; (2) 9; (3) more than nine.

   Variation. Premaxillary tooth position count does vary, and the character scored is the average value for the individuals examined. However, even in those taxa whose count did vary, the variants always possessed one fewer tooth position than the average (and modal) number. Furthermore, these nonmodal variants were rare.

   Evolution. Under both analyses, having more than nine tooth positions is an autapomorphy of *L. borneensis.* Under Analysis 1, the ancestral state is ambiguous. If it is eight or nine tooth positions, then having seven tooth positions is an autapomorphy of *P. torquatus,* and the other transformations are as described below for the case in which eight or nine is ancestral for Anguimorpha. If seven tooth positions is the ancestral state, an increased number is a synapomorphy either of Anguimorpha or of Anguidae + *Xenosaurus.* Two possibilities obtain if an increased number of either eight or nine is a synapomorphy of Anguimorpha. If eight, then having nine tooth positions is a synapomorphy of Anguidae + *Xenosaurus* and of Varanidae, and having seven tooth positions is a synapomorphy of *S. crocodilurus* + *M. ornatus.* If nine, then only the two-step transformation along the *Shinisaurus* stem need occur.

Nasal

   The nasal is unknown for *E. lancensis, R. rugosus,* and *M. ornatus.*

26. Nasal: Contacts contralateral nasal at dermal surface (0) extensively, along, at least a quarter of its medial margin (Fig. 12B); (1) barely or not at all (Fig. 2A).

Variation. In younger individuals of *V. exanthematicus*, the nasals are barely in contact, but in medium to large individuals, they show extensive contact. The nasals of *Varanus* in general are unusual in their morphology and their contacts, concomitantly with the retracted nares characteristic of the clade (McDowell and Bogert, 1954; Estes et al., 1988).

Evolution. Under both analyses, a small amount of contact is a synapomorphy of *Xenosaurus* and an autapomorphy of *V. niloticus*.

27. Nasal: Posterior tapered portion (in horizontal plane) (0) mediolaterally wider at base than long along long axis of nasal (Fig. 12C); (1) longer than wide (Fig. 12D).

    Evolution. Under Analysis 1, the longer-than-wide morphology is ancestral, with wider-than-long a synapomorphy of *Xenosaurus* + Anguidae and, within that clade, longer-than-wide a synapomorphy of the southern clade of *Xenosaurus*. Under Analysis 2, the ancestral state for Anguimorpha is ambiguous. If the ancestral state is wider-than-long, then the longer-than-wide morphology is a synapomorphy of *B. ammoskius* + *S. crocodilurus* and the southern clade of *Xenosaurus*. If the ancestral state is longer-than-wide, then wider-than-long is a synapomorphy of Anguidae. Furthermore, wider-than-long is either a synapomorphy of *E. serratus* + *Xenosaurus* and longer-than-wide a synapomorphy of the southern clade of *Xenosaurus*, or wider-than-long is an autapormophy of *E. serratus* and a synapomorphy of the northern clade of *Xenosaurus*.

28. Nasal: Osteoderms of lateral row posterior to enlarged anterolateral osteoderm (0) comparable in size to or smaller than osteoderms of medial row (Fig. 3A); (1) larger and more prominent than osteoderms of medial row; anterolateral osteoderm especially large (Fig. 12D).

    Evolution. Under both analyses, greater size and prominence of the lateral row is a synapomorphy of the northern clade of *Xenosaurus*.

29. Nasal: Anterior portion of lateral edge corresponding to underlying lateral bend of cartilaginous nasal capsule (0) with no change in angle or with deflection in horizontal plane away from the midline of a few degrees relative to the posterior portion of the lateral edge (Fig. 13A); (1) with slight deflection from posterior portion of about 10°; (2) with notable bend, deflecting from the posterior portion by about 40° (Fig. 12D).

    Evolution. Under both analyses, ancestral character states are ambiguous between a change in angle of 10° and 40° across most of the tree. Under Analysis 1, the only unambiguous synapomorphy is the lack of a change in angle uniting *Varanus*. Under Analysis 2, the ambiguity along the stem of Varanoidea shifts to no change in angle/slight change in angle.

Septomaxilla

Unfortunately, the septomaxilla is unknown in all of the extinct taxa. In general, this element is neglected in studies of squamate osteology. It received the most attention in work dealing with the complex olfactory organs of lizards (Stebbins, 1948; Bellairs, 1949; Hallerman, 1994; Bernstein, 1999). A few characters are used in current phylogenetic works on Serpentes (Lee and Scanlon, 2002). In the course of this investigation, I was able to identify a number of informative characters in the septomaxilla. In part, this stems from the unusually complex septomaxilla of *Xenosaurus*, in and upon which several canals and ridges are formed that do not appear on the septomaxillae of most other squamates.

30. Septomaxilla: Posteromedial corner of cupular portion (0) with a long para-
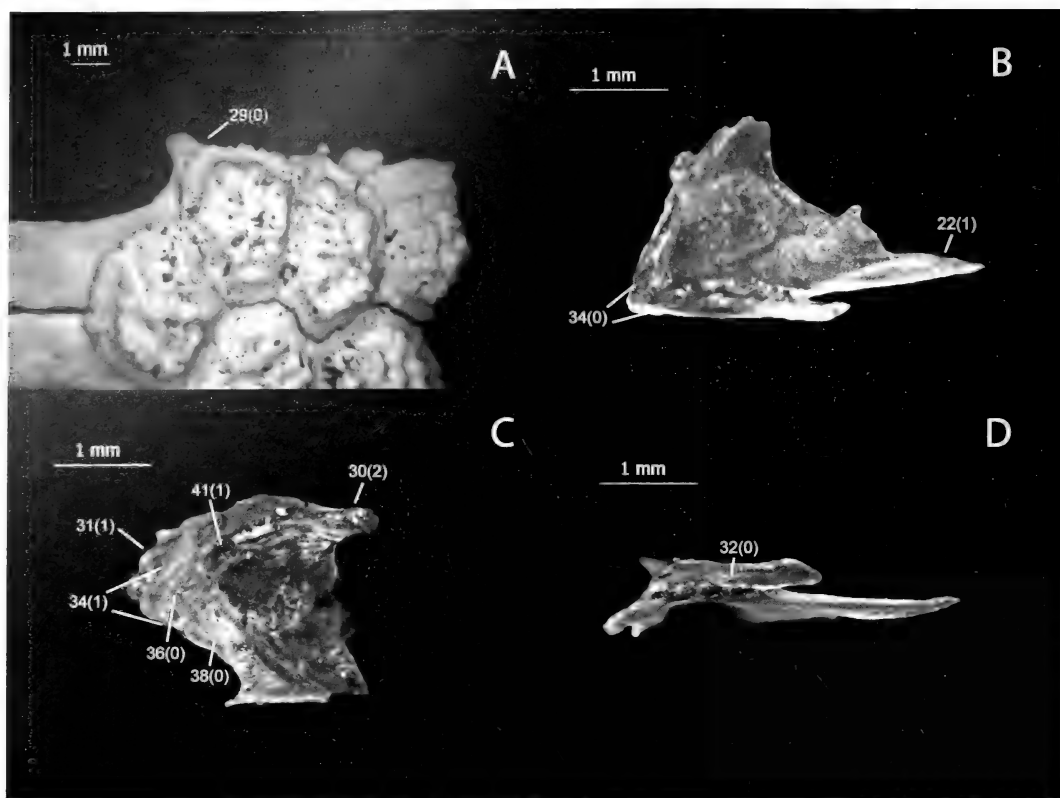
Figure 13.   A, Nasals of *Heloderma suspectum* TMM-M 9001, dorsal, anterior to the left. Illustrates character 29(0). B, Right septomaxilla of *Elgaria multicarinata* TMM-M 8958, dorsal, anterior to the left. Illustrates characters 30(0), 31(0), 34(0). C, Left septomaxilla of *Xenosaurus newmanorum* NAUQSP-JIM uncatalogued specimen, dorsal, anterior to the left. Illustrates characters 30(2), 31(1), 34(1), 36(0), 38(0), 41(1). D, Right septomaxilla of *Elgaria multicarinata* TMM-M 8958, medial, anterior to the left. Illustrates character 32(0).

septal process, several times as long as mediolaterally wide at base (Fig. 13B); (1) sending back moderate-length or short process, about twice as long as mediolaterally wide at base; (2) process absent or reduced to minor projection of corner, septomaxilla roughly an equilateral triangle in overall shape (Fig. 13C).

Variation. The process becomes longer during postnatal ontogeny, but its proportions are consistent with the scoring for most of ontogeny.

Evolution. Under both analyses, moderate length of the process is ancestral and absence is a synapomorphy of *Xenosaurus*. Under Analysis 1,

great length is a synapomorphy of Varanidae. Great length is also either a synapomorphy of Anguidae with moderate length an autapomorphy of *C. enneagrammus*, or great length is an autapomorphy of Helodermatidae and *O. ventralis* + *E. multicarinata*. Under Analysis 2, great length is a synapomorphy of Anguidae + Varanoidea, and moderate length is an autapomorphy of *C. enneagrammus*.

31. Septomaxilla: Deflection of bone away from rostral process of nasal septum to form distinct anteromedial surface (0) absent (Fig. 13B); (1) present (Fig. 13C).
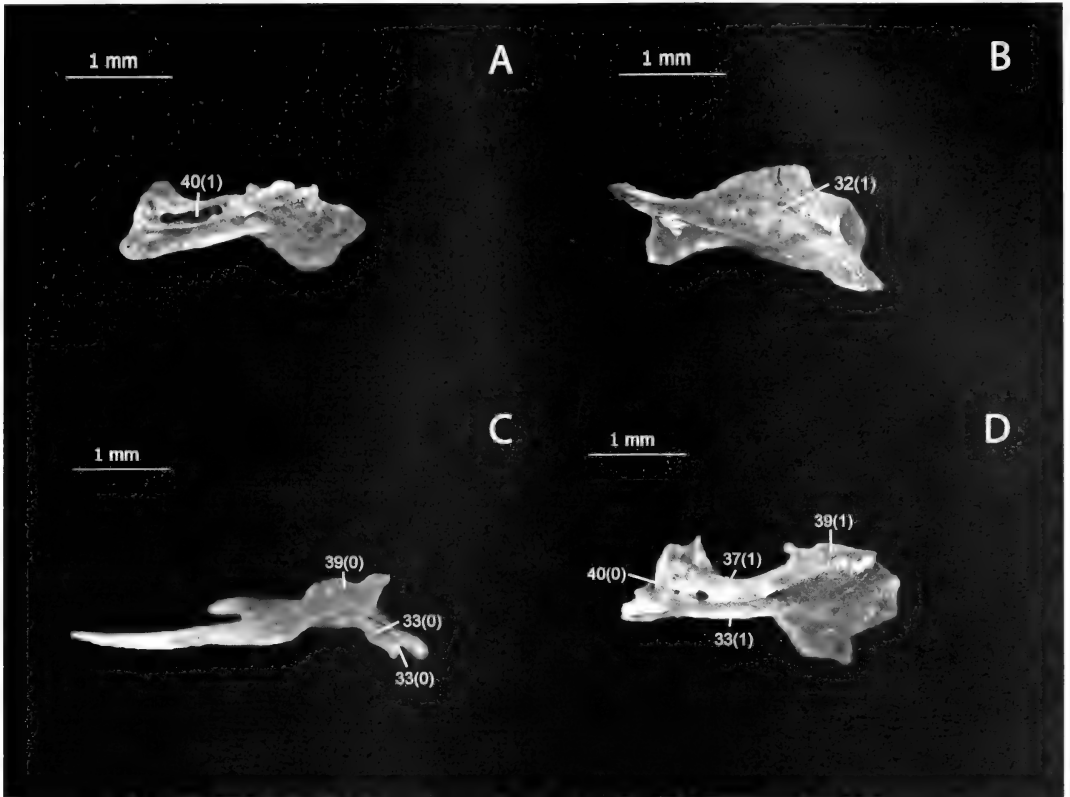
Figure 14.   A, Left septomaxilla of *Xenosaurus rackhami* UTEP-OC "MALB" 388, lateral, anterior to the left. B, Left septomaxilla of *Xenosaurus newmanorum* NAUQSP-JIM uncatalogued specimen, medial, anterior to the right. Illustrates characters 32(1), 40(1). C, Right septomaxilla of *Elgaria multicarinata* TMM-M 8958, lateral, anterior to the right. Illustrates characters 33(0), 37(0), 39(0). D, Left septomaxilla of *Xenosaurus newmanorum* NAUQSP-JIM uncatalogued specimen, lateral, anterior to the left. Illustrates characters 33(1), 37(1), 39(1), 40(0).

Evolution. Under both analyses, the presence of the anteromedial surface is a synapomorphy of *Xenosaurus*.

32. Septomaxilla: Medial ethmoidal nerves and vasculature (0) running in connective tissue near surface of septomaxilla, not enclosed by bone (Fig. 13D); (1) enclosed by septomaxilla (Fig. 3.32B).

Evolution. Under Analysis 1, enclosure is a synapomorphy of *Xenosaurus* + Anguidae and an autapomorphy of *L. borneensis.* Under Analysis 2, enclosure may be ancestral, in which case lack of enclosure is an autapomorphy of *P. torquatus* and *S. crocodilurus.* If enclo-

sure is not ancestral, it is a synapomorphy of Anguimorpha or a synapomorphy of *Xenosaurus* and of Anguidae + Varanoidea. Under any of these hypotheses of character evolution, lack of enclosure is a synapomorphy of *Varanus.*

33. Septomaxilla: Lateral ethmoidal nerves and vasculature (0) running in connective tissue near surface of septomaxilla, not enclosed by bone (Fig. 14C); (1) enclosed by septomaxilla (Fig. 14D).

Evolution. Under Analysis 1, lateral enclosure is either a synapomorphy of Anguidae + *Xenosaurus*, with lack of
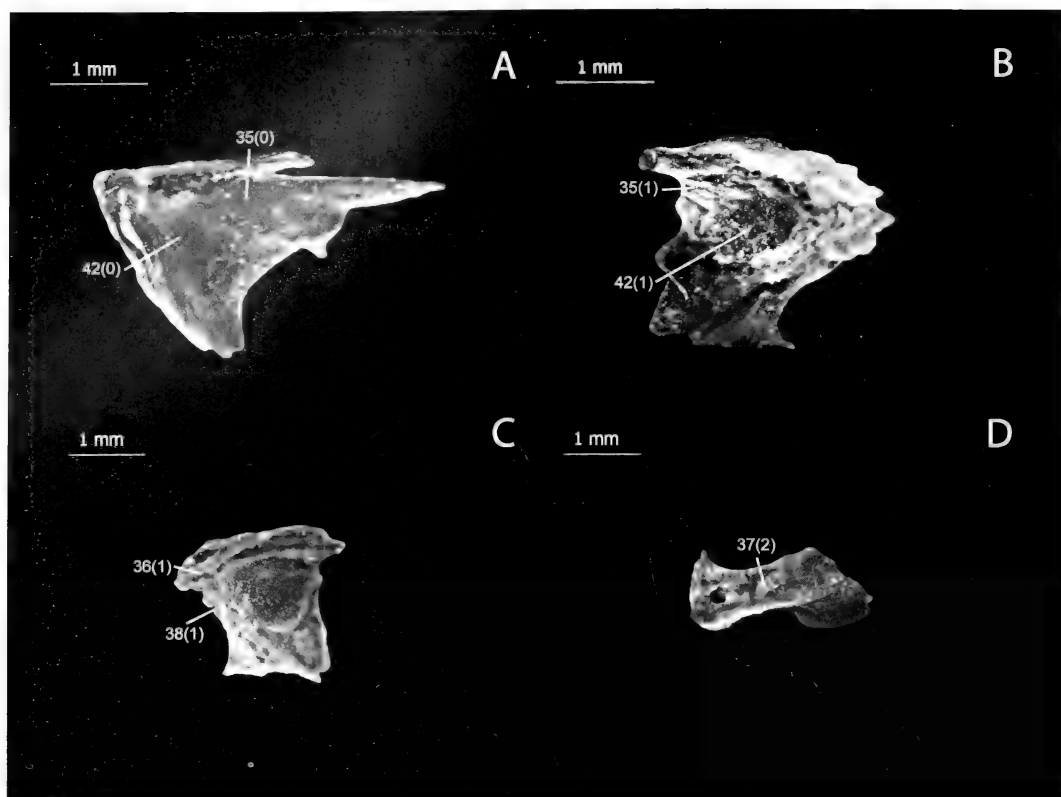
Figure 15.   A, Right septomaxilla of *Elgaria multicarinata* TMM-M 8958, ventral, anterior to the left. Illustrates characters 35(0), 42(0). B, Right septomaxilla of *Elgaria multicarinata* TMM-M 8958, lateral, anterior to the right. Illustrates characters 35(1), 42(1). C, Left septomaxilla of *Xenosaurus grandis* NAUQSP-JIM 1460, dorsal, anterior to the left. Illustrates characters 36(1), 38(1), 41(0). D, Left septomaxilla of *Xenosaurus grandis* NAUQSP-JIM 1460, lateral, anterior to the left. Illustrates character 37(0).

enclosure a synapomorphy of Anguidae, or lateral enclosure is a synapomorphy of *Xenosaurus* and an autapomorphy of Helodermatidae. Under Analysis 2, only the latter hypothesis of character evolution is most parsimonious.

34. Septomaxilla: Dorsal ridges following anterolateral and anteromedial edges (0) absent or low (Fig. 13B); (1) high and sharp (Fig. 13C).

   Evolution. Under both analyses, a high, sharp morphology is a synapomorphy of *Xenosaurus*.

35. Septomaxilla: Ventral surface posterior to vomeronasal cupula (0) smooth (Fig. 15A); (1) impressed into longitudinal grooves by vomeronasal nerve (Fig. 15B).

   Variation. The sulci become more deeply incised during ontogeny but are present in even the youngest individuals examined.

   Evolution. Under both analyses, the presence of vomeronasal nerve impressions is a synapomorphy of *Xenosaurus*.

36. Septomaxilla: Anteroposterior length of flattened dorsal region near anterior apex, in front of capsular depression. Measured as proportion of total anteroposterior length of septomaxilla from

anterior apex back along anteroposterior axis: (0) 0.35 or greater (Fig. 13C); (1) less than 0.35 (Fig. 15C).

Variation. The lamina of bone posterior to the cupular region of the septomaxilla lengthens slightly during ontogeny, so the ratios above should be taken to apply to fairly mature individuals.

Evolution. Because no other squamate possesses the flattened region, the ancestral state within *Xenosaurus* is ambiguous.

37. Septomaxilla: Ratio of dorsoventral height of anterolateral face at shortest level to anteroposterior length of face (0) less than 0.10 (Fig. 14C); (1) 0.10 to 0.50 (Fig. 14D); (2) greater than 0.50 (Fig. 15D).

Evolution. A dorsoventrally short anterolateral face with a height-to-length ratio of less than 0.10 is ancestral under both analyses. Also under both analyses, a ratio of 0.10 to 0.50 is a synapomorphy of *Xenosaurus* and a ratio greater than 0.50 is a synapomorphy of the southern clade of *Xenosaurus*.

38. Septomaxilla: Anterolateral dorsal ridge continuing from lateral wing (0) broad and rounded (Fig. 13C); (1) narrow and sharp (Fig. 15C).

Evolution. The ancestral state within *Xenosaurus* is ambiguous.

39. Septomaxilla: Ratio of anteroposterior length of lateral wing to anteroposterior length of septomaxilla along anteroposterior axis from level of anterior apex to level of back of lateral wing (0) greater than 0.55 (Fig. 14C); (1) 0.55 or less (Fig. 14D).

Evolution. Under both analyses, a ratio of 0.55 or less is a synapomorphy of the northern clade of *Xenosaurus* and an autapomorphy of Helodermatidae.

40. Septomaxilla: Anterolateral ethmoid canal (0) open only at round terminal foramina (Fig. 14D); (1) open along much of anterolateral face as long fissure (Fig. 14A).

Evolution. Under both analyses, closure is the primitive state and the existence of the fissure is a synapomorphy of the southern clade of *Xenosaurus*.

41. Septomaxilla: Canal paralleling and running lateral to the medial edge of the septomaxilla or to the anteromedial dorsal ridge (when visible) (0) absent (Fig. 15C); (1) present (Fig. 13C).

Evolution. Under both analyses, presence of the canal is a synapomorphy of the northern clade of *Xenosaurus*.

42. Septomaxilla: Ratio of mediolateral width of vomeronasal cupula at its widest level to width of septomaxilla at that level (0) 0.45 or greater (Fig. 15A); (1) less than 0.45 (Fig. 15B).

Evolution. Under both analyses, a ratio of less than 0.45 is a synapomorphy of the northern clade of *Xenosaurus*.

Maxilla

The maxilla is only partially preserved in *E. lancensis* and *M. ornatus*.

43. Maxilla: Medial premaxillary process, portion projecting beyond dental gutter, (0) anteroposteriorly very short, about twice as tall at posterior end as long (Fig. 16A); (1) short, about as tall as long; (2) intermediate length, about two-thirds as tall as long (Fig. 16B); (3) long, about half as tall as long (Fig. 16C).

Variation. The medial premaxillary process becomes slightly dorsoventrally taller during ontogeny, but despite this, no variation that would affect scoring was evident.

Evolution. Under both analyses, a very short process is ancestral for the
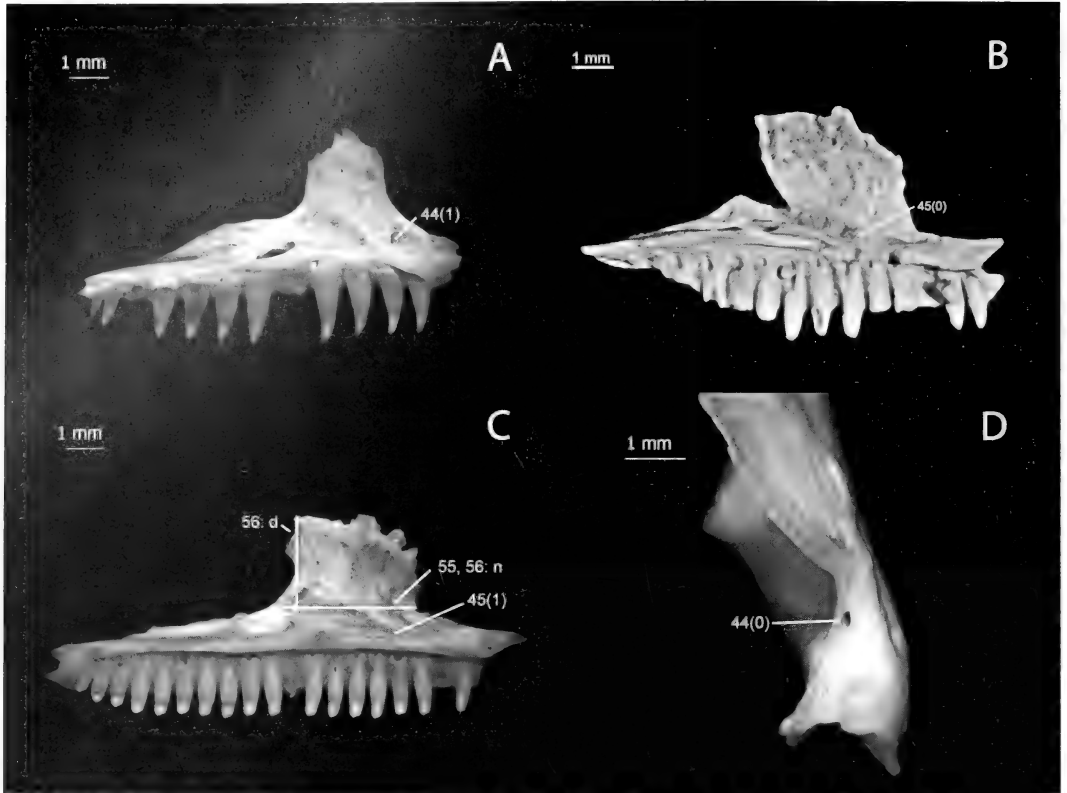
Figure 16. A, Left maxilla of *Shinisaurus crocodilurus* UF 72805, medial, anterior to the right. Illustrates characters 43(0), 44(1), 46(2), 63(1). B, Left maxilla of *Exostinus serratus*, CT scan of USNM v16565, medial, anterior to the right. Illustrates characters 43(2), 45(0), 46(1), 60(1), 63(0). C, Left maxilla of *Xenosaurus platyceps* UF 45622, medial, anterior to the right. Illustrates characters 43(3), 45(1), 55 (n for numerator, d for denominator), 56 (n for numerator, d for denominator), 60(0). D, Left maxilla of *Elgaria multicarinata* TMM-M 8958, anterior. Illustrates character 44(0).

entire group and for Anguimorpha and a long process is a synapomorphy of the northern clade of *Xenosaurus*. The ancestral states for *Xenosaurus* + *E. serratus* and *Xenosaurus* are ambiguous between short and intermediate. Under Analysis 1, the ancestral state for Anguidae + Xenosauridae is ambiguous among very short, short, and intermediate, as is that for *Xenosaurus* + *R. rugosus*. The long morphology is a synapomorphy of Anguidae + Helodermatidae, and intermediate length is an autapomorphy of *E. multicarinata*. Under Analysis 2, the ancestral states for Anguidae + Varanoidea and Varanoidea are ambiguous among very short, short, and intermediate lengths. The long morphology is a synapomorphy of *O. ventralis* + *C. enneagrammus* and an autapomorphy of . Along the other branch of Anguimorpha, the ancestral state for Xenosauridae and for *Xenosaurus* + *R. rugosus* is the very short morphology.

44. Maxilla: Major anterior foramen for contents of infraorbital canal (ethmoidal nerve and accompanying structures) (0) exiting onto lamina intercristalis, lateral to crista transversalis (Fig. 16D); (1) exiting posteromedial to crista transversalis (Fig. 16A).

Evolution. Under both analyses, the ancestral state of the character is ambiguous. However, the medial foramen is not widespread outside of Anguimorpha, and I tentatively suggest that the ancestral state is for the exit to be in the upper region of the lamina intercristalis. Under Analysis 1, a medial exit is then a synapomorphy of Anguimorpha and a lateral exit is a synapomorphy of Anguidae. Under Analysis 2, the ancestral state for Anguimorpha is ambiguous.

45. Maxilla: Anterior end of lacrimal recess (0) relatively posterior, greater than one quarter of the way to the posterior end of the facial process (Fig. 16B); (1) relatively anterior, one quarter of the way back or less (Fig. 16C).

Evolution. Under both analyses, the relatively anterior morphology is ancestral for the total group and the relatively posterior morphology is ancestral for *Xenosaurus* + *R. rugosus*, with the relatively anterior morphology a synapomorphy of *Xenosaurus*. Under Analysis 1, the ancestral state for Anguidae + *Xenosaurus* and for the clades within Anguidae is ambiguous. Under Analysis 2, the relatively posterior morphology is a synapomorphy of *O. ventralis* + *C. enneagrammus*.

46. Maxilla: Anterior portion of dorsal margin of lacrimal recess—posterodorsal rise in plane of facial process (0) shallow, 30° or less (Fig. 17A); (1) moderate, between 30° and 35° (Fig. 16B); (2) steep, 35° and greater (Fig. 16A).

Evolution. Under both analyses, a shallow angle of 30° or less is ancestral. In the absence of data for *B. ammoskius*, a steep angle of 35° or greater is an autapomorphy of *S. crocodilurus*. An angle between 30° and 35° is a synapomorphy of *Xenosaurus*, and an angle of 35° or greater is a synapomorphy of *X. agrenon* + *X. rectocollaris*.

47. Maxilla: Articular facet posterior to facial process (0) mediolaterally narrow, hardly differentiated from sharp dorsal edge of maxilla (Fig. 17B); (1) mediolaterally wide, with a distinct dorsally facing table (Fig. 17C).

Evolution. Under Analysis 1, the wide morphology is a synapomorphy of *E. serratus* + *Xenosaurus* and of *S. crocodilurus* + *B. ammoskius*. Under Analysis 2, the ancestral state for Xenosauridae is ambiguous.

48. Maxilla: Mediolaterally expanded facet posterior to facial process: (0) for lacrimal; (1) for jugal.

Evolution. Because of widespread missing data, the ancestral state for the character is ambiguous at all levels.

49. Maxilla: Width of palatal shelf at widest level (measured in horizontal plane perpendicular to axis of toothrow) (0) less than one-fifth length of maxillary toothrow (Fig. 17D); (1) one-fifth length of maxillary toothrow or greater (Fig. 18A).

Evolution. Under both analyses, a wide palatal shelf is an autapomorphy of *E. serratus*.

50. Maxilla: Posterior end of tooth row (0) relatively straight, collinear with more anterior portion (Fig. 17D); (1) medially deflected (Fig. 18A).

Evolution. Under both analyses, medial deflection is an autapomorphy of *E. serratus*.

51. Maxilla: Infraorbital canal (0) round for entire length, confined to medial, steep portion of palatal shelf (see *E. multicarinata*, The Deep Scaly Project [2007], coronal slices 35–124); (1) mediolaterally expanded and oval for portion of length, extending above flattened, horizontal lateral portion of palatal shelf (Fig. 18B).

Evolution. Under both analyses, an expanded canal is a synapomorphy of
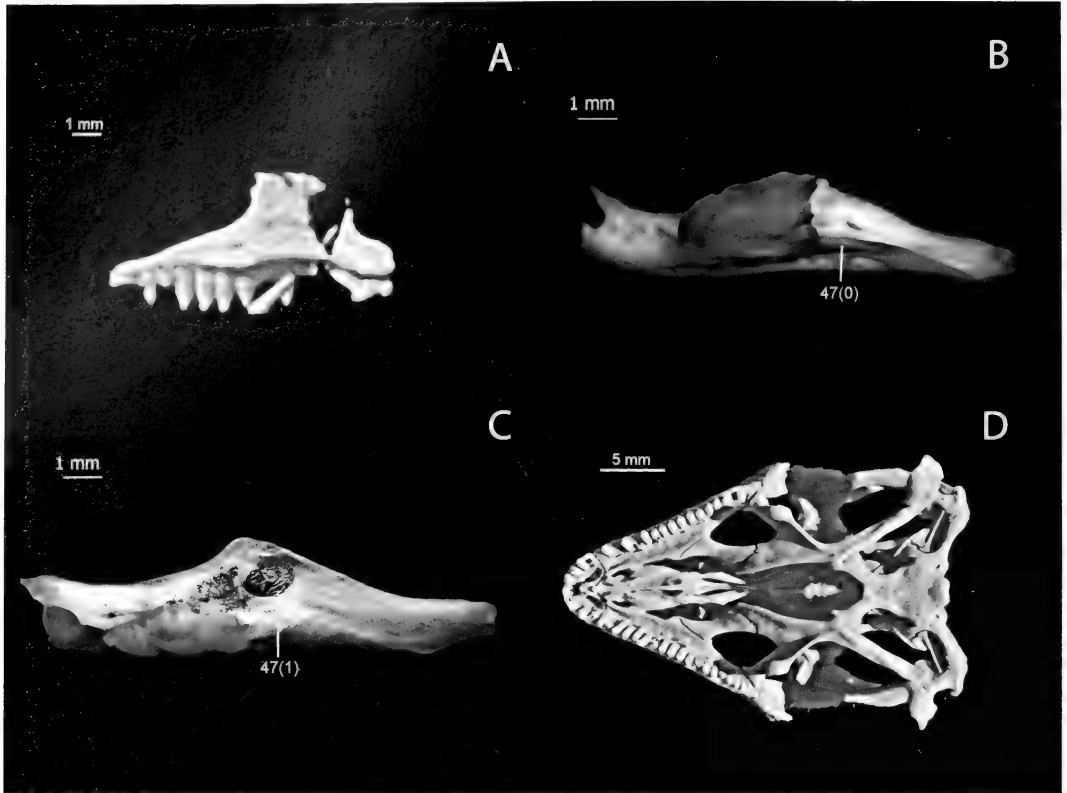
Figure 17.   A, Left maxilla of *Restes rugosus*, CT scan of YPM PU 14640, medial, anterior to the right. Illustrates character 46(0). B, Left maxilla of *Elgaria multicarinata* TMM-M 8958, dorsal, anterior to the left. Illustrates character 47(0). C, Left maxilla of *Xenosaurus grandis* NAUQSP-JIM 1460, dorsal, anterior to the left. Illustrates character 47(1). D, Skull of *Xenosaurus newmanorum*, CT scan of UMMZ 126056, ventral, anterior to the left. Illustrates characters 49(0), 50(0), 93(1).

Xenosaurus + *R. rugosus* and of *Varanus*, and an autapomorphy of *C. enneagrammus*.

52. Maxilla: Supradental thickening (0) absent (Fig. 18C); (1) weak, low ridge above teeth (Fig. 18D); (2) strong, rounded ridge above teeth, differentiated dorsally by groove (Fig. 19A).

    Variation. The ridge becomes stronger with increasing age.

    Evolution. Under both analyses, weak development is an autapomorphy of *E. serratus*. Under Analysis 1, the ancestral state for the entire group is ambiguous between absence of the thickening and the weakly developed morphology, as are the ancestral states for Anguimorpha and Anguidae + Helodermatidae. Strong development is a synapomorphy of *Xenosaurus* + *R. rugosus* and of *S. crocodilurus* + *M. ornatus*. Under Analysis 2, absence is the ancestral state for the entire group and for Anguimorpha and Anguidae + Varanoidea. Within Varanoidea, weak development is an autapomorphy of Helodermatidae. Strong development is a synapomorphy of Xenosauridae.

53. Maxilla: Major labial foramina: (0) posteriormost one or more foramina abruptly larger than others (Fig. 19B); (1) nearly the same size, with only a subtle and gradual trend of posterior enlargement (Fig. 19A).
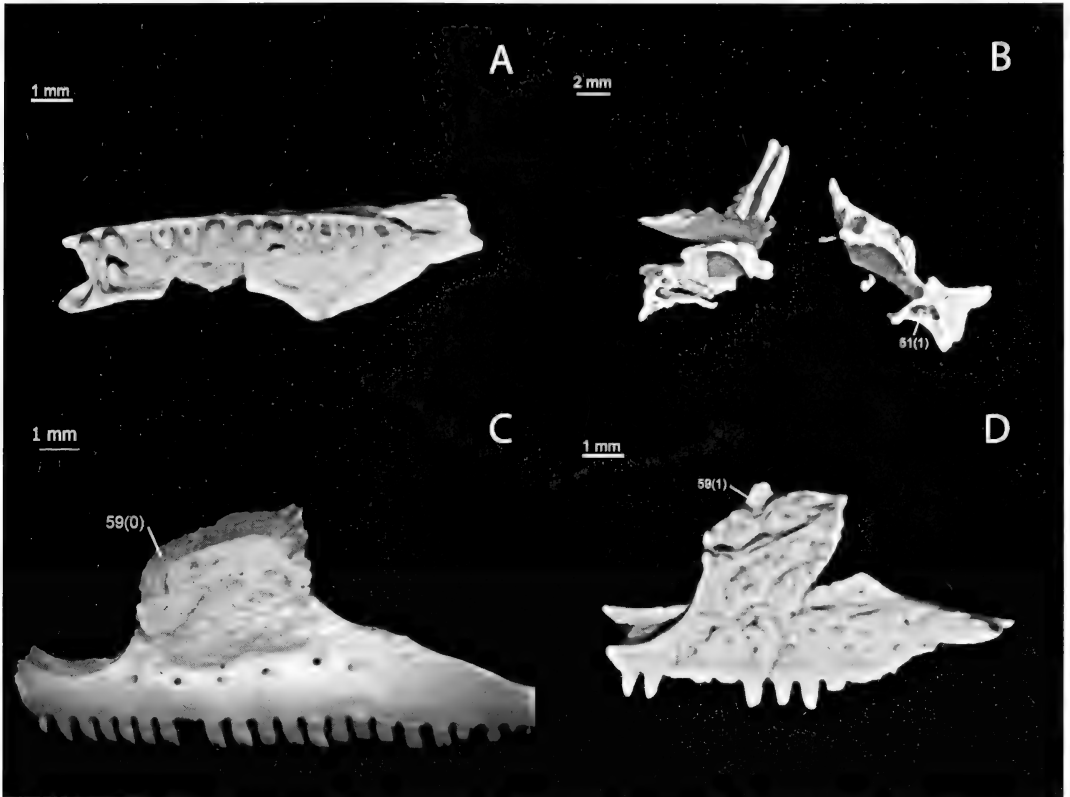
Figure 18.   A, Left maxilla of *Exostinus serratus*, CT scan of USNM v16565, ventral, anterior to the left. Illustrates characters 49(1), 50(1). B, Cutaway near posterior end of infraorbital canal of rostrum of *Exostinus serratus*, CT scan of USNM v16565, anterior. Illustrates character 51(1). C, Left maxilla of *Elgaria multicarinata* TMM-M 8993, lateral, anterior to the left. Illustrates characters 52(0), 54(0), 59(0), 61(0), 62(1). D, Left maxilla of *Exostinus serratus*, CT scan of USNM v16565 lateral, anterior to the left. Illustrates characters 52(1), 54(1), 57(0), 58(0), 59(1), 61(3), 62(4).

Evolution. Under both analyses, rough equivalence in size along the entire row is a synapomorphy of *Xenosaurus + R. rugosus*.

54. Maxilla: Foramina (0) concentrated in single row of labial foramina (Fig. 18C); (1) present in two rows—ventral labial foramina and dorsal row upon lower portion of facial process (Fig. 18D).

Evolution. Under both analyses, the ancestral state for *Xenosaurus + E. serratus* and for the southern clade of *Xenosaurus* is ambiguous, such that presence of the dorsal row could either be an autapomorphy of *E. serratus* and a synapomorphy of the southern clade of *Xenosaurus* or a synapomorphy of

Xenosaurus + E. serratus, with lack of a dorsal row a synapomorphy of the northern clade of *Xenosaurus.*

55. Maxilla: Ratio of length of facial process along base (at dorsoventral level of inflection toward horizontal between rami of lacrimal) to total length of maxilla from anterior edge of facial process at that dorsoventral level to posterior end of maxilla (Fig. 16C) (0) 0.20 to less than 0.30; (1) 0.30 to less than 0.40; (2) 0.40 to less than 0.50; (3) 0.50 to less than 0.60; (4) 0.60 to less than 0.70; (5) 0.70 to less than 0.80.

Variation. As the orbit becomes proportionally smaller during growth,
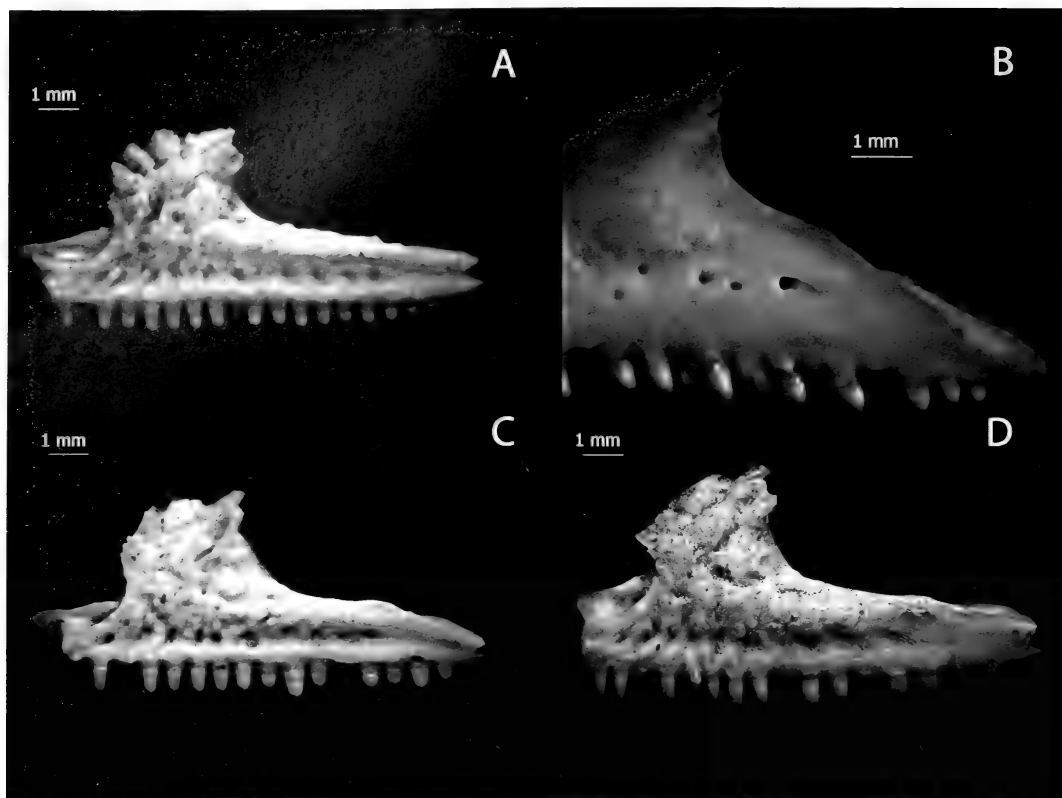
Figure 19.   A, Left maxilla of *Xenosaurus platyceps* UF 45622, lateral, anterior to the left. Illustrates characters 52(2), 53(1), 57(1), 61(2). B, Left maxilla of *Elgaria multicarinata* TMM-M 8958, lateral, anterior to the left. Illustrates character 53(0). C, Left maxilla of *Xenosaurus rackhami* UTEP-OC "MALB" 388, lateral, anterior to the left. Illustrates character 58(2). D, Left maxilla of *Xenosaurus grandis* NAUQSP-JIM 1460, lateral, anterior to the left. Illustrates character 58(3).

the posterior suborbital portion of the maxilla shortens relative to the remainder of the bone. However, this transformation occurs largely during early ontogenetic stages, and I scored this character on relatively large individuals.

Evolution. Under both analyses, state 1 is autapomorphic for *X. agrenon, X. grandis,* and *B. ammoskius,* state 4 is autapomorphic for *O. ventralis,* and state 5 is autapomorphic for *L. borneensis.* Under Analysis 1, the ancestral state for the entire group is ambiguous among state 0, state 1, state 2, and state 3. The ancestral state for Anguimorpha is ambiguous between state 2 and state 3, as is that for *S. crocodilurus* + Varanidae, Varanidae, *Varanus, Xenosaurus*

+ Anguidae, and *Xenosaurus + R. rugosus.* The ancestral state for *S. crocodilurus + B. ammoskius* is state 2, as is that for *E. serratus + Xenosaurus* and all nodes therein. Finally, the ancestral state for Anguidae is state 3, making state 2 an autapomorphy of *E. multicarinata.* Under Analysis 2, the ancestral state for the entire group is ambiguous among state 0, state 1, and state 2. The ancestral state for Xenosauridae and all nodes therein is state 2, and state 3 is autapomorphic for *R. rugosus.* The ancestral state for Anguidae + Varanoidea and for Anguidae is ambiguous between state 2 and state 3. The ancestral state for *O. ventralis + C. enneagrammus* is state 3, as is that for

Varanoidea, making state 2 autapo-morphic for *V. exanthematicus*.

56. Maxilla: Ratio of length of facial process along base (at dorsoventral level of posterior inflection toward horizontal) to greatest height posterior to nasal facet (Fig. 16C) (0) 0.50 to less than 0.75; (1) 0.75 to less than 1.00; (2) 1.00 to less than 1.25; (3) 1.25 to less than 1.50; (4) 1.50 to less than 1.75; (5) 1.75 to less than 2.00; (6) 2.00 to less than 2.25.

   Evolution. Under both analyses, state 0 is a synapomorphy of *Varanus* and state 6 is an autapomorphy of *L. borneensis* and of *O. ventralis*. State 2 is an autapomorphy of *C. enneagram-mus* and a synapomorphy of *S. crocodi-lurus* + *B. ammoskius*. Furthermore, the ancestral state for *Xenosaurus* is ambig-uous between state 3 and state 4. Within *Xenosaurus*, state 5 is autapomorphic for *X. newmanorum*, and state 2 is synapo-morphic for *X. agrenon* + *X. rectocol-laris*, with state 1 an autapomorphy of *X. agrenon*. Under Analysis 1, the ancestral state for the entire group is ambiguous among state 1, state 2, and state 3. The ancestral state for Anguimorpha is state 2. State 4 is a synapomorphy of *Xeno-saurus* + Anguidae. Under Analysis 2, the ancestral state for the entire group is ambiguous among state 0, state 1, state 2, state 3, and state 4. The ancestral states for Anguimorpha and Xenosaur-idae are ambiguous among the last three of those states. That for Anguidae + Varanoidea is state 4. The ancestral state for *Xenosaurus* + *R. rugosus* is ambigu-ous between state 3 and state 4.

57. Maxilla: Narial margin of facial process (0) dorsoventrally tall, horizontal portion about as extensive as or less extensive than vertical portion (Fig. 18D); (1) dorsoventrally short, horizontal margin more extensive than vertical portion (Fig. 19A).

   Evolution. Under both analyses, a proportionally short vertical margin is a synapomorphy of *Xenosaurus*. Under Analysis 1, a short vertical margin is a synapomorphy of Varanidae and an autapomorphy of Helodermatidae. Un-der Analysis 2, a short vertical margin is a synapomorphy of Varanoidea.

58. Maxilla: Vertical portion of narial margin of facial process (0) failing to tilt anterodorsally beyond the vertical by more than a few degrees (Fig. 18D); (1) tilting slightly beyond the vertical to form a dorsal overhang of the naris by the facial process with a slight anterior eminence (Fig. 19A); (2) tilting beyond the vertical to form a dorsal overhang with a pronounced but rounded anterior eminence (Fig. 19C); (3) tilting beyond the vertical to form a marked dorsal overhang with a pronounced and sharply pointed anterior eminence (Fig. 19D).

   Variation. Smaller individuals of *X. rackhami* do not show as much anterior projection of the overhang as large adults, which were scored.

   Evolution. Under both analyses, a slight overhang is a synapomorphy of *Xenosaurus*, a moderately pronounced overhang is a synapomorphy of *X. rackhami* + *X. grandis*, and a very pronounced overhang is an autapomor-phy of *X. grandis*.

59. Maxilla: Posterior portion of nasal facet upon facial process (0) curving smoothly in transverse plane, following general curvature of facial process (Fig. 18C); (1) distinctly folded toward the vertical relative to remainder of facial process, forming an upturned posterior tab of the nasal facet (Fig. 18D).

   Evolution. Under Analysis 1, the upturned tab is a synapomorphy of *Xenosaurus* + *R. rugosus* and of *S. crocodilurus* + *B. ammoskius*. Under Analysis 2, the upturned tab is a synapomorphy of Xenosauridae.

60. Maxilla: Highest point of facial process: (0) prominent, posterior corner between
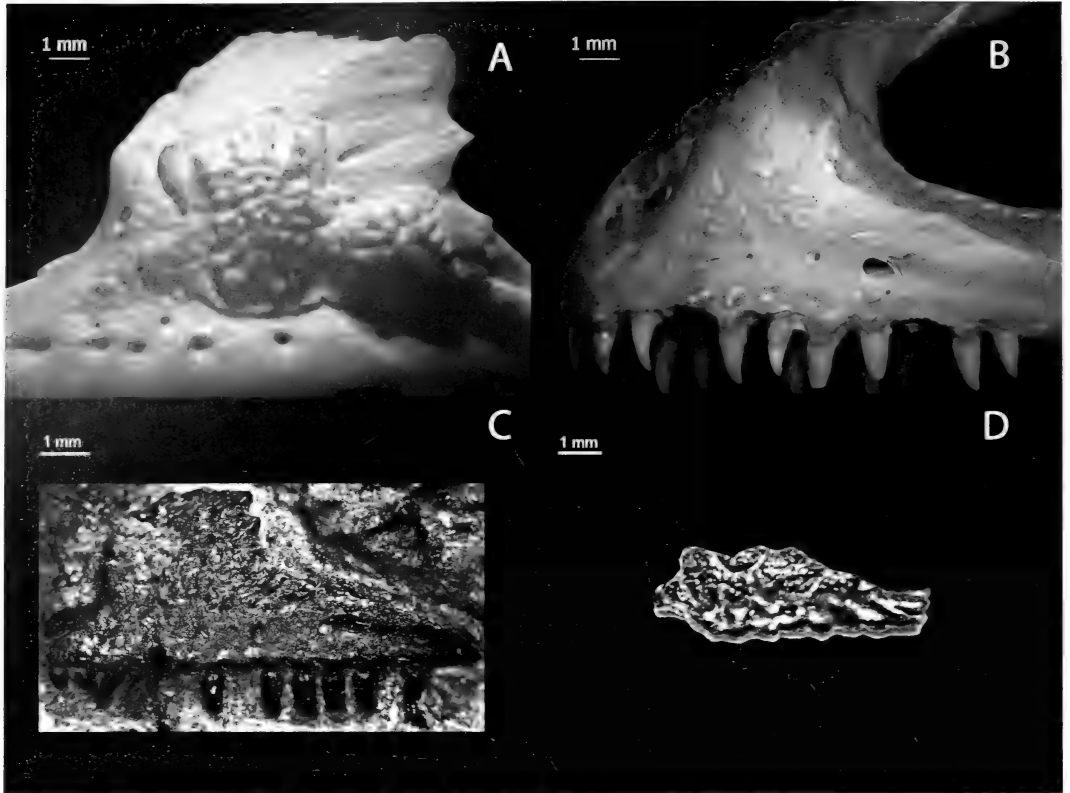
Figure 20.   A, Left maxilla of *Heloderma suspectum* TMM-M 9001, lateral, anterior to the left. Illustrates character 61(1). B, Left maxilla of *Shinisaurus crocodilurus* MVZ 204291, lateral, anterior to the left. Illustrates characters 62(0), 118(1). C, Left maxilla of *Restes rugosus* YPM PU 14640, lateral, anterior to the left. Illustrates character 62(2). D, Fragmentary left maxilla of *Exostinus lancensis* AMNH 8498, lateral, anterior to the left. Illustrates character 62(3).

prefrontal facet and orbital (posterior) edge (Fig. 16C); (1) dorsal edge of facial process nearly horizontal (Fig. 17A); (2) upturned tab of nasal facet (Fig. 16B).

Evolution. Under both analyses, the ancestral state for the entire group is for the highest point to be the corner between the prefrontal facet and orbital edge. The ancestral state for *Xenosaurus* + *R. rugosus* is a horizontal dorsal edge of the facial process, with the upturned tab of the nasal facet the highest point autapomorphically in *E. serratus* and *X. rectocollaris*. The corner between the prefrontal facet and orbital edge the highest point synapomorphically in the northern clade of *Xenosaurus*. Under

Analysis 1, the ancestral state for Anguidae + *Xenosaurus* is ambiguous between the prefrontal facet/orbital edge corner and a horizontal dorsal edge, as is the ancestral state for Anguidae + Helodermatidae. A horizontal dorsal edge is an autapomorphy of *L. borneensis*. Under Analysis 2, a horizontal dorsal edge is a synapomorphy of *Xenosaurus* + *R. rugosus*, and the ancestral state for Varanoidea is ambiguous between the prefrontal facet/orbital edge corner and a horizontal dorsal edge.

61. Maxilla: Canthal crest (0) absent (Fig. 18C); (1) minimally developed: abrupt medial fold of facial process, but no projecting ridge (Fig. 20A); (2)

projecting as a low ridge (Fig. 19A); (3) projecting as an extensive, strong ridge (Fig. 18D).

Variation. The crest, when present, becomes somewhat stronger with age, and the scoring here represents the condition in relatively large individuals.

Evolution. Under both analyses, the ancestral state for the entire group is ambiguous between slight and moderate development of the crest. The ancestral state for Anguimorpha is moderate development. Also under both analyses, lack of a crest is a synapomorphy of Anguidae, a moderately developed crest is an autapomorphy of *X. platyceps*, and an extensive crest is an autapomorphy of *E. serratus*. Under Analysis 1, the ancestral state for *S. crocodilurus* + Varanidae is ambiguous between lack of a crest and slight development. Under Analysis 2, lack of a crest is a synapomorphy of *S. crocodilurus* + *M. ornatus* and of *Varanus*.

62. Maxilla: Osteoderms upon facial process (0) absent (Fig. 20B); (1) present as nearly continuous sculptured plate or a small number of rectangular plates (Fig. 18C); (2) present as sculptured plate with sculpture concentrated into low mounds (Fig. 20C); (3) present as several low, polygonal (generally more edges than rectangles) tesserae (Fig. 20D); (4) present as pronounced mounds (Fig. 18D). This character was described and scored as "rugosity absent or present" by Conrad (2005, 2008).

Variation. Fusion of osteoderms to dermal elements proceeds during postnatal ontogeny, and mound-shaped osteoderms develop from flat lattices of bone (personal observation). Thus, relatively large individuals were scored.

Evolution. Under both analyses, the ancestral state for the entire group and for Anguimorpha is no osteodermal fusion. The ancestral state for *Xenosaurus* + *R. rugosus* is a sculptured plate concentrated into scattered low mounds. The low, polygonal, tesselated morphology is a synapomorphy of *E. lancensis* + *Xenosaurus,* and the pronounced mound-shaped morphology is a synapomorphy of *E. serratus* + *Xenosaurus* and an autapomorphy of Helodermatidae. The latter result is consistent with the presence of low, polygonal tesserae instead of pronounced mounds in primitive helodermatids (Hoffstetter, 1957). Under Analysis 1, the ancestral state for Anguidae + *Xenosaurus* is ambiguous among all four states. The ancestral state for Anguidae is ambiguous between state 0 and state 1. Under Analysis 2, the ancestral state for Xenosauridae is the absence of fused osteoderms; presence of a few large sculptured plates is an autapomorphy of *E. multicarinata*. Note, however, that the apparently primitive (Conrad, 2005, 2008) glyptosaurid anguids generally have large sculptured plate-like osteoderms fused to the facial process (Meszoely, 1970; personal observation).

63. Maxilla: Tooth height (0) short, less than half of tooth extending beyond margin of bone (Fig. 16B); (1) tall, half or more of tooth extending beyond margin of bone (Fig. 16A).

Evolution. Under both analyses, the ancestral state is ambiguous at all nodes whose branches have mixed states. However, this is largely a result of incomplete taxon sampling, as few non-anguimorph squamates have tall teeth.

64. Maxilla: Tooth count (average, rounded to nearest integer) (0) 7; (1) 8; (2) 9; (3) 10; (4) 11; (5) 12; (6) 13; (7) 14; (8) 15; (9) 16; (A) 17; (B) 18.

Variation. As noted, average values were scored. Ontogenetic increase in tooth number was previously documented for some squamates (Edmund, 1969; Ananjeva et al., 2003), but it was not in abundant evidence for the taxa I examined.
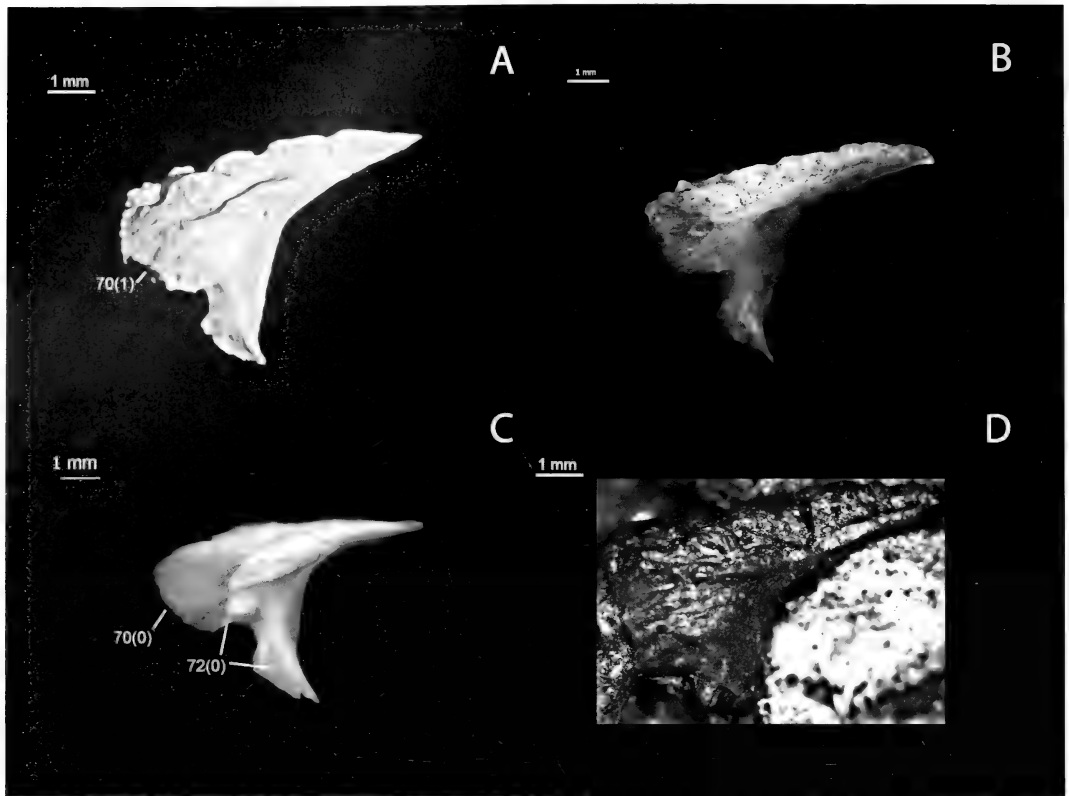
Figure 21.   A, Left prefrontal of *Exostinus serratus*, CT scan of USNM v16565 lateral, anterior to the left. Illustrates characters 65(0), 68(2), 69(2), 70(1), 71(1). B, Left prefrontal of *Xenosaurus grandis* NAUQSP-JIM 1460, lateral, anterior to the left. Illustrates characters 65(1), 68(0). C, Left prefrontal of *Elgaria multicarinata* TMM-M 8958, lateral, anterior to the left. Illustrates characters 66(0), 69(0), 70(0), 71(0), 72(0). D, Left prefrontal of *Restes rugosus* YPM PU 14640, lateral, anterior to the left. Illustrates characters 66(1), 69(1).

Evolution. Under both analyses, a count of seven is an autapomorphy of Helodermatidae, nine is an autapomorphy of *V. exanthematicus*, 12 is an autapomorphy of *E. serratus* and *S. crocodilurus*, and 17 is an autapomorphy of *E. multicarinata*. Additionally, a count of 16 is a synapomorphy of *Xenosaurus* and a count of 18 is a synapomorphy of the northern clade of *Xenosaurus*, as well as an autapomorphy of *X. rectocollaris*. Under Analysis 1, the ancestral state for the entire group is ambiguous from 13 to 16, and that for Anguimorpha is ambiguous between 13 and 14. The ancestral state for *S. crocodilurus* + Varanidae is ambiguous from 12 to 14, and a count of 15 is an autapomorphy of *B. ammoskius*. A count of 11 is a

synapomorphy of Varanidae. Along the other major anguimorph lineage, a count of 16 is a synapomorphy of *E. multicarinata* + *O. ventralis*. Under Analysis 2, the primitive state for the entire group is ambiguous from 14 to 16. A count of 11 is a synapomorphy of Varanoidea.

Prefrontal

The prefrontal is unknown for *E. lancensis* and *M. ornatus*.

65. Prefrontal: Frontal process (0) relatively short and broad-based at divergence from main body of prefrontal, about twice as long along long axis as wide at base perpendicular to long axis (Fig. 21A); (1) relatively long and nar-
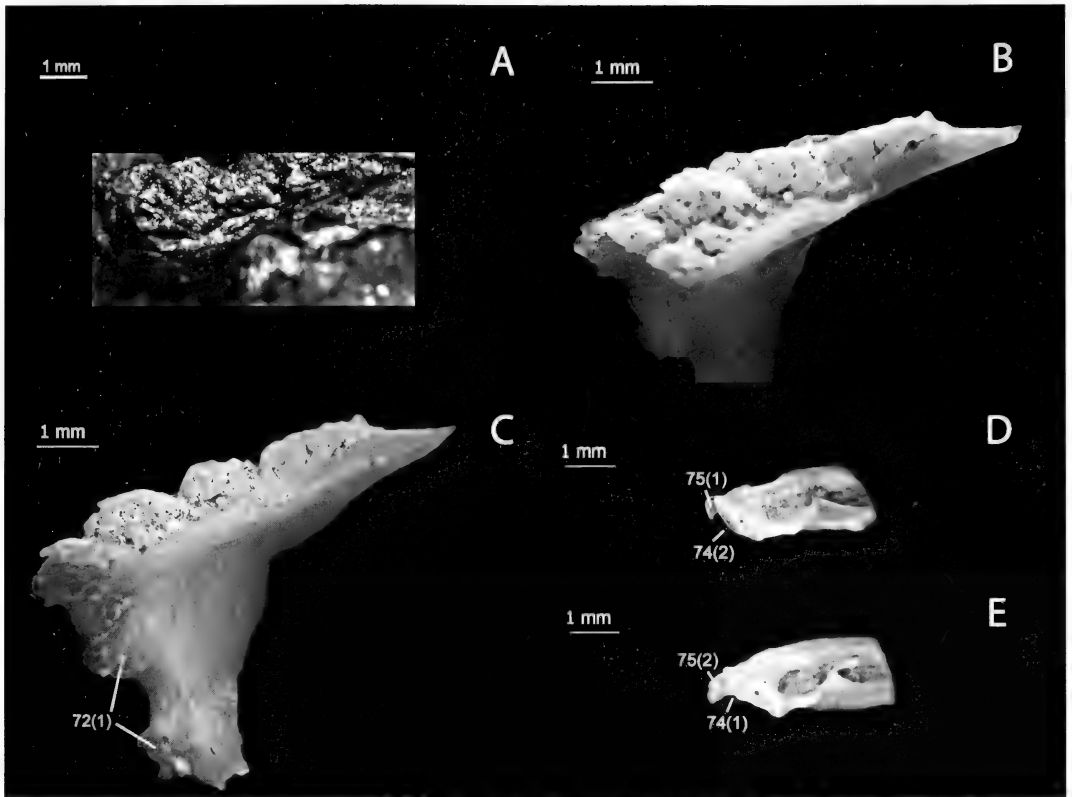
Figure 22.　A, Left prefrontal of *Restes rugosus* YPM PU 14640, dorsal, anterior to the left. Illustrates characters 67(1), 68(1). B, Left prefrontal of *Xenosaurus newmanorum* NAUQSP-JIM uncatalogued specimen, dorsolateral, anterior to the left. Illustrates character 68(3). C, Left prefrontal of *Xenosaurus newmanorum* NAUQSP-JIM uncatalogued specimen, lateral, anterior to the left. Illustrates character 72(1). D, Left vomer of *Xenosaurus grandis* NAUQSP-JIM 1460, dorsolateral, anterior to the left. E, Left vomer of *Xenosaurus newmanorum* NAUQSP-JIM uncatalogued specimen, same view. D and E illustrate characters 73(0), 73(1), 74(1), 74(2), 75(1), 76(2).

row-based, about two-and-a-half times as long as wide (Fig. 21B).

Variation. The frontal process becomes relatively shorter and more stout with age, and this character was scored on relatively large individuals. Large adults were available for all taxa scored as having long frontal processes.

Evolution. Under both analyses, a long frontal process is an autapomorphy of *O. ventralis* and of *X. newmanorum* and a synapomorphy of *X. grandis* + *X. rackhami.*

66. Prefrontal: Row of osteoderms along lateral edge of dermal surface (0) absent (Fig. 21C); (1) present (Fig. 21D).

Variation. Osteoderms fuse to the prefrontal postnatally.

Evolution. Under Analysis 1, presence of a lateral row of osteoderms is a synapomorphy of *S. crocodilurus* + *B. ammoskius* and of *Xenosaurus* + *R. rugosus.* Under Analysis 2, presence of the lateral row is a synapomorphy of Xenosauridae.

67. Prefrontal: Distinct osteodermal pattern of two small osteoderms adjacent to nasal facet and longer, lateral row of four with anteriormost laterally displaced, (0) absent (Fig. 12B); (1) present (Fig. 22A).

Variation. Osteoderms fuse to the prefrontal postnatally.

Evolution. Under both analyses, the "two and four" pattern is a synapomorphy of *Xenosaurus + R. rugosus.*

68. Prefrontal: Osteoderms (0) low, barely domed, with flat appearance (Fig. 21B); (1) moderately pronounced, with some doming (Fig. 22A); (2) pronounced with domes and low keels (Fig. 21A); (3) pronounced with high domes and sharp keels (Fig. 22B).

    Variation. Osteoderms become more domed during postnatal ontogeny, but as mentioned in the description for character 13, the keel forms early.

    Evolution. Under both analyses, the moderately pronounced morphology is ancestral. The low, barely domed morphology is a synapomorphy of *S. crocodilurus + B. ammoskius.* The ancestral states for *Xenosaurus + E. serratus* and for *Xenosaurus* are ambiguous between the moderately pronounced morphology and the domed and moderately keeled morphology. The low morphology is a synapomorphy of the southern clade of *Xenosaurus* and the highly domed and highly keeled morphology a synapomorphy of the northern clade.

69. Prefrontal: Canthal crest (0) absent (Fig. 21C); (1) present as distinct ridge (Fig. 21D); (2) present as sharp, pronounced ridge (Fig. 21A).

    Evolution. Under both analyses, a sharp, pronounced morphology is an autapomorphy of *E. serratus.* Under Analysis 1, a distinct crest is a synapomorphy of *S. crocodilurus + B. ammoskius* and of *Xenosaurus + R. rugosus.* Under Analysis 2, it is a synapomorphy of Xenosauridae.

70. Prefrontal: Emargination or straight edge in maxillary flange (0) dorsoventrally extensive, representing over half of entire edge length of flange (Fig. 21C); (1) dorsoventrally restricted, less than half of entire edge length (Fig. 21A).

Variation. The maxillary flange is extremely thin early in postnatal ontogeny, and in young individuals, it may be damaged or only partially ossified. This character is best scored on relatively large individuals.

Evolution. Under both analyses, the restricted morphology is an autapomorphy of *E. serratus* and of Helodermatidae.

71. Prefrontal: Lacrimal foramen (0) relatively unconstricted, margins remain divergent (Fig. 21C); (1) relatively constricted, margins become nearly parallel (Fig. 21A).

    Evolution. Under both analyses, the parallel morphology is an autapomorphy of *E. serratus.*

72. Prefrontal: Lacrimal facets (0) relatively smooth (Fig. 21C); (1) adorned with complex ridges and bumps (Fig. 22C).

    Variation. When the complex adorned morphology is present, it tends to be more pronounced in older individuals.

    Evolution. Under both analyses, the adorned morphology is a synapomorphy of *Xenosaurus + R. rugosus.*

Vomer

The vomer is unknown in *E. serratus, E. lancensis, R. rugosus,* and *M. ornatus.* It is not visible in the single known specimen of *B. ammoskius* (Conrad, 2006).

73. Vomer: Anterior facet for medial premaxillary process of maxilla (0) less than three times as long along its long axis as tall perpendicular to long axis (Fig. 22D); (1) three or more times as long as tall (Fig. 22E).

    Evolution. Under both analyses, the elongated morphology is a synapomorphy of the northern clade of *Xenosaurus.*

74. Vomer: Anterior facet for medial premaxillary process of maxilla (0) abruptly diverging ascending portion of ventral edge absent (Fig. 23A); (1) abruptly
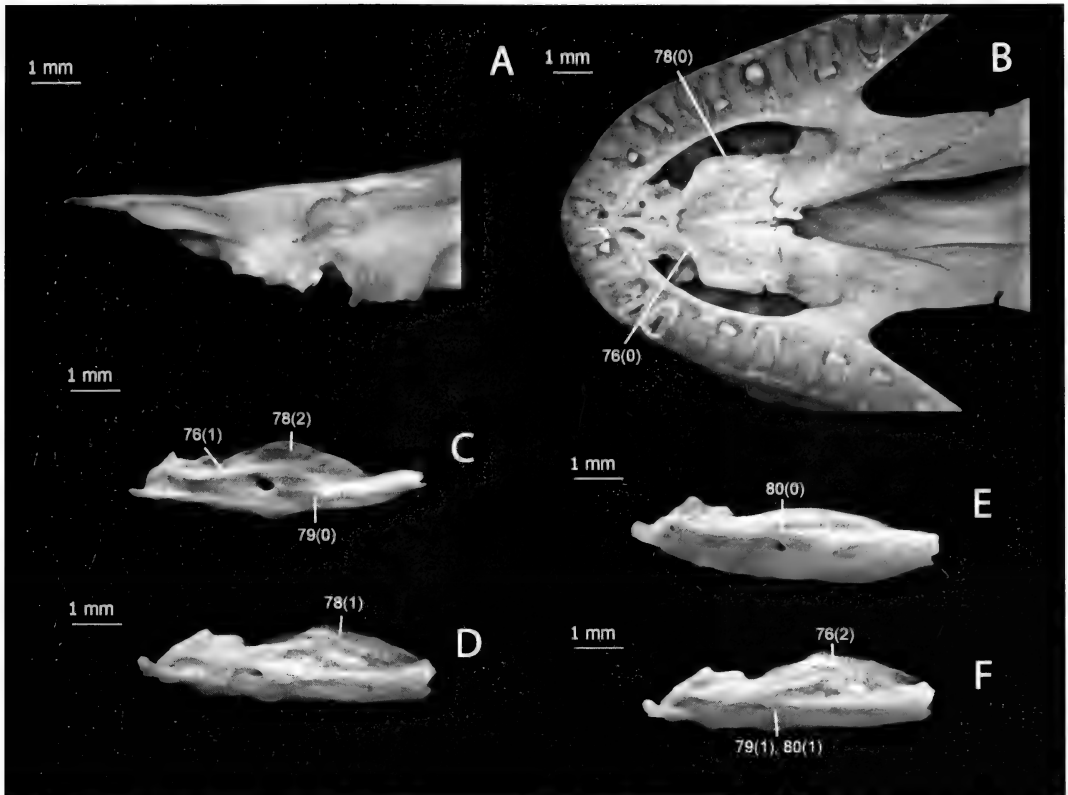
Figure 23. A, Left vomer of *Varanus exanthematicus* TMM-M 8956, dorsolateral, anterior to the left. Illustrates characters 74(0), 75(0). B, Rostrum of *Pristidactylus torquatus* CAS 85234, ventral, anterior to the left. Illustrates characters 76(0), 78(0), 87(0). C, Left vomer of *Xenosaurus rackhami* UTEP-OC "MALB" 388, ventromedial, anterior to the left. D, Left vomer of *Xenosaurus platyceps* UF 45622, same view. C and D illustrate characters 76(1), 77(0), 78(1), 78(2), 79(0), 81(0), 81(1), 82(0), 82(1), 83(0), 83(1). E, Left vomer of *Xenosaurus newmanorum* NAUQSP-JIM uncatalogued specimen, same view. F, Left vomer of *Xenosaurus platyceps* UF 45622, same view. E and F illustrate characters 76(2), 79(1), 80(0), 80(1).

diverging ascending portion of ventral edge relatively short, beginning over halfway to medial limit of facet (Fig. 22E); (2) ascending portion relatively long, beginning less than halfway to medial limit of facet (Fig. 22D).

Evolution. Under both analyses, the ancestral states for the entire group and for Anguimorpha are ambiguous between absence and the short morphology. The ancestral state for the southern clade of *Xenosaurus* is ambiguous between the short and long morphologies, and the long morphology is an autapomorphy of *E. multicarinata*. Under Analysis 1, the ancestral state for *S. crocodilurus* +

Varanidae is ambiguous between absence and the short morphology. The ancestral state for Varanidae is absence. Along the other major branch of Anguimorpha, the ancestral state for *Xenosaurus* + Anguidae is ambiguous between absence and the short morphology, but the short morphology is the ancestral state for *Xenosaurus* and for Anguidae.

75. Vomer: Anterior process from anteromedial corner (0) absent (Fig. 23A); (1) present, short—about as long along long axis as wide perpendicular to it (Fig. 22D); (2) present, long—longer along long axis than wide perpendicular to long axis (Fig. 22E).

Evolution. Under both analyses, presence of a short process is a synapomorphy of *Xenosaurus*, and a long process is a synapomorphy of the northern clade of *Xenosaurus*.

76. Vomer: Lateral parasagittal crest on ventral surface (0) short, extends about a third of the way to the back of the vomer (Fig. 23B); (1) intermediate length, extends about half of the way to the back of the vomer (Fig. 23C); (2) long, extends about two-thirds of the way to the back of the vomer (Fig. 23F).

Evolution. Under both analyses, the ancestral state for the entire group is ambiguous between short and intermediate length. The ancestral state for *Xenosaurus* is the intermediate morphology, with the short morphology an autapomorphy of *X. agrenon* and the long morphology a synapomorphy of the northern clade. Under Analysis 1, the ancestral state for Anguimorpha is ambiguous between short and intermediate length. The ancestral state for *Xenosaurus* + Anguidae is intermediate length, that for Anguidae is ambiguous between intermediate length and the long morphology, and that for Varanidae is the short morphology. Under Analysis 2, intermediate length is ancestral for Anguimorpha. The long morphology is a synapomorphy of *O. ventralis* + *C. enneagrammus*, and the short morphology is a synapomorphy of Varanidae.

77. Vomer: Lateral parasagittal crest (0) extends largely dorsoventrally (Fig. 23C); (1) folds medially as a tall flange, underhanging much of the vomer (Fig. 24A).

Evolution. Under both analyses, the medial folding is an autapomorphy of *X. agrenon*.

78. Vomer: Mediolateral width of lateral flange bordered medially by lateral parasagittal crest at widest anteroposterior level (0) narrow, less than half that of remainder of vomer (Fig. 23B); (1) intermediate, one half of that of remainder of vomer to just under equal to that of remainder of vomer (Fig. 23D); (2) wide, equal to or wider than that of remainder of vomer (Fig. 23C).

Evolution. Under both analyses, the narrow morphology is ancestral for the entire group and for Anguimorpha. The intermediate morphology is ancestral for *Xenosaurus* and the wide morphology is a synapomorphy of the southern clade of *Xenosaurus*. Under Analysis 1, the ancestral state for *Xenosaurus* + Anguidae is ambiguous between narrow and intermediate, and the ancestral state for Anguidae is ambiguous between intermediate and wide. Under Analysis 2, the ancestral state for Anguidae + Varanoidea and for Xenosauridae is narrow, making the intermediate morphology a synapomorphy of Anguidae and the wide a synapomorphy of *O. ventralis* + *C. enneagrammus*.

79. Vomer: Medial parasagittal crest (0) ends posterior to vomerine foramen (Fig. 23C); (1) ends at level of, or anterior to, vomerine foramen (Fig. 23F).

Evolution. Under both analyses, termination at or anterior to the vomerine foramen is a synapomorphy of the northern clade of *Xenosaurus*.

80. Vomer: Medial parasagittal crest extending to or past level of vomerine foramen (0) passes lateral to foramen (Fig. 23E); (1) passes medial to foramen (Fig. 23F).

Evolution. Given the restricted distribution of the character states, it is impossible to infer the ancestral state of this character.

81. Vomer: Vomerine foramen (0) small, mediolateral width less than one-eighth mediolateral width of vomer at same level (Fig. 23D); (1) large, mediolateral width one-eighth mediolateral width of vomer at same level or greater (Fig. 23C).
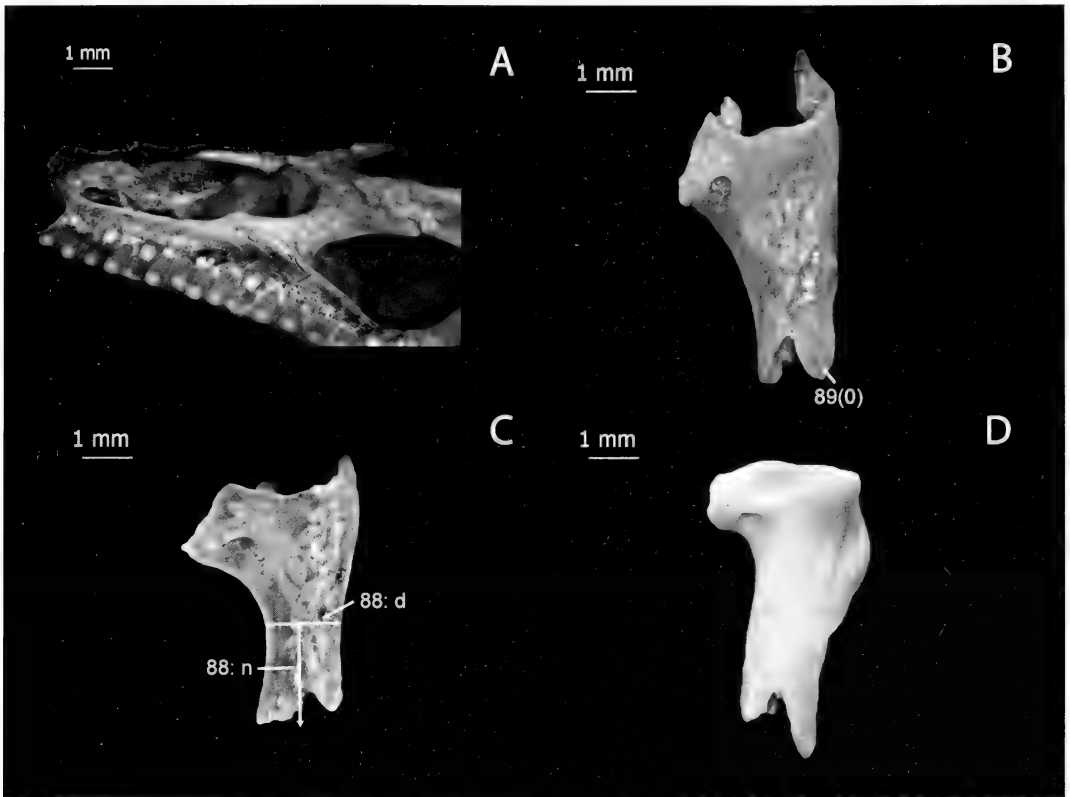
Figure 24.   A, Rostrum of *Xenosaurus agrenon* UTACV r45008, ventral, anterior to the left. Illustrates character 77(1). B, Left palatine of *Xenosaurus newmanorum* NAUQSP-JIM uncatalogued specimen, dorsal, anterior to the top. C, Left palatine of *Xenosaurus grandis* NAUQSP-JIM 1460, same view. D, Left palatine of *Elgaria multicarinata* TMM-M 8958, same view. B through D illustrate characters 84(0), 84(1), 85(0), 85(1), 85(2), 86(0), 86(1), 88 (n for numerator, d for denominator), 89(0).

Evolution. Under both analyses, a large foramen is an autapomorphy of *X. rackhami.*

82. Vomer: Posterior end of palatine process (0) nearly straight in horizontal plane (Fig. 23D); (1) bowed laterally (Fig. 23C).

   Evolution. Under both analyses, lateral bowing is a synapomorphy of *X. grandis + X. rackhami.*

83. Vomer: Palatine process, width measured by ratio of mediolateral width to widest mediolateral width of vomer, (0) mediolaterally wide, ratio 0.44 or greater (Fig. 23D); (1) mediolaterally narrow, ratio less than 0.44 (Fig. 23C).

   Evolution. Under both analyses, the ancestral state for the entire group is

the wide morphology, as is that for Anguimorpha. The ancestral state for the southern clade of *Xenosaurus* is ambiguous, with the narrow morphology either a synapomorphy of the entire clade and the wide morphology an autapomorphy of *X. rectocollaris* or the narrow morphology an autapomorphy of *X. agrenon* and a synapomorphy of *X. grandis + X. rackhami.* Under Analysis 1, the narrow morphology is an autapomorphy of *S. crocodilurus.* Under Analysis 2, the ancestral state for Xenosauridae is ambiguous.

Palatine

   The palatine is unknown in *E. serratus, E. lancensis, R. rugosus,* and *M. ornatus.* It is

not visible in the single known specimen of *B. ammoskius* (Conrad, 2006).

84. Palatine: Choanal margin (0) straight or convex anteriorly in horizontal plane (Fig. 24D); (1) concave anteriorly in horizontal plane (Fig. 24C).

Evolution. Under both analyses, anterior concavity is a synapomorphy of the northern clade of *Xenosaurus* and an autapomorphy of *X. grandis*. Under Analysis 1, anterior concavity is an autapomorphy of Helodermatidae and of *L. borneensis*. Under Analysis 2, the ancestral states for Varanoidea and Varanidae are ambiguous, with anterior concavity either a synapomorphy of Varanoidea and convexity or linearity a synapomorphy of *Varanus* or anterior concavity an autapomorphy of Helodermatidae and *L. borneensis*.

85. Palatine: Eminence in choanal margin (0) absent (Fig. 24D); (1) small and located medial to the mediolateral midpoint of the margin (Fig. 24C); (2) large, broadly curved, and located around the mediolateral midpoint of the margin (Fig. 24B).

Evolution. Under both analyses, absence of the eminence is ancestral for the entire group and the small, medial morphology is a synapomorphy of *Xenosaurus*. The large, broad morphology is a synapomorphy of the northern clade of *Xenosaurus*.

86. Palatine: Maxillary process (0) about as anteroposteriorly long as mediolaterally wide (Fig. 24D); (1) distinctly anteroposteriorly longer than mediolaterally wide (Fig. 24C).

Evolution. Under both analyses, the longer-than-wide morphology is a synapomorphy of *Xenosaurus*.

87. Palatine: Pterygoid process ventral surface (0) bearing teeth (Fig. 23B); (1) bearing midline ridge or groove (Fig. 5B); (2) smooth (Fig. 25A). Presence or absence

of palatine teeth was character 82 of Estes et al. (1988).

Variation. I did not have ontogenetic series for taxa that possess palatine teeth, but the palatal teeth upon the pterygoid of *E. multicarinata* increase in number during postnatal ontogeny.

Evolution. Under both analyses, the ancestral state for the entire group is ambiguous among the three states, but the ancestral state for Anguimorpha is absence of teeth and ridges. The presence of ridges in *X. rectocollaris*, and of teeth in *O. ventralis* and *L. borneensis*, is autapomorphic for each of these taxa.

88. Palatine: Pterygoid process, ratio of length along long axis beginning at posterior end of base of vomerine process to width perpendicular to long axis at constriction behind base of vomerine process (Fig. 24C) (0) 1.1 or less; (1) greater than 1.1 to 1.2; (2) greater than 1.2 to 1.3; (3) greater than 1.3 to 1.4; (4) greater than 1.4 to 1.5; (5) greater than 1.5.

Variation. The pterygoid process in some but not all taxa becomes relatively wider with age, and all scorings were performed on relatively large individuals.

Evolution. Under both analyses, the ancestral state for *Xenosaurus* is ambiguous between state 1 and state 2. State 0 is a synapomorphy of *X. agrenon* + *X. rectocollaris,* and state 4 is an autapomorphy of *X. rackhami.* Under Analysis 1, the ancestral state for the entire group is ambiguous among all states, as is that for Anguimorpha and *Xenosaurus* + Anguidae, as well as *Shinisaurus* + Varanidae. State 0 is a synapomorphy of Varanidae and an autapomorphy of Helodermatidae. Under Analysis 2, state 5 is ancestral for the entire group, Anguidae + Varanoidea, and Xenosauridae. State 0 is a synapomorphy of Varanoidea.
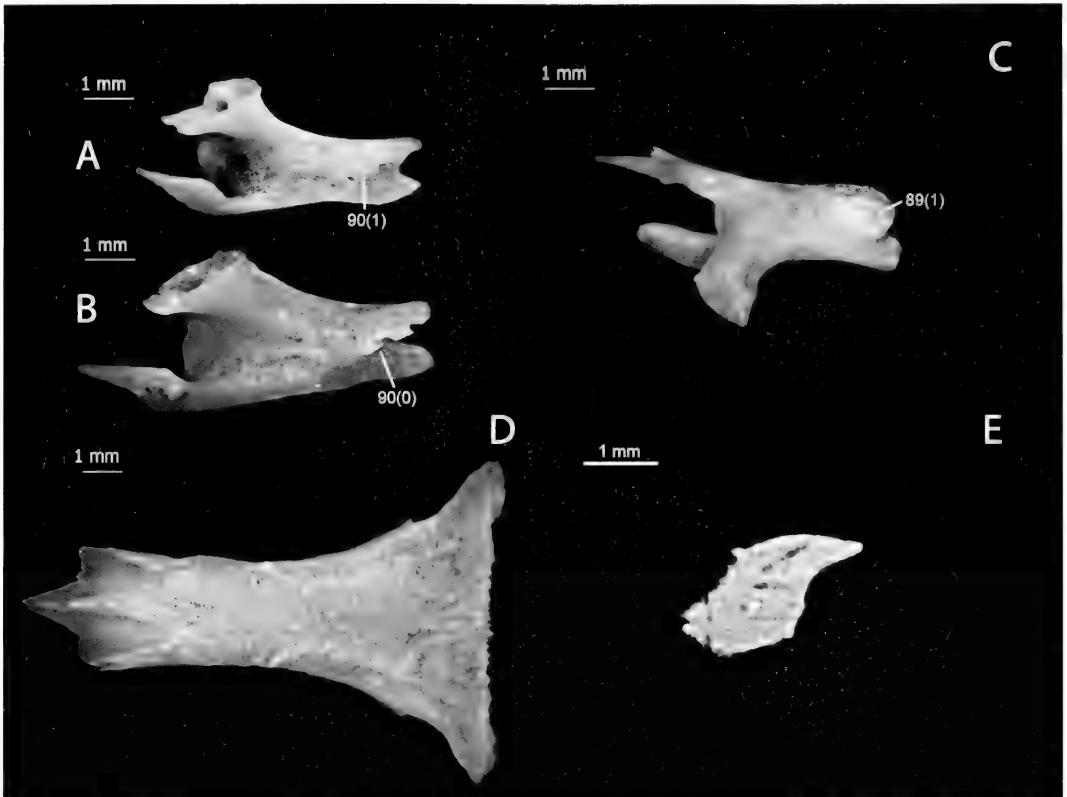
Figure 25.   A, Left palatine of *Xenosaurus rackhami* UTEP-OC "MALB" 388, ventral, anterior to the left. B, Left palatine of *Xenosaurus newmanorum* NAUQSP-JIM uncatalogued specimen, same view as A. A and B illustrate characters 87(2), 90(0), 90(1). C, Left palatine of *Xenosaurus platyceps* UF 45622, dorsal, anterior to the left. Illustrates character 89(1). D, Frontal of *Elgaria multicarinata* TMM-M 8958, dorsal, anterior to the left. Illustrates characters 91(0), 94(0), 97(0), 104(1), 108(0). E, Anterior tip of frontal of *Exostinus serratus*, CT scan of USNM v16565, ventral, anterior to the left. Illustrates character 93(0).

89. Palatine: Dorsomedial tongue for pterygoid articulation (0) anteroposteriorly longer than mediolaterally wide at base (Fig. 24B); (1) mediolaterally wider at base than long (Fig. 25C).

   Evolution. Under both analyses, the wider-than-long morphology is anautapomorphy of *X. platyceps*. Under Analysis 1, the wider-than-long morphology is a synapomorphy of Varanidae and an autapomorphy of Helodermatidae. Under Analysis 2, it is a synapomorphy of Varanoidea.

90. Palatine: Anterior to mediolateral divergence of dorsomedial and ventrolateral tongues for pterygoid articulation, medial edge of dorsoventrally diverging ventrolateral tongue (0) raised into sharp, underhanging ridge (Fig. 25B); (1) raised into low ridge with little if any underhang (Fig. 25A).

   Evolution. Under both analyses, the low, rounded morphology is a synapomorphy of the southern clade of *Xenosaurus*.

Frontal

91. Frontal: Frontals (0) remain unfused throughout ontogeny (Estes et al., 1988, Fig. 13B); (1) fuse at some point during ontogeny (Fig. 25D).

   Variation. Frontal fusion occurs during ontogeny; in the taxa (specified in Materials and Methods) for which very

young postnatal specimens were available, a seam and sometimes a split at the anterior end still remained.

Evolution. Under both analyses, the fused morphology is ancestral for the entire group. Under Analysis 1, pairing is a synapomorphy of Varanidae and of Anguidae + Helodermatidae, with the fused morphology an autapomorphy of *E. multicarinata.* Under Analysis 2, the ancestral state for Anguidae + Varanoidea is ambiguous; either the paired morphology is a synapomorphy of that clade, and fused morphology is an autapomorphy of *E. multicarinata,* or the paired morphology is a synapomorphy of *O. ventralis + C. enneagrammus* and of Varanoidea.

92. Frontal: Frontals in taxa where fusion occurs (0) remain separate for some period of time postnatally; (1) fuse prenatally.

Variation. This character depends upon the recognition of ontogenetic variation. It is possible that unrecognized individual variation occurs regarding when and whether fusion occurs, in particular among the extinct taxa.

Evolution. Under both analyses, the ancestral state for the entire group is prenatal fusion. Postnatal fusion is an autapomorphy of *E. lancensis* and of *M. ornatus.*

93. Frontal: In taxa with fused frontals, frontals fuse and raised seam at line of fusion vanishes (0) only at most advanced ontogenetic stages (Fig. 25E); (1) by attainment of approximately two-thirds of "adult" size of frontals (Fig. 17D).

Variation. As noted, this character is scored based on the nature of inferred ontogenetic variation.

Evolution. Under both analyses, the ancestral state for the entire group and for Anguimorpha is early disappearance of the seam. Under Analysis 1,

the ancestral state for *E. lancensis + Xenosaurus* and for *E. serratus + Xenosaurus* is ambiguous, and late disappearance is an autapomorphy of *M. ornatus.* Under Analysis 2, the ancestral state for Xenosauridae is ambiguous.

94. Frontal: Constriction (0) weak, ratio of widest mediolateral width of frontal table anterior to level of greatest constriction to width at greatest constriction less than 1.15 (Fig. 25D); (1) moderate, ratio 1.15 to 1.7; (2) strong, ratio greater than 1.7 (Fig. 26A).

Variation. In many taxa, including *S. crocodilurus,* the frontals in younger individuals are considerably more constricted than in older individuals, concomitant with the relatively larger size of the eyes. Individuals scored here were relatively large adults.

Evolution. Under both analyses, the ancestral state for the entire group and for Anguimorpha is moderate constriction, and weak constriction is an autapomorphy of *S. crocodilurus.* Under Analysis 1, weak constriction is a synapomorphy of Varanidae and of Anguidae + Helodermatidae, and strong constriction is a synapomorphy of *E. serratus + Xenosaurus* and an autapomorphy of *M. ornatus.* Under Analysis 2, weak constriction is a synapomorphy of Anguidae + Varanoidea, and the ancestral state for Xenosauridae is ambiguous between weak and strong constriction.

95. Frontal: Osteoderms (0) lacking keels or with weak keels (Fig. 26A); (1) strongly keeled, at least in part (Fig. 26B).

Variation. Osteoderms fuse to the frontal postnatally in most taxa, but the keel may be the first part of each osteoderm to form.

Evolution. Under both analyses, the keeled morphology is a synapomorphy of the northern clade of *Xenosaurus.*

96. Frontal: Orbital rows of osteoderms along lateral edges (0) flat and rectan-
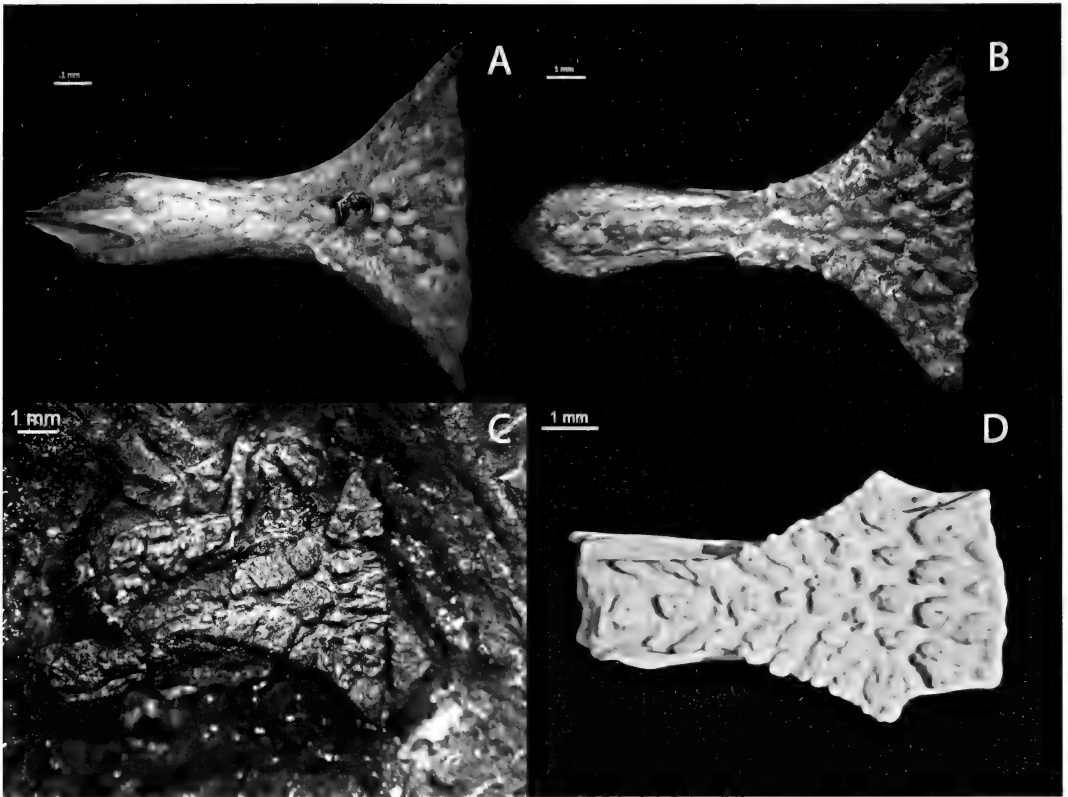
Figure 26.   A, Frontal of *Xenosaurus grandis* NAUQSP-JIM 1460, dorsal, anterior to the left. Illustrates characters 94(2), 95(0), 102(1), 103(1). B, Frontal of *Xenosaurus newmanorum* NAUQSP-JIM uncatalogued specimen, dorsal, anterior to the left. Illustrates characters 95(1), 96(1), 97(3), 98(1), 99(1), 100(0), 102(0), 103(0), 108(1). C, Frontal of *Restes rugosus* YPM PU 14640, dorsal, anterior to the left. Illustrates characters 96(0), 97(2), 98(0), 99(0). D, Frontal of *Exostinus serratus*, CT scan of AMNH 1608, dorsal, anterior to the left. Illustrates characters 98(2), 100(1), 108(2).

gular (Fig. 26C); (1) small and domed (Fig. 26B).

Variation. Osteoderms fuse to the frontal postnatally in most taxa.

Evolution. Under both analyses, the ancestral state for the entire group is ambiguous and the ancestral state for Anguimorpha is flat and rectangular. The domed morphology is a synapomorphy of *E. lancensis* + *Xenosaurus*, and the flat, rectangular morphology is an autapomorphy of *X. rectocollaris*.

97. Frontal: Osteoderms in center of expanded posterior portion of frontal (0) all flat and plate-like (Fig. 25D); (1) some flat and plate-like, others broad and domed (Klembara, 2008); (2) some flat and plate-like,

others small and domed (Fig. 26C); (3) all small and domed (Fig. 26B).

Variation. Osteoderms become fused to the frontal and become more domed during ontogeny.

Evolution. Under both analyses, the ancestral state for the entire group is ambiguous among all three states, and that for Anguimorpha is ambiguous between state 1 and state 2. State 2 is ancestral for *R. rugosus* + *Xenosaurus*, and state 3 is a synapomorphy of *E. lancensis* + *Xenosaurus* and an autapomorphy of *B. ammoskius*. Under Analysis 1, the ancestral states for *S. crocodilurus* + Varanidae and for *Xenosaurus* + Anguidae are ambiguous like Anguimorpha. State 0 is

ancestral for Anguidae + the heloderma-
tid lineage. Under Analysis 2, the ances-
tral state for Xenosauridae is ambiguous
like Anguimorpha, and the ancestral state
for Anguidae + Varanoidea is state 0.

98. Frontal: Region of strong development
of orbital rows of osteoderms along
lateral edges (0) restricted, extending
anteriorly only up to greatest constric-
tion of frontal table or ending posterior
to it (Fig. 26C); (1) intermediate, ex-
tending anteriorly past greatest con-
striction of frontal table and for less
than a third of the length of the
prefrontal facet (Fig. 26B); (2) exten-
sive, extending anteriorly past greatest
constriction of frontal table and for
about a third of the length of the
prefrontal facet (Fig. 26D).

Variation. Osteoderms fuse to the
frontal during postnatal ontogeny.

Evolution. Under both analyses, the
ancestral state for the entire group is a
restricted extent. The intermediate
morphology is a synapomorphy of *S.
crocodilurus* + *B. ammoskius* and of *E.
serratus* + *Xenosaurus*, and the exten-
sive morphology is an autapomorphy of
E. serratus.

99. Frontal: Transverse rows of osteoderms
in posterior expanded portion (0) two to
three (Fig. 26C); (1) four or more
(Fig. 26B).

Evolution. Under both analyses, the
ancestral state for the entire group is
ambiguous, and four or more rows is a
synapomorphy of *E. serratus* + *Xenosaurus*.

100. Frontal: Posteriormost transverse row
of osteoderms in posterior expanded
portion (0) similar in prominence to
more anterior rows (Fig. 26B); (1) less
prominent than more anterior rows
(Fig. 26D).

Variation. No variation affecting scor-
ing was evident, save, most likely, the
ontogenetic variation already noted in
osteoderm characters.

Evolution. Under both analyses, the
reduced prominence of the posterior-
most row is either a synapomorphy of
E. lancensis + *Xenosaurus*, with similar
prominence a synapomorphy of *Xeno-
saurus*, or it is an autapomorphy of *E.
lancensis* and of *E. serratus*.

101. Frontal: Distance from posterior end of
prefrontal facet to posterior end of
frontal (0) relatively great, 2.25 or more
times length of posterior sharply taper-
ing portion of prefrontal facet
(Fig. 27A); (1) relatively small, fewer
than 2.25 times length of posterior
portion of facet (Fig. 27B).

Evolution. Under both analyses, a
relatively small distance is an autapo-
morphy of *E. serratus*. Under Analysis
1, that character state is also an
autapomorphy of Helodermatidae and
a synapomorphy of Varanidae. Under
Analysis 2, it is a synapomorphy of
Varanoidea.

102. Frontal: Anterior mediolaterally ta-
pered tip of frontal (0) mediolaterally
wider at base than anteroposteriorly
long (Fig. 26B); (1) longer than wide
(Fig. 26A).

Evolution. Under both analyses, lon-
ger than wide is a synapomorphy of the
southern clade of *Xenosaurus*.

103. Frontal: Internasal spine (0) closely
approaching anterior tip of frontal
(Fig. 26B); (1) halting posterior to
anterior tip with frontal extending
beyond it for half or more of the length
of the spine, forming an extensive
anterior lamina (Fig. 26A).

Evolution. Under both analyses, a
posterior termination of the spine is a syn-
apomorphy of *X. rackhami* + *X. grandis*.

104. Frontal: Posteriorly, medial and lateral
edges of nasal facets converge (0) at a
relatively wide angle of 70° or greater
(Fig. 27C); (1) at a relatively narrow
angle of less than 70° (Fig. 25D).
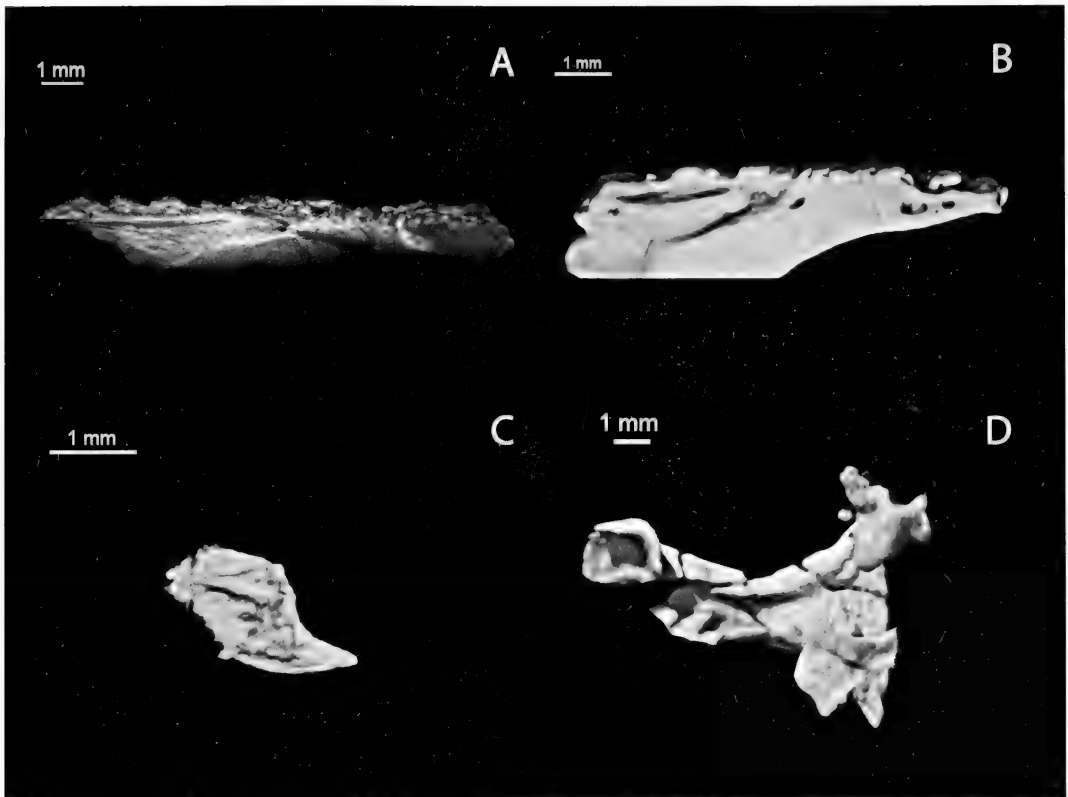
Figure 27.   A, Frontal of *Xenosaurus newmanorum* NAUQSP-JIM uncatalogued specimen, left lateral, anterior to the left. Illustrates characters 101(0), 106(0), 107(0). B, Frontal of *Exostinus serratus*, CT scan of AMNH 1608, left lateral, anterior to the left. Illustrates characters 101(1), 106(1), 107(1). C, Anterior tip of frontal of *Exostinus serratus*, CT scan of USNM v16565, dorsal, anterior to the left. Illustrates character 104(0). D, Frontal of *Restes rugosus*, CT scan of YPM PU 14640, ventral, anterior to the left. Illustrates character 105(0).

Evolution. Under Analysis 1, the ancestral states for all clades with mixed character distribution are ambiguous. Under Analysis 2, the ancestral state for the entire group is a relatively narrow angle, as is that for Anguimorpha. The ancestral state for Xenosauridae is ambiguous. On the other branch of Anguimorpha, the ancestral state for Anguidae + Varanoidea is a relatively narrow angle, with the wider morphology a synapomorphy of *C. enneagrammus + O. ventralis* and an autapomorphy of *Lanthonotus borneensis*.

105. Frontal: Ventral edges of cristae cranii, at closest approach in a horizontal plane, separated by (0) greater than

one-third of the mediolateral width of the frontal at that anteroposterior level (Fig. 27D); (1) one-third or less of the mediolateral width of the frontal (Fig. 28A).

Evolution. Under both analyses, wide separation is the primitive state for the entire group and for Anguimorpha. Under Analysis 1, close approach is a synapomorphy of *S. crocodilurus* + Varanidae and of *E. lancensis* + *Xenosaurus*. Under Analysis 2, close approach is a synapomorphy of Varanidae, and the ancestral state for Xenosauridae is ambiguous.

106. Frontal: Cristae cranii deepen anterior to expanded portion of frontal to (0)
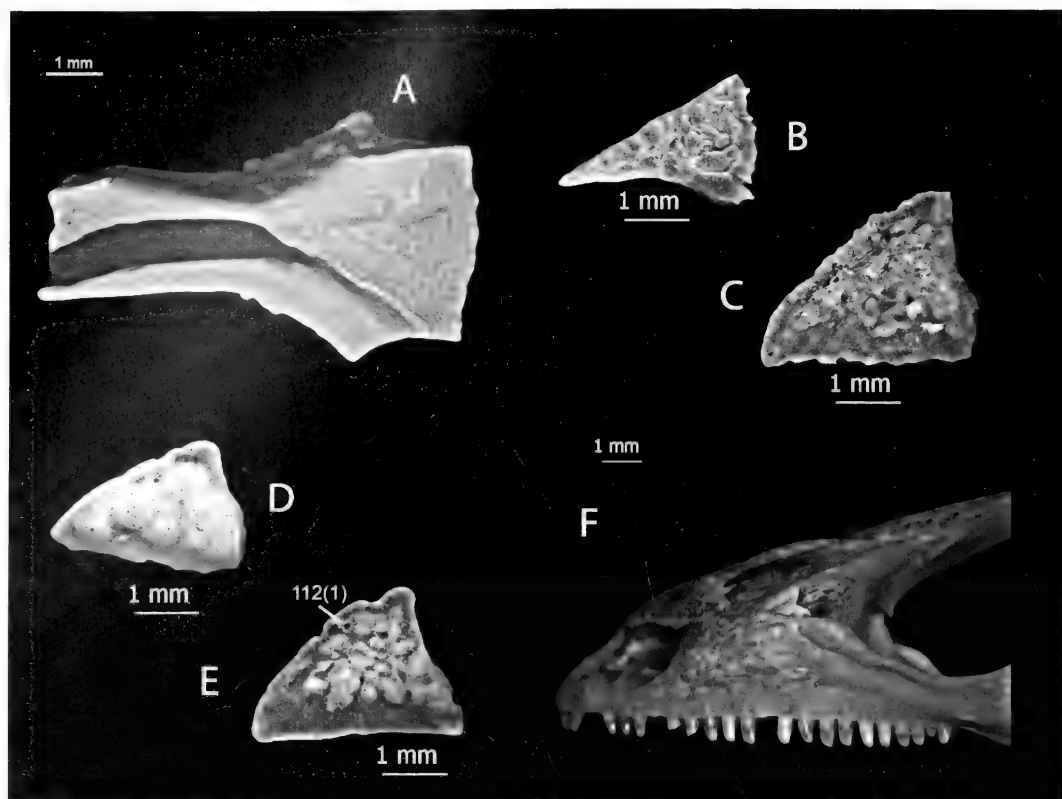
Figure 28.   A, Frontal of *Exostinus serratus*, CT scan of AMNH 1608, ventral, anterior to the left. Illustrates character 105(1). Left palpebrals, dorsal, anterior to the top: B, *Elgaria multicarinata* TMM-M 8958; C, *Xenosaurus newmanorum* NAUQSP-JIM uncatalogued specimen; D, *Xenosaurus agrenon* UTACV r45008; E, *Xenosaurus grandis* NAUQSP-JIM 1460. B through D illustrate characters 109(0), 109(1), 110(0), 110(1), 111(0), 111(1), 112(0), 112(1), 113(0), 113(1). F, Rostrum of *Elgaria multicarinata* CAS 85234, left lateral, anterior to the left. Illustrates character 114(0).

less than twice their dorsoventral height along the expanded portion (Fig. 27A); (1) equal to or greater than twice their dorsoventral height along the expanded portion (Fig. 27B).

Evolution. Under both analyses, shallow cristae cranii are ancestral for the entire group and for Anguimorpha, and the deep morphology is an autapomorphy of *E. lancensis.* Under Analysis 1, the deep morphology is a synapomorphy of Varanidae and of Anguidae + Helodermatidae. Under Analysis 2, the deep morphology is a synapomorphy of Anguidae + Varanoidea.

107. Frontal: Angle of posterior descent of cristae cranii just behind horizontal

portion of ventral edges (0) less than 40° (Fig. 27A); (1) 40° or greater (Fig. 27B).

Evolution. Under both analyses, a steep slope is an autapomorphy of *E. serratus.* Under Analysis 1, a steep slope is a synapomorphy of Varanidae and an autapomorphy of Helodermatidae. Under Analysis 2, it is a synapomorphy of Varanoidea.

108. Frontal: Cristae cranii project laterally beyond dermal table of frontal (0) not at all (Fig. 25D); (1) only in region of greatest constriction (Fig. 26A); (2) extensively beginning in region of greatest constriction and extending nearly to anterior tip of frontal (Fig. 26D).

Evolution. Under both analyses, no projection is the ancestral state for the entire group and for Anguimorpha. Moderate projection is a synapomorphy of *E. serratus* + *Xenosaurus*, and extensive projection is an autapomorphy of *E. serratus* and a synapomorphy of *Varanus*. Under Analysis 1, moderate projection is a synapomorphy of Varanidae and an autapomorphy of Helodermatidae. Under Analysis 2, moderate projection is a synapomorphy of Varanoidea.

Palpebral

The palpebral is unknown for *M. ornatus, B. ammoskius, E. lancensis,* and *E. serratus.* It is absent in *P. torquatus* and Helodermatidae and is so reduced in *L. borneensis* that its morphology in relation to the characters described here is unscorable (Maisano et al., 2002).

109. Palpebral: Overall shape: (0) mediolaterally elongate triangle with lateral constriction caused by step in posterior margin (Fig. 28B); (1) mediolaterally shorter triangle without lateral constriction caused by step in posterior margin (Fig. 28C).

Evolution. Under both analyses, the mediolaterally elongate morphology is a synapomorphy of Anguimorpha, and the more equilateral morphology is a synapomorphy of *R. rugosus* + *Xenosaurus* and an autapomorphy of *O. ventralis.*

110. Palpebral: Posterior edge (0) with relatively straight or smoothly curving margin (Fig. 28E); (1) with wavy margin (Fig. 28D); (2) with ragged margin (Fig. 28C).

Evolution. Under both analyses, the wavy morphology is an autapomorphy of *X. agrenon,* and the ragged morphology is a synapomorphy of the northern clade of *Xenosaurus.*

111. Palpebral: Fused osteoderms (0) absent (Fig. 28B); (1) present as slight dorsal rugosities (Fig. 28E); (2) present across most of dorsal surface; less coverage upon anterior two-thirds and along anterior edge (Fig. 28D); (3) strong across dorsal surface, including anterior portion, with distinct, tall row along anterior edge (Fig. 28C).

Variation. Osteodermal fusion to dermal elements, including the palpebral, occurs postnatally, although relatively small specimens of *X. platyceps* already show some dorsal rugosity.

Evolution. Under both analyses, a slight dorsal rugosity is a synapomorphy of *R. rugosus* + *Xenosaurus*, a moderately strong covering of osteoderms is a synapomorphy of *Xenosaurus*, and a strong covering is a synapomorphy of the northern clade of *Xenosaurus.*

112. Palpebral: Foramen near anterior edge, just lateral to mediolateral level of apex of slight concavity in posterior margin (0) absent (Fig. 28C); (1) present (Fig. 28E).

Evolution. Under both analyses, presence of the foramen is a synapomorphy of *X. rackhami* + *X. grandis.*

113. Palpebral: Strong s-curve to medial edge in horizontal plane, with anterior emargination and posterior bulge accompanied by dorsoventral deepening (0) absent (Fig. 28B); (1) present (Fig. 28D).

Variation. In some large adult *E. multicarinata,* the medial edge of the palpebral displays a slight s-curve, but not to the extent of the taxa scored as (1).

Evolution. Under both analyses, the ancestral state for the entire group is ambiguous, as is that for Anguimorpha. Under Analysis 1, the ancestral state for *R. rugosus* + *Xenosaurus* is presence of the s-curve, with all mixed nodes ambiguous. Under Analysis 2, the ancestral state for Xenosauridae is presence of an s-curve, and that for Anguidae + Varanoidea is absence.

Lacrimal

The lacrimal is unknown for all of the extinct taxa save *B. ammoskius,* but some of
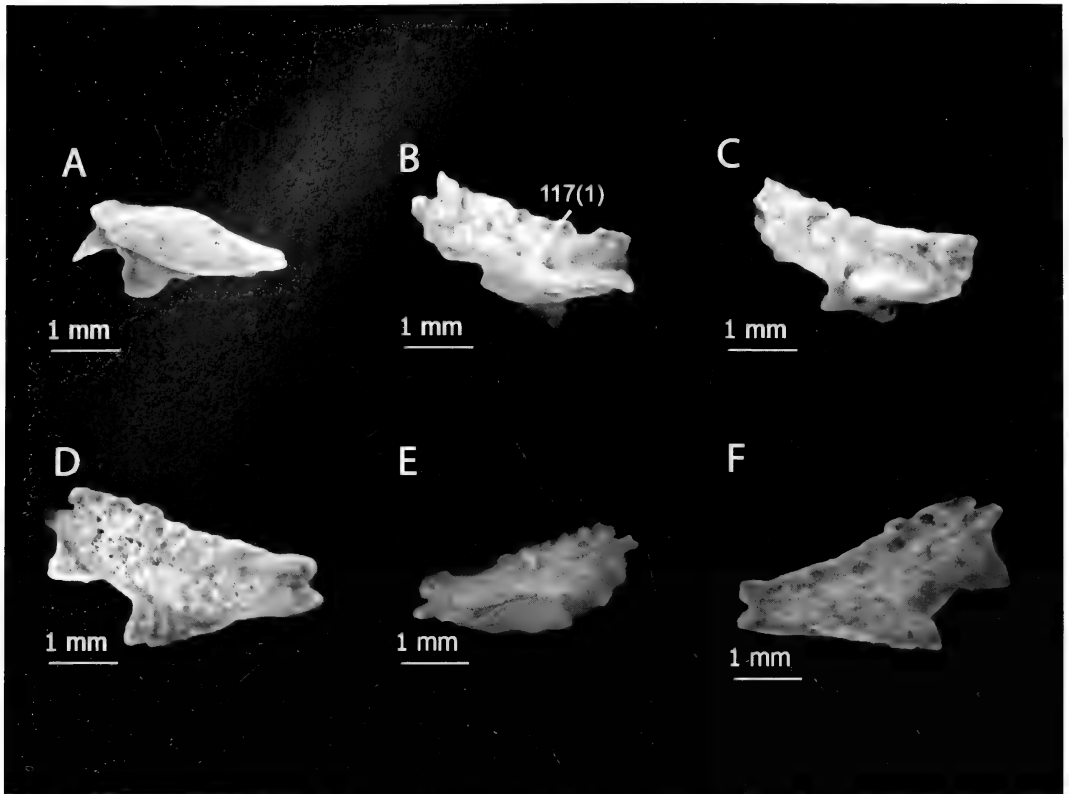
Figure 29.   Left lacrimals, lateral, anterior to the left: A, *Elgaria multicarinata* TMM-M 8958; B, *Xenosaurus newmanorum* NAUQSP-JIM uncatalogued specimen; C, *Xenosaurus agrenon* UTACV r45008; D, *Xenosaurus grandis* NAUQSP-JIM 1460. A through D illustrate characters 115(0), 115(1), 116(0), 116(1), 116(2), 116(3), 117(0), 117(1), 120(0), 120(1), 121(0), 121(1), 122(0), 122(1). Left lacrimals, medial, anterior to the right: E, *Xenosaurus platyceps* UF 45622; F, *Xenosaurus grandis* NAQSP-JIM 1460; E and F illustrate characters 119(0), 119(1), 122(0), 122(1).

its basic dimensions can be inferred from the morphology of the maxilla and prefrontal. This is the method by which character 114 is scored for all taxa.

114. Lacrimal: Size relative to maxilla (0) small, around one-quarter length of maxilla or smaller (Fig. 28F); (1) large, around one-third length of maxilla (Fig. 1C).

   Evolution. Under both analyses, a relatively large lacrimal is a synapomorphy of *R. rugosus* + *Xenosaurus*.

115. Lacrimal: Angle between antorbital and suborbital rami measured along lower margin (0) high, greater than 135° (Fig. 29A); (1) low, less than 135° (Fig. 29C).

   Evolution. Under both analyses, an angle of less than 135° is a synapomorphy of *X. rackhami* + *X. grandis*.

116. Lacrimal: Fused osteoderms (0) absent (Fig. 29A); (1) present as slight rugosities (Fig. 29C); (2) present as low mounds (Fig. 29B); (3) present as tall mounds, some of which bear keels (Fig. 29D).

   Variation. Osteoderms become fused to dermal elements postnatally.

   Evolution. Under both analyses, the presence of fused osteoderms as slight rugosities is a synapomorphy of *Xenosaurus*, low mounds is an autapomorphy of *X. grandis*, and tall, sometimes keeled

mounds is a synapomorphy of the northern clade of *Xenosaurus*.

117. Lacrimal: Subpalpebral fossa (0) absent (Fig. 29A); (1) present (Fig. 29B).

   Evolution. Under Analysis 1, the fossa is a synapomorphy of *Xenosaurus* and of *S. crocodilurus* + *B. ammoskius.* Under Analysis 2, it is a synapomorphy of Xenosauridae.

118. Lacrimal: Subpalpebral fossa (0) contained entirely in lacrimal (Fig. 1C); (1) extending onto adjacent elements (Fig. 20B).

   Evolution. Under both analyses, most nodes optimize ambiguously. The ancestral state for the southern clade of *Xenosaurus* is containment within the lacrimal.

119. Lacrimal: Lacrimal foramen (0) large, expanse at greatest extent is half or more of length of antorbital ramus of lacrimal (Fig. 29F); (1) small, less than half as extensive as antorbital ramus (Fig. 29E).

   Evolution. Under both analyses, the small, constricted morphology is an autapomorphy of *X. platyceps.*

120. Lacrimal: Dorsal and ventral prefrontal processes (0) project as prominent wedges beyond main body of lacrimal in sagittal plane (Fig. 29A); (1) barely project if at all beyond body of lacrimal in sagittal plane (Fig. 29B).

   Evolution. Under both analyses, lack of projection or minor projection is ancestral for the entire group, and projection is an autapomorphy of *X. newmanorum*, *E. multicarinata*, and *X. grandis.* Under Analysis 1, projection is an autapomorphy of Helodermatidae and a synapomorphy of Varanidae. Under Analysis 2, it is a synapomorphy of Varanoidea.

121. Lacrimal: Lacrimal canal (0) deeply incised into medial surface of lacrimal, with strong overhanging and/or underhanging ridges, the latter formed by flange of ventral prefrontal process (Fig. 29A); (1) shallowly incised, with marginal ridges only in anteriormost portion (Fig. 29B).

   Evolution. Under both analyses, the ancestral state for the entire group is ambiguous. Under Analysis 1, shallow incision is ancestral for Anguimorpha, and deep incision is a synapomorphy of Anguidae. Under Analysis 2, the ancestral state for Anguimorpha is ambiguous, as are those for Anguidae + Varanoidea and Varanoidea.

122. Lacrimal: Posteriorly, ventral prefrontal process (0) diminishes mediolaterally (Fig. 29D); (1) expands mediolaterally (Fig. 29B).

   Evolution. Under both analyses, mediolateral expansion along a posterior cline is a synapomorphy of the northern clade of *Xenosaurus.*

Jugal

   The jugal is unknown for *M. ornatus.*

123. Jugal: Postorbital ramus (0) long axis relatively straight (Fig. 3C); (1) long axis broadly curved in sagittal plane (Fig. 5C).

   Evolution. Under both analyses, sagittal curvature is an autapomorphy of *X. rectocollaris.*

124. Jugal: Fused osteoderms or osteodermal sculpturing (0) absent (Fig. 30A); (1) present on ventral two-thirds of postorbital ramus (Fig. 30B); (2) present on all of postorbital ramus (Fig. 30C). This character was scored as presence or absence of sculpturing by Estes et al. (1988).

   Variation. Osteoderms fuse to the jugal during early postnatal ontogeny.

   Evolution. Under both analyses, the ancestral state for the entire group and for Anguimorpha is a lack of sculpturing or fused osteoderms and that for *R. rugosus* + *Xenosaurus* is partial cover-
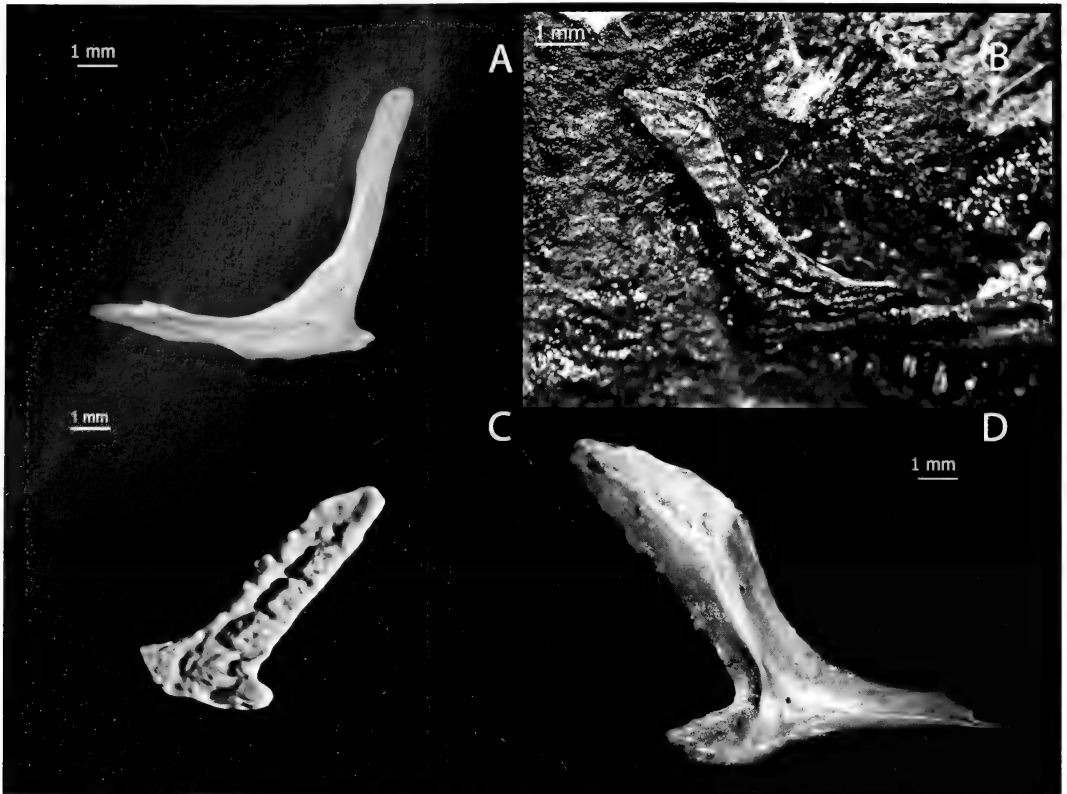
Figure 30.   A, Left jugal of *Elgaria multicarinata* TMM-M 8958, lateral, anterior to the left. Illustrates character 124(0). B, Right jugal of *Restes rugosus* YPM PU 14640, lateral, anterior to the right. Illustrates characters 124(1), 125(0), 132(2), 133(0). C, Left jugal of *Exostinus serratus*, CT scan of AMNH 1608, lateral, anterior to the left. Illustrates characters 124(2), 125(1), 132(1). D, Left jugal of *Xenosaurus newmanorum* NAUQSP-JIM uncatalogued specimen, medial, anterior to the right. Illustrates characters 126(0), 128(1).

age. Having osteoderms upon the entire dermal surface is a synapomorphy of *E. serratus* + *Xenosaurus*. Under Analysis 1, partial coverage is an autapomorphy of *S. crocodilurus*. The ancestral state for *Xenosaurus* + Anguidae and for Anguidae + Helodermatidae is ambiguous between absence and partial coverage. Under Analysis 2, partial coverage is an autapomorphy of Helodermatidae; the ancestral state for Xenosauridae and for *S. crocodilurus* + *M. ornatus* is ambiguous between absence and partial coverage.

125. Jugal: Fused osteoderms (0) relatively unconsolidated, vermiculate plate with a few mounds (Fig. 30B); (1) mostly consolidated into discrete osteoderms (Fig. 30C).

Variation. Osteoderms fuse to the jugal during early postnatal development.

Evolution. Under both analyses, all mixed internal nodes are ambiguous regarding ancestral states.

126. Jugal: Ridge between orbital and adductor surfaces (0) at or posterior to midline of postorbital ramus of jugal (perpendicular to its long axis), orbital surface relatively sagittally oriented (Fig. 30D); (1) anterior to midline, orbital surface relatively transversely oriented (Fig. 31A).

Figure 31. A, Left jugal of *Xenosaurus agrenon* UTACV r45008, medial, anterior to the right. Illustrates characters 126(1), 127(0). B, Left jugal of *Xenosaurus platyceps* UF 45622, medial, anterior to the right. Illustrates characters 127(1), 130(1), 131(1). C, Left jugal of *Exostinus serratus*, CT scan of AMNH 1608, medial, anterior to the right. Illustrates characters 126(0), 128(0), 129(1), 131(0). D, Left jugal of *Shinisaurus crocodilurus* UF 72805, medial, anterior to the right. Illustrates characters 129(0), 130(0).

Evolution. Under both analyses, the ancestral state for the entire group is a location at or posterior to the midline. The ancestral states for the southern clade of *Xenosaurus* and for *S. croco-dilurus* + *M. ornatus* are ambiguous and a location anterior to the midline is an autapomorphy of Helodermatidae.

127. Jugal: Base of postorbital ramus (0) less extensive perpendicular to its long axis than base of suborbital ramus or approximately as extensive (Fig. 31A); (1) more extensive than base of suborbital ramus (Fig. 31B).

Evolution. Under both analyses, the more extensive morphology is an autapomorphy of *X. platyceps* and of *X. grandis*.

128. Jugal: Adductor surface (0) expands ventrally (Fig. 31C); (1) diminishes ventrally, resulting in a longer quadratojugal process (Fig. 30D).

Evolution. Under both analyses, ventral diminishment is a synapomorphy of *Xenosaurus*.

129. Jugal: Foramen piercing table at junction of maxillary, orbital, and adductor surfaces (0) absent (Fig. 31D); (1) present (Fig. 31C).

Evolution. Under both analyses, the ancestral states for the entire group and for Anguimorpha are absence of the foramen. Under Analysis 1, the ancestral state for *S. crocodilurus* + Varanidae is

absence of the foramen; that for Anguidae + *Xenosaurus* is ambiguous, as is that for Helodermatidae + Anguidae and all nodes therein. Under Analysis 2, presence of the foramen is a synapomorphy of *E. serratus* + *Xenosaurus* and of *C. enneagrammus* + *O. ventralis*.

130. Jugal: Foramen piercing adductor surface just posterior to table at junction of maxillary, orbital, and adductor surfaces (0) absent (Fig. 31D); (1) present (Fig. 31B).

Evolution. Under both analyses, the ancestral states for the entire group and for Anguimorpha are ambiguous. Under Analysis 1, the ancestral state for *S. crocodilurus* + Varanidae and for Anguidae + Helodermatidae is absence of the foramen. Under Analysis 2, the ancestral state for Anguidae + Varanoidea is absence, and that for Xenosauridae is ambiguous.

131. Jugal: Anterior expansion at meeting of anterior and dorsal edges of postorbital ramus (0) absent (Fig. 31C); (1) present (Fig. 31B).

Evolution. Under both analyses, the ancestral states for *R. rugosus* + *Xenosaurus* and *E. lancensis* + *Xenosaurus* were ambiguous. The ancestral state for *Xenosaurus* is expansion. Lack of expansion is an autapomorphy of *X. rectocollaris*.

132. Jugal: Tip of postorbital ramus (0) without strong change in sagittal angle at level of postorbital facet (Estes et al., 1988, Fig. 13B); (1) moderately projected posteriorly at beginning of level of postorbital facet by less than 20° to long axis of majority of postorbital ramus (Fig. 30C); (2) strongly projected posteriorly beginning at level of postorbital facet by 20° or more to long axis of majority of postorbital ramus (Fig. 30B).

Evolution. Under both analyses, the ancestral state for the entire group and for Anguimorpha is moderate posterior projection, as is that for shinisaurs. The ancestral state for Varanidae is lack of projection, and that for *R. rugosus* + *Xenosaurus* is ambiguous between moderate and strong projection. Under Analysis 1, the ancestral state for *S. crocodilurus* + Varanidae is moderate projection, as is that for *Xenosaurus* + Anguidae. The ancestral state for Anguidae + Helodermatidae and for Anguidae is ambiguous between no and moderate projection. Under Analysis 2, the ancestral state for Anguimorpha, Anguidae + Varanoidea, and Xenosauridae is moderate projection. A lack of projection is an autapomorphy of *C. enneagrammus* and a synapomorphy of Varanoidea.

133. Jugal: Posterior edge of postorbital ramus (0) straight or smoothly curved (Fig. 30B); (1) abruptly angled toward the vertical at level of postorbital facet (Fig. 3C).

Evolution. Under both analyses, abrupt vertical angulation is a synapomorphy of *X. rackhami* + *X. grandis*.

Postorbital/Postfrontal

The postorbital and postfrontal are unknown in *M. ornatus*, *E. serratus*, and *E. lancensis*. The postorbital is unknown in *B. ammoskius*. Only the postfrontal ossifies in Helodermatidae and *L. borneensis*.

134. Postorbital/Postfrontal: Postorbital and postfrontal (0) remain separate well after hatching/birth or throughout ontogeny (Fig. 32A); (1) fuse in late prenatal or early postnatal ontogeny (Fig. 32B) (see character 14 of Estes et al., 1988).

Variation. As noted, this character involves the assessment of the ontogenetic stage of a specimen. Justifications for age assessments of the fossils were given in Materials and Methods.

Evolution. Under both analyses, the ancestral state for the entire group
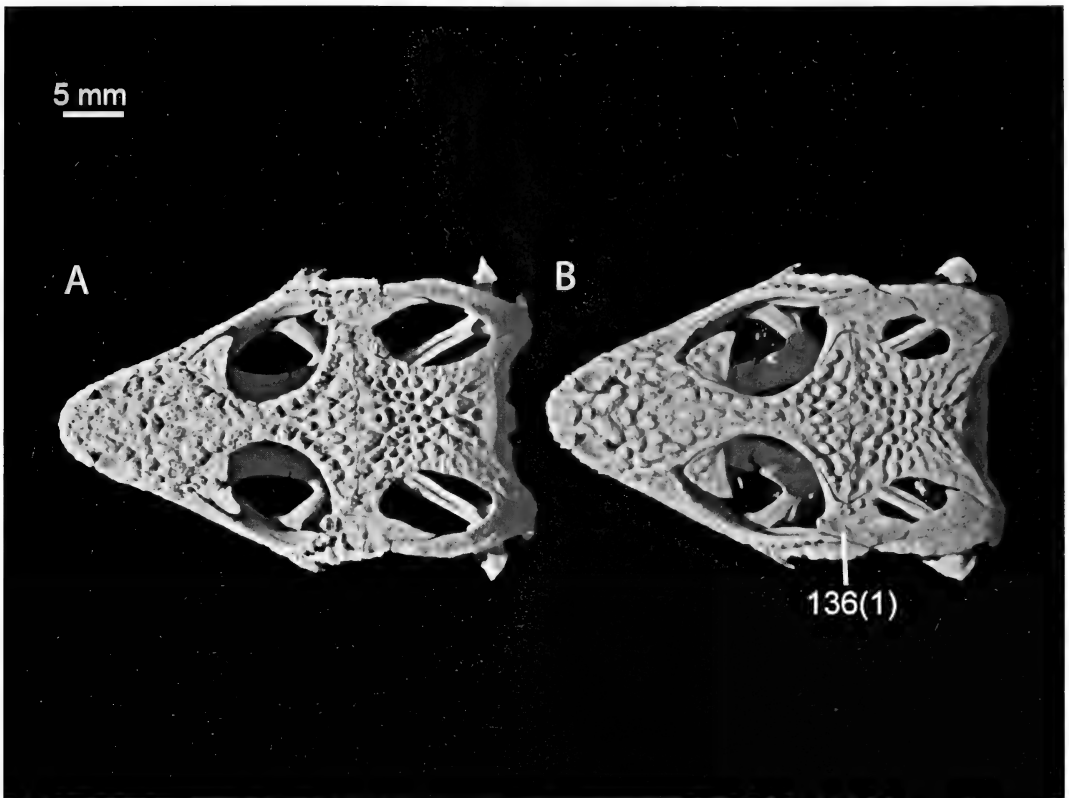
Figure 32.   Skulls, dorsal, anterior to the left: A, *Xenosaurus newmanorum*, CT scan of UMMZ 126056; B, *Xenosaurus rackhami*, CT scan of UTEP 4555. A and B illustrate characters 134(0), 134(1), 136(1), 138(0), 139(1), 139(2), 140(0), 140(1), 141(0), 141(1), 142(1), 165(1), 165(3), 166(0), 166(1).

and for Anguimorpha is lack of fusion, and early fusion is a synapomorphy of the southern clade of *Xenosaurus*. Under Analysis 1, the ancestral state for *S. crocodilurus* + Varanoidea is ambiguous. Under Analysis 2, early fusion is a synapomorphy of *Varanus* and an autapomorphy of *S. crocodilurus*.

135. Postorbital/Postfrontal: Angle of post-frontal "clasp" of frontoparietal suture (taken between long axes of anterior and posterior processes of postfrontal) (0) less than 80° (Fig. 5A); (1) 80° to 85° inclusive (Fig. 4A); (2) greater than 85° (Fig. 3A).

Evolution. Under both analyses, state 2 is ancestral for the entire group. The ancestral state for *Xenosaurus* is am-biguous between state 2 and state 1.

State 0 is a synapomorphy of *X. agrenon* + *X. rectocollaris* and an autapomorphy of *X. platyceps*.

136. Postorbital/Postfrontal: Dorsal ridge adjacent to lateral edge of postorbital (0) absent (Fig. 33A); (1) present (Fig. 32B).

Evolution. Under both analyses, ab-sence of a ridge is the ancestral state for the entire group and for Anguimorpha. Under Analysis 1, presence of a ridge is a synapomorphy of *Xenosaurus* and an autapomorphy of *S. crocodilurus*. Un-der Analysis 2, the ancestral state for Xenosauridae is ambiguous.

137. Postorbital/Postfrontal: Postorbital (0) relatively flat, lying largely in horizontal plane (Fig. 33A); (1) bearing deep
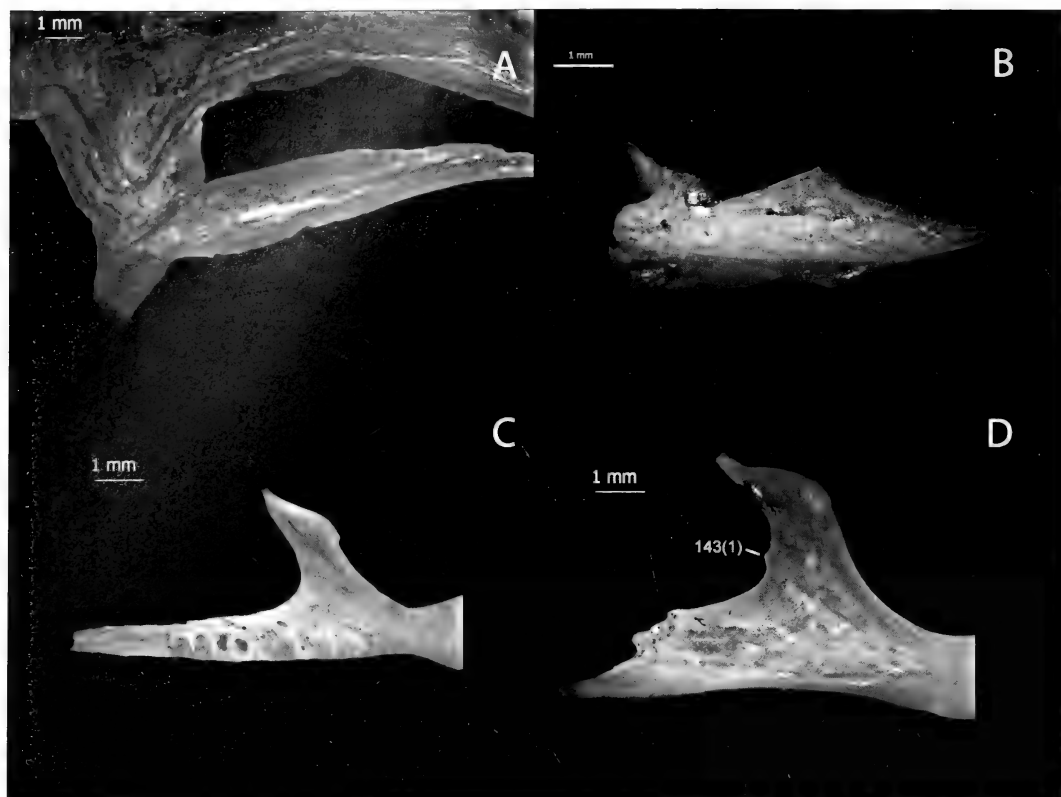
Figure 33.   A, Temporal region of *Elgaria multicarinata* CAS 85234, dorsolateral, anterior to the left. Illustrates characters 136(0), 137(0), 139(0), 142(0). B, Left postorbital of *Xenosaurus newmanorum* NAUQSP-JIM uncatalogued specimen, dorsolateral, anterior to the left. Illustrates character 137(1). C, Left pterygoid of *Shinisaurus crocodilurus* UF 72805, ventral, anterior to the left. Illustrates characters 143(0), 145(0). D, Left pterygoid of *Xenosaurus newmanorum* NAUQSP-JIM uncatalogued specimen, ventral, anterior to the left. Illustrates characters 143(1), 145(2).

flange descending from lateral edge, creating a surface in the sagittal plane, perpendicular to the main body of the bone (Fig. 33B).

Evolution. Under both analyses, the flat morphology is ancestral for the entire group and for Anguimorpha. Under Analysis 1, presence of a flange is a synapomorphy of *Xenosaurus* and an autapomorphy of *S. crocodilurus*. Under Analysis 2, the ancestral state for Xenosauridae is ambiguous.

138. Postorbital/Postfrontal: Tip of postorbital process of postfrontal (0) pointed, formed by meeting of smoothly curving medial and lateral edges (Fig. 32A); (1) squared-off because of posterior

inflection of medial edge in horizontal plane (Fig. 32B).

Evolution. Under both analyses, the ancestral state for the entire group and for Anguimorpha is pointed, and the squared-off morphology is a synapomorphy of the southern clade of *Xenosaurus* and an autapomorphy of *S. crocodilurus*. Under Analysis 1, the squared-off morphology is a synapomorphy of *Varanus* and an autapomorphy of Helodermatidae. Under Analysis 2, the ancestral state for Varanoidea is ambiguous.

139. Postorbital/Postfrontal: Narrowness of postorbital measured by ratio of anteroposterior length to mediolateral width

just posterior to divergence of posterior process of postfrontal (0) 4.0 or greater (Fig. 33A); (1) between 2.5 and 4.0 (Fig. 32A); (2) 2.5 or less (Fig. 32B).

Evolution. Under both analyses, the ancestral state of the entire group and of Anguimorpha is the narrow morphology, and the wide morphology is a synapomorphy of *X. rackhami* + *X. grandis*. Under Analysis 1, intermediate width is a synapomorphy of *Xenosaurus* and an autapomorphy of *S. crocodilurus*. Under Analysis 2, the ancestral state for Xenosauridae is ambiguous between the narrow and intermediate morphologies.

140. Postorbital/Postfrontal: Posterior end of squamosal process of postorbital (0) pointed (Fig. 32A); (1) rounded (Fig. 32B).

Evolution. Under both analyses, the rounded morphology is an autapomorphy of *X. rackhami*.

141. Postorbital/Postfrontal: Posterior end of squamosal process of postorbital (0) gently curved medially in horizontal plane or not curved medially (Fig. 32A); (1) strongly curved medially in horizontal plane, resulting in sharp change in angle of medial edge (Fig. 32B).

Evolution. Under both analyses, strong curvature is a synapomorphy of *X. rackhami* + *X. grandis*.

142. Postorbital/Postfrontal: Lateral edge of postorbital (0) straight or nearly straight in horizontal plane (Fig. 33A); (1) broadly curved in horizontal plane (Fig. 32B).

Evolution. Under both analyses, the ancestral state for *Xenosaurus* is ambiguous.

Pterygoid

The pterygoid is unknown in *E. lancensis* and *E. serratus* and is not substantially visible in *B. ammoskius*.

143. Pterygoid: Margin of pterygoid bordering infraorbital fenestra (0) smoothly curved (Fig. 33C); (1) bearing small eminence just medial of posterior apex (Fig. 33D).

Evolution. Under both analyses, presence of an eminence is a synapomorphy of the northern clade of *Xenosaurus* and an autapomorphy of Helodermatidae.

144. Pterygoid: Medial and lateral edges of vomerine process posterior to oblique anterior edge (0) weakly divergent (by 20° or less) in horizontal plane (Fig. 34A); (1) strongly divergent (by greater than 20°) in horizontal plane (Fig. 34B).

Evolution. Under both analyses, strong divergence is an autapomorphy of *R. rugosus* and of *C. enneagrammus*.

145. Pterygoid: Bears (0) large row or patch of teeth (Fig. 33C); (1) one or two small teeth, sometimes bilaterally asymmetrical (Fig. 34B); (2) no teeth (Fig. 33D). Presence or absence of pterygoid teeth was character 83 of Estes et al. (1988).

Variation. Pterygoid teeth often increase in number with age (personal observation), and observations on this character were made using relatively large individuals. Additionally, when teeth are highly reduced, their presence can vary from side to side in an individual or from individual to individual in a species (e.g., *C. enneagrammus*).

Evolution. Under both analyses, reduction of pterygoid dentition is a synapomorphy of *Xenosaurus* + *R. rugosus* and an autapomorphy of *C. enneagrammus*. Absence of pterygoid dentition is a synapomorphy of *Xenosaurus* and of *Varanus*.

Ectopterygoid

The ectopterygoid is unknown for all extinct taxa in the study (not sufficiently exposed in *B. ammoskius*).
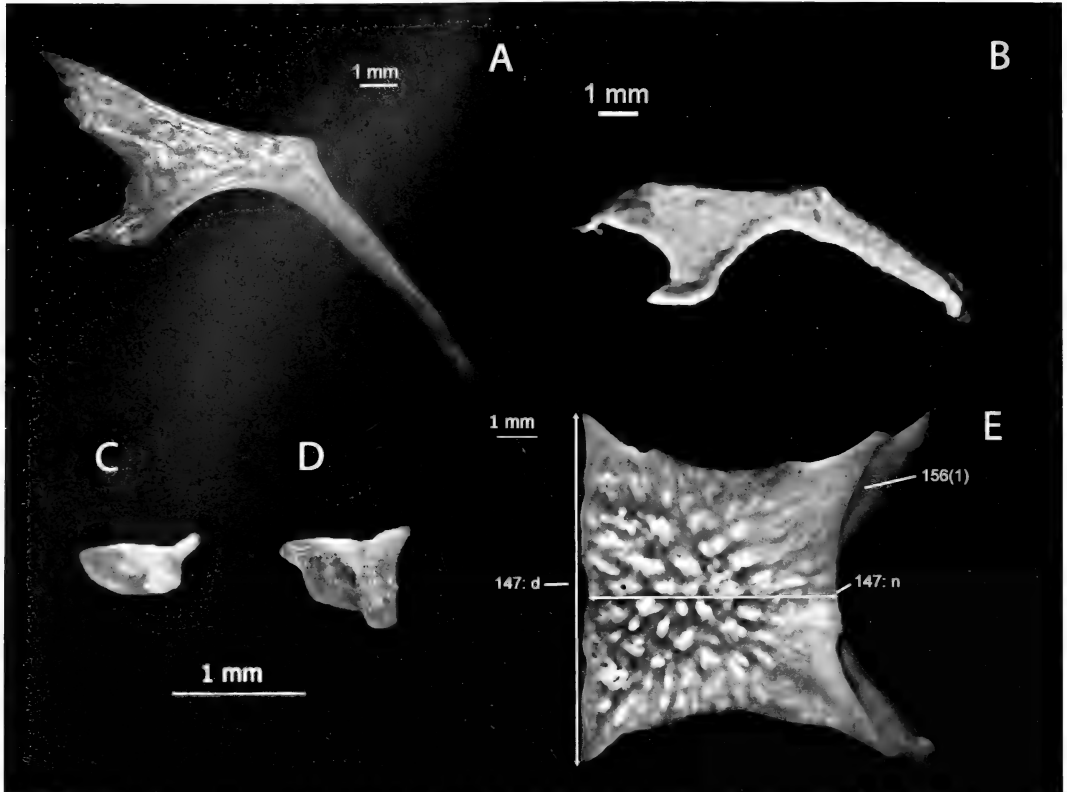
Figure 34.   Right pterygoids, ventral, anterior to the left: A, *Xenosaurus newmanorum* NAUQSP-JIM uncatalogued specimen. Illustrates character 144(0). B, *Restes rugosus*, CT scan of YPM PU 14640. Illustrates characters 144(1), 145(1). Left ectopterygoids, maxillary articulation surfaces, anterior to the left: C, *Elgaria multicarinata* TMM-M 8958; D, *Xenosaurus newmanorum* NAUQSP-JIM uncatalogued specimen. C and D illustrate characters 146(0), 146(1). E, Parietal of *Xenosaurus rackhami* UTEP-OC "MALB" 388, dorsal, anterior to the left. Illustrates characters 147 (n for numerator, d for denominator), 150(0), 151(1), 153(1), 154(1), 156(1).

146. Ectopterygoid: Prominent descending projection of maxillary process (0) absent (Fig. 34C); (1) present (Fig. 34D).

  Evolution. Under both analyses, presence of a descending projection is a synapomorphy of *Xenosaurus*.

Parietal

  The parietal is unknown in *R. rugosus* and *E. serratus*.

147. Parietal: Ratio of anteroposterior length along midline (to apex of meeting of supratemporal processes) to mediolateral width at frontoparietal suture (Fig. 34E) (0) less than 0.70; (1) 0.70 to less than 0.75; (2) 0.75 to less than 0.80; (3) 0.80 to less than 0.85; (4) 0.85 to less than 0.90; (5) 0.90 to less than 0.95; (6) 0.95 to less than 1.00; (7) 1.00 to less than 1.05; (8) 1.05 to less than 1.10; (9) 1.10 to less than 1.15; (A) 1.15 to less than 1.20; (B) 1.20 to less than 1.25; (C) 1.25 or greater.

  Variation. The length-to-width ratio of the parietal body increases with growth, especially in the earlier parts of ontogeny (personal observation). Thus, care must be taken to use relatively large adult individuals in scoring this character.

  Evolution. Under both analyses, the ancestral state for the entire group is ambiguous among state 1, state 2, state

3, and state 4. The ancestral state for Anguimorpha is ambiguous between state 3 and state 4. Additionally, the ancestral state for *S. crocodilurus* + *M. ornatus* is state 5. State 6 is a synapomorphy of *S. crocodilurus* + *B. ammoskius*, and state 9 is an autapomorphy of *S. crocodilurus*. The ancestral state for Anguidae is ambiguous between state 3 and state 4. State 7 is an autapomorphy of *O. ventralis*. State C is an autapomorphy of *E. lancensis*. The ancestral state for *Xenosaurus* is ambiguous between state 3 and state 4. A reduced ratio is a synapomorphy of the southern clade of *Xenosaurus*, whose ancestral state is ambiguous between state 1 and state 2. State 0 is a synapomorphy of *X. agrenon* + *X. rectocollaris*. State 8 is an autapomorphy of *L. borneensis*, and state 0 is an autapomorphy of *V. exanthematicus*. Under Analysis 1, the ancestral state for *S. crocodilurus* + Varanidae is ambiguous between state 4 and state 5, and that for *Varanus* is state 4. The ancestral state for *Xenosaurus* + Anguidae and for Anguidae + Helodermatidae is ambiguous between state 3 and state 4. Under Analysis 2, the ancestral state for Anguidae + Varanoidea is ambiguous between state 3 and state 4, as is that for Varanoidea and all nodes therein. The ancestral state for Xenosauridae is ambiguous among state 3, state 4, and state 5, as is that for *Xenosaurus* + *E. lancensis*.

148. Parietal: Ratio of anteroposterior length of supratemporal processes beginning at apex of their meeting to mediolateral width at widest separation of processes (Fig. 35A) (0) less than 0.20; (1) 0.20 to less than 0.25; (2) 0.25 to less than 0.30; (3) 0.30 to less than 0.35; (4) 0.35 to less than 0.40; (5) 0.40 to less than 0.45; (6) 0.45 to less than 0.50; (7) 0.50 or greater.

Variation. The posterior portion of the parietal becomes relatively more elongate with growth, especially in early ontogeny (personal observation), so it is important to score this character on relatively large adults.

Evolution. Under both analyses, the ancestral state for Varanidae is state 5, and state 7 is an autapomorphy of *L. borneensis*. State 7 is a synapomorphy of Anguidae. The ancestral state for *S. crocodilurus* + *M. ornatus* is state 4, and state 3 is an autapomorphy of *S. crocodilurus*. Finally, the ancestral state for *Xenosaurus* is ambiguous between state 2 and state 3. The ancestral state for the northern clade of *Xenosaurus* is state 2, and state 0 is an autapomorphy of *X. newmanorum*. In the southern clade, state 1 is an autapomorphy of *X. grandis*. Under Analysis 1, the ancestral state for the entire group, Anguimorpha, *S. crocodilurus* + Varanidae, and *Xenosaurus* + Anguidae is ambiguous between state 4 and state 5. Under Analysis 2, the ancestral state for the entire group, Anguimorpha, Anguidae + Varanoidea, and Varanoidea is state 5. State 4 is an autapomorphy of Helodermatidae. On the other branch of Anguimorpha, state 4 is a synapomorphy of Xenosauridae.

149. Parietal: Attachment areas for adductor musculature (0) dorsolateral or lateral, without extensive overhanging flange; (1) ventral, roofed over by flange of parietal table (Fig. 35B) (see character 54 of Estes et al., 1988).

Variation. Although the overhanging flange in those taxa with ventral origin often becomes relatively more extensive with age, I did not observe intraspecies variation that would alter the scoring of the character.

Evolution. Under both analyses, the ancestral state for *Xenosaurus* + *E. lancensis* is ventral origin. Under Analysis 1, the ancestral state for the entire group and for Anguimorpha is dorsal origin, and ventral origin is a synapomorphy of *Xenosaurus* + Anguidae.
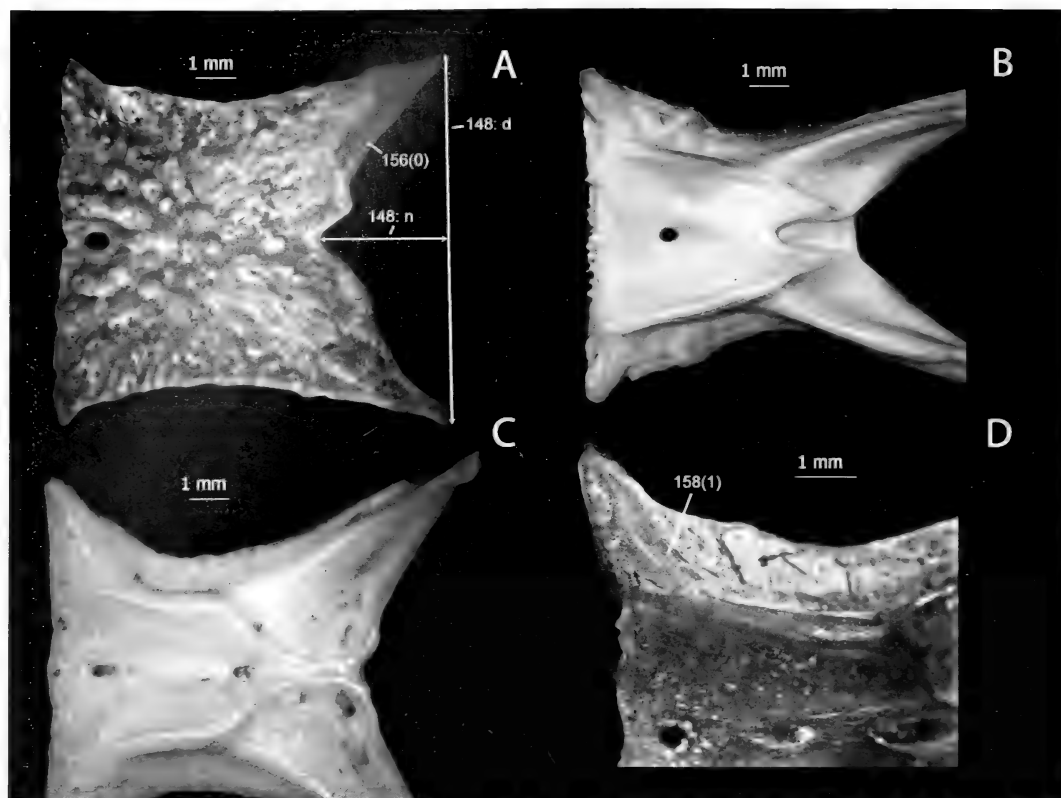
Figure 35. A, Parietal of *Xenosaurus agrenon* UTACV r45008, dorsal, anterior to the left. Illustrates characters 148 (n for numerator, d for denominator), 150(1), 152(1), 153(0), 155(2), 156(0). B, Parietal of *Elgaria multicarinata* TMM-M 8958, ventral, anterior to the left. Illustrates characters 149(1), 152(0), 155(0), 157(0). C, Parietal of *Xenosaurus platyceps* UF 45622, ventral, anterior to the left. Illustrates characters 154(2), 155(1), 157(1). D, Parietal of *Xenosaurus newmanorum* NAUQSP-JIM uncatalogued specimen, ventral, anterior to the left. Illustrates characters 154(3), 158(1).

Note that this is dependent upon the use of an iguanian as the immediate anguimorph outgroup. Most sclero-glossans show ventral origin (Estes et al., 1988). Under Analysis 2, the ancestral state for all mixed nodes is ambiguous.

150. Parietal: Lateral edges forming margins of supratemporal fenestrae (0) strongly curved in a horizontal plane (Fig. 34E); (1) weakly curved, especially anterior to apex of temporal emargination (Fig. 35A).

Variation. In the taxa showing lateral or dorsolateral origin of the adductor musculature (character 149-0), the degree of emargination increases with age as the braincase becomes relatively smaller and the adductor chamber relatively larger.

Evolution. Under both analyses, relatively weak curvature is an autapomorphy of *X. agrenon*.

151. Parietal: Number of osteoderms on each side lateral to midline osteoderm just posterior to parietal foramen (0) three (Fig. 1A); (1) two (Fig. 34E); (2) one (Conrad, 2006, fig. 2A).

Evolution. Under both analyses, the ancestral state for the entire group is ambiguous between three osteoderms and two osteoderms. The ancestral

state for shinisaurs is two osteoderms and one osteoderm is an autapomorphy of *M. ornatus*.

152. Parietal: Parietal foramen (0) set far back from frontoparietal suture, considerably posterior to anterolateral extensions of parietal bearing postfrontal facets (Fig. 35B); (1) set close to frontoparietal suture, at anteroposterior level of anterolateral extensions bearing postfrontal facets (Fig. 35A).

Variation. State 0 reportedly occurs in some *S. crocodilurus* (J. L. Conrad, personal communication), although not in the specimens examined.

Evolution. Under both analyses, the ancestral state for the entire group and for Anguimorpha is ambiguous. Under Analysis 1, the ancestral state for *Xenosaurus* + Anguidae and for Helodermatidae + Anguidae is ambiguous. The ancestral state for *E. multicarinata* + *O. ventralis* is relatively posterior placement. Under Analysis 2, the ancestral state for *S. crocodilurus* + Varanoidea is the relatively posterior placement, with placement close to the frontoparietal suture an autapomorphy of *S. crocodilurus*. The ancestral state for Anguidae + Helodermatidae is ambiguous. Under Analysis 2, the ancestral state for Anguidae + Varanoidea is relatively posterior placement.

153. Parietal: Parietal foramen (0) relatively large (Fig. 35A); (1) small, barely larger than tiny nutrient foramina (Fig. 34E).

Evolution. Under both analyses, the small morphology is an autapomorphy of *X. rackhami*.

154. Parietal: Anterior edge in horizontal plane (0) convex (Conrad, 2006, fig. 2A); (1) relatively straight (Fig. 34E); (2) slightly concave (Fig. 35C); (3) strongly concave (Fig. 35D).

Evolution. Under both analyses, the ancestral state for the entire group is ambiguous among straight, slightly concave, and strongly concave. The ancestral state for shinisaurs is relatively straight and a convex morphology is an autapomorphy of *B. ammoskius*. The ancestral state for Anguidae and xenosaurs is also straight, with convex an autapomorphy of *E. lancensis*, slightly concave a synapomorphy of the northern clade of *Xenosaurus*, and strongly concave an autapomorphy of *X. newmanorum*. Strongly concave is an autapomorphy of *L. borneensis*. Under Analysis 1, the relatively straight morphology is ancestral for Anguimorpha, and slightly concave is an autapomorphy of Helodermatidae. Under Analysis 2, the ancestral state for Anguimorpha is ambiguous between relatively straight and slightly concave.

155. Parietal: Notch in posterior edge of parietal at meeting of medial edges of supratemporal processes (0) absent (Fig. 35B); (1) weak, more than four times as mediolaterally wide as anteroposteriorly long (Fig. 35C); (2) strong, four times or less as mediolaterally wide as anteroposteriorly long (Fig. 35A).

Evolution. Under both analyses, the ancestral state for the entire group and for Anguimorpha is ambiguous between weakly notched and strongly notched, as are the ancestral states for Varanidae and Anguidae. The absence of a notch is a synapomorphy of shinisaurs and an autapomorphy of *E. multicarinata*, Helodermatidae, and *V. exanthematicus*. The ancestral state for *E. lancensis* + *Xenosaurus* is weakly notched. The strongly notched morphology is a synapomorphy of *X. agrenon* + *X. rectocollaris*, and absence of a notch is a synapomorphy of *X. rackhami* + *X. grandis*. Under Analysis 1, the ancestral state for shinisaurs + Varanidae is ambiguous between weakly and strongly notched, as is that for *Xenosaurus* + Anguidae. Under Analysis 2, the ancestral state for Xenosauridae is weakly notched.
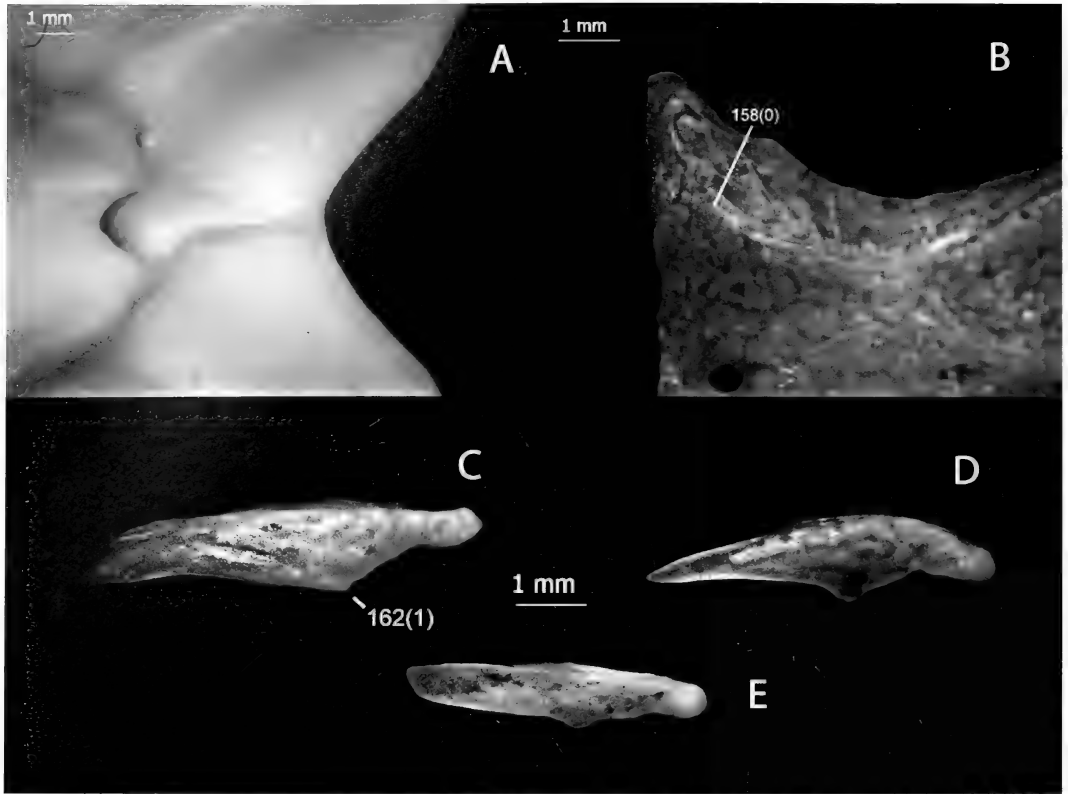
Figure 36.   Parietals, ventral, anterior to the left: A, *Heloderma suspectum* TMM-M 9001. Illustrates character 157(2). B, *Xenosaurus grandis* NAUQSP-JIM 1460. Illustrates character 158(0). Left supratemporals, lateral, anterior to the left: C, *Xenosaurus newmanorum* NAUQSP-JIM uncatalogued specimen; D, *Xenosaurus grandis* NAUQSP-JIM 1460. E, *Xenosaurus agrenon* UTACV r45008. C through E illustrate characters 159(0), 159(1), 160(0), 160(1), 161(1), 162(1), 163(0), 163(1), 163(2).

156. Parietal: Dorsal fossae for m. articulo-parietalis attachment (0) shallow, only slightly stepped down from parietal table (Fig. 35A); (1) deep, divided from parietal table by sharp ridge along at least part of fossa (Fig. 34E).

Variation. The relative depth of the fossae increases somewhat with age, most prominently in the early stages of postnatal ontogeny.

Evolution. Under both analyses, the ancestral condition for the entire group is ambiguous, and the deep morphology is a synapomorphy of *X. rackhami* + *X. grandis* and an autapomorphy of *C. enneagrammus.* Under Analysis 1, the ancestral state for Anguimorpha is ambiguous, and the ancestral state for

Xenosaurus + Anguidae is the shallow morphology. Under Analysis 2, the ancestral state for Anguimorpha is the shallow morphology, and the deep morphology is a synapomorphy of Varanidae.

157. Parietal: Ventral excavations on supra-temporal processes for transversospinalis group muscles (0) widely separated by sulcus processi ascendentis (Fig. 35B); (1) moderately separated; bridged by flange of parietal extending posteriorly past sulcus processi ascendentis but do not approach each other closely, leaving between them a broad triangular wedge of cerebral table (Fig. 35C); (2) approach each other closely, leaving between them only a thin ridge of cerebral table (Fig. 36A).

Evolution. Under both analyses, widely separated is the ancestral state for the entire group and for Anguimorpha. The ancestral state for *E. lancensis* + *Xenosaurus* is moderately separated, and that for the southern clade of *Xenosaurus* is ambiguous between moderately separated and closely approaching. Closely approaching is an autapomorphy of Helodermatidae. Under Analysis 1, the ancestral state for *Xenosaurus* + Anguidae is ambiguous between closely approaching and moderately separated. Under Analysis 2, the ancestral state for Xenosauridae is widely separated, and moderately separated is a synapomorphy of *Xenosaurus* + *E. lancensis*.

158. Parietal: Ventral ridges contacting taeniae marginales (0) also bound adductor attachment surface medially for entire length (Fig. 35D); (1) diverge just posterior to level of prefrontal facet from ridge delineating medial margin of adductor attachment surface (Fig. 36B).

    Evolution. Under both analyses, divergence is a synapomorphy of the northern clade of *Xenosaurus*.

Supratemporal

The supratemporal is unknown for all extinct taxa save *B. ammoskius*, in which a negligible amount of its morphology is visible.

159. Supratemporal: Anterior edge (0) dorsoventrally short, less than half greatest height of supratemporal (Fig. 36D); (1) dorsoventrally tall, more than half greatest dorsoventral height of supratemporal (Fig. 36C).

    Evolution. Under both analyses, the ancestral state for the entire group and for Anguimorpha is the short morphology. Under Analysis 1, the ancestral state for *Xenosaurus* is ambiguous, and the tall morphology is an autapomorphy of *S. crocodilurus*. Under Analysis 2, the tall morphology is a synapomorphy of Xenosauridae and the short mor-

phology is a synapomorphy of *X. rackhami* + *X. grandis*.

160. Supratemporal: Foramen piercing lateral surface near ridge dividing squamosal facet and adductor attachment surface about two-thirds of the way to posterior end of supratemporal (0) present (Fig. 36E); (1) absent (Fig. 36D).

    Evolution. Under both analyses, the ancestral state for the entire group is ambiguous, and absence of the foramen is a synapomorphy of *X. rackhami* + *X. grandis*. Under Analysis 1, the ancestral state for Anguimorpha is ambiguous, and the ancestral state for *Xenosaurus* + Anguidae is presence of the foramen. Under Analysis 2, the ancestral state for Anguimorpha is presence of the foramen, and absence is a synapomorphy of Varanidae and of *X. rackhami* + *X. grandis*.

161. Supratemporal: Foramen piercing lateral surface (0) above (Fig. 37A); (1) below ridge dividing squamosal facet and adductor attachment surface (Fig. 36E).

    Evolution. Under both analyses, a ventral position is a synapomorphy of *Xenosaurus*.

162. Supratemporal: Ventral flange wrapping under supratemporal process of parietal (0) smoothly curved along ventromedial edge (Fig. 37A); (1) produced into wedge (Fig. 36C).

    Evolution. Under both analyses, the ancestral state for the entire group and Anguimorpha is smoothly curved. Under Analysis 1, production into a wedge is an autapomorphy of *S. crocodilurus* and a synapomorphy of *Xenosaurus*. Under Analysis 2, production into a wedge is a synapomorphy of Xenosauridae.

163. Supratemporal: Wedge-shaped ventral flange wrapping under supratemporal process of parietal (0) small and nub-like (Fig. 36E); (1) squat, obtuse wedge
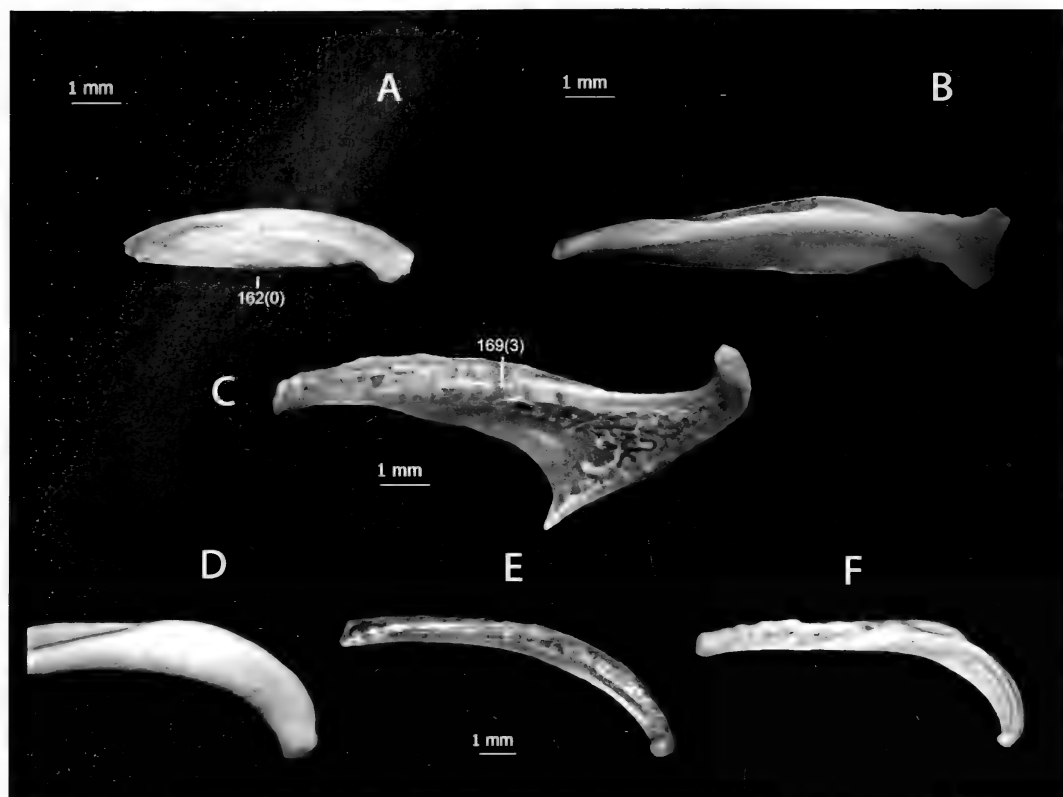
Figure 37.   A, Left supratemporal of *Elgaria multicarinata* TMM-M 8958, lateral, anterior to the left. Illustrates characters 161(0), 162(0). Left squamosals, ventral, anterior to the left: B, *Elgaria multicarinata* TMM-M 8958. Illustrates character 164(0). C, *Xenosaurus newmanorum* NAUQSP-JIM uncatalogued specimen. Illustrates characters 164(1), 167, 169(3). Left squamosals, lateral, anterior to the left: D, TMM-M 8956. Illustrates characters 165(0), 168(0), 169(0). E, *Xenosaurus newmanorum* NAUQSP-JIM uncatalogued specimen; F, *Xenosaurus grandis* NAUQSP-JIM 1460. E illustrates 168(1) and F illustrates 168(2).

(Fig. 36C); (2) sharp, more acute wedge (Fig. 36D).

Evolution. Under both analyses, the ancestral state is squat and obtuse. The small, nub-like morphology is a synapomorphy of *X. agrenon* + *X. rectocollaris,* and the sharp, acute morphology is a synapomorphy of *X. rackhami* + *X. grandis.*

Squamosal

The squamosal is unknown for all of the extinct taxa.

164. Squamosal: Posterior portion (0) unexpanded mediolaterally (Fig. 37B); (1) mediolaterally expanded (Fig. 37C). The presence or absence of a canthal

crest in the temporal region was mentioned as a possible synapomorphy of Xenosauridae by Estes et al. (1988).

Evolution. Under both analyses, expansion is the ancestral state for the entire group and for Anguimorpha. Under Analysis 1, narrowness is a synapomorphy of Varanidae and of Anguidae + Helodermatidae. Under Analysis 2, narrowness is a synapomorphy of Anguidae + Varanoidea.

165. Squamosal: Dorsal ridge adjacent to lateral edge (0) absent (Fig. 37D); (1) relatively low (Fig. 32A); (2) intermediate height (Fig. 5A); (3) pronounced (Fig. 32B).

Evolution. Under both analyses, presence of a low ridge is a synapomorphy of *Xenosaurus,* presence of a ridge of intermediate height is a synapomorphy of the southern clade of *Xenosaurus,* and presence of a sharp ridge is an autapomorphy of *X. rackhami.*

166. Squamosal: Dorsal ridge adjacent to lateral edge (0) most prominent posteriorly (Fig. 32A); (1) most prominent anteriorly (Fig. 32B).

Evolution. Under both analyses, anterior prominence is an autapomorphy of *X. agrenon* and of *X. rackhami.*

167. Squamosal: Width, assessed by ratio of mediolateral width at anteroposterior level of closure of supratemporal fenestra to anteroposterior length of squamosal (Fig. 37C) (0) 0.15 or less; (1) 0.15 to 0.30; (2) 0.30 to 0.40; (3) 0.40 or above.

Evolution. Under both analyses, the ancestral state for the entire group and for Anguimorpha is ambiguous between state 1 and state 2. The ancestral state for *Xenosaurus* is state 2, and state 3 is a synapomorphy of *X. rackhami* + *X. grandis.* Under Analysis 1, the ancestral state for *Shinisaurus* + Varanidae is state 1, and state 0 is a synapomorphy of Varanidae. Under Analysis 2, state 0 is a synapomorphy of Anguidae + Varanoidea.

168. Squamosal: Suspensorial end curvature in a sagittal plane (0) without abrupt terminal hook (Fig. 37D); (1) terminal hook present and reaches the vertical or only slightly beyond the vertical (Fig. 37E); (2) terminal hook progresses well beyond the vertical, folding under the remainder of the squamosal and extending anteriorly for a short distance (Fig. 37F).

Evolution. Under both analyses, curvature of the hook to near the vertical is a synapomorphy of *Xenosaurus,* and curvature well beyond the vertical is a synapomorphy of *X. rackhami* + *X. grandis.*

169. Squamosal: Ventral ridge dividing attachment surface for m. anguli oris 1a and m. adductor mandibularis externus superficialis 1b from that for m. adductor mandibularis externus medialis and m. adductor mandibularis externus profundus (0) absent (Fig. 37D); (1) uniformly weak (Fig. 38A); (2) sharp only in posterior portion of squamosal (Fig. 38B); (3) sharp and well-defined for most of length of squamosal (Fig. 37C).

Evolution. Under both analyses, absence of a ridge is ancestral for the entire group and for Anguimorpha. A sharp ridge is an autapomorphy of *E. multicarinata,* and a ridge of mixed prominence is ancestral for *X. rackhami* + *X. grandis,* whereas a weak ridge is an autapomorphy of *X. rackhami.* Under Analysis 1, a sharp ridge is an autapomorphy of *S. crocodilurus.* The ancestral state for *Xenosaurus* is ambiguous between a ridge of mixed prominence and a sharp ridge, as is that for the southern clade of *Xenosaurus.* Under Analysis 2, a sharp ridge is a synapomorphy of Xenosauridae, and a ridge of mixed prominence is a synapomorphy of *X. rackhami* + *X. grandis.*

Quadrate

The quadrate is unknown in the fossil xenosaurs and in *M. ornatus.*

170. Quadrate: Two-thirds or more of the way down its dorsoventral height, lateral edge of tympanic crest (0) abruptly angles medially in plane of the crest, possibly associated with attachment of lateral collateral ligament and other connective tissue (Fig. 38C); (1) curves smoothly without abrupt medial angulation (Fig. 38E).

Evolution. Under both analyses, lack of a medial deflection is a synapomorphy of Varanidae and of *X. agrenon + X.*
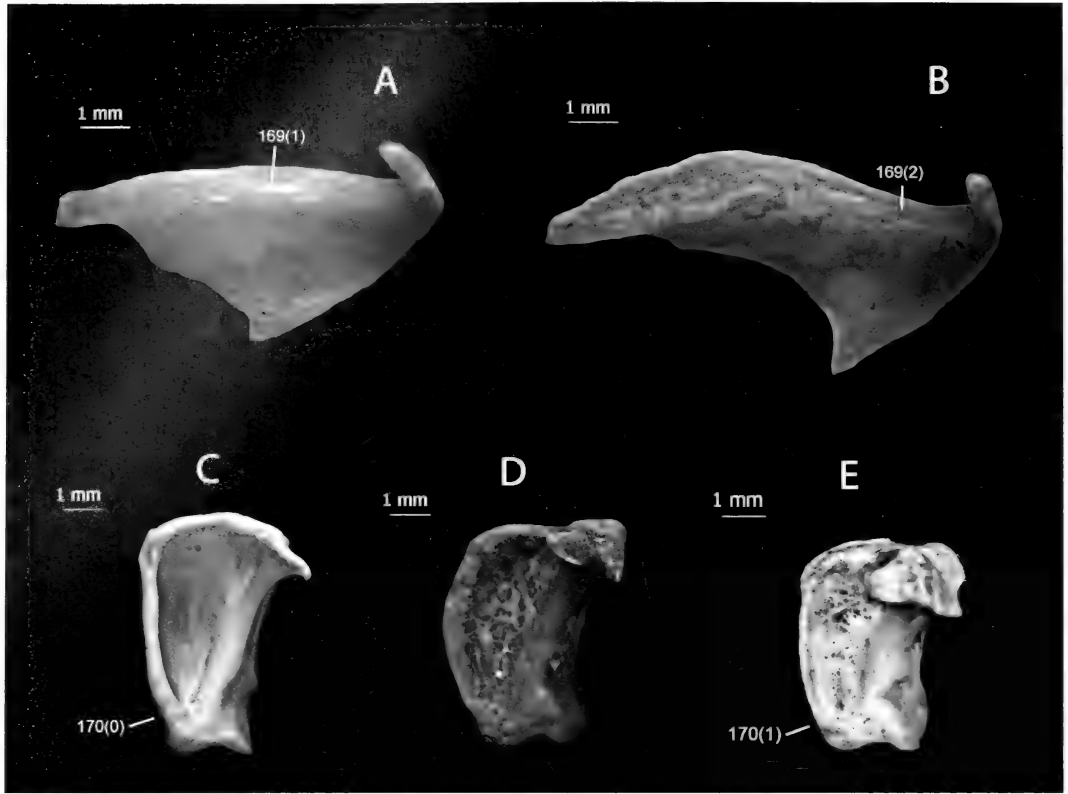
Figure 38.   Left squamosals, ventral, anterior to the left: A, *Xenosaurus rackhami* UTEP-OC "MALB" 388. Illustrates character 169(1). B, *Xenosaurus grandis* NAUQSP-JIM 1460. Illustrates character 169(2). Left quadrates, posterior: C, *Elgaria multicarinata* TMM-M 8958; D, *Xenosaurus newmanorum* NAUQSP-JIM uncatalogued specimen. C and D illustrate characters 170(0), 173(0), 173(1). E, *Xenosaurus agrenon* UTACV r45008. Illustrates character 170(1).

rectocollaris. Under Analysis 1, the ancestral state for Anguidae is ambiguous. Under Analysis 2, lack of a deflection is a synapomorphy of *C. enneagrammus + O. ventralis*.

171. Quadrate: Anteromedial emargination of dorsal surface of cephalic condyle (0) relatively deep, enclosing angle of 35° or more (Fig. 39A); (1) relatively shallow, enclosing angle of less than 35° (Fig. 39C).

   Evolution. Under both analyses, the shallow morphology is a synapomorphy of *X. agrenon + X. rectocollaris*.

172. Quadrate: Posterior eminence from lateralmost portion of dorsal surface of cephalic condyle (0) small, rounded

bump (Fig. 39A); (1) pronounced wedge (Fig. 39B).

   Evolution. Under both analyses, the ancestral state for the entire group is ambiguous; that for Anguimorpha is the small, bump-like morphology; and the wedge morphology is a synapomorphy of *X. rackhami + X. grandis*.

173. Quadrate: Depression for tympanic cavity (0) strong, deeply concave posteriorly in horizontal plane (Fig. 38C); (1) weak, weakly concave posteriorly in horizontal plane (Fig. 38D).

   Variation. The depression for the tympanic cavity deepens with age, but relative differences can still be observed in early postnatal individuals.
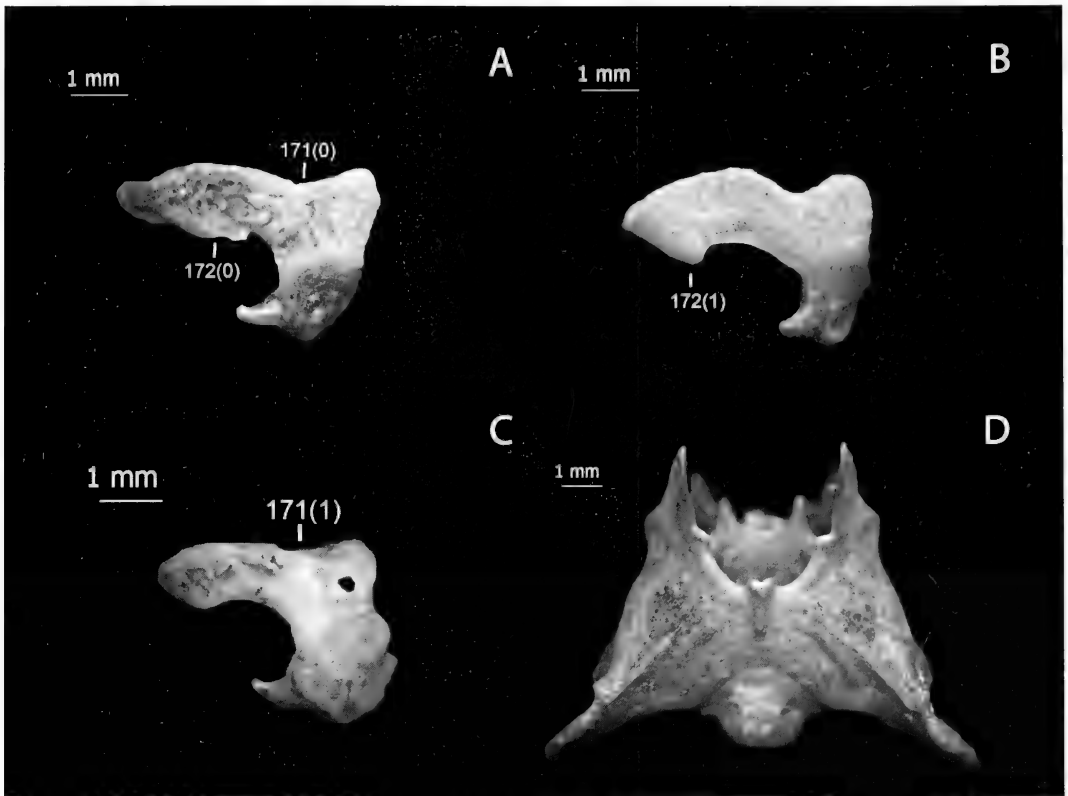
Figure 39. Left quadrates, dorsal, anterior to the top: A, *Xenosaurus newmanorum* NAUQSP-JIM uncatalogued specimen; B, *Xenosaurus grandis* NAUQSP-JIM 1460. A and B illustrate characters 171(0), 172(0), 172(1). C, *Xenosaurus agrenon* UTACV r45008. Illustrates character 171(1). D, Braincase of *Xenosaurus newmanorum* NAUQSP-JIM uncatalogued specimen, dorsal, anterior to the top. Illustrates characters 174, 181(0).

Evolution. Under both analyses, the shallow morphology is a synapomorphy of *Xenosaurus* and of Varanidae.

Braincase

The braincase is unknown for all extinct taxa save *B. ammoskius*, in which it is largely obscured.

174. Braincase: Ratio of greatest mediolateral width to anteroposterior length from posterior end of paroccipital process anteriorly to level of anterior end of alar process (Fig. 39C) (0) 1.20 or less; (1) between 1.20 and 1.50; (2) 1.50 or greater.

Variation. The proportions of the braincase vary significantly during ontogeny (Barahona and Barbadillo, 1998; Bever et al., 2005). In particular, the paroccipital processes become relatively longer with the relative expansion of the adductor chamber relative to the brain, and the alar processes of the prootic lengthen. This character must be evaluated on relatively large, adult individuals with fused braincases.

Evolution. Under both analyses, a ratio of 1.20 or less is an autapomorphy of *X. newmanorum*. Under Analysis 1, the ancestral state for the entire group and for Anguimorpha is 1.50 or greater. A ratio of 1.20 to 1.50 is an autapomorphy of *S. crocodilurus*, a synapomorphy of Anguidae, and a synapomorphy of *X. rackhami* + *X. grandis*. A ratio of 1.20 or
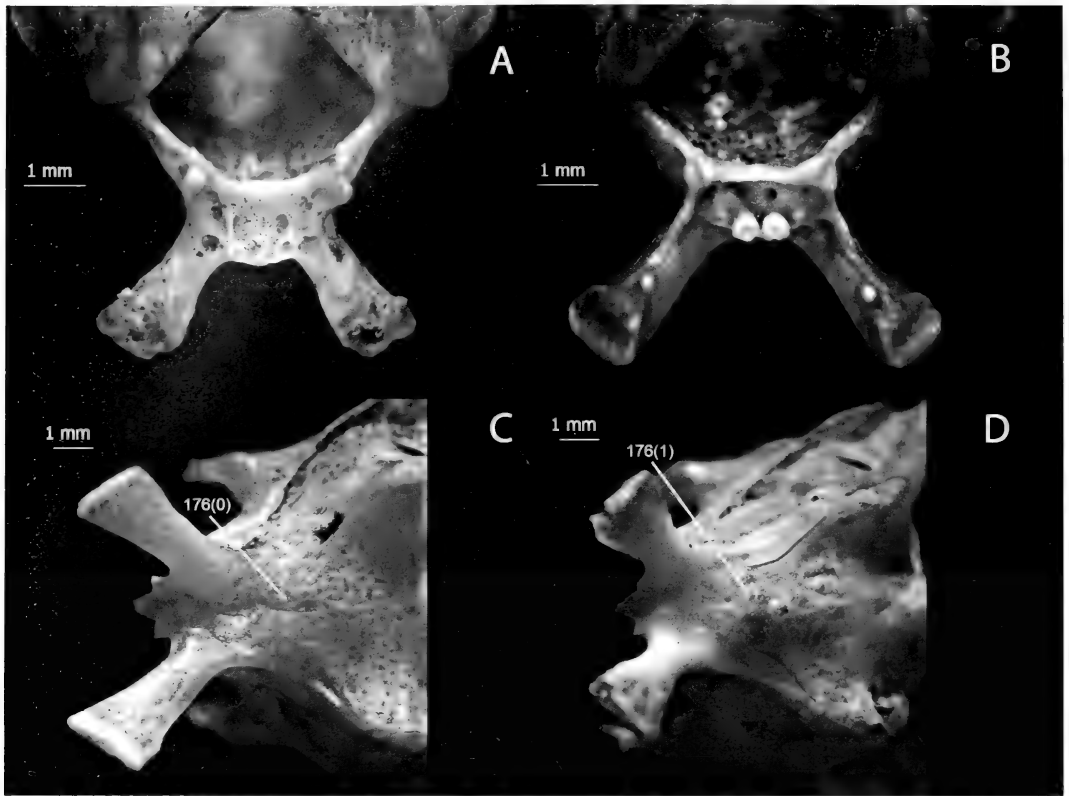
Figure 40. A, Braincase of *Xenosaurus agrenon* UTACV r45008, anterior. Illustrates character 175(0). B, Braincase of *Xenosaurus platyceps* UF 45622, anterior. Illustrates character 175(1). C, Braincase of *Xenosaurus grandis* NAUQSP-JIM 1460, ventral, anterior to the left. Illustrates character 176(0). D, Braincase of *Xenosaurus agrenon* UTACV r45008, ventral, anterior to the left. Illustrates character 176(1).

less is a synapomorphy of *E. multicarinata + O. ventralis*. Under Analysis 2, the ancestral state for the entire group and Anguimorpha is ambiguous between 1.20 to 1.50 and 1.50 or greater. The ancestral state for Anguidae is ambiguous between 1.20 or less and 1.20 to 1.50.

175. Braincase: Carotid fossa and retractor pits (0) shallow, barely excavated (Fig. 40A); (1) deeply excavated (Fig. 40B).

  Variation. The carotid fossa and retractor pits deepen somewhat with age, and only relatively large adults were scored.

  Evolution. Under both analyses, the shallow morphology is the ancestral state for the entire group and for

Anguimorpha and the ancestral state for *Xenosaurus* is ambiguous. Under Analysis 1, the ancestral state for *Xenosaurus* + Anguidae and all mixed nodes therein is ambiguous. Under Analysis 2, the ancestral state for Xenosauridae and for Anguidae + Varanoidea is the shallow morphology. The deep morphology is an autapomorphy of *O. ventralis* and of Helodermatidae.

176. Braincase: Domed portion of ventral surface spanning sphenoid/basioccipital suture (0) divided into bilateral swellings with median groove (Fig. 40C); (1) projected into a single swelling without midline groove, bearing small tubercle slightly posterior to apex of dome in basioccipital region (Fig. 40D).
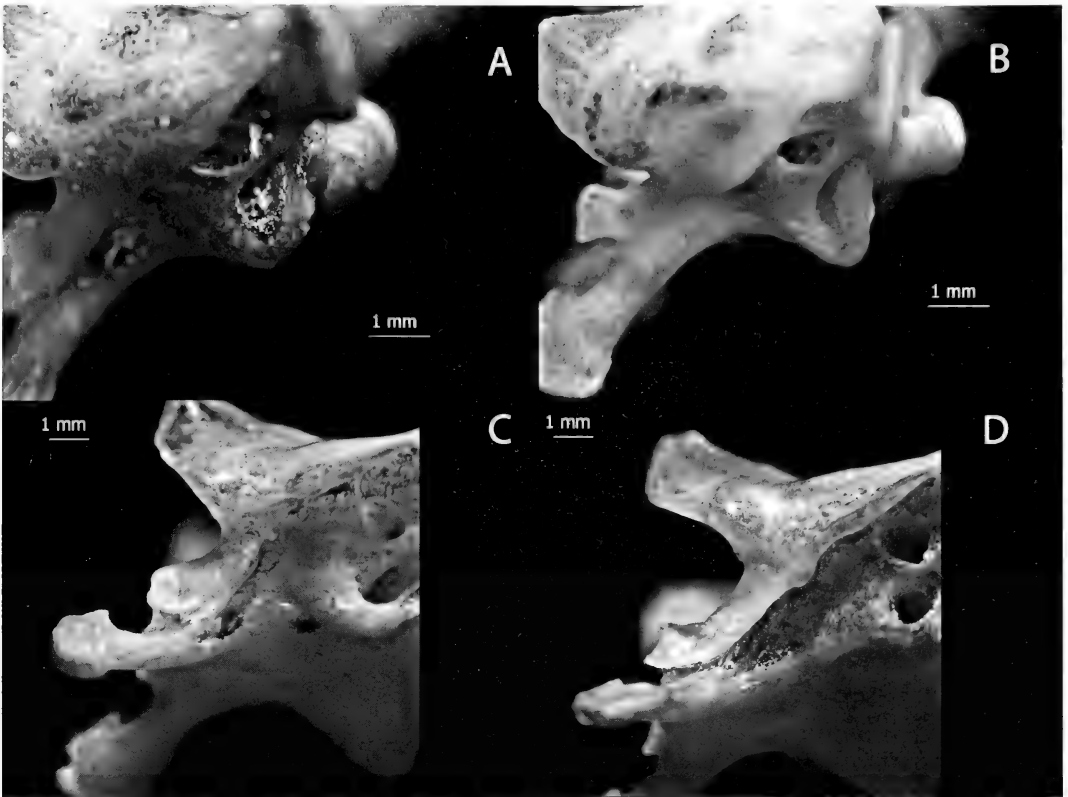
Figure 41.   A, Braincase of *Xenosaurus newmanorum* NAUQSP-JIM uncatalogued specimen, left lateral, anterior to the left. Illustrates character 170(0). B, Braincase of *Xenosaurus rackhami* UTEP-OC "MALB" 388, left lateral, anterior to the left. Illustrates character 177(1). C, Braincase of *Xenosaurus grandis* NAUQSP-JIM 1460, left ventrolateral, anterior to the left. Illustrates character 178(0). D, Braincase of *Xenosaurus newmanorum* NAUQSP-JIM uncatalogued specimen, left ventrolateral, anterior to the left. Illustrates character 178(1).

Evolution. Under both analyses, the undivided morphology is an autapomorphy of *C. enneagrammus* and a synapomorphy of *X. agrenon* + *X. rectocollaris*. Under Analysis 1, the ancestral state for the entire group and for Anguimorpha is ambiguous. The ancestral state for *Xenosaurus* + Anguidae is the divided morphology. Under Analysis 2, the ancestral state for the entire group, Anguimorpha, Xenosauridae, and Anguidae + Varanoidea is the divided morphology.

177. Braincase: Sphenooccipital tubercles (0) rounded and blunt (Fig. 41A); (1) acutely pointed (Fig. 41B).

Variation. The sphenooccipital tubercles become more prominent with age, and their terminal shape forms in the later stages of postnatal ontogeny; this character should be scored on relatively large adults with fused braincases.

Evolution. Under both analyses, the pointed morphology is an autapomorphy of *O. ventralis* and of *X. rackhami*.

178. Braincase: Recessus vena jugularis (0) ends anteriorly behind anterior tip of alar process of sphenoid (Fig. 41C); (1) extends along entirety of lateral surface of alar process (Fig. 41D).

Variation. The recessus vena jugularis and the alar process of the sphenoid
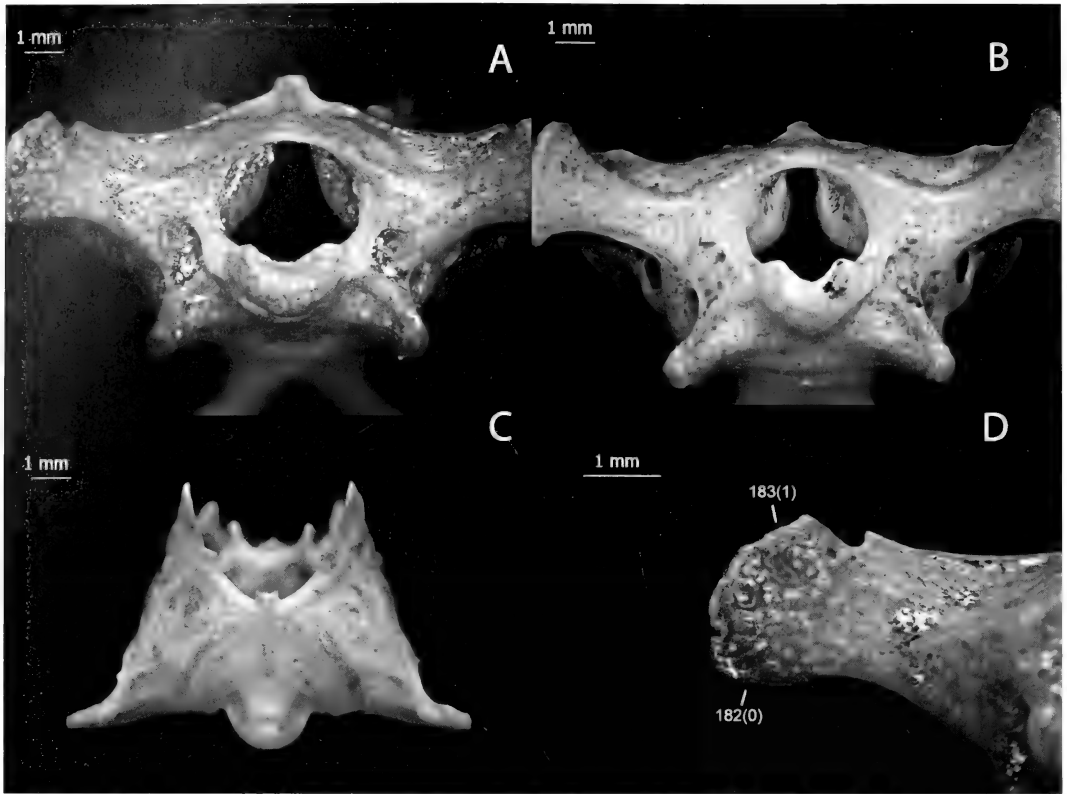
Figure 42.   A, Braincase of *Xenosaurus newmanorum* NAUQSP-JIM uncatalogued specimen, posterior. Illustrates characters 179(0), 180(0). B, Braincase of *Xenosaurus grandis* NAUQSP-JIM 1460, posterior. Illustrates characters 179(1), 180(1). C, Braincase of *Xenosaurus rackhami* UTEP-OC "MALB" 388, dorsal, anterior to the top. Illustrates character 181(1). D, Braincase of *Xenosaurus newmanorum* NAUQSP-JIM uncatalogued specimen, posterior. Illustrates characters 182(0), 183(1).

both develop largely after hatching. This character should be scored on relatively large adults.

Evolution. Under Analysis 1, extension to the anterior end of the alar process is an autapomorphy of *S. crocodilurus* and a synapomorphy of the northern clade of *Xenosaurus*. Under Analysis 2, the ancestral state for Xenosauridae is ambiguous and the ancestral state for the southern clade of *Xenosaurus* is ending posterior to the tip of the alar process.

179. Braincase: Constriction of odontoid recess (notochordal groove) in dorsal margin of occipital condyle, measured by angle through highest points of notch and deepest point (0) greater

than 120° (Fig. 42A); (1) 120° or less (Fig. 42B).

Variation. The recess becomes somewhat more constricted with age and should be scored on relatively large adults.

Evolution. Under both analyses, an angle of 120° or less is an autapomorphy of *O. ventralis* and a synapomorphy of *X. rackhami* + *X. grandis*.

180. Braincase: Cava capsulares within braincase (0) leave relatively wide space between them—mediolateral separation at closest approach greater than one-quarter mediolateral width of foramen magnum at that dorsoventral level (Fig. 42A); (1) approach closely— mediolateral separation at closest ap-
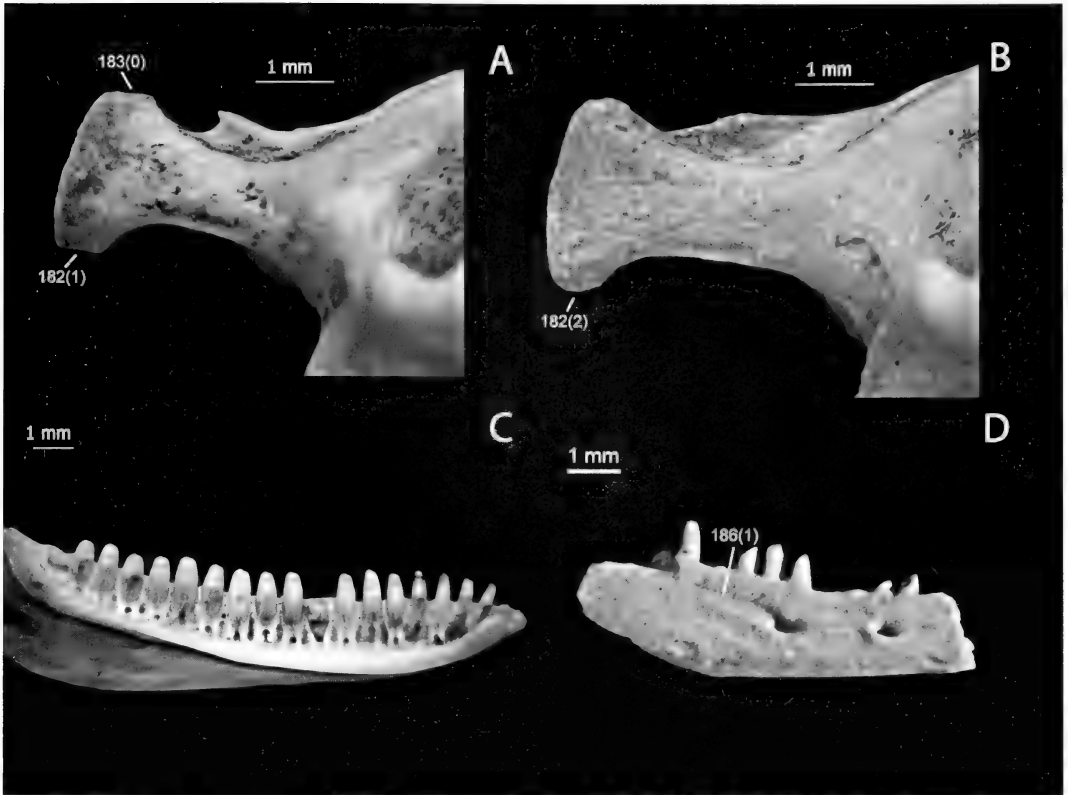
Figure 43.   A, Braincase of *Xenosaurus agrenon* UTACV r45008, posterior. Illustrates characters 182(1), 183(0). B, Braincase of *Xenosaurus grandis* NAUQSP-JIM 1460, posterior. Illustrates character 182(2). C, Left dentary of *Xenosaurus rackhami* UTEP-OC "MALB" 388, medial, anterior to the right. Illustrates characters 185(0), 197(1). D, Right dentary of *Exostinus serratus*, CT scan of AMNH 1608, lateral, anterior to the right. Illustrates characters 185(1), 186(1), 195(1), 196(1).

proach one-quarter or less mediolateral width of foramen magnum at that dorsoventral level (Fig. 42B).

Variation. The approach of the cava capsulares increases somewhat with age and should be scored in relatively large adults.

Evolution. Under both analyses, close approach is an autapomorphy of *O. ventralis* and of *X. grandis.*

181. Braincase: Paroccipital processes (0) distinctly posterolaterally directed (Fig. 39D); (1) only slightly posterolaterally directed, nearly oriented mediolaterally (Fig. 42C).

Variation. The posterior direction of the paroccipital processes tends to

increase with age and should be scored in relatively large adults.

Evolution. Under Analysis 1, the ancestral state for the entire group and Anguimorpha, as well as all internal mixed nodes, is ambiguous. Under Analysis 2, the ancestral state for the entire group and for Anguimorpha is lateral extension. Posterolateral extension is a synapomorphy of *C. enneagrammus* + *O. ventralis* and an autapomorphy of *L. borneensis.* The ancestral state for Xenosauridae is ambiguous.

182. Braincase: Expanded tips of paroccipital processes—ventral projections (0) absent (Fig. 42D); (1) present, squared off or blunt (Fig. 43A); (2) present, long and pointed (Fig. 43B).

Variation. The projections become more prominent during early postnatal ontogeny and should be scored in relatively large adults.

Evolution. Under both analyses, absence of projections is an autapomorphy of *S. crocodilurus* and of *X. newmanorum*. Under Analysis 1, the ancestral state for the entire group and for Anguimorpha is ambiguous between squared off and long and pointed, as is that for *S. crocodilurus* + Varanidae, *Xenosaurus* + Anguidae, and *Xenosaurus*. Under Analysis 2, the ancestral state for the entire group and for Anguimorpha is long and pointed. Blunt or squared-off is an autapomorphy of Helodermatidae and a synapomorphy of Xenosauridae. Within Xenosauridae, the long and pointed state is a synapomorphy of *X. rackhami* + *X. grandis*.

183. Braincase: Expanded tips of paroccipital processes—dorsal projections (0) present as blunt or squared off tab (Fig. 43A); (1) low, barely divergent (Fig. 42D).

Variation. Dorsal projections tend to become more prominent during postnatal ontogeny and should be scored in relatively large adults.

Evolution. Under Analysis 1, the ancestral state for the entire group and all mixed nodes therein is ambiguous. Under Analysis 2, the ancestral state for the entire group and for Anguimorpha is presence of relatively extensive projections. The low and rounded morphology is a synapomorphy of Varanoidea and the northern clade of *Xenosaurus* and an autapomorphy of *C. enneagrammus*.

Dentary

184. Dentary: Anterior tip of dentary (0) relatively pointed in sagittal plane (Fig. 1A); (1) blunt, truncated, with steeply rising "chin" (genioglossus attachment area).

Evolution. Under both analyses, the ancestral state for the entire group and for Anguimorpha is the relatively pointed morphology. The ancestral state for *E. lancensis* + *Xenosaurus* is ambiguous, and the ancestral state for *Xenosaurus* is pointed.

185. Dentary: Posterior, rising section of dorsal edge of dentary extends for (0) more than six tooth positions (Fig. 43C); (1) six or fewer tooth positions (Fig. 43D).

Evolution. Under Analysis 1, the ancestral state for the entire group is ambiguous, and the ancestral state for Anguimorpha is six or fewer tooth positions. More than six tooth positions is a synapomorphy of *O. ventralis* + *E. multicarinata* and an autapomorphy of *M. ornatus*. The ancestral state for *Xenosaurus* + *E. lancensis* is ambiguous, as is that of *Xenosaurus* + *E. serratus*. Under Analysis 2, the ancestral state for the entire group and for Anguimorpha is more than six tooth positions. Six or fewer tooth positions is a synapomorphy of Varanoidea and *S. crocodilurus* + *B. ammoskius* and an autapomorphy of *C. enneagrammus*, *R. rugosus*, and *E. serratus*.

186. Dentary: Groove anterior to coronoid facet on lateral surface of dentary (0) shallow and short, not approaching posteriormost mental foramen (Fig. 44A); (1) deep and long, approaching or running to posteriormost mental foramen (Fig. 43D).

Evolution. Under both analyses, the ancestral state for the entire group and for Anguimorpha is the shallow, short morphology. Under Analysis 1, the deep, long morphology is a synapomorphy of *Xenosaurus* + *R. rugosus* and an autapomorphy of *S. crocodilurus*. Under Analysis 2, the deep, long morphology is a synapomorphy of Xenosauridae.
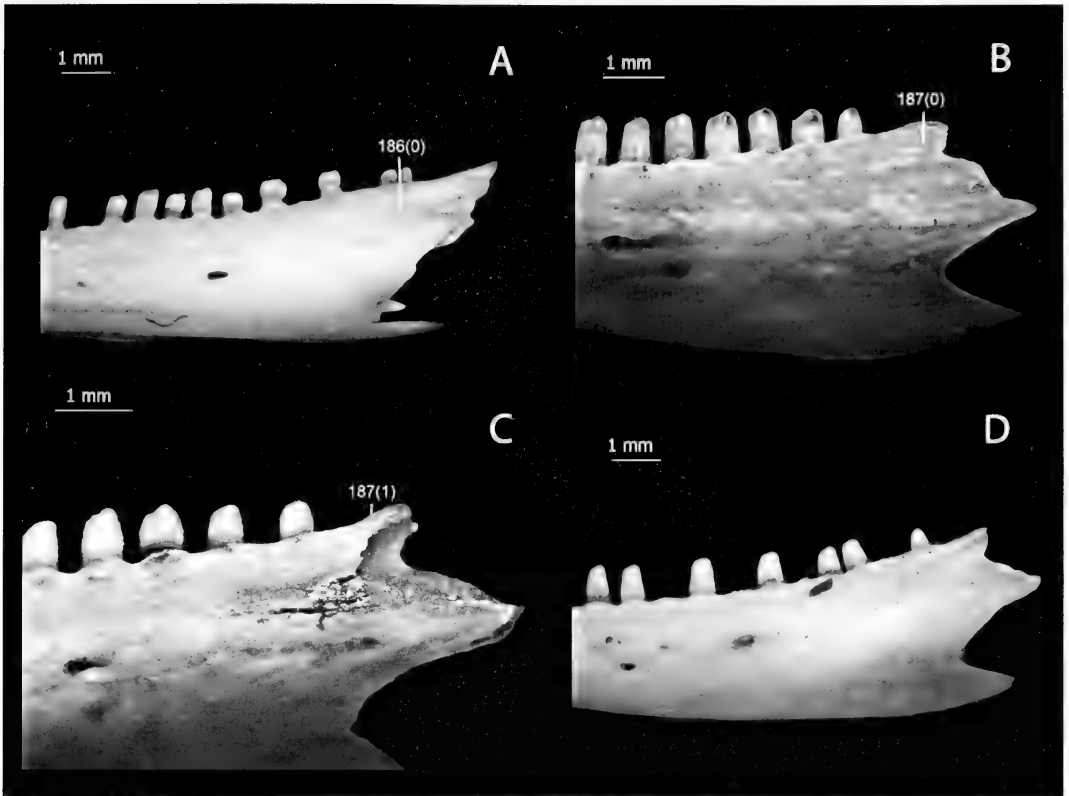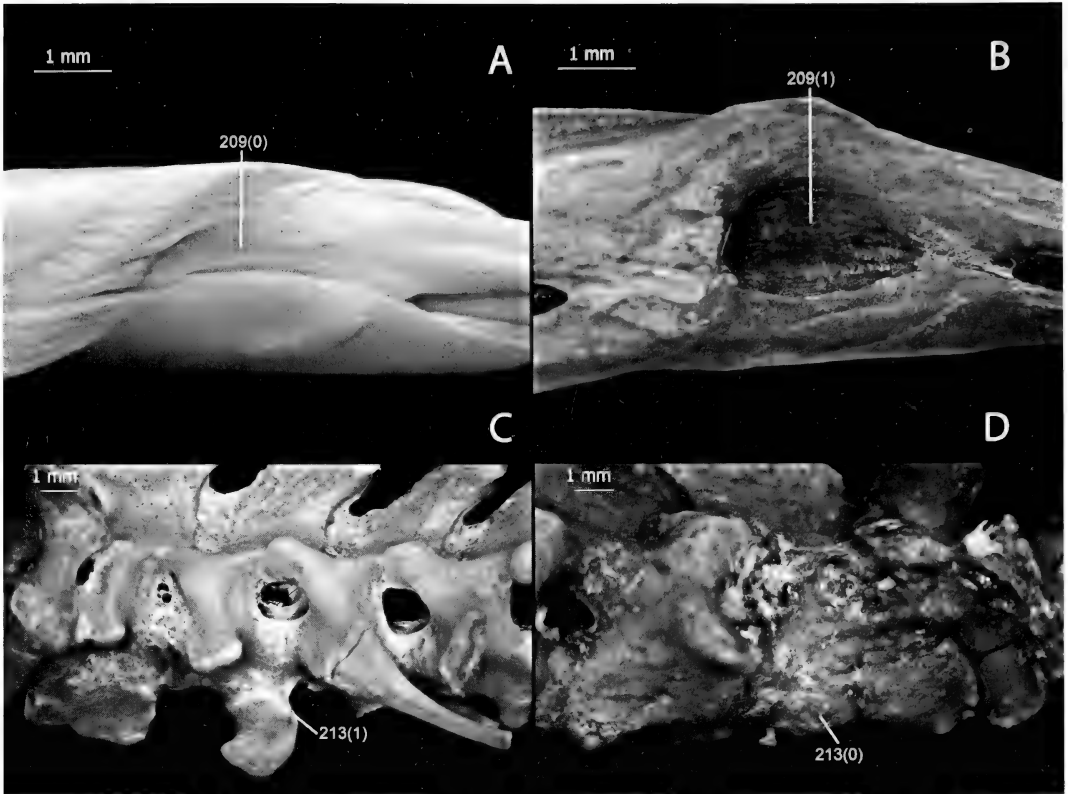
Figure 44.   A, Left dentary of *Elgaria multicarinata* TMM-M 8958, lateral, anterior to the left. Illustrates characters 186(0), 188(0). B, Left dentary of *Xenosaurus grandis* NAUQSP-JIM 1460, lateral, anterior to the left. Illustrates characters 187(0), 190(0). C, Left dentary of *Xenosaurus newmanorum* NAUQSP-JIM uncatalogued specimen, lateral, anterior to the left. Illustrates character 187(1). D, Left dentary of *Xenosaurus agrenon* UTACV r45008, lateral, anterior to the left. Illustrates characters 188(1), 189(1), 190(1).

187. Dentary: Lateral coronoid facet (0) shallowly impressed, surrounded dorsally and anteriorly by low ridge (Fig. 44B); (1) deeply impressed, surrounded by sharp ridge (Fig. 44C).

Evolution. Under both analyses, deep impression with a sharp ridge is a synapomorphy of the northern clade of *Xenosaurus* and an autapomorphy of *C. enneagrammus*.

188. Dentary: Coronoid process (0) extending posteriorly beyond surangular process (Fig. 44A); (1) ending anterior to tip of surangular process (Fig. 44D).

Evolution. Under both analyses, the ancestral state for the entire group is ambiguous, and that for Anguimorpha is extension beyond the surangular process. Ending anterior to the surangular process is a synapomorphy of *X. agrenon* + *X. rectocollaris* and an autapomorphy of *S. crocodilurus* and of Helodermatidae.

189. Dentary: Surangular notch between surangular and angular process (0) absent (Estes et al., 1988, fig. 11B); (1) present (Fig. 44D). Presence or absence of a surangular notch was character 63 of Estes et al. (1988).

Evolution. Under both analyses, the ancestral state of the entire group is ambiguous.

190. Dentary: Tip of angular process (0) pointed (Fig. 44B); (1) blunt and slightly bifurcated (Fig. 44D).
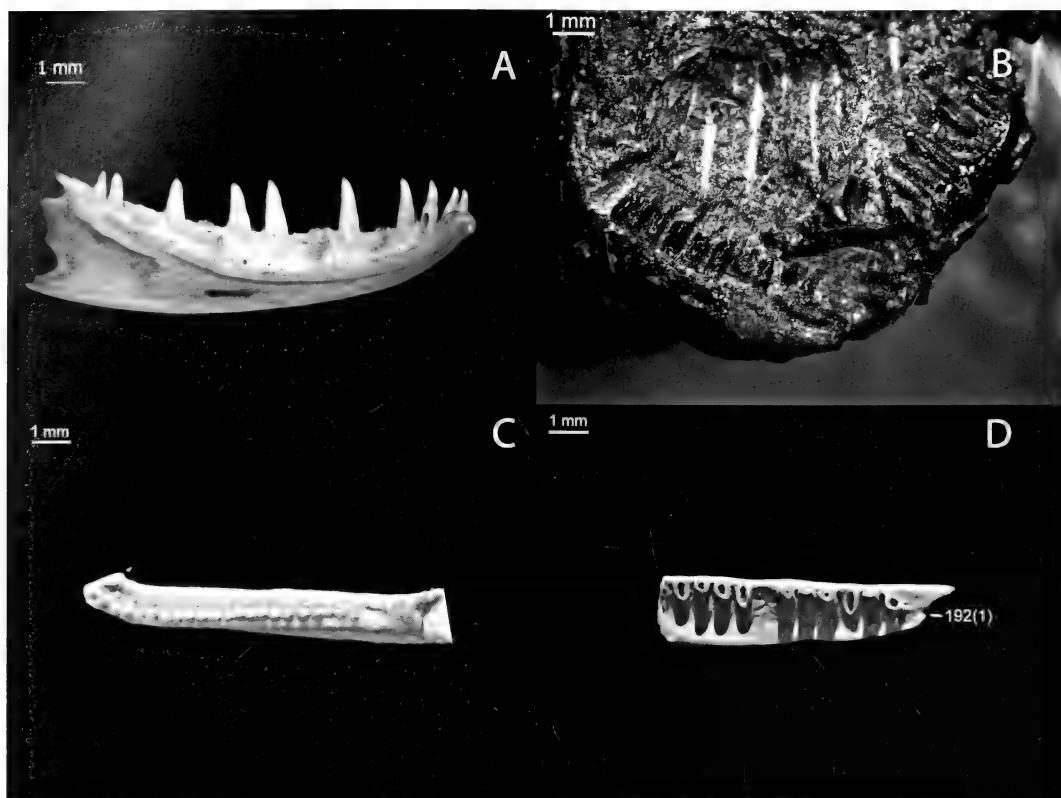
Figure 45.   A, Left dentary of *Shinisaurus crocodilurus* UF 72805, medial, anterior to the right. Illustrates characters 191(0), 193, 195(2). B, Left and right dentaries of *Restes rugosus* YPM PU 14640, lateral and medial, respectively, anterior to the left. Illustrates character 191(1). C, Left dentary of *Xenosaurus rectocollaris*, CT scan of UF 51443, dorsal, anterior to the left. Illustrates characters 192(0), 194(0). D, Right dentary of *Exostinus serratus*, CT scan of AMNH 1608, dorsal, anterior to the left. Illustrates characters 192(1), 194(1).

Evolution. Under both analyses, a blunt, slightly bifurcated angular process is a synapomorphy of *X. agrenon* + *X. rectocollaris.*

191. Dentary: Suprameckelian lip (0) becomes dorsoventrally taller anteriorly, but Meckel's groove remains fairly widely open (Fig. 45A); (1) becomes dorsoventrally tall anteriorly, restricting Meckel's groove to thin slit (Fig. 45B).

Evolution. Under both analyses, the ancestral state for *Xenosaurus* + *R. rugosus* and *Xenosaurus* + *E. lancensis* was ambiguous.

192. Dentary: Wedge-shaped process extending posteriorly from suprameckelian lip near posterior end of dental gutter (0) absent (Fig. 45C); (1) present (Fig. 45D).

Evolution. Under both analyses, the presence of a wedge-shaped process is an autapomorphy of *E. serratus.*

193. Dentary: Apex of posterior u-shaped emargination in intramandibular septum (Fig. 45A) at level of (0) third or fewer tooth position from back of dentary; (1) fourth tooth position from back; (2) fifth tooth position from back; (3) sixth or more tooth position from back.

Evolution. Under both analyses, the ancestral state for *Xenosaurus* + *R. rugosus* is at the level of the fourth tooth position from the back, and the

state for *Xenosaurus* + *E. lancensis* and *Xenosaurus* + *E. serratus* is ambiguous between the fourth and fifth tooth position from the back. The ancestral state for *Xenosaurus* is the fifth tooth position from the back. A position at the level of the fourth tooth position from the back is an autapomorphy of *X. grandis*, and one at the level of the sixth from the back is an autapomorphy of *X. new-manorum*. Finally, a position at the level of the sixth from the back is an autapomorphy of *E. multicarinata*. Under Analysis 1, the ancestral state for the entire group, for Anguimorpha, *S. croco-dilurus* + Varanidae, *Xenosaurus* + Anguidae, and Anguidae + Helodermatidae, is the third or fewer tooth position from the back. A position at the level of the fourth tooth position from the back is a synapomorphy of *Xenosaurus* + *R. rugo-sus*, of *E. multicarinata* + *O. ventralis* and of *S. crocodilurus* + *M. ornatus*. Under Analysis 2, the ancestral state for the entire group and for Anguimorpha is ambiguous between the third and fourth tooth positions from the back. That for Xenosauridae is the fourth tooth position from the back, and that for Varanoidea is the third from the back.

194. Dentary: Posterior end of tooth row in horizontal plane (0) relatively straight or with slight medial inflection (Fig. 45C); (1) with marked medial inflection (Fig. 45D).

Evolution. Under both analyses, medial inflection is an autapomorphy of *E. serratus*.

195. Dentary: Tooth height (0) short, with one-third or less of most teeth extending above dorsal margin of dentary (Fig. 45A); (1) intermediate height, between one-third and half of most teeth extending above dorsal margin of dentary (Fig. 46A); (2) tall, with half or more of most teeth extending above dorsal margin of dentary (Fig. 46B).

Evolution. Under both analyses, the ancestral state for the entire group is

ambiguous between tall and intermediate height, and the ancestral state for Anguimorpha is intermediate height. The ancestral state for *Xenosaurus* + *R. rugosus* is intermediate height, and the short morphology is a synapomorphy of *Xenosaurus*. Under Analysis 1, the ancestral state for *Xenosaurus* + Anguidae is intermediate height. The tall morphology is a synapomorphy of *S. crocodilurus* + Varanidae and an autapomorphy of Helodermatidae. Under Analysis 2, the ancestral state for Anguidae + Varanoidea and for Xenosauridae is intermediate height. The tall morphology is a synapomorphy of shinisaurs and of Varanoidea.

196. Dentary: Tooth height (0) declines drastically posteriorly, with two or three teeth anterior to most posterior tooth about half to two-thirds the height of tallest dentary teeth (Fig. 46A); (1) declines less, with teeth just anterior to most posterior tooth nearly the same height as tallest dentary teeth (Fig. 43D).

Evolution. Under both analyses, a precipitous decline is the ancestral state for the entire group and for Anguimorpha. Lack of a decline is ancestral for *Xenosaurus* + *R. rugosus* and for shinisaurs. A precipitous decline is a synapomorphy of *Xenosaurus*. Under Analysis 1, lack of a decline is a synapomorphy of *Xenosaurus* + *R. rugosus* and of shinisaurs. Under Analysis 2, lack of a decline is a synapomorphy of Xenosauridae.

197. Dentary: Shafts of teeth (0) do not change drastically in diameter posteriorly, save at anterior tip in premaxillary–maxillary occlusal transition (Fig. 46A); (1) increase markedly in diameter posteriorly (Fig. 43C).

Variation. The differentiation of shaft widths becomes more pronounced with age.

Evolution. Under both analyses, a marked posterior increase in diameter
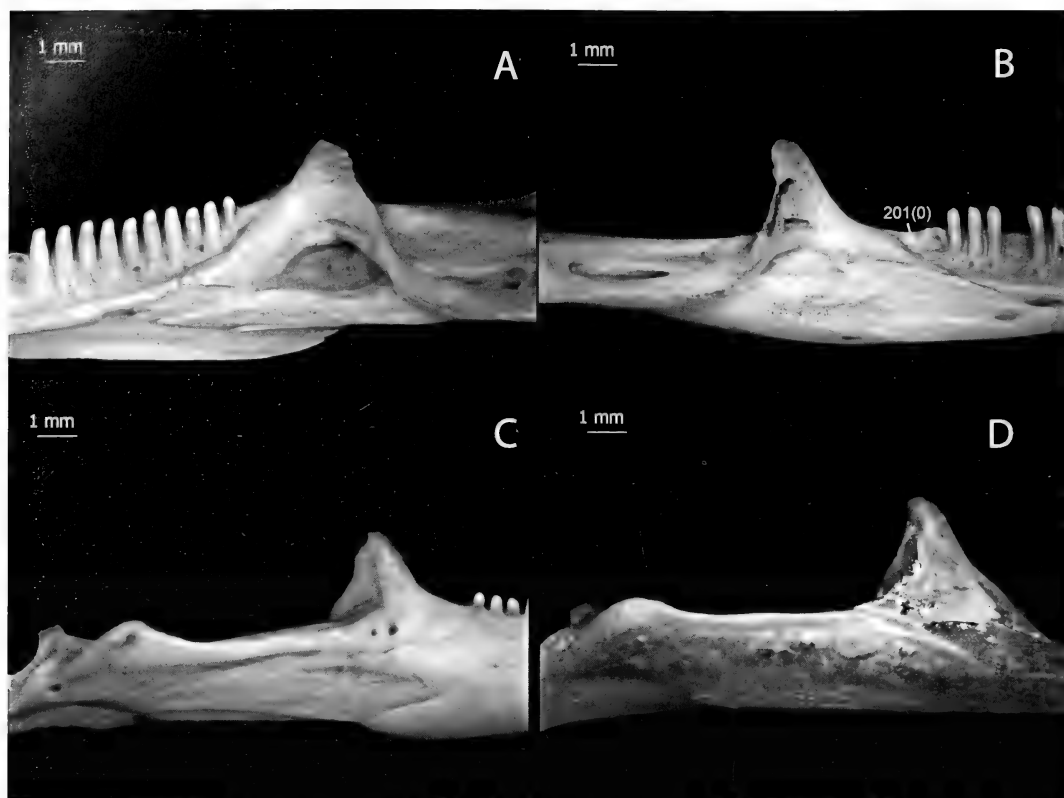
Figure 46.   A, Right mandible of *Xenosaurus platyceps* UF 45622, medial, anterior to the left. Illustrates characters 195(0), 196(0), 197(0), 200(1), 201(1), 202(1), 203(0), 204(0). B, Left mandible of *Elgaria multicarinata* CAS 54241, medial, anterior to the right. Illustrates characters 195(1), 200(0), 201(0). C, Right mandible of *Xenosaurus platyceps* UF 45622, lateral, anterior to the right. Illustrates characters 198(0), 199(1), 205(2), 206(1), 208(1). D, Right mandible of *Xenosaurus newmanorum* NAUQSP-JIM uncatalogued specimen, lateral, anterior to the right. Illustrates characters 198(1), 206(0), 207(1).

is a synapomorphy of *X. rackhami* + *X. grandis.*

Coronoid

The coronoid is unknown for *E. lancensis* and *M. ornatus.*

198. Coronoid: Anterolateral process (0) anteroposteriorly longer than dorsoventrally tall at base (Fig. 46C); (1) taller than long (Fig. 46D).

Evolution. Under both analyses, taller than long is an autapomorphy of *X. newmanorum,* of *X. agrenon,* and of *X. grandis.*

199. Coronoid: Posterolateral process: (0) ventral margin directed posterodorsally, resulting in taper for entire length

(Fig. 47A); (1) ventral margin directed straight posteriorly for most of length, resulting in a dorsoventrally extensive process (Fig. 46C).

Evolution. Under both analyses, a straight ventral margin and tall posterolateral process is a synapomorphy of *Xenosaurus.*

200. Coronoid: Posteromedial process (0) trending posteroventrally without strong bend toward the vertical (Fig. 46B); (1) becoming nearly vertical at tip, resulting in highly bowed appearance of coronoid arch (Fig. 47B).

Evolution. Under Analysis 1, the ancestral state for the entire group and
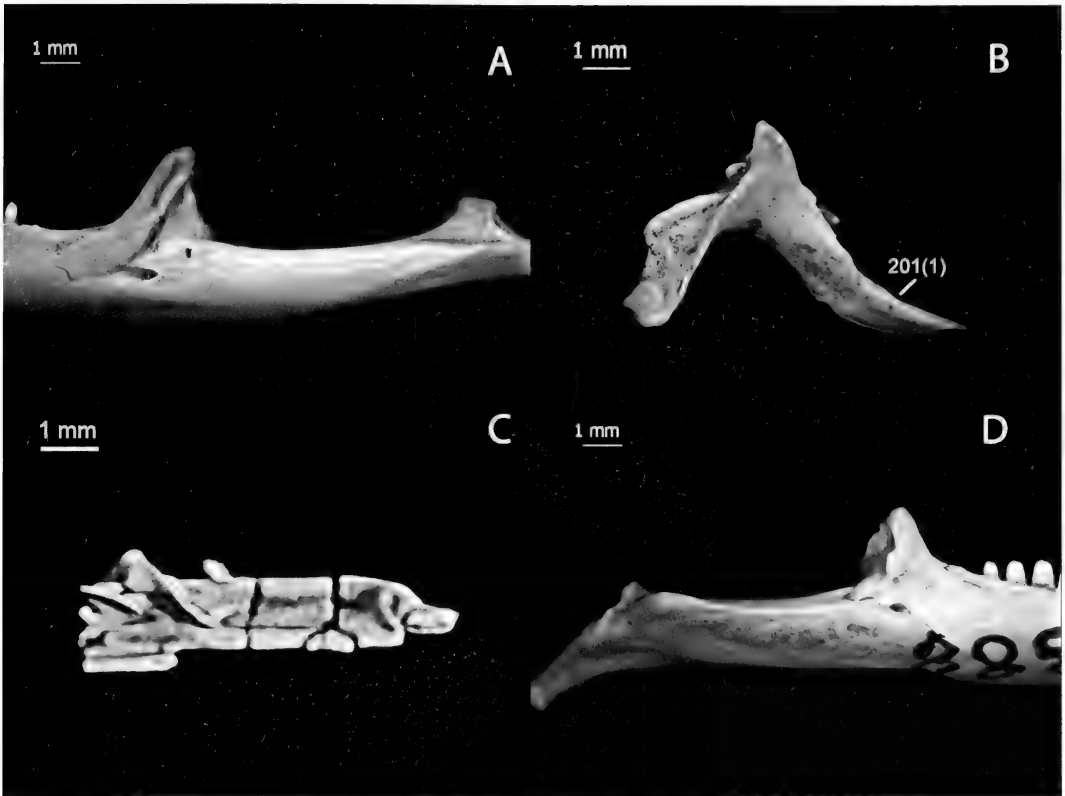
Figure 47.   A, Left mandible of *Elgaria multicarinata* CAS 54241, dorsolateral, anterior to the left. Illustrates characters 199(0), 205(0), 207(0), 208(0). B, Left coronoid of *Xenosaurus agrenon* UTACV r45008, medial, anterior to the right. Illustrates characters 200(1), 201(1), 202(0), 203(1). C, Right mandible of *Restes rugosus*, CT scan of YPM PU 14640, medial, anterior to the left. Illustrates character 204(1). D, Right mandible of *Xenosaurus rackhami* UTEP-OC "MALB" 388, lateral, anterior to the right. Illustrates character 205(1).

for Anguimorpha is ambiguous. The ancestral state for Anguidae + Helodermatidae is the relatively straight morphology. Under Analysis 2, the ancestral state for the entire group and for Anguimorpha is the bowed morphology. The straight morphology is a synapomorphy of Anguidae + Varanoidea and an autapomorphy of *R. rugosus*.

201. Coronoid: Anteromedial process (0) with abrupt constriction of dorsal and ventral margins about a third of the way toward anterior tip followed by continued taper (Fig. 46B); (1) gradually tapering without abrupt constriction or with slight step in dorsal, but not ventral, margin (Fig. 47B).

Evolution. Under both analyses, a gradual taper is a synapomorphy of *Xenosaurus* and of *Varanus*.

202. Coronoid: Anteromedial process (0) more than twice as long along long axis as tall perpendicular to long axis at widest level (Fig. 47B); (1) twice as long as tall or less, with thickened process restricting exposed portion anteriorly (Fig. 46A).

Evolution. Under both analyses, twice as long as tall or shorter is a synapomorphy of the northern clade of *Xenosaurus*. Under Analysis 1, twice as long as tall or shorter is a synapomorphy of *Varanus* and an autapomorphy of Helodermatidae. Under Analysis 2,

twice as long as tall or shorter is a synapomorphy of Varanoidea.

203. Coronoid: Medially facing flange extending posteriorly from posteromedial process for attachment of bodenaponeurosis; ratio of greatest width perpendicular to long axis to length along long axis (0) 0.25 or less (Fig. 46A); (1) greater than 0.25 (Fig. 47B).

    Evolution. Under both analyses, an extensive flange is a synapomorphy of *X. agrenon* + *X. rectocollaris.*

204. Coronoid: Posterior end of posteromedial process (0) extends for short distance along prearticular (ventromedial) rim of adductor fossa (Fig. 46A); (1) ends anterior to adductor fossa (Fig. 47C).

    Evolution. Under both analyses, termination anterior to the adductor fossa is a synapomorphy of the southern clade of *Xenosaurus* and an autapomorphy of *R. rugosus.*

205. Coronoid: Anterior surangular foramen (0) not overlapped by coronoid (Fig. 47A); (1) partially overlapped by coronoid, forming emargination in ventral margin of bone (Fig. 47D); (2) fully overlapped by coronoid, piercing through the bone (Fig. 46C).

    Evolution. Under both analyses, partial overlap is an autapomorphy of *L. borneensis.* Complete overlap is a synapomorphy of *Xenosaurus,* and partial overlap is an autapomorphy of *X. rackhami.*

206. Coronoid: Anterior surangular foramen in coronoid (0) single (Fig. 46D); (1) double (Fig. 46C).

    Evolution. Under both analyses, the paired morphology is an autapomorphy of *X. platyceps.*

Surangular/Prearticular/Articular

The surangular/prearticular/articular complex is unknown in *E. lancensis* and *M. ornatus.*

207. Surangular/prearticular/articular: Strong dorsal crest on surangular lateral to m. adductor externus medialis attachment table (0) absent (Fig. 47A); (1) present (Fig. 46D).

    Variation. The crest becomes more prominent with age, and only relatively large adults should be scored.

    Evolution. Under both analyses, presence of a crest is a synapomorphy of *Xenosaurus* and an autapomorphy of Helodermatidae.

208. Surangular/prearticular/articular: Posterior surangular foramen (0) anterior to articular (Fig. 47A); (1) at anteroposterior level of anterior edge of articular (Fig. 46C).

    Evolution. Under both analyses, a position at the anterior edge of the articular is a synapomorphy of *Xenosaurus.*

209. Surangular/prearticular/articular: Fossa ventral to arc of medial coronoid facet (subcoronoid fossa) (0) shallow, only slightly impressed (Fig. 48A); (1) deep, forming a strongly impressed bowl-shaped cavity (Fig. 48B).

    Evolution. Under both analyses, a deep subcoronoid fossa is a synapomorphy of *Xenosaurus* + *E. serratus.*

210. Surangular/prearticular/articular: Subcoronoid fossa (0) with no medial overhang at posterior end or only slight ridge developed there (Fig. 48A); (1) posteriorly continuing into bone as a blind pocket, sometimes pierced by a foramen, such that a portion of the medial wall of the surangular bearing the facet for the posteromedial process of the coronoid overhangs it (Fig. 48B).

    Evolution. Under both analyses, lack of overhang is the ancestral state for the entire group and for Anguimorpha, and presence of an overhang is the ancestral state for *Xenosaurus* + *R. rugosus.* Under Analysis 1, the ancestral state for *Xenosaurus* + Anguidae and for Anguidae + Helodermatidae is ambiguous, and over-

Figure 48.   A, Left postdentary elements of *Elgaria multicarinata* TMM-M 8958, medial, anterior to the right. Illustrates characters 209(0), 210(0). B, Left postdentary elements of *Xenosaurus grandis* NAUQSP-JIM 1460, medial, anterior to the right. Illustrates characters 209(1), 210(1). C, Cervical vertebrae of *Shinisaurus crocodilurus* MVZ 204291, left lateral, anterior to the left. Illustrates characters 212(0), 213(1). D, Cervical vertebrae of *Heloderma suspectum* CAS 513, right ventrolateral, anterior to the right. Illustrates characters 212(1), 213(0).

hang is an autapomorphy of *L. borneensis*. Under Analysis 2, overhang is a synapomorphy of *Xenosaurus* + *R. rugosus*, and the ancestral state for Varanoidea and Varanidae is ambiguous.

211. Surangular/prearticular/articular: Subcoronoid fossa (0) without foramina; (1) pierced by one or more small foramina; (2) pierced by one large posterior foramen serving as exit for canal from adductor fossa.

Evolution. Under both analyses, the ancestral state for the entire group is ambiguous, and that for Anguimorpha is one or more small foramina. A single large posterior foramen is a synapomorphy of *Xenosaurus*.

Cervical Skeleton

Most or all of the cervical skeleton is lacking in all fossils save *B. ammoskius*.

212. Cervical skeleton: Intercentra three and four (0) dorsoventrally taller than anteroposteriorly long (Fig. 48C); (1) anteroposteriorly longer than dorsoventrally tall (Fig. 48D).

Evolution. Under both analyses, the ancestral state for the entire group and for Anguimorpha is taller than long. Under Analysis 1, the ancestral state for *Xenosaurus* + Anguidae and for Anguidae + Helodermatidae is ambiguous. Under Analysis 2, longer than tall is a synapomorphy of
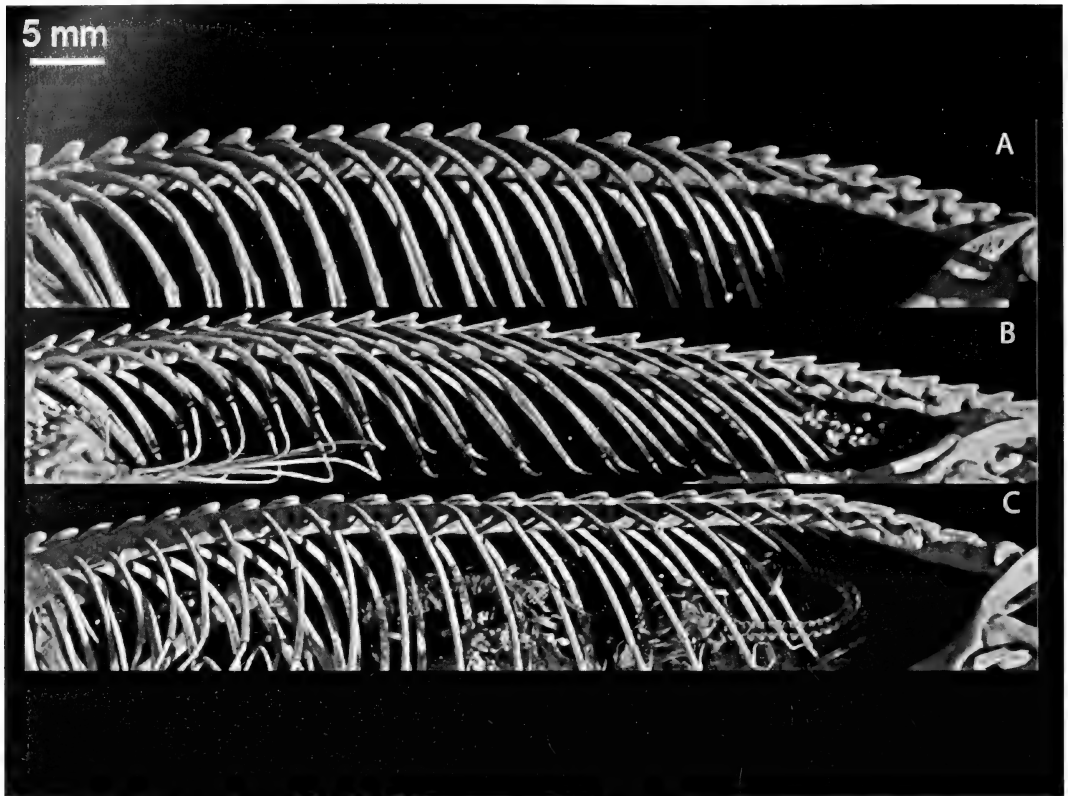
Figure 49.   Trunk skeletons, left lateral, anterior to the left: A, *Xenosaurus newmanorum*, CT scan of UMMZ 126057; B, *Xenosaurus platyceps*, CT scan of UF 25005; C, *Xenosaurus rectocollaris*, CT scan of UF 51443. A illustrates 214(1), 215(1), and 216(0). B illustrates 214(2), 215(2), and 216(0). C illustrates 214(2), 215(0), and 216(1).

Xenosaurus and an autapomorphy of Helodermatidae.

213. Cervical skeleton: Intercentra three and four (0) lateral surfaces gently contoured (Fig. 48D); (1) lateral surfaces bearing small transverse processes (Fig. 48C) (see Estes, 1983).

Evolution. Under both analyses, absence of transverse processes is the ancestral state for the entire group and for Anguimorpha. Under Analysis 1, presence of transverse processes is a synapomorphy of *Xenosaurus* and an autapomorphy of *S. crocodilurus*. Under Analysis 2, longer presence of transverse processes is a synapomorphy of Xenosauridae.

Trunk Skeleton

The trunk skeleton is unknown for all fossil taxa save *B. ammoskius* and *R. rugosus*. In the latter, only a few disarticulated vertebrae are preserved.

214. Trunk skeleton: Thoracic vertebral column, neural spines (0) tall, anterior edges sloping at about 45° to centrum; (1) spines in posterior third of thoracic column bearing long ribs low, anterior edges sloping at well under 45° (Fig. 49A); (2) all thoracic neural spines low, sloping at under 45° (Fig. 49B).

Variation. Neural spines heighten with age, especially during early postnatal ontogeny. This character should be scored on relatively large adults.

Evolution. Under both analyses, the low morphology in the posterior portion of the dorsal column is a synapomorphy of *Xenosaurus* + *R. rugosus.* The uniformly low morphology in the thoracic dorsal column is an autapomorphy of *X. platyceps* and of *X. rectocollaris.*

215. Trunk skeleton: Neural spines, posterodorsal projection formed by anteroventral slope of posterior edges (0) absent on most vertebrae, posterior edges of neural spines vertical or sloping posteroventrally (Fig. 49C); (1) well-developed, tip of neural spine blunt or rectangular (Fig. 49A); (2) well-developed, tip of neural spine produced into narrow finger-like process (Fig. 49B).

Variation. Neural spines grow substantially during early postnatal ontogeny and so this character should not be scored on individuals less than about half of adult size.

Evolution. Under both analyses, the ancestral state for the entire group and for Anguimorpha is the well-developed, blunt morphology. Absence is an autapomorphy of *X. rectocollaris,* and long, narrow production is an autapomorphy of *X. platyceps.*

216. Trunk skeleton: Lumbar neural spines (0) posteriorly sloped, anterior and posterior edges sloped with an anteroventral/posterodorsal orientation (Fig. 49A); (1) low, flat rectangles with weak, if any, slope (Fig. 49C).

Evolution. Under both analyses, the low, rectangular morphology is a synapomorphy of *X. agrenon* + *X. rectocollaris.*

Caudal Skeleton

The caudal skeleton is unknown for all fossils save *B. ammoskius.*

217. Caudal skeleton: Caudal vertebral count (average, rounded to nearest integer) (0)

35 to 39; (1) 40 to 44; (2) 45 to 49; (3) 50 to 54; (4) 55 to 59; (5) 60 to 64; (6) 65 to 69; (7) 70 to 74; (8) 75 to 79; (9) 80 to 84; (A) 85 to 89; (B) 90 to 94.

Variation. As noted, the values scored above are averages. A small amount of variation in caudal vertebral counts occurs. Furthermore, intact tails are present in a small fraction of specimens from modern skeletal collections and a smaller fraction still of fossils.

Evolution. Under both analyses, the ancestral state for *Xenosaurus* is 40 to 44 and that for the southern clade of *Xenosaurus* is ambiguous between 35 to 39 and 40 to 44. A count of 60 to 64 is a synapomorphy of Varanidae, and a count of 90 to 94 a synapomorphy of *Varanus* or an autapomorphy of *V. exanthematicus.* A count of 65 to 69 is an autapomorphy of *O. ventralis,* and 35 to 39 is an autapomorphy of Helodermatidae. Under Analysis 1, the ancestral state for the entire group and for Anguimorpha is ambiguous between 40 to 44 and 45 to 49, as is that for *Xenosaurus* + Anguidae and Anguidae + Helodermatidae. A count of 50 to 54 is a synapomorphy of *E. multicarinata* + *O. ventralis.* The ancestral state for *S. crocodilurus* + Varanidae is 45 to 49. Under Analysis 2, the ancestral state for the entire group and for Anguidae is ambiguous between 45 to 49 and 50 to 54, as is that for Anguidae + Varanoidea and for Varanoidea. The ancestral state for Anguidae is 50 to 54. The ancestral state for Xenosauridae is 45 to 49, and 40 to 44 is a synapomorphy of *Xenosaurus.*

218. Caudal skeleton: Caudal autotomy planes (0) present (Fig. 50A); (1) absent (Fig. 164). (See character 103 of Estes et al., 1988).

Variation. Autotomy planes are formed in most taxa by the time of hatching.
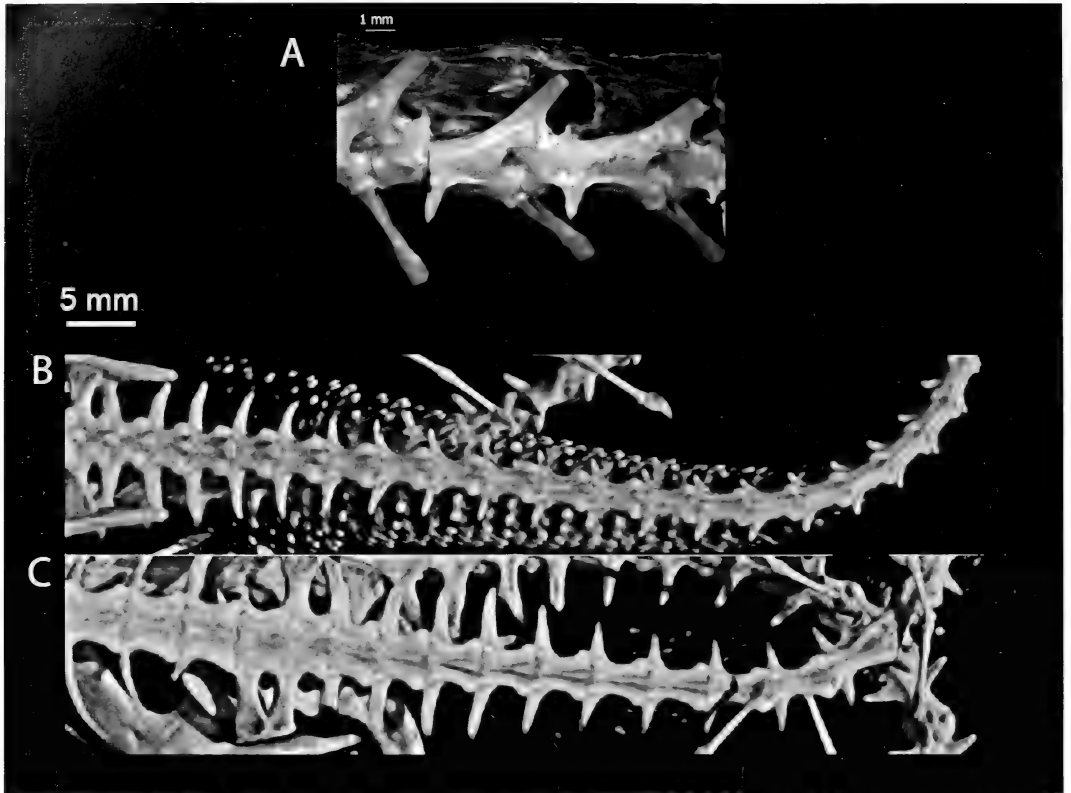
Figure 50.   A, Caudal vertebrae of *Shinisaurus crocodilurus* MVZ 204291, left lateral, anterior to the left. Illustrates character 218(0). Caudal vertebrae, dorsal, anterior to the left: B, *Xenosaurus newmanorum*, CT scan of UMMZ 126057; C, *Xenosaurus platyceps*, CT scan of UF 25005. B and C illustrate characters 218(1), 268(0), 268(1).

Evolution. Under Analysis 1, the ancestral state for the entire group and for Anguimorpha is ambiguous. Under Analysis 2, the ancestral state for the entire group and for Anguimorpha is presence of autotomy planes, and their absence is a synapomorphy of *Xenosaurus* and of Varanoidea.

Pectoral Girdle

The pectoral girdle is unknown for all extinct taxa save *B. ammoskius*.

219. Pectoral girdle: Scapulocoracoid emargination: (0) dorsal and ventral margins strongly diverging for most of length (Fig. 51A); (1) dorsal and ventral margins weakly diverging or nearly parallel for most of length (Fig. 51B).

Evolution. Under both analyses, weak or no divergence is a synapomorphy of the northern clade of *Xenosaurus* and of *Varanus*, as well as an autapomorphy of *C. enneagrammus*.

220. Pectoral girdle: Scapulocoracoid emargination; ratio of greatest height perpendicular to long axis to length along long axis (0) 0.70 or greater (Fig. 51C); (1) less than 0.70 (Fig. 51D).

Evolution. Under both analyses, the ancestral state for Anguidae is ambiguous, and a ratio of less than 0.70 is a synapomorphy of the northern clade of *Xenosaurus*.
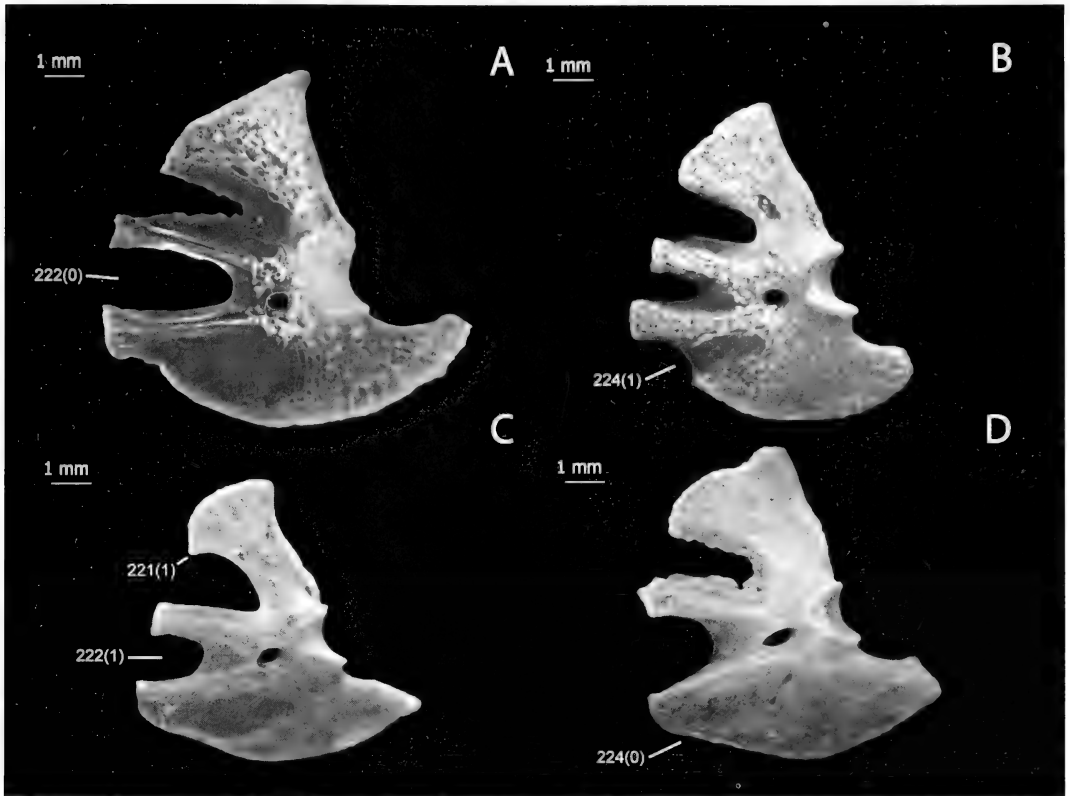
Figure 51.   A, Left scapulocoracoid of *Elgaria multicarinata* TMM-M 8993, lateral, anterior to the left. Illustrates characters 219(0), 222(0), 223. B, Left scapulocoracoid of *Xenosaurus newmanorum* NAUQSP-JIM uncatalogued specimen, lateral, anterior to the left. Illustrates characters 219(1), 221(0), 224(1). C, Left scapulocoracoid of *Xenosaurus rackhami* UTEP-OC "MALB" 388, lateral, anterior to the left. Illustrates characters 220(0), 221(1), 222(1), 225(0). D, Left scapulocoracoid of *Xenosaurus platyceps* UF 45622, lateral, anterior to the left. Illustrates characters 220(1), 224(0), 225(1).

221. Pectoral girdle: Sharp hook-like overhang of scapulocoracoid emargination by scapula (0) absent (Fig. 51B); (1) present (Fig. 51C).

Evolution. Under both analyses, presence of an overhang is a synapomorphy of *X. rackhami* + *X. grandis.*

222. Pectoral girdle: Length of anterior coracoid emargination along long axis from apex of emargination to anterior end of dorsal margin (0) equal to or greater than length of remainder of scapulocoracoid along line of axis continued posteriorly from apex (Fig. 51A); (1) less than length of remainder of scapulocoracoid (Fig. 51C).

Evolution. Under Analysis 1, the ancestral state for the entire group and for Anguimorpha is ambiguous, as is that for all mixed internal nodes. Under Analysis 2, the ancestral state for the entire group and Anguimorpha is as long or longer than the remainder of the scapulocoracoid. Shorter than the remainder is a synapomorphy of *Xenosaurus* and of Varanoidea.

223. Pectoral girdle: Anterior coracoid emargination; ratio of greatest height perpendicular to long axis to length along long axis (Fig. 51B) (0) 0.50 or less; (1) between 0.50 and 0.85; (2) 0.85 or greater.

Evolution. Under both analyses, the ancestral state for the entire group and for Anguimorpha is between 0.50 and 0.85. The state 0.50 or less is an autapomorphy of *X. newmanorum*, whereas 0.85 or greater is an autapomorphy of *X. platyceps* and of *L. borneensis*. Under Analysis 1, the ancestral state for Anguidae + Helodermatidae and for Anguidae is ambiguous between 0.50 or less and between 0.50 and 0.85. The state 0.50 or less is a synapomorphy of *Varanus*. Under Analysis 2, the ancestral state for Anguidae + Varanoidea is ambiguous between states 0.50 or less and between 0.50 and 0.85.

224. Pectoral girdle: Posterior coracoid emargination (0) absent, ventral margin of coracoid curves smoothly (Fig. 51D); (1) present at least as abrupt anterior change in angle of ventral margin of coracoid toward the horizontal and straightening of curve (Fig. 51B) (see character 112 of Estes et al., 1988).

Evolution. Under both analyses, the ancestral state for the entire group is ambiguous, and that for Anguimorpha is absence of the emargination. Presence of the emargination is an autapomorphy of *X. newmanorum*, of *C. enneagrammus*, and of *L. borneensis*.

225. Pectoral girdle: Posterior end of coracoid (0) terminating in a point (Fig. 51C); (1) squared-off or blunt, attenuate (Fig. 51D).

Evolution. Under both analyses, the squared-off or blunt morphology is a synapomorphy of the northern clade of *Xenosaurus*.

226. Pectoral girdle: Clavicle, flattened tip of sternal ramus (0) in plane parallel or oblique to that of flattened portion of scapular ramus; (1) in plane nearly perpendicular to that of flattened portion of scapular ramus.

Evolution. Under both analyses, the nearly perpendicular morphology is a synapomorphy of the northern clade of *Xenosaurus*.

227. Pectoral girdle: Clavicle, corner between rami (0) projected into long, narrow process (Fig. 52A); (1) produced into distinct, moderately long eminence (Fig. 52B); (2) produced only slightly into small thickening or bump (Fig. 52C).

Evolution. Under both analyses, the ancestral state for the entire group and for Anguimorpha is ambiguous between production into a moderately long eminence and slight production. The long morphology is an autapomorphy of *S. crocodilurus* and of *E. multicarinata*. Under Analysis 1, the ancestral state for *S. crocodilurus* + Varanidae is ambiguous in the same way as Anguimorpha. The ancestral state for *Xenosaurus* + Anguidae is slight production, and moderate production is a synapomorphy of *X. rackhami* + *X. grandis*.

228. Pectoral girdle: Interclavicle, lateral processes (0) without proximal change in angle (Fig. 52A); (1) extending perpendicular to longitudinal body of interclavicle for short proximal stretch before abruptly angling backward (Fig. 52B).

Evolution. Under both analyses, the morphology involving a proximal transverse stretch and a posterior inflection is a synapomorphy of *Xenosaurus*.

229. Pectoral girdle: Interclavicle, angle of distal portion of lateral process to longitudinal body (0) 65° or less (Fig. 52B); (1) greater than 65° (Fig. 52C).

Evolution. Under both analyses, an angle greater than 65° is a synapomorphy of the northern clade of *Xenosaurus* and an autapomorphy of *X. rectocollaris* and of *L. borneensis*.

230. Pectoral girdle: Interclavicle, ratio of length of lateral process to length of posterior process (including section
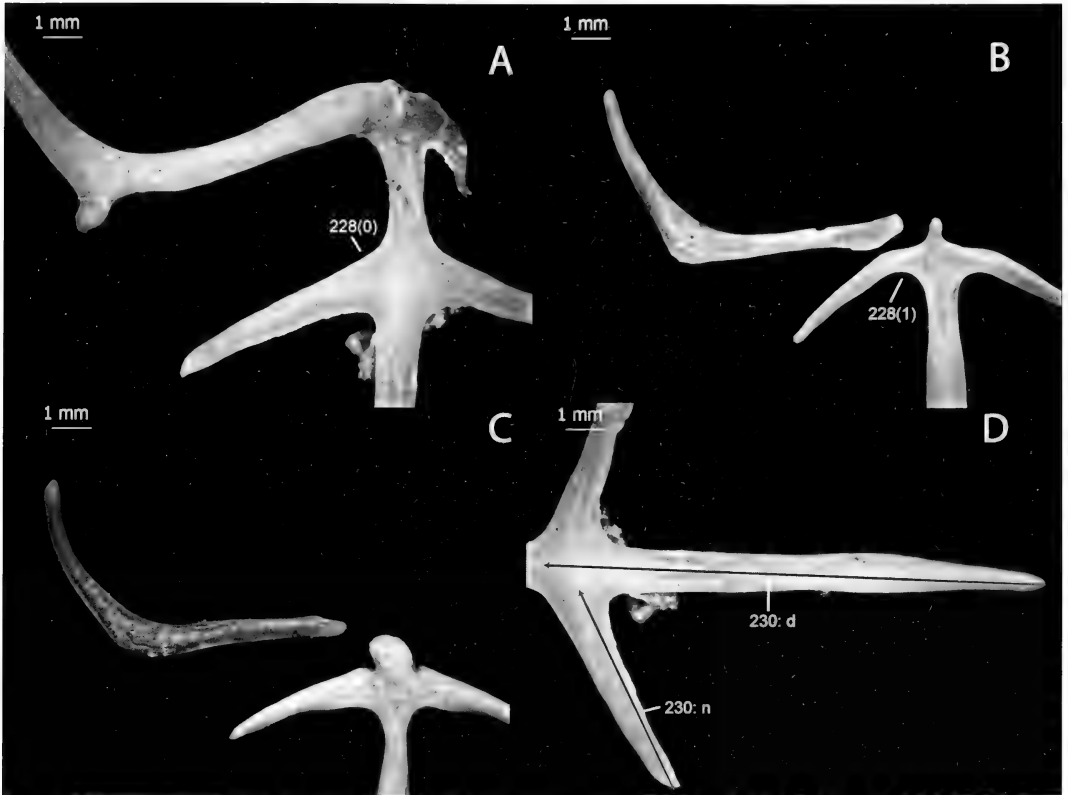
Figure 52. A, Interclavicle and right clavicle of *Shinisaurus crocodilurus* MVZ 204291, ventral, anterior to the top. Illustrates characters 227(0), 228(0), 231(0). B, Interclavicle and right clavicle of *Xenosaurus rackhami* UTEP-OC "MALB" 388, ventral, anterior to the top. Illustrates characters 227(1), 229(0), 228(1). C, Interclavicle and right clavicle of *Xenosaurus newmanorum* NAUQSP-JIM uncatalogued specimen, ventral, anterior to the top. Illustrates characters 227(2), 229(1), 231(1). D, Interclavicle of *Shinisaurus crocodilurus* MVZ 204291, ventral, anterior to the left. Illustrates character 230 (n for numerator, d for denominator).

between lateral processes) (Fig. 52D) (0) 0.55 or greater; (1) less than 0.55.

Evolution. Under both analyses, the ancestral state for the entire group and for Anguimorpha is less than 0.55, and 0.55 or greater is an autapomorphy of *S. crocodilurus*. Under Analysis 1, the ancestral state for Anguidae + Helodermatidae and for Anguidae is ambiguous. Under Analysis 2, a ratio of 0.55 or greater is an autapomorphy of *E. multicarinata* and of Helodermatidae.

231. Pectoral girdle: Interclavicle, anterior process (0) prominent, several times as long as wide (Fig. 52A); (1) present as small eminence or absent (Fig. 52C)

(see character 120 of Estes et al., 1988).

Evolution. Under both analyses, the ancestral state for the entire group and for Anguimorpha is small size or absence. Prominence is a synapomorphy of Anguidae and an autapomorphy of *S. crocodilurus*.

Forelimb

The forelimb is unknown for all fossils but *B. ammoskius*.

232. Forelimb: Ulna, ratio of width perpendicular to long axis at narrowest part of shaft to length along long axis (0) 0.07 or less (Fig. 53A); (1) greater than 0.07 (Fig. 53B).

Figure 53.   Left ulnae, anterior, distal to the left: A, *Xenosaurus newmanorum* NAUQSP-JIM uncatalogued specimen; B, *Xenosaurus platyceps* UF 45622. A and B illustrate characters 232(0), 232(1). Right ilia, lateral, anterior to the right: C, *Xenosaurus newmanorum* NAUQSP-JIM uncatalogued specimen. Illustrates character 233(0). D, *Shinisaurus crocodilurus* MVZ 204291. Illustrates character 233(1).

Evolution. Under both analyses, relative width with a ratio greater than 0.07 is an autapomorphy of *X. platyceps*.

Pelvic Girdle

The pelvic girdle is unknown for *E. serratus*, *E. lancensis*, and *M. ornatus*. Only the ilium is preserved in *R. rugosus*; the taxon cannot be scored for the other elements. *Ophisaurus ventralis* has a vestigial pelvic girdle and could not be scored for these characters.

233. Pelvic girdle: Narrowing at tip of ilium (0) primarily resulting from change in angle in ventral margin of ilium (Fig. 53C); (1) primarily resulting from

change in angle in dorsal margin (Fig. 53D).

Evolution. Under both analyses, tapering resulting from a dorsal change in angle is a synapomorphy of *S. crocodilurus* + *B. ammoskius*.

234. Pelvic girdle: Thyroid fenestra, ratio in plane of fenestra of longest anteroposterior length parallel to symphysis to widest mediolateral width perpendicular to symphysis (Fig. 54A) (0) less than 0.95; (1) from 0.95 to less than 1.20; (2) 1.20 or greater.

Evolution. Under both analyses, the ancestral state for the entire group and for Anguimorpha is between 0.95 and 1.20. A ratio of less than 0.95 is an
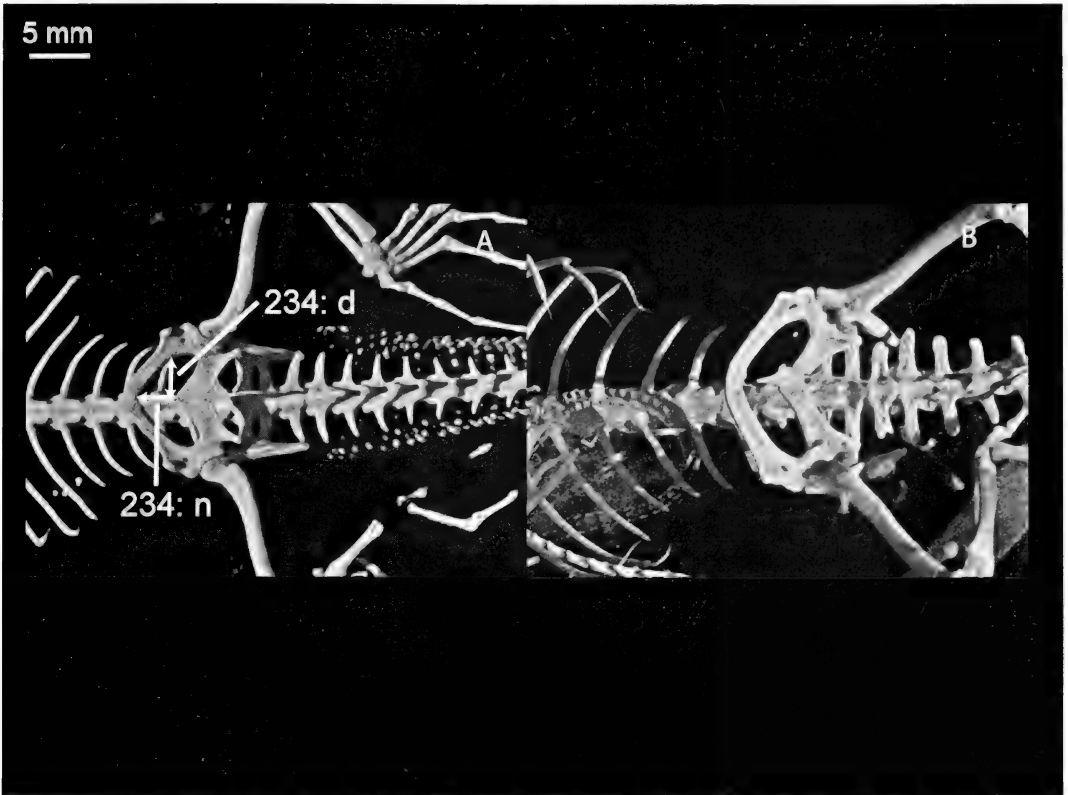
Figure 54.   Pelvic girdles and posterior axial skeletons, ventral, anterior to the left: A, *Xenosaurus newmanorum*, CT scan of UMMZ 126057; B, *Xenosaurus rectocollaris*, CT scan of UF 51443. A illustrates 234 (n for numerator, d for denominator), 235(1), 236(0), and 267(1). B illustrates 235(0), 236(1), and 267(2).

autapomorphy of *X. newmanorum*, of *X. rectocollaris*, and of *C. enneagrammus*. A ratio of 1.20 or greater is an autapomorphy of *X. platyceps*.

235. Pelvic girdle: Pubis, ratio of width perpendicular to long axis just medial to pectineal tubercle to length along long axis from tubercle to symphysis (0) greater than 0.38 (Fig. 54B); (1) 0.38 or less (Fig. 54A).

Evolution. Under both analyses, a ratio of 0.38 or less is an autapomorphy of *X. newmanorum* and of *C. enneagrammus*.

236. Pelvic girdle: Ischium (0) flat, broadly plate-like with constriction near mediolateral midpoint (Fig. 54A); (1) narrow, tapering medially with constriction

absent or weakly present far medially (Fig. 54B).

Evolution. Under both analyses, the narrow, tapering, unconstricted morphology is an autapomorphy of *X. rectocollaris*.

Hind Limb

The hind limb is unknown for all extinct taxa save *B. ammoskius*.

237. Hind limb: Femur, femoral neck in plane of knee flexion (0) wider perpendicular to long axis than long (Fig. 55A); (1) longer along long axis than wide (Fig. 55B).

Evolution. Under both analyses, longer-than-wide is an autapomorphy of *X. platyceps*.
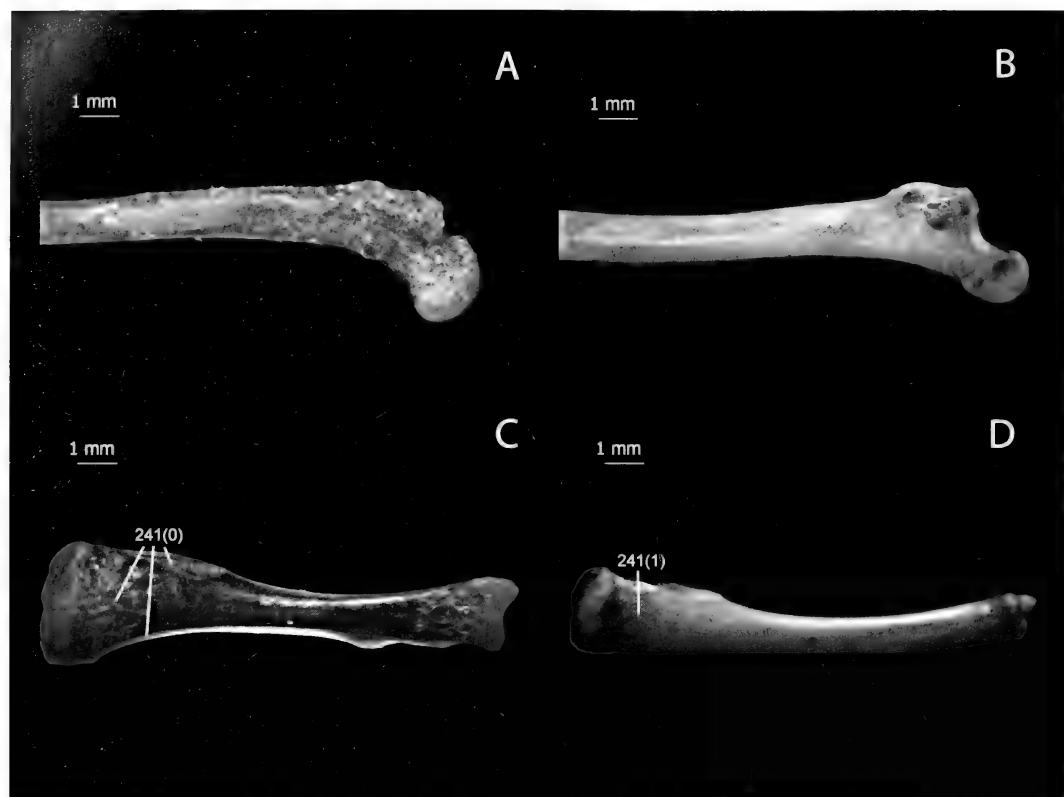
Figure 55.   Left femora, anterior, distal to the left: A, *Xenosaurus grandis* NAUQSP-JIM 1460; B, *Xenosaurus platyceps* UF 45622. A and B illustrate characters 237(0), 237(1). Left tibiae, flexor view, distal to the right: C, *Xenosaurus newmanorum* NAUQSP-JIM uncatalogued specimen; D, *Elgaria multicarinata* TMM-M 8958. C and D illustrate characters 238(0), 238(1), 239(0), 239(1), 240(0), 241(0), 241(1).

238. Hind limb: Tibia, width measured by ratio of anteroposterior length across extensor surface at proximal end, just distal to epiphysis, to proximodistal length (0) wide, 0.25 or greater (Fig. 55C); (1) narrow, less than 0.25 (Fig. 55D).

Evolution. Under both analyses, the ancestral state for the entire group and for Anguimorpha is ambiguous. Under Analysis 1, the ancestral state for *S. crocodilurus* + Varanidae and for Anguidae + Helodermatidae is 0.25 or greater. The ancestral state for *Xenosaurus* + Anguidae is ambiguous. Under Analysis 2, the ancestral state for Anguidae + Varanoidea is 0.25 or greater and that for Xenosauridae is ambiguous.

239. Hind limb: Tibia, anterior crest margin (0) straight or slightly convex (Fig. 55C); (1) concave in plane of crest (Fig. 55D).

Evolution. Under both analyses, the concave morphology is a synapomorphy of the northern clade of *Xenosaurus* and an autapomorphy of *X. agrenon*.

240. Hind limb: Tibia, anterior crest occupies (0) about one-quarter of shaft of tibia (Fig. 55C); (1) about one-fifth of shaft of tibia; (2) minimal portion of shaft, crest reduced to small distal eminence (Fig. 56A).

Evolution. Under both analyses, the ancestral state for the entire group is ambiguous among all three states. That
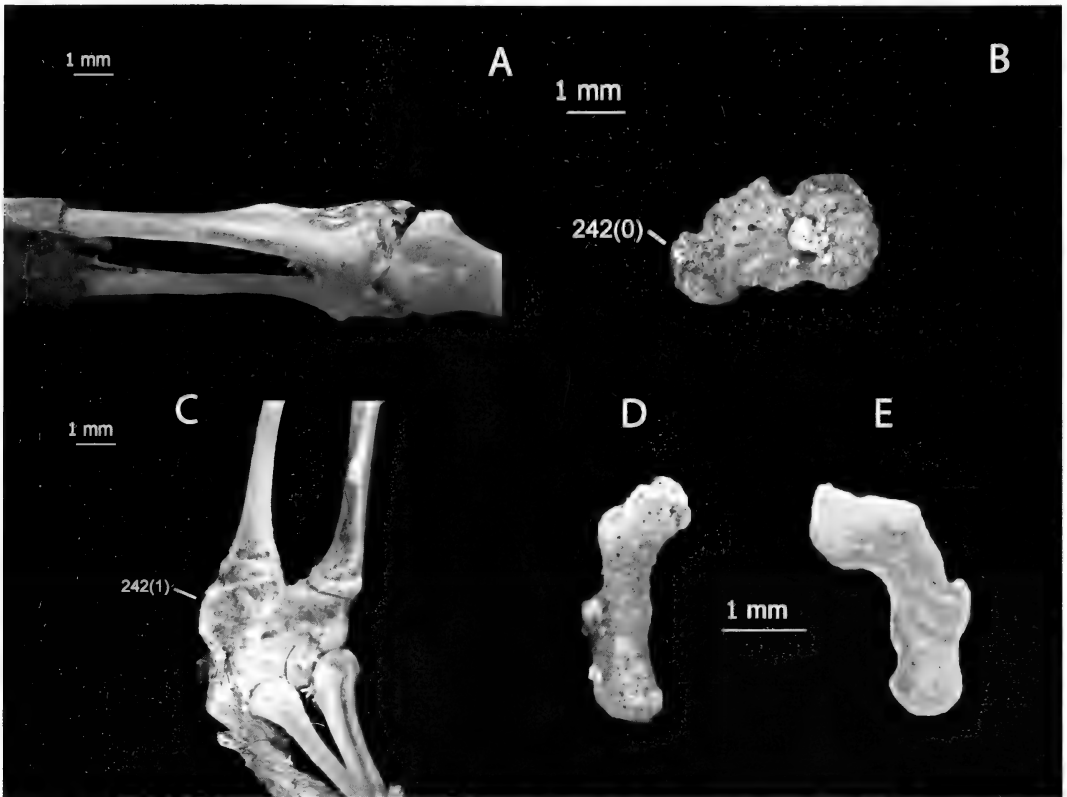
Figure 56.   A, Right lower hind limb of *Xenosaurus rackhami* MCZ 54317, flexor view, distal to the left. Illustrates character 240(2). B, Left astragalocalcaneum of *Xenosaurus newmanorum* NAUQSP-JIM uncatalogued specimen, flexor view, distal toward the bottom. Illustrates character 242(0). C, Left astragalocalcaneum of *Xenosaurus grandis* MVZ 128947, flexor view, distal toward the bottom. Illustrates character 242(1). Fifth metatarsals, extensor view, distal toward the bottom: D, left, *Xenosaurus newmanorum* NAUQSP-JIM uncatalogued specimen; E, right, *Elgaria multicarinata* TMM-M 8958.

for Anguimorpha is occupation of one-quarter of the shaft. Occupation of one-fifth of the shaft is an autapomorphy of *X. platyceps* and of *B. ammoskius*. Occupation of a minimal portion of the shaft as a small nub or eminence is an autapomorphy of *X. rackhami*.

241. Hind limb: Tibia, proximal sulci on flexor surface for attachment of m. semimembranosus and m. tibialis posterior among other muscles (0) forming distinct, shallow grooves (Fig. 55C); (1) barely incised, represented only by a flattening of tibial surface (Fig. 55D).

Evolution. Under both analyses, the simple, flattened morphology is ancestral

for the entire group and for Anguimorpha. Under Analysis 1, deep incision is a synapomorphy of *Varanus* or Varanidae and of Anguidae. Under Analysis 2, the ancestral state for Anguidae + Varanoidea is ambiguous.

242. Hind limb: Calcaneum, length of calcaneal heel measured by ratio of anteroposterior length to proximodistal width (0) long, 0.50 or greater (Fig. 56B); (1) short, less than 0.50 (Fig. 56C).

Evolution. Under both analyses, the ancestral state for the entire group is ambiguous, and that for Anguimorpha is the long morphology. The short

morphology is a synapomorphy of the southern clade of *Xenosaurus* and an autapomorphy of *L. borneensis*.

243. Hind limb: Fifth metatarsal, flexo-extensor bending such that metatarsal is concave in the extensor direction (0) strongly arched, in part because of heavy development of expanded proximal end (Fig. 56E); (1) weak, creating a gentle, nearly horizontal arc (Fig. 56D).

Evolution. Under both analyses, a weak flexo-extensor arch is a synapomorphy of *Xenosaurus*.

244. Hind limb: Fifth metatarsal, anteroposterior expansion of head measured by ratio of anteroposterior length at longest proximodistal level to proximodistal length of metatarsal (0) relatively great, 0.65 or greater (Fig. 56E); (1) relatively slight, less than 0.65 (Fig. 56D).

Evolution. Under both analyses, the ancestral state for the entire group and for Anguimorpha is slight expansion. Under Analysis 1, relative expansion is a synapomorphy of Anguidae + Helodermatidae and of *Varanus*. Under Analysis 2, it is a synapomorphy of Anguidae + Varanoidea, and slight expansion is an autapomorphy of *L. borneensis* within that clade.

245. Hind limb: Fifth metatarsal, lateral plantar tubercle (0) nearly perpendicular to medial plantar tubercle in plane perpendicular to long axis of metatarsal; (1) at an acute angle to medial plantar tubercle.

Evolution. Under both analyses, an acute angle is a synapomorphy of the southern clade of *Xenosaurus* and of Varanidae.

Osteoderms, General

These notes apply to all osteoderm character categories. Osteoderms could only be visualized on species of *Xenosaurus*, save *X. agrenon*, *S. crocodilurus*, *L. borneensis* from published x-rays (McDowell and Bogert,

1954) and CT scans (Maisano et al., 2002), Anguidae, and Helodermatidae, as well as the postcranium of *B. ammoskius*. When the southern clade of *Xenosaurus* is mentioned as having a character state in the osteoderm section, it should be understood that the state for *X. agrenon* is inferred. *Varanus* has osteoderms (McDowell and Bogert, 1954), but they are too small to visualize reliably with CT scanning, and alternative preparations were unavailable. Osteoderms are unknown for the remaining fossil anguimorphs, save some isolated osteoderms associated with *M. ornatus* (Klembara, 2008). *Pristidactylus torquatus* does not have significant free osteoderms as an adult; the condition in juveniles is unknown.

Regarding osteodermal variation, it is obvious that osteoderm patterns vary slightly with scalation patterns. Additionally, osteoderms develop postnatally for the most part; thus, it is important to score osteoderm characters on relatively large adult individuals.

246. Osteoderms: Domed osteoderms (0) absent; (1) largely circular; (2) some circular, but largely oval or obovate (see Conrad, 2005, 2008).

Evolution. Under both analyses, the ancestral state for *Xenosaurus* + *R. rugosus* is domed and circular. Domed and circular plus oval is an autapomorphy of *E. lancensis*. Under Analysis 1, the ancestral state for the entire group and for Anguimorpha is domed and circular. Lack of domed osteoderms is a synapomorphy of *S. crocodilurus* + Varanidae and of Anguidae. Under Analysis 2, the ancestral state for the entire group and for Anguimorpha is ambiguous between absent and largely circular.

Cranial Osteoderms

247. Cranial osteoderms: Fused cranial osteoderms (0) absent; (1) present (Fig. 1A).

Evolution. Under both analyses, absence of fused cranial osteoderms is a synapomorphy of Varanidae.

248. Cranial osteoderms: Supraorbital osteo-
derm longitudinal rows (0) five
(Fig. 2A); (1) four (Fig. 1A); (2) three
(Fig. 5A); (3) two (Fig. 4A).

　　Evolution. Under both analyses, two
rows is ancestral for Anguimorpha.
Three rows is an autapomorphy of *C.
enneagrammus*. The ancestral state for
Xenosaurus is ambiguous between
three and two rows. Four rows is a
synapomorphy of the northern clade of
Xenosaurus, and five rows is an auta-
pomorphy of *X. platyceps*.

249. Cranial osteoderms: Full supraorbital
osteoderms in longitudinal row bearing
largest osteoderms (0) eight (Fig. 1A);
(1) seven; (2) six; (3) five (Fig. 5A); (4)
four; (5) three; (6) two (Fig. 3A).

　　Evolution. Under both analyses, a
count of eight is a synapomorphy of the
northern clade of *Xenosaurus*. Two is an
autapomorphy of *X. rackhami* and of *L.
borneensis*. Four is an autapomorphy of
E. multicarinata, and three is an autapo-
morphy of Helodermatidae. Six is an
autapomorphy of *S. crocodilurus*. Under
Analysis 1, the ancestral state for Angu-
imorpha is five, as is that for *S. crocodi-
lurus* + Varanidae, *Xenosaurus* + Angu-
idae, and Anguidae + Helodermatidae.
Under Analysis 2, the ancestral state for
Anguimorpha is ambiguous among six,
five, and four. The ancestral state for
Xenosauridae is ambiguous between six
and five. The ancestral state for Anguidae
+ Varanoidea is ambiguous between five
and four, as is that for Anguidae. Three is
a synapomorphy of Varanoidea

250. Cranial osteoderms: Supraorbital osteo-
derms in longitudinal row bearing
largest osteoderms—largest osteo-
derms (0) less than twice as extensive
along long axis as perpendicular to long
axis (Fig. 2A); (1) twice as extensive or
more along long axis as perpendicular
to long axis (Fig. 4A).

　　Evolution. Under Analysis 1, the
ancestral state for the entire group

and for Anguimorpha is less than twice
as long as wide. Twice as long as wide
or more is a synapomorphy of the
southern clade of *Xenosaurus* and an
autapomorphy of *S. crocodilurus*. Un-
der Analysis 2, the ancestral state for
the entire group and for Anguimorpha
is ambiguous. The ancestral state for
Anguidae + Varanoidea is less than
twice as long as wide.

251. Cranial osteoderms: Dorsal temporal
osteoderms, peripheral rims (0) present
(Fig. 1A); (1) absent (Fig. 4A).

　　Evolution. Under both analyses,
presence of rims is a synapomorphy of
the northern clade of *Xenosaurus* and
an autapomorphy of Helodermatidae.

252. Cranial osteoderms: Dorsal temporal
osteoderms (0) overlie entirety of dorsal
temporal fenestra and dorsal surfaces of
upper temporal arch bones (Fig. 1A);
(1) overlie entirety of dorsal temporal
fenestra and partially overlie dorsal
surfaces of upper arch bones, but
posterodorsal tip of jugal, lateral edge
of postorbitofrontal, and anterolateral
portion of squamosal lateral to medio-
lateral level of external edge of post-
orbitofrontal are exposed (Fig. 5A); (2)
overlie dorsal temporal fenestra but
leave exposed elements described in
state 1 plus postfrontal portion of
postorbitofrontal and most of squamosal
(Fig. 4A); (3) only few and isolated,
overlying dorsal temporal fenestra and
posterior, median portion of postorbito-
frontal (Fig. 3A); (4) absent.

　　Evolution. Under both analyses, the
ancestral state for the entire group is
ambiguous among all four states. The
ancestral state for Anguimorpha is 0. State
4 is a synapomorphy of *Varanus*, state 1 is
a synapomorphy of the southern clade of
Xenosaurus, and state 2 is a synapomor-
phy of *X. rackhami* + *X. grandis*.

253. Cranial osteoderms: Transverse rows of
osteoderms behind posterior edge of

parietal (0) spanning most of width of parietal (Fig. 2A); (1) restricted to mediolateral area spanned by notch at meeting of supratemporal processes (Fig. 5A); (2) absent (Fig. 4A).

Evolution. Under both analyses, absence is a synapomorphy of *X. rackhami* + *X. grandis*. Under Analysis 1, a span of most of the width of the parietal is ancestral for Anguimorpha, and a restricted span is a synapomorphy of the southern clade of *Xenosaurus*. Absence is an autapomorphy of *S. crocodilurus*. Under Analysis 2, the ancestral state for Anguimorpha and for Xenosauridae is ambiguous between a wide and a restricted span. The ancestral state for Anguidae + Varanoidea is a wide span.

254. Cranial osteoderms: Number of transverse rows of osteoderms behind posterior edge of parietal (0) two (Fig. 5A); (1) three (Fig. 2A).

Evolution. Under both analyses, three rows is an autapomorphy of *X. platyceps.* Under Analysis 1, three rows is an autapomorphy of Helodermatidae and of *L. borneensis.* Under Analysis 2, three rows is a synapomorphy of Varanoidea.

255. Cranial osteoderms: Lateral temporal osteoderms, peripheral rims (0) absent (Fig. 5C); (1) present (Fig. 1C).

Evolution. Under both analyses, the presence of rims is a synapomorphy of *Xenosaurus.* It is also an autapomorphy of *X. grandis* and of Helodermatidae.

256. Cranial osteoderms: Lateral temporal osteoderms, spacing—(0) closely packed (Fig. 1C); (1) separated by small gaps (Fig. 5C); (2) separated by gaps of one scale or more (Fig. 4C); (3) present only as small slivers of ossification (Fig. 3C); (4) absent.

Evolution. Under both analyses, the ancestral state for the entire group is ambiguous among the last four states. That for Anguimorpha is ambiguous

between separation by small and large gaps. Presence as only small slivers of ossification is autapomorphic for *X. rackhami.* Under Analysis 1, the ancestral state for *S. crocodilurus* + Varanidae is ambiguous between separation by small and large gaps. The ancestral state for *Xenosaurus* + Anguidae is ambiguous between close packing and separation by small gaps. Close packing is the ancestral state for Anguidae + Helodermatidae. Separation by small gaps is ancestral for the southern clade of *Xenosaurus,* and separation by large gaps is a synapomorphy of *X. rackhami* + *X. grandis.* Under Analysis 2, the ancestral state for Anguidae + Varanoidea is ambiguous between closely packed and separated by small gaps.

257. Cranial osteoderms: Lateral temporal osteoderms, coverage of quadratojugal region posterior to quadratojugal process of jugal (0) present (Fig. 1C); (1) absent (Fig. 5C).

Evolution. Under both analyses, noncoverage of the quadratojugal region is a synapomorphy of the southern clade of *Xenosaurus.*

258. Cranial osteoderms: Mandibular osteoderms (0) absent; (1) most of dentary exposed; only portions of postdentary bones extensively covered; (2) covering part of lateral face of mandible, including dentary and postdentary bones, but leaving large areas of dentary and postdentary bones exposed (Fig. 5B, C); (3) covering most of lateral face of mandible save for retroarticular process and pterygoideus insertion on surangular, present in three major longitudinal rows (Figs. 1B, C); (4) as with state 3 but with four major longitudinal rows (Figs. 2B, C).

Evolution. Under both analyses, the ancestral state for Anguimorpha is ambiguous between state 1 and state 2. The ancestral state for *Xenosaurus* is 2, and state 3 is a synapomorphy of

the northern clade of *Xenosaurus*, with state 4 an autapomorphy of *X. platyceps*. State 3 is also a synapomorphy of Anguidae. The ancestral state of most other nodes under both analyses is ambiguous between state 1 and state 2.

259. Cranial osteoderms: Mandibular osteoderms (0) with strong, sharp keels (Fig. 1B, C); (1) unkeeled or subtly keeled (Fig. 5B, C).

  Evolution. Under both analyses, strong keeling of the mandibular osteoderms is a synapomorphy of the northern clade of *Xenosaurus*.

260. Cranial osteoderms: Intermandibular osteoderms (0) present, well-developed (Fig. 1B); (1) present as multiple small ossifications (Fig. 2B); (2) present as one or two small ossifications (Fig. 5B); (3) absent (Fig. 4B).

  Evolution. Under both analyses, the well-developed morphology is an autapomorphy of *X. newmanorum*, and absence is a synapomorphy of *X. rackhami + X. grandis*. Under Analysis 1, the ancestral state for the entire group is ambiguous among multiple small ossifications, one or two small ossifications, and absence, and that for Anguimorpha is ambiguous between multiple and one or two small ossifications. The well-developed morphology is a synapomorphy of Anguidae + Helodermatidae and an autapomorphy of *L. borneensis*. Under Analysis 2, the ancestral state for the entire group is ambiguous between one or two small ossifications and absence. That for Anguimorpha is one or two small ossifications. The well-developed morphology is a synapomorphy of Anguidae + Varanoidea, and presence as multiple small ossifications is a synapomorphy of the northern clade of *Xenosaurus*.

261. Cranial osteoderms: Intermandibular osteoderms, well-developed portion (0) in posterior half of mandible; (1) in anterior half of mandible (Fig. 1A).

  Evolution. Under Analysis 1, posterior development is ancestral, and development in the anterior half of the mandible is a synapomorphy of the northern clade of *Xenosaurus* or of all xenosaurs. Under Analysis 2, the ancestral state is ambiguous across most of the tree, but the ancestral state of Varanoidea is posterior development.

262. Cranial osteoderms: Intermandibular osteoderms, lateral rows (0) present along entirety of tooth-bearing region of dentaries (Fig. 1B); (1) present only along anterior portion (Fig. 2B).

  Evolution. The ancestral state of the character is entirely ambiguous.

263. Cranial osteoderms: Intermandibular osteoderms (0) spanning mandibular rami for large portion of anteroposterior extent (Fig. 1B); (1) developed only laterally for most of extent (Fig. 2B).

  Evolution. Under both analyses, the ancestral state for Anguimorpha is ambiguous. Under Analysis 1, most internal nodes are ambiguous, save that the ancestral state for Anguidae + Helodermatidae is extensive development. Under Analysis 2, the ancestral state for Anguidae + Varanoidea is extensive development, and that for Xenosauridae is lateral development, making the extensive development in *X. newmanorum* an autapomorphy of that taxon.

Cervical Osteoderms

264. Cervical osteoderms: Cervical osteoderms (0) present dorsally in each scale (The Deep Scaly Project, 2007); (1) present dorsally in regularly spaced pattern, but not in each scale; (2) present dorsally as small ossifications concentrated anteriorly with occasional larger osteoderms interspersed (Fig. 1A); (3) present dorsally as small
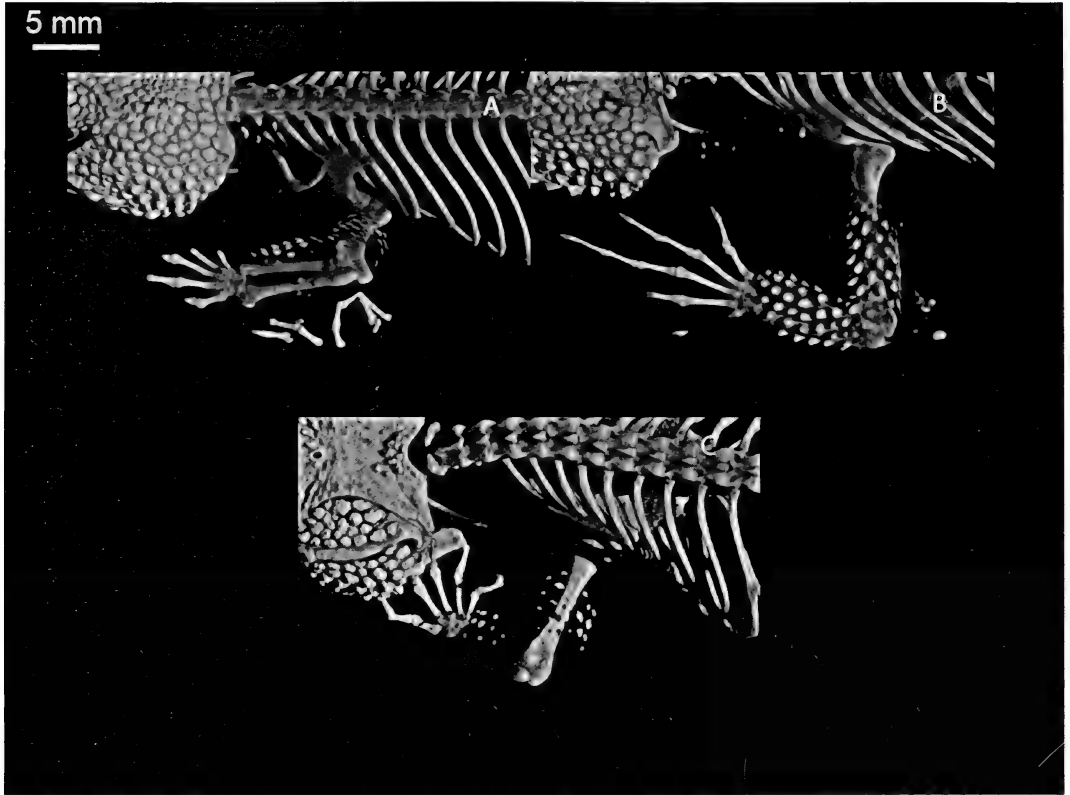
Figure 57.   Left pectoral limbs, extensor view, anterior to the left: A, *Xenosaurus newmanorum*, CT scan of UMMZ 126057; B, *Xenosaurus platyceps*, CT scan of UF 25005; C, *Xenosaurus rectocollaris*, CT scan of UF 51443. A illustrates 265(1) and 266(1). B illustrates 265(0) and 266(1). C illustrates 265(0) and 266(2).

ossifications (Fig. 3A); (4) absent (Fig. 5A).

Evolution. Under both analyses, the ancestral state for the entire group is ambiguous among the last four states, and that for Anguimorpha is ambiguous between 1 and 2. The ancestral state for *Xenosaurus* is 2, and state 3 is a synapomorphy of the southern clade of *Xenosaurus*. State 4 is an autapomorphy of *X. rectocollaris*. Under Analysis 1, the ancestral state for *S. crocodilurus* + Varanidae is 2, and that for Anguidae + Helodermatidae is 0. Under Analysis 2, the ancestral state for Anguidae + Varanoidea is ambiguous between 0 and 1, and that for Xenosauridae is ambiguous between 1 and 2.

Pectoral Osteoderms

265. Pectoral osteoderms: Osteoderms on pectoral limb (0) present on most of extensor surfaces of stylopod and zeugopod and more lightly distributed on flexor surface (Fig. 57B); (1) present on central two-thirds or more of extensor surfaces, but only marginally on flexor surfaces (Fig. 57A); (2) present only as narrow central band (about central one-third) of extensor surfaces, save for a few scattered ossifications over elbow (Fig. 57C); (3) absent.

Evolution. Under both analyses, the ancestral state for the northern clade of *Xenosaurus* is 1, and state 0 is an autapomorphy of *X. platyceps*. The ancestral state for the southern clade

of *Xenosaurus* is 2, and state 3 is a synapomorphy of *X. rackhami* + *X. grandis*. Under Analysis 1, the ancestral state for the entire group is ambiguous among 1, 2, and 3. That for Anguimorpha is ambiguous between 1 and 2. The ancestral state for Anguidae + Helodermatidae is 0. Under Analysis 2, the ancestral state for the entire group is ambiguous between 2 and 3, and that for Anguimorpha is 2. State 0 is a synapomorphy of Anguidae + Varanoidea, and state 1 is a synapomorphy of the northern clade of *Xenosaurus*.

266. Pectoral osteoderms: Osteoderms on pectoral limb (0) present as small nubs of ossification; (1) present as large rounded ossifications (Fig. 57A); (2) present as large rounded ossifications and in places as cone-shaped spicules (Fig. 57B).

Evolution. Under both analyses, the ancestral state for the entire group is presence as large rounded ossifications. Presence as small nubs of ossification is an autapomorphy of *S. crocodilurus*, and presence as large rounded ossifications plus cone-shaped ossifications is an autapomorphy of *X. platyceps*.

Pelvic Osteoderms

267. Pelvic osteoderms: Osteoderms on pelvic limb (0) present on extensor surface of stylopod and scattered on flexor surface (McDowell and Bogert, 1954, plate 4); (1) present only on extensor surface of stylopod (Fig. 54A); (2) absent.

Evolution. Under both analyses, the ancestral state for the northern clade of *Xenosaurus* is extensor presence only, and presence on the extensor and flexor surfaces is an autapomorphy of *X. platyceps*. Under Analysis 1, the ancestral state for the entire group and for Anguimorpha is ambiguous between presence on the extensor surface and absence. Presence on the flexor

and extensor surfaces is a synapomorphy of Anguidae + Helodermatidae and an autapomorphy of *L. borneensis*. Under Analysis 2, the ancestral state for the entire group and for Anguimorpha is absence, and presence on the extensor and flexor surfaces is a synapomorphy of Anguidae + Varanoidea. Presence on the extensor surface is a synapomorphy of the northern clade of *Xenosaurus*.

Caudal Osteoderms

268. Caudal osteoderms: Caudal osteoderms (0) in complete or nearly complete rings around anterior portion of tail and scattered over more posterior portion (Fig. 50B); (1) scattered in anterior portion of tail, sparse in more posterior portion (Fig. 50C); (2) absent.

Evolution. Under both analyses, the ancestral state for the entire group is ambiguous between scattered and absent. That for Anguimorpha is scattered, as is that for *Xenosaurus*. Absence of cadual osteoderms is a synapomorphy of the southern clade of *Xenosaurus*, and complete rings thereof is an autapomorphy of *X. newmanorum*. Under Analysis 1, complete rings is a synapomorphy of Anguidae + Helodermatidae and an autapomorphy of *L. borneensis*. Under Analysis 2, complete rings is a synapomorphy of Anguidae + Varanoidea.

Scalation

Scalation is not informatively preserved on any of the extinct taxa.

269. Scalation: Canthus temporalis (0) scales no larger or more prominent than lateral and dorsal temporal scales, or barely so (Fig. 58A); (1) scales markedly larger and more prominent, canthus well-developed (Fig. 58B).

Evolution. Under both analyses, the ancestral state for the entire group and for Anguimorpha is a lack of
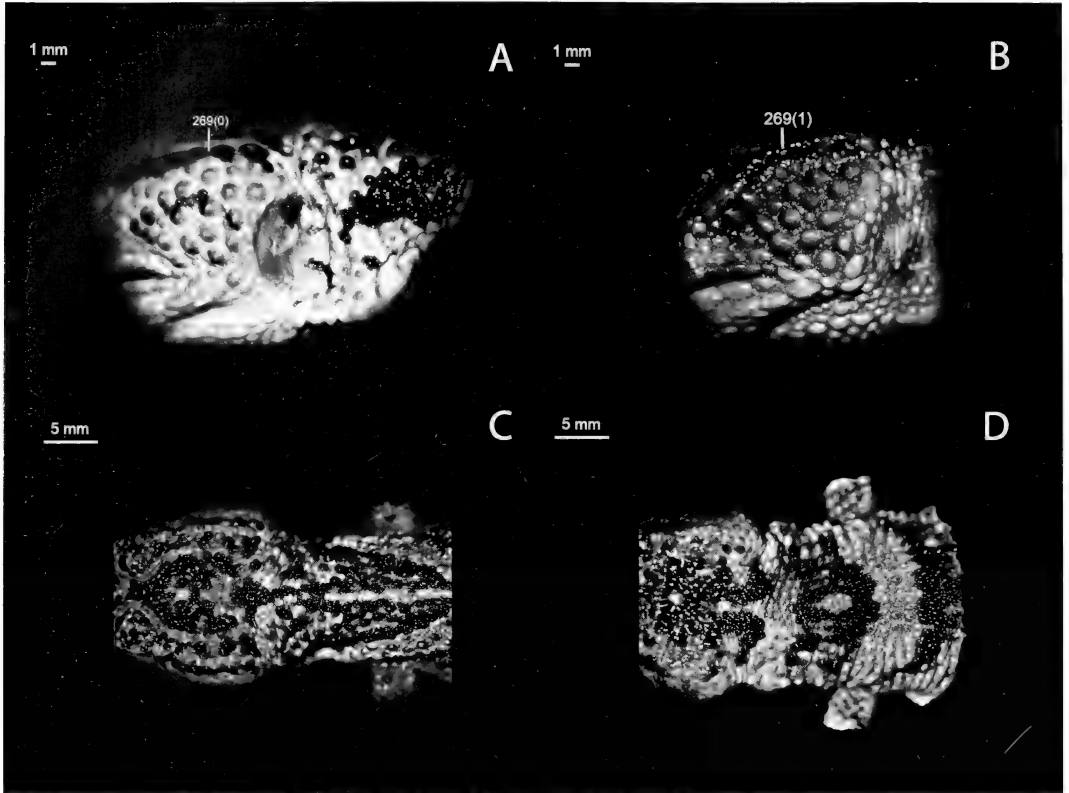
Figure 58.   Temporal and tympanic regions, left lateral, anterior to the left: A, *Xenosaurus newmanorum* UF 25006. Illustrates characters 269(0), 270(1). B, *Xenosaurus rackhami* UTEP 4555. Illustrates characters 269(1), 270(2). Necks, dorsal, anterior to the left: C, *Xenosaurus newmanorum* UF 25006. Illustrates character 271(0). D, *Xenosaurus rectocollaris* UF 51443. Illustrates character 271(1).

prominence. Under Analysis 1, the ancestral state for *S. crocodilurus* + Varanidae is ambiguous, and prominence of the canthus is a synapomorphy of the southern clade of *Xenosaurus*. Under Analysis 2, the ancestral state for Xenosauridae is ambiguous, and prominence is an autapomorphy of *L. borneensis*.

270. Scalation: Tympanum (0) unscaled; (1) covered with thin scales, becoming thinner toward middle of tympanum (Fig. 58A); (2) covered with thick scales but still differentiated from surrounding skin (Fig. 58B); (3) covered with thick scales and undifferentiated from surrounding skin (McDowell and Bogert, 1954, plate 1).

Variation. In *S. crocodilurus*, small juveniles have a tympanum that appears naked to the eye (Sprackland, 1993; Mägdefrau, 1997; Bever et al., 2005). It is possible that a thin layer of scales covers it, as in juvenile *X. grandis*. Relatively large adults should be scored for this character.

Evolution. Under both analyses, the nondifferentiated covering of thick scales in *L. borneensis* is an autapomorphy of that taxon. Under Analysis 1, the ancestral state for the entire group and for Anguimorpha is ambiguous between unscaled and covered with thin scales. A thick scaly covering is an autapomorphy of *S. crocodilurus*. The ancestral state for Anguidae + Helo-

dermatidae is unscaled, and the ancestral state for *Xenosaurus* is thinly scaled, with thickly scaled but differentiated a synapomorphy of the southern clade of *Xenosaurus*. Under Analysis 2, the ancestral state for the entire group and for Anguimorpha is unscaled, and increased scalation is a synapomorphy of Xenosauridae, whose ancestral state is ambiguous between lightly scaled and heavily scaled but differentiated.

271. Scalation: Skin around neck (0) conforms relatively tightly to underlying muscular structure (Fig. 58C); (1) puffs out considerably, such that neck appears wide and little differentiated from back of head (Fig. 58D).

  Evolution. Under both analyses, the loose collar-like morphology is an autapomorphy of *X. rectocollaris.*

272. Scalation: Lateral fold (0) absent; (1) present, relatively weakly developed, discontinuous; (2) present, well-developed, continuous along body. (Scored as lateral fold absent or present in Estes et al., 1988).

  Evolution. Under both analyses, lack of a fold is the ancestral state for the entire group and for Anguimorpha. Presence of a weak fold is a synapomorphy of *Xenosaurus*, and a strong fold is a synapomorphy of the southern clade of *Xenosaurus*. Under Analysis 1, a well-developed fold is a synapomorphy of *E. multicarinata* + *O. ventralis*. Under Analysis 2, the ancestral state for Anguidae is ambiguous among absent, weakly developed, and strongly developed.

273. Scalation: Dark markings on venter (0) absent; (1) present peripherally; (2) present across most of venter.

  Evolution. Under both analyses, lack of markings is the ancestral state for the entire group and for Anguimorpha. Under Analysis 1, peripheral markings

are an autapomorphy of *S. crocodilurus* and the ancestral state for the southern clade of *Xenosaurus* is ambiguous among absence, peripheral presence, and extensive presence, as is the state for *X. agrenon* + *X. rectocollaris.*

274. Scalation: Epidermal ridge microstructure (0) polygonal; (1) not arranged in regular polygons.

  Evolution. This character was scored from the work of Harvey (1991, 1993). Under both analyses, the ancestral state for the entire group and for Anguimorpha is polygonal microstructure. Under Analysis 1, a lack of polygonal arrangement is a synapomorphy of Anguidae + Helodermatidae. Under Analysis 2, the ancestral state for Anguidae + Varanoidea is ambiguous.

RESULTS

Ingroup Topology and Effects of Ordering

  Analysis 1 and Analysis 2 yielded the same fully resolved topology for *Xenosaurus* and its extinct relatives (Figs. 6, 7). In the single recovered topology, *R. rugosus* is sister to all other xenosaurs, and *E. lancensis* is sister to *E. serratus* + *Xenosaurus*. Within *Xenosaurus*, the northern clade of *X. newmanorum* + *X. platyceps* is sister to the southern clade, which is divided into two additional clades: *X. agrenon* + *X. rectocollaris* and *X. rackhami* + *X. grandis*. Bootstrap values greater than 50% are given at the internal nodes. For both trees, all internal nodes for the ingroup had bootstrap values greater than 50%.

  Analysis 1 yielded a single most parsimonious tree with a length of 924 steps (Fig. 6). Of the 274 characters used in the analysis, 253 were parsimony-informative and 21 were parsimony-uninformative. The tree consistency index was 0.4708 (0.3147 rescaled and 0.4573 excluding uninformative characters), the homoplasy index was 0.5292 (0.5427 excluding uninformative characters), and the retention index was

0.6685. The parametric bootstrap test resulted in values of greater than 50% for all ingroup nodes and for the nodes within the shinisaur clade. The other nodes were constrained.

Analysis 2 yielded a single most parsimonious tree with a length of 875 steps (Fig. 7). Of the 274 characters used in the analysis, 253 were parsimony-informative and 21 were parsimony-uninformative. The tree consistency index was 0.4971 (0.3488 rescaled and 0.4836 excluding uninformative characters), the homoplasy index was 0.5029 (0.5164 excluding uninformative characters), and the retention index was 0.7017. The parametric bootstrap test resulted in values of greater than 50% for all ingroup nodes, for Xenosauridae, for Anguidae + Varanoidea, and for Varanoidea and all nodes therein.

A comparison of the Analysis 1 and Analysis 2 trees using a Templeton test with the Analysis 2 tree as the best or unconstrained instance (see Materials and Methods) demonstrated that the toplogies were significantly different ($P < 0.0001$, Wilcoxon signed-rank statistic 556.0, $N = 70$, $Z = -4.3500$). As expected, the tree length of the unconstrained tree (Analysis 2) was less than that of the constrained tree (Analysis 1), and the consistency and retention indices were higher in the unconstrained tree, which also had a lower homoplasy index. The number of parsimony-informative and parsimony-uninformative characters was consistent between the two analyses, despite the differing outgroup topologies. Finally, in both analyses, bootstrap values for the ingroup nodes were all greater than 50%, with the lowest support (the only values less than 80%) being for the *Xenosaurus* + *E. serratus* node and the *Xenosaurus* + *E. lancensis* node. The internode bounded by these nodes was the only branch to collapse when characters were run unordered, as described below. Ingroup topologies were identical between the two trees.

When the matrix was run with all characters unordered, the internode be-tween *E. serratus* + *Xenosaurus* and *E. lancensis* + *Xenosaurus* collapsed. This somewhat unexpected result emphasizes that the position of *R. rugosus* as sister to all other xenosaurs here included is fairly robust, and that *E. lancensis* is known from specimens representing a relative paucity of phylogenetic information. At a glance, the loss of resolution of *E. serratus* + *Xenosaurus* seems absurd; *E. serratus* is nearly identical to *Xenosaurus* in several unique features. Notable among these is the highly domed form of the maxillary osteoderms, as opposed to the primitively flat osteoderms of *E. lancensis*. That distinction is represented in the scorings of character 62, a multistate character representing a morphocline from a flat plate-like morphology to a broken-up domed morphology. The nature of the problem lies in the status of *E. lancensis* as a "transitional form," uniquely displaying a broken-up but undomed morphology. In an unordered scheme, the transitional nature of this morphology is not recognized, and it instead becomes simply an autapomorphy. Indeed, a simplification of the character scoring to two states (not domed and *Xenosaurus*-like, or domed and *Xenosaurus*-like) results in a majority-rule consensus identical to the ingroup tree produced by the ordered data. Two other multistate characters, 46 (the steepness of the slanted dorsal margin of the lacrimal recess) and 108 (the lateral projection of the cristae cranii), likewise have states that are unambiguous synapomorphies of *E. serratus* + *Xenosaurus*, whereas *E. lancensis* has an intermediate state.

Outgroup Topology

The alliance of *S. crocodilurus* and the fossil *B. ammoskius* was established by Conrad (2005, 2006) and Conrad et al. (2011). My study also agrees with Conrad et al. (2011) in placing *M. ornatus* Klembara 2008 as sister to a *Shinisaurus* + *Bahndwivici* clade in a phylogenetic analysis. All other relationships were set using a constraint tree to generate Analysis 1 (see

Materials and Methods). However, Analysis 2 was generated by specifying only *P. torquatus* as an outgroup for the analysis and therefore generated a hypothesis of anguimorph relationships (Fig. 7). Under Analysis 2, the initial split of Anguimorpha is between the traditional Xenosauridae, including the *Xenosaurus* clade and the shinisaurs, and an Anguidae + Varanoidea clade. Anguidae consists of an Anguinae + Diploglossinae clade to the exclusion of Gerrhonotinae, and Varanoidea has its traditional topology of Helodermatidae + Varanidae, with Varanidae consisting of *L. borneensis* and *Varanus*.

Character States Supporting Clades and Terminal Taxa

Following are lists of character states supporting the focal clades in this study (synapomorphies) and terminal taxa (autapomorphies) under each hypothesis. Starred states (*) are unambiguous. Clade numbering is arbitrary, but clades common to both hypotheses (clades 1 to 22) have the same number under both listings. Character states unique to one hypothesis are denoted with a capital "U" (not marked as such when state being transitioned from is different), and states that differ between analyses in ambiguity are denoted with a lowercase "u."

When dealing with scores of ?, accelerated transformation (ACCTRAN) optimization is assumed. My character descriptions are worded with neither accelerated transition nor delayed transformation (DELTRAN) optimization in mind, and they are thus more complete guides to character distribution than the following lists. One exception obtains in the case of the character descriptions and in the lists below—when data are truly missing, instead of a character being inapplicable to the taxon (see Strong and Lipscomb, 1999), I use a DELTRAN-type assumption, placing ambiguous synapomorphies at more exclusive nodes instead of assuming early transformation. Those transformations are listed in brackets following the other transformations optimized at the

nodes in question. Specifically, those nodes are all of those for which one branch is completely extinct and therefore represented by incomplete fossils: *Xenosaurus* + *R. rugosus*, *Xenosaurus* + *E. lancensis*, *Xenosaurus* + *E. serratus*, *S. crocodilurus* + *M. ornatus*, and *S. crocodilurus* + *B. ammoskius*. Additionally, I use the same approach for the osteodermal characters of *X. agrenon* at the *X. agrenon* + *X. rectocollaris* node because data were unavailable regarding the osteoderms of *X. agrenon*.

Analysis 1

1. *Xenosaurus* + *Restes rugosus*: 1 0-2*; 51 0-1*; 52 1-2 U*; 53 0-1*; 59 0-1 U*; 64 6-7 U; 66 0-1 U*; 67 0-1*; 69 0-1 U*; 72 0-1*; 97 1-2; 109 0-1*; 111 0-1*; 113 0-1 U; 114 0-1*; 131 0-1; 132 1-2; 145 0-1*; 184 0-1; 186 0-1 U*; 191 0-1; 193 0-1 U*; 196 0-1 U*; 214 0-1*;

2. *Restes rugosus*: 43 2-0 U; 125 1-0 U; 144 0-1*; 204 0-1*

3. *Xenosaurus* + *Exostinus lancensis*: 62 2-3*; 93 1-0; 96 0-1*; 97 2-3*; 100 0-1; 105 0-1 U*; 185 1-0 U; 193 1-2 [152 0-1];

4. *Exostinus lancensis*: 1 2-1; 92 1-0*; 147 4-C*; 154 1-0*; 246 1-2*

5. *Xenosaurus* + *Exostinus serratus*: 46 0-1*; 54 0-1; 62 3-4*; 93 1-0; 98 0-1*; 99 0-1*; 108 0-1*; 191 1-0 [7 1-2; 8 0-3; 9 0-1; 11 0-1; 19 0-1; 22 0-1 U; 47 0-1 U; 55 3-2 U; 63 1-0; 130 0-1; 68 1-2; 94 1-2 U; 111 1-2; 124 1-2; 200 0-1 U; 209 0-1]

6. *Exostinus serratus*: 49 0-1*; 50 0-1*; 52 2-1*; 60 1-2*; 61 1-3*; 64 7-5*; 69 1-2*; 70 0-1*; 71 0-1*; 98 1-2*; 101 0-1*; 106 0-1*; 107 0-1*; 108 1-2*; 131 1-0; 132 2-1; 185 0-1 U; 192 0-1*; 193 2-0*; 194 0-1*

7. *Xenosaurus*: 2 0-1*; 8 3-4*; 9 1-2*; 10 0-1; 17 0-1*; 21 2-3*; 23 0-1*; 26 0-1*; 45 0-1*; 56 4-3; 57 0-1*; 58 0-1*; 64 7-9*; 93 0-1*; 100 1-0; 104 0-1; 128 0-1*; 184 1-0; 195 1-0*; 196 1-0*; 201 0-1* [30 1-2; 31 0-1; 34 0-1; 35 0-1; 37 0-1; 75 0-1; 85 0-1; 86 0-1; 116 0-1; 117 0-1 U; 135 2-1; 136 0-1; 137 0-1 U; 139 0-1 U; 142 0-1; 145 1-2; 146 0-1; 147 4-3; 148 4-2;

159 0-1 U; 161 0-1; 162 0-1 U; 165 0-1; 167 1-2; 168 0-1; 169 0-3 U; 173 0-1; 199 0-1; 205 0-2; 207 0-1; 208 0-1; 211 1-2; 213 0-1 U; 228 0-1; 238 0-1; 243 0-1; 248 3-2; 260 0-1 U; 261 0-1 U; 263 0-1 U; 264 1-2; 265 0-1 U; 268 0-1 U; 272 0-1]

8. Northern clade of *Xenosaurus*: 13 0-1*; 16 0-1*; 18 0-1; 20 1-0*; 21 3-4*; 22 1-2*; 28 0-1*; 29 1-2; 39 0-1*; 41 0-1*; 42 0-1*; 43 2-3*; 54 1-0; 60 1-0*; 64 9-B*; 68 2-3*; 73 0-1*; 75 1-2*; 76 1-2*; 79 0-1*; 84 0-1*; 85 1-2*; 95 0-1*; 110 0-2*; 111 2-3*; 116 1-3*; 122 0-1*; 143 0-1*; 154 1-2*; 158 0-1*; 178 0-1 U*; 187 0-1*; 202 0-1*; 219 0-1*; 220 0-1*; 225 0-1*; 226 0-1*; 229 0-1*; 239 0-1*; 248 2-1*; 249 3-0*; 251 0-1*; 255 0-1*; 258 2-3*; 259 1-0*; 267 2-1*

9. *Xenosaurus newmanorum*: 56 3-5*; 65 0-1*; 88 1-2; 135 1-2; 147 3-4; 148 2-0*; 154 2-3*; 174 2-0*; 181 1-0; 182 1-0*; 198 0-1*; 223 1-0*; 224 0-1*; 234 1-0*; 235 0-1*; 237 0-1*; 260 1-0*; 263 1-0 u; 268 1-0 u

10. *Xenosaurus platyceps*: 61 1-2*; 80 0-1; 89 0-1*; 118 0-1; 119 0-1*; 120 0-1*; 127 0-1*; 135 1-0*; 193 2-3*; 206 0-1*; 214 1-2*; 215 1-2*; 223 1-2*; 232 0-1*; 234 1-2*; 240 0-1*; 248 1-0*; 254 0-1*; 258 3-4*; 262 0-1; 265 1-0 u; 266 1-2*; 267 1-0*

11. Southern clade of *Xenosaurus*: 11 1-2*; 12 0-1*; 27 0-1 u*; 36 0-1; 37 1-2*; 38 0-1; 40 0-1*; 43 2-1; 68 2-0*; 74 1-2; 78 1-2*; 83 0-1 U; 90 0-1*; 102 0-1*; 126 0-1; 134 0-1*; 138 0-1*; 147 3-1*; 151 0-1; 157 1-2; 165 1-2*; 183 1-0 U; 204 0-1*; 217 1-0; 242 0-1*; 245 0-1*; 250 0-1 U*; 252 0-1*; 253 0-1 U*; 256 0-1 U*; 257 0-1*; 260 1-2 U*; 264 2-3*; 265 1-2 U*; 268 1-2*; 269 0-1 U*; 270 1-2 U*; 272 1-2*; 273 0-2

12. *Xenosaurus agrenon* + *Xenosaurus rectocollaris*: 46 1-2*; 56 3-2*; 88 1-0*; 135 1-0*; 142 1-0; 147 1-0*; 155 1-2*; 163 1-0*; 170 0-1*; 171 0-1*; 175 1-0; 176 0-1*; 188 0-1*; 190 0-1*; 203 0-1*; 216 0-1*;

13. *Xenosaurus agrenon*: 55 2-1*; 56 2-1*; 74 2-1; 76 1-0*; 77 0-1*; 110 0-1*; 148 2-3; 150 0-1*; 166 0-1*; 181 1-0; 198 0-1*; 217 0-1; 239 0-1*

14. *Xenosaurus rectocollaris*: 8 4-0*; 16 0-1*; 60 1-2*; 64 9-B*; 83 1-0; 87 2-1*; 96 1-0*; 123 0-1*; 131 1-0*; 148 2-1*; 214 1-2*; 215 1-0*; 229 0-1*; 234 1-0*; 236 0-1*; 271 0-1*; 273 2-0 [264 3-4]

15. *Xenosaurus grandis* + *Xenosaurus rackhami*: 5 0-1*; 15 0-1*; 58 1-2*; 65 0-1*; 82 0-1*; 103 0-1*; 112 0-1*; 115 0-1*; 133 0-1*; 139 1-2*; 141 0-1*; 151 1-2*; 155 1-0*; 156 0-1*; 159 1-0 u; 160 0-1*; 163 1-2*; 167 2-3*; 168 1-2*; 169 3-2 u; 172 0-1*; 174 2-1 U*; 179 0-1*; 182 1-2 u; 197 0-1*; 221 0-1*; 227 2-1 u*; 248 2-3; 252 1-2*; 253 1-2*; 256 1-2*; 260 2-3*; 265 2-3*

16. *Xenosaurus rackhami*: 56 3-4; 81 0-1*; 88 1-4*; 126 1-0; 135 1-2; 140 0-1*; 148 2-3; 153 0-1*; 165 2-3*; 166 0-1*; 169 2-1*; 177 0-1*; 205 2-1*; 240 0-2*; 249 3-6*; 252 2-3*; 256 2-3*

17. *Xenosaurus grandis*: 55 2-1*; 58 2-3*; 84 0-1*; 116 1-2*; 120 0-1*; 127 0-1*; 147 1-2; 157 2-1; 180 0-1*; 181 1-0; 193 2-1*; 198 0-1*; 255 0-1*

18. *Shinisaurus crocodilurus* + *Merkurosaurus ornatus*: 20 1-2*; 22 0-1 U; 25 2-0; 52 1-2 U*; 155 1-0*; 193 0-1 U*; 196 0-1 U*

19. *Shinisaurus crocodilurus* + *Bahndwivici ammoskius*: 47 0-1 U*; 98 0-1*; 147 5-6* [29 1-2; 55 3-2 U; 59 0-1 U; 66 0-1 U; 69 0-1 U; 117 0-1 U; 200 0-1 U; 218 1-0 U; 233 0-1]

20. *Merkurosaurus ornatus*: 7 1-0; 23 0-1*; 92 1-0*; 94 1-2 U*; 185 1-0 U*

21. *Bahndwivici ammoskius*: 22 1-0 U; 55 2-1*; 64 5-8* U; 97 1-3*; 134 1-0 U; 151 2-3*; 154 1-0*; 240 0-1*

22. *Shinisaurus crocodilurus*: 5 0-1*; 94 1-0*; 124 0-1 U*; 138 0-1*; 147 6-9*; 148 4-3*; 152 0-1 u* [14 1-0 U; 46 0-2; 83 0-1 U; 88 1-5 U; 93 0-1; 113 0-1 U; 126 0-1; 136 0-1 U; 137 0-1 U; 139 0-1 U; 159 0-1 U; 169 0-3 U; 174 2-1 U; 178 0-1 U; 182 1-0; 183 1-0 U; 186 0-1 U; 188 0-1; 213 0-1 U; 222 1-0 U; 227 2-0; 230 1-0;

231 1-0; 249 3-2 U; 250 0-1 U; 253 0-2; 256 1-2; 258 2-1; 260 0-2 U; 263 0-1 U; 265 0-2 U; 266 1-0; 268 0-1 U; 273 0-1 U]

23. *Xenosaurus* + Anguidae: 27 1-0*; 32 0-1*; 33 0-1; 43 0-2; 45 1-0; 56 2-4*; 60 0-1; 62 0-2; 78 0-1; 124 0-1; 125 0-1; 129 0-1; 149 0-1*; 157 0-1; 175 0-1; 210 0-1; 212 0-1

Analysis 2

1. *Xenosaurus* + *Restes rugosus*: 1 0-2*; 45 1-0 U*; 51 0-1*; 53 0-1*; 60 0-1 U*; 62 0-2 U*; 67 0-1*; 72 0-1*; 97 1-2; 109 0-1*; 111 0-1*; 114 0-1*; 131 0-1; 132 1-2; 145 0-1*; 191 0-1; 210 0-1 U*; 214 0-1*

2. *Restes rugosus*: 55 2-3 U*; 105 1-0 U; 136 1-0 U; 137 1-0 U; 139 1-0 U; 144 0-1*; 185 0-1 U*; 200 1-0 U*; 204 0-1*

3. *Xenosaurus* + *Exostinus lancensis*: 62 2-3*; 93 1-0; 96 0-1*; 97 2-3*; 100 0-1; 111 1-2; 125 0-1 U; 193 1-2 [152 0-1; 157 0-1 U; 184 0-1]

4. *Exostinus lancensis*: 1 2-1; 92 1-0*; 147 5-C*; 154 1-0*; 246 1-2*

5. *Xenosaurus* + *Exostinus serratus*: 46 0-1*; 54 0-1; 62 3-4*; 93 1-0; 98 0-1*; 99 0-1*; 108 0-1*; 191 1-0 [7 1-2; 8 0-3; 9 0-1; 11 0-1; 14 0-1 U; 19 0-1; 43 0-2 U; 63 1-0; 68 1-2; 124 1-2; 129 0-1 U; 130 0-1; 209 0-1]

6. *Exostinus serratus*: 49 0-1*; 50 0-1*; 52 2-1*; 60 1-2*; 61 1-3*; 64 7-5*; 69 1-2*; 70 0-1*; 71 0-1*; 98 1-2*; 101 0-1*; 106 0-1*; 107 0-1*; 108 1-2*; 131 1-0; 132 2-1; 185 0-1 u*; 192 0-1*; 193 2-0*; 194 0-1*

7. *Xenosaurus*: 2 0-1*; 8 3-4*; 9 1-2*; 10 0-1; 17 0-1*; 21 2-3*; 23 0-1*; 26 0-1*; 45 0-1*; 56 4-3; 57 0-1*; 58 0-1*; 64 7-9*; 93 0-1*; 100 1-0; 104 0-1; 128 0-1*; 184 1-0; 195 1-0*; 196 1-0*; 201 0-1* [30 1-2; 31 0-1; 33 0-1 U; 34 0-1; 35 0-1; 37 0-1; 75 0-1; 78 0-1 U; 85 0-1; 86 0-1; 88 5-1 U; 116 0-1; 135 2-1; 142 0-1; 145 1-2; 146 0-1; 147 5-3; 148 4-2; 161 0-1; 165 0-1; 167 1-2; 168 0-1; 173 0-1; 175 0-1 U; 199 0-1; 205 0-2; 207 0-1; 208 0-1; 211 1-2; 212 0-1 U; 217 2-1 U; 218 0-1 U; 222 0-1 U; 228 0-1; 238 0-1; 243 0-1; 248 3-2; 264 1-2; 272 0-1]

8. Northern clade of *Xenosaurus*: 13 0-1*; 16 0-1*; 18 0-1; 20 1-0*; 21 3-4*; 22 1-2*; 28 0-1*; 29 1-2; 39 0-1*; 41 0-1*; 42 0-1*; 43 2-3*; 54 1-0; 60 1-0*; 64 9-B*; 68 2-3*; 73 0-1*; 75 1-2*; 76 1-2*; 79 0-1*; 83 1-0 U; 84 0-1*; 85 1-2*; 95 0-1*; 110 0-2*; 111 2-3*; 116 1-3*; 122 0-1*; 143 0-1*; 154 1-2*; 158 0-1*; 183 0-1 U*; 187 0-1*; 202 0-1*; 219 0-1*; 220 0-1*; 225 0-1*; 226 0-1*; 229 0-1*; 239 0-1*; 248 2-1*; 249 2-0*; 250 1-0 U; 251 0-1*; 253 1-0 U; 255 0-1*; 256 1-0 U; 258 2-3*; 259 1-0*; 260 2-1 U; 265 2-1 U; 267 2-1*; 269 1-0 U; 270 2-1 U; 273 1-0 U

9. *Xenosaurus newmanorum*: 56 3-5*; 65 0-1*; 88 1-2; 135 1-2; 147 3-4; 148 2-0*; 154 2-3*; 174 1-0*; 181 1-0; 182 1-0*; 198 0-1*; 223 1-0*; 224 0-1*; 234 1-0*; 235 0-1*; 237 0-1*; 260 1-0*; 263 1-0 u*; 268 1-0 u*

10. *Xenosaurus platyceps*: 61 1-2*; 80 0-1; 89 0-1*; 118 0-1; 119 0-1*; 120 0-1*; 127 0-1*; 135 1-0*; 174 1-2 U; 193 2-3*; 206 0-1*; 214 1-2*; 215 1-2*; 223 1-2*; 232 0-1*; 234 1-2*; 240 0-1*; 248 1-0*; 254 0-1*; 258 3-4*; 262 0-1; 265 1-0 u*; 266 1-2*; 267 1-0*

11. Southern clade of *Xenosaurus*: 11 1-2*; 12 0-1*; 27 0-1 u; 36 0-1; 37 1-2*; 38 0-1; 40 0-1*; 43 2-1; 68 2-0*; 74 1-2; 78 1-2*; 90 0-1*; 102 0-1*; 126 0-1; 134 0-1*; 138 0-1*; 147 3-1*; 151 0-1; 157 1-2; 165 1-2*; 178 1-0 U; 204 0-1*; 217 1-0; 242 0-1*; 245 0-1*; 249 2-3 U; 252 0-1*; 257 0-1*; 264 2-3*; 268 1-2*; 272 1-2*; 273 1-2

12. *Xenosaurus agrenon* + *Xenosaurus rectocollaris*: 46 1-2*; 56 3-2*; 88 1-0*; 135 1-0*; 142 1-0; 147 1-0*; 155 1-2*; 163 1-0*; 170 0-1*; 171 0-1*; 174 1-2 U; 175 1-0; 176 0-1*; 188 0-1*; 190 0-1*; 203 0-1*; 216 0-1*

13. *Xenosaurus agrenon*: 55 2-1*; 56 2-1*; 74 2-1; 76 1-0*; 77 0-1*; 110 0-1*; 148 2-3; 150 0-1*; 166 0-1*; 181 1-0; 198 0-1*; 217 0-1; 239 0-1*

14. *Xenosaurus rectocollaris*: 2-0*; 16 0-1*; 60 1-2*; 64 9-B*; 83 1-0; 87 2-1*; 96 1-0*; 123 0-1*; 131 1-0*; 148 2-1*; 214

1-2*; 215 1-0*; 229 0-1*; 234 1-0*; 236 0-1*; 271 0-1*; 273 2-0 [264 3-4]

15. *Xenosaurus grandis + Xenosaurus rackhami*: 5 0-1*; 15 0-1*; 58 1-2*; 65 0-1*; 82 0-1*; 103 0-1*; 112 0-1*; 115 0-1*; 133 0-1*; 139 1-2*; 141 0-1*; 151 1-2*; 155 1-0*; 156 0-1*; 159 1-0 u*; 160 0-1*; 163 1-2*; 167 2-3*; 168 1-2*; 169 3-2 u*; 172 0-1*; 179 0-1*; 182 1-2 u*; 197 0-1*; 221 0-1*; 227 2-1 u; 248 2-3; 252 1-2*; 253 1-2*; 256 1-2*; 260 2-3*; 265 2-3*

16. *Xenosaurus rackhami*: 56 3-4; 81 0-1*; 88 1-4*; 126 1-0; 135 1-2; 140 0-1*; 148 2-3; 153 0-1*; 165 2-3*; 166 0-1*; 169 2-1*; 177 0-1*; 205 2-1*; 240 0-2*; 249 3-6*; 252 2-3*; 256 2-3*

17. *Xenosaurus grandis*: 55 2-1*; 58 2-3*; 84 0-1*; 116 1-2*; 120 0-1*; 127 0-1*; 147 1-2; 157 2-1; 180 0-1*; 181 1-0; 193 2-1*; 198 0-1*; 255 0-1*

18. *Shinisaurus crocodilurus + Merkurosaurus ornatus*: 20 1-2*; 25 2-0; 61 1-0 U*; 149 1-0 U; 151 0-2 U; 155 1-0*; 195 1-2*

19. *Shinisaurus crocodilurus + Bahndwivici ammoskius*: 94 2-1 U; 98 0-1*; 147 5-6*; 185 0-1 U*; [27 0-1 U; 29 1-2; 48 0-1 U; 56 4-2 U; 68 1-0 U; 118 0-1 U; 126 0-1; 233 0-1]

20. *Merkurosaurus ornatus*: 7 1-0; 23 0-1*; 47 1-0 U; 92 1-0*

21. *Bahndwivici ammoskius*: 22 1-0 U*; 55 2-1*; 64 5-8 U; 97 1-3*; 124 1-0 U; 151 2-3*; 154 1-0*; 240 0-1*

22. *Shinisaurus crocodilurus*: 5 0-1*; 64 7-5 U*; 94 1-0*; 134 0-1 U*; 138 0-1*; 147 6-9*; 148 4-3*; 152 0-1 U [32 1-0 U; 46 0-2; 93 0-1; 182 1-0; 188 0-1; 227 2-0; 230 1-0; 231 1-0; 253 1-2; 256 1-2; 258 2-1; 266 1-0]

23. Xenosauridae: 3 0-1*; 6 0-1*; 7 0-1; 22 0-1*; 24 0-1*; 47 0-1; 52 0-2*; 59 0-1*; 66 0-1*; 69 0-1*; 83 0-1; 93 1-0; 94 1-2; 104 1-0; 105 0-1; 113 0-1; 117 0-1*; 124 0-1; 136 0-1; 137 0-1; 139 0-1; 147 4-5; 148 5-4*; 159 0-1*; 162 0-1*; 169 0-3*; 178 0-1; 181 0-1; 182 2-1*; 186 0-1*; 196 0-1*; 213 0-1*; 250 0-1; 253 0-1; 256 0-1; 260 0-2; 261 0-1; 263 0-1; 265 0-2; 268 0-1; 269 0-1; 270 0-2*; 273 0-1

DISCUSSION

Relation to Previous Studies and Taxonomic Issues Raised

Under both starting hypotheses, xenosaurs formed a clade within Anguimorpha when allowed to vary across the entire tree, supporting the monophyly of the ingroup of six extant species of *Xenosaurus* and three extinct taxa relative to the other included taxa. The relationship of the extinct taxa to *Xenosaurus* is thus consistent with historical descriptions of the fossils suggesting xenosaur affinities. Of the two prior studies presenting explicitly phylogenetic hypotheses of relationships among extinct and extant xenosaurs, the position of *R. rugosus* outside of a clade including *Xenosaurus* and *E. serratus* is consistent with those of both Gauthier (1982) and Conrad (2005, 2008). *Restes rugosus* as sister to all other xenosaurs is specifically consistent with Conrad (2005, 2008). However, *E. serratus* as the immediate sister to *Xenosaurus* was suggested by Gauthier (1982) but not Conrad (2005, 2008), who recovered a monophyletic *Exostinus*. Note that the relationships of xenosaurs were a primary focus of Gauthier's but not Conrad's work (J. Conrad, 2008; personal communication).

A single recent study suggests an alliance of the Mongolian Cretaceous taxon *C. intermedia* with xenosaurs (Conrad, 2008). A full analysis using the characters identified in the present work will have to proceed after examination of fossil material, and in particular CT scans, of *C. intermedia*. More recent work has indicated that *C. intermedia* might not be an anguimorph (J. A. Gauthier, personal communication); thus, a broader spread of scleroglossan characters and taxa than used in this study might be required to establish its phylogenetic position.

As predicted by previous studies (Gauthier, 1982; Estes, 1983; Conrad, 2008), I recovered *Exostinus* as a paraphyletic group consisting of two successive sister taxa to *Xenosaurus*. Notwithstanding concerns about the assignment of specimens to *E.*

lancensis, that taxon would then require a new genus name, and *Exostinus* would become monotypic, including only *E. serratus*. I propose to resurrect the name *Harpagosaurus*, applied by Gilmore (1928) to a maxilla now referred to *E. lancensis* (Estes, 1964, 1983). A more formal definition will require further study of known material of *E. lancensis*, which may represent several taxa (Gao and Fox, 1996).

As already discussed, the recovery of a monophyletic Xenosauridae in generating Analysis 2 is consistent with most morphological phylogenetic hypotheses, but not with studies based on molecular structure or with hypotheses proposed by Conrad (2005, 2008). Aside from this result, the close relationship of *B. ammoskius* to *S. crocodilurus* was again confirmed (Conrad, 2006). Moreover, *M. ornatus*, *B. ammoskius* + *Shinisaurus* as recovered by Conrad et al. (2011). That result provides support for the shinisaur affinities of the taxon (Klembara, 2008).

Temporal Implications

Exostinus serratus, sister to *Xenosaurus*, is nearly identical to the crown clade in most aspects of its known anatomy. Many of the character states appearing in the crown clade had thus arisen by the age of the Orellan sediments from which *E. serratus* was collected (Swisher and Prothero, 1990). Thus far, no extinct taxa that fall within the crown clade *Xenosaurus* have been identified. This "genus" may be very ancient indeed, like some anguid "genera" (Estes, 1983; personal observation). *Exostinus lancensis*, from the Late Cretaceous, is the oldest extinct taxon on the stem of *Xenosaurus* according to this study. The known fossil record of Anguidae and Helodermatidae, the putative sister groups to the xenosaur lineage in Analysis 1, are consistent with a Mesozoic split. *Odaxosaurus piger* is a primitive glyptosaur from the Cretaceous (Meszoely, 1970; Gauthier, 1982; Estes, 1983), and the primitive helodermatids *G. pulchra* and *P. nessovi*

are from the Upper Cretaceous of Mongolia and the Albian-Cenomanian of Utah, respectively. (If *P. nessovi* is indeed a helodermatid, its presence in the Early Cretaceous would suggest significant ghost lineages for xenosaurs and anguids.) The fossil record of shinisaurs extends back to the late Paleocene/early Eocene (Smith, 2006b), leaving a longer ghost lineage for the shinisaur branch of the Xenosauridae in Analysis 2. However, a number of North American Cretaceous "platynotan" taxa known from fragmentary remains have yet to be fully examined in a phylogenetic context, and among these might be found part of the missing shinisaur lineage (Estes, 1983; K. T. Smith, personal communication; personal observation).

Some notable stratigraphic incongruities are present in the phylogenetic hypotheses recovered here. The Paleocene *R. rugosus* is sister to all remaining xenosaurs, including the Cretaceous *E. lancensis*. The *R. rugosus* lineage has yet to be recovered from the Mesozoic. However, *R. rugosus* itself appears to be exceedingly rare in Paleogene faunas (Smith, 2006b; K. T. Smith, personal communication), and this may apply to its predecessors, as well. The second incongruity is the closer relationship of *B. ammoskius* from the North American Eocene to the extant Asian *S. crocodilurus* than *Merkurosaurus ornatus* from the European Miocene (Conrad, 2006; Klembara, 2008). This might suggest an early Paleogene transatlantic dispersal of the *Merkurosaurus* lineage, much like that which has been suggested to have resulted in the appearance of the primitive helodermatid *E. gallicum* in the Eocene of France (Hoffstetter, 1957) and the iguanian *Geiseltaliellus* in the Eocene of Germany (K. T. Smith, personal communication). One would then expect to find the *Merkurosaurus* lineage in earlier European deposits and in Early Paleogene or Mesozoic North American deposits. The former has not yet been reported, but the latter expectation may be fulfilled by the host of shinisaur-related taxa being identified from screenwashed early

Eocene and late Paleocene North American microfaunas (Smith, 2006b). Alternatively, in the case of both shinisaurs and helodermatids, the North American and European representatives could have been derived from an unknown Asian stock. Primitive helodermatids were present in present-day Mongolia during the Late Cretaceous (Gao and Norell, 2000).

Finally, taxa farther down the stem of *Xenosaurus* than *R. rugosus* are notably lacking. As noted already, relatively primitive helodermatids and shinisaurs have been found, but another frustrating absence exists along the stem of Anguidae. The highly derived glyptosaurs are the only putative stem anguids known, and even that placement is not strongly supported, for they already possess most of the derived features of anguids (Conrad, 2005, 2008; Conrad et al., 2011; J. A. Gauthier, personal communication).

Biogeography of Xenosaurs

There is a striking difference in latitude between the locations of collections of the stem xenosaurs in this study, all of which were found in Colorado, Wyoming, and farther north still, and the present distribution of *Xenosaurus* in central and southern Mexico. That pattern obtains for other squamate taxa, as well—notably diploglossine anguids (Gauthier, 1982; Smith, 2006b; personal observation) and polychrotine iguanians (Smith, 2006a, 2006b). The apparent contraction of the ranges of parts of clades has been convincingly attributed to the contraction of megathermal climate zones during the global cooling following the Paleocene/Eocene thermal maximum by Smith (2006b).

Xenosaurus are, with few exceptions, crevice-dwelling lizards and are distributed along the great north–south-extending mountain ranges of Mexico. The initial split within *Xenosaurus* is a division between a northern clade, consisting of *X. newmanorum* and *X. platyceps* in the Sierra Madre Oriental, and a southern clade, consisting of the remaining taxa (King and Thompson,

1968; Canseco Márquez, 2005), of which the *X. agrenon* + *X. rectocollaris* clade is more to the west and the *X. grandis* + *X. rackhami* clade is more to the east, extending into Central America. *Xenosaurus rackhami* has a particularly wide distribution, and I observed more intraspecies variation in that species of *Xenosaurus* than in the others for which I had sample sizes larger than one or two. Further details of the biogeography of *Xenosaurus* were provided by Canseco Márquez (2005).

Comments on Ingroup Clades

Xenosauridae. Analysis 2, the unconstrained analysis, strongly recovered a monophyletic Xenosauridae in the classical sense, as also suggested, but not cladistically tested, by Smith (2006b). Many of the characters supporting the clade were not used by Conrad (2005, 2008). Two characters, the subpalpebral fossa and the mediolaterally expanded facet on the maxilla, are present in association with slightly different elements in the two taxa, but this does not invalidate their potential homology according to the tree. Several other characters, including the upfolded tab of the facial process of the maxilla, are unique within Squamata. Part of the difficulty of resolving the degree of relatedness between xenosaurs and shinisaurs is the poor fossil record along the stem of Anguimorpha. It is quite possible that the character states that seem so peculiar to the classical Xenosauridae are in fact ancestral for Anguimorpha as a whole.

Xenosaurus + *Restes rugosus.* The most inclusive clade of the xenosaur lineage already has the characteristic dentition of the group. Among the bones surrounding the nasal capsule, the maxilla shows a combination of plesiomorphic and derived features, notably a primitively platey, continuous osteodermal covering. The palpebral and prefrontal already display typical xenosaur morphologies. Likewise, the frontal and jugal bear several synapomorphies with the other xenosaurs, but they are

primitive in various respects, as well. What is preserved of the palate is intermediate between *Xenosaurus* and the remainder of Anguimorpha, in particular the persistence of remnants of the pterygoid dentition. *Restes rugosus* is the only fossil xenosaur to preserve any of the palate. The primitively long, narrow postorbital suggests that the supratemporal arch was not expanded and heavily ornamented as in *Xenosaurus*. It is thus likely that the general flattening of the head and possibly the body evident in the crown clade was not as developed in the ancestor of this more inclusive clade.

Differences in synapomorphies supporting the clade between Analysis 1 and Analysis 2 have largely to do with the issue of xenosaurid monophyly. In Analysis 1, several features shared by xenosaurs and shinisaurs optimize as convergent and are added to the apomorphy list for *Xenosaurus* + *R. rugosus*.

Restes rugosus. *Restes rugosus* displays a host of plesiomorphic characters for xenosaurs, exhibiting few obvious autapomorphies in its known anatomy. The most obvious of its autapomorphies is the unusually large angle of divergence of the medial and lateral edges of the palatine process of the pterygoid. It is unclear whether that morphology indicates a similarly peculiar morphology for the remainder of the palate, which is not preserved. In *Xenosaurus*, despite the widening of the head, the palatine process of the pterygoid is not particularly expanded.

Xenosaurus + Exostinus lancensis. *Exostinus lancensis* is not a well-known taxon, and this clade is supported largely by the more broken-up osteoderms on the maxilla and the *Xenosaurus*-like domed osteoderms of the frontal. The frontal is still unconstricted interorbitally compared with *E. serratus* and *Xenosaurus*, but the cristae cranii approach each other more closely than in *R. rugosus*. *Exostinus lancensis* is the only fossil xenosaur, unfortunately, to preserve the parietal. The supratemporal processes are broken and so could not be scored, but they appear to have been short as in *Xenosaurus*.

Exostinus lancensis. This is a difficult taxon for reasons already stated, relating to incompleteness and difficulty in the assignment of specimens. Its recovered position closer to the crown clade than *R. rugosus* requires a reversal in tooth form from slightly bicuspid to unicuspid. However, despite the assertion of the most recent description that all teeth in *E. lancensis* are unicuspid (Gao and Fox, 1996), some AMNH specimens I examined for this study show an apical, longitudinal groove like that which extends basally from the division between the smaller mesial and the larger distal cusps in those xenosaurs that have a bicuspid morphology (e.g., AMNH 15366). The apices of the teeth of all of these specimens are damaged. Furthermore, although the skull roof osteoderms of *E. lancensis* are domed like those of *E. serratus* and *Xenosaurus*, their form is unusual. They are oval or obovate and on the parietal show a concentric distribution unique to *E. lancensis*.

Xenosaurus + Exostinus serratus. These two taxa are nearly identical in many aspects of their osteology, although only the rostral portions of the skull are known for *E. serratus*, and these incompletely. The osteoderms in general are of the characteristic *Xenosaurus* form and distribution. The dentition also has the form seen in primitive parts of the crown clade. However, the nares are primitively large and elongate; concomitantly, the nasal process of the premaxilla, although expanded, is not so expanded as in *Xenosaurus*, and the slope of the narial margin of the maxilla is gentler and longer. Unfortunately, premaxillae are unknown from other fossil xenosaurs.

Exostinus serratus. This is essentially a short-faced xenosaur, its rostrum autapomorphically short, reflected in features such its reduced tooth count. Additionally, the unusually wide palatal shelf of the maxilla suggests a particularly wide skull with the maxillae diverging from each other at a high angle. The lack of a posterior expansion of

the jugal is another strange autapomorphy. The various unique features of this taxon raise the question of whether xenosaurs were relatively diversified earlier than the crown radiation. In turn, it is unclear where less autapomorphic lineages more similar to the crown might be found.

Xenosaurus. *Xenosaurus*, in part because constituents are extant and thus much more completely known, is supported by a large number of synapomorphies. Notable are the mediolateral expansions of the nasal process of the premaxilla and the squamosal and the relative mediolateral widening of the parietal. Several bones, such as the septomaxilla and coronoid, are expanded and enclose more nerves and vasculature than the primitive state. The body is flattened and the neural spines relatively low; various other axial and appendicular synapomorphies also exist, such that the postcranium of *Xenosaurus* is fairly distinct among anguimorphs.

Northern clade of Xenosaurus. The northern clade of *Xenosaurus*, widely separated geographically from the remaining species, retains a number of ancestral characters that the southern clade has lost, notably the proportions of the skull roof bones. However, the taxa within the northern clade are united by a consistent suite of synapomorphies—more than the southern taxa. Among these synapomorphies are several features of the anterior maxilla and premaxilla. Furthermore, the heavy osteodermal armor of the northern clade optimizes as primitive if the heavily armored helodermatids and anguids are the immediate sister taxon to xenosaurs. However, it optimizes as derived or ambiguous if the more lightly armored shinisaurs are used.

Xenosaurus newmanorum. This is a large-bodied species (King and Thompson, 1968). Other than its large size, it is in general the less autapomorphic of the two examined species from the northern clade. It has a particularly tall head for *Xenosaurus*, possibly a primitive feature (Herrel et al., 2001). As the less autapomorphic part of the northern clade, which itself retains a number of ancestral characters, *X. newmanorum*

might be a better taxon to include in phylogenetic analyses than the commonly used *X. grandis* and *X. platyceps* (e.g., Conrad, 2008, who noted the shortcomings of scoring a composite "*Xenosaurus*" from *X. grandis* and *X. platyceps*—although these two taxa do bracket the clade).

Xenosaurus platyceps. This is the flattest species of *Xenosaurus*, in head and body. Several autapomorphies of the maxilla and skull roof relate to the particularly flat, wide head of the taxon, and unusual morphologies of the axial and appendicular skeletons might also relate to this marked dorsoventral compression.

Southern clade of Xenosaurus. The southern clade of *Xenosaurus* is united by a large number of synapomorphies, most of them relatively subtle, such as the proportions of osteodermal sculpturing and proportions of articular parts of the dermal cranial roof and sidewall. The ranges of some of the taxa within are considerably greater than those of the species within the northern clade (i.e., *X. rackhami*; King and Thompson, 1968), and the individual species as a whole are more morphologically divergent than the relatively similar *X. newmanorum* and *X. platyceps*.

Xenosaurus agrenon + Xenosaurus rectocollaris. This clade, consisting of two little-known taxa for which I had but one specimen each, is supported by the fewest synapomorphies of the clades within *Xenosaurus*. Nevertheless, some of these synapomorphies (e.g., the unusual notch in the posterior region of the parietal, the morphology of the central region of the basisphenoid, and the bizarre flattened neural spines of the lumbar region) are striking and unique, and the clade appears robust. In general, this clade shares several ancestral character states with the northern clade that are no longer present in the well-supported *X. rackhami* + *X. grandis* clade. In contrast to the meager osteodermal armor of the latter clade, the *X. agrenon* + *X. rectocollaris* clade shares relatively heavy armor with the northern clade.

Xenosaurus agrenon. This species is particularly little known, appearing exter-

nally very similar to *X. grandis*, but internally sharing a number of synapomorphies with *X. rectocollaris*. A distinct form of the supratemporal arch is one of the few autapomorphies distinguishing it from its common ancestor with that taxon.

Xenosaurus rectocollaris. This is the most unusual of the species of *Xenosaurus* at first glance. Its head is particularly short and stout, although the shortening appears to involve the postorbital dermal bones of the adductor/otic region, instead of the bones surrounding the nasal capsule as in *E. serratus*. Externally, the taxon is distinguished by a bold dark-on-light color pattern different from the light-on-dark patterns of the other species of *Xenosaurus*, and it bears a strange cuff of puffy tissue around its neck. It would be interesting to investigate possible ecological correlations of the singular anatomy of this animal.

Xenosaurus rackhami + Xenosaurus grandis. These two species share a number of synapomorphies, most strikingly a dramatic reduction of cranial osteoderms (postcranial osteoderms are absent). Certain other features distinct to *Xenosaurus*, such as the anteroposterior expansion of the tip of the jugal and the mediolateral expansion of the supratemporal arch, are at their most extreme in these two taxa, which are also perhaps the best represented in U.S. museum collections.

Xenosaurus rackhami. This species is slender of head and body compared with other *Xenosaurus*, and some individuals have particularly flat heads. In *X. rackhami*, the reduction of osteoderms is the extreme among examined *Xenosaurus*, and several peculiar autapomorphies of the skull roof and supratemporal bar, as well as the dentition, also obtain.

Xenosaurus grandis. This is a relatively unusual species of *Xenosaurus*, stout and robust where its sister taxon is slim and slight. The reduction of osteoderms is less extreme in *X. grandis*, and some of the autapomorphies of the taxon relate to its generally stout form. *Xenosaurus grandis* is the most common species of *Xenosaurus* in

U.S. collections, and the most heavily figured and described (notably by Barrows and Smith, 1947). It is generally used as the exemplar for *Xenosaurus*, and sometimes for the classical Xenosauridae as a whole (Wever, 1978; Estes et al., 1988). Considering the large number of apomorphies between *X. grandis* and the *Xenosaurus* ancestor, it is not the ideal choice. Only one recent study (Conrad, 2008; extended in Conrad et al., 2011) included a prudent combination of *X. grandis* and *X. platyceps*, bracketing *Xenosaurus*.

Morphological Characters in Phylogenetic Analysis and Specific Issues of Character Evolution

My analysis includes an unusual number of characters for such a restricted group of lizards (compared with, e.g., Rieppel and Zaher [2002] for uropeltid snakes, a group of similar size and high specialization). The surfeit of characters owes in part to my discovery of a number of informative features in previously unappreciated elements, such as the septomaxilla and the palpebral— these discoveries in turn owing to the availability of disarticulated skeletal material. Characters such as small foramina in these diminutive bones were remarkably invariant within taxa, and the fact that this seems counterintuitive suggests that a large number of characters dealing with subtle differences in anatomy are arbitrarily neglected in gross anatomical phylogenetics. Further work, in particular, on subtle features of disarticulated bones, could be immensely profitable in increasing the number of gross-scale characters to achieve greater parity with the size of molecular-scale datasets (Chippindale and Wiens, 1994). Already, work on subtle and tiny foramina dotting the dermatocranial elements of certain mammals has shown that the clustering of these foramina are consistent within taxa and appear to be phylogenetically informative (Wible, 2003; Kearney et al., 2005).

In addition to hypotheses of relationships, phylogenetic analyses provide a thorough

catalogue of anatomical changes in the structures utilized, whether at the gross, histological, or molecular scale—they are in some ways "shorthand" descriptions of anatomy. Several characters or character systems here examined stand out as potentially fruitful for additional study. The enclosure of the ethmoid nerves within the premaxilla (character 6) is unusual within Squamata. It is interesting that xenosaurs show both this character and very heavy osteodermal sculpturing—as do very old individuals of *E. multicarinata*. The appearance of xenosaur-like features in very late stage *E. multicarinata* might suggest a heterochronic relationship, wherein some characters of xenosaurs are peramorphic with respect to those of anguids and perhaps other anguimorphs.

The increased number of foramina in the premaxilla (characters 7 and 8) and maxilla (characters 53 and 54) in xenosaurs might suggest an increased acuity of integumentary sensation, perhaps related to the decreased utility of sight in the dark environments frequented at least by individuals of *Xenosaurus*. Increased numbers of foramina on the face have been suggested to imply great tactile acuity in amphisbaenians, as well (Kearney et al., 2005). The increased diameter of the infraorbital canal within xenosaurs (character 51) indicates an increase in the size of the contained neurovascular bundle, which includes the V_2 division of the trigeminal nerve. An enlarged canal for V_3 is associated with the enormously elaborated sensory capabilities of the platypus snout (Rowe et al., 2008).

The various septomaxillary characters identified herein are remarkably phylogenetically useful and consistent with regard to variation, considering the general neglect of this skeletal element in the non-snake squamate literature. Clearly the septomaxilla is complex and evolutionarily labile, and I predict that it will prove a rich source of characters for other clades, as well. The morphology in *Xenosaurus*, with its fully enclosed medial and lateral canals, is especially remarkable, and one wonders at the possible soft tissue and sensory correlates. The complete enclosure of the lateral canal in *Xenosaurus* and *Heloderma* recalls the sister taxon relationship between those taxa suggested by some analyses in molecular-scale studies (Townsend et al., 2004).

Several transformations in the temporal region, notably the lateral and ventral expansion of the postorbital and squamosal and the anteroposterior expansion of the jugal, occur along the stem of *Xenosaurus*. Seemingly accompanying these changes are the strong surangular crest and the subcoronoid fossa. Possibly these features are variously related to the enormously elaborated adductor musculature of *Xenosaurus* (Haas, 1960). If they are so related, they may together represent a complex of characters that are not fully independent from each other.

Finally, *Xenosaurus* shows a lack of depression in the posterior end of the quadrate for the tympanic cavity (character 173). Varanidae also display this character, but the quadrates of those taxa are heavily modified. Possibly the lack of depression is related to a reduction of the tympanic cavity also associated with the scaling over (and thus apparent functional impedance) of the tympanum (character 270). However, the depression remains in *Shinisaurus*, whose tympanum is also scaled over in adulthood.

Character nonindependence is a recurring problem in phylogenetic analysis (Martins and Garland, 1991; Schaffer et al., 1991; Huelsenbeck and Nielsen, 1999; McCracken et al., 1999). Given the level of integration among the parts of a multicellular (or unicellular) organism, it is unlikely that characters can ever be fully independent. Nevertheless, studies such as mine could profit from careful analysis of character correlation, taking into account ontogeny and the soft tissue relations of bones. The character list I provided is arranged by sensory capsule, for example, because most dermatocranial elements are involved in sheathing one of the three capsular regions (with the otic region being more complicated because of the additional

presence of the adductor chamber). Significant changes in the basic structure of one of the sensory capsules surely would produce complementary changes in multiple sheathing bones. Considering the ingroup of this study, a few other potential sources of nonindependence arise. The head of *Xenosaurus* is unusually wide, and this general change may be related to the mediolateral expansion of several dermatocranial elements and even the capture of previously external vascular and nervous structures by the septomaxilla. In *E. serratus*, the shortness and width of the snout could be related to several autapomorphies of the taxon. Osteodermal development obviously shows general trends, with most regions of osteoderms reduced, for example, in *X. grandis* + *X. rackhami*. However, these trends are not always uniform, preventing the scoring of a single combined character for the various potentially related transformations. For instance, cranial osteoderms are best developed in *X. newmanorum* and *X. platyceps*, especially in the former. Limb osteoderms, however, are more prominent and numerous in *X. platyceps*, whereas caudal osteoderms are more developed in *X. newmanorum*. Thus, neither taxon can been scored overall as having the most "highly developed" osteoderms, even if cranial and postcranial categories are established.

Finally, an initial foray into studies of the intraspecies variation of characters is made herein, although the attempt is basically limited to an effort to justify character selection and scoring. A great deal of additional work needs to be done on intraspecies variation in all vertebrates, for this variation is the raw material of evolution (Darwin, 1859; Bever, 2006 and references therein). In particular, compared with the attempts made here, further studies must incorporate larger sample sizes, greater ontogenetic spreads, and careful control of localities/populations and the temporal aspect of collection. *Xenosaurus* provides an interesting case study for population studies because populations of the species are spatially restricted, often occupying a single rock cliff (Ballinger et al., 2000). That spatial restriction may account for the relatively large number of species of *Xenosaurus*, and it is not clear whether significant gene flow occurs among isolated populations (Lemos-Espinal et al., 2004). On a larger scale, aspects of variation can provide additional characters for phylogenetic analysis. In short, morphological characters for phylogenetic analysis are by no means exhausted, even in the most heavily studied clades. A push for careful, thorough anatomical analysis of as much of the body as possible, ranging from the microscopic scale to aspects of variation and behavior, will yield a vast number of additional characters. The limited exercise provided by this work demonstrates that even a thorough, bone-by-bone analysis of the skeleton alone can yield hundreds of novel characters and produce a fully resolved phylogeny with high support values. In this case, congruence with DNA-based analyses allows further confidence in the results, but considering the number of the characters and the high support for the morphological tree, incongruence would necessitate careful reconsideration not only of the morphological but also of the molecular data and analyses.

ACKNOWLEDGMENTS

LITERATURE CITED

ANANJEVA, N. B., E. M. SMIRINA, AND N. G. NIKITINA. 2003. Dentition of *Phrynocephalus melanurus*. Does tooth number depend on body size and/or age? *Russian Journal of Herpetology* **10**: 1–6.

ARISTOTLE. 350 BCEa. Categories. The Internet Classics Archive; c1995–2001 [cited 2008 August 25]. Available from: http://classics.mit.edu/Aristotle/categories.html.

ARISTOTLE. 350 BCEb. Physics. The Internet Classics Archive; c1995–2001 [cited 2008 August 25]. Available from http://classics.mit.edu/Aristotle/physics.html.

AST, J. C. 2001. Mitochondrial DNA evidence and evolution in Varanoidea (Squamata). *Cladistics* **17**: 211–226.

BALLINGER, R. E., G. R. SMITH, AND J. A. LEMOS-ESPINAL. 2000. *Xenosaurus. Catalogue of American Amphibians and Reptiles* **712**: 1–3.

BARAHONA, F., AND L. J. BARBADILLO. 1998. Inter- and intraspecific variation in the post-natal skull of some lacertid lizards. *Journal of Zoology of the Zoological Society of London* **245**: 393–405.

BARROWS, S., AND H. M. SMITH. 1947. The skeleton of the lizard *Xenosaurus grandis* (Gray). *The University of Kansas Science Bulletin* **31**(2): 227–281.

BELLAIRS, A. D'A. 1949. Observations on the snout of *Varanus*, and a comparison with that of other lizards and snakes. *Journal of Anatomy* **83**: 116–146 + 1 plate.

BERNSTEIN, P. 1999. Morphology of the nasal capsule of *Heloderma suspectum* with comments on the systematic position of helodermatids (Squamata:). *Acta Zoologica (Stockholm)* **80**: 219–230.

BEVER, G. S. 2005. Variation in the ilium of North American *Bufo* (Lissamphibia; Anura) and its implications for species-level identification of

fragmentary anuran fossils. *Journal of Vertebrate Paleontology* **25**: 548–560.

BEVER, G. S. 2006. Studies on post-natal variation and variability in the vertebrate skeleton and its paleontological implications [unpublished Ph.D. dissertation]. Austin: The Univ. of Texas.

BEVER, G. S. 2008. Comparative growth in the postnatal skull of the extant North American turtle *Pseudemys texana* (Testudinoidea: Emydidae) *Acta Zoologica* **89**: 107–131.

BEVER, G. S., C. J. BELL, AND J. A. MAISANO. 2005. The ossified braincase and cephalic osteoderms of *Shinisaurus crocodilurus* (Squamata, Shinisauridae). *Palaeontologia Electronica* **8**: 1–36.

BHULLAR, B.-A. S. 2006. Postnatal ontogenetic changes in the cranium of *Varanus exanthematicus* with comparisons to other varanoids and applications to the fossil record. *Journal of Vertebrate Paleontology* **26**: 42A.

BHULLAR, B.-A. S. 2007. The enigmatic fossils *Exostinus* and *Restes*: resolving the stem and the crown of *Xenosaurus*, the knob-scaled lizards. *Journal of Vertebrate Paleontology* **27**: 48A.

BHULLAR, B.-A. S. 2008. Anatomy and phylogeny of *Xenosaurus* and its extinct relatives [unpublished M.S. thesis]. Austin: The Univ. of Texas.

BHULLAR, B.-A. S. 2010. Cranial osteology of *Exostinus serratus* (Squamata: Anguimorpha), fossil sister taxon to the enigmatic clade *Xenosaurus*. *Zoological Journal of the Linnean Society* **159**: 921–953.

BHULLAR, B.-A. S, AND K. T. SMITH. 2008. Helodermatid lizard from the Miocene of Florida, the evolution of the dentary in, and comments on dentary morphology in, Varanoidea. *Journal of Herpetology* **42**: 286–302.

BORSUK-BIALYNICKA, M. 1984. Anguimorphans and related lizards from the Late Cretaceous of the Gobi Desert, Mongolia. *Palaeontologia Polonica* **46**: 1–105 + 13 plates.

CANSECO MÁRQUEZ, L. 2005. Filogenia de las Lagartijas del Genero *Xenosaurus* Peters (Sauria: Xenosauridae) Basada en Morfologia Externa [unpublished M.S. thesis]. Mexico City: Univ. Nacional Autonoma de Mexico.

CHIPPINDALE, P. T., AND J. J. WIENS. 1994. Weighting, partitioning, and combining characters in phylogenetic analysis. *Systematic Biology* **43**: 278–287.

CONRAD, J. L. 2004. Skull, mandible, and hyoid of *Shinisaurus crocodilurus* Ahl (Squamata, Anguimorpha). *Zoological Journal of the Linnean Society* **141**: 399–434.

CONRAD, J. L. 2005. Shinisaur osteology and the evolution of Squamata [unpublished Ph.D. dissertation]. Chicago: Univ. of Chicago.

CONRAD, J. L. 2006. An Eocene shinisaurid (Reptilia, Squamata) from Wyoming, U.S.A. *Jounral of Vertebrate Paleontology* **26**: 113–126.

CONRAD, J. L. 2008. Phylogeny and systematics of Squamata (Reptilia) based on morphology. *Bulletin of the American Museum of Natural History*, **310**: 1–182.

CONRAD, J. L., J. C. AST, S. MONTANARI, AND M. A. NORELL. 2011. A combined evidence phylogenetic analysis of Anguimorpha (Reptilia: Squamata). *Cladistics* **27**: 230–277.

DARWIN, C. 1859. *On the Origin of Species by Means of Natural Selection*. London: John Murray.

DEEP SCALY PROJECT, THE. 2007. "*Elgaria multicarinata*," Digital Morphology [Internet]. Austin, Texas: DigiMorph; c2002 [cited 2008 August 28]. Available from: http://digimorph.org/specimens/Elgaria_multicarinata.

EDMUND, A. G. 1969. Dentition, pp. 117–200. *In* C. Gans, A. D'A. Bellairs, and T. S. Parsons (eds.), *Biology of the Reptilia*. Vol. 1. London and New York: Academic Press.

ESTES, R. 1964. Fossil vertebrates from the Late Cretaceous Lance Formation eastern Wyoming. *University of California Publications in Geological Sciences* **49**: 1–180 + 5 plates.

ESTES, R. 1965. Notes on some Paleocene lizards. *Copeia* **1965**: 104–106.

ESTES, R. 1983. *Sauria Terrestria, Amphisbaenia*. Stuttgart; New York: Gustav Fischer Verlag.

ESTES, R., K. DE QUEIROZ, AND J. GAUTHIER. 1988. Phylogenetic relationships within Squamata, pp. 119–281. *In* R. Estes and G. Pregill (eds.), *Phylogenetic Relationships of the Lizard Families: Essays Commemorating Charles L. Camp*. Stanford, California: Stanford Univ. Press.

EVANS, S. E. 1980. The skull of a new eosuchian reptile from the Lower Jurassic of South Wales. *Zoological Journal of the Linnean Society* **70**: 203–264.

EVANS, S. E., AND L. J. BARBADILLO. 1998. An unusual lizard (Reptilia: Squamata) from the Early Cretaceous of Las Hoyas, Spain. *Zoological Journal of the Linnean Society* **124**: 235–265.

EVANS, S. E., Y. WANG, AND C. LI. 2005. The Early Cretaceous lizard genus *Yabeinosaurus* from China: resolving an enigma. *Journal of Systematic Palaeontology* **3**: 319–335.

FRASER, N. C. 1982. A new rhynchocephalian from the British Upper Trias. *Palaeontology* **25**: 709–725 + plates 769–771.

FULLER, S., P. BAVERSTOCK, AND D. KING. 1998. Biogeographic origins of goannas (Varanidae): a molecular perspective. *Molecular Phylogenetics and Evolution* **9**: 294–307.

GAO, K., AND R. C. FOX. 1996. Taxonomy and evolution of Late Cretaceous lizards (Reptilia: Squamata) from western Canada. *Bulletin of Carnegie Museum of Natural History* **33**: 1–107.

GAO, K., AND M. A. NORELL. 1998. Taxonomic revision of *Carusia* (Reptilia: Squamata) from the Late Cretaceous of the Gobi Desert and phylogenetic relationships of anguimorphan lizards. *American Museum Novitates* **3230**: 1–51.

GAO, K., AND M. A. NORELL. 2000. Taxonomic composition and systematics of Late Cretaceous lizard assemblages from Ukhaa Tolgod and adjacent localities, Mongolian Gobi Desert. *Bulletin of

the American Museum of Natural History **249**: 1–118.

GAUTHIER, J. A. 1982. Fossil xenosaurid and anguid lizards from the Early Eocene Wasatch Formation, southeast Wyoming, and a revision of the Anguioidea. *Contributions to Geology, University of Wyoming* **21**: 7–54.

GAUTHIER, J., A. G. KLUGE, AND T. ROWE. 1988. Amniote phylogeny and the importance of fossils. *Cladistics* **4**: 105–209.

GILMORE, C. W. 1928. Fossil lizards of North America. *Memoirs of the National Academy of Sciences* **22**: 1–169 + 27 plates.

GILMORE, C. W. 1942. Paleocene faunas of the Polecat Bench Formation, Park County, Wyoming, part II. lizards. *Proceedings of the American Philosophical Society* **85**: 159–167.

GRAY, J. E. 1856. Notice of a new species of nocturnal lizard from Mexico. *Annals and Magazine of Natural History* **2**: 270.

HAAS, G. 1960. On the trigeminus muscles of the lizards *Xenosaurus grandis* and *Shinisaurus crocodilurus*. *American Museum Novitates* **2017**: 1–54.

HALLERMAN, J. 1994. Zur Morphologie der Ethmoidalregion der Iguania (Squamata)—Eine vergleichend-anatomische Untersuchung. *Bonner Zoologische Monographien* **35**: 1–133.

HARVEY, M. B. 1991. The microstructure and evolution of scale surfaces in xenosaurid lizards [unpublished Master's thesis]. Arlington: The Univ. of Texas.

HARVEY, M. B. 1993. Microstructure, ontogeny, and evolution of scale surfaces in xenosaurid lizards. *Journal of Morphology* **216**: 161–177.

HERREL, A., E. DE GRAUW, AND J. A. LEMOS-ESPINAL. 2001. Head shape and bite performance in xenosaurid lizards. *Journal of Experimental Zoology* **290**: 101–107.

HOFFSTETTER, R. 1957. Un saurien helodermatidé (*Eurheloderma gallicum* nov. gen. et ap.) dans la faune fossile des phosphorites du Quercy. *Bulletin de la Société Géologique de la France* **7**: 775–786.

HUELSENBECK, J. P., AND R. NIELSEN. 1999. Effect of nonindependent substitution on phylogenetic accuracy. *Systematic Biology* **48**: 317–328.

KEARNEY, M., J. A. MAISANO, AND T. ROWE. 2005. Cranial anatomy of the extinct amphisbaenian *Rhineura hatcherii* (Squamata, Amphisbaenia) based on high-resolution x-ray computed tomography. *Journal of Morphology* **264**: 1–33.

KING, W., F. G. THOMPSON. 1968. A review of the American lizards of the genus *Xenosaurus* Peters. *Bulletin of the Florida State Museum* **12**: 93–123.

KLEMBARA, J. 2008. A new anguimorph lizard from the Lower Miocene of north-west Bohemia, Czech Republic. *Palaeontology* **51**: 81–94.

LARSON, A. 1994. The comparison of morphological and molecular data in phylogenetic systematics, pp. 371–390. *In* B. Schierwater, B. Streit, G. P. Wagner, and R. DeSalle (eds.), *Molecular Ecology and Evolution: Approaches and Applications.* Basel: Birkhauser Verlag.

LEE, M. S. Y. 1998. Convergent evolution and character correlation in burrowing reptiles: towards a resolution of squamate relationships. *Biological Journal of the Linnean Society* **65**: 369–453.

LEE, M. S. Y., AND J. D. SCANLON. 2002. Snake phylogeny based on osteology, soft anatomy and ecology. *Biological Reviews* **77**: 333–401.

LEMOS-ESPINAL, J. A., G. R. SMITH, AND R. E. BALLINGER. 2004. Aspects of the ecology of a distinct population of *Xenosaurus platyceps* from Queretaro, Mexico. *Amphibia-Reptilia* **25**: 204–210.

MACEY, J. R., J. A. SCHULTE, II., A. LARSON, B. S. TUNIYEV, N. ORLOV, AND T. J. PAPENFUSS. 1999. Molecular phylogenetics, tRNA evolution, and historical biogeography in anguid lizards and related taxonomic families. *Molecular Phylogenetics and Evolution* **12**: 250–272.

MADDISON, W. P., AND D. R. MADDISON. 2008. Mesquite: a modular system for evolutionary analysis. Version 2.5 [Internet] Available from: http://mesquiteproject.org.

MÄGDEFRAU, H. 1997. Biologie, Haltung und Zucht der Krokodilschwanz-Höckerechse (*Shinisaurus crocodilurus*). *Zeitschrift des Kölner Zoo* **40**: 55–60.

MAISANO, J. A., C. J. BELL, J. A. GAUTHIER, AND T. ROWE. 2002. The osteoderms and palpebral in *Lanthanotus borneensis* (Squamata: Anguimorpha). *Journal of Herpetology* **36**: 678–682.

MARTINS, E. P., AND T. GARLAND, JR.. 1991. Phylogenetic analyses of the correlated evolution of continuous characters: a simulation study. *Evolution* **45**: 534–557.

McCRACKEN, K. G., J. HARSHMAN, D. A. McCLELLAN, AND D. A. AFTON. 1999. Data set incongruence and correlated character evolution: an example of functional convergence in the hind-limbs of Stifftail Diving Ducks. *Systematic Biology* **48**: 683–714.

McDOWELL, S. B., JR., AND C. M. BOGERT. 1954. The systematic position of *Lanthanotus* and the affinities of the anguimorphan lizards. *Bulletin of the American Museum of Natural History* **105**: 1–142 + 16 plates.

MESZOELY, C. A. M. 1970. North American fossil anguid lizards. *Bulletin of the Museum of Comparative Zoology* **139**: 87–149.

NORELL, M. A., AND K. GAO. 1997. Braincase and phylogenetic relationships of *Estesia mongoliensis* from the Late Cretaceous of the Gobi Desert and the recognition of a new clade of lizards. *American Museum Novitates* **3211**: 1–25.

NORELL, M. A., M. C. McKENNA, AND M. J. NOVACEK. 1992. *Estesia mongoliensis*, a new fossil varanoid from the Late Cretaceous Barun Goyot Formation of Mongolia. *American Museum Novitates* **3045**: 1–24.

NYDAM, R. L. 2000. A new taxon of helodermatid-like lizard from the Albian-Cenomanian of Utah. *Journal of Vertebrate Paleontology* **20**: 285–294.

Pianka, E. R., and D. R. King. 2004. *Varanoid Lizards of the World*. Bloomington and Indianapolis: Indiana University Press.

Rieppel, O. 1980. The phylogeny of anguinomorph lizards. *Denkschriften der Schweizerischen Naturforschenden Gesellschaft* **94:** 1–86.

Rieppel, O., and H. Zaher. 2002. The skull of the Uropeltinae (Reptilia, Serpentes), with special reference to the otico-occipital region. *Bulletin of the Natural History Museum of London (Zoology)* **68:** 123–130.

Rowe, T. 1986. Osteological diagnosis of Mammalia, L.1758, and its relationship to extinct Synapsida [unpublished Ph.D. dissertation]. Berkely: Univ. of California.

Rowe, T., T. H. Rich, P. Vickers-Rich, M. Springer, and M. O. Woodburne. 2008. The oldest platypus and its bearing on divergence timing of the platypus and echidna clades. *Proceedings of the National Academy of Sciences* **105:** 1238–1242.

Schaffer, H. B., J. M. Clark, and F. Kraus. 1991. When molecules and morphology clash: a phylogenetic analysis of the North American ambystomatid salamanders (Caudata: Ambystomatidae). *Systematic Zoology* **40:** 284–303.

Scotland, R. W., R. G. Olmstead, and J. R. Bennett. 2003. Phylogeny reconstruction: the role of morphology. *Systematic Biology* **52:** 539–548.

Smith, H. M., and J. B. Iverson. 1993. A new species of knobscale lizard (Reptilia: Xenosauridae) from Mexico. *Bulletin of the Maryland Herpetological Society* **29:** 51–66.

Smith, K. T. 2006a. A diverse new assemblage of Late Eocene squamates (Reptilia) from the Chadron Formation of North Dakota, U.S.A. *Palaeontologia Electronica* **9:** 1–44.

Smith, K. T. 2006b. Horizontal and vertical aspects of species diversity in the fossil record: alpha, beta, and the temporal nature of the richness-temperature relation [unpublished Ph.D. dissertation]. New Haven, Connecticut: Yale Univ.

Sprackland, R. G. 1993. The biology of the Chinese crocodile lizard in captivity. *The Reptilian Magazine* **4**(2): 9–15.

Stebbins, R. C. 1948. Nasal structure in lizards. *American Journal of Anatomy* **83:** 183–221.

Strong, E. E., and D. Lipscomb. 1999. Character coding and inapplicable data. *Cladistics* **15:** 363–371.

Swisher, C. C., III., and D. R. Prothero. 1990. Single crystal ^{40}Ar/^{39}Ar dating of the Eocene–Oligocene transition in North America. *Science* **249:** 760–762.

Swofford, D. L. 2001. *PAUP*: Phylogenetic Analysis Using Parsimony (*and Other Methods), Version 4 0b10*. Sunderland, Massachusetts: Sinauer Associates.

Taylor, E. H. 1949. A preliminary account of the herpetology of the state of San Luis Potosi, Mexico. *The University of Kansas Science Bulletin* **33**(Part 1): 169–215.

Templeton, A. R. 1983. Phylogenetic inference from restriction endonuclease cleavage site maps with particular reference to the evolution of humans and the apes. *Evolution* **37:** 221–244.

Townsend, T., A. Larson, E. Louis, and J. Macey. 2004. Molecular phylogenetics of Squamata: the position of snakes, amphisbaenians, and dibamids, and the root of the squamate tree. *Systematic Biology* **53:** 735–757.

Vidal, N., and S. B. Hedges. 2005. The phylogeny of squamate reptiles (lizards, snakes, and amphisbaenians) inferred from nine nuclear protein-coding genes. *Comptes Rendus Biologies* **328:** 1000–1008.

Wever, E. G. 1978. The Reptile Ear: Its Structure and Function. Princeton, New Jersey: Princeton Univ. Press.

Whiteside, D. I. 1986. The head skeleton of the Rhaetian sphenodontid *Diphydontosaurus avonis* gen. et sp. nov. and the modernizing of a living fossil. *Philosophical Transactions of the Royal Society of London B* **312:** 379–430.

Wible, J. R. 2003. On the cranial osteology of the short-tailed opossum *Monodelphis brevicaudata* (Didelphidae, Marsupialia). *Annals of Carnegie Museum* **72:** 137–202.

Wiens, J. J. 2001. Character analysis in morphological phylogenetics: problems and solutions. *Systematic Biology* **50:** 689–699.

Wiens, J. J., and J. L. Slingluff. 2001. How lizards turn into snakes: a phylogenetic analysis of body-form evolution in anguid lizards. *Evolution* **55:** 2303–2318.

Bulletin
of the
Museum of Comparative Zoology

Cryptic species within the *Dendrophidion vinitor* complex in Middle America (Serpentes: Colubridae)

JOHN E. CADLE

CRYPTIC SPECIES WITHIN THE *DENDROPHIDION VINITOR* COMPLEX IN MIDDLE AMERICA (SERPENTES: COLUBRIDAE)

JOHN E. CADLE[1]

CONTENTS

ABSTRACT. Snakes previously referred to *Dendrophidion vinitor* from southern Mexico to eastern Panama comprise three sibling species primarily distinguishable by substantial differences in hemipenial morphology and some subtle aspects of color pattern. *Dendrophidion vinitor* Smith is here restricted to populations from southern Mexico to Belize. *Dendrophidion apharocybe* new species is distributed from Honduras to Panama, primarily on the Atlantic versant. *Dendrophidion crybelum* new species is known from middle elevations of the Río Coto Brus valley in southwestern Costa Rica (Pacific versant). Hemipenes of *D. vinitor* and *D. apharocybe* are similar in overall shape (short, bulbous) but the former has a highly ornate apex with membranous ridges and an unusual apical boss, whereas *D. apharocybe* has a largely nude apex strongly inclined toward the sulcate side. *Dendrophidion crybelum* has an elongate cylindrical hemipenis with a large number of spines. In general, these species are not distinguishable by standard scutellation characters. Hemipenial and other characters suggest that these species are a monophyletic group within *Dendrophidion* and have the following relationships: (*vinitor* (*apharocybe*, *crybelum*)). Some aspects of the systematics and biogeography of *Dendrophidion* are discussed. Divergence among the three species is associated with two geological features important to speciation in Middle America, the northern Motagua–Polochíc fault zone (Guatemala–Belize) and the southern Cordillera Talamanca (Costa Rica–Panama).

Key words: Snakes, New Species, Central America, Mexico, Systematics, Costa Rica, Hemipenis, Morphology

RESUMEN. Las serpientes anteriormente referidas a *Dendrophidion vinitor* desde el sur de México hasta Panamá oriental se componen tres especies hermanas que se distinguen por differencias importantes en la morfología de los hemipenes y aspectos sutiles de coloración. *Dendrophidion vinitor* Smith se limita a las poblaciones del sur de México, Guatemala, y Belice. *Dendrophidion apharocybe*, nueva especie, se encuentra desde Honduras hasta Panamá primariamente en la vertiente Atlántica. *Dendrophidion crybelum*, nueva especie, se concoce solamente de elevaciones medias del valle del Río Coto Brus en el suroeste de Costa Rica (vertiente Pacífica). Los hemipenes de *D. vinitor* y *D. apharocybe* son similares en forma (corte, buloso) pero el primero tiene un ápice muy ornamentado con crestas membranosas y una protuberancia apical, mientras *D. apharocybe* tiene el ápice mayormente nudo y fuertemente inclinado al lado sulcado. *Dendrophidion crybelum* tiene un hemipene alargado y cilíndrico con muchas espinas. Generalmente, estas especies no se distinguen por characteres estandarizados de escutelación. Los característicos de los hemipenes y otros caracteres sugieren que estas especies se componen un grupo monofilético dentro *Dendrophidion* con las relaciones siguientes: (*vinitor*

[1] Research Associate, Department of Herpetology, California Academy of Sciences, 55 Music Concourse Drive, Golden Gate Park, San Francisco, California 94118 (jcadle@calacademy.org).

(*apharocybe, crybelum*)). Se discuten algunos aspectos de la sistemática y biogeografía de *Dendrophidion*. La divergencia entre las tres especies es asociada con dos rasgos geológicos importantes para la especiación en América Central, la falla Motagua–Polochíc (Guatemala–Belice) en el norte y la Cordillera Talamanca (Costa Rica–Panamá) en el sur.

INTRODUCTION

The Neotropical snake genus *Dendrophidion* Schlegel currently comprises eight or nine recognized species (Lieb, 1988; McCranie, 2011). Despite considerable progress in clarifying the taxonomy and species limits over the last three-quarters of a century (Smith, 1941; Peters and Orejas-Miranda, 1970; Lieb, 1988; Savage, 2002), it is clear that additional work is needed. Smith (1941) described *D. vinitor* (type locality: Piedras Negras, Guatemala) to accommodate a Mexican and Middle American species with a single anal plate, a relatively low number of subcaudals, and strongly keeled scales. His primary objective was to distinguish this species from the catch-all earlier name *D. dendrophis* (Duméril, Bibron, and Duméril) (type locality: Cayenne, French Guiana), which had been widely applied to Middle American forms of *Dendrophidion* with an undivided anal plate. In doing so, Smith helped clarify the presence and characters of four species of *Dendrophidion* in Central America: *D. clarkii* Dunn, *D. paucicarinatum* (Cope), *D. percarinatum* (Cope), and *D. vinitor*. Lieb (1988) synonymized *D. clarkii* with *D. nuchale* (W. Peters; type locality: Caracas, Venezuela). However, McCranie (2011) resurrected the name *clarkii* (type locality: El Valle de Antón, Panama) for application to Middle American and western Colombian/Ecuadorian populations of this group based on patterns of geographic variation described by Lieb (1988). Nonetheless, further revision of *D. nuchale/clarkii* is necessary (see comments on name usage in Materials and Methods). Apart from continuing ambiguity concerning *D. nuchale/clarkii*, the taxonomy of Central American species has been stable since Smith's (1941) revisions.

Smith (1941) had referred specimens from southern Mexico to central Panama to *D. vinitor* and thought that the distribution was continuous throughout this area. However, Lieb (1988, 1991) thought the distribution was highly fragmented, with disjunct segments in southern Veracruz, Mexico; Oaxaca, Mexico, to northern Guatemala; Nicaragua to western Panama on the Atlantic versant; southwestern Costa Rica; and Darién, Panama, to northwestern Colombia. Researchers since have considered *D. vinitor* a widespread, if discontinuously distributed, species of the Central American herpetofauna. Lieb (1988) considered *D. vinitor* a member of his "*Dendrophidion dendrophis* species group," which is defined on the basis of hemipenial characters, strong keeling on the dorsal scales, and the point of reduction of the dorsocaudal scales.

During my examination of Costa Rican material referred to *D. vinitor*, it was apparent that specimens from the Atlantic and Pacific versants differed substantially in hemipenial morphology. Furthermore, both of the hemipenial morphs of the Costa Rican specimens were quite distinct from hemipenes of specimens from the northern part of the range of *D. vinitor* (Mexico). Further study indicated that "*Dendrophidion vinitor*" comprised three very similar species distinguishable primarily by strong differences in hemipenial morphology and by a few subtle external characters. The three species occupy geographically discrete distributions, with no contiguity or overlap currently known. The purpose of this paper is to redefine and diagnose *D. vinitor* and to describe the two new species within this complex. Available data on the natural history of these species are summarized, and detailed descriptions of their hemipenes are presented.

MATERIALS AND METHODS

General methodology and methods of recording meristic data and measurements follow procedures previously described (e.g., Cadle, 2005, 2007), but I here amplify

some of the characters particularly useful for the three species covered in this paper. Dorsocaudal reductions were recorded as the subcaudal at which the reduction from eight to six dorsal scale rows on the tail occurred (Lieb, 1988). The point of posterior reduction of the dorsal scales was scored on each side of selected specimens as the ventral scute number at which the reduction occurred and the dorsal rows involved. For purposes of analyzing intraspecific differences in mean snout–vent length (SVL) of adult males and females, specimens with SVL > 450 mm were considered adults (Goldberg, 2003; Stafford, 2003). Similarly, because relative tail length increases proportionally with SVL, the range of adult relative tail length (RTL) was assessed for individuals with SVL > 300 mm because analyses showed that RTL approaches an asymptote at approximately this size. When measurements or meristic data for particular specimens are referred to in the text, these data are based on my examinations (data encountered in the literature sometimes differ).

Intraspecific mean differences between male and female sizes and scale counts were tested for significance using *t* tests after testing for homogeneity of variances. *P*-values reported for intraspecific comparisons are two-tailed pairwise comparisons; in the few cases in which there was a priori expectation for one sex or the other to have a greater value for a character (e.g., males having a longer tail or more subcaudals than females), *p*-values for one-tailed tests did not differ from the two-tailed comparison. Similar procedures and two-tailed tests were used for interspecific comparisons, which were analyzed separately for each sex except in cases in which intraspecific sexual differences were nonsignificant (sexes pooled in these cases). Means, standard deviations, and results of intraspecific statistical comparisons for most meristic counts are presented in Table 1, and only summaries are given in the text.

For determining tail breakage frequencies, I counted as "broken" only tails with a clearly healed cap on the stump; thus, I record the frequency of "broken/healed" tails. In my survey of literature, it was apparent that some authors included any specimens with a tail fracture in their tail breakage frequency calculations (e.g., at least one paper recorded multiple fracture points in a high percentage of specimens). However, this method artificially inflates estimates of tail breakage frequencies because of the inclusion of snakes whose tails were broken during or after capture, or even subsequent to storage in a museum jar. Although these specimens may offer clues as to the fragility of the tail in a particular species, they are not especially useful for comparative purposes.

I scored the number of keeled dorsal scale rows on the neck, at midbody, and just anterior to the vent. Keels in all species of *Dendrophidion* are best developed (i.e., encompassing more dorsal rows) on the posterior body, but the number of keeled rows on the neck or at midbody often show interspecific differences that provide discriminating characters. The three species covered in this paper are similar in their patterns of keeling. The basic pattern of temporal scales in *D. vinitor* and the new species here described is 2+2 (two primary, two secondary). However, temporal scales were often divided by a vertical suture (usually dividing the scale asymmetrically), or, less commonly, two temporal scales were fused or a temporal was fused with a supralabial. I recorded these divisions or fusions separately from the basic pattern. For example, a specimen might be recorded as having 2+2 temporals but with the upper primary and upper secondary fused on one side. Because of frequent asymmetry, temporal scales and supra- and infralabials were scored on each side of a specimen, and each side was treated as an independent observation; the total count of observations for these scale characters (Table 1) is thus about twice the number of specimens examined (damage sometimes prevented scoring on one or both sides of a given specimen).

TABLE 1. SCALE COUNTS, MEASUREMENTS, AND OTHER DATA FOR THE THREE SPECIES OF THE *DENDROPHIDION VINITOR* COMPLEX. BODY PROPORTIONS, VENTRAL AND SUBCAUDAL COUNTS, AND NUMBER OF PALE BANDS ARE GIVEN AS RANGE FOLLOWED BY MEAN ± SD. BILATERAL COUNTS ARE SEPARATED BY A SLASH (/). FOR PRIMARY AND SECONDARY TEMPORALS AND SUPRA- AND INFRALABIAL SCALES, EACH SIDE OF EACH SPECIMEN WAS COUNTED AS AN INDEPENDENT OBSERVATION. SVL, SNOUT–VENT LENGTH; MEASUREMENTS IN MILLIMETERS. SAMPLE SIZES IN PARENTHESES. ASTERISKS INDICATE STATISTICAL SIGNIFICANCE OF INTRASPECIFIC DIFFERENCES BETWEEN MEANS OF MALE AND FEMALE SIZE, PROPORTIONS, OR MERISTIC COUNTS (* $p <$ 0.05; ** $p < 0.01$; *** $p < 0.001$); NO ASTERISK INDICATES NONSIGNIFICANCE.

	Dendrophidion vinitor Smith, 1941	*Dendrophidion apharocybe* New Species	*Dendrophidion crybelum* New Species
Largest specimens: total length, SVL	997, 636 ♂ 847+, 595 ♀	1040, 653 ♂ 1045, 672 ♀	985, 625 ♂ 893+, 631 ♀
Tail length/total length	0.35–0.37 ♂ 0.36 ± 0.006 (8) **	0.35–0.38 ♂ 0.37 ± 0.008 (15) ***	0.34–0.36 ♂ 0.35 ± 0.0007 (7) *
	0.33–0.36 ♀ 0.34 ± 0.012 (8)	0.33–0.36 ♀ 0.35 ± 0.010 (21)	0.34–0.35 ♀ 0.34 ± 0.003 (3)
Tail length/SVL	0.53–0.59 ♂ 0.56 ± 0.019 (8) **	0.53–0.61 ♂ 0.57 ± 0.021 (15) ***	0.51–0.58 ♂ 0.55 ± 0.021 (7) *
	0.49–0.56 ♀ 0.53 ± 0.025 (8)	0.49–0.57 ♀ 0.54 ± 0.025 (21)	0.50–0.54 ♀ 0.52 ± 0.02 (3)
Maxillary teeth	38–45 40.8 ± 1.96 (13)	33–44 39.1 ± 2.39 (29)	38–44 40.8 ± 1.91 (8)
Dorsal scales	17–17–15 (29)	17–17–15 (60)	17–17–15 (16)
Ventrals	147–156 ♂ 152.0 ± 3.09 (12) ***	149–160 ♂ 153.9 ± 2.84 (31) ***	150–153 ♂ 151.6 ± 0.92 (8) ***
	153–162 ♀ 158.1 ± 2.93 (17)	152–168 ♀ 160.8 ± 3.79 (34)	156–162 ♀ 160.0 ± 2.27 (8)
Subcaudals	112–125 ♂ 118.6 ± 3.53 (11) 109–122 ♀ 116.8 ± 3.58 (13)	115–127 ♂ 121.1 ± 3.79 (23) 111–129 ♀ 119.9 ± 4.47 (29)	112–119 ♂ 116.9 ± 2.29 (8) 115–119 ♀ 117.2 ± 1.85 (6)
Dorsocaudal reduction, 8 to 6 (subcaudal number)	40–65 ♂ 52.6 ± 7.49 (12) **	32–63 ♂ 47.8 ± 7.35 (29) ***	43–58 ♂ 49.0 ± 4.69 (8)
	34–59 ♀ 45.3 ± 5.61 (17)	26–52 ♀ 41.5 ± 7.43 (31)	42–56 ♀ 48.6 ± 5.53 (8)
Dorsal scales, posterior reduction (ventral number)	85–96 ♂ 92.8 ± 2.75 (18) ***	85–102 ♂ 94.6 ± 3.89 (36) ***	93–99 ♂ 96.0 ± 1.65 (12) ***
	93–106 ♀ 99.0 ± 3.64 (24)	93–105 ♀ 99.3 ± 3.83 (36)	99–104 ♀ 102.1 ± 1.96 (9)
Preoculars	1/1 (28)	1/1 (65)	1/1 (16)
Postoculars	2/2 (28)	2/2 (63) 2/3 (2)	2/2 (16)
Primary temporals	2 (58)	1 (5) 2 (125)	2 (32)
Secondary temporals	2 (58)	1 (5) 2 (125)	2 (32)
Supralabials, supralabials touching eye	8, 3–5 (2) 9, 4–6 (54) 10, 5–7 (2)	8, 3–5 (2) 8, 4–6 (2) 9, 4–6 (119) 9, 5–6 (1) 9, 5–7 (1) 10, 4–7 (3) 10, 5–7 (2)	8, 3–5 (1) 9, 4–6 (31)

TABLE 1. CONTINUED.

	Dendrophidion vinitor Smith, 1941	*Dendrophidion apharocybe* New Species	*Dendrophidion crybelum* New Species
Infralabials	9 (52)	7 (1)	9 (32)
	10 (3)	8 (7)	
	11 (1)	9 (116)	
		10 (5)	
No. of pale bands on body	51–70	46–69	36–62
	60.3 ± 4.69 (28)	54.4 ± 4.48 (54)	48.2 ± 7.53 (13)

The width of the pale neck bands has been important in distinguishing "*Dendrophidion vinitor*" auctorum from other species. However, neck bands, particularly the first two behind the head (which are often broader than other bands), can be very irregular in outline. Bands on the posterior two-thirds of the body are more uniform and narrower than the anterior bands (and less easily discriminate species). Thus, in scoring the width of neck bands, I used the third and fourth band behind the head as references and counted the scales or fractions thereof encompassed by the pale portion of the band (not including the dark bordering stipple) in the dorsolateral region at the level of dorsal scale rows 6 and 7. I counted scales in a horizontal line, not along the diagonal, as is often counted while doing dorsal scale counts; this was to minimize the effect of irregularities in band shape (e.g., zigzag or not) on scoring width. Thus, my summaries of band widths are somewhat less than some of those encountered in the literature. For example, Costa Rican "*D. vinitor*" are sometimes said to have pale bands 2–3 scale rows wide (Savage, 2002: 655), whereas in my scorings, most specimens have bands 1–2.5 rows wide.

Maxillary dentition is similar in the three species covered in this paper. Teeth gradually enlarge anterior to posterior, but typically, four posterior teeth are abruptly enlarged (and nongrooved). The enlarged teeth are not offset, and a diastema is absent (e.g., see Fig. 8). However, there is some variation within all three species in the abruptness with which the enlarged posterior teeth transition to the smaller anterior

series. I assessed some specimens as having either three or five posterior enlarged teeth (recognizing some subjectivity as to what constitutes an "enlarged" tooth). My impression is that posterior teeth in *D. vinitor*, as redefined herein, are not enlarged to the same degree or as abruptly as in the new species, *D. apharocybe* and *D. crybelum*. However, this is a subjective impression only—something that is difficult to quantify with wet preparations given the apparent variation. I have not attempted to assess this more fully, although I comment on some of the noticeable variation in the species accounts. Tooth counts are the total number of maxillary teeth, including empty tooth sockets and the enlarged posterior teeth.

Everted hemipenes described in detail and illustrated herein were fully everted in the field at the time of collection. For detailed study they were removed from the specimen and inflated with colored jelly (Myers and Cadle, 2003); manual eversion was used for a few specimens for comparative purposes. Retracted hemipenes were slit midventrally and pinned flat for study. In addition to the hemipenes described in detail, I made reference to others that were everted to varying degrees and studied in situ. Hemipenial measurements were taken with dial vernier calipers to the nearest 0.1 mm. In the species accounts, I give brief characterizations of the hemipenes, emphasizing salient features only. For ease of comparison, detailed descriptions of everted and retracted organs of all three species are deferred to a separate section at the end. However, because these species are most notably distinguished by

details of hemipenial morphology, the detailed descriptions should be considered integral parts of the species accounts. Hemipenial terminology is explained in the detailed accounts.

"*Dendrophidion vinitor*" is discussed in many regional faunistic works for Central America, some of which are cited in the synonymies in the species accounts. However, with few exceptions, the variational data (e.g., scale count ranges or color notes) in these works seem to derive from other sources (e.g., Lieb, 1988). Thus, it is usually not clear whether a particular account is based on specimens from the focal region. For example, Taylor (1954: 729–730) gave data on size, meristics, and color in life "taken from field notes" for "*D. vinitor*" in his account of Costa Rican snakes. However, the color notes he quoted are those for the holotype, which is from Guatemala (Smith, 1941) and the Costa Rican form is a different species described herein. The size and meristic data of Taylor (1954) are a summary from throughout the range given in Smith (1941; Mexico to Panama), with no indication that that is the case. Unless it seems clear that descriptive comments apply to a specific geographic area, I do not cite them here because three species have been confused in previous literature. Similar caveats apply to some natural history data.

Despite progress in understanding the systematics of *Dendrophidion* reviewed in the introduction, my own preliminary study makes it clear that further revisions are necessary. For purposes of this work, some taxonomic conventions, which will ultimately be modified as revisionary work proceeds, are necessary. For convenience in the diagnoses, I use the two species groups of *Dendrophidion* recognized by Lieb (1988): the *D. percarinatum* group comprising *D. bivittatum*, *D. brunneum*, *D. paucicarinatum*, and *D. percarinatum*; and the *D. dendrophis* group comprising *D. dendrophis*, "*D. nuchale/clarkii*," and *D. vinitor* (and by extension, the two new species described here). Lieb did not assign the

Colombian endemic *D. boshelli* to a species group. Species in the *D. percarinatum* group differ from those in the *D. dendrophis* group in having a dorsocaudal reduction from 8 to 6 anterior to subcaudal 25 (posterior to subcaudal 25 in the *D. dendrophis* group, further refined for three species herein), by less strongly keeled dorsal scales, and often by smaller hemipenial spines, among other characters (Lieb, 1988). In addition, I recognize as the "*Dendrophidion vinitor* complex" the two new species described herein along with *D. vinitor* as restricted here. McCranie (2011) resurrected the name *D. clarkii* for part of "*D. nuchale*" *sensu* Lieb (1988), but further revision will be necessary before the application of names in this complex becomes clear; see comments in Savage (2002: 655) and McCranie (2011: 106–107). Thus, in this paper, I refer to the complex of species represented by the names *D. nuchale* and *D. clarkii* as "*D. nuchale* auctorum." Additional comments on taxonomy and character distributions are given in the discussion.

Specimens of *D. vinitor* as restricted herein are listed in Appendix 1, which also includes museum abbreviations used throughout this paper. Specimens of the new species are listed in their species accounts since this material comprises the type series. Notes on the localities and coordinates for specimens examined and for selected localities from literature are in Appendix 2.

Redescription of *Dendrophidion vinitor* Smith, 1941

Figures 1, 2A, 3–4, 6, 18–19

Drymobius dendrophis. Günther, 1885–1902: 127 (part; Guatemala); Boulenger, 1894: 15–16 (part; specimens *b, d, f* from "Vera Paz" and "Guatemala"). See discussion of historical records under Distribution.

Dendrophidion dendrophis. Duméril et al., 1870–1909: 730–732 (part; specimens from "Peten" and "Vera Paz"). The

"Peten" specimen (MNHN 7353), illustrated by Lieb (1988: fig. 1), is a syntype of *Herpetodryas poitei* Duméril, Bibron, and Duméril, 1854. See discussion of historical records under Distribution.

Dendrophidium dendrophis. Dugés, 1892: 100–101 + pl. (Motzorongo [Veracruz], Mexico). See Smith (1943: 416) and discussion of historical records under Distribution herein.

Dendrophidion vinitor. Smith, 1941: 74–75 (type locality: Piedras Negras, Guatemala) (part; holotype and paratypes from Guatemala and Mexico). Smith, 1943: 415–416 + fig. 13. Taylor, 1944: 184 (EHT-HMS 27496–98). Smith and Taylor, 1945: 46. Stuart, 1948: 63. Smith and Taylor, 1950: 318 (holotype). Stuart, 1950: 23. Darling and Smith, 1954: 191 (UIMNH 33862). Taylor, 1954: 729–730 (part; color description of holotype and some meristic data quoted from Smith, 1941). Cochran, 1961: 172 (part; holotype and paratypes, USNM 110662, 7099, 46589). Duellman, 1963: 246. Stuart, 1963: 94 (part; Mexico and Guatemala). Peters and Orejas-Miranda, 1970: 79 (part). Alvarez del Toro, 1972: 142, 144. Johnson et al. "1976" [1977]: 134, 136–137. Perez-Higareda, 1978: 69, 72. Alvarez del Toro, 1982: 190–191. Pérez-Higareda et al., 1987: 16. Smith, 1987: xxxvii (part; based on Günther's "*Drymobius dendrophis*"). Flores and Gerez, 1988: 218–219, 261. Lieb, 1988: 171 (part). Villa et al., 1988: 63 (part). Campbell and Vannini, 1989: 11. Johnson, 1989: 64. Lieb, 1991: 522.1–522.2 (part). Pérez-Higareda and Smith, 1991: 31, pl. 4. Flores-Villela, 1993: 30. Lee, 1996: 310–311 (Yucatan, base). Campbell, 1998: 207, fig. 127 (part; specimen from Veracruz, Mexico). Lee, 2000: 282–283, fig. 315 (part; Belize). Stafford and Meyer, 2000: 199–200 (Belize). Savage, 2002: 655–656 (part). Köhler, 2003: 200 (part). Meerman and Lee, 2003: 67, 70. Stafford, 2003: 111 (part; specimens from Mexico, Guatemala). Guyer and Donnelly, 2005: 185 (part). McCranie et al., 2006: 147–148 (part). Köhler, 2008: 215 (part). Savage and Bolaños, 2009: 14 (part). McCranie, 2011: 111 (part).

Holotype (Fig. 1). USNM 110662, from Piedras Negras [El Petén], Guatemala. Collected 21 May 1939 by Hobart M. Smith and Rozella B. Smith (field number 7280) as part of collections assembled during tenure of the Walter Rathbone Bacon Traveling Scholarship (Smith, 1943: 416). The holotype is presently in fair condition. I did not examine it directly but inspected dorsal and ventral photographs provided by USNM and had selected characters verified by USNM personnel. According to Smith (1941), it is a subadult female 510+ mm total length, 169+ mm incomplete tail length (341 mm SVL). The holotype has several irregular longitudinal ventral incisions from the anterior body nearly to the vent and on the anterior ventral part of the tail. The tail tip is missing. Smith (1941) described the holotype in detail, but one character in his description is apparently in error: "nine supralabials, 3rd, 4th and 5th entering orbit"—a character found in no other specimen (Table 1). Both sides of the holotype in fact have nine supralabials but it is the 4th, 5th, and 6th that touch the eye on both sides (verified by Steve Gotte, March 2011), which is the near-universal condition in the specimens I examined (Table 1).

Etymology. The specific name *vinitor* is a Latin noun meaning "vine cultivator" or "vine dresser." Latin lexicons show that the word is derived from the noun *vinum* (wine). The complete derivation therefore is the stem *vin-* + connective *-i-* + the suffix *-tor*. The termination is a classic noun suffix meaning an agent or doer of something (vine care and pruning in this case). The name was not a good choice for a forest-dwelling snake.

Hobart Smith gave no etymological information in the original description, but

Figure 1.   Holotype of *Dendrophidion vinitor* Smith (USNM 110662) from Piedras Negras, Guatemala (Petén Department). Scale = 5 cm.

provided different intended meanings to other taxonomists: Lee (1996: 311) quoted Smith as stating that the name means "a dweller in vines"; McCranie (2011: 113) quoted Smith as stating that he could not know for sure what he had in mind but that he had intended "vine-climber." In any case, Lee (1996: 311) was incorrect in stating that *vinitor* is derived from "*vinea*," which is both an adjective pertaining to wine and a substantive meaning vineyard or vines.

Diagnosis. Dendrophidion vinitor is characterized by (1) Dorsocaudal reduction from 8 to 6 occurring posterior to subcaudal 30 (range, 34–65); (2) single anal plate (rarely divided); (3) relatively low subcaudal counts (<130 in males and females); (4) pale dorsal crossbands usually less than one dorsal row wide and bordered posteriorly (often anteriorly as well) by dark brown or black; (5) immaculate ventrals and subcaudals except for lateral dark pigment common to all species of *Dendrophidion*; and

(6) a bulbous hemipenis with a highly ornate apex, including: asulcate flounces; a series of free-standing membranous ridges, the median one of which is taller than others and bisects the apex; and a raised rounded boss or protuberance on the sulcate edge of the apex (the sulcus spermaticus ends beneath its free edge). The combination of few subcaudals and (in most individuals) a single anal plate will distinguish *D. vinitor* from all other species of *Dendrophidion* except *D. apharocybe*, *D. crybelum*, and *D. paucicarinatum*.

Dendrophidion vinitor differs from the four species of the *D. percarinatum* group in having the dorsocaudal reduction from 8 to 6 posterior to subcaudal 30 and more strongly keeled dorsal scales, and from all species of the *D. percarinatum* group except some individuals of *D. paucicarinatum* in having a single anal scale. *Dendrophidion paucicarinatum* usually has a more uniformly colored dorsum lacking distinct pale crossbands, has narrow dark lines across
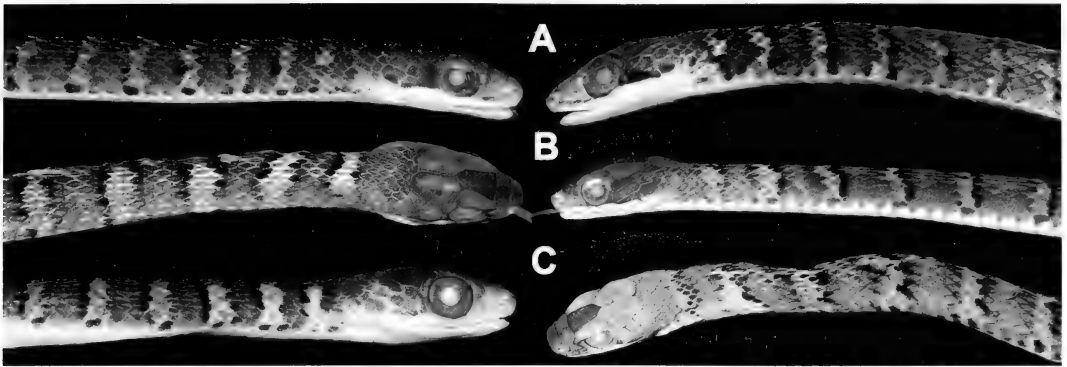
Figure 2.　Comparison of pale bands on the anterior body of representative specimens of the *Dendrophidion vinitor* complex. Each pair (left, right) representative of one species. (A) *Dendrophidion vinitor* as restricted herein (UMMZ 121145, UMMZ 122767; both Veracruz, Mexico). (B) *Dendrophidion apharocybe* new species (KU 112974, Nicaragua; LACM 148593, Costa Rica [holotype]). (C) *Dendrophidion crybelum* new species (LACM 114108, LACM 148599 [holotype]; both Costa Rica).

the venter in adults and many juveniles, and has a higher number of ventrals (>175 compared with <170 in *D. vinitor*). *Dendrophidion vinitor* differs from *D. boshelli* in having 17 midbody scale rows (15 in *D. boshelli*). *Dendrophidion vinitor* has fewer subcaudals (<130) and usually a shorter adult relative tail length (<60% of SVL) than *D. nuchale* auctorum and *D. dendrophis* (>130 and usually >60% of SVL, respectively); the anal plate may be either single or divided in these last two species.

Dendrophidion vinitor differs from the new species described herein, *D. apharocybe* and *D. crybelum*, in having narrower pale bands on the neck/anterior body (Fig. 2). Although "*Dendrophidion vinitor*" is often stated to have broader bands than other congeners, such as *D. percarinatum* (e.g., Savage, 2002: 655), those statements are based on a comparison of the two new species described herein, *D. apharocybe* and/or *D. crybelum*, with other species. *Dendrophidion vinitor* as redefined here has narrow pale crossbands, generally one scale row or less in width (as pointed out by Smith [1941] for the holotype), compared with crossbands more than one row wide in *D. apharocybe* and *D. crybelum* (Fig. 2). In *D. vinitor*, the crossbands become indistinct posteriorly or restricted to the dorsolateral/vertebral region, whereas in *D. apharocybe* and *D. crybelum*, the posterior crossbands

usually become invested with dark pigment so that each crossband appears as a transverse dark band with embedded pale ocelli. These patterns of *D. apharocybe* and *D. crybelum* are easily seen in the color plates of Savage (2002: pl. 416), Solórzano (2004, fig. 60), Figure 9 herein for *D. apharocybe*, and Figures 15 and 16 herein for *D. crybelum*. *Dendrophidion vinitor* has a significantly greater mean number of pale bands on the body than either *D. apharocybe* (p < 0.001) or *D. crybelum* (p < 0.001), although the ranges of band numbers overlap broadly among the three species (Table 1).

Additionally, *Dendrophidion vinitor* differs from *D. apharocybe* and *D. crybelum* in hemipenial morphology (see detailed descriptions). The everted hemipenis of *D. vinitor* is rather short and stout and has a highly ornate bulbous apex ornamented with largely nonanastomosing (free-standing) membranous ridges (reduced remnants of calyces primitively present). The apex has a prominent rounded protuberance, or *apical boss*, on the sulcate side; the centrolineal sulcus spermaticus ends underneath its free edge. One of the free-standing ridges bisects the apex in a line from the front edge of the apical boss directly across the apex to the asulcate side. The other ridges extend obliquely outward toward the asulcate side from this median ridge.

Dendrophidion apharocybe has a hemipenis similar in shape to that of *D. vinitor*, but the apex is strongly inclined toward the sulcate side, lacks an apical boss, and, in contrast to *D. vinitor*, is nude except for low rounded ridges. *Dendrophidion crybelum* has a relatively long cylindrical hemipenis with a small, nonbulbous apex bearing short ridges, and a large number of enlarged spines (≥70) on the hemipenial body compared with <50 in *D. vinitor*.

Description (12 males, 17 females). Table 1 summarizes size, body proportions, and meristic data for *D. vinitor*. Largest specimen (UIMNH 37165) a male 997 mm total length, 636 mm SVL. Largest female (UIMNH 35546) 847+ mm total length, 595 mm SVL. Tail 35–37% of total length (53–59% of SVL) in males; 33–36% of total length (49–56% of SVL) in females. Dorsal scales in 17–17–15 scale rows, the posterior reduction usually by fusion of rows 2+3 at the level of ventrals 85–106 (see sexual dimorphism below). Ventrals 147–156 (averaging 152) in males, 153–162 (averaging 158.1) in females; usually one preventral anterior to ventrals (about 33% of specimens have two preventrals; rarely, preventrals were absent). Anal plate nearly always single (divided in two of 29 specimens). Subcaudals 112–125 (averaging 118.6) in males, 109–122 (averaging 116.8) in females. Dorsocaudal reduction at subcaudals 40–65 in males (mean 52.6), 34–59 in females (mean 45.3). Preoculars 1, postoculars 2, primary temporals 2, secondary temporals 2, supralabials usually 9 with 4–6 bordering the eye (occasionally 8 with 3–5 bordering the eye or 10 with 5–7 bordering the eye), infralabials usually 9 (low frequency of 10 or 11). Maxillary teeth 38–45 (averaging 41), typically with four posterior teeth abruptly enlarged; sometimes the enlargement appears more gradual and with three or five somewhat enlarged. Smith (1943: 416) illustrated head scalation for EHT-HMS 27496 (now UIMNH 17632).

Two apical pits present on dorsal scales. About 85% of specimens have keels on all dorsal rows of the neck except row 1; the others lack keels on row 2 additionally. Virtually all specimens have all dorsal rows except row 1 keeled at mid- and posterior body; an exception is a small juvenile female (294 mm SVL) in which all rows are keeled at mid- and posterior body (keels very weak on row 1 in both positions). Fusions or divisions of temporal scales were moderately common, with the following frequencies: upper primary divided (10), upper secondary divided (10), upper or lower primary + secondary fused (3), lower primary divided (2), lower secondary fused with ultimate supralabial (1), upper + lower secondary fused (1, partial fusion).

Hemipenis unilobed with a somewhat bulbous apex; spinose region followed distally by flounces, poorly developed calyces, and a highly ornate apex, including free-standing spinulate ridges and an apical boss on the sulcate side. Sulcus spermaticus simple, centrolineal, with a slightly flared tip in everted organs.

Geographic and Other Variation. Tails are proportionally shorter in small individuals. Specimens less than 300 mm SVL have tail lengths 29–34% of total length, 40–51% of SVL (*N* = 8, males and females combined). No strong geographic trends were evident among the characters examined. Johnson et al. "1976" [1977] reported a male from near Ocozocuautla (Chiapas, Mexico) with 157 ventrals and 127 subcaudals, which are slightly greater than counts for specimens I examined (Table 1). The posterior reduction of the dorsal scales always involves lateral rows, but in addition to the rows most commonly involved (2+3), reduction occasionally occurs by fusion of rows 3+4 and rarely by loss of row 3 or fusion of rows 1+2.

Two specimens from Guatemala (UTACV 22155, 22755), both from the same general locality, have divided anal plates and are the only specimens examined having this condition (the only known specimen from nearby in Belize, KU 300784, has a single anal plate). Ordinarily, a divided anal plate in northern specimens of *Dendrophidion* suggests an identity with *D. nuchale* auc-

torum but the color pattern and low subcaudal counts (115–116) of these specimens confirms their identity as *D. vinitor*. Whether this is a peculiarity of this population or whether divided anal plates occur with low frequency in others is unknown (but see comments on historical records in Distribution). No other characteristic of these specimens is particularly unusual, although in UTACV 22755, the last ventral plate is also divided. At least three other species of *Dendrophidion* (*D. dendrophis*, *D. nuchale* auctorum, *D. paucicarinatum*) are variable in the single/divided nature of the anal plate.

Sexual Dimorphism. A few characters showed significant sexual dimorphism (Table 1). Although the largest specimen is a male, mean sizes of adult males (542 mm SVL) and females (535 mm SVL) are not significantly different (with the caveat that sample sizes are small and sample variances high). Females have significantly greater ventral counts than males and the posterior reduction of the dorsal scales occurs farther posteriorly in females (mean ventral 99.0, $N = 24$) than in males (mean ventral 92.8, $N = 18$; $p < 0.001$). In males, the dorsocaudal reduction (8 to 6) occurs at a significantly more posterior position than in females. Males also have a proportionally longer tail than females, but males and females do not differ in subcaudal counts.

Coloration in Life. Color photographs of *D. vinitor* from Veracruz, Mexico, were published by Pérez-Higareda and Smith (1991, pl. 4) and Campbell (1998, fig. 127) and from Belize by Lee (2000, fig. 315; = KU 300784 fide Julian C. Lee, personal communication). Alvarez del Toro (1972, fig. 133; 1982, fig. 143) illustrated a specimen from Chiapas, Mexico, in black and white, and Dugés (1892) provided a somewhat stylized colorized drawing of a specimen from Veracruz.

Smith (1941) gave detailed color notes for the holotype in life (repeated virtually verbatim by Taylor [1954: 729–730]), here paraphrased: Head and temporal region down to upper edges of two postocular labials and all of the last labial brownish gray, the sutures darker and with a slightly reddish tinge (lower edge of head cap dark brown, mixed with dull brownish brick-red); upper parts of anterior supralabials with a reddish tinge; supralabials below the head cap pure white; 59 bands on body, 54 on tail; bands on neck covering one scale length, brownish gray laterally, yellow dorsally and bordered anteriorly, posteriorly, or both by narrow irregular areas of black; size of yellow dorsal area in light bands decreasing and eventually disappearing posteriorly; light bands gradually disappearing posteriorly; tail bands and those on posterior part of body black; black borders of light bands interspersed or themselves bordered by brick-red, this color especially prominent medially; central ground color between bands brownish gray anteriorly, becoming light brown tinged with red on middle and posterior body; tail with a stripe of dark brown (black) interspersed with brick-red, involving edges of subcaudals and lower half of first dorsocaudal row; gular region white; belly yellow; subcaudals yellow, paler posteriorly.

Alvarez del Toro (1972: 144) described a specimen from Chiapas, Mexico: "general coloration reddish brown, a little grayish toward the sides. On the neck are three yellow bands, and an additional 62 yellowish ones on the body; all the bands or bars bordered posteriorly by narrow black bands. The lips and throat are white, the venter yellow orange" (description repeated by Alvarez del Toro [1982: 191] except the neck bands are said to be orange).

Coloration in Preservative. Dorsal ground color of preserved specimens yellowish brown, brown, or gray (smaller specimens usually paler than larger ones). Pale crossbands yellowish brown to gray. In adults, posterior pale crossbands become indistinct, marked only by dark transverse stippling with occasional pale flecks dorsolaterally and indistinct or absent on the flanks (Fig. 3). The number of pale bands/ocelli on the body ranged from 51 to 70 with a mean and median of 60 and a mode of 59
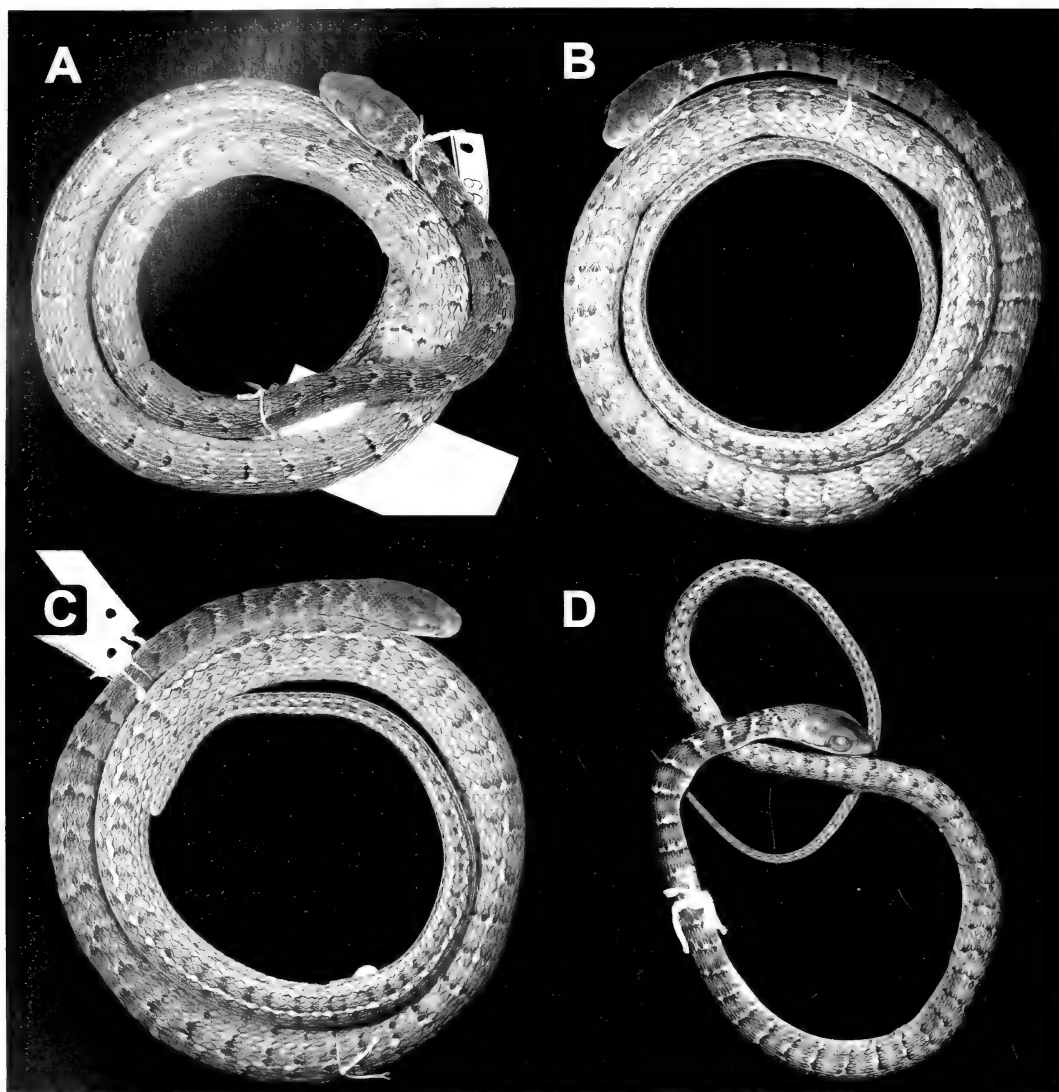
Figure 3.   Representative specimens of *Dendrophidion vinitor* from Mexico. (A) AMNH R-66845 (Oaxaca). (B) UMMZ 122767 (Veracruz). (C) UMMZ 121145 (Veracruz). (D) UCM 39912 (Oaxaca; juvenile, 218 mm SVL).

(posterior indistinct bands included; no significant difference between males and females). In about 85% of the specimens neck bands were one scale row or less in width; in the remainder, the neck bands were 1–1.5 rows wide. Vertebral region usually retains whitish spots that sometimes form a more or less continuous vertebral streak punctuated by larger irregular pale spots (like beads on a string) at the position

of crossbands (Figs. 3B, 3C, 4). The dark ventrolateral tail stripe mentioned by Smith (1941; see Fig. 1) varies from distinct to indistinct. On the posterior body most specimens have a series of small, widely spaced dark spots on scale row 2 or the suture line between rows 2–3 (occasionally forming a more or less broken line). This line is often highlighted by paler scales in rows 3–4 on the posterior body (e.g.,
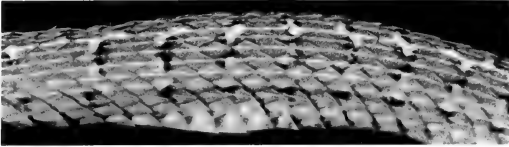
Figure 4.   A typical posterior body pattern of *Dendrophidion vinitor* (AMNH R-66845). Section is from the posterior third of the body. The vertebral row is marked by a whitish line punctuated with larger blotches at the position of pale crossbands which, on the posterior body, are mainly restricted to a dorsolateral position and heavily invested with dark pigment.

Fig. 3B). Venter yellowish to whitish and immaculate except for lateral dark pigment. Most juveniles have more distinct pale crossbands on the posterior body than do adults, and in general, their patterns are more contrasting than those in adults (Fig. 3D).

Distribution (Fig. 5). Central Veracruz state, Mexico, eastward to southeastern Guatemala and southern Belize. *Dendrophidion vinitor* occurs on the Atlantic and Pacific versants of the Isthmus of Tehuantepec but otherwise appears to be restricted to the Atlantic versant. The northernmost record is from Las Minas, Veracruz (Pérez-Higareda and Smith, 1991), assuming I have identified the locality correctly. Recorded elevations for specimens I examined are

lowland (<100 m) to about 800 m on the slopes of Volcán San Martín in southern Veracruz (most localities 400–600 m), with the single Belize specimen from slightly higher, between 940 and 1,035 m (see Appendix 2, Little Quartz Ridge).

Several historical records of *D. vinitor* deserve comment because they document localities from which no recent specimens are available. Dugés (1892; "*Dendrophidium dendrophis*") gave a detailed description and color illustration of a specimen from Motzorongo, Veracruz, which leaves little doubt about its identity as *D. vinitor*. Specimens from Guatemala are scarce, and I am aware of only two specimens obtained since the holotype was collected in 1939 (Appendix 1), despite considerable biological inventory of that country (e.g., Duellman, 1963; Stuart, 1963; Campbell, 1998). There has been controversy about the origin and identity of several specimens obtained in Guatemala during the 19th century (see synonymy under the names *Drymobius dendrophis* and *Dendrophidion dendrophis*).

Duméril et al. (1870–1909: 730–732) reported a specimen obtained by Arthur Morelet from "Peten" and two others ("seen alive," collector not indicated) from "Vera
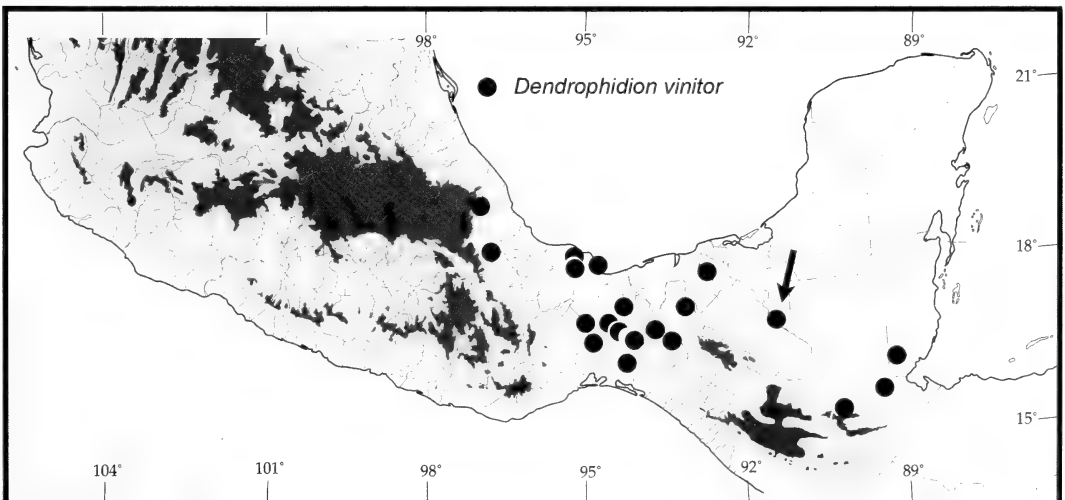
Figure 5.   Distribution of *Dendrophidion vinitor* in southern Mexico, Guatemala, and Belize. A few symbols represent multiple contiguous localities. Arrow indicates the type locality.

Paz"; their composite *"Dendrophidion dendrophis"* also included specimens from northern South America. Some details in their account (e.g., single anal plate and low subcaudal counts [119–127]), suggest *D. vinitor*, although Lieb (1988: 164–165) pointed out some confusion in their subcaudal counts and tail lengths. The "Peten" specimen is one of three syntypes of *H. poitei* Duméril et al. (1854: 208), a name that Lieb (1988: 165) made an objective junior synonym of *D. dendrophis* (Schlegel) by designating MNHN 41 from French Guiana as the lectotype of both names, thus preserving Smith's name *D. vinitor* for the Central American species. Lieb (1988, fig. 1) illustrated the "Peten" syntype of *H. poitei*, whose banding pattern is consistent with *D. vinitor* (pale bands becoming restricted dorsolaterally on the posterior body).

Lieb (1991: 522.1) thought the Petén specimen of Duméril et al. (1870–1909) "almost certainly originated from … Flores [Guatemala], where [Morelet's] collectors were most active." I think it's far from certain that Morelet's specimen came from Flores, although he spent a long sojourn there. Morelet traveled extensively in the Mexican states of Tabasco and northern Chiapas, ascending the Río Usumacinta to near the present Guatemalan border (all within the known range of *D. vinitor*) before traveling overland to Flores (Morelet, 1871). The specimen could have come from anywhere along this route, and I discount the "Flores" locality based on this historical material. Owing to its accessibility and location along a major route, perhaps more biologists have passed through Flores than any other part of Petén. Duellman (1963: 246) listed *D. vinitor* as "hypothetical" in southern Petén but obtained no material during a 2-week survey of rainforests there, nor did Stuart (1934, 1935, 1958) working in the same region. Thus, apart from western Petén along the Río Usumacinta (type locality), the presence of *D. vinitor* in Petén is unsubstantiated.

Günther (1885–1902) reported four specimens from "Vera Paz, between Cobán and Lanquín" (in present-day Alta Verapaz province) and another from "Guatemala" collected by Osbert Salvin. Their identity has been questioned mainly on the basis of scale counts and a divided anal plate reported by Günther. It should be noted that Boulenger (1894: 16, specimens *b–f*) gave ventral and subcaudal counts for the same specimens, in some cases substantially different from Günther's. Based on Boulenger's subcaudal counts, it seems likely that only specimens *b*, *d*, and *f* (subcaudals 113, 116, 119, respectively) are *D. vinitor* because it is the only *Dendrophidion* from that area with such low subcaudal counts (counts of the other two specimens are consistent with *D. nuchale* auctorum, which is known from the region). The only character seeming to disallow the identity of the three Salvin specimens as *D. vinitor* is the divided anal plate reported by Günther (not recorded by Boulenger). However, the only two recently collected Guatemalan specimens of *D. vinitor* are from near Salvin's Alta Verapaz locale and have divided anal plates (see above Description), so this character is no longer an obstacle. Thus, I accept this locality and include it in Figure 5. I am aware of only one published reference based on a re-examination of Salvin's material (Stafford, 2003; see Appendix 1), but Stafford cited only one of the specimens in his study.

I confirmed several erroneous reports of *"Dendrophidion vinitor"* from Belize and the outer Yucatán Peninsula first pointed out by Lieb (1991): Wilson (1966; based on LSUMZ 8901–03; = *D. nuchale* auctorum); McCoy (1970; UCM 25708, 25794, 25805–06, 25846–47, 25874; = *D. nuchale* auctorum); and Lee (1980: 34, 65; UCM 28122; = *Mastigodryas melanolomus*). However, a recently collected specimen documents *D. vinitor* in southern Belize (KU 300784; Fig. 6). KU 300784 is a female, and its identification as *D. vinitor* is based on the narrow pale crossbands on the neck and other features of coloration, 119 subcaudals, and dorsocaudal reduction at subcaudal 47. This specimen is the basis for the record reported as a personal communication by
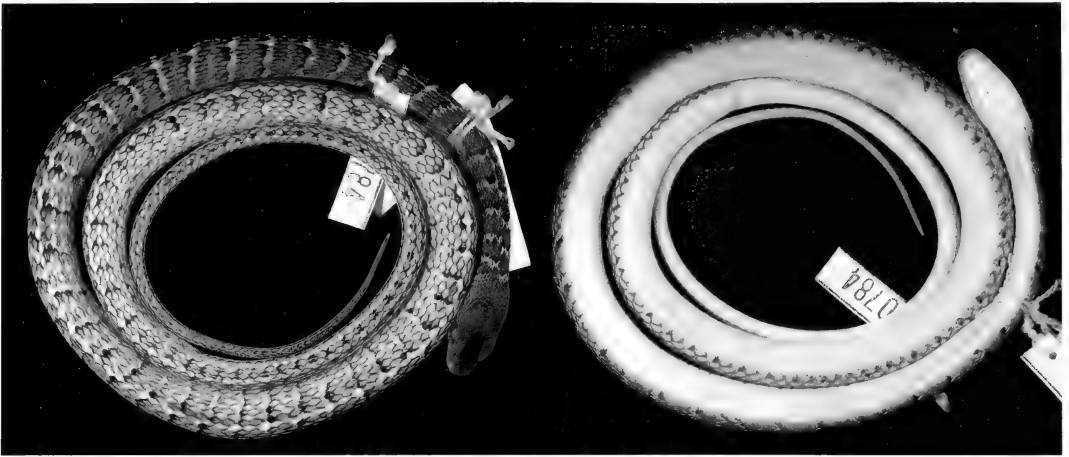
Figure 6.   *Dendrophidion vinitor* (KU 300784), the only known specimen from Belize. A color photograph of this specimen in life is in Lee (2000: fig. 315).

Stafford and Meyer (2000: 200) and for the color photograph in Lee (2000, fig. 315; Julian C. Lee, personal communication, January 2011); see Meerman and Lee (2003).

Natural History. The few specimens of *D. vinitor* accompanied by habitat information suggest that it inhabits relatively intact forests, variously described as "rainforest" or "lower montane rainforest" (e.g., Duellman, 1960: 34, for Donají, Oaxaca; Johnson, 1989: 64, for Chiapas). Goodwin (1969: 259) gave brief habitat notes on Oaxacan localities for specimens collected by Thomas MacDougall, as follows: La Gloria (coffee plantations, milpas, rainforest; elevation about 1,500 ft.); Cerro Azul ("cloud forest," high north-facing slopes swept by gale-force winds, elevation of peaks to about 8,000 ft., collections from 4,000 to 7,000 ft.); Cerro Atravesado (open pine stands, grass and rocks, patches of "cloud forest" at north end, some ranches on lower slopes. Elevation about 4,750 ft.).

Few natural history or behavioral data seem to have been recorded for *D. vinitor*. Darling and Smith (1954: 191) found a juvenile coiled by a trail during the day on Volcán San Martín, Veracruz, Mexico. Two specimens (FMNH 126554–55) are accompanied by notes indicating they were "in heavy shade, in daytime, on ground." Johnson et al. "1976" [1977] reported a male from near Ocozocuautla (Chiapas, Mexico) actively foraging on the forest floor at 3:30 p.m. on 28 December 1974. Alvarez del Toro (1972, 1982) reported *D. vinitor* as "relatively common" in the hills surrounding Presa Malpaso, a large hydroelectric reservoir in the Río Grijalva basin of northern Chiapas, Mexico; he stated that it inhabits the shady parts of the forest and rapidly hides in the leaf litter upon disturbance. At Los Tuxtlas Biological Station Perez-Higareda (1978) encountered *D. vinitor* much more frequently in the dry season and first half of the rainy season (April–October), with a peak encounter rate in October, than in the period of more consistent heavier rains (November–March). Stomach contents of two specimens I examined (576 and 248 mm SVL) each comprised a single small frog (*Pristimantis* or *Craugastor*; 20 and 15 mm SVL, respectively). In contrast to some species of *Dendrophidion*, the frequency of broken/healed tails in *D. vinitor* is relatively low—13.7% of the specimens examined compared with 30% or more in some species (Stafford, 2003; Cadle, 2010); this may indicate a less easily pseudautotomic tail than other species or differential predation intensities.

Stafford (2003) included specimens of *D. vinitor* as redefined herein in a study of morphology, diet, and reproduction of

Dendrophidion spp., but most of his specimens actually are the two new species described in this paper. Among specimens I examined, a gravid female from Veracruz (491 mm SVL; KU 27564) was collected 30 March 1949. UCM 41162 from Oaxaca (567 mm SVL) had vitellogenic ova 3–5 mm in length and was collected 5 May 1967. UTACV 22755 from Guatemala (427 mm SVL), a female (? adult) with thin, nonconvoluted oviducts, was collected 16 October 1987. The two smallest individuals were 199 mm SVL (Veracruz; collected 19 September 1965) and 218 mm SVL (Oaxaca; collected July to September 1968).

Vernacular names for *D. vinitor* given in various regional works include *zumbadora aquillada de barras* (Guatemala), *culebra barrada* (Guatemala and Mexico), *kuyun kan* (Lacandón Maya), and *sabanerita* (Belize) (Alvarez del Toro, 1972; Lee, 1996: 310; Campbell, 1998: 207; Stafford and Meyer, 2000).

Dendrophidion apharocybe **New Species**

Figures 2B, 7–10, 13B, 13D, 14C, 14D, 20, 21

Dendrophidion dendrophis (part). Gaige et al., 1937: 12 (UMMZ 79765–66). Dunn and Bailey, 1939: 15 (two specimens from Pequení–Esperanza ridge = MCZ R-42782–83).
Dendrophidion vinitor. Smith, 1941: 74–75 (part; paratypes from Nicaragua, Costa Rica, Panama). Barbour and Loveridge, 1946: 99–100 (paratypes from Nicaragua, Costa Rica, Panama). Peters, 1952: 43 (paratypes from Nicaragua). Taylor, 1954: 729–730 (part; Costa Rica). Smith, 1958: 223 (Panama). Cochran, 1961: 172 (part; paratypes from Nicaragua). Peters and Orejas-Miranda, 1970: 79 (part). Savage, 1973: 14 (part), 1980: 92 (part). Scott et al., 1983: 372 (part; "La Selva"). Kluge, 1984: 54 (Nicaragua: UMMZ 79766). Wilson and Meyer, 1985: 41 (key). Savage and Villa, 1986: 17, 148, 169 (part). Lieb, 1988: 171 (part). Villa et al., 1988: 63 (part). Pérez-Santos and Moreno, 1989: 4 (part; Colombia listed but no details given). Ibáñez and Solís, "1991" [1993]: 30, 33 (Panama). Lieb, 1991: 522.1–522.2 (part). Perez-Santos et al, 1993: 116. Guyer, 1994: 382 (Costa Rica). Auth, 1994: 16 (part). Ibáñez et al., "1994" [1995]: 26 (Panama). Lee, 1996: 310–311 (part). Campbell, 1998: 207 (part). Stafford, 1998: 16–17. Lee, 2000: 282–283 (part). Stafford and Meyer, 2000 (part; specimen from Costa Rica), pl. 113. Savage, 2002 (part): 655–656, pl. 416. Goldberg, 2003: 298–300 (part). Köhler, 2003: 200, figs. 478 (Panama) and 479 (Costa Rica) (part). Stafford, 2003: 111 (part; specimens from Nicaragua, Costa Rica, Panama). Wilson et al., 2003: 18. Solórzano, 2004: 236–239, fig. 60 (part). Guyer and Donnelly, 2005: 185, pl. 149 (part). McCranie et al., 2006: 147–148 (part). Wilson and Townsend, 2006, tables 1, 3. Köhler, 2008: 215, figs. 580–581 (Panama, Nicaragua) (part). McCranie, 2009: 12. Savage and Bolaños, 2009: 14 (part). Bolaños et al., 2010: 12 (part). McCranie, 2011: 111 (part).

Holotype (Figs. 2B, 7, 14C). LACM 148593, an adult male from Finca La Selva, 40 m elevation, Heredia Province, Costa Rica. Collected 9 December 1974 by C. Dock, Carl Lieb, and Catherine Toft. Formerly CRE (Costa Rica Expeditions) 8598. The holotype is 908 mm total length; 574 mm SVL; 334 mm tail length (complete). It has 152 ventrals and 123 subcaudals. The left hemipenis is nearly fully everted (small portion of apex uneverted); right hemipenis everted to the base of the apex just beyond the flounces. Most of the stratum corneum is missing from the dorsal scales. The middle half of the venter has a long midventral slit exposing the viscera; a shorter irregular slit (about 100 mm long) begins about 35 mm in front of the vent.
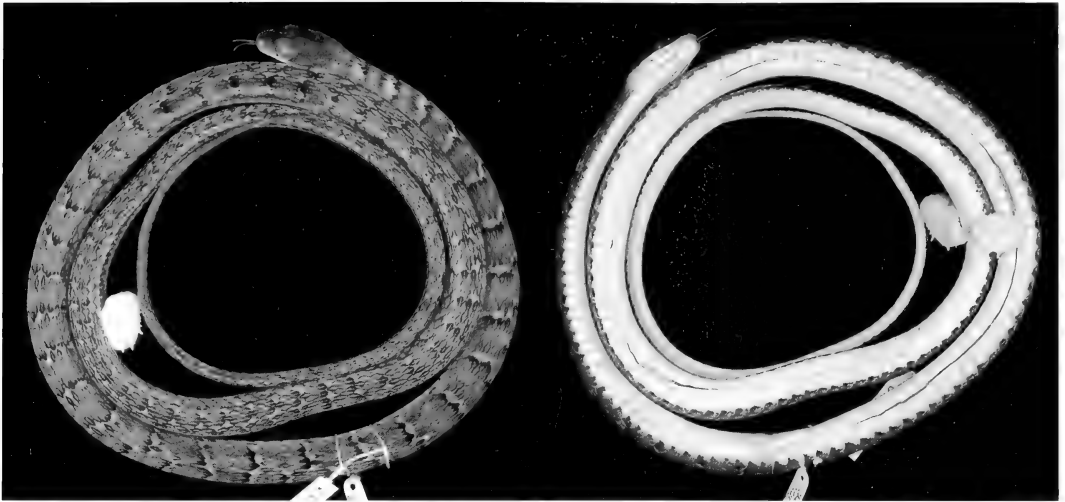
Figure 7.   Holotype of *Dendrophidion apharocybe* (LACM 148593) from La Selva, Costa Rica (Heredia Province).

Paratopotypes. LACM 148591, 148595, 148597–98, 148603–05, 148609–11, 148616, 148619, 148621; CM 53948.

Other Paratypes. **Honduras:** *Gracias a Dios:* Bodega de Río Tapalwás, 190 m, USNM 559615, 561032. Caño Awalwás (camp), 100 m, USNM 559616. Crique Ibantara, 70 m, USNM 559617. Warunta Tingni Kiamp, 150 m, USNM 561920. Hiltara Kiamp, 150 m, USNM 562874. Sachin Tingni, 150 m, USNM 562875. Near Crique Wahatingni, USNM 562876. Near Crique Yulpruan, 140 m, USNM 563303. *Olancho:* Planes de San Esteban, 1,100 m, USNM 565534. **Nicaragua:** Eastern Nicaragua, ANSP 22863–64 (paratypes of *D. vinitor* Smith). [*Atlántico Norte*]: Musawas, Waspuc River, AMNH R-75223. [*Atlántico Sur*]: Cara de Mono, KU 112974. Recreo, Río Mico, UMMZ 79766 (paratype of *D. vinitor* Smith; see Appendix 2 for locality clarification). Río Mico, 10 mi above Recreo, UMMZ 79765 (see Appendix 2 for locality clarification). *Matagalpa:* Hacienda La Cumplida, 19 km N of Matagalpa, 2,500 ft. [762 m], UMMZ 115259. Matagalpa, MCZ R-9561 (paratype of *D. vinitor* Smith), UMMZ 90670 (paratype of *D. vinitor* Smith, formerly MCZ R-17117). **Costa Rica:** *Alajuela:* Poco Sol de La Tigre,

540 m, LACM 148601. *Cartago:* ca. 2.5 km N Pavones, 700 m, LACM 148594. Pavones, near Turrialba, KU 140055. *Guanacaste:* Cacao Biological Station, 729–1,528 m, LACM 148589. Silencio, 10 km SES [? SSE] from La Casa, 875–940 m, LACM 148607. *Heredia:* Río Puerto Viejo near junction with Río Sarapiquí, KU 35639. 10 km WSW Puerto Viejo de Sarapiquí, MVZ 217610. Zona Protectora, La Selva, trail from 1,000-m camp to 1,500-m camp, 990 m, LACM 148600. *Limón:* Pandora, 50 m, LACM 148618. Suretka, MCZ R-19342 (paratype of *D. vinitor* Smith). Near Suretka, Mt. Mirador, KU 35638. **Panama:** *Bocas del Toro:* Almirante, 10 m, KU 80223. 11 km NW Almirante, 600 ft. [183 m], FMNH 153653, 154038–39. South end of Isla Popa, 1 km E of Sumwood Channel, USNM 347352. La Loma, W. Panama, MCZ R-19344 (paratype of *D. vinitor* Smith). Peninsula Valiente, Bluefields, 70 m, KU 107646. Peninsula Valiente, Quebrada Hido, USNM 338624. *Coclé:* Continental divide N El Copé, 600–700 m, AMNH R-115922. *Darién:* North slope of Cerro Malí, 700–1,200 m elev., AMNH R-119377. Laguna, 820 m, KU 75680. [*Panamá*]: Pequshowní–Esperanza ridge, near head of Río Pequshowní, 2,000 ft. [610 m], MCZ

R-42782 (paratype of *D. vinitor* Smith). Pequení–Esperanza ridge, junction main divide, 1,200 ft. [366 m], MCZ R-42783 (paratype of *D. vinitor* Smith). *Panamá:* Cerro Azul region, Río Piedra, AMNH R-119878. Cerro Campana, 3,000 ft. [915 m], UMMZ 155745. S slope of Cerro Campana, 900–950 m, AMNH R-108693. *San Blas:* Border of Darién, summit site, 320 m, 08°55′N, 77°51′W, FMNH 170138. *Veraguas:* Cerro Delgadito, 2–4 mi. W Santa Fe, AMNH R-147806–07. Cerro Arizona above Alto de Piedra, North of Santa Fe, 4,700 ft. [1,433 m], UMMZ 155725.

Other Referred Specimens and Locality Records from Literature (specimens not seen except LACM 148622). **Costa Rica:** *Heredia:* Finca La Selva (type locality), LACM 148622 (fragmentary skin), LACM 163285–87 (skeletons). *Limón:* Guápiles, UCR 6327 (Lieb, 1988). 7 km NW Penshurst, San Clemente, UCR 7545 (Lieb, 1988). **Honduras:** *Gracias a Dios:* Las Marías (McCranie, 2011: 114). **Nicaragua:** No specific locality, USNM 14215 (paratype of *D. vinitor* Smith) (another paratype of *D. vinitor* from an unspecified locality in Nicaragua, USNM 14220, was reidentified as "*D. nuchale*" by Stafford [2002, 2003], but that identity seems not to have been independently verified). [*Chontales*]: Santo Domingo, Chontales Mines, 2,000 ft. [610 m], BMNH 94.10.1.19–20 (Stafford, 2003). [*Río San Juan*]: Río San Juan (Köhler, 2008, fig. 581). **Panama:** *Bocas del Toro:* South end of Isla Popa, 1 km E Sumwood Channel, USNM 319234 (skin + skeleton). Savage (2002: 656) plotted additional Costa Rican localities for *D. apharocybe* based on specimens that I did not see (mainly at UCR), but see comments under Distribution on two erroneous lowland Pacific localities indicated by Savage.

Etymology. The species name is a feminine noun in apposition derived from the Greek words *aphares* (ἀφαρής), meaning naked or unclad, and *kybe* (κύβη), meaning head. The "naked head" refers to the distinctive unadorned apex of the hemipenis of *D. apharocybe* compared with its sibling species.

Diagnosis. Dendrophidion apharocybe is characterized by (1) dorsocaudal reduction from 8 to 6 occurring posterior to subcaudal 25 (range, 26–63); (2) single anal plate; (3) relatively low subcaudal counts (<130 in males and females); (4) black-edged pale crossbands on the neck nearly always more than one scale row wide; (5) immaculate ventrals and subcaudals except for lateral dark pigment; (6) a relatively short hemipenis with a bulbous apex strongly inclined toward the sulcate side (asulcate edge of apex higher than sulcate edge) and largely devoid of ornamentation (apex nude). The combination of few subcaudals and a single anal plate will distinguish *D. apharocybe* from all other species of *Dendrophidion* except *D. vinitor*, *D. crybelum*, and *D. paucicarinatum*.

Dendrophidion apharocybe differs from species of the *D. percarinatum* group (*D. bivittatum*, *D. brunneum*, *D. paucicarinatum*, *D. percarinatum*) in having the dorsocaudal reduction from 8 to 6 usually posterior to subcaudal 30 (26–30 in some specimens from Costa Rica and Panama; see Sexual Dimorphism and Geographic Trends). A single anal plate will distinguish *D. apharocybe* from all of these except some individuals of *D. paucicarinatum* (anal plate variable in this species). *Dendrophidion paucicarinatum* usually has a more uniformly colored dorsum lacking distinct crossbands, has narrow dark lines across the venter in adults and many juveniles, has a higher number of ventrals (>175 compared with <170 in *D. apharocybe*), and has more weakly keeled dorsal scales. *Dendrophidion apharocybe* differs from *D. boshelli* in having 17 midbody scale rows (15 in *D. boshelli*). *Dendrophidion apharocybe* has fewer subcaudals (<130) and usually a shorter adult relative tail length (<60% of SVL) than *D. nuchale* auctorum and *D. dendrophis* (>130 and usually >60% of SVL, respectively); the anal plate may be either single or divided in these last two species, and their venters are often heavily marked with dark pigment (immaculate in *D. apharocybe*).

Dendrophidion apharocybe previously has been confused with another new species, *D. crybelum*, and with *D. vinitor* as redefined herein. *Dendrophidion apharocybe* differs from *D. crybelum* (characters in parentheses) in the following hemipenial characters: hemipenis rather short and with a bulbous apex comprising well over one-third the length of the organ (longer and cylindrical, without a distinctly expanded apex that comprises one-fourth or less the length of the hemipenis); apex strongly inclined toward the sulcate side and nude (not inclined and ornamented with many free-standing membranous ridges having embedded spinules); hemipenis with relatively few moderately enlarged spines, total enlarged spines <45 (many greatly enlarged spines, total enlarged spines >70). *Dendrophidion apharocybe* and *D. crybelum* are very similar in color patterns, but *D. apharocybe* has immaculate ventrals and subcaudals, whereas adult *D. crybelum* have small dark spots on the posterior ventrals and the subcaudals (juveniles sometimes have only dark suffusion on the subcaudals); see species account for *D. crybelum* for details. *Dendrophidion apharocybe* averages more pale body bands (Table 1) than *D. crybelum* ($p < 0.001$) and fewer than *D. vinitor* ($p < 0.001$), but the ranges overlap greatly in each case.

Hemipenes of *D. apharocybe* and *D. vinitor* are similar in overall shape, but the apex of the former is nude and strongly inclined toward the sulcate side, and it lacks an apical boss. The hemipenis of *D. vinitor* has a highly ornate apex, including an apical boss, and it is not strongly inclined (see detailed hemipenial descriptions). Additionally, these two species differ in aspects of color pattern (see species account for *D. vinitor*).

Description (31 males, 34 females). Table 1 summarizes size, body proportions, and meristic data for *D. apharocybe*; McCranie (2011) summarized data for 10 Honduran specimens, most of which are also included in this summary. Largest specimen (KU 35638) a female 1,045 mm

total length, 672 mm SVL. Largest male (KU 80223) 1,040 mm total length, 653 mm SVL (another male, LACM 148601, was also 653 mm SVL but had an incomplete tail). Tail 35–38% of total length (53–61% of SVL) in males; 33–36% of total length (49–57% of SVL) in females. Dorsal scales in 17–17–15 scale rows, the posterior reduction by fusion of rows 2+3 (40%) or 3+4 (54%) or loss or row 3 (6%) at the level of ventrals 85–105 (see Sexual Dimorphism below). Ventrals 149–160 (averaging 153.9) in males, 152–168 (averaging 160.8) in females; 1 or 2 preventrals anterior to ventrals (preventrals rarely absent). Anal plate single. Subcaudals 115–127 (averaging 121.1) in males, 111–129 (averaging 119.9) in females. Dorsocaudal reduction at subcaudals 32–63 in males (mean 47.8), 26–52 in females (mean 41.5). Preoculars 1, postoculars nearly always 2 (rarely 3), primary temporals usually 2 (rarely 1), secondary temporals usually 2 (rarely 1), supralabials usually 9 with 4–6 bordering the eye (range 8–10 with other combinations bordering the eye; Table 1), infralabials usually 9 (range 7–10). Maxillary teeth 33–44 (averaging 39), typically with four posterior teeth abruptly enlarged; sometimes the enlargement appeared more gradual and with three or five somewhat enlarged (Fig. 8).

Two apical pits present on dorsal scales. Nearly 60% of specimens have all dorsal rows except row 1 keeled on the neck (in about half of those, keels on row 2 were scored as weak); another 34% of specimens lacked keels on rows 1 and 2 on the neck (in one-quarter of those keels were weak on row 3); the remaining specimens lacked keels on rows 1–3 on the neck (these proportions differ from *D. crybelum*; see species account). In all except five specimens, keels were present on all dorsal rows except row 1 at mid- and posterior body; in the five exceptions (four from Panama, one from Costa Rica) keels were present additionally on scale row 1 posteriorly (sometimes weak). Fusions or divisions of temporal scales were common, with the following
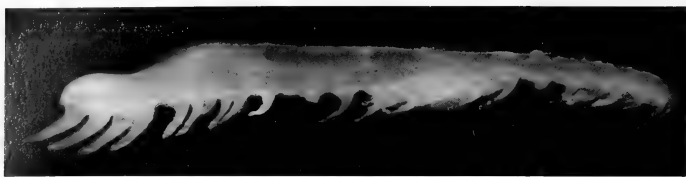
Figure 8.   Maxillary dentition of *Dendrophidion apharocybe*. Right maxilla of LACM 148597 showing four enlarged posterior teeth (anterior to the right). The gap anterior to the enlarged posterior teeth is an empty tooth position, not a diastema.

frequencies: upper primary divided (5), upper secondary divided (5), upper primary + secondary fused (5), lower primary divided (2), lower secondary fused with the last supralabial (4), upper + lower secondary fused (2), upper + lower primary fused (2), lower secondary divided (1). On eight sides, a dorsal projection of the lower primary temporal extended between the upper primary and secondary temporals, separating them and contacting the parietal scale. In one specimen supralabials 6–8 were fused on one side. In LACM 148616 subcaudals 3–16 are entire or only partially divided.

Hemipenis unilobed with a bulbous apex. Sulcus spermaticus simple, centrolineal, with a distinctly flared tip. Central part of hemipenis ornamented with spines, distal to which is a series of flounces (about four on the sulcate side to about seven on the asulcate side). The broad apex is strongly inclined toward the sulcate side and entirely nude except for some low rounded ridges (noticeable only with magnification).

Geographic Variation, Ontogenetic Variation, and Sexual Dimorphism. No strong geographic trends were evident except in the point of dorsocaudal reduction, which is more distal in northern compared with southern specimens. The mean subcaudal number at the point of reduction for Honduran–Nicaraguan specimens is 45.4 and 50.8 (females and males, respectively). In Panamanian specimens these means are 35.6 and 43.8 (the means for all non-Panamanian specimens combined are 43.5 and 49.3 for females and males, respectively). Dorsocaudal reductions anterior to subcaudal 30 occurred only in females from Panama and Costa Rica (uni- or bilateral

reductions at subcaudals 26–29 in five specimens). Relative tail length increases with body size in subadults. Specimens <300 mm SVL have tail lengths 30–35% of total length, 44–53% of SVL (N = 15, males and females combined); see Table 1 for adult proportions.

Patterns of sexual dimorphism in *D. apharocybe* are similar to those in *D. vinitor* (Table 1). Mean sizes of adult males (571 mm SVL) and females (575 mm SVL) are not significantly different (N = 19 males, 23 females). Females have a significantly greater ventral count than males and the posterior reduction of the dorsal scales occurs farther posteriorly in females (mean ventral 99.3) than in males (mean ventral 94.6; $p < 0.001$). The dorsocaudal reduction occurs at a significantly more posterior position in males than in females. Males have a proportionally longer tail than females but the sexes do not differ in subcaudal counts.

Coloration in Life. Color photographs of *D. apharocybe* from the type locality are published in Savage (2002, pl. 416), Solórzano (2004, fig. 60), and Guyer and Donnelly (2005, pl. 149); from other Costa Rican localities in Stafford and Meyer (2000, pl. 113) and Köhler (2003, fig. 479); from Honduras in Wilson et al. (2003, fig. 4; same photograph but with distinctly red/orange tones in McCranie et al. [2006, pl. 120]) and McCranie (2011, pl. 6D); from Nicaragua in Köhler (2008, fig. 581); and from Panama in Köhler (2003, fig. 478; 2008, fig. 580). A black and white photograph of the head/neck (La Selva, Costa Rica) is in Lieb (1991).

Salient characteristics of adult coloration in life, as described by Stafford (1998),
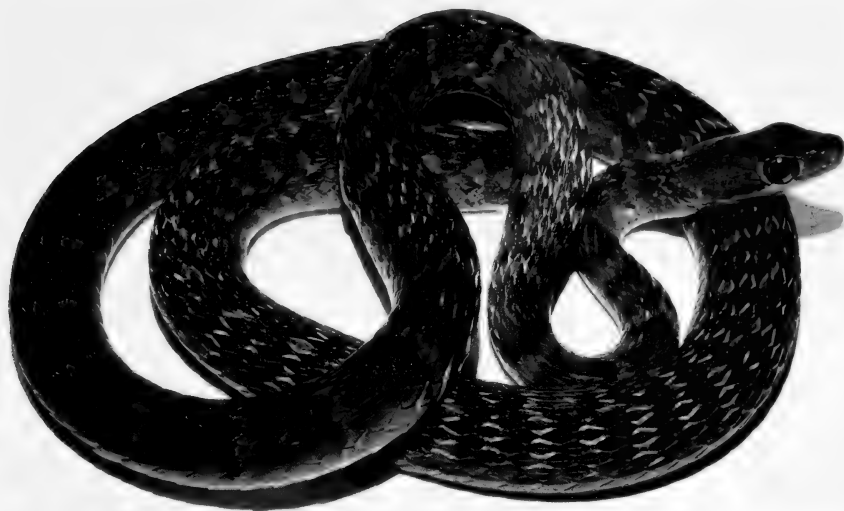
Figure 9.   *Dendrophidion apharocybe* in life. AMNH R-115922 from continental divide N of El Copé, Panama (Coclé Province). Adult female, 666 mm SVL. From color slide by Charles W. Myers. A reverse image of the same photo was published in Köhler (2003: fig. 478, 2008: fig. 580).

Savage (2002: 656), Guyer and Donnelly (2005: 185), McCranie et al. (2006: 148), McCranie (2011: 112), and Charles W. Myers (field notes for KU 107646; AMNH R-108693, R-115922, R-119377) include a gray to brown dorsum with a series of dark-edged pale grayish to pale brown crossbands (ground color or crossbands often with reddish or orange tones, especially on head, anterior and midbody). Posteriorly, pale bands tend to become invested with dark pigment, forming transverse series of pale ocelli set within darker pigment. Posterior ocelli are not mentioned in all color descriptions, but they are visible in virtually every published photo from throughout the range. Often a pale vertebral line posteriorly. Usually a narrow lateral dark line on dorsal rows 2 and/or 3 on the posterior body (sometimes indistinct) and a similar dark line at the subcaudal/dorsocaudal border. Skin between the anterior dorsal scales pale blue or bluish white. Top of head brown, sometimes invested with reddish or greenish tones. Supralabials and throat pale to bright yellow. Venter in adults whitish to yellow, often with an orangish or greenish wash. Juveniles similar to adults but reddish or orange tones in dorsal ground color reduced or absent; venter usually whitish, greenish white, or orange/yellow.

Guyer and Donnelly (2005: 185) described specimens from the type locality as follows: Dorsum gray brown anteriorly, shading to brown posteriorly. Crossbands pale grayish tan bordered by dark. Anterior-most interspace between pale bands rusty red, the rest gray brown. Skin between the anterior dorsal scales pale blue, creating a bluish tint to the light bands or, when the lung is expanded, a blue band. Posterior body middorsal tan stripe interrupted by thin, dark bands that shade to gray laterally. Venter immaculate white to light yellow. Head gray brown. Supralabials brownish anteriorly, white to pale yellow posteriorly.

Figure 9 illustrates an adult female *D. apharocybe* from Panama, whose coloration in life was described thus (Charles W. Myers, field notes): Head brown, turning gray-brown on neck and then greenish brown over rest of body. Pale crossbands gray anteriorly, pale orange at midbody, pale brown posteriorly. Skin within cross-
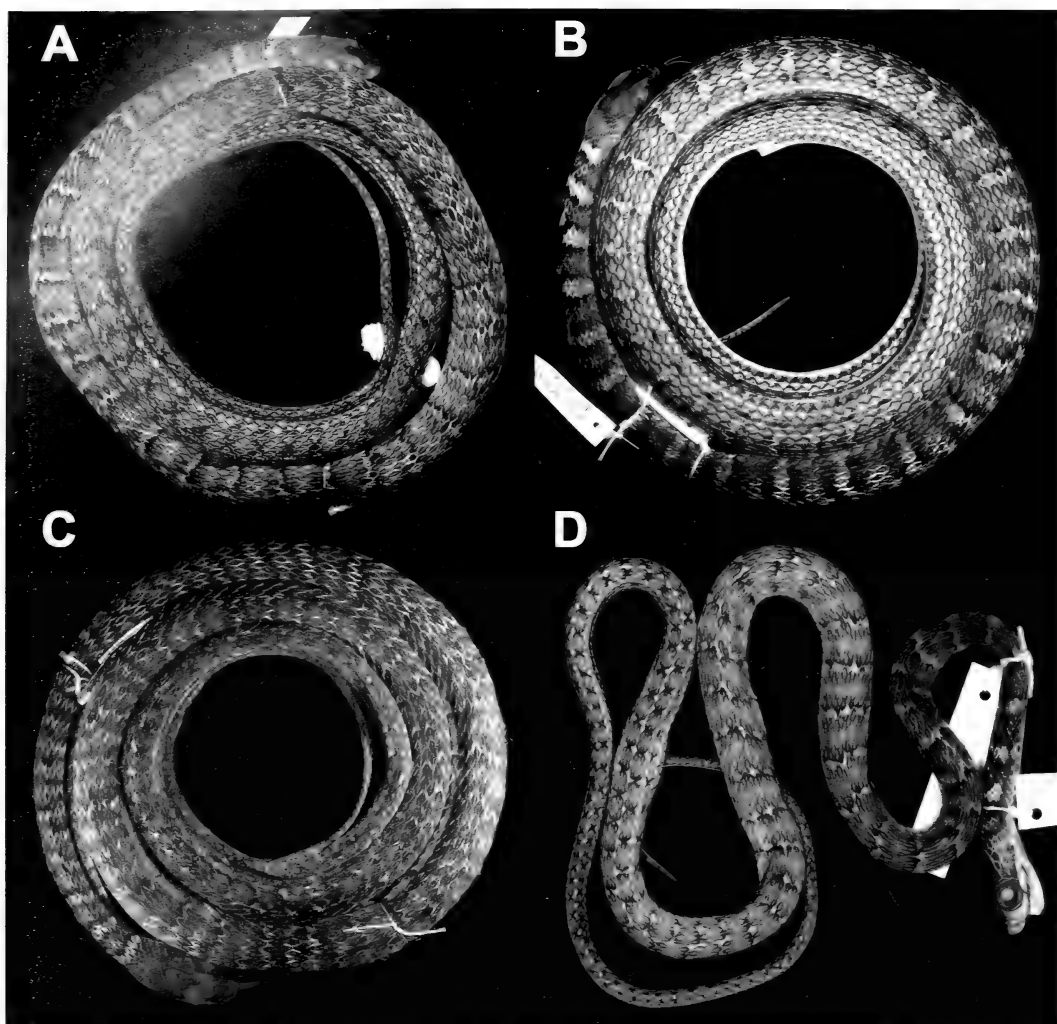
Figure 10. Representative specimens of *Dendrophidion apharocybe*. (A) USNM 562874 (Honduras). (B) KU 112974 (Nicaragua). (C) UMMZ 115259 (Nicaragua; primary banding pattern obscured by formation of secondary bands). (D) FMNH 153653 (Panama; juvenile, 275 mm SVL).

bands bright yellow except on anterior one-third of body, where it is orange for a short distance just behind the head and bluish white thereafter. Labials, underside of head, and neck golden yellow, turning golden orange over rest of venter. Upper one-fourth of iris tan, lower three-quarters gray brown with a few darker brown spots. Tongue, including fork, black.

Coloration in Preservative. Dorsum gray to brown with pale gray or brown cross-bands (sometimes offset), broader on the neck than more posteriorly (specimens with intact stratum corneum tend to be brown, those without, gray) (Fig. 10). Each cross-band bordered posteriorly by narrow irregular blackish border; a less distinct border on anterior edge. The number of pale bands/ocelli on the body ranged from 46 to 69 with a mean and median of 54 and a mode of 53. Neck bands in about 80% of the specimens were 1 to 1.5 scale rows in width;

in another 18% the bands were up to 2.5 rows wide; in one specimen, the neck bands were three rows wide and in another they were less than one row wide. In some preserved specimens (e.g., Fig. 10C) the pale dorsal bands are indistinct posteriorly, seemingly because of secondary lightening of the interspaces between the pale bands.

Crossbands extend down to lateral edges of ventrals and merge with dark pigment on the lateral edges of the ventral scales. Posterior crossbands become invested with dark pigment so that each crossband is broken into a transverse series of vertebral and lateral pale spots (ocelli) separated by dark pigment (lateral ocelli on dorsal rows 3–5 and comprising adjacent parts of three or four scales). Narrow broken blackish lateral stripe on suture line between dorsal rows 2–3 on posterior third or more of body; distinctness and extent of interruption of this stripe varies. Ventrolateral blackish tail stripe on suture between subcaudals and dorsocaudal row 1. The dark posterolateral and tail stripes are indistinct in some specimens.

Top of head uniform brown or gray down to upper edges of supralabials. Ill-defined postocular stripe extending across top edge of penultimate supralabial. Rest of supralabials and gular region immaculate whitish. Venter immaculate except for fairly pale brown/gray speckling (often containing some larger dark spots) on extreme lateral edges. Subcaudals immaculate; no investing dark pigment or spots on subcaudals or posterior ventrals (compare *D. crybelum*). One specimen from Costa Rica (KU 35638) has an unusual ventral pattern: in addition to lateral dark blotches, the anterior third of the body has short dark lateral lines across the anterior edges of the ventral plates. These lines are never complete (as in some other *Dendrophidion*, e.g., *D. paucicarinatum*), the extensions occupying only the lateral portions of the plates.

Juveniles are similar to adults but color tones are lighter. Anterior ground color medium to pale brown (unlike juvenile *D. crybelum*). Ocelli on the posterior body are poorly defined because the investment of pale bands with dark pigment is much less in small juveniles than in adults.

Distribution (Fig. 11). Atlantic versant of Central America from extreme eastern Honduras to eastern Panama at the Colombia border; upland Pacific drainages in northwestern Costa Rica (Cordillera de Tilarán and Cordillera de Guanacaste) and in Panama. The elevational range derived from data associated with specimens is 10 to 1,433 m (most records <200 m). Records from the Pacific lowlands of Costa Rica (Savage, 2002: 656; Laurencio and Malone, 2009) are erroneous, as discussed below. The distributions of *D. vinitor* and *D. apharocybe* are separated by about 400 km at their closest localities in Guatemala/Belize and Honduras, respectively (Fig. 11).

Savage (2002: 656, map 11.79) indicated two lowland localities of "*Dendrophidion vinitor*" on the Pacific side of Costa Rica (denoted by "×" in Fig. 17). I conclude that both are based on mistaken identities (I am indebted to Jay M. Savage for pointing me toward the source of the records and to Gerardo Cháves for information and photographs of UCR specimens). The first, due east of the tip of the Nicoya Peninsula (Savage, 2002: 656, map 11.79), is based on UCR 14406 and 14620, which were obtained during a survey of Carara National Park (Laurencio and Malone, 2009; David Laurencio, personal communication, March 2011). These specimens were initially identified as "*D. vinitor*," but both have divided anal plates and pattern characters of *D. percarinatum* rather than "*D. vinitor*" (characters confirmed from photos provided by Gerardo Cháves, who also examined the specimens at my request, May 2011). The second erroneous record is from the Pacific lowlands due north of the Osa Peninsula (Savage, 2002: 656, map 11.79), purportedly based on UCR 7235 cited by Lieb (1988) from Cajón (north bank of the Río Térraba, about 80 m, Puntarenas Province). However, that UCR number is seemingly in error, and the UCR collection currently has no specimens of "*D. vinitor*" from Puntarenas
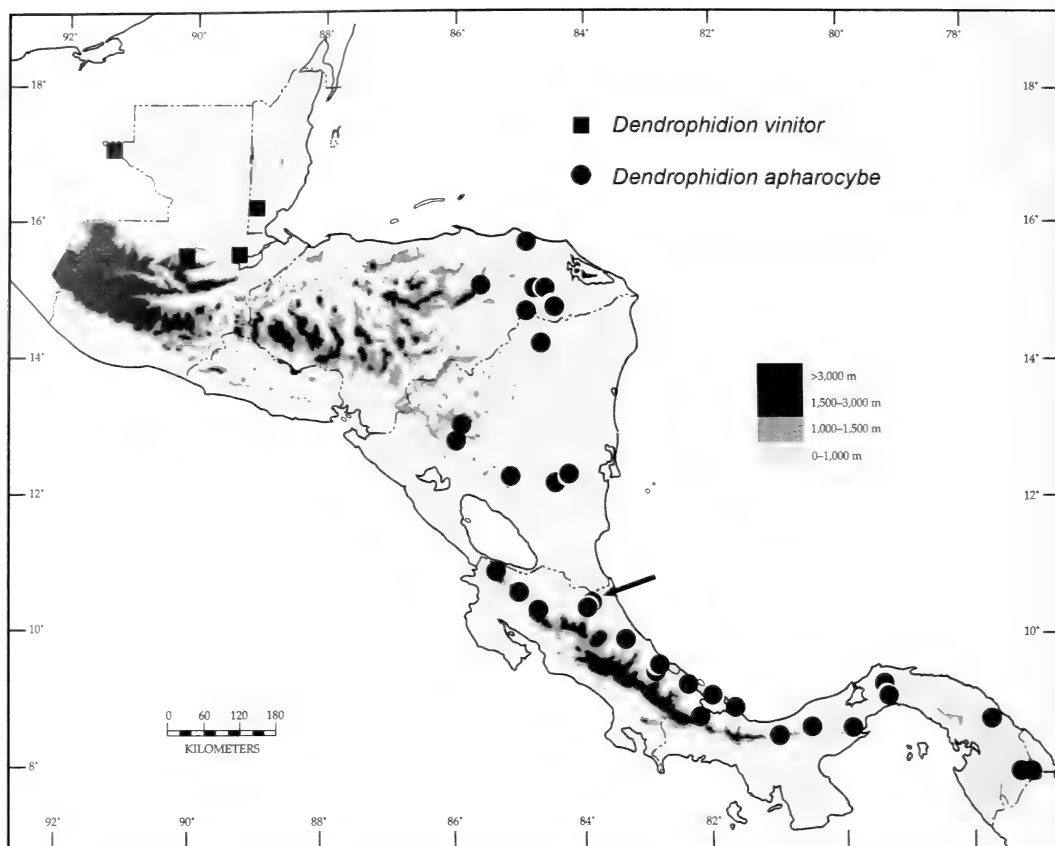
Figure 11.   Distribution of *Dendrophidion apharocybe*, with adjacent localities for *D. vinitor* in Guatemala and Belize shown (see Fig. 5 for complete distribution of *D. vinitor*). A few symbols represent multiple contiguous localities. A detail of the distribution of *D. apharocybe* in Costa Rica is shown in Figure 17 for comparison with that of *D. crybelum*. Arrow indicates the type locality of *D. apharocybe*.

Province other than the above-cited mis-identified specimens from Carara National Park. Another specimen from a locality near Cajón, LACM 148592, was previously identified as *D. vinitor* in the LACM catalogs, but I identify this specimen as *D. percarinatum* (again based on a divided anal plate, pattern characters, and a more proximal dorsocaudal reduction). Thus, there are no confirmed records of "*D. vinitor*" from the Pacific lowlands of Costa Rica.

Dendrophidion apharocybe undoubtedly occurs in northwestern Colombia (Chocoan region) given the proximity of definite Panamanian localities (Fig. 11). However, I have been unable to document a definitive Colombian record, although several authors have listed the species for Colombia (as "*D. vinitor*"). Pérez-Santos and Moreno (1989) included it in "addenda and corrigenda" to Pérez-Santos and Moreno (1988) but listed its distribution in Colombia as "desconocida." Lieb (1988) included Colombia as part of the distribution but listed no Colombian material; he later (Lieb, 1991) plotted a locality well into western Colombia on a distribution map for "*D. vinitor*" but queries to identify the source of the record went unanswered. Stafford (2003: 111) identified LACM 45443 (from Chocó, Colombia) as "*D. vinitor*," but this specimen is a member of the *D. percarinatum*

group (personal observation). Several other works have cited Colombia as part of the distribution apparently based on these sources. Likewise, Lieb (1991) indicated a locality on the tip of the Azuero Peninsula (Cerro Hoya area) on the Pacific side of western Panama, which is far from any locality from which I have seen specimens (Fig. 11). According to Jay M. Savage (personal communication, March 2011), this locality is based on a misidentified specimen.

Natural History. Dendrophidion apharocybe is a diurnal snake found in humid forests (lowland to montane rainforests, cloud forests) and is the best known species of the *D. vinitor* complex owing to incidental or focused attention by students of the Costa Rican herpetofauna. Most natural history data for *D. apharocybe* come from the relatively well-studied La Selva Biological Station, the type locality, operated by the Organization for Tropical Studies (all literature references to "*D. vinitor*"); the La Selva ecosystem is described in McDade et al. (1994) and Holdridge et al. (1971, under the name "Sarapiquí"). Guyer (1994: 382) and Guyer and Donnelly (2005) reported *D. apharocybe* as common and semiarboreal, and Guyer and Donnelly (1990) summarized data on size, mass, and body proportions for this population. Guyer and Donnelly (2005: 185) further observed that *D. apharocybe* is "typically observed crossing trails in primary and secondary forest. It is wary … usually races away when approached … [and is] an adept climber… found at night coiled in understory shrubs and trees. At La Selva this snake consumes … [*Craugastor*] *bransfordii* and … [*Dendropsophus*] *ebraccata*."

In the Cordillera de Guanacaste, Costa Rica (750–850 m elevation), Stafford (1998) found two juveniles (about 250 mm total length) active at 10:00 a.m. and "late morning" on sunny June days after rain. Stafford reported that *D. apharocybe* is wary and swift and, when alarmed, raises the head and forebody high off the ground (as shown by photographs in Stafford and Meyer [2000, pl. 113] and Köhler [2003, fig. 479]).

Goldberg (2003) reported reproductive data for "*Dendrophidion vinitor*" in Costa Rica based on a mix of specimens of *D. apharocybe* and *D. crybelum*. Because he reported data for individual specimens, it is possible to extract data for *D. apharocybe*, all of which are from the type locality. A gravid female (LACM 148598, 567 mm SVL) collected 11 December 1974 had a clutch size of five estimated from yolked ovarian follicles >12 mm length. A female (LACM 148609, 657 mm SVL) collected in June 1983, although "not undergoing yolk deposition" (Goldberg, 2003), has swollen convoluted oviducts (personal observation), suggesting that it had perhaps recently laid a clutch. Males undergoing spermiogenesis were collected in April, May, November, and December ($N = 4$); the smallest actively spermiogenic male, collected in May, was 420 mm SVL but a smaller individual (402 mm SVL) also showed some evidence of spermatid transformation. Goldberg (2003) inferred that sperm production may proceed year-round. Stafford (2003) included specimens of *D. apharocybe* in an ecological study of *Dendrophidion* spp. but presented summary data only, making it impossible to disentangle data specific to *D. apharocybe* from the other two species of this complex. Other natural history data for *D. apharocybe* and *D. crybelum* combined were summarized by Savage (2002) and Solórzano (2004).

I made incidental observations of reproductive condition in several other specimens (eggs not counted unless previous incisions in a given specimen permitted thorough study): a female with enlarged (20 mm) oviductal eggs collected 21 June 1967 (KU 140055, Costa Rica; 612 mm SVL); a female with three large shelled oviductal eggs collected 23 February–6 March 1967 (FMNH 170138, Panama; 583 mm SVL); a female with five large nonoviductal eggs about 25 mm long collected in June 1963 (KU 75680, Panama; 534 mm SVL). The smallest individual of *D. apharocybe* (from

Panama) was 172 mm SVL and collected 4 April 1980; two others from Panama were 200 mm SVL (collected 23 January 1953 and 24 January 1975), and one individual was 204 mm SVL (collected 4 April 1980). The smallest specimens from La Selva, Costa Rica, 209–219 mm SVL, were collected between 30 June and 26 August. The smallest specimen from the northern part of the range (Honduras) was 228 mm SVL, collected in February 2006.

Reports from other parts of the range give portraits of *D. apharocybe* similar to Costa Rican populations. In Honduras this species is infrequently encountered from 30 to 1,100 m elevation in Lowland Moist and Premontane Wet forests (Wilson et al., 2003: 18; McCranie et al., 2006: 148; Wilson and Townsend, 2006. tables 1, 3; McCranie, 2011: 113). Honduran habitats are discussed and illustrated by McCranie (2011: 22–25, pl. IA–B). Two specimens were active about midday and late afternoon on forest floor; two others were sleeping at night on understory vegetation in forest. Two specimens inflated the anterior body when disturbed, exposing the pale blue skin between the dorsal scales (McCranie, 2011: 113).

Ibáñez et al. ("1994" [1995]: 26) reported *Dendrophidion apharocybe* as "infrequent, unpredictable" in eastern Panama, and it has not been recorded for the well-known herpetofauna of Barro Colorado Island, Panama (Rand and Myers, 1990). A juvenile from Cerro Campana (AMNH R-108693, 203 mm SVL) regurgitated the remains of an adult *Eleutherodactylus* [now *Diasporus*] *diastema* (Charles W. Myers, field notes). Myers (1969: 24–25; see also Anthony [1916: 358–363]) described the environment at Cerro Malí (Darién Province, Panama), from which he obtained a specimen of *D. apharocybe* (AMNH R-119377): "Cerro Malí is high (about 1,410 meters [AMNH R-119377 from 700 to 1,200 m]) and wet, but is affected by the dry season and much of its forest is possibly no more than transition to cloud forest. … the forest contains many small trees, including palms,

reaching heights of ± 12 meters. Larger trees up to ± 30 meters are scattered through the forest. There is an understory of bushes and ferns. Most of the trees have a thin covering of moss on the trunks. There is a thick mulch layer on the ground and many rotting logs. Many bromeliads and a few orchids present; few tree ferns."

Like the other species of the *D. vinitor* complex (see species accounts), snakes with broken/healed tails in *D. apharocybe* were of low frequency (13.3%) compared with some other species of *Dendrophidion* (>30%, e.g., Stafford, 2003; Cadle, 2010). *Dendrophidion apharocybe* is sympatric with at least two other species of *Dendrophidion* in some parts of its range. The distributions of *D. apharocybe* and *D. percarinatum* broadly overlap from Honduras through Panama, and both species occur at some localities (e.g., near Recreo, Nicaragua, and La Selva, Costa Rica). *Dendrophidion apharocybe* is also broadly sympatric with *D. nuchale* auctorum in Costa Rica and Panama, and both species have been collected together at some localities (e.g., Laguna, Darién, Panama, and La Selva, Costa Rica, where both occur with *D. percarinatum*). *Dendrophidion nuchale* auctorum has not been formally reported from La Selva (Guyer, 1994; Guyer and Donnelly, 2005), but I identify as this species a color photograph in Guyer and Donnelly (2005, pl. 148, "Brown Forest Racer" = *D. percarinatum* according to the authors); the specimen was photographed and released at La Selva (Craig Guyer, personal communication, December 2010). Solórzano (2004) used the vernacular name *corredora quillada* for *D. apharocybe* in Costa Rica.

Because its diet comprises small terrestrial frogs almost exclusively (e.g., Stafford, 2003), populations of *D. apharocybe* in Costa Rica and Panama are undoubtedly affected to some extent by well-documented declines in amphibian populations in lower Central America. For example, populations of prey species of frogs at La Selva, the type locality, collectively have declined by about
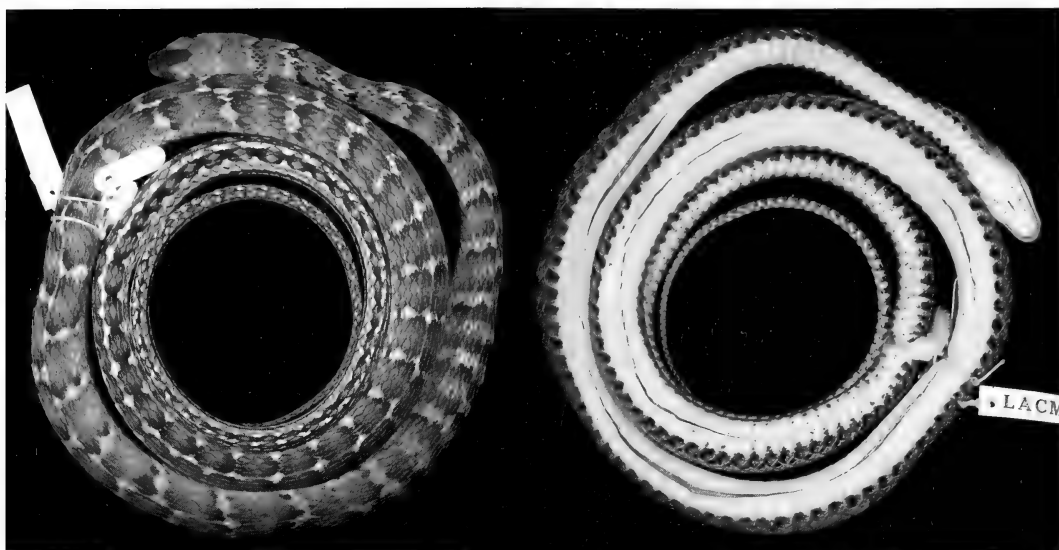
Figure 12.   Holotype of *Dendrophidion crybelum* (LACM 148599) from Finca Las Cruces, Costa Rica (Puntarenas Province).

75% since 1970, probably due to climate-driven changes in the amount of surface leaf litter (Whitfield et al., 2007). Several localities in western Panama from which *D. apharocybe* is documented (e.g., El Copé and Santa Fe) have experienced precipitous declines in amphibian populations due to disease. Lips et al. (2006) documented >90% decline in abundance and >60% decline in amphibian species richness at El Copé. All of these declines involved species of *Pristimantis*, *Craugastor*, and *Diasporus*, which are the predominant prey for *Dendrophidion* (Stafford, 2003). These prey declines and associated climate changes have unknown effects on snake predators such as *D. apharocybe*, but they deserve study.

Dendrophidion crybelum **New Species**

Figures 2C, 12, 13A, 13C, 14A, 14B, 15, 16, 22, 23

? *Drymobius dendrophis*, part. Boulenger, 1894: 15–16 (? specimen *g* from "Chiriqui"). See comments under Distribution.

Dendrophidion vinitor, part (southwestern Costa Rica mentioned explicitly or implicitly as part of the distribution, or listing of specimens in the type series). Savage, 1973: 14. Savage, 1980: 92. Scott et al., 1983: 372 ("Las Cruces"). Savage and Villa, 1986: 17, 148, 169. Lieb, 1988: 171. Villa et al., 1988: 63. Lieb, 1991: 522.1–522.2. Auth, 1994: 16. Lee, 1996, fig. 164 (illustration of head scales of CRE 5099; = LACM 148612). Savage, 2002: 655–656. Goldberg, 2003: 298–300. Stafford, 2003: 111. Solórzano, 2004: 236–239. Guyer and Donnelly, 2005: 185. McCranie et al., 2006: 147–148. Köhler, 2008: 215. Savage and Bolaños, 2009: 14. McCranie, 2011: 111 (part).

Holotype (Figs. 2C, 12, 14B). LACM 148599, an adult male from Finca Las Cruces, near San Vito de Java, 4 km S San Vito, 1,200 m elevation, Puntarenas Province, Costa Rica. Collected in September 1972 by James E. DeWeese and Ron T. Harris. Formerly CRE 3182. The holotype is 850 mm total length, 552 mm SVL,

298 mm tail length (complete), and has fully everted hemipenes (the left one removed for description and illustration). It has 152 ventrals and 115 subcaudals. Supralabial 2 on the left side is partially divided by a suture on its upper edge. The left and right upper primary temporal and the right lower primary temporal are divided by a vertical suture. Three long midventral slits through the body wall (one on anterior body, two posterior to attached collection tags). Most of the stratum corneum is missing from the dorsal scales. A histological study of the reproductive system indicated active spermiogenesis (Goldberg, 2003).

Paratopotypes. LACM 114106–08, 148596, 148602, 148606, 148608, 148613–15, 148617. The stated localities for the topotypes vary somewhat among the specimens according to the LACM catalogues (different collectors over a period of years). All have the basic locality "Finca Las Cruces" with little more specific information. Elevations associated with paratopotypes range from 1,100 to 1,300 m.

Other Paratypes. LACM 148590, 148620 from Finca Loma Linda, 2 km SSW Canas Gordas, 1,170 m, Puntarenas Province, Costa Rica. LACM 148612 from Finca Las Alturas, vicinity of main plaza and surrounding streams and forests, 1,330 m, Puntarenas Province, Costa Rica. UF 16425 from Finca Mellizas, 14 km ENE La Unión, near the Panama border [approximately 1,310 m], Puntarenas Province, Costa Rica.

Etymology. The species name is derived from the Greek adjective *krybelos* (κρύβηλος) meaning "hidden" or "secret." Transliteration to Latin yields *crybelum* (with neuter gender ending to agree with the neuter generic name). It recognizes the cryptic nature of this species and the fact that it remained unrecognized for so long in a well-studied herpetofauna.

Diagnosis. Dendrophidion crybelum is characterized by (1) dorsocaudal reduction from 8 to 6 occurring posterior to subcaudal 40 (range, 42–58); (2) single anal plate; (3) low subcaudal counts (<120 in males and females); (4) black-edged pale crossbands on the neck nearly always more than one scale row wide; (5) pale crossbands continuing to the vent but posteriorly tending to become invested with dark pigment, forming a lateral and vertebral series of ocelli within dark bands; (6) in adults, a tendency for small dark spots and flecks on subcaudals and posterior ventrals; (7) a relatively long cylindrical hemipenis with a large number of spines (>70) and a short, nonbulbous apex ornamented with freestanding membranous ridges. The combination of few subcaudals and a single anal plate will distinguish *D. crybelum* from all other species of *Dendrophidion* except *D. vinitor, D. apharocybe,* and *D. paucicarinatum.*

Additional distinguishing characters and comparisons include the following. *Dendrophidion crybelum* differs from species of the *D. percarinatum* group (*D. bivittatum, D. brunneum, D. paucicarinatum, D. percarinatum*) in having the dorsocaudal reduction from 8 to 6 occurring posterior to subcaudal 40. A single anal plate will distinguish *D. crybelum* from all of these except some individuals of *D. paucicarinatum* (anal plate variable in this species), but *D. paucicarinatum* lacks distinct pale crossbands in adults; has narrow dark lines across the venter; and a large number of ventrals (>175 compared with <165 in *D. crybelum*). In addition to having a divided anal scale, *D. percarinatum* has narrow pale crossbands (<1.5 scale rows wide) on the neck. *Dendrophidion bivittatum* and *D. brunneum* have divided anal scales and different color patterns (posterior blackish dorsolateral and lateral stripes in *D. bivittatum* and uniform greenish or with a combination of paravertebral stripes or spots, or indistinct crossbands in *D. brunneum*; see Cadle, 2010). *Dendrophidion crybelum* differs from *D. boshelli* in having 17 midbody scale rows (15 in *D. boshelli*).

Dendrophidion crybelum differs from two other members of the *D. dendrophis* group, *D. dendrophis* and *D. nuchale auctorum* (characteristics in parentheses), in having fewer subcaudal scales (≥130); a
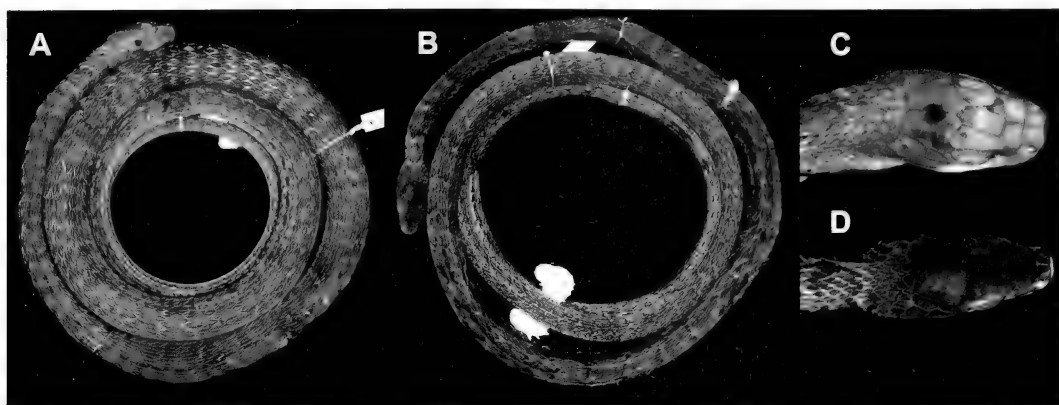
Figure 13.   Comparison of closely size-matched males of (A, C) *Dendrophidion crybelum* (LACM 148590, 625 mm SVL) and (B, D) *D. apharocybe* (LACM 148601, 653 mm SVL). (A) and (B) are to the same scale, (C) and (D) to the same scale. Relative to body size, *Dendrophidion crybelum* has a more robust body and a broader head than *D. apharocybe*.

venter without extensive dark pigment, usually only scattered spots on the most posterior ventrals (venter often heavily marked with dark pigment, especially posteriorly); smaller body size (adults commonly more than 1 m in total length); a shorter relative tail length in adults, <60% of SVL (tail usually more than 60% of SVL); and in hemipenial morphology (hemipenes bulbous rather than long and cylindrical; a spinose battery followed distally by several transverse flounce-like structures). In *D. dendrophis* and *D. nuchale* auctorum the anal plate may be either single (as in *D. crybelum*) or divided.

Dendrophidion crybelum differs from *D. apharocybe* and *D. vinitor* most notably in hemipenial morphology, including overall shape (elongate and cylindrical vs. shorter and bulbous in the last two species), number of spines (>70 vs. <45), and apical morphology (narrow and with reduced calycular structures vs. nude and strongly inclined in *D. apharocybe*, or with well developed membranous ridges and an apical boss in *D. vinitor*). See complete descriptions for details.

Other characteristics distinguishing *D. crybelum* from *D. apharocybe* and *D. vinitor* are subtle. *Dendrophidion crybelum* is a more robust animal than either *D. apharocybe* or *D. vinitor*, which is most

easily seen in side-by-side comparisons of individuals of comparable body length, as shown for two males illustrated at the same scale in Figure 13. The body of *D. crybelum* is more massive, and the head is larger and more angular, than similar sized specimens of *D. apharocybe* or *D. vinitor*.

Adults of *D. crybelum* have fine dark speckling on the subcaudal scales, often concentrated along suture lines, and small dark flecks and spots on the posterior ventral plates (Fig. 14). However, these features vary among adults (very distinct and numerous to only scattered flecks), and they appear to develop ontogenetically. Juveniles often have only a fine peppering on the distal subcaudals forming a dark suffusion easily visible only with magnification. On the other hand, apart from lateral dark pigment on the ventrals and subcaudals common to all species of *Dendrophidion*, the ventral plates and subcaudals of *D. apharocybe* and *D. vinitor* are immaculate (Fig. 14; see Fig. 6 for *D. vinitor*). *Dendrophidion crybelum* averages fewer pale bands on the body than *D. apharocybe* or *D. vinitor* (Table 1; $p < 0.01$ and $p < 0.001$, respectively), although the ranges overlap greatly. The pale neck bands in *D. crybelum* are typically broader than those of *D. vinitor* (Fig. 2).

Description (8 males, 8 females). Table 1 presents standard meristic and mensural
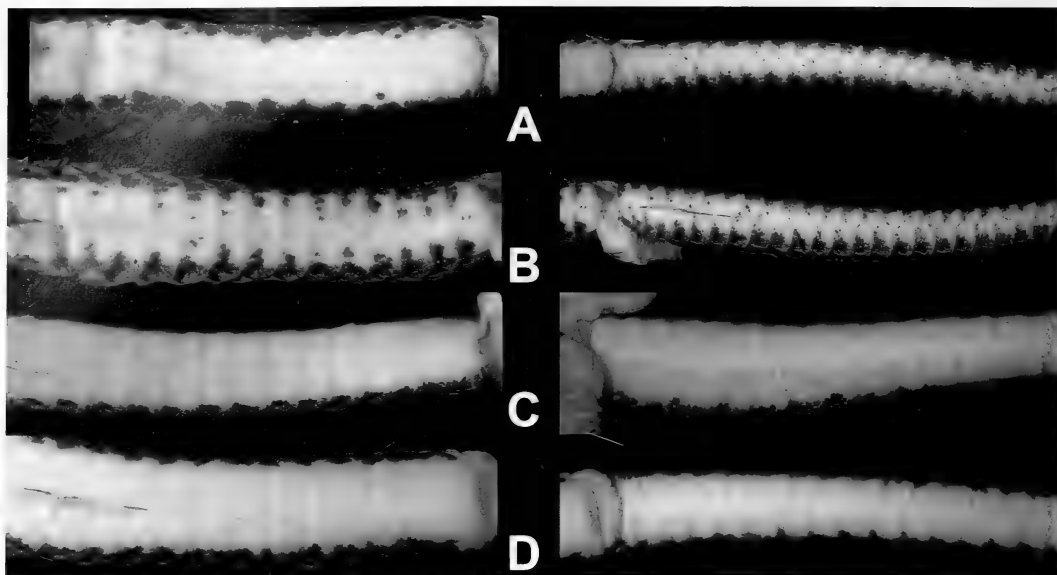
Figure 14.   Comparison of posterior ventral and subcaudal patterns of *Dendrophidion crybelum* and *D. apharocybe. Left series:* Ventral plates immediately anterior to the vent. *Right series:* Tail base immediately posterior to the vent. Vent toward the center in each series. (A, B) *D. crybelum* (LACM 114107 and LACM 148599 [holotype], respectively). (C, D) *D. apharocybe* (LACM 148593 [holotype] and LACM 148609, respectively). Posterior ventrals and subcaudals of *D. crybelum* have fine dark spots and speckling compared with the immaculate ventrals and subcaudals of *D. apharocybe.* The specimen in panel A is atypical for adult *D. crybelum* in having only a few widely scattered spots on the ventral scutes, but its subcaudals were extensively speckled; the ventral spotting of the specimen in panel B is more typical. *Dendrophidion vinitor* is similar to *D. apharocybe* in having immaculate posterior ventral and subcaudal patterns (see Fig. 6 for an example).

data for *D. crybelum.* Largest male (LACM 148590) 985 mm total length, 625 mm SVL; largest female (LACM 114107) 631 mm SVL, 893+ mm total length (tail incomplete; a female 621 mm SVL was 956 mm total length). Tail 34–36% of total length (51–58% of SVL) in males; 34–35% of total length (50–54% of SVL) in females. Dorsal scales in 17–17–15 scale rows, the posterior reduction usually by fusion of rows 3+4 (90%; remainder 2+3) at the level of ventrals 93–104 (see Sexual Dimorphism below). Ventrals 150–153 (averaging 151.6) in males, 156–162 (averaging 160) in females; 1 or 2 preventrals anterior to ventrals. Anal plate divided. Subcaudals 112–119 (mean 116.9) in males, 115–119 (mean 117.2) in females. Dorsocaudal reduction at subcaudals 43–58 in males (mean 49), 42–56 in females (mean 48.6). Preoculars 1, postoculars 2, primary temporals 2, secondary temporals 2. Supralabials nearly always 9 with supralabials 4–6

bordering the eye (rarely 8 with 3–5 bordering eye). Infralabials 9. Maxillary teeth 38–44, usually with the last four (occasionally three) enlarged.

Two apical pits present on dorsal scales. In most specimens (including juveniles) all dorsal rows except row 1 are keeled from the neck to the vent. In occasional specimens (juveniles and adults) all rows are keeled at midbody and posteriorly (in these cases scales in row 1 usually have very weak keels and sometimes not every scale in row 1 has a detectable keel); one adult lacked keels on rows 1–3 on the neck only. Divisions (but no fusions) of temporal scales were recorded as follows: upper primary divided (5), upper secondary divided (6), lower primary divided (4).

Hemipenis cylindrical, much longer than wide, lacking a bulbous apex. Sulcus spermaticus simple, centrolineal, and with a flared tip. Hemipenial body dominated by a great number of enlarged spines. Spines
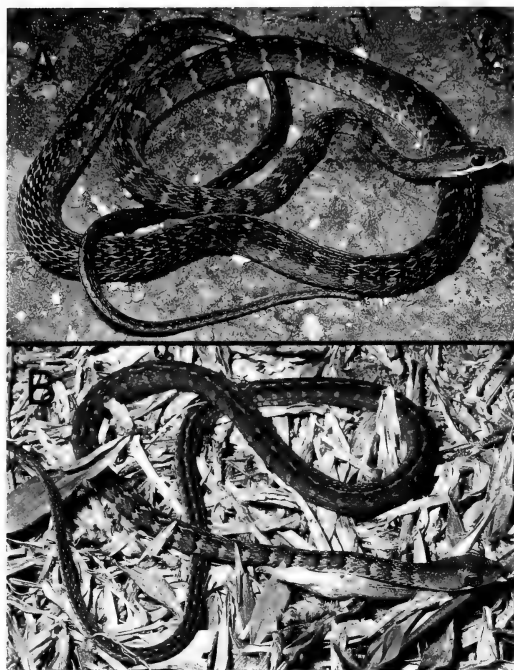
Figure 15. *Dendrophidion crybelum* in life from the type locality (paratypes). (A) LACM 114107 (adult female, 631 mm SVL). (B) LACM 114108 (juvenile female, 298 mm SVL). From color slides by Roy W. McDiarmid.

followed distally by a very short apex ornamented with a crowded series of flounces, calyces, and (on the apex proper) free-standing ridges. Small apical region essentially covered with these ornaments (i.e., nude areas very small).

Sexual Dimorphism and Ontogenetic Variation. Small sample sizes hamper a full exploration of sexual dimorphism, and the only statistically significant standard scale count differences are the greater number of ventrals in females compared with males ($p \ll 0.001$; Table 1) and a different point of dorsal scale reduction (mean ventral numbers 96 and 102.1 for males and females, respectively; $p < 0.001$). Males and females do not differ significantly in mean adult SVL (581 mm and 574 mm SVL, respectively), subcaudal number, or the point of dorsocaudal reduction. The difference between male and female relative tail lengths is marginally significant ($p = 0.045$). The

mean points of dorsocaudal reduction in male and female *D. crybelum* differ by less than one scale, and this character presents a departure from the pattern of sexual dimorphism in *D. vinitor* and *D. apharocybe*, which are sexually dimorphic for this character (Table 1). Specimens <300 mm SVL have relatively shorter tails (31–34% of total length, 46–52% of SVL; $N = 4$, males and females combined) than larger specimens (Table 1).

Coloration In Life. I am unaware of previously published photographs of *D. crybelum*. Figure 15 presents photographs of *D. crybelum* in life from color slides by Roy W. McDiarmid. An adult female (LACM 114107, Fig. 15A; the same specimen is illustrated in Fig. 16A) has a deep chocolate brown ground color; pale bands washed with orange on the neck and the posterior two-thirds of the body, grayish in between, and invested irregularly with black (tendency for the bands to form transverse series of ocelli posteriorly); a pale vertebral line washed with orange; and whitish lips. The juvenile (LACM 114108, Fig. 15B) is patterned similarly but has a pale brown ground color (somewhat tan); pale bands/ocelli and pale vertebral line grayish anteriorly, invested with yellowish brown posteriorly and on the first two or three bands on the neck. McDiarmid's slide collection also has a photo of LACM 114106 in life, an adult female with clouded eyes (preparing to shed). Its coloration appears similar to that of LACM 114107 except perhaps a paler brown ground color (not as pale as the juvenile described above) and more orangish wash in the pale bands. The venter of LACM 148614 (339 mm SVL) was described as "yellowish" (Roy W. McDiarmid, field note).

Coloration in Preservative. Overall dorsal coloration predominantly grays and browns (tendency for brown with stratum corneum intact, grays without). A series of pale gray to pale brown crossbands (sometimes offset) on the body from the neck to the vent, continuing onto the tail as a variably distinct series of pale dorsolateral spots (Fig. 16).
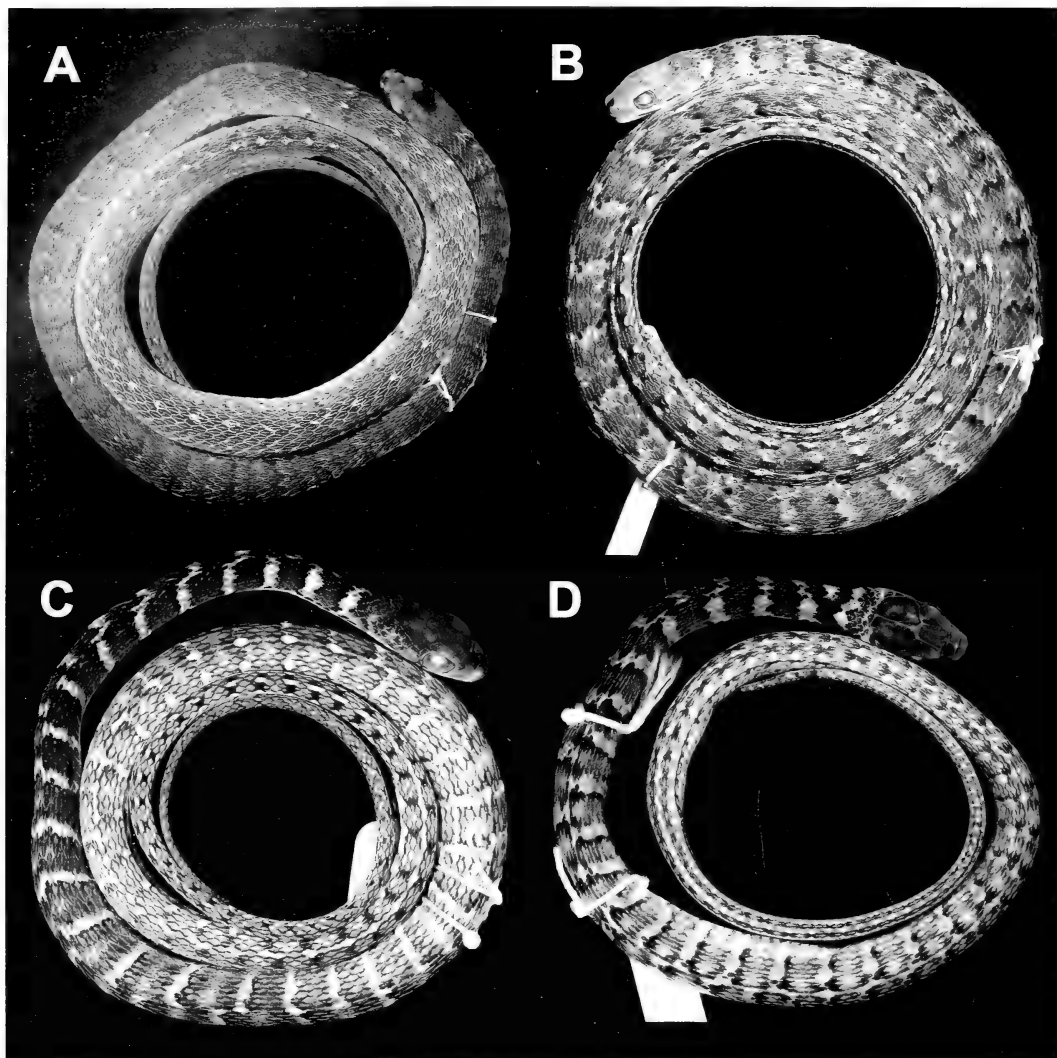
Figure 16.   Representative specimens of *Dendrophidion crybelum*. (A) LACM 114107 (primary banding pattern obscured partly by formation of secondary bands and darkening of primary bands during preservation; compare Fig. 15A). (B) LACM 148596. (C) LACM 148613 (juvenile, 304 mm SVL). (D) LACM 148620 (juvenile, 185 mm SVL).

The number of pale bands/ocelli on the body ranged from 36 to 62 (mean 48.2). In about 58% of the specimens neck bands were 1.5–2 scale rows in width; in another 25% the bands were 1–1.5 rows wide; in the remainder, the neck bands were more than two scale rows wide or less than one row wide.

Crossbands bordered anteriorly and posteriorly by irregular black pigment forming narrow jagged border (usually better developed on posterior edges). Posterior crossbands become invested with greater amount of dark pigment, usually becoming fragmented into a lateral and vertebral series of ocelli (lateral ocelli occupy parts of four adjacent scales on rows 3–5); less distinct ventrolateral ocelli sometimes on row 1. Crossbands extend to lateral edges of ventrals, which are marked with dark gray

and brown or black irregular spots. The first few bands on the neck and anterior body are broader than more posterior bands. Narrow broken blackish lateral stripe (or series of dashes/spots) occurs on the suture line between rows 2 and 3 on the posterior one-third of body. Black ventrolateral tail stripe on suture line between subcaudals and dorsocaudal row 1 extends to tail tip.

Two specimens (LACM 148596, 148599) have more vivid banding pattern than others; these two also tend to be grayer than others, which are browner. Crossbands obscure in other preserved adults (LACM 148590, 114106–07) seemingly because they are invested with brown pigment (except for neck bands) nearly the same color as the ground color and the crossband borders are not distinctly marked with pigment darker than ground color. Specimens with a dark brown ground color and contrasting pale bands in life may have obscure bands when preserved (compare Figs. 15A and 16A).

Top of head more or less uniform gray or brown down to superior edge of supralabials (last two supralabials mostly gray or brown). Faint blackish postocular stripe extends diagonally down across penultimate supralabial. Gular region immaculate.

Lateral portions of ventrals with dense grayish black pigment, within which are darker irregular spots. Remainder of most ventrals immaculate. However, posterior ventrals (up to about the 20th ventral anterior to the vent) have small scattered irregular black spots that vary in number from relatively many (LACM 148596, 148599) to almost none (LACM 114106–07) (Fig. 14). Subcaudals with ventrolateral stripe (described above) and generally with dense blackish/gray pigment investing subcaudals, especially along suture lines, and scattered irregular small round black spots on many subcaudals (Fig. 14).

Juveniles similar to adults but pale bands/ocelli are much better defined. Spotting or stippling on posterior ventrals and proximal subcaudals very faint, but even relatively small specimens have fine speckling of dark pigment on posterior portion of tail (e.g.,
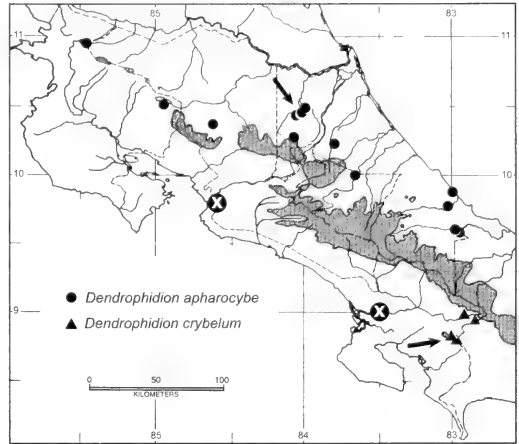
Figure 17. Distribution of *Dendrophidion crybelum* and of *D. apharocybe* in Costa Rica; see Savage (2002) for a more complete representation of localities. Arrows indicate type localities. A few symbols represent multiple contiguous localities. Two localities indicated by "×" within dots in western (Pacific) Costa Rica are erroneous localities for "*D. vinitor*" indicated by Savage (2002: 656); see species account for *D. apharocybe*.

LACM 114108, 298 mm SVL), especially on suture lines and laterally. Anterior ground color dark brown to blackish (contrasting greatly with pale crossbands), becoming lighter posteriorly (pale brown to tan on posterior half to two-thirds of body). Posterior lateral stripe broken; tail stripe quite distinct. Secondary pale bands between the primary crossbands already evident in LACM 148613–14. Width of pale dorsal bands in LACM 148614, 148617 is no more than about one scale wide. Juvenile *Dendrophidion crybelum* have a more contrasting pattern and well-developed ocelli on the posterior body compared with juvenile *D. apharocybe*.

Distribution (Fig. 17). Definitely known only from middle elevations (1,100–1,330 m) at the eastern end of the Fila Costeña and the south slope of the Cordillera Talamanca in southwestern Costa Rica. All known localities are in the uplands of the upper Río Coto Brus, separated from the lowlands of the Osa Peninsula–Golfo Dulce by the Fila Costeña. Despite relatively intensive surveys, "*D. vinitor*" has not been recorded

from lowland sites on the Osa Peninsula (Scott et al., 1983; McDiarmid and Savage, 2005). See the species account for *D. apharocybe* for discussion of two lowland Pacific localities erroneously attributed to "*D. vinitor*."

Given the proximity of Costa Rican localities (Fig. 17), *D. crybelum* undoubtedly occurs on the adjacent Pacific versant of western Panama (Chiriquí province), where similar environments occur. Savage (2002) included "adjacent western [Pacific] Panama" in his distribution summary for *D. vinitor*, the basis being a specimen from "Chiriquí" listed in E. R. Dunn's notes as having 121 subcaudals and a single anal plate (Jay M. Savage, personal communication, March 2011). This may be the same specimen listed by Boulenger (1894: 16; specimen g collected by Godman in Chiriquí, now BMNH 94.5.17.8), although Boulenger's subcaudal count is 128. No one seems to have re-examined the specimen recently, so the presence of *D. crybelum* in Panama remains likely, though unsubstantiated. Nonetheless, *D. crybelum* probably has a very restricted distribution in southwestern Costa Rica and adjacent Panama.

Southwestern Costa Rica (Golfo Dulce region) has long been known for both high species diversity and high herpetofaunal endemism (e.g., Duellman, 1966: 712, 716; Savage, 1966: 758, 2002: 85, 813–814). Hence, the presence of a narrowly endemic species of *Dendrophidion* in this region comes as little surprise. In terms of overall species composition (Duellman, 1966) and historical biogeographic origins (Savage, 1966, 2002), the herpetofauna of the Golfo Dulce region shows ties to Atlantic lowland herpetofaunas of Costa Rica and Panama. Many closely related species pairs or conspecific populations of amphibians and reptiles show disjunct distributions in these two areas. Moreover, paleoenvironmental modeling (Chan et al., 2011: 528–531) shows that the Río Coto Brus valley has had a long history of environmental stability. The Pacific populations are isolated by the

presence of subhumid habitats north and south of this area (Savage, 2002). The biogeographic events responsible for these disjunctions are explored in the discussion.

Natural History. Most confirmed specimens of *D. crybelum* come from sites on the north side of the Fila Costeña (separating the Río Coto Brus Valley from the Golfo Dulce) that have been intensively studied by investigators associated with the Organization for Tropical Studies (OTS) and others (e.g., Janzen, 1973; Scott, 1976; Fauth et al., 1989; Santos-Barrera et al., 2008). Other close-by localities are on the southern slope of the Cordillera Talamanca. The type locality (Las Cruces) is classified as Premontane Wet Forest in the Holdridge system; other localities span a range of forest types, including Premontane and Lower Montane Wet Forest and Rainforest (Holdridge, 1967; Holdridge et al. 1971).

Scott (1976: 44, 53, table 1) described the site of quantitative herpetofaunal sampling at Finca Las Cruces (1,200 m) as having a 12-year average rainfall of 4,000 mm/yr, a brief "dry" period January–March, and moderate to steep slopes. Compared with the lowlands, Las Cruces has shorter, smaller trees, more understory, and deeper litter (5–7 cm deep depending on the season). Janzen (1973: 675) added further details: "The overstory canopy is about 30 m high and densely intertwined with vines and heavily laden with epiphytes. … The understory is rich in palms, Cyclanthaceae, ferns, Marantaceae, and cycads, and appears in general very similar to that of the Osa [Peninsula lowland] primary forest sites except that the [Las Cruces] understory appears to have a much heavier epiphyllae load, the tree trunks have heavy layers of lower plants, and there seems to be a slightly reduced species richness of plants in the 0.3 to 2 m height range. … *Quercus*, *Prunus*, and *Alnus* are more prominent than in nearby lowland sites."

The discovery of specimens of *D. crybelum* in Costa Rica came relatively late, the first specimens from the type locality collected by Jay M. Savage and colleagues

in 1964. (A paratype from another locality, UF 16425, was obtained in 1962 and is the earliest known specimen.) Even in the early 1970s Janzen (1973: 675) reported considerable deforestation of lower montane forest in the vicinity of the type locality, which is now a patchwork of severely human-altered habitats (Santos-Barrera et al., 2008). According to Savage (personal communication, March 2011) good primary forest and additional second growth parcels still remain at the type locality (266 ha; now an OTS field station and Wilson Botanical Garden) and nearby indigenous reserves. Forested habitat at Finca Loma Linda is considerably altered, whereas Las Alturas is on the margin of La Amistad Biosphere Reserve, where substantial montane forest still exists (the habitat patchwork of this area is especially well shown on Google Earth).

Unfortunately, the region where *D. crybelum* occurs has also experienced considerable amphibian population declines (Lips, 1998, 1999; Lips et al., 2003, 2006; Santos-Barrera et al., 2008), a fact relevant to sustainability of *Dendrophidion* since leaf litter frogs comprise a major portion of the diet in all species (Stafford, 2003). The declining species documented by Lips and coworkers included species of *Pristimantis*, *Craugastor*, and *Diasporus*, which are major prey for *Dendrophidion*. The effects of extirpation of such prey species on the population biology of their snake predators are, as yet, little understood (Whitfield et al., 2007). In contrast to the population declines at La Selva (see species account for *D. apharocybe*), the amphibian declines at Las Cruces and nearby sites were precipitous and due primarily to the amphibian pathogen *Batrachochytrium*. A recent herpetofaunal inventory of Las Cruces and surrounding areas (Santos-Barrera et al., 2008) recovered two specimens of *D. percarinatum* but none of the three other species of *Dendrophidion* recorded there historically (*D. crybelum*, *D. nuchale* auctorum, and *D. paucicarinatum*; Scott et al., 1983, and personal observations of specimens in LACM). The last specimen of *D.*

crybelum held in U.S. collections was obtained in 1987.

The holotype and most paratypes of *D. crybelum* were included (as "*D. vinitor*") in a study of reproductive cycles in *Dendrophidion* from Costa Rica (Goldberg, 2003) and range-wide, Mexico to Panama (Stafford, 2003; as summary statistics only, along with specimens of *D. vinitor* and *D. apharocybe*). Four males in Goldberg's study (552–625 mm SVL) were undergoing spermiogenesis in April, June, August, and September. Two females (621–631 mm SVL) collected in May and July each had four oviductal eggs. Of the specimens I examined, a female collected 19 June from Las Alturas (LACM 148612, 480 mm SVL), has swollen and convoluted oviducts but no vitellogenic ova, suggesting that it had recently laid a clutch. The two smallest individuals (185 and 206 mm SVL) were collected 6 June and in September, respectively, and their umbilical scars were nearly completely closed. The umbilical scar of the next larger (251 mm SVL) was completely closed, and in two individuals of 304 and 339 mm SVL the umbilical scars were no longer evident. Like the other two species of the *D. vinitor* complex, there is a low frequency of snakes with broken/healed tails in *D. crybelum* (6.7% of the specimens examined).

HEMIPENIAL MORPHOLOGY

An Introduction to *Dendrophidion* Hemipenes

The initial recognition of the new species described herein depended to a great extent on differences in hemipenial morphology. However, *Dendrophidion* hemipenes are peculiar in ways that have never been fully described; thus, it seems pertinent to provide an overview of their general structure and characteristics. I have examined retracted and everted hemipenes of all currently described species of *Dendrophidion* except *D. boshelli*, for which no material has been available. Hemipenes of other species will be described elsewhere. Stuart

(1932) long ago recognized some unusual characteristics of *Dendrophidion* hemipenes, but a detailed description of only one species, *D. brunneum*, is as yet available (Cadle, 2010). Hemipenial terminology follows Dowling and Savage (1960), Myers (1974), Myers and Campbell (1981), Myers and Cadle (1994, 2003), Savage (1997), and Zaher (1999), but the terminology useful in describing certain unusual structures in *Dendrophidion* is further discussed here. Except where noted, these comments apply equally to the *D. dendrophis* and *D. percarinatum* groups (*sensu* Lieb, 1988).

The hemipenis of *Dendrophidion* is either unilobed or slightly bilobed but the overall shape varies considerably among species—from short, bulbous, and cylindrical forms described here to longer, slender and clavate shapes. A short basal nude section (*pedicel* in the terminology of Savage [2002: 539]) is followed by a broader section usually ornamented with minute spines; there are no nude pockets or basal lobes (some organs have round basal bulges when everted). The relatively unadorned base is followed by an array of closely spaced spines that are enlarged to varying degrees and in patterns that are species specific. In general, hemipenial spines in the *D. dendrophis* species group are larger than those in the *D. percarinatum* group. Although hemipenes of the *D. dendrophis* group are sometimes said to have enlarged "basal hooks" or "basal spines" (e.g., Dunn, 1933: 78; Lieb, 1988; Savage, 2002: 654), their enlarged spines are not basal in the same sense as in some snakes, in which enlarged spines are truly positioned at the base of the organ. Rather, they are attached along the central portion of the hemipenial body (truncus in the terminology of Savage [2002: 539]). In some species of both the *D. dendrophis* and *D. percarinatum* groups, a pair of spines much larger than any others is positioned near the sulcus spermaticus at the proximal edge of the array of spines (one on each side of the sulcus); this pair is relatively much larger in *D. dendrophis* and *D. nuchale* auctorum than in other species

in which they occur (*D. dendrophis* and *D. nuchale* auctorum also have an additional pair of enlarged spines positioned toward the asulcate side). Species of the *D. vinitor* complex lack such conspicuously enlarged spines.

Distal to the spines are structures that range from more or less definitive calyces (cuplike structures with both longitudinal and transverse walls) to flounces (transverse ridges lacking longitudinal connecting walls), with an array of intermediate structures that are neither definitive calyces nor flounces. For example, the hemipenial apex in two species of the *D. vinitor* complex has long, relatively free-standing ridges that don't conform to strict definitions of either calyces (because they do not form reticulating networks) or flounces (because they are not transverse in orientation). Nonetheless, the morphological similarity among all of these structures is clear and they undoubtedly have similar developmental origins. Further reductions of calyxlike structures result in low fleshy ridges or entirely nude apical areas. Proximal calyces/flounces have broader walls than more distal ones. These descriptors refer to structures visible in everted or retracted hemipenes. In addition, retracted hemipenes may have *pseudocalyces*, which are calyxlike structures visible in retracted organs that disappear upon eversion and full inflation (Myers and Cadle, 1994: 13–14; Cadle, 2010: 19–20). The tip of the apex in *Dendrophidion* has a combination of reduced calyces, free-standing ridges, and/or nude areas in patterns that are species-specific.

Flounces, calyces, and other similar structures are ornamented with mineralized spinules, at least proximally, but spinules are usually reduced or absent in distal calyxlike structures. Most spinules in *Dendrophidion* are atypical in that they lack a tip projecting from atop the calycular walls. Instead, they consist of a mineralized rod completely enclosed by the wall tissue. I refer to these as *embedded spinules* (see also Cadle, 2010: 16 [fig. 6], 19); they are relatively straight and more or less the same thickness throughout.

A general pattern in the arrangement of calyxlike structures seems common to all species of *Dendrophidion*, regardless of the overall pattern in a given species. Calyces are most fully developed on the asulcate side in comparison to the sulcate side, which has few or no full-fledged calyces. On the asulcate side in most species, a calyculate region extends to the tip of the apex, sometimes as far as its midpoint. Additionally, at the proximal edge of the calyculate region, at least one pair of transverse flounces encircles the hemipenis in all species (some species have more than one pair). Transitions between flounces and calyces or calyxlike structures occur abruptly within a single organ.

The sulcus spermaticus in *Dendrophidion* is centrolineal and usually has a slightly flared tip with divergent sulcus lips, but the sulcus is terminally divided in an undescribed species of the *D. percarinatum* group and in *D. dendrophis* (a detailed discussion of this morphology will be presented elsewhere). Savage (2002: 539) introduced the term *semicentripetal* for sulcus conditions such as those *Dendrophidion* with a simple sulcus on a unilobed organ in which the sulcus extends to the tip of the hemipenis with minimal deviation from the midline of the sulcate surface (e.g., hemipenes described herein). This term is unnecessary because it embodies several aspects of hemipenial morphology for which vocabulary already exists, namely the overall hemipenial form (unilobed vs. bilobed), sulcus morphology (simple vs. bifurcate), and sulcus orientation (centrifugal, centrolineal, or centripetal). Because these three aspects of hemipenial morphology can be combined in various ways, I prefer to employ terms that keep the descriptive concepts separate. Thus, I use *centrolineal* to refer to simple or bifurcate sulci that pass distally with little deviation from the middle of the sulcate side of a hemipenis, whether unilobed or bilobed. Other authors (e.g., Zaher [1999] and Myers [2011]) have also used *centrolineal* in this broader sense.

The use of the term *semicentripetal* has other awkward consequences. First, *semi-centripetal* suggests a relationship to centripetal sulci seen on many bifurcate hemipenes. This relationship is unclear given that simple sulci can be derived in several ways from distinct bifurcate morphologies (centripetal, centrolineal, or centrifugal), and hemipenes in colubrids may have sulci in any of these orientations (Cadle, 2010: 18–19; see also Myers, 2011: 22–24). Secondly, some genera (e.g., *Dendrophidion*, *Leptodeira*, *Taeniophallus*) have species with both divided and simple sulci spermatici on unilobed to slightly bilobed organs; see Schargel et al. (2005, fig. 8) for an example from *Taeniophallus* and Myers (2011: 22–24) for *Leptodeira*. Using *semicentripetal* for those species with a simple sulcus and *centrolineal* for those with a divided sulcus has the undesirable consequence of applying different names to sulcus orientations that are basically the same, the only difference being the simple or divided nature of the sulcus overall. The different terms obscure the clear relation between the simple and divided sulcus conditions within such genera.

The use of *centrolineal* for forked or simple sulci on either bilobed or unilobed hemipenes means that the term applies to a broader array of sulcus topologies than would be the case if it were used exclusively for forked sulci on uni- or bilobed organs (its original definition, used in conjunction with describing the morphology of some dipsadids; Myers and Campbell, 1981: 16). I believe this is a nonissue inasmuch as I use the terms *centrolineal*, *centripetal*, and *centrifugal* to refer *only to the position of the sulcus* on the hemipenis overall, regardless of variations in other aspects of hemipenial morphology such as lobation or whether the sulcus is bifurcate or simple. Other variations, such as deflections of a simple (centrolineal) sulcus to the right (as in Colubridae) or left (in Natricidae) lobe, can simply be described or accommodated by terms already in use (e.g., dextral and sinistral, respectively; Rossman and Eberle, 1977; Myers, 2011: 14). I believe that using terms such as *centrolineal* for discrete

aspects of morphology (in this case *sulcus position only*), rather than combinations of several aspects, is more straightforward and more directly communicates morphological details.

The *retractor penis magnus* in *Dendrophidion* may or may not have a short division at the insertion. In species of the *D. vinitor* complex, some specimens seemed to have a very short separation of muscle fibers at the insertion, but I failed to detect such a separation in others. Whether this reflects true morphological variation or simple difficulty of determination in very short divisions is unclear. On everted hemipenes, two internal points of insertion of the retractor can often be discerned through the apical tissue; the spacing between these points may reflect the degree of division of the muscle.

Dendrophidion vinitor

Everted (UMMZ 121145, Veracruz state, Mexico; Figs. 18, 19). Hemipenis unilobed and with a somewhat bulbous apex. Total length about 17 mm; about 7.5 mm across the widest point (apex). Sulcus spermaticus simple, centrolineal, with a very slightly expanded tip. The tip of the sulcus is near the sulcate side of the apex and entirely hidden beneath the free edge of a raised knob of tissue, the *apical boss* described below.

Short proximal portion of the hemipenial body mostly nude, having only a band of scattered minute spines on the asulcate side and a few adjacent to the sulcus spermaticus just proximal to the array of enlarged spines. Central region of hemipenial body with short, robust, strongly hooked spines arranged in four to five more or less regular transverse rows all around. Total spines in the array 46. Spines are shorter on the sulcate side and longer on the asulcate side but there is little proximal-to-distal size differentiation.

Distal to the spines four or five flounces completely encircle the hemipenis. On the apex, these flounces grade into calyxlike structures and free-standing ridges that are more fully described below. The flounces have a short, thick, fleshy base and a wider outer membranous portion (within which are embedded spinules). Flounces somewhat wider on the asulcate side than on the sulcate side, and they gradually narrow in width distally. There is an abrupt transition between the array of spines and the flounces, but in some places, particularly adjacent to the sulcus spermaticus, spines in the distalmost row are incorporated into the proximal pair of flounces (most evident in the proximal flounce) and appear as especially robust spinules (Figs. 18A, 19B). These incorporated spines have a more strongly projecting and hooked distal tip compared with other spinules.

On the distal portion of the asulcate side are eight to 10 poorly developed calyces between the distal three flounces (i.e., four to five between the distal two flounces, and another four to five between the penultimate and antepenultimate flounce). Longitudinal walls of calyces much lower than transverse walls (which make up the flounces). Among the proximal three flounces on the asulcate side are a few other poorly developed longitudinal walls, which form very large irregular calyces (obscured by the overhanging flounces in Fig. 18A).

All flounces, calyces, and similar structures (including those on the apex) have embedded spinules. Adjacent to the sulcus spermaticus the spinules have a short projecting tip, but away from the sulcus the spinules are completely embedded. Spinules near the sulcus are also hooked (probably represents transitional structure to spines in the array), but they are relatively straight away from the sulcus.

Tip of the apex with a complex series of free-standing ridges similar to flounces except that they extend mostly obliquely across the apex from a median axis (Figs. 18A, 19A, B). Around the periphery of the apex, especially on the asulcate side, a few poorly developed connections among the apical ridges form rudimentary calyces. One of the apical ridges (the *median bisecting ridge*) is taller than the others
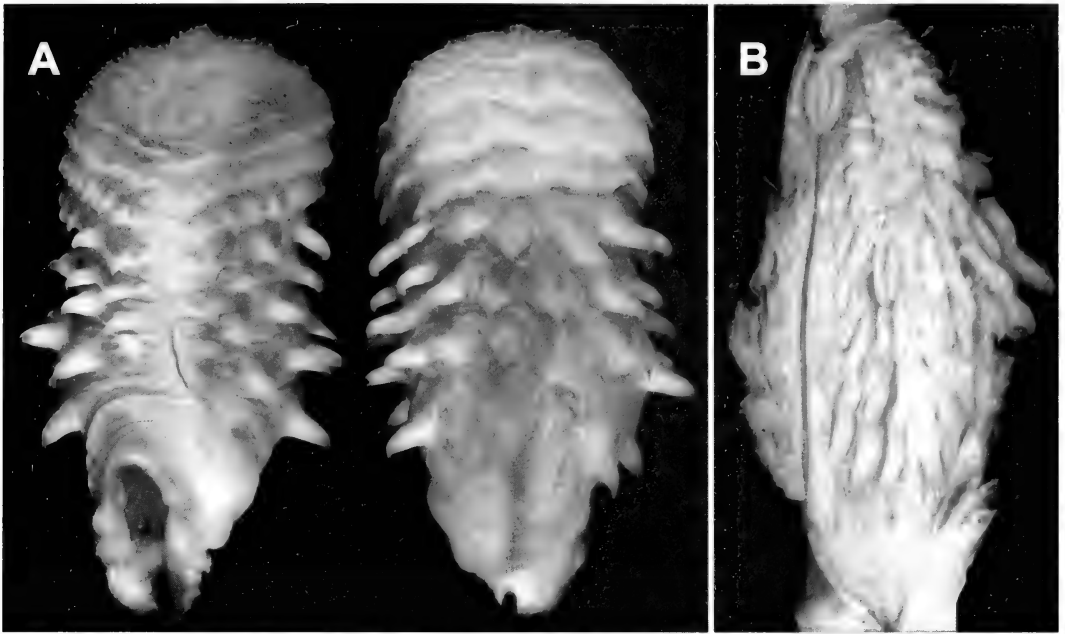
Figure 18.   Hemipenes of *Dendrophidion vinitor*. (A) Everted organ in sulcate and asulcate views (UMMZ 121145; Veracruz, Mexico; right hemipenis). (B) Retracted organ slit midventrally and spread flat (UIMNH 35547; Oaxaca, Mexico; left hemipenis). See Figure 19 for details of apical morphology.

and bisects the apex in a line extending from above the tip of the sulcus spermaticus directly across the middle of the apex; it is not straight, but undulates, and has well-developed embedded spinules (Fig. 19B). A series of shorter, lower ridges runs obliquely outward from the median bisecting ridge toward the asulcate side. These also have

embedded spinules but the spinules are less regularly developed than on the median ridge. On its sulcate end the median bisecting ridge continues across a prominent bulbous knob (the *apical boss*), bisecting it as well (seen in Figs. 18A and 19A as a line of denser whitish tissue extending across the middle of the boss). The borders
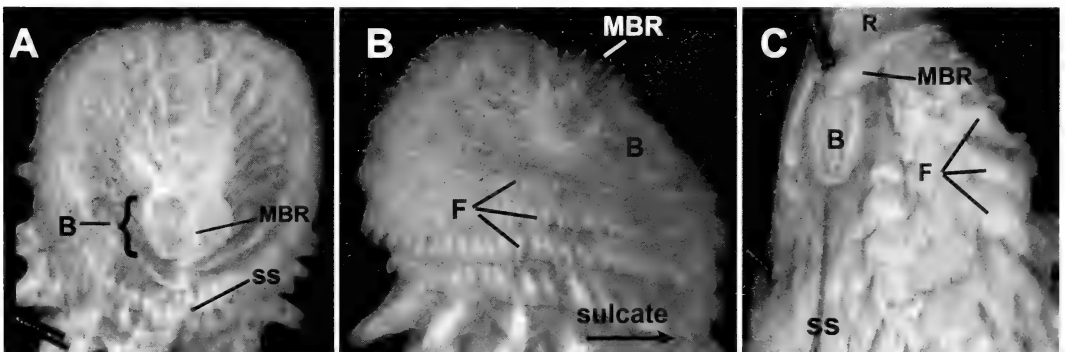
Figure 19.   Details of apical morphology of the hemipenis of *Dendrophidion vinitor*. (A) Apical view of UMMZ 121145 (everted, sulcate edge of apex toward bottom). (B) Lateral view of UMMZ 121145 (everted, sulcate side to the right). (C) Apical region of a retracted organ (UIMNH 35547; distal toward the top). *Abbreviations:* B, apical boss; F, flounces; MBR, median bisecting ridge; R, retractor penis magnus; ss, sulcus spermaticus. Compare Figure 18.

of the boss are well-defined and raised. The sulcate edge of the boss is elevated above the apical tissue and the sulcus spermaticus ends beneath it.

Retracted (UIMNH 35547, Oaxaca state, Mexico; Figs. 18B, 19B). Hemipenis extends to the middle of subcaudal 8. There appeared to be a slight separation of muscle fibers at the insertion of the *retractor penis magnus*. Extreme proximal portion of hemipenial body nude, followed by a band of scattered minute spines proximal to the array of enlarged spines (minute spines perhaps a bit denser around the sulcus and on the asulcate side). Ornamentation of the body dominated by an array of enlarged spines (45 total); enlarged spines robust, hooked at the tip, larger proximally and on the asulcate side, gradually decreasing in size distally. Each side of the sulcus spermaticus bordered by a line of seven to nine much smaller spines (small spines one-fourth or one-fifth the size of the enlarged spines in the array).

Three flounces on sulcate side of organ, increasing to five or more on the asulcate side; these grade into the apical freestanding ridges. All flounces/ridges with embedded spinules. Proximal flounces broader than the more distal ones and mainly membranous rather than fleshy. Some low and weak connections extend between adjacent distal flounces, especially on the asulcate side, and form poorly developed calyces.

At the tip of the organ is a prominent tissue ridge (equivalent to the median bisecting ridge and associated oblique ridges in the everted organ) extending from the asulcate side across the apex and bisecting the apical boss, which lies at the tip of the sulcus spermaticus (Fig. 19C). The boss has a prominent ridge delimiting its border but is nude apart from this border and the bisecting ridge; its morphology in the retracted organ is similar to that in the everted state. The bordering ridge has a few crenulations, which seem to have short embedded spinules. A few loose folds (presumably forming the oblique ridges in

the everted organ) lie lateral and distal to the boss and bisecting ridge; tissue mainly lateral and proximal to the boss is nude.

Sulcus spermaticus simple, in the dorsolateral wall of organ, ending distally beneath the sulcate edge of the apical boss. Tip of the sulcus not expanded, the groove actually appearing to narrow slightly at its terminus. The sulcus lips also do not appear to diverge distally.

There is some variation in the length of retracted hemipenes. Of nine retracted hemipenes examined superficially in situ, four ended between the suture of subcaudals 7/8 and the suture of subcaudals 8/9; four ended between the middle of subcaudal 9 and the middle of subcaudal 10; and one extended to the middle of subcaudal 11. The major retractor muscle appeared undivided in four specimens, but three others appeared to have a slight separation of muscle fibers at the insertion.

Dendrophidion apharocybe

Everted (LACM 148600, Heredia province, Costa Rica; Fig. 20). Hemipenis short, stout, with a slightly bulbous apex having an asulcate indentation, giving a somewhat cordate shape to the apex when viewed from the sulcate side. Total length about 21 mm. Length of base proximal to spine array on sulcate side about 3.5 mm. Length of apex from proximalmost flounce to tip on sulcate side about 13 mm. Maximum width of organ 11.5 mm (across middle of apex). Sulcus spermaticus simple, centrolineal, with a distinctly flared tip.

Base of organ proximal to the array of enlarged spines very short, ornamented with minute spines. The relatively unornamented base is followed by a central section with enlarged spines. Thirty-six spines form the array and a line of very small spines lies on each side of the sulcus just proximal to the apex. Spines arranged in somewhat irregular oblique rows on the sulcate side but no particular arrangement on the asulcate side (appear scattered, irregular). Spines on the asulcate side are much larger than those on

Figure 20.   Everted hemipenis of *Dendrophidion apharocybe* (LACM 148600 from near the type locality, left hemipenis) in sulcate, asulcate, and lateral views. Note flared tip of the sulcus spermaticus and the nude apical tip strongly inclined toward the sulcate side (sulcate to the right in lateral view).

the sulcate side. Some small spines are incorporated into the first flounce on the sulcate side. On the sulcate side all spines are more or less the same size (perhaps slightly larger proximally). On the asulcate side, the distal spines are slightly larger than the more proximal ones.

Four flounces on the sulcate side broaden to about seven on the asulcate side. The proximal flounce on the sulcate side becomes the 3rd flounce on the asulcate side (two proximal flounces added on the asulcate side). Flounces curve distad toward the asulcate side, reflecting the inclination of the apex toward the sulcate side (Fig. 20, lateral view). No distinct calyces except for a couple of irregular ones distally on the right asulcate side (i.e., the right side viewed looking toward the asulcate side; see Fig. 20, asulcate view). These calyces are asymmetrical (no comparable ones on the left side). Several other weak calyces present between the first pair of flounces on the asulcate side (weakly developed longitudinal walls between these two flounc-

es). Flounces have a thick fleshy base and an outer membranous part. All flounces have embedded spinules, the tips of which occupy weak scallops on their edges; spinules occupy mainly the membranous part but enter the fleshy part slightly. Scalloping becomes progressively less distally and medially.

Apex strongly inclined so that its distal surface faces toward the sulcate side (flounces extending distad much farther on the asulcate than the sulcate side). Central part of the apex occupied by a prominent bulge, which slopes gradually to meet the asulcate edge of the apex but drops off sharply on the sulcate side (Fig. 20, lateral view). The sulcus ends near the sulcate side of the organ just beneath the bulge. Apex nude except for low rounded ridges that occupy the central bulge. These ridges have the same general pattern as the membranous ridges on the hemipenis of *D. vinitor* (see above description). That is, they extend obliquely outward toward the asulcate side from a median axis; toward the sulcus the

ridges converge on a point on the bulge distal to the tip of the sulcus. An indication of these ridges can be seen in Figure 20 (sulcate view) as oblique darker streaks alternating with wider whitish streaks just lateral to the central part of the apex. Small areas lateral to the sulcus tip are smooth and without ridges. Toward the asulcate edge of the apex some of the oblique ridges are connected by very low additional ridges, forming a series of indistinct reticulating structures (highly reduced calyces).

Retracted (MVZ 217610, Heredia province, Costa Rica; Fig. 21). Hemipenis extends to about the middle of subcaudal 7. Sulcus spermaticus simple, extending distally in dorsolateral wall of the organ and ending short of the tip. At the tip of the sulcus are fine loose folds of tissue within the sulcus groove that presumably expand upon eversion to form the expanded tip of the sulcus in the everted organ.

Extreme basal portion of hemipenis under subcaudal 1 appears to be nude. About three rows of enlarged spines begin at level of the proximal edge of subcaudal 2 and extend to the distal edge of subcaudal 3. About 34 total spines on the organ, with 10–12 of these very large. These spines have a somewhat unusual flattened form with a tiny point at the tip.

About seven or eight rows of calyces/flounces located primarily on the asulcate side (medial and ventral sides of the retracted organ) begin at the level of the proximal edge of subcaudal 4. Only the proximal three flounces extend all the way to the sulcus spermaticus (more distal flounces stop short of the sulcus). Thus, the asulcate surface of the hemipenis is flounced almost to the tip of the organ, whereas on the sulcate side the flounces stop well short of the tip. Distal to the three proximal flounces adjacent to the medial side of the sulcus, the tissue of the hemipenis is smooth and nude and formed into low longitudinal folds. A few calyces are nestled within the distal longitudinal folds, mostly on the asulcate side. On the lateral side of the sulcus are enlarged spines up to
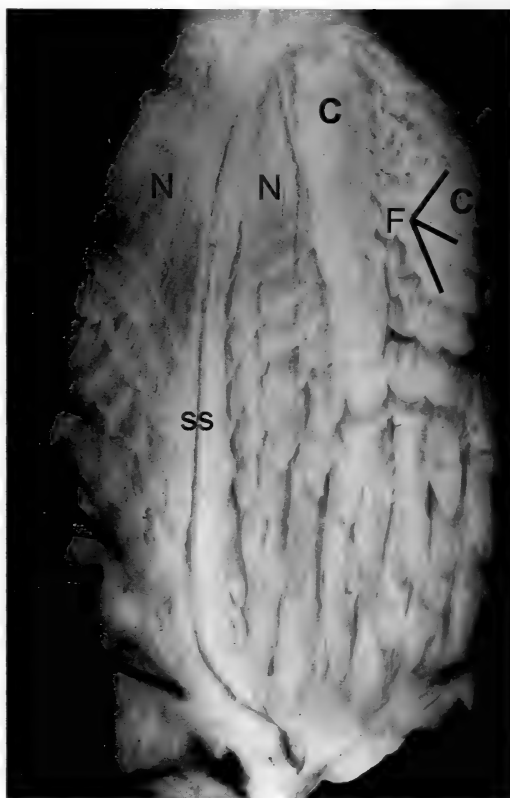
Figure 21.   Retracted left hemipenis of *Dendrophidion apharocybe* (MVZ 217610 from near the type locality). Apex toward the top. *Abbreviations:* C, thick cords composed of closely appressed flounces on each side of the apical nude area; F, asulcate flounces; N, expanse of nude tissue on each side of the sulcus spermaticus that forms the nude sulcate face of the apex in the everted organ; ss, sulcus spermaticus. Note the lack of an apical boss and large area of apical nude tissue (compare Figs. 18B, 19C, *D. vinitor*).

about the middle of subcaudal 5, distal to which the hemipenis is nude, smooth, and in low longitudinal folds.

The calyces/flounces are tightly bound, pleated tissue, with adjacent flounces barely overlapping. The flounces are gathered into a pair of thick "cords," one on each side of the apical nude tissue in the intact retracted organ (Fig. 21; in the figure, both cords are on one side of the nude tissue because of the position at which the hemipenis was slit). Between the cords is thinner tissue in which the flounces are individually discrete (the thinner tissue makes up the asulcate

flounces in the everted organ). A few weakly developed longitudinal connections are present between the distal two or three flounces. The flounces seem tightly bound to one another because of sturdy longitudinal connections that occur periodically between adjacent ones. Their free edges are very slightly crenulate and have embedded spinules. The spinules extend to the edge of the flounces but do not seem to extend entirely to their bases. In the most proximal flounce, bunches of four to five spinules are separated by thinner, narrower tissue, such that the edge of this flounce is undulating. The bunches of four or five spinules grade almost imperceptibly into the enlarged spines more proximally.

Variation and Remarks. A consistent and unusual hemipenial morphology is primary evidence that the populations from Honduras to Panama here referred to *D. apharocybe* comprise a single species. Sample sizes from different parts of this range of either fully everted organs or hemipenes everted sufficiently to see the configuration of the apex are 4 (Honduras), 2 (Nicaragua), 7 (Costa Rica), 1 (Panama). In addition, I studied the internal morphology of one retracted organ each from Nicaragua, Costa Rica, and Panama. There is little variation in basic morphology or ornamentation from throughout the range (particularly the distinctive inclination of the apex, asulcate flounces, and large apical nude expanse). The number of enlarged spines in the spine array is variable (23–40) but shows no particular geographic trend. For example, two organs with 23 spines were from Honduras and Panama and two hemipenes with 28 and 40 spines were both from Nicaragua. In large part, the strong consistency of hemipenial morphology throughout the geographic range of *D. apharocybe* lends integrity to the concept of this species as distinct from *D. vinitor* and *D. crybelum.*

Eight retracted hemipenes of *Dendrophidion apharocybe* from Honduras to Panama were superficially examined. Their distal endpoints were between the end of sub-

caudal 6 and the proximal edge of subcaudal 10, with four ending at or proximal to the middle of subcaudal 7. The major retractor muscle appeared undivided in two specimens and with a slight division in two others.

Dendrophidion crybelum

Everted (LACM 148599, holotype, Puntarenas province, Costa Rica; Fig. 22). Hemipenes of the holotype were the only fully everted organs studied in detail. One other was more or less fully everted (LACM 148590); it is essentially identical to the holotype but a few differences are noted. Hemipenis cylindrical, much longer than wide, and lacking a distinctly bulbous apex. Total length about 21.5 mm; width about 6 mm (about 3.6× longer than wide). Sulcus spermaticus, simple, centrolineal, with an expanded tip that broadens and then narrows, forming a tear drop–shaped expanse of nude tissue. The distal narrowing may be an artifact of the field eversion preparation, perhaps slight desiccation (it seems as if some slight folds between the distal lips might expand to form an openly expanded sulcus tip as in other *Dendrophidion* hemipenes). In LACM 148590 the sulcus tip appears to expand in normal fashion and then has a narrow distal nude extension. The distally divergent lips of the sulcus seemingly end short of the nude extension.

Extreme base nude but scattered minute spines occur in a band around the organ proximal to the enlarged spines. A great number of enlarged spines dominate the ornamentation of the hemipenial body (about 90–95 in LACM 148599; about 70–75 spines in LACM 148590). About 12 much smaller spines form a line on each side of the sulcus spermaticus for most of its length. Spines are larger proximally, gradually decreasing in size distally, and somewhat larger on the asulcate compared with the sulcate side.

Distally, spines are followed by a short, nonbulbous apex ornamented with flounces
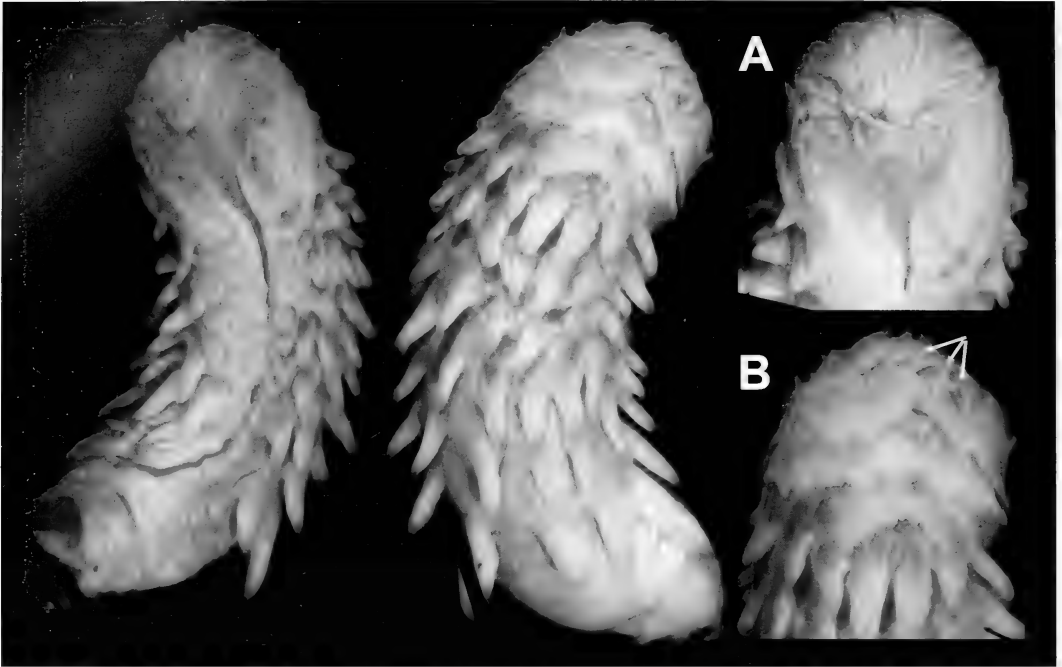
Figure 22. Everted hemipenis of *Dendrophidion crybelum* (LACM 148599, holotype), sulcate and asulcate views. (A) Detail of apical region showing closely packed apical ridges and flared tip of the sulcus spermaticus. (B) Asulcate side of apex showing flounces and rudimentary calyces (arrows).

and calyces. Two flounces adjacent to the sulcus, broadening to four on the asulcate side (the most proximal on asulcate side is short, poorly developed, and asymmetrically placed in about the middle of the asulcate side). The two additional flounces on the asulcate side are proximal to the two on the sulcate side and form from connections among spines in a transverse row (the spines then becoming relatively robust spinules within the flounce). Flounces contain embedded spinules, which span their membranous parts and extend into the outer portion of their fleshy parts (these flounces mostly consist of membranous part, very little fleshy base). On the asulcate side between the distal pair of flounces are several poorly developed calyces with very low, underdeveloped longitudinal walls; these are mostly not visible except by lifting and separating the flounces forming their transverse walls. These calyces are more fully developed on the right side of the apex than the left

(Fig. 22B; similar to the pattern of development in *D. apharocybe*).

Apex with many freestanding ridges containing embedded spinules and very little nude tissue (a small amount on the sulcate side around the tip of the sulcus spermaticus). The ridges generally have the same pattern as the apical ridges in *D. vinitor* (i.e., a median bisecting, somewhat taller ridge from which less prominent ones extend obliquely toward the asulcate side). These ridges are much lower and seem fleshier than the more membranous ridges in *D. vinitor*. They have slightly scalloped edges, and, because the apex is much narrower in *D. crybelum*, the ridges are more tightly packed. Toward the sulcate side, the ridges converge toward a point just distal to the tip of the sulcus spermaticus.

No definitive apical boss such as that in *D. vinitor* is apparent. However, the sulcate tip of the median bisecting ridge has a thickened nodule and, on each side, a short
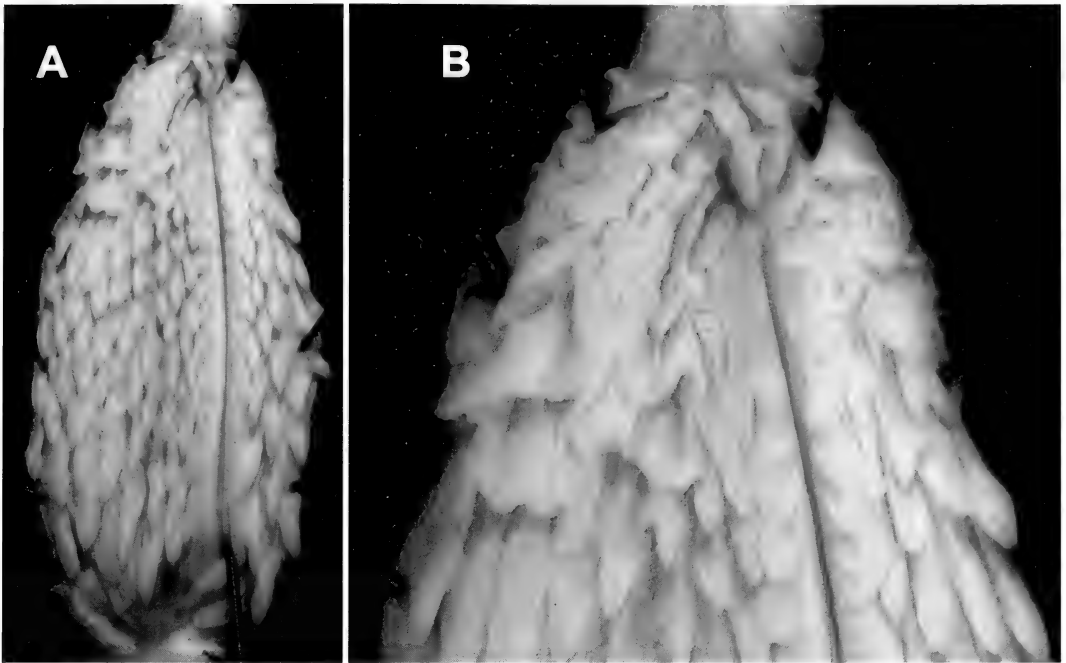
Figure 23. (A) Retracted right hemipenis of *Dendrophidion crybelum* (LACM 148608). (B) Detail of the apex of the same specimen.

segment of calycular tissue with somewhat thickened peripheral edges; the segment on the right side of the sulcus is partially fused with the median bisecting ridge, whereas the one on the left is detached. Toward their asulcate ends, the segments are attached to one of the oblique apical ridges by a constriction in the tissue, which separates them somewhat from the main part of the oblique ridge. The general configuration of this area is reminiscent of the apical boss in *D. vinitor* and may be a less fully developed, but homologous structure. Both hemipenes of *D. crybelum* examined, LACM 148590 and LACM 148599, have similar configurations in this area.

Retracted (LACM 148608, Topotype, Puntarenas province, Costa Rica; Fig. 23). Hemipenis extends to the suture between subcaudals 9 and 10. No division of the major retractor was detected. The base of the organ is nude and followed by a very short region ornamented with minute spines. Hemipenial body dominated by

approximately 92 enlarged spines; a series of much smaller spines lines each side of sulcus spermaticus. Individual spines are robust, very long, with a small hooked spike at tip. The spinose region is followed distally by flounces/calyces; they are more calyxlike on the asulcate side (very deep calyces here), where they extend onto the apical region. All flounces/calyces have embedded spinules.

Sulcus spermaticus simple and in the dorsolateral wall of organ; seemingly not flared at tip, but there is a long very fine ridge of tissue extending along the midline between the sulcus lips at the tip of the organ (may expand upon eversion to form flared tip). Sulcus ends beneath the tips of a pair of membranous ridges (reduced calyx walls) at the sulcate edge of the bisecting apical ridge (the bisecting ridge extends toward the sulcate side and divides, forming a pair of flaps resembling the apical boss in *D. vinitor*; these two flaps are connected by a low transverse ridge extending between

them). The entire sulcus spermaticus between the origin of the enlarged spines and the flounces/calyces is bordered on each side by a line of closely spaced small spines.

Three other retracted hemipenes of *D. crybelum* extended to the middle and end of subcaudal 9 and to the proximal edge of subcaudal 10.

DISCUSSION

Species Groups and Relationships

The recognition of three cryptic species within the *D. vinitor* complex, a detailed understanding of their hemipenial morphology, and comparative data on other species of *Dendrophidion* provide a framework for understanding some aspects of *Dendrophidion* systematics and biogeography. I will elsewhere present detailed hemipenial descriptions of other species of *Dendrophidion* and, for present purposes, mention only a few salient features necessary for understanding hemipenes of the *D. vinitor* complex. Characters suggested here as unifying groups of species are provisional apomorphies pending broader comparative work.

One hemipenial character has been used to define the *D. dendrophis* species group (*D. dendrophis*, *D. nuchale* auctorum, and the three species of the *D. vinitor* complex as defined herein): the presence of "basal spines or elongate hooked villi" or "large basal hooks" (Lieb, 1988; Savage, 2002: 654, 656). As pointed out in the introduction to *Dendrophidion* hemipenes, none of the enlarged spines in *Dendrophidion* hemipenes are truly basal. However, details of hemipenial morphology in the *D. vinitor* complex allow some refinement of hemipenial characterizations of this group. Within the *D. dendrophis* group, only *D. dendrophis* and *D. nuchale* auctorum have a pair of sulcate spines at the proximal edge of the spine array that are enormously enlarged beyond the size of most spines in the array (these two species also have up to two other moderately enlarged spines). These greatly enlarged spines correspond

to the "basal spines" of other authors and are much larger than any other spines on the hemipenis of these two species (unpublished data; see Stuart, 1932).

In contrast, other than a size asymmetry noted below, species of the *D. vinitor* complex have no spines enormously enlarged beyond the majority of "enlarged" spines on the hemipenial body, a detail noted by Smith (1941) in his description of *D. vinitor*. Thus, only part of the *D. dendrophis* species group is characterized by greatly enlarged hemipenial spines. Moreover, although hemipenial spines in the *D. dendrophis* species group are generally larger than those in the *D. percarinatum* group, this generalization does not hold for all species. For example, hemipenial spines in some specimens of *D. percarinatum* are approximately the same relative size as those in *D. vinitor*. While there is great interspecific variation in the absolute sizes of spines in *Dendrophidion*, all species have an array containing "enlarged" spines but the variation in spine size does not clearly distinguish the two species groups. Until more thorough comparative studies of hemipenial morphology within *Dendrophidion* demonstrate consistent differences between the *D. dendrophis* and *D. percarinatum* groups, statements about differences in relative spine enlargement need qualification to account for intragroup variation. The point of dorsocaudal reduction and the prominence of keels on the dorsal scales still provide convenient characters for distinguishing the two species groups of *Dendrophidion*, although whether this convenience reflects phylogeny ultimately should be reexamined.

Is the *D. vinitor* complex monophyletic? Within the *D. dendrophis* group, species of the *D. vinitor* complex share several hemipenial characters compared with *D. dendrophis* and *D. nuchale* auctorum (characters in parentheses): (1) Calyxlike structures reduced to flounces, especially on the asulcate side (Figs. 18, 20, 22) (calyces reduced, but fully formed cuplike structures present on both the sulcate and asulcate

sides); (2) increased number of flounces on the asulcate side compared with the sulcate side (flounces/calyces not increased on asulcate side, perhaps reduced); (3) enlargement of spines within the battery conspicuously asymmetrical, with asulcate spines noticeably larger than sulcate spines, seen especially well in Figure 20, lateral view (no conspicuous general asymmetry in spine enlargement [a pair of enormously enlarged spines on the sulcate side and often another pair toward the asulcate side]); (4) series of freestanding apical ridges with a primarily oblique orientation from a central axis, the median bisecting ridge (freestanding ridges absent; calyces and/or low reticulating ridges may be present). As indicated in the detailed hemipenial descriptions, the freestanding ridges in *D. apharocybe* are reduced to only low rounded ridges, but the pattern of oblique orientation is evident even in such a reduced form (Fig. 20, sulcate view). These characters, plus the absence of several characters uniquely shared by *D. dendrophis* and *D. nuchale* auctorum (e.g., greatly enlarged sulcate spines, a very regular distal row of enlarged spines within the spine array) can be taken as provisional evidence for the monophyly of the *D. vinitor* complex.

Among the three species of the *D. vinitor* complex, the hemipenis of *D. crybelum* stands out because of its unique cylindrical form and great number of enlarged spines. My current assessment is that both of these characters are autapomorphies of *D. crybelum* because the short, bulbous hemipenial form and fewer spines shared by *D. vinitor* and *D. apharocybe* are more widespread within *Dendrophidion*, including the other members of the *D. dendrophis* group, *D. dendrophis* and *D. nuchale* auctorum. On the other hand, *D. apharocybe* and *D. crybelum* share several hemipenial characters relative to *D. vinitor*: (1) reductions in the apical free-standing ridges (more completely reduced in *D. apharocybe* than in *D. crybelum*); (2) poorly developed asulcate calyces that are asymmetrically placed on the right asulcate side; (3) a more strongly

flared tip to the sulcus spermaticus. In addition, *D. apharocybe* and *D. crybelum* are more similar in having wider pale bands that are usually distinct the entire body length and which tend to form pale ocelli on the posterior body. These characters provide evidence suggesting that *D. apharocybe* and *D. crybelum* are more closely related within the *D. vinitor* complex. The apical boss of *D. vinitor* and the nude and strongly inclined apex of *D. apharocybe* are then seen as autapomorphies of these two species.

Apart from hemipenial differences, the three species of the *D. vinitor* complex are exceedingly similar in scutellation and other features generally useful for distinguishing snake species (Table 1). Few of the interspecific comparisons of ventrals, subcaudals, relative tail lengths, maxillary tooth counts, or the point of dorsocaudal reduction were statistically significant. Even in cases in which means were significantly different, the absolute differences were minimal and character ranges overlap substantially, sometimes completely. For example, mean subcaudal number is significantly different between *D. apharocybe* and each of the other two species, but the magnitude of the difference between means in each comparison was only 2.7 or 3.4 (sexes combined). In general, the means for intraspecific differences between males and females were more substantial and of greater statistical significance than interspecific comparisons by sex. The lack of substantive differences in these systematic characters emphasizes the cryptic nature of these species and lends credence to their hypothesized close relationship within *Dendrophidion*.

Biogeography

Considerable progress has been made in understanding biogeographic patterns within Middle America in the last decade. Many of the patterns have been elucidated by comprehensive understanding of phylogeographic patterns shown by Central Ameri-

can snakes, which in many cases have confirmed or refined prior assessments based on patterns of endemism and diversity (reviewed by Daza et al., 2010). Daza et al. (2010) correlated phylogeographic patterns with the history of major tectonic units and concluded that vicariance associated with tectonic events was a predominant agent causing speciation in Middle American snake lineages. Two critical geologic events associated with divergences in snakes are the Motagua–Polochíc fault zone (suture of the Maya and Chortis blocks) in present-day Guatemala (3–8 million years ago [MYA]) and the uplift of the Cordillera de Talamanca in Costa Rica and Panama (2.5–3.9 MYA). Other important events are associated with the Isthmus of Tehuantepec, the Nicaraguan Depression, and the primary Middle–South American transition; however, the temporal span of divergences in these areas are broader than the first two, perhaps because geological events in these areas had differential effects in different lineages.

The distributions and relationships of species in the *D. vinitor* complex proposed here fit nicely into this paradigm. *Dendrophidion vinitor*, the proposed sister taxon to *D. apharocybe*–*D. crybelum*, is distributed entirely north of the Motagua–Polochíc fault zone, and its isolation there most likely reflects the estimated late Miocene–Pliocene divergence in other snake taxa across this zone (Daza et al., 2010). The more recent divergence between *D. apharocybe* and *D. crybelum* accompanied the vicariance of Atlantic and Pacific slope faunas resulting from elevation of the Cordillera Talamanca in the late Pliocene. Chan et al. (2011: 328–331), in an elegant analysis of relationships among populations of the hylid frog *Dendrosophus ebraccatus* across the Talamanca disjunction in Costa Rica and Panama, found the most strongly supported model to be that suggested here for *D. apharocybe*–*crybelum*. At the level of the species concepts developed here, no differentiation has resulted from the other major Central American tectonic events outlined by Daza et al. (2010). Nonetheless, finer scale genetic studies could show some intraspecific differentiation due to these last events.

insights. Craig Guyer, Toby Hibbitts, and David Laurencio exchanged information, photographs, and observations on *Dendrophidion* they collected. Gerardo Cháves provided crucial data on, and photographs of, specimens in the UCR; these helped resolve some enigmatic localities and identities. I am grateful to Roy W. McDiarmid for information on *D. crybelum* and for copies of his color slides, which were scanned and checked by James Poindexter. Charles W. Myers provided copies of his field notes and color slides of Panamanian *Dendrophidion* and saved me from a *nomen deforme* and other calamities. Myers and McDiarmid graciously permitted the use of their photographs in Figures 9 and 15. Colin J. McCarthy provided copies of BMNH ledger pages relevant to *Dendrophidion*. Robert M. Timm (KU) verified data for specimens from the original field notes of Walter Dalquest. I am grateful to all for their help. For comments on the manuscript I thank Roy W. McDiarmid, Charles W. Myers, and Jay M. Savage; they didn't always agree with my presentation but their comments sharpened my thinking and improved the manuscript substantially.

APPENDIX 1. SPECIMENS EXAMINED AND LITERATURE RECORDS FOR *DENDROPHIDION VINITOR* SMITH

Museum abbreviations used throughout are the following: AMNH—American Museum of Natural History (New York). ANSP—Academy of Natural Sciences of Philadelphia. BMNH—British Museum (Natural History) (London). CM—Carnegie Museum (Pittsburgh). KU—University of Kansas Museum of Natural History (Lawrence). LACM—Natural History Museum of Los Angeles County (California). MCZ—Museum of Comparative Zoology (Cambridge). MNHN—Muséum National d'Histoire Naturelle (Paris). TCWC—Texas Cooperative Wildlife Collection, Texas A&M University (College Station). UAZ—University of Arizona Museum of Natural History (Tucson). UCM—University of Colorado Museum of Natural History (Boulder). UCR—Universidad de Costa Rica Museo de Zoología (San José). UF—Florida Museum of Natural History, University of Florida (Gainesville). UIMNH—University of Illinois Museum of Natural History (Urbana). UMMZ—University of Michigan Museum of Zoology (Ann Arbor). USNM—National Museum of Natural History, Smithsonian Institution (Washington, DC). UTACV—University of

Texas at Arlington Collection of Vertebrates (Arlington). UTEP—University of Texas at El Paso Centennial Museum (El Paso).

Bracketed data associated with localities here and elsewhere in the text are inferences derived from sources other than the original data associated with specimens as recorded in literature, museum or collectors' catalogues, or specimen labels. Some museum databases (e.g., USNM) unfortunately do not distinguish "original" and "inferred" locality information in this era of databasing and georeferencing, and I have of necessity in most cases taken these sources at face value.

Belize: *Toledo:* Little Quartz Ridge [summit, 940–1,035 m], KU 300784 (Fig. 6). **Guatemala:** "Vera Paz" (Duméril et al. 1870–1909: 732; see comments under Distribution). [*Alta Verapaz*]: between Cobán and Lanquín, BMNH 64.1.26.21 (Stafford, 2003; specimen not seen; see comments under Distribution). *Izabal:* Sierra de Santa Cruz, Semococh, 8 km W Finca Semuc headquarters, UTACV 22155. Sierra de Santa Cruz, Finca Semuc, Serujijá Mountain, 15°37′09″N, 89°22′05″W, 600 m, UTACV 22755. *Petén:* "Peten," no specific locality (Duméril et al. 1854: 208, = MNHN 7353 fide Lieb, 1988: 164, Fig. 1; specimen not seen); Duméril et al. 1870–1909: 732; see comments under Distribution). Piedras Negras, USNM 110662 (holotype; Fig. 1). **Mexico:** No specific locality, USNM 7099 (paratype of *D. vinitor* Smith, specimen not seen; Smith, 1941). *Chiapas:* Presa Malpaso (Alvarez del Toro, 1972: 142, 1982: 191). 26 km N Ocozocuautla (Johnson et al. "1976" [1977], presumably UTEP 6038 cited by Lieb, 1988; specimen not seen). Approximately 8 km S Solosuchiapa, camp on Rio Teapa, ca. 400 ft. [120 m], UAZ 24161. *Oaxaca:* Río Chicapa near El Atravesado, 1,600 ft. [488 m], AMNH R-66845. Donají, Mije [province], UCM 39911–12, 44481. La Gloria (north of Niltepec), 1,500 ft. [457 m], FMNH 126554–55. La Gloria, UIMNH 17632, 35546–47, 37094–95, 37165; TCWC 12797. La Gloria-Cerro Azul, UIMNH 35548. Río Negro (Grijalva), Juchitán [province], UCM 41162. *Tabasco:* Teapa, USNM 46589 (paratype of *D. vinitor* Smith, 1941; specimen not seen). *Veracruz:* Bastonal (8 mi E of Cuatzelapa, Lago Catemaco), CM 41478. Forest at Cascapel, upper Uzpanapa river, Isthmus of Tehuantepec, BMNH 1936.6.6.8 (Stafford, 2003; specimen not seen); see Appendix 2 for comments. Near Coyame, 1,400 ft. [427 m], UMMZ 111450. Coyame, 9–10 mi E Catemaco, UIMNH 39154, 82444. Isla (Perez-Higareda and Smith, 1991: 31). 60 km SE Jesus Carranza, 450 ft. [137 m], KU 23965. 25 km SE Jesus Carranza, 250 ft. [76 m], KU 27564. Las Minas (Perez-Higareda and Smith, 1991: 31). Los Tuxtlas (Perez-Higareda and Smith, 1991: 31). Motzorongo (Dugés 1892). Tesechoacan (Perez-Higareda and Smith, 1991: 31). Uxpanapa (Perez-Higareda and Smith, 1991: 31). SE slope Volcán San Martín, approximately 2,600 ft. [793 m], UMMZ 121145. Volcán San Martín near base, UMMZ 122767. Volcán San Martín, UIMNH 33862. Volcán San Martín, El Tular Station, UIMNH 35472.

APPENDIX 2. GAZETTEER

Except where otherwise stated, coordinates for place names are from the National Geospatial-Intelligence Agency (NGA) online gazetteer (GEOnet Names Server): http://earth-info.nga.mil/gns/html/. A few coordinates were taken from Google Earth (GE). Many specimens of *Dendrophidion vinitor* were obtained by Thomas MacDougall, field biologist extraordinaire, whose collections significantly advanced many fields of Mexican zoology and botany (Stix, 1975). Goodwin (1969) reported MacDougall's mammal collections, and I quote from his brief characterizations of various Oaxacan localities before human alteration in the last half century; Goodwin had the opportunity to work directly with MacDougall's notes (Root, 1975). The three northern countries harboring *D. vinitor* are listed first, followed by an alphabetical listing of other Middle American countries with the other two members of the *D. vinitor* complex.

BELIZE AND GUATEMALA (*Dendrophidion vinitor*)

Cobán to Lanquín (Guatemala: Alta Verapaz). Approximately 15°34′N, 90°09′W (coordinates arbitrarily about midway along the route between the two places). Cobán (approximately 1,320 m elevation) and Lanquín (approximately 335 m) lie about 43 airline kilometers apart in the Río Cahabón basin (north side of the Sierra de Santa Cruz and near Finca Semuc, whence come the only recent Guatemalan records of *D. vinitor*).

Finca Semuc, Serujijá Mountain, Sierra de Santa Cruz, 600 m (Guatemala: Izabal). 15°37′09″N, 89°22′05″W (coordinates from 1:50,000 topographic map, Instituto Geográfico Nacional, Guatemala; provided by the collector of UTACV 22755, Eric N. Smith).

Little Quartz Ridge (Belize: Toledo). 16°24′N, 89°05′W. The single known Belize specimen of *D. vinitor* was collected at the summit of the ridge, given as "940–1035 m elevation" (Meerman and Lee, 2003, table 1). The environment of the area is described in Meerman and Matola (2003).

Piedras Negras (Guatemala: Petén). 17°11′N, 91°15′W. Type locality of *D. vinitor* Smith.

Semococh, 8 km W Finca Semuc headquarters, Sierra de Santa Cruz (Guatemala: Izabal). This locality is seemingly none of several "Semococh" indexed by NGA, most of which are in Alta Verapaz department. Presumably close to coordinates for Finca Semuc listed above.

MEXICO (*Dendrophidion vinitor*)

Bastonal (8 mi E of Cuatzelapa, Lago Catemaco) (Veracruz). 18°19′N, 94°54′W.

Cascapel, upper Uzpanapa river, Isthmus of Tehuantepec (Veracruz). Not located. The spelling "Cascapel" seems clear in BMNH ledgers, as listed by Stafford (2003). This may be a transcription error for "Cascajal" (or El Cascajal), a village on the upper Río Uxpanapa in extreme southeastern Veracruz near the Oaxaca border (17°37′N, 94°08′W).

Cerro Azul (Oaxaca). See La Gloria.

Coyame, 9–10 mi E Catemaco (Veracruz). 18°26′N, 95°00′W. (and Near Coyame, 1,400 ft. [427 m]).

Donají, Mije [province] (Oaxaca; MacDougall). 17°13′53″N, 95°03′40″W. 90 m elevation in "rainforest" fide Duellman (1960: 34).

El Atravesado (Oaxaca). See Río Chicapa.

El Tular (Veracruz). See Volcán San Martín.

Isla (Veracruz). At least three localities with this name are in Veracruz: 18°36′N, 96°09′W and 18°02′N, 95°31′30″W (NGA); and "La Isla": 17°25′N, 94°01′W (Esparza-Torres, undated).

Jesús Carranza. 60 km SE, 450 ft. [137 m] (KU 23965); and 25 km SE, 250 ft. [76 m] (KU 27564) (both Veracruz). These are localities of Walter W. Dalquest (see Hall and Dalquest, 1963). Original KU catalogue data for the "60 km" locality gave the compass direction as "SW" from Jesús Carranza, which would place the locality in Oaxaca rather than Veracruz. However, according to Robert M. Timm, Dalquest's field catalogue in the Mammal Division at KU has the locality corrected by hand (presumably by Dalquest himself) to "60 km SE Jesús Carranza." According to the itinerary given in Hall and Dalquest (1963: 177), Dalquest worked out of a village (Zapotal) on the Río Coatzacoalcos during the period when KU 23965 was collected. His field notes for mammals collected at the same time indicate that he traveled upriver via the Río Chalchijapa and then Río Solosuchil. Coordinates from the gazetteer of Hall and Dalquest (1963: 184) are: junction of the Río Chalchijapa with the Río Coatzacoalcos (approximately 17°27′N, 94°50′W); junction of the Río Solosuchil with the Río Chalchijapa (approximately 17°23′N, 94°47′W); and "Río Solosuchil" (17°14′N, 94°28′W). Coordinates for the river junctions are quite accurate, as verifiable using Google Earth. The "Río Solosuchil" locale is in southern Veracruz at its headwaters near the Oaxaca border, and close to 60 airline kilometers from Jesús Carranza in an ESE direction (perusal of Hall and Dalquest [1963] suggests they used a fairly loose interpretation of compass directions). This is perhaps the approximate location of KU 23965 (it is not clear whether Dalquest used airline or river distances). In any case, KU 23965 was apparently collected along the Río Solosuchil in southern Veracruz.

La Gloria (north of Niltepec), 1,500 ft. [457 m] (Oaxaca; MacDougall). 16°47′17″N, 94°36′40″W. Located 7 mi S of Santa María Chimalapa in Juchitán district (Goodwin, 1969: 259). Usually stated simply "La Gloria," this is the origin of more specimens of *D. vinitor* in U.S. collections than any other single locality (rivaled only by Volcán San

Martín in Veracruz). Cerro Azul, associated with La Gloria in one specimen locality, is a local name for high parts of the Sierra Madre of Oaxaca–Chiapas, 25 mi NW of Santo Domingo Zanátepec, also in Juchitán district (Goodwin, 1969: 257); this is not the same "Cerro Azul" indexed by NGA. All of the La Gloria specimens were obtained by Thomas MacDougall. Habitats at La Gloria include "coffee plantations, milpas, rainforest," whereas Cerro Azul harbors "cloud forest" (Goodwin, 1969: 257).

Las Minas (Veracruz). 19°42′N, 97°07′W.

Los Tuxtlas (Veracruz). 18°30′N, 95°10′W.

Motzorongo (Veracruz) 18°39′N, 96°44′W. Goldman (1951: 277) gives the elevation as 800 ft. (244 m) but in steeply dissected country with hills rising locally to 1,500 ft. (457 m). Goldman (1951: 277–278, 316) briefly describes the vegetation ("fairly uniformly covered with evergreen forest"), which he classified as "Humid Lower Tropical Zone."

Ocozocuautla, 26 km N (Chiapas). About 16°55′N, 93°27′W.

Presa Malpaso (Chiapas). 17°08′N, 93°30′W. Also known as Presa Netzahualcóyotl.

Río Chicapa near El Atravesado, 1,600 ft. [488 m] (Oaxaca; MacDougall). Pacific drainage. El Atravesado (16°41′N, 94°35′W) is a village near a mountain of the same name. This is an inland locality on the Río Chicapa, not the coastal locality between Unión Hidalgo and the river's mouth in Laguna Superior indexed by Goodwin (1969: 262). Cerro Atravesado is a "large flat-topped hill 18 mi S of Santa Maria Chimalapa [with] open pine stands, grass and rocks, patches of "cloud forest" at the north end" (Goodwin, 1969: 257).

Río Negro (Grijalva), Juchitán [district] (Oaxaca; MacDougall). Atlantic drainage. Goodwin (1969: 262) gives two MacDougall localities with this designation: "[Río Grijalva system at] Junction of Río Negro with Río 'Porta Monedo' [sic] near Chiapas border 29 mi north of Tapanatepec," and 5 mi west of this junction. The "Río Porta Moneda" is in the headwaters of the Río Encajonado system (Goodwin, 1969: 262). Coordinates from NGA: Río Negro, 16°49′36″N, 94°01′25″W; Río Portamonedas, 16°41′15″N, 94°08′22″W. Goodwin (1969) notes "heavy shade of trees in river flat" for the river junction and "many tree ferns … rainforest [and] tapir trails" for the nearby camp.

Solosuchiapa, approximately 8 km S; camp on Rio Teapa, ca. 400 ft. [122 m] (Chiapas). 17°24′N, 93°01′W.

Teapa (Tabasco). 17°33′N, 92°57′W. 800 ft. [244 m] in the Humid Lower Tropical Zone fide Goldman (1951: 257–259).

Tesechoacan (Veracruz). 18°08′N, 95°40′W.

Uxpanapa (Veracruz). A name associated with several locations in southeastern Veracruz, including a major river and at least three towns.

Volcán San Martín (Veracruz). 18°33′N, 95°12′W. A number of localities on the slopes of this volcano (near the base; SE slope, approximately 2,600 ft. [793 m]). The volcano is now part of the Los Tuxtlas Biosphere Reserve. Several places in southern Veracruz have the name El Tular, El Tular station being on the southwestern flank of the Volcán San Martín within the boundaries of the reserve (approximately 18°30′N, 95°13′W, 600 m). Goldman (1951: 283) stated that virgin [rainforest] covered the mountain and that "from the sloping plain the heavy forest, full of small palms, vines, and other undergrowth up to about 4,800 feet changed but little."

COSTA RICA (*Dendrophidion apharocybe* and *D. crybelum*)

Cacao Biological Station, 729–1,528 m (Guanacaste). 10°56′N, 85°28′W. Part of the Area de Conservación Guanacaste, the station is on the southwestern slope of Volcán Cacao at about 1,000 m. Montane rainforest to cloud forest on the upper slopes, transitioning to dry forest on the western lower slopes.

Carara National Park (Puntarenas and San José). 09°46′30″N, 84°36′25″W. Near the Pacific coast in northern Puntarenas and extreme western San José provinces. Origin of two specimens erroneously referred to "*Dendrophidion vinitor*" (Laurencio and Malone, 2009) indicated on the distribution map of Savage (2002: 656). These specimens are *D. percarinatum*. See Distribution in the *D. apharocybe* species account and Figure 17.

Cajón, N bank of Río Térraba (Puntarenas). 08°56′30″N, 83°20′W, about 80 m. Source of an apparently erroneous lowland Pacific locality for "*D. vinitor*" indicated by Savage (2002: 656). See text discussion under Distribution in species account for *D. apharocybe*.

Finca La Selva (Heredia). 10°26′N, 83°59′W, 35–137 m (McDade and Hartshorn, 1994). Now the La Selva Biological Station of the Organization for Tropical Studies. Type locality of *D. apharocybe*.

Finca Las Alturas, 1,330 m (Puntarenas). 08°57′N, 82°50′W. Presently the Las Alturas Biological Station operated by the Organization for Tropical Studies.

Finca Las Cruces, near San Vito de Java, 4 km S San Vito, 1,200 m (Puntarenas). 08°47′35″N, 82°57′30″W (Wake et al., 2007: 557). Presently the Las Cruces Biological Station operated by the Organization for Tropical Studies. Type locality of *D. crybelum*.

Finca Mellizas, 14 km ENE La Unión near Panama border (Puntarenas). 08°53′08″N, 82°46′42″W, approximately 1,310 m (GE).

Finca Loma Linda, 2 km SSW Canas Gordas, 1,170 m (Puntarenas). 08°43.3′N, 82°54.3′W (Wake et al., 2007).

Guápiles (Limón). 10°17'N, 83°46'W.

La Selva (Heredia). See Finca La Selva.

Mt. [Cerro] Mirador near Suretka (Limón). 09°36'N, 82°57'W.

Pandora, 50 m (Limón). 09°44'N, 82°58'W.

Pavones, ca. 2.5 km N, 700 m (Cartago). Near Turrialba. 09°57'N, 083°37'W.

Poco Sol de La Tigre, 540 m (Alajuela). 10°22'N, 84°37'W.

Puerto Viejo de Sarapiquí, 10 km WSW (Heredia). 10°28'N, 84°01'W.

San Clemente, 7 km NW Penshurst (Limón). 09°50'N, 82°56'W.

Silencio, 875–940 m (Guanacaste). 10°28'N, 84°54'W.

Suretka (Limón). 9°34'N, 82°56'W. See also Mt. Mirador.

Río Puerto Viejo near junction with Río Sarapiquí (Heredia). 10°28'N, 84°02'W.

Zona Protectora, La Selva, trail from 1,000 m camp to 1,500 m camp, 990 m (Heredia). Approximately 10°17'N, 84°04'W. See Pringle et al. (1984).

HONDURAS (*Dendrophidion apharocybe*)

Bodega de Río Tapalwás, 190 m (Gracias a Dios). 14°55'39"N, 84°32'02"W. About 20 km NW Rus Rus. Wilson et al. (2003: 18); McCranie et al. (2006: 265).

Caño Awalwás (camp), 100 m (Gracias a Dios). 14°49'N, 84°52'W. Wilson et al. (2003: 18). McCranie et al. (2006: 261).

Crique Ibantara, 70 m (Gracias a Dios). 14°47'N, 84°27'W. A tributary of the Río Rus Rus. Wilson et al. (2003: 18); McCranie et al. (2006: 263).

Crique Wahatingni, near (Gracias a Dios). Tributary of Río Tapalwás, 200 m. McCranie et al. (2006: 265).

Crique Yulpruan, near; 140 m (Gracias a Dios). 14°54'N, 84°31'W. Tributary of Río Tapalwás, 200 m. McCranie et al. (2006: 266).

Hiltara Kiamp, 150 m (Gracias a Dios). 14°57'N, 84°40'W. Along the upper portion of the Río Warunta (McCranie, 2011: 615).

Las Marías, 20 m (Gracias a Dios). 15°40'N, 84°53'W (GE). A village along the Río Plátano (McCranie, 2011: 620). Figures transposed in latitude given by McCranie (2011: 620; 15°04'N).

Planes de San Esteban, 1,100 m (Olancho) 15°05'N, 85°42'W. Northern slope of the Sierra de Agalta (McCranie, 2011: 609).

Sachin Tingni, 150 m (Gracias a Dios). 14°57'N, 84°40'W. Tributary of Río Warunta (McCranie, 2011: 633).

Warunta Tingni Kiamp, 150 m (Gracias a Dios). 14°55'20"N, 84°41'28"W. Campsite along upper portion of Río Warunta (McCranie et al., 2006: 266).

NICARAGUA (*Dendrophidion apharocybe*)

Cara de Mono (Atlántico Sur), ca. 120 m. 12°07'N, 84°28'W.

Hacienda La Cumplida, 19 km N of Matagalpa, 2,500 ft. [762 m] (Matagalpa). 13°00'N, 85°51'W.

Matagalpa (Matagalpa). 12°55'N, 85°55'W.

Musawas, Waspuc River (Atlántico Norte). 14°08'59.6"N, 84°42'18.4"W.

Recero. See Recreo.

Recreo, Río Mico (Atlántico Sur). About 50 m. 12°10'N, 84°19'W. Gaige et al. (1937; see especially pp. 2–3) referred to this place as "Recero" in text and an accompanying map from information provided by Morrow J. Allen, the collector of UMMZ specimens, based in turn on a "U.S. Marine Corps survey map ca. 1930." The field notebooks of Allen at UMMZ also refer to the place as Recero (Gregory E. Schneider, personal communication, January 2011). No independent sources I have seen refer to the place as "Recero," which seems to be in the same location as "Recreo" or "El Recreo" in gazetteers and on modern maps (e.g., NGA and Google Earth). "Recero" appears in no geographic reference on Nicaragua that I consulted, including maps and gazetteers contemporary with and earlier than Gaige et al. (1937). However, the place is listed as "Recreo" in several other taxonomic works (e.g., Smith [1941: 74, 76], Smith and Taylor [1950: 320], Dunn and Stuart [1951: 58]). All of these seem ultimately to trace back to Allen's material or to Gaige et al. (1937).

Río Mico, 10 mi above Recreo (Atlántico Sur). Approximately 12°07'N, 84°28'W. See locality notes for Recreo above.

Río San Juan (Río San Juan). River along the frontier between eastern Nicaragua and Costa Rica.

Santo Domingo, Chontales Mines, 2,000 ft. (610 m) (Chontales). 12°16'N, 85°05'W. The locale was made famous by Belt (1874), who described the environment and geology of the area.

PANAMA (*Dendrophidion apharocybe*)

Almirante, 10 m (Bocas del Toro). 09°18'N, 82°24'W. 11 km NW Almirante, 600 ft. [183 m] (Bocas del Toro); about 09°21'N, 82°28'W.

Cerro Arizona above Alto de Piedra, North of Santa Fe (Veraguas). Not located. Alto de Piedra is a small village about 3 airline kilometers NW (not strictly N as in the original locality data) of the town of Santa Fe (8°31'N, 81°04'W).

Cerro Azul region, Río Piedra (Panamá). 09°13'N, 79°18'W (Fairchild and Handley, 1966).

Cerro Campana, 900–950 m (Panamá). 08°41'N, 79°56'W (Fairchild and Handley, 1966). Myers (1969: 28) described the area, paraphrased here: Small area of cloud forest above 870 m. Forest of moderate height, with few large trees, many small trees, a scattering of tree ferns and small palms, a few stilt palms. Dense cover of bushes, herbs, ferns. Once abundant tree and ground bromeliads and other epiphytes have been reduced. Disturbed vegetation on the top.

Cerro Delgadito, 2–4 mi W Santa Fe (Veraguas). Approximately 08°30′N, 81°07′W (GE).

Cerro Malí (Darién). 08°07′N, 77°14′W (Fairchild and Handley, 1966). According to Myers (1969: 25) Cerro Malí is about 1,410 m elevation and southeast of Cerro Tacarcuna and the headwaters of the Río Pucro (= Río Pucuro; see Myers and Lynch, 1997, figs. 1 and 2). It lies at the southeastern end of the Serranía del Darién, a ridge separating the Pacific-draining Río Tuira system from the Atlantic lowlands of eastern Panama and northern Colombia (the international border follows the continental divide along this ridge). Myers (1969: 24–25) described the general topography and environment. Additional perspectives and details are in Anthony (1916, 1923), Gentry (1983), and Myers and Lynch (1997).

El Copé, continental divide north of, 600–700 m (Coclé). The village of El Copé is at 08°37′N, 80°35′W (Fairchild and Handley, 1966). El Copé (Omar Torrijos) National Park now encompasses the continental divide.

Isla Popa, south end of, 1 km E of Sumwood Channel (Bocas del Toro). Approximately 09°09′N, 82°08′W.

Laguna, 820 m (Darién). 08°04′N, 77°19′W (Fairchild and Handley, 1966). According to Charles W. Myers (personal communication), this locality is on a "ridge south of the Río Tacarcuna (upper tributary of Río Pucuro, Tuira drainage)." Also referred to as "La Laguna," it is not the village of the same name near the coast in southwestern Darién Province (e.g., as indexed in the NGA), with which it is sometimes confused.

La Loma, W Panama (Bocas del Toro). 08°50′N, 82°12′W. Also known as Buenavista. 1,200 ft. elevation (366 m) on the Atlantic slope along a trail from Chiriquí Lagoon to David (Dunn, 1942: 478).

Peninsula Valiente, Bluefields, 70 m (Bocas del Toro). 09°11′N, 81°55′W. Peninsula Valiente delimits the eastern side of the Laguna de Chiriquí.

Peninsula Valiente, Quebrada Hido (Bocas del Toro). Not located.

Pequení–Esperanza ridge, near head of Río Pequení, 2,000 ft. [610 m] (Panamá). Approximately 09°29′N, 79°24′W. Now within Parque Nacional Chagres. A ridge northeast of Lago Alajuela (Madden Lake), running roughly northeast to southwest and separating the Chagres–Esperanza river system from the Pequení–Boquerón system (Dunn and Bailey, 1939: 4, 15). Cadle and Myers (2003: 15–17) described some of the geography of the area as altered by damming associated with construction of the Panama Canal. Ibáñez et al. ("1994" [1995], fig. 1) provided an outline map of the major rivers of the region.

Pequení–Esperanza ridge, junction main divide, 1,200 ft. [366 m] (Panamá). Approximately 09°20′N, 79°20′W. Location not precisely indicated by Dunn and Bailey (1939) but presumably at a lower elevation along the ridge closer to Lago Alajuela than the above-listed locality near the head of the Río Pequení (see above cited references).

Summit site, border of Darién, 320 m (San Blas). 08°55′N, 77°51′W (coordinates from the collector of FMNH 170138, Michael Duever). Also known as Camp Summit, a canal survey camp in the Serranía del Darién discussed by Myers (1969: 26–27, fig. 1), who gave the elevation as 358 m.

LITERATURE CITED

ALVAREZ DEL TORO, M. 1972. *Los Reptiles de Chiapas.* Segunda edition. Tuxtla Gutierrez, Chiapas, Mexico: Gobierno del Estado de Chiapas.

ALVAREZ DEL TORO, M. 1982. *Los Reptiles de Chiapas.* Tercera edition. Tuxtla Gutierrez, Chiapas, Mexico: Instituto de Historia Natural.

ANTHONY, H. E. 1916. Panama mammals collected in 1914–1915. *Bulletin of the American Museum of Natural History* **35**: 357–376 + foldout map.

ANTHONY, H. E. 1923. In the footsteps of Balboa. *Natural History* **23**: 312–324.

AUTH, D. L. 1994. Checklist and bibliography of the amphibians and reptiles of Panama. *Smithsonian Herpetological Information Service* **98**: 1–59.

BARBOUR, T., AND A. LOVERIDGE. 1946. First supplement to typical reptiles and amphibians. *Bulletin of the Museum of Comparative Zoology* **96**: 59–214.

BELT, T. 1874. *The Naturalist in Nicaragua, a Narrative of a Residence at the Gold Mines of Chontales; Journeys in the Savannahs and Forests; with Observations on Animals and Plants in Reference to the Theory of Evolution of Living Forms.* London: John Murray.

BOLAÑOS, F., J. M. SAVAGE, AND G. CHÁVES. 2010. Anfibios y reptiles de Costa Rica (versión: 18 de Agosto del 2010). *Listas Zoológicas Actualizadas UCR.* San Pedro: Museo de Zoología, Universidad de Costa Rica. Available from: http://museo.biologia.ucr.ac.cr/ Listas/LZAPublicaciones.htm. Accessed 1 January 2011.

BOULENGER, G. A. 1894. *Catalogue of the snakes in the British Museum (Natural History).* Volume 2. London: British Museum (Natural History).

CADLE, J. E. 2005. Systematics of snakes of the *Dipsas oreas* complex (Colubridae: Dipsadinae) in western Ecuador and Peru, with revalidation of *D. elegans* (Boulenger) and *D. ellipsifera* (Boulenger). *Bulletin of the Museum of Comparative Zoology* **158**: 67–136.

CADLE, J. E. 2007. The snake genus *Sibynomorphus* (Colubridae: Dipsadinae: Dipsadini) in Peru and Ecuador, with comments on the systematics of

Dipsadini. *Bulletin of the Museum of Comparative Zoology* **158**: 183–284.

CADLE, J. E. 2010. Systematics, natural history, and hemipenial morphology of *Dendrophidion brunneum* (Günther), a poorly known snake from the Andes of Ecuador and Peru. *Zootaxa* **2433**: 1–24.

CADLE, J. E., AND C. W. MYERS. 2003. Systematics of snakes referred to *Dipsas variegata* in Panama and western South America, with revalidation of two species and notes on defensive behaviors in the Dipsadini Colubridae). *American Museum Novitates* **3409**: 1–47.

CAMPBELL, J. A. 1998. *Amphibians and Reptiles of Northern Guatemala, the Yucatan, and Belize.* Norman: University of Oklahoma Press.

CAMPBELL, J. A., AND J. P. VANNINI. 1989. Distribution of amphibians and reptiles in Guatemala and Belize. *Proceedings of the Western Foundation of Vertebrate Zoology* **4**: 1–21.

CHAN, L. M., J. L. BROWN, AND A. D. YODER. 2011. Integrating statistical genetic and geospatial methods brings new power to phylogeography. *Molecular Phylogenetics and Evolution* **59**: 523–537.

COCHRAN, D. M. 1961. Type specimens of reptiles and amphibians in the U.S. National Museum. *Bulletin of the United States National Museum* **220**: 1–291.

DARLING, D. M., AND H. M. SMITH. 1954. A collection of reptiles and amphibians from eastern Mexico. *Transactions of the Kansas Academy of Science* **57**: 180–195.

DAZA, J. M., T. A. CASTOE, AND C. L. PARKINSON. 2010. Using regional comparative phylogeographic data from snake lineages to infer historical processes in Middle America. *Ecography* **33**: 343–354.

DOWLING, H. G., AND J. M. SAVAGE. 1960. A guide to the snake hemipenis: a survey of basic structure and systematic characteristics. *Zoologica* **45**: 17–31.

DUELLMAN, W. E. 1960. A distributional study of the amphibians of the Isthmus of Tehuantepec, Mexico. *University of Kansas Publications, Museum of Natural History* **13**: 19–72.

DUELLMAN, W. E. 1963. Amphibians and reptiles of the rainforests of southern El Petén, Guatemala. *University of Kansas Publications, Museum of Natural History* **15**: 205–249.

DUELLMAN, W. E. 1966. The Central American herpetofauna: an ecological perspective. *Copeia* **1966**: 700–719.

DUGÉS, A. 1892. El *Dendrophidium dendrophis* Schl. Fitz. Syst. Rept. 1843. *La Naturaleza* ser. 2, **2**: 100–101 + 1 pl.

DUMÉRIL, A. H. A., M.-F. BOCOURT, AND F. MOCQUARD. 1870–1909. *Mission Scientifique au Mexique et dans l'Amérique Centrale. Recherches Zoologiques, Troisième Partie, Première Section: Études sur les Reptiles.* Paris: Imprimerie Impériale.

DUMÉRIL, A. M. C., G. BIBRON, AND A. H. A. DUMÉRIL. 1854. *Erpétologie Générale ou Histoire Naturelle Complète des Reptiles.* Tome 7. Paris: Librairie Encyclopédique de Roret.

DUNN, E. R. 1933. Amphibians and reptiles from El Valle de Anton, Panama. *Occasional Papers of the Boston Society of Natural History* **8**: 65–79.

DUNN, E. R. 1942. The American caecilians. *Bulletin of the Museum of Comparative Zoology* **91**: 437–540.

DUNN, E. R., AND J. R. BAILEY. 1939. Snakes from the uplands of the Canal Zone and of Darien. *Bulletin of the Museum of Comparative Zoology* **86**: 1–22.

DUNN, E. R., AND L. C. STUART. 1951. Comments on some recent restrictions of type localities of certain South and Central American amphibians and reptiles. *Copeia* **1951**: 55–61.

ESPARZA-TORRES, H. F. Undated [ca. 1977]. *Estado de Veracruz* [Map of the state of Veracruz]. Mexico City: Librería Patria.

FAIRCHILD, G. B., AND C. O. HANDLEY, JR. 1966. Gazetteer of collecting localities in Panama, pp. 9–20 + map. *In* R. L. Wenzel and V. J. Tipton (eds.), *Ectoparasites of Panama.* Chicago: Field Museum of Natural History.

FAUTH, J. E., B. I. CROTHER, AND J. B. SLOWINSKI. 1989. Elevational patterns of species richness, evenness, and abundance of the Costa Rican leaf-litter herpetofauna. *Biotropica* **21**: 178–185.

FLORES-VILLELA, O. 1993. Herpetofauna Mexicana. Lista anotada de las especies de anfibios y reptiles de México, cámbios taxonómicos recientes, y nuevas especies. *Carnegie Museum of Natural History, Special Publication* **17**: iv + 73 pp.

FLORES VILLELA, O., AND P. GEREZ. 1988. *Conservación en México: Síntesis sobre Vertebrados Terrestres, Vegetación, y Uso del Suelo.* Xalapa, Veracruz, Mexico: Instituto Nacional de Investigaciones sobre Recursos Bióticos.

GAIGE, H. T., N. HARTWEG, AND L. C. STUART. 1937. Notes on a collection of amphibians and reptiles from eastern Nicaragua. *Occasional Papers of the Museum of Zoology, University of Michigan* **357**: 1–18.

GENTRY, A. H. 1983. A biological exploration of Cerro Tacarcuna. *National Geographic Research Reports* **15**: 233–235.

GOLDBERG, S. R. 2003. Reproduction in four species of *Dendrophidion* from Costa Rica (Serpentes: Colubridae). *Transactions of the Illinois State Academy of Science* **96**: 295–300.

GOLDMAN, E. A. 1951. *Biological Investigations in México* (Smithsonian Miscellaneous Collections 115). Washington, DC: Smithsonian Institution.

GOODWIN, G. G. 1969. Mammals from the state of Oaxaca, Mexico, in the American Museum of Natural History. *Bulletin of the American Museum of Natural History*, **141**: 1–270 + pls. 1–40.

GÜNTHER, A. C. L. G. 1885–1902. *Biologia Centrali-Americana, Reptilia and Batrachia* [SSAR reprint 1987]. Ithaca, New York: Society for the Study of Amphibians and Reptiles.

GUYER, C. 1994. The reptile fauna: diversity and ecology, pp. 210–216 + appendix 6. *In* K. S. Bawa, G. S. Hartshorn, H. A. Hespenheide, and L. A. Macdade (eds.), *La Selva: Ecology and Natural*

History of a Neotropical Rainforest. Chicago: The University of Chicago Press.

GUYER, C., AND M. A. DONNELLY. 1990. Length-mass relationships among an assemblage of tropical snakes in Costa Rica. *Journal of Tropical Ecology* **6**: 65–76.

GUYER, C., AND M. A. DONNELLY. 2005. *Amphibians and Reptiles of La Selva, Costa Rica, and the Caribbean Slope: A Comprehensive Guide.* Berkeley: University of California Press.

HALL, E. R., AND W. W. DALQUEST. 1963. The mammals of Veracruz. *University of Kansas Publications, Museum of Natural History,* **14**: 165–362.

HOLDRIDGE, L. R. 1967. *Life Zone Ecology.* Revised edition. San José, Costa Rica: Tropical Science Center.

HOLDRIDGE, L. R., W. C. GRENKE, W. H. HATHEWAY, T. LIANG, AND J. A. TOSI, JR. 1971. *Forest Environments in Tropical Life Zones, a Pilot Study.* Oxford, United Kingdom: Pergamon Press.

IBÁÑEZ, D. R., F. A. AROSEMENA, F. A. SOLÍS, AND C. A. JARAMILLO. "1994" [1995]. Anfibios y reptiles de la Serranía Piedras-Pacora, Parque Nacional Chagres. *Scientia (Panamá)* **9**: 17–31.

IBÁÑEZ, D. R., AND F. A. SOLÍS. "1991" [1993]. Las serpientes de Panamá: lista de especies, comentarios taxonómicos y bibliografía. *Scientia (Panamá)* **6**: 27–52.

JANZEN, D. H. 1973. Sweep samples of tropical foliage insects: description of study sites, with data on species abundances and size distributions. *Ecology* **54**: 659–686.

JOHNSON, J. D. 1989. A biogeographic analysis of the herpetofauna of northwestern Nuclear Central America. *Milwaukee Public Museum Contributions in Biology and Geology* **76**: 1–66.

JOHNSON, J. D., C. A. ELY, AND R. G. WEBB. "1976" [1977]. Biogeographical and taxonomic notes on some herpetozoa from the northern highlands of Chiapas, Mexico. *Transactions of the Kansas Academy of Science* **79**: 131–139.

KLUGE, A. G. 1984. Type-specimens of reptiles in the University of Michigan Museum of Zoology. *Miscellaneous Publications of the Museum of Zoology, University of Michigan* **167**: 1–85.

KÖHLER, G. 2003. *Reptiles of Central America.* English edition. Offenbach, Germany: Herpeton.

KÖHLER, G. 2008. *Reptiles of Central America.* 2nd English edition. Offenbach, Germany: Herpeton.

LAURENCIO, D., AND J. H. MALONE. 2009. The amphibians and reptiles of Parque Nacional Carara, a transitional herpetofaunal assemblage in Costa Rica. *Herpetological Conservation and Biology* **4**: 120–131.

LEE, J. C. 1980. An ecogeographic analysis of the herpetofauna of the Yucatan Peninsula. *University of Kansas Museum of Natural History, Miscellaneous Publications,* **67**: 1–75.

LEE, J. C. 1996. *The Amphibians and Reptiles of the Yucatán Peninsula.* Ithaca: Comstock Publishing Associates.

LEE, J. C. 2000. *A Field Guide to the Amphibians and Reptiles of the Maya World, the Lowlands of Mexico, Northern Guatemala, and Belize.* Ithaca: Cornell University Press.

LIEB, C. S. 1988. Systematic status of the Neotropical snakes *Dendrophidion dendrophis* and *D. nuchalis* (Colubridae). *Herpetologica* **44**: 162–175.

LIEB, C. S. 1991. *Dendrophidion vinitor.* Catalogue of American Amphibians and Reptiles, **522**: 522.1–522.2.

LIPS, K. R. 1998. Decline of a tropical montane amphibian fauna. *Conservation Biology* **12**: 106–117.

LIPS, K. R. 1999. Mass mortality and population declines of anurans at an upland site in western Panama. *Conservation Biology* **13**: 117–125.

LIPS, K. R., F. BREM, R. BRENES, J. D. REEVE, R. A. ALFORD, J. VOYLES, C. CAREY, L. LIVO, A. P. PESSIER, AND J. P. COLLINS. 2006. Emerging infectious disease and the loss of biodiversity in a Neotropical amphibian community. *Proceedings of the National Academy of Sciences, USA* **103**: 3165–3170.

LIPS, K. R., D. E. GREEN, AND R. PAPENDICK. 2003. Chytridiomycosis in wild frogs from southern Costa Rica. *Journal of Herpetology* **37**: 215–218.

McCOY, C. J. 1970. The snake fauna of Middlesex, British Honduras. *Journal of Herpetology* **4**: 135–140.

McCRANIE, J. R. 2009. Amphibians and reptiles of Honduras (versión 12 November 2009). *Listas Zoológicas Actualizadas UCR.* San Pedro: Museo de Zoología, Universidad de Costa Rica. Available from: http://museo.biologia.ucr.ac.cr/Listas/LZAPublicaciones.htm. Accessed 1 January 2011.

McCRANIE, J. R. 2011. *Snakes of Honduras: Systematics, Distribution, and Conservation.* Ithaca: Society for the Study of Amphibians and Reptiles.

McCRANIE, J. R., J. H. TOWNSEND, AND L. D. WILSON. 2006. *The Amphibians and Reptiles of the Honduran Mosquitia.* Malabar, Florida: Krieger Publishing Co.

McDADE, L. A., K. S. BAWA, H. A. HESPENHEIDE, AND G. S. HARTSHORN. 1994. *La Selva: Ecology and Natural History of a Neotropical Rain Forest.* Chicago: University of Chicago Press.

McDADE, L. A., AND G. S. HARTSHORN. 1994. La Selva Biological Station, pp. 6–14. *In* K. S. Bawa, G. S. Hartshorn, H. A. Hespenheide, and L. A. Macdade (eds.), *La Selva: Ecology and Natural History of a Neotropical Rainforest.* Chicago: The University of Chicago Press.

McDIARMID, R. W., AND J. M. SAVAGE. 2005. The herpetofauna of the Rincón area, Península de Osa, Costa Rica, a Central American lowland evergreen forest site, pp. 366–427. *In* M. A. Donnelly, B. I. Crother, C. Guyer, M. H. Wake, and M. E. White (eds.), *Ecology and Evolution in the Tropics, a Herpetological Perspective.* Chicago: University of Chicago Press.

MEERMAN, J. C., AND J. C. LEE. Undated [published 2003]. Amphibians and reptiles of the Columbia

River Forest Reserve, pp. 66–70. *In* J. C. Meerman and S. Matola (eds.), *The Columbia River Forest Reserve Little Quartz Ridge Expedition, A Biological Assessment*. Belize City: Wildlife Trust.

MEERMAN, J. C., AND S. MATOLA (eds.). Undated [published 2003]. *The Columbia River Forest Reserve Little Quartz Ridge Expedition, A Biological Assessment*. Belize City: Wildlife Trust.

MORELET, A. 1871. *Travels in Central America, Including Accounts of Some Regions Unexplored since the Conquest* [translated from the French by M. F. Squier]. London: Trübner and Co [French edition, 2 vols., 1857].

MYERS, C. W. 1969. The ecological geography of cloud forest in Panama. *American Museum Novitates* **2396**: 1–52.

MYERS, C. W. 1974. The systematics of *Rhadinaea* (Colubridae), a genus of New World snakes. *Bulletin of the American Museum of Natural History* **153**: 1–262.

MYERS, C. W. 2011. A new genus and new tribe for *Enicognathus melanauchen* Jan, 1863, a neglected South American snake (Colubridae: Xenodontinae), with taxonomic notes on some Dipsadinae. *American Museum Novitates* **3715**: 1–33.

MYERS, C. W., AND J. E. CADLE. 1994. A new genus for South American snakes related to *Rhadinaea obtusa* Cope (Colubridae) and resurrection of *Taeniophallus* Cope for the "*Rhadinaea*" *brevirostris* group. *American Museum Novitates* **3102**: 1–33.

MYERS, C. W., AND J. E. CADLE. 2003. On the snake hemipenis, with notes on *Psomophis* and techniques of eversion: a response to Dowling. *Herpetological Review* **34**: 295–302.

MYERS, C. W., AND J. A. CAMPBELL. 1981. A new genus and species of colubrid snake from the Sierra Madre del Sur of Guerrero, Mexico. *American Museum Novitates* **2708**: 1–20.

MYERS, C. W., AND J. D. LYNCH. 1997. *Eleutherodactylus laticorpus*, a peculiar new frog from the Cerro Tacarcuna Area, Panamanian-Colombian frontier. *American Museum Novitates* **3196**: 1–12.

PÉREZ-HIGAREDA, G. 1978. Reptiles and amphibians from the Estación de Biología Tropical "Los Tuxtlas" (U.N.A.M.), Veracruz, México. *Bulletin of the Maryland Herpetological Society* **14**: 67–74.

PÉREZ-HIGAREDA, G., AND H. M. SMITH. 1991. *Ofidiofauna de Veracruz, Análisis Taxonómico y Zoogeográfico/ Ophidiofauna of Veracruz, Taxonomical and Zoogeographical Analysis* [Publicaciones Especiales del Instituto de Biología no. 7]. Los Tuxtlas, México: Universidad Nacional Autónoma de México.

PÉREZ-HIGAREDA, G., R. C. VOGT, AND O. A. FLORES-VILLELA. 1987. *Lista anotada de los anfibios y reptiles de la región de Los Tuxtlas, Veracruz. Los Tuxtlas*. Veracruz, México: Estación de Biología Tropical Los Tuxtlas, Instituto de Biología, Universidad Nacional Autónoma de México.

PÉREZ-SANTOS, C., AND A. G. MORENO. 1988. *Ofidios de Colombia*. Torino: Museo Regionale di Scienze Naturali.

PÉREZ-SANTOS, C., AND A. G. MORENO. 1989. Addenda y corrigenda al libro "Ofidios de Colombia." *Bollettino del Museo Regionale di Scienze Naturali, Torino* **7**: 1–17.

PÉREZ-SANTOS, C., A. G. MORENO, AND A. GEARHART. 1993. Checklist of the snakes of Panama. *Revista Española de Herpetología* **7**: 113–122.

PETERS, J. A. 1952. Catalogue of type specimens in the herpetological collections of the University of Michigan Museum of Zoology. *Occasional Papers of the Museum of Zoology, University of Michigan* **539**: 1–55.

PETERS, J. A., AND B. OREJAS-MIRANDA. 1970. Catalogue of the Neotropical Squamata: Part I. Snakes. *Bulletin of the United States National Museum* **297**: 1–347.

PRINGLE, C. M., I. CHACON, M.GRAYUM, H. W. GREENE, G. HARTSHORN, R. SCHATZ, G. STILES, C. GOMEZ, AND M. RODRIGUEZ. 1984. Natural history observations and ecological evaluation of the La Selva Protection Zone, Costa Rica. *Brenesia* **22**: 189–206.

RAND, A. S., AND C. W. MYERS. 1990. The herpetofauna of Barro Colorado Island, Panama: an ecological summary, pp. 386–409. *In* A. H. Gentry (ed.), *Four Neotropical Rainforests*. New Haven, Connecticut: Yale University Press.

ROOT, N. J. 1975. The Thomas Baillie MacDougall collection in the American Museum of Natural History Library. *Curator* **18**: 270–276.

ROSSMAN, D. A., AND W. G. EBERLE. 1977. Partition of the genus *Natrix*, with preliminary observations on evolutionary trends in natricine snakes. *Herpetologica* **33**: 34–43.

SANTOS-BARRERA, G., J. PACHECO, F. MENDOZA-QUIJANO, F. BOLAÑOS, G. CHÁVES, G. C. DAILY, P. R. EHRLICH, AND G. CEBALLOS. 2008. Diversity, natural history and conservation of amphibians and reptiles from the San Vito region, southwestern Costa Rica. *Revista de Biología Tropical* **56**: 755–778.

SAVAGE, J. M. 1966. The origins and history of the Central American herpetofauna. *Copeia* **1966**: 719–766.

SAVAGE, J. M. 1973. *A Preliminary Handlist of the Herpetofauna of Costa Rica*. Lawrence, Kansas: American Society of Ichthyologists and Herpetologists.

SAVAGE, J. M. 1980. *A Handlist with Preliminary Keys to the Herpetofauna of Costa Rica*. Los Angeles: Allan Hancock Foundation.

SAVAGE, J. M. 1997. On terminology for the description of the hemipenes of squamate reptiles. *Herpetological Journal* **7**: 23–25.

SAVAGE, J. M. 2002. *The Amphibians and Reptiles of Costa Rica, a Herpetofauna between Two Continents, between Two Seas*. Chicago: The University of Chicago Press.

SAVAGE, J. M., AND F. BOLAÑOS. 2009. A checklist of the amphibians and reptiles of Costa Rica: additions and nomenclatural revisions. *Zootaxa* **2005**: 1–23.

SAVAGE, J. M., AND J. VILLA. 1986. *Introduction to the Herpetofauna of Costa Rica/Introducción a la Herpetofauna de Costa Rica*. Ithaca, New York: Society for the Study of Amphibians and Reptiles.

SCHARGEL, W. E., G. RIVAS FUENMAYOR, AND C. W. MYERS. 2005. An enigmatic new snake from cloud forest of the Península de Paria, Venezuela (Colubridae: genus *Taeniophallus*?). *American Museum Novitates* **3484**: 1–22.

SCOTT, N. J., JR. 1976. The abundance and diversity of the herpetofaunas of tropical forest litters. *Biotropica* **8**: 41–58.

SCOTT, N. J., JR., J. M. SAVAGE, AND D. C. ROBINSON. 1983. Checklist of reptiles and amphibians, pp. 367–374. *In* D. H. Janzen (ed.), *Costa Rican Natural History*. Chicago: University of Chicago Press.

SMITH, H. M. 1941. A new name for the Mexican snakes of the genus *Dendrophidion*. *Proceedings of the Biological Society of Washington*, **54**: 73–76.

SMITH, H. M. 1943. Summary of the collections of snakes and crocodilians made in Mexico under the Walter Rathbone Bacon traveling scholarship. *Proceedings of the United States National Museum*, **93**: 393–504 + pl. 32.

SMITH, H. M. 1958. Handlist of the snakes of Panama. *Herpetologica* **14**: 222–224.

SMITH, H. M. 1987. Current nomenclature for the names and material cited in Günther's Reptilia and Batrachia volume of the *Biologia Centrali-Americana*, pp. xv–li. *In* K. Adler (ed.), *Albert C. A. G. Günther, Biologia Centrali-Americana, Reptilia and Batrachia*. Ithaca, New York: Society for the Study of Amphibians and Reptiles.

SMITH, H. M., AND E. H. TAYLOR. 1945. An annotated checklist and key to the snakes of Mexico. *Bulletin of the United States National Museum* **187**: 1–239.

SMITH, H. M., AND E. H. TAYLOR. 1950. Type localities of Mexican reptiles and amphibians. *University of Kansas Science Bulletin* **33, pt. 2**: 313–380.

SOLÓRZANO, A. 2004. *Serpientes de Costa Rica: Distribución, Taxonomía e Historia Natural/ Snakes of Costa Rica: Distribution, Taxonomy and Natural History*. Eagle Mountain, Utah: Eagle Mountain Publishing, LC.

STAFFORD, P. J. 1998. Amphibians and reptiles of the Cordillera de Guanacaste, Costa Rica: a field list with notes on colour patterns and other observations. *British Herpetological Society Bulletin* **62**: 9–19.

STAFFORD, P. J. 2002. Record of the colubrid snake *Dendrophidion nuchale* (Peters) from Nicaragua. *Southwestern Naturalist* **47**: 615–616.

STAFFORD, P. J. 2003. Trophic ecology and reproduction in three species of Neotropical forest racer (*Dendrophidion*; Colubridae). *Herpetological Journal* **13**: 101–111.

STAFFORD, P. J., AND J. R. MEYER. 2000. *A Guide to the Reptiles of Belize*. San Diego: Academic Press.

STIX, J. S. 1975. Thomas Baillie MacDougall—naturalist and collector. *Curator* **18**: 270–276.

STUART, L. C. 1932. Studies on Neotropical Colubrinae. I. The taxonomic status of the genus *Drymobius* Fitzinger. *Occasional Papers of the Museum of Zoology, University of Michigan* **236**: 1–16.

STUART, L. C. 1934. A contribution to a knowledge of the herpetological fauna of El Petén, Guatemala. *Occasional Papers of the Museum of Zoology, University of Michigan* **292**: 1–18.

STUART, L. C. 1935. A contribution to a knowledge of the herpetology of a portion of the savanna region of Central Petén, Guatemala. *Miscellaneous Publications of the Museum of Zoology, University of Michigan* **29**: 1–56.

STUART, L. C. 1948. The amphibians and reptiles of Alta Verapaz, Guatemala. *Miscellaneous Publications of the Museum of Zoology, University of Michigan* **69**: 1–109.

STUART, L. C. 1950. A geographic study of the herpetofauna of Alta Verapaz, Guatemala. *Contributions from the Laboratory of Vertebrate Biology, University of Michigan* **45**: 1–77.

STUART, L. C. 1958. A study of the herpetofauna of the Uaxactún–Tikal area of northern El Petén, Guatemala. *Contributions from the Laboratory of Vertebrate Biology, University of Michigan* **75**: 1–30.

STUART, L. C. 1963. A checklist of the herpetofauna of Guatemala. *Miscellaneous Publications of the Museum of Zoology, University of Michigan* **122**: 1–150.

TAYLOR, E. H. 1944. Present location of certain herpetological and other type specimens. *University of Kansas Science Bulletin* **30, part 1**: 117–187.

TAYLOR, E. H. 1954. Further studies on the serpents of Costa Rica. *University of Kansas Science Bulletin* **36, part 2**: 673–801.

VILLA, J., L. D. WILSON, AND J. D. JOHNSON. 1988. *Middle American Herpetology—A Bibliographic Checklist*. Columbia: University of Missouri Press.

WAKE, D. B., J. M. SAVAGE, AND J. HANKEN. 2007. Montane salamanders from the Costa Rica–Panama border region, with descriptions of two new species of *Bolitoglossa*. *Copeia* **2007**: 556–565.

WHITFIELD, S. M., K. E. BELL, T. PHILIPPI, M. SASA, F. BOLAÑOS, G. CHÁVES, J. M. SAVAGE, AND M. A. DONNELLY. 2007. Amphibian and reptile declines over 35 years at La Selva, Costa Rica. *Proceedings of the National Academy of Sciences, USA* **104**: 8352–8356.

WILSON, L. D. 1966. *Dendrophidion vinitor*, an addition to the snake fauna of British Honduras. *Journal of the Ohio Herpetological Society* **5**: 103.

WILSON, L. D., J. R. McCRANIE, S. GOTTE, AND J. H. TOWNSEND. 2003. Distributional comments on some members of the herpetofauna of the Mosquitia, Honduras. *Herpetological Bulletin* **84**: 15–19.

WILSON, L. D., AND J. R. MEYER. 1985. *The Snakes of Honduras*, 2nd edition. Milwaukee: Milwaukee Public Museum.

WILSON, L. D., AND J. H. TOWNSEND. 2006. The herpetofauna of the rainforests of Honduras. *Caribbean Journal of Science* **42**: 88–113.

ZAHER, H. 1999. Hemipenial morphology of the South American xenodontine snakes, with a proposal for a monophyletic Xenodontinae and a reappraisal of colubroid hemipenes. *Bulletin of the American Museum of Natural History* **240**: 1–168.

Bulletin
of the
Museum of Comparative Zoology

On the Cyphophthalmi (Arachnida, Opiliones) types from the Museo Civico di Storia Naturale "Giacomo Doria"

RONALD CLOUSE AND GONZALO GIRIBET

ON THE CYPHOPHTHALMI (ARACHNIDA, OPILIONES) TYPES FROM THE MUSEO CIVICO DI STORIA NATURALE "GIACOMO DORIA"

RONALD CLOUSE[1] AND GONZALO GIRIBET[2]

ABSTRACT. The Museo Civico di Storia Naturale "Giacomo Doria," Genoa, hosts one of the most important historical collections of the Opiliones suborder Cyphophthalmi, including all the known specimens for the type species of the genera *Leptopsalis* (Stylocellidae), *Miopsalis* (Stylocellidae), and *Parogovia* (Neogoveidae), as well as several other types in the families Ogoveidae and Stylocellidae (it is unclear whether specimens in Pettalidae and Sironidae constitute types). These specimens were recently made available to us for study, and given their importance, we discuss and illustrate them here. Study of this collection allows confirmation of the validity of *Leptopsalis*, considered a synonym of *Stylocellus* for more than a century, and of *Miopsalis*, considered a nomen dubium in the most recent catalogue of the group. It furthermore helps to clarify the identity of several other species in the family Stylocellidae. Here we formally resurrect the genera *Miopsalis* Thorell, 1890, and *Leptopsalis* Thorell, 1882, and transfer several species to these genera: *M. collinsi* (Shear, 1993) comb. nov.; *M. gryllospeca* (Shear, 1993) comb. nov.; *M. lionota* (Pocock, 1897) comb. nov.; *M. sabah* (Shear, 1993) comb. nov.; *M. silhavyi* (Rambla, 1991) comb. nov.; *M. tarumpitao* (Shear, 1993) comb. nov.; *L. dumoga* (Shear, 1993) comb. nov.; *L. hillyardi* (Shear, 1993) comb. nov.; *L. javana* Thorell, 1882; *L. lydekkeri* (Clouse & Giribet, 2007) comb. nov.; *L. modesta* (Hansen & Sørensen, 1904) comb. nov.; *L. novaguinea* (Clouse & Giribet, 2007) comb. nov.; *L. ramblae* (Giribet, 2002) comb. nov.; *L. sulcata* (Hansen & Sørensen, 1904) comb. nov.; *L. tambusisi* (Shear, 1993) comb. nov.; *L. thorellii* (Hansen & Sørensen, 1904) comb. nov.; *L. weberii* (Hansen & Sørensen, 1904) comb. nov.

Key words: Neogoveidae, Ogoveidae, Sironidae, Stylocellidae, Museum collections

---

[1] Division of Invertebrate Zoology, American Museum of Natural History, Central Park West at 79th Street, New York, New York 10024 (rclouse@amnh.org).
[2] Museum of Comparative Zoology, Department of Organismic and Evolutionary Biology, Harvard University, 26 Oxford Street, Cambridge, Massachusetts 02138. Author for correspondence (ggiribet@oeb.harvard.edu).

INTRODUCTION

One of the worst impediments of taxonomy is, along with the loss of expertise (e.g., Rodman and Cody, 2003), the dependence on type specimens that are not properly described or documented; hence the importance of well-funded museums to ensure that collections are properly maintained and specimens are made available to the scientific community (Suarez and Tsutsui, 2004). But proper cataloguing and revisionary taxonomy often require examinations of large numbers of type specimens scattered in institutions around the world. These are usually in museums and university collections but are sometimes in private collections that may not be up to curatorial standards, especially after the researcher passes away and the collection burdens surviving family members. Many important collections have been lost this way, including some of the Opiliones collections of interest to us, most prominently the collection of Julio A. Rosas Costa, with his Cyphophthalmi types (Rosas Costa, 1950) becoming lost to science for the time being. Unfortunately, as exemplified by the arachnid order Opiliones, many types are often simply unavailable.

Here we study a collection of the harvestman suborder Cyphophthalmi and document the specimens deposited at the Museo Civico di Storia Naturale "Giacomo Doria," Genoa, Italy (MCSN), which we had not examined until recently. The importance of this collection is without parallel in many respects, as it includes types and nontypes of many of the earliest cyphophthalmid species.

Types of the suborder Cyphophthalmi are deposited in approximately 30 museums around the world (Giribet, 2000). A visit to half of these museums would allow one to study around 85% of the known species (a large number of recently described species are deposited in the collection of Ivo Karaman, University of Novi Sad, Serbia, but they are not available for study to the broader community). In terms of historical collections, many of the oldest types are deposited at The Natural History Museum, London, which includes 15 primary types, although their collections are not especially large. The Muséum national d'Histoire naturelle, Paris, includes numerous types (mostly from Christian Juberthie and most New Caledonian species), as well as a large general collection. The American Museum of Natural History, New York, includes 15 types and one of the largest general collections of Cyphophthalmi, with nearly all families represented. Currently, the largest collection in terms of diversity and including representatives of all families is that of the Museum of Comparative Zoology, Harvard University, with ca. 800 lots, most of it recently collected, DNA-grade specimens. It also contains more types than any other institution, although few are "historical" types. Te Papa Tongarewa, Wellington, with 26 types, and the Canterbury Museum, Christchurch, with 11 types, are indispensable visits for those studying the New Zealand fauna. The size of the MCSN collection is small compared with these other collections; however, its importance lies in the species available there, including the primary (and only) types of six species, in addition to a few other specimens, including additional type specimens. Among them are the type species for two of the five currently recognized genera in the family Stylocellidae, including the only described specimens in the yet-monotypic genus *Miopsalis* Thorell, 1890 (Clouse et al., 2009; Clouse and Giribet, 2010). The featured species are: *Parogovia sironoides* Hansen, 1921; *Ogovea nasuta* (Hansen, 1921); *Miopsalis pulicaria* Thorell, 1890; *Leptopsalis beccarii* Thorell, 1882; *Leptopsalis javana* Thorell, 1882; *Leptopsalis*

thorellii (Hansen and Sørensen, 1904); and *Leptopsalis weberii* (Hansen and Sørensen, 1904).

The MCSN collection is of exceptional importance due to several factors. First is the fact that the prolific Swedish arachnologist Tord Tamerlan Teodor Thorell studied arachnology with Giacomo Doria at the MCSN. In addition to describing more than 1,000 spider species from 1850 to 1900, Thorell described two stylocellid genera (*Leptopsalis* Thorell, 1882 and *Miopsalis* Thorell, 1890) and three stylocellid species, types of which are deposited at MCSN. Although *Leptopsalis* was synonymized with *Stylocellus* Westwood, 1874 by Thorell himself (1890b), and has remained in synonymy for more than a century, a clade containing the type species was recently found to be sufficiently distinct from the type species of *Stylocellus* for them to be kept in separate genera (Clouse and Giribet, 2010; Clouse et al., 2009, 2011). *Leptopsalis* was thus informally revalidated by Clouse et al. (2009: 525), and the genus has been used in subsequent papers on stylocellid (Clouse et al., 2011) and cyphophthalmid (Giribet et al., 2011) phylogenetics. *Miopsalis* is currently a nomen dubium (Giribet, 2000), although it has recently been postulated to be the identity of a distinct clade that diversified mostly in Borneo (Clouse and Giribet, 2010; Clouse et al., 2009, 2011; Giribet et al., 2011). However, the identity of this clade as the genus *Miopsalis* was based on its inclusion of small species that closely match the description of *M. pulicaria*, but it could not be confirmed without examination of the type (and sole known specimen) of this species.

Second, the great Italian explorer Leonardo Fea became an assistant at the MCSN, and his expeditions to the Gulf of Guinea yielded important specimens, including the type species of the genus *Parogovia* Hansen, 1921 and the second species of the genus *Ogovea* Hansen & Sørensen, 1921. Finally, the collection also received specimens from Eugène Simon and Gustav Joseph, including specimens of

the type species of the genera *Cyphophthalmus* Joseph, 1868 and *Parasiro* Hansen & Sørensen, 1904, and it acquired some other specimens of Hansen and Sørensen's species, including a juvenile of *Purcellia illustrans* Hansen & Sørensen, 1904. Few museums had, by the beginning of the 20th century, a collection as complete as the one of the MCSN. By 1921, 19 species of Cyphophthalmi had been described, and the MCSN had 10 of these represented in its collection, including eight or more types. By that time the British Museum of Natural History, London (later to become The Natural History Museum), the largest museum of natural history in the world, had only types of seven cyphophthalmid species, some of these being type series shared with the MCSN. In spite of this importance, the MCSN collection of Cyphophthalmi has not been documented using modern imaging techniques, so here we provide high-resolution images of the most important specimens and discuss long-standing questions about their morphology and taxonomy.

MATERIALS AND METHODS

Specimens were cleaned in a Branson 200 Ultrasonic cleaner and imaged under a Leica MX12.5 stereomicroscope, PLAN 0.5x, with images taken at different planes with a JVC 3-CCD digital camera KY-F75U and integrated with the software Auto-Montage Pro version 5.02.0096 from Syncroscopy.

Data provided for each specimen are a transcription of the specimen label. Modern localities and additional data are provided in the discussion of the specimens.

Abbreviations:

AMNH: American Museum of Natural History, New York, United States.

BMNH: The Natural History Museum, London, United Kingdom.

MCSN: Museo Civico di Storia Naturale "Giacomo Doria," Genoa, Italy.

MCZ: Museum of Comparative Zoology, Harvard University, Cambridge, Massachusetts, United States.

MNHN: Muséum national d'Histoire naturelle, Paris, France.

ZMUC: Zoologisk Museum, Statens Naturhistoriske Museum, Københavns Universitet, Copenhagen, Denmark.

ANNOTATED TAXONOMIC SECTION

Family Neogoveidae:

Parogovia sironoides Hansen, 1921
Figures 1–3

Specimen in good condition with some appendages detached (Fig. 1):

Parogovia sironoides Hansen, 1921
Type: Male
Island of Fernando Poo: Punta Frailes
leg. L. Fea, X–XI 1901

Specimen in poor condition, with white residue on exterior (Fig. 2):

Parogovia sironoides Hansen, 1921
Type: Female
Island of Fernando Poo: Basilè (400–600 m)
leg. L. Fea, VIII–IX 1901

The latter specimen above originally labeled incorrectly as male.

Detached appendages: basichelicerite, distal cheliceral segments, palp, leg I, leg IV (Fig. 3):

Parogovia sironoides Hansen, 1921
Type: Male
Five detached parts

Genitalia (spermatopositor and ovipositor), not photographed:

Parogovia sironoides Hansen, 1921
Type: Female, male
Penis and ovopositor slide
Mounted by G. Legg, 1986
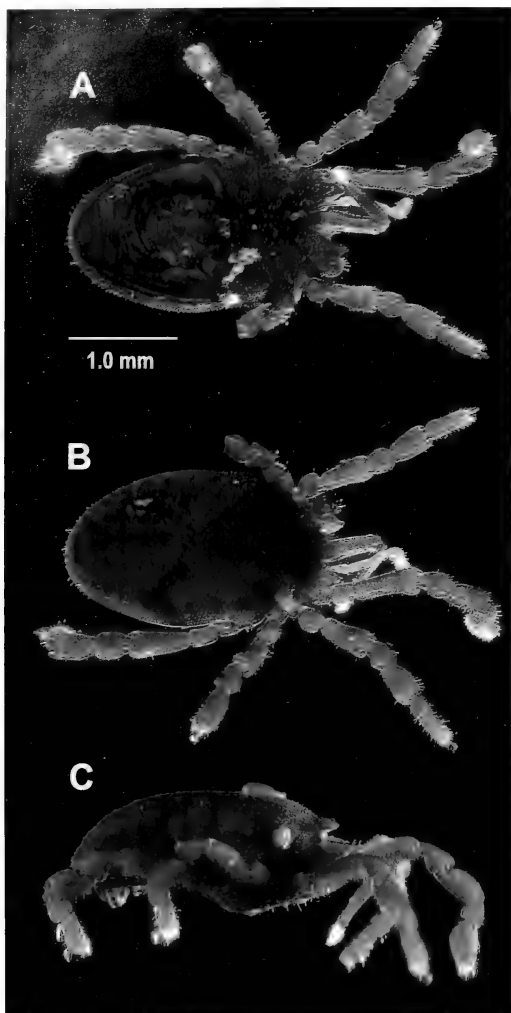
Figure 1.   *Parogovia sironoides* Hansen, 1921, male para-lectotype in ventral (A), dorsal (B), and lateral (C) views.

Figure 2.   *Parogovia sironoides* Hansen, 1921, female para-lectotype in ventral view.

spermatopositor and ovipositor, was studied by Gerald Legg in 1986 (Legg, 1990).

Punta Frailes, the locality of one of the syntypes, is of unknown identity; it is not found on current maps of Bioko, it is not known to local biologists interviewed by G.G., and it was not seen in a study of old maps of the former Spanish Colony of Fernando Poo. This is, however, one of the localities surveyed by the Italian explorer Leonardo Fea during his collecting trip to the Gulf of Guinea and Portuguese West Africa, and it is the type locality of several other species of arthropods and vertebrates. Basilé refers to Pico Basilé (Mt. Basilé), formerly Pico de Santa Isabel, the highest mountain on the island of Bioko, with an altitude of 3,011 m. It is the summit of the largest and highest of three overlapping basaltic shield volcanoes that form the

Parogovia sironoides, the type species of the genus *Parogovia* Hansen, 1921, was described on the basis of two specimens from Bioko (formerly Fernando Poo), Equatorial Guinea, one male from Punta Frailes collected by Leonardo Fea in October–November 1901, and one female from Basilé, collected by Leonardo Fea in August–September 1901, at an altitude of 400–600 m. The male was profusely illustrated by Hansen (1921: pl. IV, fig. 2a–l). The type material, including a preparation of the

Figure 3.   *Parogovia sironoides* Hansen, 1921, detached appendages of lectotype male. From top to bottom, left to right: chelicera, distal articles; chelicera, basal article; palp; leg I; leg IV.

island. From the summit, Mt. Cameroon can be seen to the northeast. Bioko was formed along the Cameroon line, a major northeast-trending geologic fault that runs from the Atlantic Ocean into Cameroon. This line includes other volcanic islands in the Gulf of Guinea such as the island territory of Annobón, the island nation of São Tomé and Príncipe, and the massive stratovolcano of Mt. Cameroon, the latter of which also has one or more undescribed species of *Parogovia* (authors' unpublished data).

Specimens identified as *Parogovia sironoides* (erroneously spelled *Paragovia sironoides* in earlier publications) from Río Campo, Continental Region of Equatorial Guinea, have been used in several taxonomic and phylogenetic studies of Cyphophthalmi and Opiliones (Giribet and Boyer, 2002; Giribet and Prieto, 2003; de Bivort and Giribet, 2004; Boyer et al., 2005; Schwendinger and Giribet, 2005). Collections of *Parogovia* specimens in the Continental Region and on Pico Basilé in 2003 led us to correct this possible misidentification and to refer to the continental specimens as *P.* cf. *sironoides*, while we apply the name *P. sironoides* for the specimens collected on Pico Basilé (Boyer et al., 2007; Boyer and Giribet, 2007; Clouse and Giribet, 2007; Giribet et al., 2010, 2011). Additional collecting in Cameroon in 2009 and subsequent phylogenetic analysis show that these are two distinct species, and that they are not even sister species (Giribet et al., 2011). This can now be confirmed by the study of the type material from MCSN.

Family Ogoveidae:

Ogovea nasuta (Hansen, 1921)
Figures 4–6

Three specimens in optimal condition (Figs. 4–6):

Ogovia nasuta Hansen, 1921
Types: Female, male, juvenile
Island of Fernando Poo: Musola (400–500 m)
leg. L. Fea, I-1902
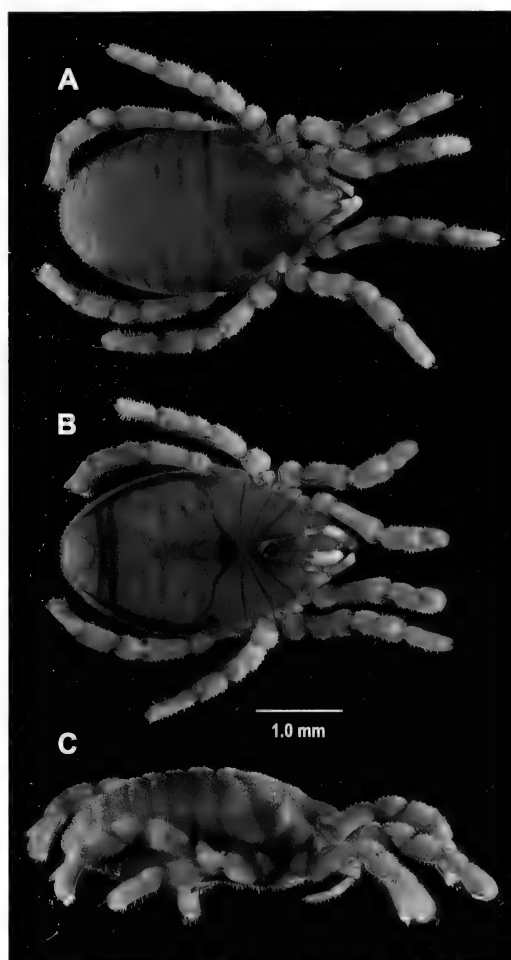
Figure 4.   *Ogovea nasuta* (Hansen, 1921), male lectotype in dorsal (A), ventral (B), and lateral (C) views.

Disarticulated specimen, not photographed:

Ogovia nasuta Hansen, 1921
Types
Detached parts for figures

Ogovea nasuta, originally spelled *Ogovia nasuta* Hansen, 1921, was described on the basis of three males, one female, and one juvenile syntype from Bioko, in Equatorial Guinea, at an altitude of 400–500 m, near Musola, collected by Leonardo Fea in January 1902 (Hansen, 1921). One male and one juvenile were illustrated by Hansen
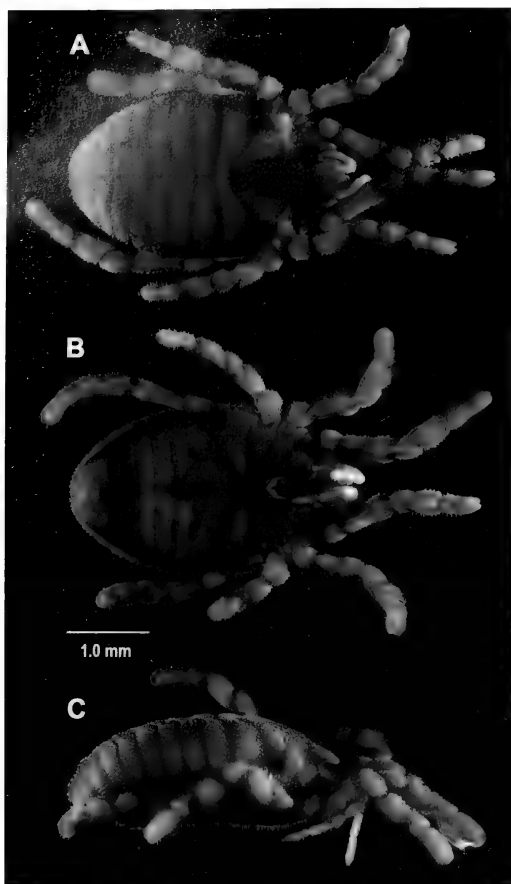
Figure 5.   *Ogovea nasuta* (Hansen, 1921), female paralecto-type in dorsal (A), ventral (B), and lateral (C) views.

(1921: pl. IV, fig. 1a–f). Three intact specimens and the detached appendages used for the original figures are deposited in the MCSN. Another disassembled male, the spermatopositor of which was studied by W. A. Shear, was deposited at the ZMUC (Shear, 1980; Giribet and Prieto, 2003).

Here we designate the male deposited at the MCSN as the lectotype of *Ogovia nasuta* Hansen, 1921, all other syntypes becoming paralectotypes.

Family Pettalidae:

Purcellia illustrans Hansen & Sørensen, 1904

The MCSN collection also includes an immature female specimen of *Purcellia*
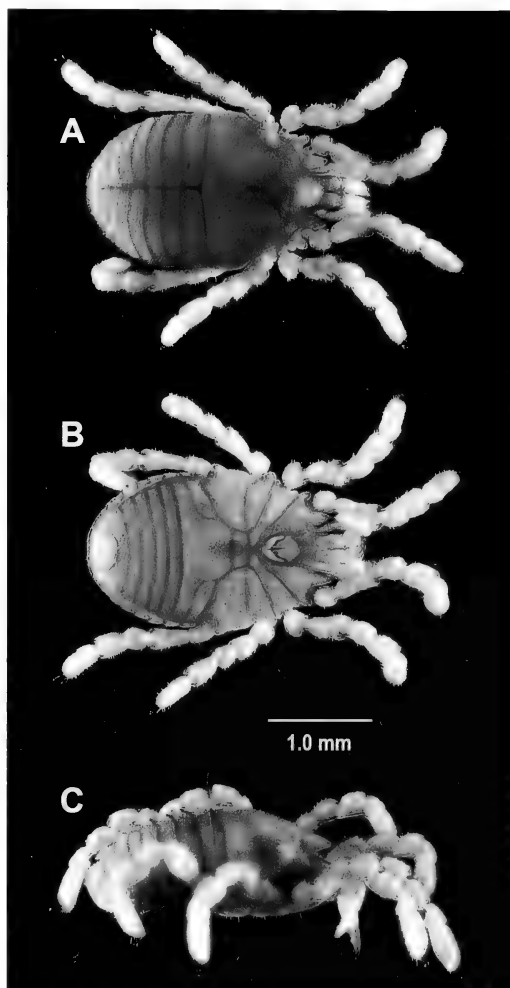
Figure 6.   *Ogovea nasuta* (Hansen, 1921), juvenile paralec-totype in dorsal (A), ventral (B), and lateral (C) views.

illustrans Hansen & Sørensen, 1904, collected by Purcell on Table Mountain, Cape Town; it may form part of the type series of the species and was determined by H. J. Hansen and W. Sørensen. Other specimens of the type series are deposited at the Zoological Museum, University of Copenhagen and at The Natural History Museum, London (BMNH 10.9.19.1-6).

Purcellia illustrans Hansen & Sørensen, 1904
Female juvenile
Caput Bonae Spei

Purcell all leg.
Det. H.J.H. & W.S.

Family Sironidae:

Parasiro corsicus (Simon, 1872)

The prolific French arachnologist (and ornithologist) Eugène Simon described *Cyphophthalmus corsicus*, a species later designated the type of the genus *Parasiro* Hansen & Sørensen, 1904, from the coast of Porto-Vecchio, Corsica (Simon, 1872). Simon did not specify the number of specimens he examined, but Hansen and Sørensen (1904) studied two males and two females, currently deposited at the ZMUC. Sixteen additional specimens are deposited at the MNHN (10 males, 6 females) and one female specimen is deposited at the AMNH. An additional two specimens (male and female) from the Simon collection are deposited at the BMNH (BMNH 02.11. 18.89). The specimens deposited at the MCSN were identified by Simon in 1880, and therefore it is unlikely that they belong to the type series. It is also unclear which of the listed specimens are syntypes.

One male and one female:

Siro corsicus
Corsica
Det. Simon, 1880–N. 338

The above female specimen was attached to the cotton stopper. It is not conspecific with the male but belongs to a smaller species (photograph not shown).

Cyphophthalmus duricorius Joseph, 1868

Cyphophthalmus duricorius Joseph, 1868 was the second cyphophthalmid species described, after *Siro rubens* Latreille, 1802 (see Kury, 2010). The holdings of the MCSN collection include two vials with specimens of *C. duricorius* from Joseph's collection, examined both by Hansen and Sørensen and by Simon.

Siro duricorius   Male
Carniola=Kranjska

Leg. et det. Joseph
Det. H.J.H. & W.S.

Siro duricorius   Female
Carniola=Kranjska
Det. Simon, 1880–N. 170

Family Stylocellidae:

Miopsalis pulicaria Thorell, 1890
Figures 7, 8

Miopsalis pulicaria was described by Thorell (1890a) on the basis of a single female specimen from Pulo Pinang (Penang Island), West Malaysia. The specimen was collected by Lamberto Loria and Leonardo Fea in February 1889. Before the great expedition of L. Loria to New Guinea, he met L. Fea in Pulo Pinang, who was returning from his expedition to Myanmar; both went for a hike and collected arachnids at an altitude between 2,000 and 2,600 "English" feet (609 to 792 m) on Penang Hill (Thorell, 1890a). Among the 49 arachnids collected, 8 were Opiliones, including *M. pulicaria*.

The genus *Miopsalis* was used by Roewer (1916, 1923) for his Japanese species *Miopsalis sauteri* Roewer, 1916, for which Juberthie (1970) erected the monotypic genus *Suzukielus* Juberthie, 1970.

Shear (1993), in his monumental study of Stylocellidae describing 11 new species, reports a blind female of an undescribed species from Borneo that "may shed light on the somewhat mysterious name *Miopsalis pulicaria*," and in his catalogue of Cyphophthalmi species Giribet (2000) considered *Miopsalis* Thorell, 1890 a nomen dubium. In different molecular phylogenetic analyses of Stylocellidae, the name *Miopsalis* has been associated with small, blind stylocellids that group with most of the species on Borneo (including some of the largest Cyphophthalmi known), starting with what we called a "Borneo + *Miopsalis* clade"(Clouse and Giribet, 2007). However, we later concluded (Clouse and Giribet, 2010: 1116) that *Miopsalis* "is both poorly understood and has little chance of remaining a valid name in the future." In the latter
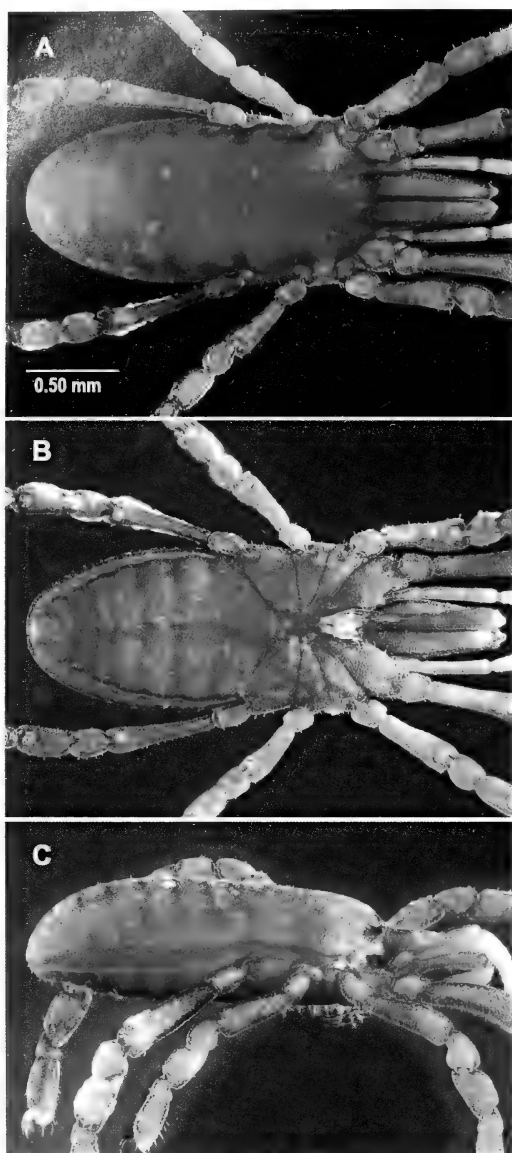
Figure 7.   *Miopsalis pulicaria* Thorell, 1890, female holotype in dorsal (A), ventral (B), and lateral (C) views.

Figure 8.   *Miopsalis pulicaria* Thorell, 1890, female holotype: ventral posterior (A), ventral anterior (B), lateral anterior part of body (C), and disarticulated distal part of left chelicera (D).

paper we again recovered a clade of predominantly Bornean species, called "clade B," which also included tiny species from Sumatra, Peninsular Malaysia, and Borneo. This clade was also corroborated in an analysis that incorporated morphological characters and type specimens for which molecular data were unavailable

(Clouse et al., 2009), but *Miopsalis pulicaria* was not included in that study, since at that time the specimen was not available, and its description lacks illustrations and detailed measurements. In follow-up studies, after receiving the *Miopsalis* specimen from

MCSN, we have used the name *Miopsalis* for the mostly Bornean clade, currently recognized as one of five stylocellid genera (Clouse et al., 2011; Giribet et al., 2011). However, no formal taxonomic action has been taken with respect to *Miopsalis*, and the MCSN specimen is the only one so far known for this species. Now that we have been able to examine the type specimen for the genus, we can tell that many details of its shape closely resemble an even smaller, also blind species that has been collected from Gunung Mulu, in Sarawak, on Borneo. Under the monikers "*Miopsalis* 101513" (Clouse and Giribet, 2007) and "Borneo sp. 15" (Clouse and Giribet, 2010), this Sarawak species was found to be a member of the mostly Bornean clade, and thus we would consider *M. pulicaria* as also belonging to this clade, thus confirming earlier suspicions about the taxonomic identity of the Bornean clade.

Here we formally transfer the most stable and unequivocal members of the Bornean clade to *Miopsalis*, which thus includes: *Miopsalis pulicaria* Thorell, 1890, the type species; *M. collinsi* (Shear, 1993) comb. nov.; *M. gryllospeca* (Shear, 1993) comb. nov.; *M. lionota* (Pocock, 1897) comb. nov.; *M. sabah* (Shear, 1993) comb. nov.; *M. silhavyi* (Rambla, 1991) comb. nov.; and *M. tarumpitao* (Shear, 1993) comb. nov., in addition to several undescribed species (Clouse, 2010; Clouse and Giribet, 2007, 2010; Clouse et al., 2009, 2011).

Specimen photographed (Figs. 7, 8):

Miopsalis pulicaria Thorell 1890
Type: Female
Pulo Pinang
Leg. L. Loria and L. Fea, 1889

Leptopsalis beccarii Thorell, 1882
Figures 9–12

The genus *Leptopsalis* Thorell, 1882, and the species *L. beccarii* Thorell, 1882, were described by Thorell (1882) on the basis of specimens from Sumatra. The MCSN collection has two specimens identified as "*Probably type series*" from Mt. Singalang
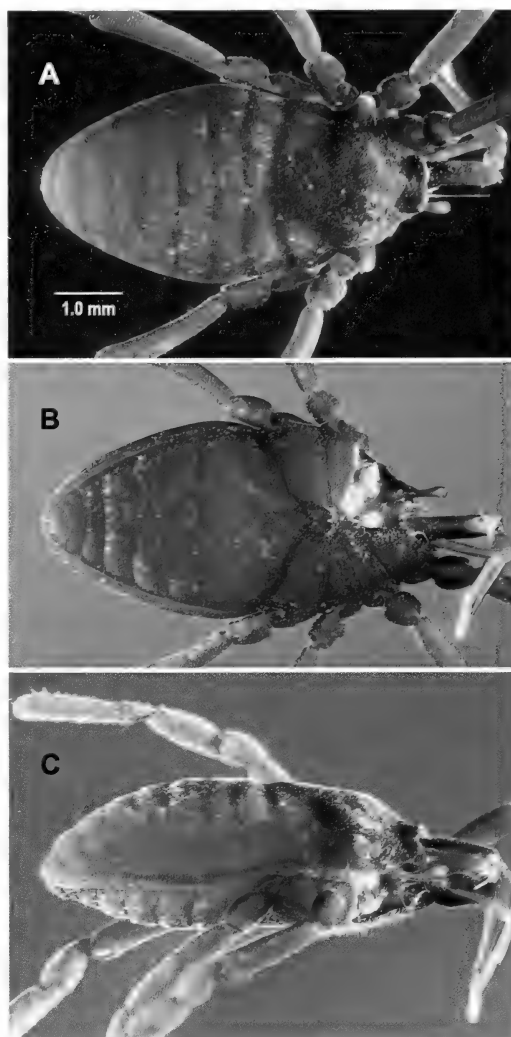
Figure 9.   *Leptopsalis beccarii* Thorell, 1882, male lectotype, showing dorsal (A), ventral (B), and lateral (C) views.

(current spelling: Singgalang), a male (Fig. 9) and a female (Fig. 10). These were collected by Odoardo Beccari on Sumatra in July 1878, during the famous expedition on which he discovered the titan arum (*Amorphophallus titanum*), the largest unbranched inflorescence. Also collected on this expedition and deposited in the MCSN collection is a female that later became the type of *Stylocellus thorellii* Hansen & Sørensen, 1904. In addition, the MCSN
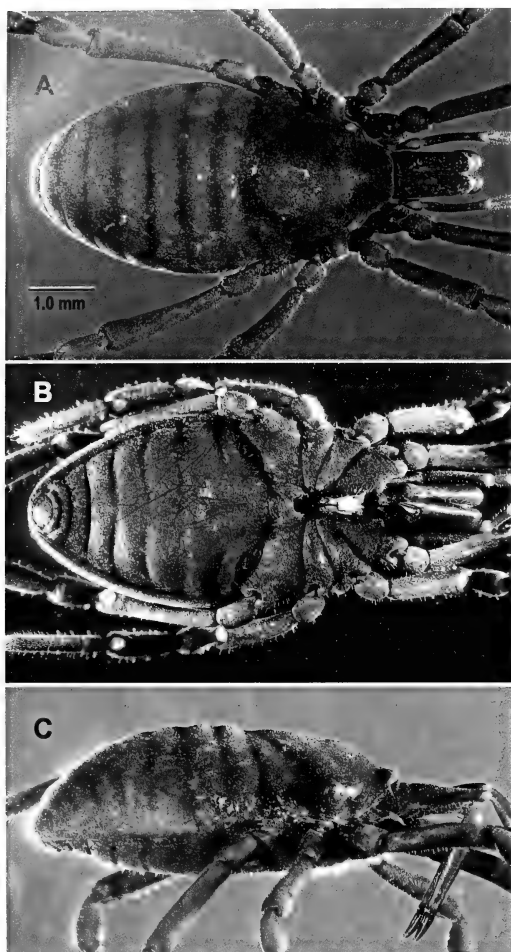
Figure 10. *Leptopsalis beccarii* Thorell, 1882, female para-lectotype, showing dorsal (A), ventral (B), and lateral (C) views.
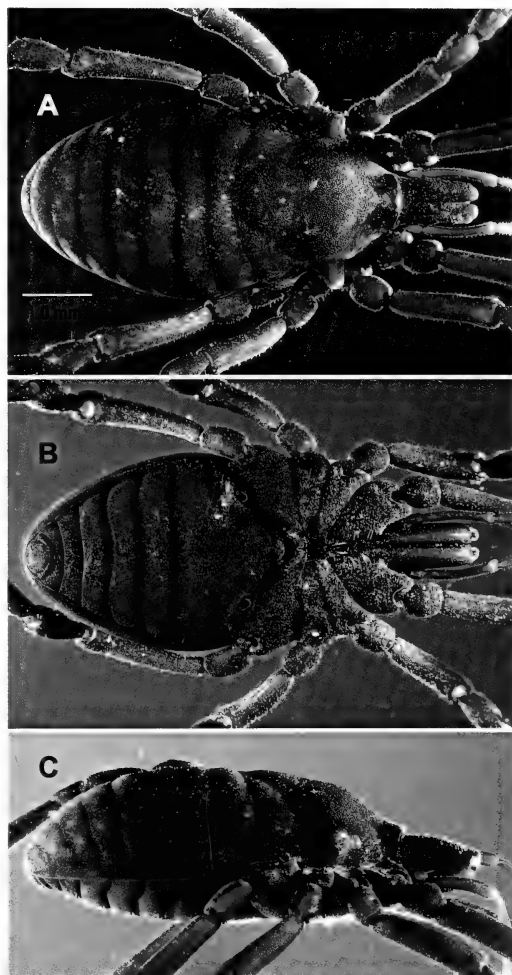
Figure 11. *Leptopsalis beccarii* Thorell, 1882, first male para-lectotype, showing dorsal (A), ventral (B), and lateral (C) views.

has four male specimens identified as "*Cotypes*" (Figs. 11, 12), which were also collected by O. Beccari on Sumatra, but no date or specific locality is given; they appear to belong to *L. beccarii*.

Here we designate the male deposited at the MCSN (Fig. 9) and previously designated as *Probably type series* as the lectotype of *L. beccarii* Thorell, 1882, all other specimens in the MCSN (the female also designated previously as *Probably type series* and the four males identified previously as *Cotypes*) becoming paralectotypes.

Leptopsalis beccarii is the type species of the genus, although this species was soon

synonymized with *Stylocellus sumatranus* Westwood, 1874 by Thorell (1890b). Later, Hansen and Sørensen (1904) recognized both species as valid, although they maintained the synonymy of *Leptopsalis* with *Stylocellus*, as did Roewer (1923) and Rosas Costa (1950). Giribet's (2000) catalogue, before examining either type, also left *L. beccarii* in synonymy with *S. sumatranus*, following Thorell (1890b), but the distinction between the species was recognized soon thereafter (Giribet, 2002). A molecular and continuous morphological phylogenetic analysis including *S. sumatranus* (but without
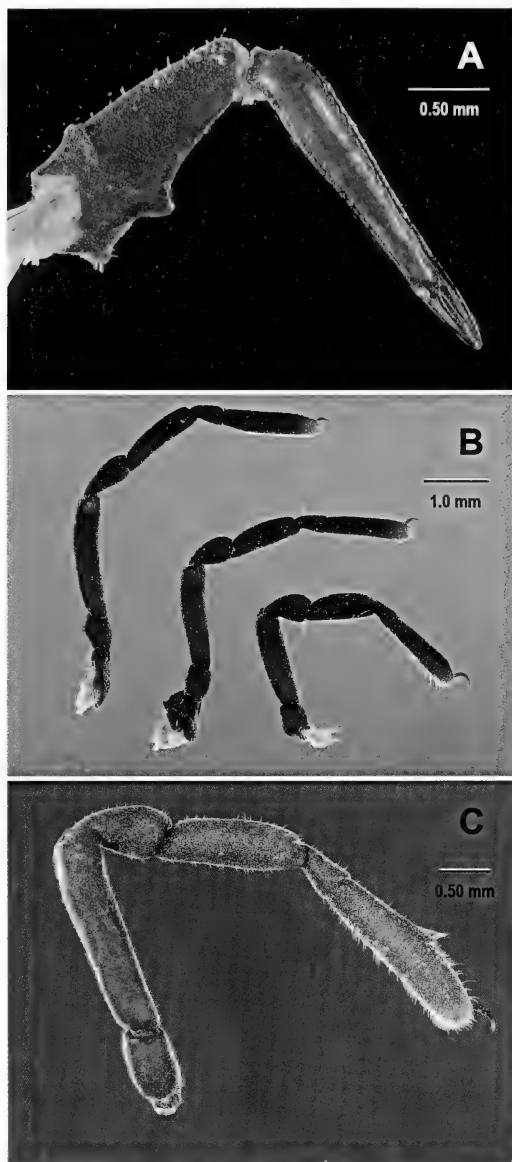
Figure 12.   *Leptopsalis beccarii* Thorell, 1882, second male paralectotype: disarticulated right chelicera (A), right legs I–III (B, left to right, respectively), and right leg IV (C).

Meghalaya and *Fangensis* (Clouse et al., 2009). It is possible that *Stylocellus* remains restricted to the type species of the genus. In contrast, our phylogenetic analysis shows that a large clade of stylocellids originating on Borneo and diversifying on the Thai–Malay Peninsula, Sumatra, Java, Sulawesi, and New Guinea includes several large Sumatran species closely resembling the type of *Leptopsalis* (Clouse and Giribet, 2007; Clouse, 2010; Clouse and Giribet, 2010; Clouse et al., 2009, 2011), and we formally resurrect this genus here and transfer the most stable members of this clade to *Leptopsalis*. These include *L. beccarii* Thorell, 1882, the type species; *L. dumoga* (Shear, 1993) comb. nov.; *L. hillyardi* (Shear, 1993) comb. nov.; *L. javana* Thorell, 1882; *L. lydekkeri* (Clouse & Giribet, 2007) comb. nov.; *L. modesta* (Hansen & Sørensen, 1904) comb. nov.; *L. novaguinea* (Clouse & Giribet, 2007) comb. nov.; *L. ramblae* (Giribet, 2002) comb. nov.; *L. sulcata* (Hansen & Sørensen, 1904) comb. nov.; *L. tambusisi* (Shear, 1993) comb. nov.; *L. thorellii* (Hansen & Sørensen, 1904) comb. nov.; and *L. weberii* (Hansen & Sørensen, 1904) comb. nov.

One male and one female specimens photographed (Figs. 9, 10):

Leptopsalis beccarii Thorell, 1882
Probably type series
Sumatra, Mt. Singalang
leg. O. Beccari VII-1878

Two male specimens whole, one photographed (Fig. 11). Two male specimens dissected, one with legs and chelicerae available, photographed (Fig. 12):

Leptopsalis beccarii Thorell, 1882
Cotypes
Sumatra
leg. O. Beccari

A male specimen collected by Elio Modigliani in Sipora Island (off the coast of Sumatra) in 1891 was erroneously identified by Carl Friedrich Roewer as *L. beccarii* in 1935 (at that time recombined in

molecular data for this species) suggests that it branches out before the split between *Miopsalis* and *Leptopsalis*, although its exact position is uncertain, and it shares key characters with members of the genera
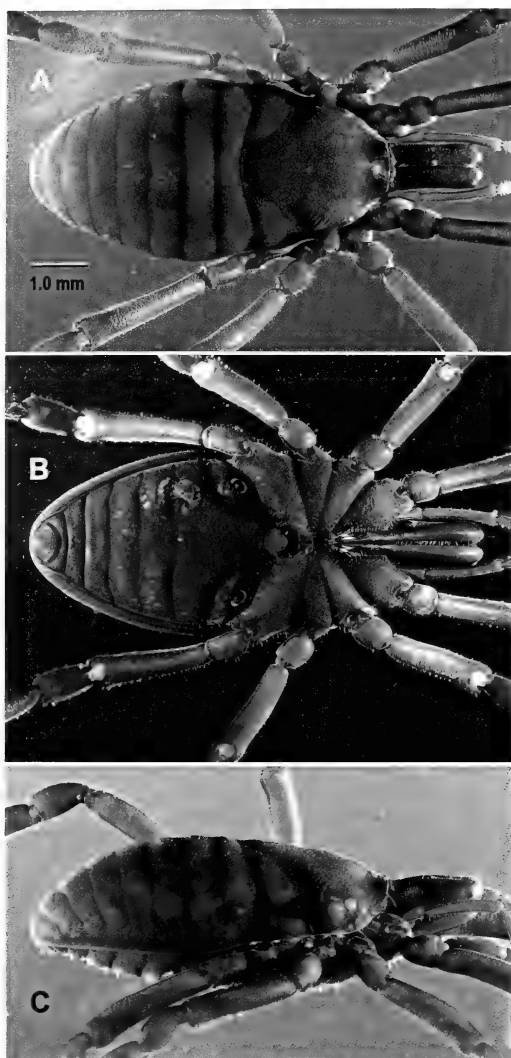
Figure 13. An undescribed male from Sipora Island (near Sumatra), collected in 1891, showing dorsal (A), ventral (B), and lateral (C) views.
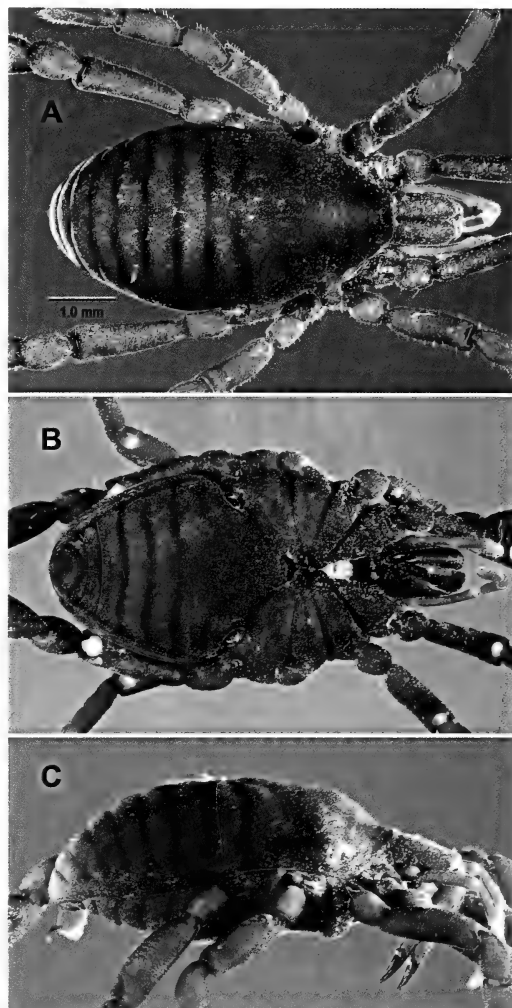
Figure 14.   *Leptopsalis javana* Thorell, 1882, male holotype in dorsal (A), ventral (B), and lateral (C) views.

Stylocellus). It is clearly affiliated with other large Sumatran *Leptopsalis*, of which we have seen several undescribed species, but it is distinctly larger than the lectotype of *L. beccarii*. Specimen photographed (Fig. 13):

> *Stylocellus beccarii* Hansen & Sør.
> Mentawei: Sereinu
> Leg. E. Modigliani, 1891
> Det. Roewer, 1935–N. 10202

Leptopsalis javana Thorell, 1882
Figures 14, 15

Leptopsalis javana was described by Thorell (1882) along with *L. beccarii* on the basis of a single male specimen from Tcibodas (Cibodas), Java, collected by Odoardo Beccari.

We collected what appears to be *L. javana* at the Cibodas Botanical Garden, at the base of Gunung Gedé-Pangrango N.P., in Java. This was included in recent studies of stylocellid phylogenetics as "Java sp. 10"

Figure 15. *Leptopsalis javana* Thorell, 1882, male holotype: detailed views of the anal plate and surrounding ventral posterior region (A), distal parts of chelicerae, lateral view (B), and gonostome (C).

Figure 16. *Leptopsalis thorellii* (Hansen & Sørensen, 1904), female holotype in dorsal (A), ventral (B), and lateral (C) views.

(Clouse et al., 2009; Clouse and Giribet, 2010). A BMNH specimen from Tcibodas that we have examined is identified as *Stylocellus javanus* but appears to be misidentified; it is actually more similar to other large species found in western Java and recently included in our molecular phylogenetic analyses.

Male specimen photographed (Figs. 14, 15):

Leptopsalis javana Thorell, 1882
Type
Giava, Tcibodas
leg. O. Beccari, X-1874

Leptopsalis thorellii (Hansen & Sørensen, 1904)
Figures 16, 17

Stylocellus thorellii was described by Hansen and Sørensen (1904) on the basis of a single female specimen from Mt. Singalang (current spelling: Singgalang), Sumatra, Indonesia. It was also originally
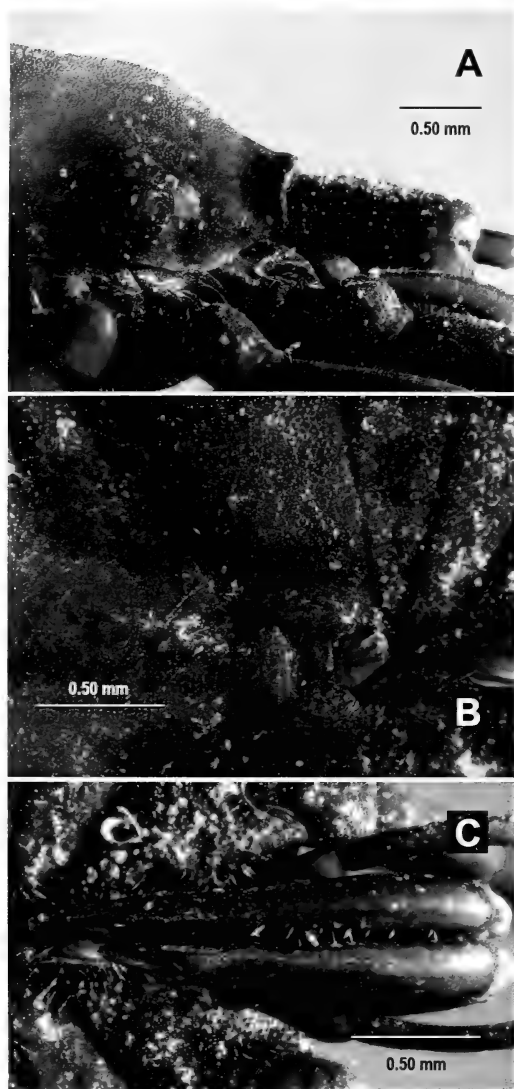
Figure 17. *Leptopsalis thorellii* (Hansen & Sørensen, 1904), female holotype: detailed views of the anterior lateral region (A), gonostome (B), and chelicerae (C).

Figure 18. *Leptopsalis* cf. *weberii* (Hansen & Sørensen, 1904), male in dorsal (A), ventral (B), and lateral (C) views.

included in the type series that was used for the description of the very similar *L. beccarii* (1882), although phylogenetically these two species have been recovered in different *Leptopsalis* clades (Clouse et al., 2009), highlighting the uncertainties of morphological characters in this large genus.

Stylocellus thorellii Hansen & Sør., 1904

Type: Female holotype

Sumatra, Mt. Singalang
leg. O. Beccari, VIII-1878
(*Stylocellus beccarii* Thor. *partim*)

Leptopsalis cf. *weberii* (Hansen & Sørensen, 1904)
Figures 18, 19

Stylocellus weberii was described by Hansen and Sørensen (1904) on the basis of a single male specimen collected by Max Weber at Manindjau (Lake Maninjau), Sumatera Barat, Sumatra, Indonesia. The MCSN contains one male and two females from a different locality on Sumatra, identified as *S. weberii*, although these specimens have not been contrasted with the
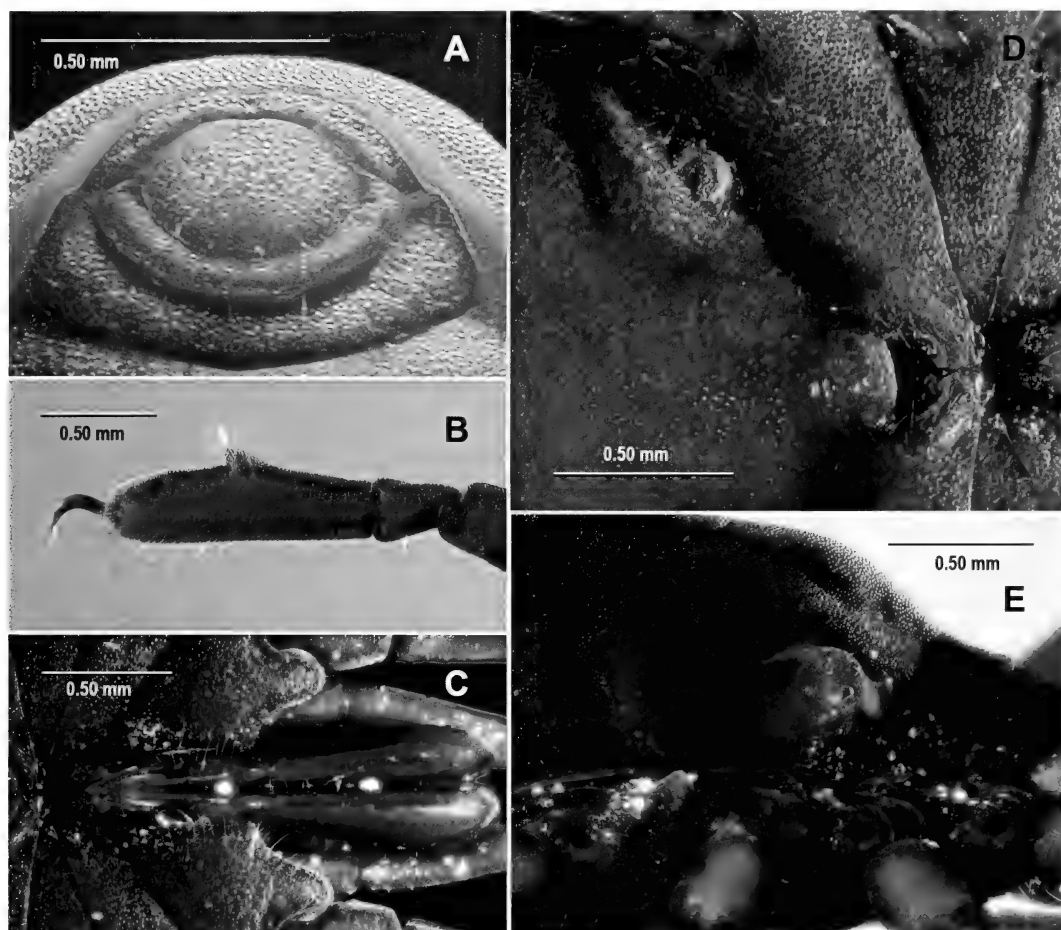
Figure 19. *Leptopsalis* cf. *weberii* (Hansen & Sørensen, 1904), male showing detailed views of the anal plate (A), tarsus IV (B), chelicerae (C), gonostome (D), and lateral anterior part of body (E).

type specimen from Maninjau, supposedly deposited in the Zoological Museum Amsterdam (Giribet, 2000).

Specimen photographed (Figs. 18, 19):

Stylocellus weberi Hansen & Sør.
One male, two females
leg. E. Modigliani, 1891
Sumatra: Pangherang
Det: Roewer, 1935–N. 10201

FINAL REMARKS

We provide here bibliographic and taxonomic details as well as high-definition photographs of important type specimens in the Opiliones suborder Cyphophthalmi deposited in the MCSN. These specimens are of special importance due to their constituting the type species of three genera (in the families Neogoveidae and Stylocellidae), having primary types of five species, and being among the oldest cyphophthalmid specimens known. The study of this material allows us to confirm the validity of the genus *Miopsalis*, considered a nomen dubium in the most recent catalogue of Cyphophthalmi, and confidently re-erect the genus *Leptopsalis*, in synonymy with *Stylocellus* for over a century. Several

described species are here assigned to both genera. Finally, this article aims at showing the importance of natural history collections for continuing the painstaking task of describing and documenting the biological diversity of our planet and how this work cannot progress in many taxonomic groups until type specimens are made available to the community.

ACKNOWLEDGMENTS

LITERATURE CITED

BOYER, S. L., R. M. CLOUSE, L. R. BENAVIDES, P. SHARMA, P. J. SCHWENDINGER, I. KARUNARATHNA, and G. GIRIBET. 2007. Biogeography of the world: a case study from cyphophthalmid Opiliones, a globally distributed group of arachnids. *Journal of Biogeography* **34**: 2070–2085.

BOYER, S. L., and G. GIRIBET. 2007. A new model Gondwanan taxon: systematics and biogeography of the harvestman family Pettalidae (Arachnida, Opiliones, Cyphophthalmi), with a taxonomic revision of genera from Australia and New Zealand. *Cladistics* **23**: 337–361.

BOYER, S. L., I. KARAMAN, and G. GIRIBET. 2005. The genus *Cyphophthalmus* (Arachnida, Opiliones, Cyphophthalmi) in Europe: a phylogenetic approach to Balkan Peninsula biogeography. *Molecular Phylogenetics and Evolution* **36**: 554–567.

CLOUSE, R. M. 2010. *Molecular and Morphometric Phylogenetics and Biogeography of a Southeast Asian Arachnid Family (Opiliones, Cyphophthalmi, Stylocellidae).* Ph.D. Thesis. Pp. 121. Cambridge, Massachusetts: Department of Organismic and Evolutionary Biology. Harvard University.

CLOUSE, R. M., B. L. DE BIVORT, and G. GIRIBET. 2009. A phylogenetic analysis for the Southeast Asian mite harvestman family Stylocellidae (Opiliones : Cyphophthalmi)—a combined analysis using morphometric and molecular data. *Invertebrate Systematics* **23**: 515–529.

CLOUSE, R. M., D. M. GENERAL, A. C. DIESMOS, and G. GIRIBET. 2011. An old lineage of Cyphophthalmi (Opiliones) discovered on Mindanao highlights the need for biogeographical research in the Philippines. *Journal of Arachnology* **39**: 147–153.

CLOUSE, R. M., and G. GIRIBET. 2007. Across Lydekker's Line—first report of mite harvestmen (Opiliones :

Cyphophthalmi : Stylocellidae) from New Guinea. *Invertebrate Systematics* **21**: 207–227.

CLOUSE, R. M., and G. GIRIBET. 2010. When Thailand was an island—the phylogeny and biogeography of mite harvestmen (Opiliones, Cyphophthalmi, Stylocellidae) in Southeast Asia. *Journal of Biogeography* **37**: 1114–1130.

DE BIVORT, B. L., and G. GIRIBET. 2004. A new genus of cyphophthalmid from the Iberian Peninsula with a phylogenetic analysis of the Sironidae (Arachnida : Opiliones : Cyphophthalmi) and a SEM database of external morphology. *Invertebrate Systematics* **18**: 7–52.

GIRIBET, G. 2000. Catalogue of the Cyphophthalmi of the World (Arachnida, Opiliones). *Revista Ibérica de Aracnología* **2**: 49–76.

GIRIBET, G. 2002. *Stylocellus ramblae,* a new stylocellid (Opiliones, Cyphophthalmi) from Singapore, with a discussion of the family Stylocellidae. *Journal of Arachnology* **30**: 1–9.

GIRIBET, G., and S. L. BOYER. 2002. A cladistic analysis of the cyphophthalmid genera (Opiliones, Cyphophthalmi). *Journal of Arachnology* **30**: 110–128.

GIRIBET, G., and C. E. PRIETO. 2003. A new Afrotropical *Ogovea* (Opiliones, Cyphophthalmi) from Cameroon, with a discussion on the taxonomic characters in the family Ogoveidae. *Zootaxa* **329**: 1–18.

GIRIBET, G., L. VOGT, A. PÉREZ GONZÁLEZ, P. SHARMA, and A. B. KURY. 2010. A multilocus approach to harvestman (Arachnida: Opiliones) phylogeny with emphasis on biogeography and the systematics of Laniatores. *Cladistics* **26**: 408–437.

GIRIBET, G., P. P. SHARMA, L. R. BENAVIDES, S. L. BOYER, R. M. CLOUSE, B. L. DE BIVORT, D. DIMITROV, G. Y. KAWAUCHI, J. Y. MURIENNE, and P. J. SCHWENDINGER. 2011. Evolutionary and biogeographic history of an ancient and global group of arachnids (Arachnida, Opiliones, Cyphophthalmi) with a new taxonomic arrangement. *Biological Journal of the Linnean Society* **105**: 92–130.

HANSEN, H. J. 1921. Studies on Arthropoda I. The Pedipalpi, Ricinulei, and Opiliones (exc. Op. Laniatores) collected by Mr. Leonardo Fea in tropical West Africa and adjacent Islands. Copenhagen: Gyldendalske Boghandel.

HANSEN, H. J., and W. SØRENSEN. 1904. *On Two Orders of Arachnida: Opiliones, Especially the Suborder Cyphophthalmi, and Ricinulei, Namely the Family Cryptostemmatoidae.* Cambridge, United Kingdom: Cambridge University Press.

JUBERTHIE, C. 1970. Sur *Suzukielus sauteri* (Roewer, 1916) opilion cyphophthalme du Japon. *Revue d'Écologie et de Biologie du Sol* **7**: 563–569.

KURY, A. B. 2010. Opilionological Record—a chronicle of harvestman taxonomy. Part 1: 1758–1804. *Journal of Arachnology* **38**: 521–529.

LEGG, G. 1990. *Parogovia pabsgarnoni,* sp. n. (Arachnida, Opiliones, Cyphophthalmi) from Sierra Leone, with notes on other African species of

Parogovia. Bulletin of the British Arachnological Society **8**: 113–121.

Rodman, J. E., and J. H. Cody. 2003. The taxonomic impediment overcome: NSF's partnerships for enhancing expertise in taxonomy (PEET) as a model. *Systematic Biology* **52**: 428–435.

Roewer, C. F. 1916. 7 neue Opilioniden des Zoolog. Museums in Berlin. *Archiv für Naturgeschichte* **81**: 6–13.

Roewer, C. F. 1923. *Die Weberknechte der Erde. Systematische Bearbeitung der bisher bekannten Opiliones.* Jena: Verlag von Gustav Fisher.

Rosas Costa, J. A. 1950. Sinopsis de los géneros de Sironinae, con la descripción de dos géneros y una especie nuevos (Opiliones, Cyphophthalmi). *Arthropoda* **1**: 127–151.

Schwendinger, P. J., and G. Giribet. 2005. The systematics of the Southeast Asian genus *Fangensis* Rambla (Opiliones : Cyphophthalmi : Stylocellidae). *Invertebrate Systematics* **19**: 297–323.

Shear, W. A. 1980. A review of the Cyphophthalmi of the United States and Mexico, with a proposed reclassification of the suborder (Arachnida, Opiliones). *American Museum Novitates* **2705**: 1–34.

Shear, W. A. 1993. New species in the opilionid genus *Stylocellus* from Malaysia, Indonesia and the Philippines (Opiliones, Cyphophthalmi, Stylocellidae). *Bulletin of the British Arachnological Society* **9**: 174–188.

Simon, E. 1872. Notice sur les Arachnides cavernicoles et hypogés. *Annales de la Société entomologique de France. 5e série* **2**: 215–244.

Suarez, A. V., and N. D. Tsutsui. 2004. The value of museum collections for research and society. *BioScience* **54**: 66–74.

Thorell, T. 1882. Descrizione di alcuni Aracnidi inferiori dell' Arcipelago Malese. *Annali del Museo civico di Storia naturale di Genova* **18**: 21–69.

Thorell, T. 1890a. Aracnidi di Pinang raccolti nel 1889 dai Sig.ri L. Loria e L. Fea. *Annali del Museo civico di Storia naturale di Genova (Ser. 2a)* **10**: 269–383.

Thorell, T. 1890b. Aracnidi di Nias e di Sumatra raccolti nel 1886 dal Sig. E. Mondigliani. *Annali del Museo civico di Storia naturale di Genova (Ser. 2a)* **10**: 5–106.

Bulletin
of the
Museum of Comparative Zoology

Systematics of the Neotropical Snake *Dendrophidion percarinatum* (Serpentes: Colubridae), with Descriptions of Two New Species From Western Colombia and Ecuador and Supplementary Data on *D. brunneum*

JOHN E. CADLE

SYSTEMATICS OF THE NEOTROPICAL SNAKE *DENDROPHIDION PERCARINATUM* (SERPENTES: COLUBRIDAE), WITH DESCRIPTIONS OF TWO NEW SPECIES FROM WESTERN COLOMBIA AND ECUADOR AND SUPPLEMENTARY DATA ON *D. BRUNNEUM*

JOHN E. CADLE[1]

CONTENTS

[1] Department of Herpetology, California Academy of Sciences, 55 Music Concourse Drive, Golden Gate Park, San Francisco, California 94118 (jcadle@calacademy.org).

ABSTRACT. *Dendrophidion percarinatum* (Cope) is redefined on the basis of standard and new characters to distinguish it from two new South American species with which it has previously been confused. The redefined *D. percarinatum* is distributed from Honduras through Central America to western Colombia, with a seemingly outlying locality in extreme western Venezuela. One new species, *D. prolixum*, is sympatric with *D. percarinatum* at a few localities in central western Colombia and the distribution of the new species continues southward into northwestern Ecuador. A second new species, *D. graciliverpa*, occurs throughout western Ecuador, where its distribution extensively overlaps that of *D. brunneum* (Günther). Hemipenes of the two new species are unusually long and slender (gracile morphotype), a morphology distinct from other described *Dendrophidion* hemipenes, which are shorter and more robust (robust morphotype). Additionally, the new species differ from *D. percarinatum* in color patterns but not in standard scutellation characters such as segmental counts. Similarly, the two new species differ from one another in coloration but not in scutellation or hemipenial morphology. Hemipenes of *D. percarinatum* and the new species are described in detail. The holotype of *D. brunneum* is redescribed to ensure the proper application of that name. New specimens document the widespread occurrence of *D. brunneum* in the lowlands of western Ecuador and apparent extensive pattern polymorphism, including unicolor, striped, crossbanded, and punctate forms; more data on coloration in life are needed. Some previous records of "*D. percarinatum*" from interandean valleys of the Río Cauca/Magdalena system are from mistaken identities. However, several specimens from the Río Magdalena resemble *D. percarinatum* in scutellation but differ in color pattern; their status needs further study.

Key words: Colombia, Ecuador, systematics, Chocó, Central America, South America, *Dendrophidion*, snakes, new species, hemipenis, morphology

RESUMEN.   *Dendrophidion percarinatum* (Cope) se redefine sobre la base de caracteres estandarizados y nuevos para distinguirlo de dos nuevas especies sudamericanos con que se confundieron anteriormente. El redefinido *D. percarinatum* se encuentra desde Honduras por América Central hasta el oeste de Colombia, con una localidad aparentemente alejada en el extremo occidental de Venezuela. Una nueva especie, *D. prolixum*, es simpátrica con *D. percarinatum* a pocas localidades en el centro-occidental de Colombia; la distribución de la nueva especie continua hacia el sur hasta el noroeste de Ecuador. Una segunda nueva especie, *D. graciliverpa*, occurre en todo del Ecuador occidental, donde su distribución traslapa la distribución de *D. brunneum* (Günther). Los hemipenes de ambas nuevas especies son exceptionalmente alargados y delgados (morfotipo esbelto). Es una morfología distinta de los otros hemipenes de *Dendrophidion*, que son más corto y robusto (morfotipo robusto). Además, las nuevas especies se distinguen de *D. percarinatum* por la coloración pero no se distinguen en caracteres estandarizados de escutellación como cuentas segmentales. De modo parecido, las dos nuevas especies se distinguen por coloración pero no por la escutellación ni la morfología de los hemipenes. Se describen los hemipenes de *D. percarinatum* y las nuevas especies. Para asegurar la aplicación apropiada del nombre *D. brunneum* se redescribe el holotipo de esta especie. Nuevas especímenes documentan la ocurrencia amplia de *D. brunneum* en las tierras bajas del Ecuador occidental y también polimorfismo extenso de patrones, incluyendo patrones unicolor, rayado, con bandas, y con manchas; se necesitan más datos sobre la coloración de vida. Algunos registros anteriores de "*D. percarinatum*" desde los valles interandinos de la sistema Ríos Cauca/Magdalena son de identidades equivocadas. Sin embargo, existen especímenes del Río Magdalena que son parecidos a *D. percarinatum* en la escutellación pero son distintos en coloración; su estatus merece más estudio.

INTRODUCTION

At the time of his death in 1972, James A. Peters had been accumulating data in preparation for a revision of the Neotropical snake genus *Dendrophidion* Fitzinger and he indicated that the account given by Peters and Orejas-Miranda (1970: 79) would "be rather thoroughly changed upon completion of the review." Forty years hence there still has been no comprehensive review of *Dendrophidion*, although various workers have chipped away at particular geographic or taxonomic segments of the genus. Lieb (1988), working in part from Peters' unpublished data, resurrected *D.*

nuchale (W. Peters) from the synonymy of *D. dendrophis* (Schlegel), stabilized the application of the last name by designating a lectotype for it, and clarified the application of other names in the much-confused literature on these snakes. Lieb (1988) also briefly summarized characters and distributions for the nine species of *Dendrophidion* he recognized and apportioned eight of them between two species groups. McCranie (2011) resurrected the name *D. clarkii* Dunn for application to Central American members of the complex including *clarkii* and *nuchale*. Cadle (2010) reviewed the systematics, natural history, and hemipenial morphology of *D. brunneum* based on new material and field observations, and Cadle (2012) partitioned *D. vinitor* by describing two new cryptic species previously confused with it. Freire et al. (2010) described another new species of the *D. dendrophis* group from northeastern Brazil. Other taxonomic issues still need resolution.

This paper focuses on *Dendrophidion percarinatum*, which according to current taxonomy is distributed from Honduras to Ecuador and Venezuela. During my review of *D. brunneum* (Cadle, 2010), I had examined material referred to "*D. percarinatum*" from western Colombia and Ecuador and indicated that revision of *D. percarinatum* appeared necessary (Cadle, 2010: 2, 24). Further investigation has confirmed that suggestion and has caused me to revise some of my earlier assessments concerning *D. brunneum*. In particular, I came to realize that most specimens previously referred to "*D. percarinatum*" in western Colombia and Ecuador were, in fact, distinct species. *Dendrophidion percarinatum* is widespread in Central America, but other than a few localities around the Golfo de Urabá in northern Colombia, it is definitely known from only a handful of localities in the Chocó region and one in extreme western Venezuela.

In this paper I review the systematics of *Dendrophidion percarinatum* with special reference to populations in western Colombia and Ecuador. Two species previously

confused with *D. percarinatum* from the last two areas are described as new. Hemipenes of the three species are described. The review of western Ecuadorian specimens of *Dendrophidion* also resulted in the discovery that the distribution of *D. brunneum* includes previously unrecognized lowland localities and broadly overlaps the distribution of one of the new species in western Ecuador. The holotype and new material of *D. brunneum* are reviewed to supplement the earlier account (Cadle, 2010) and to ensure proper application of this name.

MATERIALS AND METHODS

Methods follow procedures described in Cadle (2005, 2007, 2012). Methods for scoring dorsocaudal reductions, dorsal keeling, aspects of color pattern, and statistical methods are described by Cadle (2012) for other *Dendrophidion*. Additional comments on characters especially relevant to *D. percarinatum* and the new species described herein are detailed below. Measurements (in mm) of hemipenes and for a loreal scale character in the section on *Dendrophidion brunneum* were made with Helios dial calipers to the nearest 0.01 mm under a dissecting microscope. For purposes of analyzing intraspecific differences in mean SVL of adult males and females, specimens >400 mm snout to vent length (SVL) were considered adults because sexual maturation occurs at 400–500 mm SVL (Goldberg, 2003; Stafford, 2003). Similarly, because relative tail length increases proportionally with SVL, the range of adult relative tail length (RTL) was assessed for individuals with SVL > 300 mm because RTL approaches an asymptote at approximately this size. Methods of hemipenial study are covered in the introduction to that section.

My sampling of *Dendrophidion percarinatum* has not been even from throughout the range. Sample sizes of *D. percarinatum* as redefined here from throughout the range are as follows (number of males, number of females): Honduras (10, 12),

Nicaragua (3, 3), Costa Rica (29, 26), Panama (56, 37), Colombia (7, 4). I also examined the lectotype of *D. percarinatum* and the holotype and additional specimens of *D. brunneum*. Hemipenial morphology offered some early insights into the systematics of these species, and I examined everted hemipenes from throughout the range of *D. percarinatum* and the internal morphology of retracted organs of selected specimens. I also examined all available everted hemipenes of the two new species and the internal morphology of other retracted organs.

Except where specifically qualified (e.g., "*Dendrophidion percarinatum sensu* Lieb 1988"), I use the name *Dendrophidion percarinatum* to refer to this snake as redefined herein, which excludes certain populations in western Colombia and Ecuador that have been included in other literature (e.g., Lieb, 1988, 1996; Savage, 2002; Stafford, 2003; Cadle, 2010). I refer to *D. percarinatum* plus the two new species described herein as the "*Dendrophidion percarinatum* complex" with no assumption that the complex is monophyletic within *Dendrophidion*. These species plus *D. brunneum* and *D. paucicarinatum* comprise the *D. percarinatum* species group of Lieb (1988). Unresolved systematic issues pertain to other species names within *Dendrophidion*, and I use the name "*D. nuchale* auctorum" for the complex of species represented by this name, as explained in Cadle (2012: 188; see also Savage, 2002: 655; McCranie, 2011: 106–107).

Appendix 1 lists specimens examined of *Dendrophidion percarinatum*, *D. brunneum* (Ecuadorian specimens identified subsequent to Cadle [2010] only), and several specimens of uncertain status (*D. species inquirendum*). Specimens of the new species are listed in the text. The accounts of new species include some specimens listed as "other referred specimens" rather than paratypes. These specimens are all juvenile or adult females, which are sometimes difficult to identify from preserved specimens (depending on state of preservation

and/or characters of individual specimens). These difficulties are discussed in the species accounts. Scutellation data from the referred specimens were included in the data summaries except as noted (e.g., Table 1). Appendix 2 contains coordinates and notes on the localities for the new species. Coordinates, some elevations, and other information on localities were derived primarily from Brown (1941; Ecuador), Fairchild and Handley (1966; Panama), Paynter (1993, 1997; Ecuador and Colombia), Lynch and Duellman (1997; Ecuador), McCranie (2011; Honduras), and the National Geospatial-Intelligence Agency (NGA, 2010-2012) online gazetteer (GEOnet). There have been changes in Ecuadorian administrative divisions associated with some well-known localities in western Ecuador (e.g., Santo Domingo de los Colorados). Two new provinces, Santo Domingo de los Tsáchilas and Santa Elena, were created in 2007 from portions of Pichincha and Guayás provinces, respectively. I record both provinces for these localities to prevent confusion when cross-referencing with other taxonomic literature on this area.

Table 1 presents summary taxonomic and morphological data for species of the *Dendrophidion percarinatum* complex. Data summarized therein for *D. percarinatum* are for specimens from throughout the geographic range of this species (Honduras to western Colombia). Geographic variation for some characters of *D. percarinatum* is discussed in the species account (see also Tables 2 and 3). Hemipenial characters are discussed in the section devoted to them after the species accounts.

TAXONOMIC CHARACTERS OF SPECIAL RELEVANCE TO THE *DENDROPHIDION PERCARINATUM* COMPLEX

At the outset it is appropriate to discuss the primary character systems used in my assessments of species boundaries within the *Dendrophidion percarinatum* complex.

Although many of the same character systems relevant to the systematics of the *D. vinitor* complex (Cadle, 2012) are pertinent to *D. percarinatum*, the informative aspects of variation are sometimes a bit different. For example, color patterns are relevant to differentiating species in both groups, but the aspects of coloration of particular value in each group differ. The following sections discuss variation in several character systems as they pertain to the *D. percarinatum* complex.

Color Pattern. Dendrophidion percarinatum as conceived in previous works is highly variable in coloration and pattern (Lieb, 1988, 1996; Savage, 2002). However, little attention has been given to the relationship of this variation to geography or its potential systematic implications. During my review it became clear that, although pattern variation within *D. percarinatum* in Central America is comparatively minor, in northern South America several distinct color patterns were present. Further consideration suggested that these distinct color patterns had both geographic integrity (i.e., discrete geographic distributions) and were correlated in some cases with other characters (e.g., hemipenial morphology) suggestive of systematic distinction. Thus, color pattern variation played a significant role in my assessment of species boundaries within the *D. percarinatum* complex, particularly in the absence of strong differentiation using standard scale characters (Lieb, 1988; Cadle, 2010, 2012; documented herein). Unfortunately, coloration in life is available for relatively few specimens. Changes induced by preservation and perhaps differences in preservation techniques make it impossible to correlate preserved coloration to colors in life with any ease. Some pattern elements seemingly become more prominent upon preservation (e.g., pale crossbands) even as others become more obscure. Other factors, such as the integrity of the stratum corneum on a given specimen, also affect the appearance of preserved specimens.

Narrow pale crossbands are expressed in some individuals of all species of the

TABLE 1.   TAXONOMIC DATA FOR *DENDROPHIDION PERCARINATUM* (RANGEWIDE SUMMARY) AND TWO NEW SPECIES. BODY PROPORTIONS, SEGMENTAL COUNTS, SCALE REDUCTIONS, MAXILLARY TEETH, AND NUMBER OF PALE BANDS ARE GIVEN AS RANGE FOLLOWED BY MEAN ± SD. BILATERAL COUNTS ARE SEPARATED BY A SLASH (/). FOR TEMPORALS AND LABIAL SCALES, EACH SIDE OF A SPECIMEN WAS COUNTED AS AN INDEPENDENT OBSERVATION. SAMPLE SIZES IN PARENTHESES. ASTERISKS INDICATE STATISTICAL SIGNIFICANCE OF INTRASPECIFIC DIFFERENCES BETWEEN MEANS OF MALE AND FEMALE SIZE, PROPORTIONS, OR MERISTIC COUNTS (* $p < 0.05$; ** $p < 0.01$; *** $p < 0.001$); NO ASTERISK INDICATES NONSIGNIFICANCE.

	Dendrophidion percarinatum (Cope) Rangewide Summary	*Dendrophidion prolixum* New Species	*Dendrophidion graciliverpa* New Species
Largest specimens: total length, SVL (mm)			
Male	1,358+, 852 [1,236, 747][†]	1,003+, 650 [1,037, 642][†]	1,054+, 676 [964, 605][†]
Female	1,300, 778	976+, 675 [1,116, 662][†]	922+, 663 [1,027, 631][†]
Mean adult SVL (mm)			
Male	401–852	455–650	409–605
	577.3 ± 93.18 (73)	582.6 ± 61.95 (10)	517.5 ± 58.30 (16)***
Female	437–778	425–675	543–663
	604.4 ± 74.63 (51)	604.3 ± 76.15 (15)	615.5 ± 37.92 (11)
Tail length/total length			
Male	0.38–0.45	0.38–0.40	0.37–0.42
	0.42 ± 0.019 (52)**	0.39 ± 0.009 (5)	0.39 ± 0.0002 (9)**
Female	0.37–0.43	0.38–0.41	0.36–0.39
	0.40 ± 0.014 (24)	0.40 ± 0.012 (6)	0.37 ± 0.014 (6)
Tail length/SVL			
Male	0.62–0.82	0.62–0.67	0.59–0.72
	0.72 ± 0.054 (52)***	0.65 ± 0.021 (5)	0.65 ± 0.038 (9)**
Female	0.59–0.75	0.63–0.69	0.56–0.64
	0.68 ± 0.039 (24)	0.66 ± 0.026 (6)	0.59 ± 0.035 (6)
Maxillary teeth	33–42	36–42	33–44
	37.1 ± 1.84 (59)	38.5 ± 1.65 (22)	38.8 ± 2.40 (23)
Dorsal scales	17–17–15 (180)	17–17–15 (37)	17–17–15 (27)
	other patterns (4)		17–19–17 (1)
Ventrals			
Male	147–170	150–164	153–163
	155.8 ± 3.51 (103)***	157.7 ± 4.63 (17)*	157.5 ± 2.15 (22)***
Female	156–167	152–164	152–166
	160.2 ± 2.42 (80)	160.9 ± 3.42 (17)	160.7 ± 3.37 (23)
Subcaudals			
Male	137–163	134–150	132–153
	150.7 ± 6.32 (71)***	140.5 ± 5.15 (11)	142.3 ± 6.41 (12)**
Female	133–157	133–150	120–143
	145.6 ± 5.26 (46)	143.3 ± 5.07 (9)	133.5 ± 7.32 (13)
Total segmental counts (ventrals + subcaudals)			
Male	293–323	284–310	290–309
	306.6 ± 6.19 (72)	297.3 ± 8.49 (11)	299.3 ± 7.01 (12)
Female	293–321	285–313	275–304
	305.9 ± 5.60 (46)	303.4 ± 7.89 (9)	293.0 ± 9.42 (12)
Dorsocaudal reduction, 8 to 6 (subcaudal number)			
Male	8–26	16–26	12–27
	16.0 ± 3.60 (103)***	19.8 ± 3.05 (17)***	20.3 ± 3.69 (21)***
Female	5–24	8–24	7–19
	10.4 ± 3.02 (81)	12.4 ± 4.50 (17)	12.0 ± 3.53 (23)
Dorsal scales, posterior reduction (ventral number)			
Male	84–102	84–99	78–95
	92.6 ± 3.85 (88)***	92.9 ± 4.27 (32)***	90.8 ± 3.73 (30)***
Female	91–106	91–110	90–101
	96.8 ± 3.30 (54)	98.7 ± 3.93 (32)	94.9 ± 9.59 (24)

TABLE 1.   CONTINUED.

	Dendrophidion percarinatum (Cope) Rangewide Summary	*Dendrophidion prolixum* New Species	*Dendrophidion graciliverpa* New Species
Preoculars	1/1 (186)	1/1 (34)	1/1 (43)
	1/2 (2)		
Postoculars	1/1 (1)	2/2 (32)	2/2 (37)
	1/2 (2)	2/3 (2)	2/3 (2)
	2/2 (182)		3/3 (4)
	2/3 (2)		
	3/3 (1)		
Primary temporals	1 (2)	1 (1)	2 (84)
	2 (370)	2 (61)	3 (2)
		3 (1)	
Secondary temporals	1 (1)	2 (61)	2 (85)
	2 (362)	3 (2)	1 (1)
	3 (3)		
Supralabials, supralabials touching eye	8, 3–5 (1)	9, 4–6 (67)	8, 3–5 (5)
	8, 4–5 (1)	10, 4–7 (1)	8, 4–5 (1)
	8, 4–6 (2)		9, 4–5 (2)
	9, 4–6 (363)		9, 4–6 (76)
	10, 5–7 (9)		
Infralabials	8 (1)	8 (3)	8 (3)
	9 (17)	9 (16)	9 (13)
	10 (321)	10 (28)	10 (54)
	11 (32)	11 (20)	11 (12)
	12 (2)	12 (1)	12 (1)
Supralabial/ temporal pattern	G, 6.8%	G, 76%	G, 66.7%
	P, 82.8%	P, 4.5%	P, 2.9%
	irregular/ambiguous, 10.4% (221)	irregular/ambiguous, 19.4% (67)	irregular/ambiguous, 30.4% (69)
No. of pale bands on body	71–96	49–57	57–87
	81.2 ± 6.87 (45)	53.0 ± 2.59 (12)	70.5 ± 8.81 (26)
Hemipenial characters	robust morphotype	gracile morphotype	gracile morphotype
	< 40 enlarged spines	> 60 enlarged spines	> 60 enlarged spines

† The largest specimens in these cases had incomplete tails. Measurements of the largest specimens with complete tails in brackets.

Dendrophidion percarinatum complex. Juveniles have more distinct crossbands than adults, in which the bands may be either distinct or indistinct. The number of pale crossbands on the body (neck to vent) is useful in distinguishing one of the new species described herein compared with the other two members of the complex. However, because crossbands are not always evident over the entire body in some specimens of all three species, this character cannot always be scored. The width of the pale bands is not useful for distinguishing the two new species from one another or from *D. percarinatum* (the bands are typically one dorsal row or less in width in all three species), but the number of scale rows *separating* pale bands on the neck is helpful when the bands are evident on the neck. In these cases, the counts were made as described in Cadle (2012) for scoring the width of pale bands in the *D. vinitor* complex (except that rows between bands, rather than rows encompassed by bands, were counted). Neck bands can sometimes be discerned under magnification and good lighting even on excessively darkened preserved specimens (the dark borders to the bands are often better clues than the pale band itself); such observations are best made with the specimen submerged in alcohol. These comments apply to preserved museum specimens, but a caveat is that observations presented herein for the two new species suggest that the appearance of pale crossbands can be *enhanced* in

preserved specimens compared with the live snakes.

Other elements of pattern are highly variable within and between species. The venter of the two new species in the *Dendrophidion percarinatum* complex develops narrow dark transverse lines across the anterior edge of each ventral scale (a character also found in some other species of *Dendrophidion*). There is seemingly an ontogenetic component to this variation: larger individuals typically have more fully developed lines in those species in which they occur. Nonetheless, some juveniles have ventral lines, and considerable variation in the prominence of the lines exists in adults as well. These lines seem to develop first on the posterior venter and eventually can encompass nearly all the ventral scutes. Superficially, these lines might appear to be on the posterior edges of the ventral scutes, but close examination shows that they are on the anterior edges of the scales and merely show through the nearly transparent posterior edge of the adjacent anterior scute.

I also examined other aspects of color pattern, such as the dark dorsal longitudinal stripes in the dorsolateral region and flanks seen in many specimens of *Dendrophidion percarinatum*. There is considerable variation in these features, and I did not find them useful for discriminating the three species of the *D. percarinatum* complex. I refer to some other coloration features, particularly with reference to *D. brunneum*.

Supralabial/Temporal Pattern. The arrangement of scales on the lateral surfaces of the head behind the eye is a useful aid in distinguishing species of the *Dendrophidion percarinatum* complex (perhaps more broadly within *Dendrophidion*, but this needs further study). I stress *useful aid* because it is not an infallible character. Some cases are ambiguous because the configuration of these scales is influenced by irregularities such as scale fusions, divisions, or other anomalous patterns. In other cases the patterns are downright misleading (i.e., some specimens have the atypical arrangement for the taxon to which I refer them). For this reason I do not include the supralabial patterns in the list of characters at the beginning of the diagnoses, although I do use them for comparative purposes when they seem useful.

The relevant scales are the lower primary and secondary temporals and their relationship to the penultimate and ultimate supralabials. I distinguish two basic configurations (Fig. 1), which were scored on both sides of a sampling of each species. Frequencies of the patterns are given in Table 1. Early in my work on the *percarinatum* complex I designated these patterns as *P* and *G* for *D. percarinatum* and *D. graciliverpa*, the first pair of species that I distinguished by this character. Atypical or ambiguous configurations were coded separately from the basic configurations.

P-Pattern or percarinatum *Pattern* (Fig. 1A). (As a mnemonic, *P* could also refer to the pentagonal shape of the penultimate supralabial in this pattern.) Penultimate supralabial (nearly always the eighth) broadly contacts the lower secondary temporal, separating the lower primary temporal from the ultimate (ninth) supralabial. The penultimate supralabial is relatively tall and usually in the shape of an irregular pentagon, with the vertical dimension of the posterior part greater than that of the anterior part. The posterior border of the penultimate supralabial is usually even with, or posterior to, the posterior border of the lower primary temporal.

G-Pattern or graciliverpa *Pattern* (Fig. 1B). (As a mnemonic, the first "r" in *graciliverpa* could also refer to the rectangular shape of the penultimate supralabial in this pattern.) Penultimate supralabial (nearly always the eighth) separated from the lower secondary temporal by contact between the lower primary temporal and the ultimate (ninth) supralabial. The penultimate supralabial is usually relatively narrow and homogeneous in vertical dimension and in the shape of an elongate rectangle (sometimes squarish). The posterior border of the penultimate

supralabial is usually anterior to the posterior border of the lower primary temporal.

Hemipenial Characters. Detailed descriptions of hemipenes of the species described herein are presented in a separate section at the end. However, hemipenial characters play a fundamental role in the recognition of the new species described here and in the application of the name *Dendrophidion brunneum* (Günther) discussed later. Thus, a few comments on hemipenial length and overall shape are pertinent here. Cadle (2012: 217–220) provided a general overview of *Dendrophidion* hemipenes. Detailed descriptions and discussion of morphological variation of hemipenes in other species are in Cadle (2010: 14–20; 2012: 220–228).

Most *Dendrophidion* hemipenes are of what may be termed the "robust (or compact) morphotype" (Fig. 2). Hemipenes of this form are relatively short. The narrow proximal portion of the hemipenial body bearing minute spines is short, and the distal section bearing enlarged spines, calyces and/or flounces, and other apical ornamentation is greatly expanded. The distal bulbous section comprises half or more of the length of everted organs.

In contrast, the two new species described herein are characterized a hemipenial morphology that may be called "gracile morphotype" (Fig. 2). Compared with hemipenes of other species of *Dendrophidion* with the possible exception of *D. bivittatum*, gracile hemipenes are exceptionally long. A long, slender proximal section of the hemipenial body bears minute spines, distal to which is a moderately bulbous region bearing enlarged spines, calyces and/or flounces, and other apical ornamentation. The bulbous region of gracile hemipenes is not expanded to the extent that it is in robust organs, and it comprises much less than half of the total length of everted organs. *Dendrophidion bivittatum* seemingly has gracile hemipenial morphology, but I have seen only one somewhat desiccated everted organ of this species; its proportions in retracted organs is similar to the gracile hemipenes described here, though perhaps not quite as

long as in the two species described herein (see Stuart, 1932: pl. I, fig. 2 for an illustration of a retracted organ of *D. bivittatum*).

The compact and gracile morphologies are easily discerned in everted organs (Fig. 2). However, in retracted hemipenes, the overall length of the organ (number of subcaudals subtended) is a reliable indicator of the morphology, even when the internal morphology is not examined and despite some variation in the length of retracted organs (detailed in the section on hemipenial morphology). "Robust" organs generally subtend fewer than 10 subcaudals, whereas "gracile" organs usually subtend 10 or more subcaudals (up to 15 in the specimens I examined). If the internal morphology of retracted hemipenes is examined, the relative proportions of the relatively unadorned base compared with the distal section differentiate the two morphotypes (Fig. 3). For this purpose the distal section comprises the section of enlarged spines (using the most proximal sulcate enlarged spine as a landmark) + flounces/calyces + apical region. The bulbous distal section comprises a much greater proportion of the length of retracted robust organs compared with gracile organs.

REDEFINITION AND DESCRIPTION OF *DENDROPHIDION PERCARINATUM* (COPE)

Figures 1A, 1C, 2, 4–8, 12A, 13A, 19, 38–41

Drymobius percarinatus Cope "1893" (1894): 344 (two syntypes from Boruca and Buenos Ayres, Costa Rica); "1894" [1895]: 427; 1895: 205.

Drymobius dendrophis: Boulenger, 1894: 16 (part). Günther, 1885–1902: 127 (? part; Nicaragua, Costa Rica). Amaral "1929" [1930]: 154 (part). Dunn and Emlen, 1932: 31 (Honduras; ANSP 20817). Schmidt "1933" [1935]: 15 (Panama; USNM 54080).

Cacocalyx percarinatus: Cope "1894" (1895): 427; 1895: 205 + pl. 19, fig. 2; 1900: 778, 781 + pl. 17, fig. 2.
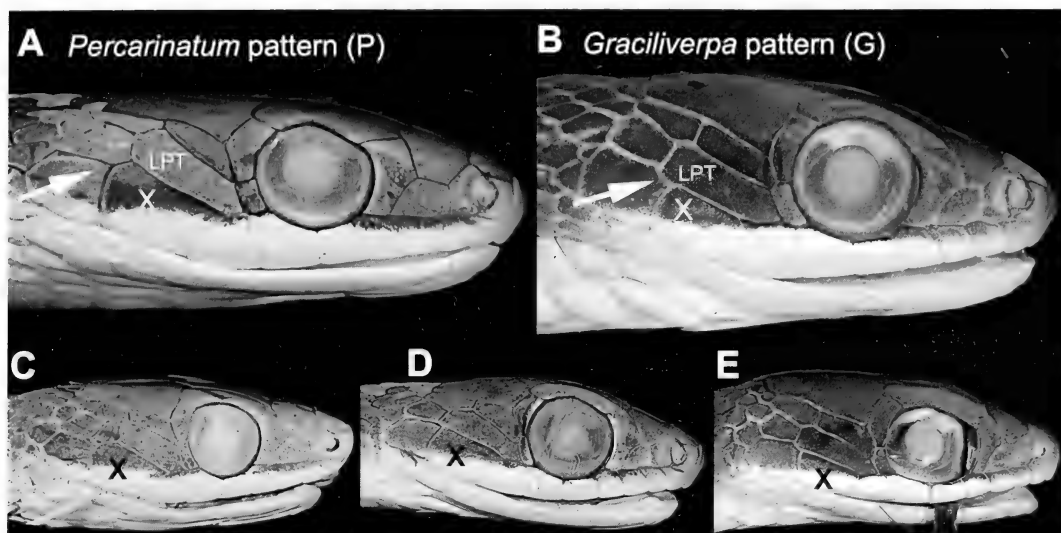
Figure 1.   Contrasting configurations of scales in the posterior supralabial and lower temporal regions in the *Dendrophidion percarinatum* complex. (A) Stereotypical *percarinatum* (*P*) configuration (*D. percarinatum*, LACM 148558); (B) Stereotypical *graciliverpa* (*G*) configuration (*D. graciliverpa*, AMNH R-110585). Bottom panel shows other representations of the typical patterns: (C) *D. percarinatum*, AMNH R-17374, *P* pattern with lower secondary temporal divided vertically; (D) *D. prolixum*, AMNH R-109724, *G* pattern; (E) *D. graciliverpa*, UIMNH 92244, *G* pattern. Panels C, D, and E are left sides reversed. *Abbreviations and symbols:* X, penultimate supralabial (nearly always the eighth); LPT, lower primary temporal. *Arrows* indicate the lack of contact between the lower primary temporal and ultimate supralabial in the *P* pattern, and contact between these two scales in the *G* pattern (arrows lie diagonally across the ultimate labials). Note contrasting shapes of the penultimate supralabial in the *P* (pentagonal) and *G* (rectangular) patterns. See text for further discussion and variation.

Dendrophidion dendrophis: Gaige et al., 1937: 12 (part). Nicéforo María, 1942: 87 (part; ?specimen from Sasaima; see comments under Distribution). Taylor, 1951: 92 (Costa Rica). ?Pérez-Santos and Moreno, 1988: 134 (part; Pacific lowlands of Colombia); 1991b: 135 (part; "lower Central America and northern South America").

Dendrophidion percarinatus. Stuart, 1932: 6. Smith, 1941; 1958: 223. Taylor, 1954: 727 (lectotype designated: "the adult specimen from Boruca" [= AMNH R-17366]). Smith and Grant, 1958: 210. Sexton and Heatwole, 1965: 41. Peters and Orejas-Miranda, 1970: 80. Pérez-Santos and Moreno, 1988: 135 (Colombia).

Dendrophidion percarinatum Dunn, 1944: 477 (? part). Savage, 1973: 14; 1980: 92; 2002: 657 + pl. 418 (part). Wilson and Meyer, 1985: 41. Scott et al., 1983: 372. Savage and Villa, 1986: 148, 169. Villa et al., 1988: 63. Lieb, 1988: 172 (part); 1996:

636.1 (part). Pérez-Santos and Moreno, 1988: 135 (part); 1989: 3 (part); 1991a: 138 (part). Rand and Myers, 1990: 395. Ibáñez and Solís, "1991" [1993]: 30, 33. Pérez-Santos et al., 1993: 116. Auth, 1994: 16. Guyer, 1994: 382. Ibáñez et al, "1994" [1995]: 26. Pérez-Santos, 1999: 99, 102. Nicholson et al., 2000: 29. McCranie et al., 2002: 27; 2006: 147, 229, 237 (part). Goldberg, 2003. Köhler, 2003: 200; 2008: 215. Stafford, 2003 (part). Solórzano, 2004: 234–236 + fig. 59 (part). Guyer and Donnelly, 2005: 184 (part). McCranie and Castañeda, 2005: 8 (part). McDiarmid and Savage, 2005: 391, 421 (part). Wilson and Townsend, 2006: 96, 106; 2007: 136, 139. Rojas-Runjaic and Rivero, 2008. Santos-Barrera et al., 2008: 766. Laurencio and Malone, 2009: 126. McCranie, 2009: 12; 2011: 108. Savage and Bolaños, 2009: 14. Bolaños et al., 2010. Cadle, 2010 (part).
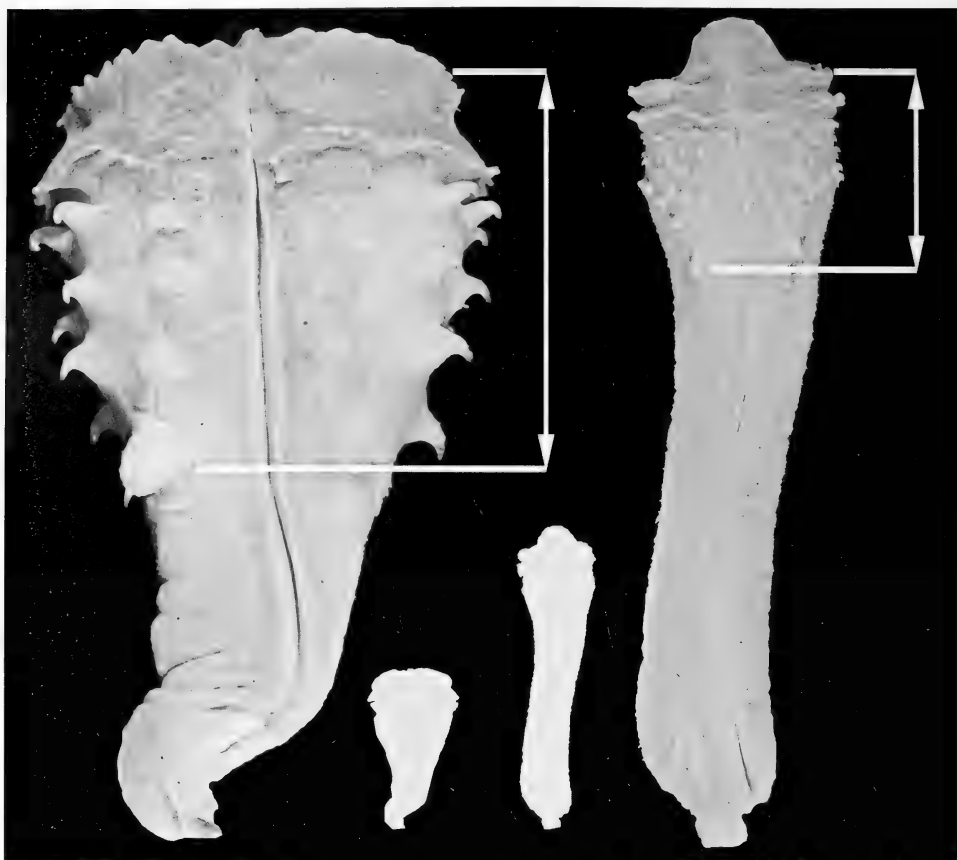
Figure 2.   Comparison showing proportional differences between the "robust" (left) and "gracile" (right) hemipenial morphotypes within *Dendrophidion*. The robust hemipenis photograph was scaled to the same length as the gracile organ. Horizontal lines are placed at the level of the proximal enlarged sulcate spine and the distal flounce in each organ (assumed to be homologous morphological markers). The apical region so delimited is a much greater proportion of the hemipenial body and relatively broader in the robust hemipenis than in the gracile one. Reverse silhouettes at bottom center show actual sizes of the organs. The representative hemipenes are *D. percarinatum* (robust, USNM 559611) and *D. graciliverpa* (gracile, AMNH R-110584 [holotype]).

Lectotype of Dendrophidion percarinatum (Figs. 4–6). Cope ("1893" [1894]) described *Drymobius percarinatus* from two Costa Rican specimens, an adult from "Boruca" collected 13 December 1891 (now AMNH R-17366; Figs. 4–5) and a young specimen from "Buenos Ayres" (originally AMNH R-9561 but now apparently missing). Both were sent to Cope by George K. Cherrie, a resident of San José who worked for a time for the national museum of Costa Rica. Myers (1982: 23) explained the history of these collections and their acquisition by the American Museum of Natural History. Recent liter-

ature (e.g., Lieb, 1996; McCranie, 2011) continues to refer to "syntypes" of *D. percarinatus* but Taylor (1954: 727) had designated AMNH R-17366 as the lectotype by referring to this specimen as "the type," in accordance with requirements for lectotype designations before 2000 (International Commission on Zoological Nomenclature, 1999: Article 74.5). The type locality, Boruca, is a small town in the foothills of the Fila Costeña on the north side of the Río Grande de Térraba where that river divides the coast range in southern Puntarenas Province (southwestern Pacific versant of Costa Rica).
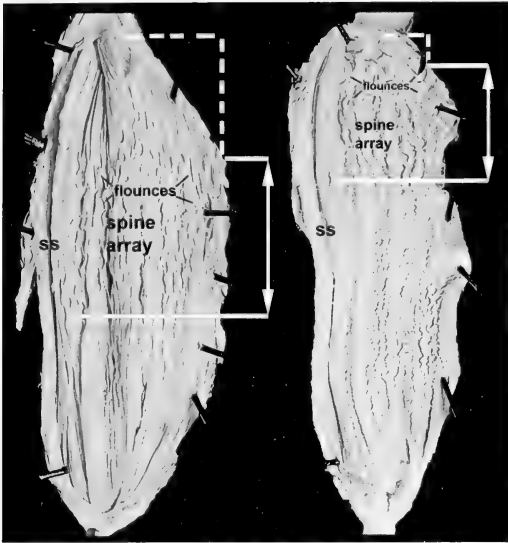
Figure 3. "Robust" (left) and "gracile" (right) hemipenial morphotypes as they appear in retracted organs (scaled to the same length, distal toward the top). Horizontal solid lines placed as in Figure 2. Dashed lines delimit the extent of apical tissue distal to the flounces. The hemipenes are *Dendrophidion brunneum* (robust, USNM 237060) and *D. graciliverpa* (gracile, UIMNH 77347). *Abbreviations and labels:* ss, sulcus spermaticus; spine array, compact tissue bearing the enlarged spines. The flounces appear as zigzag transverse lines of tissue distal to the spine array. *Dendrophidion brunneum* has an extensive area of nude apical tissue in the everted hemipenis, which accounts for the large area of pleated apical tissue in the retracted organ (left; Cadle [2010] illustrated the everted hemipenis of this species).

AMNH R-17366 is an adult male in good condition; the tail tip is missing and approximately the distal one-third of the remaining tail is broken off and tied to the specimen (Fig. 4). There is a midventral incision in the base of the tail. Total length 834+ mm; tail length 363+ mm; SVL 471 mm. 154 ventrals (2 preventrals); 143+ subcaudals; anal plate divided; 37 maxillary teeth with the last 3 somewhat enlarged; dorsocaudal reduction from 8 to 6 at subcaudal 23; dorsal scale reduction from 17 to 15 at ventral 93; 9/9 supralabials (2–4 touching the loreal; 4–6 touching the eye); 2/2 postoculars; 2+2 temporals; 10/10 infralabials. The supralabial/temporal pattern is the *P* pattern on both sides, as described above (Fig. 5A).

Narrow (<1 scale row wide) pale crossbands over the entire body (less distinct on

the neck) narrowly bordered by dark brown flecks, which often tend to invest the pale portion of the bands. Dorsal crossbands peter out on the anterior portion of the tail. Narrow dark brown lateral stripe along the suture line of dorsal rows 2–3 on the posterior half of body (Fig. 5B). Ventrolateral tail stripe at the dorsocaudal/subcaudal junction (Fig. 5C) + dusky median four rows of dorsocaudals on the anterior part of the tail (dusky continues onto posterior body, where the three paravertebral rows on each side are dusky). Venter immaculate except for narrow triangular encroachment of dorsal pigment onto lateral edges of ventral scutes. Head cap extends down to top of supralabials except the last (covers two-thirds of this scale) and the penultimate (covers somewhat less than half of this scale).

Hemipenis of the Lectotype. Because of the critical importance of hemipenial characters to the systematics of *Dendrophidion*, the left hemipenis of the lectotype of *D. percarinatum* was manually everted using methods of Myers and Cadle (2003) (the right hemipenis had been damaged by a previous incision into the tail base). The manual eversion was successful (Fig. 6), although, as is typical in many manually everted hemipenes, it is not maximally expanded (Myers and Cadle, 2003). In particular, the apex is much narrower than in everted organs described later herein, resulting in a different shape from field-everted organs. Nonetheless, the ornamentation of the entire everted organ except for the very tip of the apex can be studied. Before excision, the retracted left hemipenis extended to the proximal portion of subcaudal 7. The *retractor penis magnus* was proximally undivided.

Approximate measurements of the manually everted organ: total length, 15.3 mm. Length from base to the right enlarged sulcate spine, 6.8 mm. Length of apex (spinose part to tip), 8.5–9 mm. Sulcus spermaticus simple, centrolineal. Just distal to the distal flounce is a single calyx on each side of the sulcus (distal flounce forms proximal border of each calyx). Sulcus continues to center of apex; could not really

determine well whether the tip of the sulcus was expanded (flared) or not.

Hemipenis with narrow base, distally expanded (but shape is not as bulbous as field-everted organs). One pair of spines at proximal edge of spine array (one on each side of sulcus, right one somewhat more proximal than the left one), each somewhat larger than other spines in the array. Spine array three rows across adjacent to sulcus and on the asulcate side, narrowing slightly to two to three rows on lateral sides in between. Thirty-two spines in the array including the two enlarged sulcate spines. Individual spines are of typical form (see later hemipenial section for relevance), strongly mineralized, hooked at the tip. A narrow circumferential section of the hemipenial body immediately proximal to the spine array is ornamented with minute spines/spinules; hemipenial body proximal to minute spines is nude.

Distal to the spine array the hemipenis is encircled by two flounces having scalloped edges, between which are a few low longitudinal ridges (more concentrated on the asulcate side). On the asulcate side distal to the distalmost flounce and extending toward the apical tip are several calyces in about two rows (transverse walls of these calyces are more strongly developed than the longitudinal walls); from these calyces a raised triangular area extends to the center of the apical tip. The tip of the apex is not fully everted, and I did not attempt full eversion because of the fragility of the specimen. Apart from the sulcus and its associated pair of calyces, and the asulcate triangular extension of raised tissue, the apex is nude.

Diagnosis. *Dendrophidion percarinatum* is characterized by (1) dorsocaudal reduction from 8 to 6 occurring anterior to subcaudal 27 (range, 5–26); (2) divided anal plate; (3) subcaudal counts >130 in males and females; (4) subadults with narrow pale bands or transverse rows of ocelli (<1 dorsal row wide throughout the body) separated by fewer than three dorsal rows on the neck (bands retained or become obscure in adults, often heavily invested

with dark pigment); total number of pale bands on the body >70 (range, 71–96); (5) ventrals immaculate except for lateral dark blotches or mottling; (6) in life, dorsal coloration various shades of brown or gray and usually including dark-bordered pale crossbands anteriorly (sometimes indistinct) and dark brown or blackish stripes posteriorly (often a broader pair of paravertebral stripes and a narrow lateral stripe on dorsal rows 2 and/or 3); venter without extensive dark spots or transverse lines (scattered small spots may be present), and (7) everted hemipenis of the "robust" morphology, with a relatively short, narrow hemipenial body proximal to a bulbous region bearing spines, calyces, and other apical ornamentation (retracted hemipenis usually extending to between subcaudals 6 to 9, rarely reaching subcaudal 10); total number of enlarged spines on hemipenis <45 (range, 26–40).

Dendrophidion percarinatum differs from species of the *D. dendrophis* species group (*D. dendrophis*, *D. atlantica*, *D. nuchale* auctorum, *D. apharocybe*, *D. crybelum*, *D. vinitor*) in having a more proximal reduction in the dorsocaudal scales (nearly always >30 in the *D. dendrophis* group). A high number of subcaudals and divided anal plate will distinguish it from *D. apharocybe*, *D. crybelum*, and *D. vinitor* (<130 subcaudals and anal plate nearly always single in these species). *Dendrophidion dendrophis*, *D. atlantica*, and *D. nuchale* auctorum have different color patterns (often with extensive dark ventral spots and flecks; see Duellman, 1978: 236–237, 2005: pl. 175; Savage, 2002: 654–655, fig. 11.39c, pls. 413–415), attain greater sizes than *D. percarinatum*, and have several enormously enlarged hemipenial spines (not so enlarged in *D. percarinatum*). *Dendrophidion percarinatum* differs from *D. boshelli* in having 17 midbody scale rows (15 in *D. boshelli*).

Dendrophidion percarinatum differs from *D. paucicarinatum* in having pale dorsal crossbands (variably distinct), often has dark longitudinal stripes on the posterior body, and has an immaculate venter. *Dendrophidion paucicarinatum* usually has
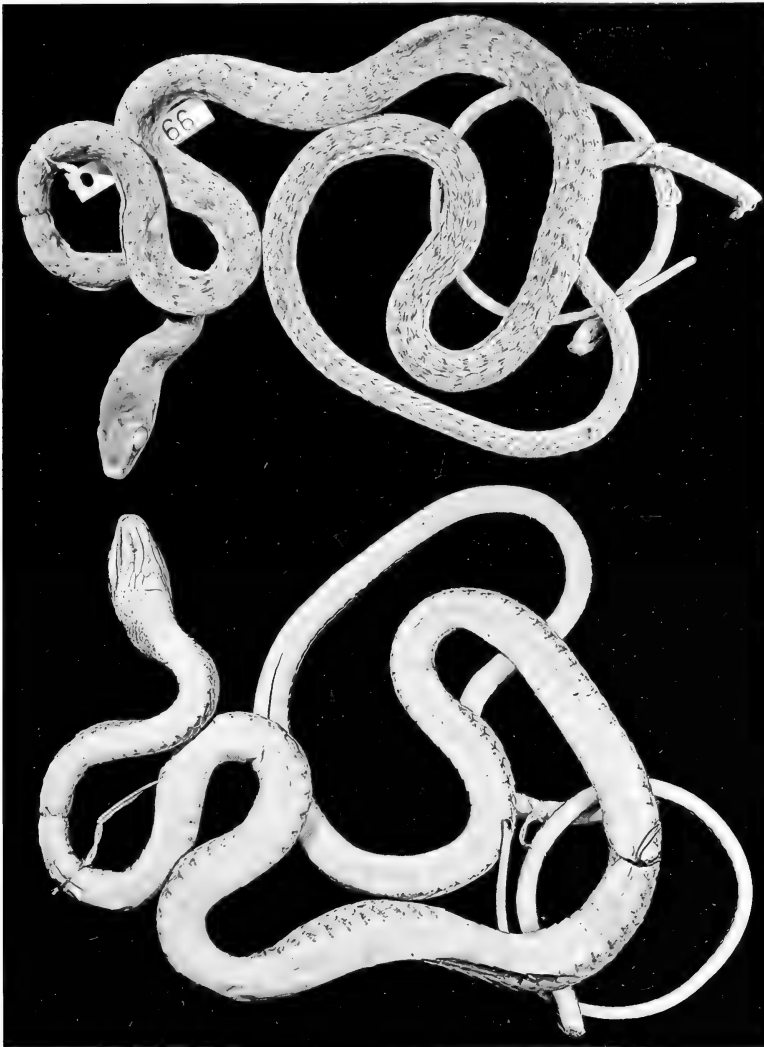
Figure 4.   Lectotype of *Dendrophidion percarinatum* (Cope), AMNH R-17366, from Boruca, Puntarenas Province, Costa Rica.

a more uniformly colored dorsum lacking distinct pale crossbands, has narrow dark lines across the venter in adults and many juveniles, and has a higher number of ventrals (>175) than *D. percarinatum* (nearly always <170 except occasional individuals from Panama and Colombia; see discussion of geographic variation). *Dendrophidion paucicarinatum* may have either a single or divided anal plate.

   Dendrophidion bivittatum differs from *D. percarinatum* in having a color pattern consisting of prominent blackish dorsal stripes on the posterior body and a greenish dorsal ground color. *Dendrophidion bivittatum* also has a shorter tail and fewer subcaudals (<60% of SVL and usually <130, respectively) than *D. percarinatum*. *Dendrophidion brunneum* has a greenish to brownish dorsum generally without pale crossbands in adults (often with dark stripes or paravertebral punctations and often with dark transverse lines and other markings on the venter).
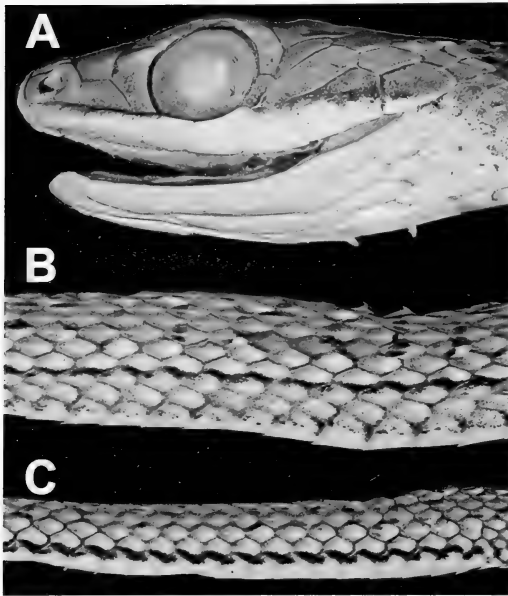
Figure 5. Lectotype of *Dendrophidion percarinatum* (Cope), AMNH R-17366. (A) Head, left side. Note the typical *P* pattern of the supralabials/temporals (see Fig. 1). (B) Posterior lateral stripe on dorsal rows 2–3. (C) Ventrolateral tail stripe.
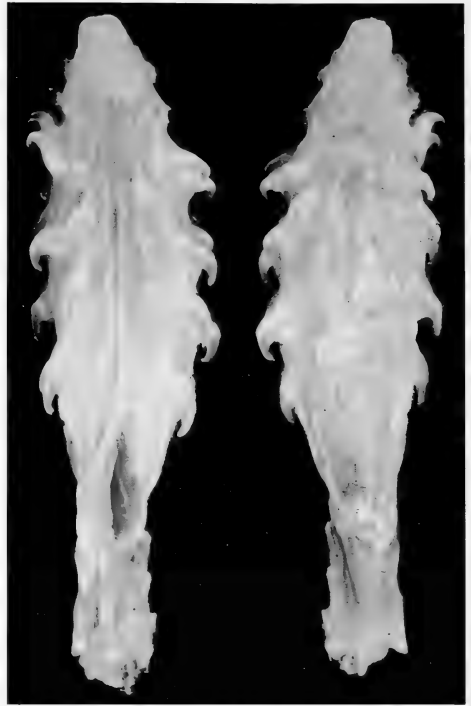
Figure 6. Manually everted hemipenis of the lectotype of *Dendrophidion percarinatum*, AMNH R-17366, in sulcate and asulcate views. The spinose region and apex are not fully inflated even though the hemipenis is virtually fully everted.

Dendrophidion percarinatum differs from the two new species described herein (*D. prolixum* and *D. graciliverpa*) in having a "robust" hemipenial morphotype as characterized herein ("gracile" in the last two species). *Dendrophidion percarinatum* also differs from these species in coloration. *Dendrophidion prolixum* and *D. graciliverpa* are green on the anterior body (sometimes restricted to the head) and often have narrow dark transverse lines on the anterior edges of ventral scutes, especially on posterior body. Additional differentiating characters and comparisons are given in the diagnoses for the new species.

Description (104 males, 85 females). Table 1 summarizes size, body proportions, and meristic data for *Dendrophidion percarinatum* throughout its geographic range; geographic variation and sexual dimorphism in some characters are summarized in the next sections. Largest specimen (AMNH R-119376 from Panama) a male 1,358+ mm total length, 852 mm SVL (largest male with a complete tail, 1,236 mm total length,

747 mm SVL). Largest female (MCZ R-20552 from Panama) 1,300 mm total length, 778 mm SVL. Tail 38–45% of total length (62–82% of SVL) in males; 37–43% of total length (59–75% of SVL) in females. Dorsal scales in 17–17–15 scale rows, the posterior reduction usually by fusion of rows 2 + 3 (*N* = 92), 3 + 4 (*N* = 19), or loss of row 3 (*N* = 11) at the level of ventrals 84–106. Ventrals 147–170 (averaging 155.8) in males, 156–167 (averaging 160.2) in females; usually 2 preventrals anterior to ventrals (about 9% of specimens have 1 preventral; rarely, 3 preventrals were present). Anal plate divided. Subcaudals 137–163 (averaging 150.7) in males, 133–157 (averaging 145.6) in females. Dorsocaudal reduction at subcaudals 8–26 in males (mean 16.0), 5–24 in females (mean 10.4). Preoculars 1, postoculars 2, primary temporals 2, secondary temporals 2, supralabials usually 9 with 4–6 bordering the eye (occasionally 8 with 3–5 bordering

the eye or 10 with 5–7 bordering the eye), infralabials usually 9 (low frequency of 10 or 11). Maxillary teeth 33–42 (averaging 37), typically with 3 or 4 posterior teeth enlarged (occasionally only 2 teeth or up to 5 posterior teeth were enlarged). Enlarged teeth are ungrooved, not offset, and there is no diastema.

Two apical pits present on dorsal scales. About 39% of specimens have keels only on the vertebral or vertebral + 1 or 2 paravertebral dorsal rows on the neck (usually at least 4–6 rows lack keels on the neck and occasionally keels are absent). At midbody, 52% of specimens lack keels only on dorsal row 1; another 38% lack keels on rows 1 and 2, and the remainder lack keels on the first 3 or 4 dorsal rows. On the posterior body, 91% of specimens lack keels only on row 1 (sometimes weak on row 2); the remainder lack keels on rows 1 and 2. Fusions or divisions of temporal scales were moderately common, with the following frequencies (counting each side separately): upper or lower primary or secondary divided (30%), irregular fusions or divisions or fragmentation (8.7%), other divisions or fusions (0.8%). Eighty-three percent of scorings for the supralabial/temporal pattern were *P*, whereas only 6.8% were *G* (the remaining were ambiguous or irregular).

Hemipenis unilobed with a bulbous apex; overall morphology "robust" as characterized herein. Spinose region followed distally by two flounces and poorly developed calyces. Apex delimited by the distal flounce. The apex has an asulcate roughly triangular raised area bearing calyces on the asulcate side, and a thick pad of raised tissue on each side of the distal portion of the sulcus spermaticus; lateral to the raised sulcate and asulcate areas the apex is nude. Sulcus spermaticus simple, centrolineal, extending to the center of the apex, and having a slightly flared tip in everted organs. There is considerable variation in the development of the calycular structures (from fully formed to much more rudimentary) and spines (see details in the hemipenial descriptions). Retracted hemipe-

nis usually extending to subcaudals 7–9 and only rarely extending to subcaudal 10 or beyond.

Sexual Dimorphism, Geographic Differentiation, and Other Variation. Tails are proportionally shorter in small individuals. Specimens <300 mm SVL have tail lengths 36–42% of total length, 57–74% of SVL (*N* = 43, males and females combined). Rare individuals have 15, 16, or 18 dorsal scale rows on the neck (one individual each), and one specimen had 15 dorsal rows at midbody.

Considering the rangewide sample, males and females differ significantly in relative tail lengths (male longer), ventral counts (female greater), subcaudal counts (male greater), the point of dorsocaudal reduction (male more distal), and the point of dorsal scale reduction (female more posterior) (Table 1). The sexes do not differ in adult body size. These are common patterns in other species of *Dendrophidion* (Cadle, 2012) and are found widely among other snakes. These patterns hold when samples are analyzed by geographic origin, except that samples from Panama-Colombia are not significantly dimorphic in relative tail lengths (Table 2). This nonsignificance is due to the fact that males from Panama-Colombia average much shorter relative tail lengths than males farther north; females from throughout the range are similar in relative tail lengths.

There is minor geographic variation in size, body proportions, and segmental counts in *Dendrophidion percarinatum* (Table 2). Mean body size increases from north to south in both males and females, whereas relative tail length and subcaudal counts decrease in the same pattern. The point of dorsocaudal reduction in males from Panama and Colombia is more proximal than in specimens from north of Panama. For most characters the greatest quantitative change in mean character values occurs between Costa Rica and Panama-Colombia rather than farther north (e.g., between Honduras-Nicaragua compared with Costa Rican specimens). For

TABLE 2.   GEOGRAPHIC VARIATION IN SELECTED CHARACTERS OF *DENDROPHIDION PERCARINATUM*. DATA PRESENTATION FOLLOWS THE FORMAT IN TABLE 1.

	Honduras-Nicaragua, 13 Males, 15 Females	Costa Rica, 29 Males, 26 Females	Panama-Colombia, 62 Males, 41 Females
Adult body size (mm, SVL)			
Male	407–595	401–652	419–852
	511.7 ± 52.15 (13)	549.5 ± 65.91 (20)*	613.5 ± 100.95 (39)
Female	437–635	457–695	465–778
	553.0 ± 65.37 (9)	599.7 ± 61.58 (21)	631.0 ± 80.40 (21)
Tail/total length			
Male	0.42–0.45	0.42–0.44	0.38–0.43
	0.44 ± 0.008 (10)***	0.44 ± 0.002 (12)***	0.40 ± 0.011 (30)
Female	0.41	0.39–0.43	0.37–0.43
	0.41 ± 0.0 (3)	0.41 ± 0.014 (8)	0.40 ± 0.015 (13)
Tail/SVL			
Male	0.74–0.82	0.72–0.80	0.62–0.77
	0.78 ± 0.024 (10)***	0.77 ± 0.025 (12)***	0.68 ± 0.031 (30)
Female	0.69–0.71	0.64–0.75	0.59–0.75
	0.70 ± 0.010 (3)	0.70 ± 0.039 (8)	0.67 ± 0.040 (13)
Ventrals			
Male	151–156	147–158	152–170
	153.7 ± 1.60 (13)***	153.4 ± 2.95 (28)***	157.4 ± 3.14 (62)***
Female	157–160	157–164	156–167
	158.8 ± 1.31 (14)	159.8 ± 2.06 (26)	160.9 ± 2.70 (40)
Subcaudals			
Male	153–163	148–161	137–160
	157.4 ± 2.76 (10)***	155.2 ± 3.34 (15)***	147.8 ± 5.66 (46)*
Female	143–151	133–157	135–156
	147.8 ± 2.76 (8)	147.4 ± 7.27 (11)	144.3 ± 4.57 (27)
Dorsocaudal reduction			
Male	14–22	10–26	8–22
	17.0 ± 2.74 (13)***	18.9 ± 3.24 (27)***	14.5 ± 3.09 (62)***
Female	5–15	7–24	6–17
	9.7 ± 2.87 (15)	11.2 ± 3.50 (25)	10.2 ± 2.71 (41)

example, for both sexes, mean RTL of Honduran-Nicaraguan specimens is similar to that of Costa Rican specimens, but mean RTL for Panamanian-Colombian specimens is less. In general, males show stronger geographic differentiation than females for the same character.

Ventral and subcaudal counts and relative tail lengths reported by Rojas-Runjaic and Rivero (2008) for the male from western Venezuela are similar to Panama-Colombian males (Table 2): 157 ventrals, 146 subcaudals (ventrals + subcaudals, 303), and relative tail length 41% of total length, 69% of SVL. This specimen has several uncommon scutellation features (1/2 pre-oculars, 2+3 temporals, and 9 supralabials with only supralabials 5 and 6 touching the eye); its dorsocaudal reduction at subcaudals 24–26 is greater than the range I observed in specimens from Panama-Colombia (Table 2).

The Cordillera de Talamanca of Costa Rica and western Panama is a strong biogeographic barrier to many groups of organisms and separates differentiated populations or closely related species on the Atlantic and Pacific versants in lower Middle America (Daza et al., 2010; Chan et al., 2011). Within *Dendrophidion*, this mountain range separates sibling species within the *D. vinitor* complex and presum-

Table 3.   Geographic differences in selected characters of Atlantic vs. Pacific populations of *Dendrophidion percarinatum* in Costa Rica. Data presentation follows the format in Table 1. None of the Atlantic/Pacific character differences were significant in comparisons by sex.

	Atlantic Versant, (10 Males, 8 Females)	Pacific Versant, (19 Males, 18 Females)
Adult body size, SVL (mm)		
Male	531–596	401–652
	556.8 ± 21.38 (8)	534.3 ± 80.14 (12)
Female	567–670	457–695
	607.9 ± 33.88 (8)	594.7 ± 74.70 (13)
Tail/total length		
Male	0.43–0.44	0.42–0.44
	0.44 ± 0.006 (3)	0.44 ± 0.007 (10)
Female	0.41	0.39–0.43
	0.41 ± 0.0 (3)	0.41 ± 0.019 (5)
Tail/SVL		
Male	0.75–0.80	0.72–0.80
	0.78 ± 0.029 (3)	0.77 ± 0.022 (10)
Female	0.69–0.71	0.64–0.75
	0.70 ± 0.011 (3)	0.69 ± 0.050 (5)
Ventrals		
Male	149–156	147–158
	152.3 ± 2.45 (10)	154.3 ± 2.93 (19)
Female	157–162	157–164
	159.6 ± 1.71 (8)	159.9 ± 2.22 (18)
Subcaudals		
Male	152–158	148–161
	154.0 ± 2.83 (4)	156.2 ± 3.56 (13)
Female	143–153	133–157
	147.7 ± 5.03 (3)	147.3 ± 8.26 (8)
Dorsocaudal reduction		
Male	10–21	14–26
	18.2 ± 3.29 (10)	19.2 ± 3.49 (19)
Female	7–15	8–24
	10.6 ± 2.72 (8)	11.4 ± 3.86 (17)

ably played a role in their speciation (Cadle, 2012). Thus, it was of interest to compare character differentiation between populations of *D. percarinatum* inhabiting the Atlantic and Pacific versants in Costa Rica (Table 3). In contrast to the *D. vinitor* complex, in which sibling species on the Atlantic and Pacific versants are differentiated by color pattern and hemipenial morphology but not scutellation (Cadle, 2012), no such differentiation is apparent in *D. percarinatum*. None of the standard scutellation characters are significantly different between snakes of the Atlantic and Pacific versants, and I detected no consis-

tent differences in coloration or hemipenial morphology between these population segments. Thus, at least as reflected by standard external characters, Atlantic and Pacific populations of *D. percarinatum* in lower Middle America show no population divergence, even though the southwestern Costa Rican populations may be isolated from the Atlantic versant populations (see Distribution).

Coloration in Life. A sampling of color photographs of *Dendrophidion percarinatum* from Costa Rica includes Savage (2002: pl. 418), Solórzano (2004: 236, pl. 59), and Köhler, 2008 (fig. 582). Photographs of
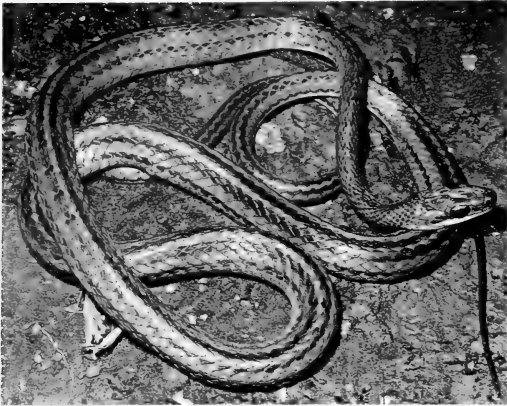
Figure 7.   *Dendrophidion percarinatum* in life. LACM 114102 from Finca Las Cruces, Puntarenas province, Costa Rica. From a color slide by Roy W. McDiarmid.

Honduran specimens include Köhler (2003: fig. 480), McCranie et al. (2006, pl. 119), and McCranie (2011, pls. 6B, C). Guyer and Donnelly (2005) identified their plate 148 as *D. percarinatum* ("Brown Forest Racer"), but I identify this photograph as *D. nuchale* auctorum based on its color pattern (the specimen was photographed and released at the La Selva Biological Station, Costa Rica; Craig Guyer, personal communication). Black and white photographs of *D. percarinatum* from Costa Rica are in Taylor (1954: 728) and Lieb (1996). A color photograph of a specimen from southwestern Costa Rica (near the type locality) is shown in Figure 7.

Specimens from Honduras and Costa Rica are brown to yellowish brown or grayish brown with narrow dark-bordered pale brown crossbands anteriorly grading to dark crossbands posteriorly and often dark stripes or alternating dark and pale stripes posteriorly and on the tail (Savage, 2002: 658; Solórzano, 2004: 234; Guyer and Donnelly, 2005: 184; McCranie, 2011: 109). The venter is immaculate, except for lateral dark pigment common to all *Dendrophidion*, and white or with a yellowish to orange wash. Some specimens apparently have a more uniformly colored dorsum (see also Coloration in Preservative). Overwhelmingly, the predominant dorsal colors of *Dendrophidion percarinatum* are shades

of brown and with a general absence of extensive green colors (compare the two new species described herein). Color notes for specimens from the southern part of the range (given below) are similar to that just described. For many specimens it appears that the dark borders to the pale crossbands are more prominent than the pale portions of the bands, which are sometimes not mentioned in individual descriptions.

The following color notes are extracted from the field notes of Charles W. Myers for specimens from Panama and Colombia (AMNH R-108468 only). Specimens are listed roughly in order of increasing SVL:

AMNH R-109643 (female, 199 mm SVL): Lateral light bars pale yellow on neck, pale grayish brown on body. Venter white, with a yellowish tinge on throat. Iris pale tan upper quarter sector, dark brown below. Tongue black with an orangish tinge near base of fork.

AMNH R-129757 (male, 213 mm SVL): Upper quarter sector of iris tan, lower three quarters dark brown. Tongue dark brown with black fork.

KU 107656 (male, 229 mm SVL): Color like [KU 107652], except venter white instead of yellow, light dorsal spots pale brown rather than gray, and yellow of scale bases is light, not bright.

KU 107647 (male, 236 mm SVL): Brown above with tan light areas. Venter white. Iris pale bronze with red-brown half moons either side of pupil.

KU 107645 (male, 258 mm SVL): Anterior part of body with pink cast to the brown background. Trace of yellow on supralabials and on neck along lower scales and first 6 ventrals. Venter immaculate white. Iris pale tan with red brown half moons.

KU 107659 (male, 329 mm SVL): Brown with yellowish dark-bordered crossbars anteriorly and black crossbars posteriorly, where there are also lateral dark lines and a vertebral light yellowish area. A yellow tinge in neck region followed by an orangish cast to entire dorsum (brown) to a bit past midbody. Labials and anterior venter white except for a yellow tinge on venter, turning pale grayish near anus and under tail. Iris

rich brown, except upper one-third, which is pale orangish tan. Tongue orangish brown with gray tips.

KU 107651 (female, 536 mm SVL): Reddish brown above, turning gray-brown on posterior one-third of body and tail; scales on anterior two-thirds of body with bright yellow anterior margins (tip of base has a small black spot). Entire body with black and lighter brown crossbanding of an odd pattern. Labials and chin white, turning yellow-green on ventrals and yellow on subcaudals. Upper one-fifth of iris light tan; lower parts brown.

KU 107650 (male, 604 mm SVL): Brown above, white below.

KU 75678 (female, 641 mm SVL): Dorsum brown with transverse black markings; bases of scales on anterior two-thirds of body yellow. Labials and underside of head white, changing to greenish white on anterior three-fourths of belly and to pale yellow on posterior one-fourth. Subcaudals bright yellow. Iris tan above, brown below.

KU 107652 (female, 651 mm SVL): Brown with grayish spotting and black crossbars. Anterior bases of scales bright yellow on anterior two-thirds of body, especially noticeable on neck where the skin does not have to be stretched to show a yellow cast. There seems to be no special behavioral display associated with this hidden color. Labials and ventrals greenish white, turning light yellow on posterior one-third of body and bright orange-yellow under tail. Upper quarter section of iris light brown and lower part dark brown. No dark stripes, even on tail.

KU 107654–55 (male and female, 543 and 720 mm SVL): Color like [KU 107652] except stripes are present and greenish white of anterior ventrals not extending under head and on labials, which are white. Tongue red with black tips in -54 [?], all black in other.

KU 107653 (male, 703 mm SVL): Color much like [KU 107652] except the dorsal ground is darker and conspicuous stripes are present posteriorly.

AMNH R-119376 (male, 852 mm SVL): Head greenish gray, neck yellowish brown (anterolateral scale bases bright yellow), turning brown on body. Underside of head and most of belly white, turning pale yellow toward tail and yellow under tail. Iris brown except that upper quarter sector is pale tan. Tongue deep red with black fork.

AMNH R-108468 (Colombia; male 615 mm SVL): Dull brown with indistinct black stripes. Anterior bases of scales are yellow in the neck region and then pale green to slightly past midbody, after which the scale bases are not differently colored. Supralabials and underside of head white; first 20 ventrals are yellow, then venter turns greenish white and, on last few dozen ventrals and on subcaudals, yellowish orange. Tongue dark. Iris pale brown on top quarter sector, dark brown on lower three-quarters.

Coloration in Preservative. Generally, the color pattern described above for living specimens is maintained in well-preserved specimens, but color tones become dull brown, olive, or gray. There is considerable variability in the distinctness of the pale crossbands and their dark edging (from virtually absent to very distinct) (Fig. 8). The extent to which this reflects color pattern in life or differences in preservation is unknown. The vertebral scale row is often distinctly paler than paravertebral rows, especially on the posterior body. In some specimens this results in the appearance of longitudinal paravertebral stripes. There is usually a lateral dark brown stripe posteriorly on dorsal rows 2 and/or 3; this varies from very prominent to indistinct. Occasional specimens from Costa Rica and Panama (and perhaps other parts of the range) have a very subdued pattern in preservative (Fig. 8B) and presumably in life as well. In these individuals pale anterior bands are absent, and the dark stripes on the body and tail nearly match the dorsal ground color, rendering a pale grayish or grayish brown dorsum with obscure dark lines. These individuals are otherwise typical of *Dendrophidion percarinatum* in other characters (two examples I have seen are females), and I assume they represent color variants within the species.
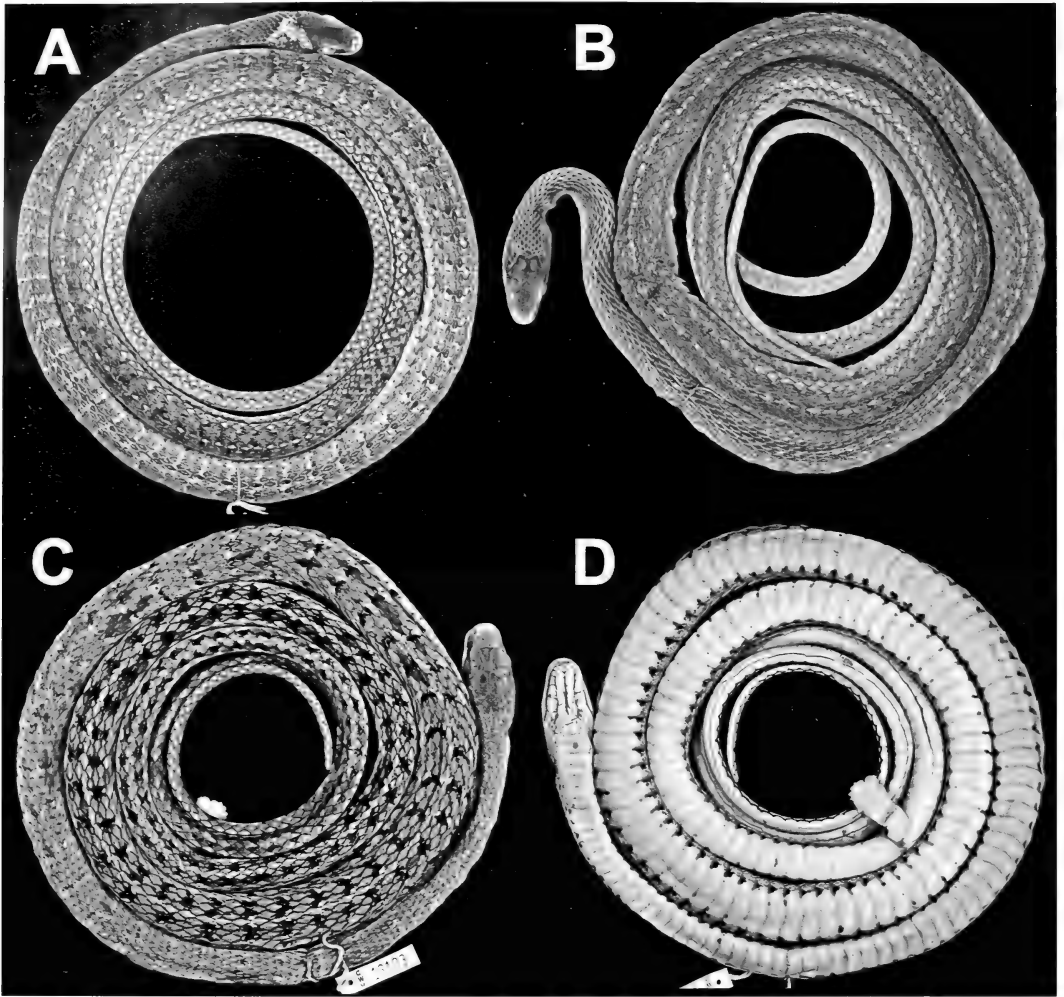
Figure 8.   Representative specimens of *Dendrophidion percarinatum*. (A) UMMZ 79764 (Nicaragua). (B) UMMZ 63762 (Panama). (C) and (D) AMNH R-119376, dorsal and ventral (Panama).

The venter sometimes has scattered small dark spots.

Distribution. Northern Honduras (Atlántida Province; McCranie, 2011) eastward and south throughout Central America to northern Colombia and northwestern Venezuela (Rojas-Runjaic and Rivero, 2008), and western Colombia (Chocoan region) to the vicinity of the Bahía de Buenaventura. *Dendrophidion percarinatum* occurs on the Pacific versant only in Costa Rica, Panama, and Colombia. Most localities are <1,000 m elevation but *D. percarinatum* occurs up to 1,200 m in southwestern Costa Rica (Río Coto Brus valley). In Honduras the maximum elevation attained is 685 m (McCranie, 2011: 110), and other elevational records derived from specimens I examined are 930 m (Panama), 520 m (Nicaragua), and 200 m (Colombia; but see below for a potentially much higher record). McCranie (2011: 109) and Savage (2002: 657) mapped localities for Honduras and Costa Rica, respectively. Lieb (1996) mapped the rangewide distribution, but the localities and range he gave for *D. percarinatum* in South America need correcting with the taxonomic
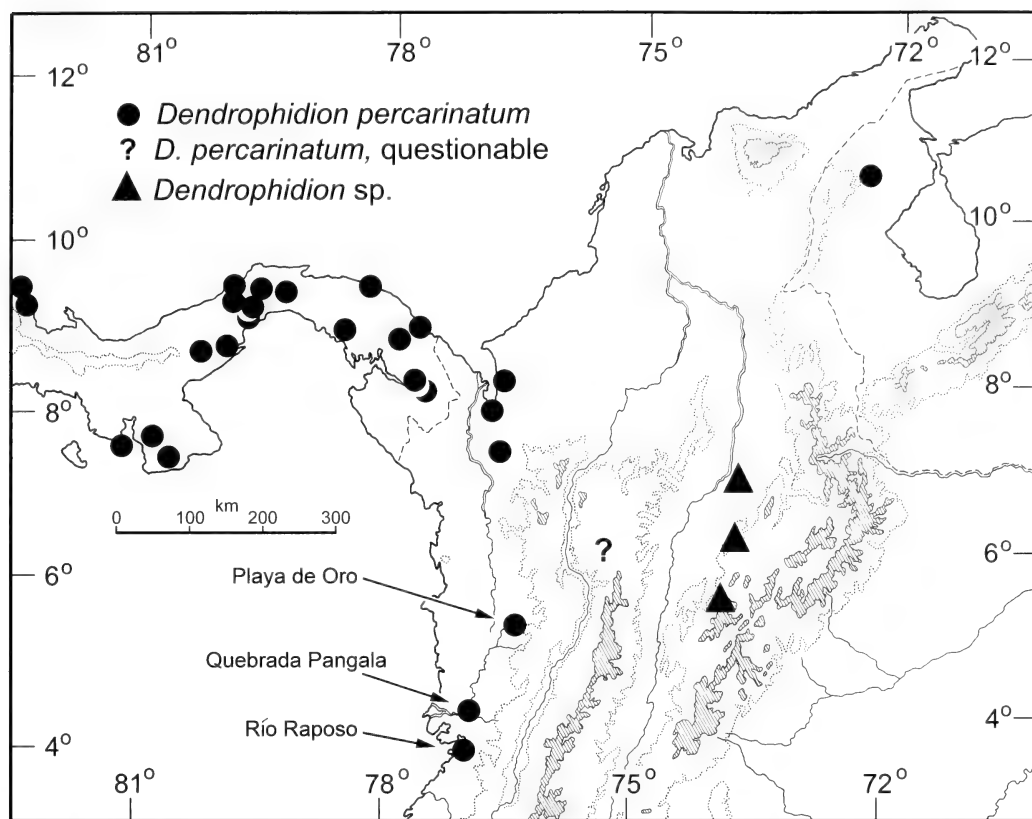
Figure 9.   Distribution of *Dendrophidion percarinatum* in Panama and northwestern South America. All known South American localities are plotted. Three labeled localities in western Colombia (*arrows*) are sites where *D. percarinatum* is sympatric with *D. prolixum*. Locality in western Venezuela (about 10°40′N, 72°30′W) is from Rojas-Runjaic and Rivero (2008). *?* in the Río Cauca valley is Medellín, a questioned locality for *D. percarinatum* (see text). *Triangles* in central Colombia (Río Magdalena valley) are localities for specimens similar to *D. percarinatum* in segmental counts, but which may represent differentiated populations or a distinct species; see *Distribution* in the *D. percarinatum* account and Appendix 1 (*Dendrophidion species inquirendum*).

revisions herein, about which more is said shortly. Figure 9 shows the distribution of *D. percarinatum* in Panama and South America as I presently understand it.

The southernmost specimen in western Colombia that I refer to *Dendrophidion percarinatum* is USNM 151658, a juvenile from the vicinity of the Bahía de Buenaventura (approximately 3°45″N; see Figs. 12A, 13A, and discussion in the account for *D. prolixum*). However, few specimens of any species of *Dendrophidion* in U.S. collections seem to have been collected between this point and the Ecuadorian frontier. Some difficulties in distinguishing juveniles of *D. percarinatum* and

the two new species are discussed in the account for *D. prolixum*.

Sympatry between *Dendrophidion percarinatum* and the new species *D. prolixum* is documented at three localities in western Colombia (Fig. 9): Playa de Oro, Quebrada Pangala, and the Río Raposo just south of Buenaventura. At each locality the specimens documenting each species have the distinctive color pattern characters of each; exemplars are illustrated in the account for *D. prolixum* (see Distribution). At Playa de Oro the documenting specimens are both males with everted hemipenes, which are described and illustrated later (see Figs. 39A, 42).

Populations of *Dendrophidion percarinatum* in southwestern Costa Rica (Río Coto Brus valley and Golfo Dulce/Osa Peninsula, including the type locality) are seemingly isolated from populations of the Atlantic versant and uplands of northwestern Costa Rica (Savage, 2002: 657). Carara National Park is the only documented lowland locality on the Pacific versant north of the Osa Peninsula region. Despite this apparent disjunction, Atlantic and Pacific populations in Costa Rica do not differ substantively in standard external morphological characters (see above discussion of geographic variation). Similarly, *D. percarinatum* seemingly has a somewhat spotty distribution in Panama, a not-infrequent pattern for Panamanian snakes (Myers, 2003; Myers et al., 2007: 12–14). The identities of *D. percarinatum* and *D. prolixum* have previously been confused in western Colombia (see discussion in the next section), where their distributions overlap. Areas of sympatry of these two species are discussed in the species account for *D. prolixum*.

Previous Records of Dendrophidion percarinatum *in Colombia and Venezuela.* Because of the confused identity of South American specimens previously referred to *Dendrophidion percarinatum*, I briefly comment on a few South American references to this species (Ecuadorian specimens are referred to in the species account for *D. graciliverpa*). Lieb (1988: 166) correctly inferred that records for "*D. percarinatum*" reported by Alemán (1953; "*D. dendrophis*") from western Venezuela and by Roze (1966) from the Cordillera de la Costa of northern Venezuela were misidentified specimens of *D. nuchale* auctorum. Many specimens of *D. nuchale* auctorum are available from the Cordillera de la Costa. The four specimens reported by Alemán (cited by Roze) are from Zulía state in western Venezuela near the recently reported "first record" of *D. percarinatum* from Venezuela (Rojas-Runjaic and Rivero, 2008). The last authors did not mention the specimens listed by Alemán (1953), who reported segmental counts and body pro-

portions consistent with either *D. percarinatum* or *D. nuchale* auctorum. These four specimens were apparently examined, and their identity confirmed as the last species, by James R. Dixon in 1981 (Fernando Rojas-Runjaic, personal communication).

The scalation data and color details given by Rojas-Runjaic and Rivero (2008) for the "first valid record" of *D. percarinatum* from western Venezuela are consistent with that species as redefined herein, even though some of the reported head scutellation is rare in my sample (see above section on variation). These authors also described the anterior dorsum of the specimen as "grayish green uniform," which is seemingly unlike most descriptions of Central American specimens (brown, yellowish brown, reddish brown; see *Coloration in Life*). The specimen is a male with everted hemipenes according to the authors, and hemipenial characters could confirm its identity. Other Venezuelan records of "*D. percarinatum*" (e.g., Test et al., 1966; Lancini, 1979) undoubtedly refer to *D. nuchale* auctorum, as recognized by Lieb (1988).

Lieb (1996) included as part of the distribution of *Dendrophidion percarinatum* two localities in the interandean valleys of the Río Cauca and Río Magdalena of northern Colombia, stating some equivocation as to their identity: "Isolated populations tentatively referred to [*D. percarinatum*] occur in the Departments of Antioquia and Cundinamarca in north-central Colombia; these snakes are somewhat divergent in the anterior body color pattern from *D. percarinatum* in other parts of the range" (Lieb, 1996: 636.1–636.2). These records are apparently based in part on MCZ R-21984 (Sonsón, Antioquia department) and MCZ R-42185 (Villeta, Cundinamarca department), which Lieb (1988: 174) cited as specimens of *D. percarinatum*; he indicated at least the first locality (Sonsón) on an accompanying map (Lieb, 1988: fig. 5). However, both of these specimens are unequivocally *D. bivittatum* (personal observations of both specimens, and Stuart [1932] for MCZ R-21984).

I am aware of only one specimen of *Dendrophidion percarinatum* potentially from the deeper interandean portion of the Río Cauca: BMNH 1897.11.12.10, collected by A. E. Pratt and said to be from "Medellín." If the locality is the well-known Andean city of that name, and is truly the point of origin of the specimen (rather than a shipping point), then this would be an elevational record for the species (1,440–1,540 m). As a cautionary note, the NGA (2010-2012) online gazetteer (GEONet) lists six other place names "Medellín" in the northern Colombian departments of Córdoba, Sucre, Magdalena, and Bolívar—any of which are at lower elevations and would bridge the lowland distributional "gap" between the northern Colombian localities for *D. percarinatum* around the Golfo de Urabá (about 8°N) and the westernmost Venezuelan locality (Fig. 9). In the absence of other documented specimens from this area, I am hesitant to include the interandean city "Medellín" as a documented locality for *D. percarinatum*.

Several specimens with segmental counts similar to *Dendrophidion percarinatum* are known from 150–1,242 m elevation in the Río Magdalena valley (Fig. 9; Appendix 1, "*Dendrophidion* species inquirendum"; see also Dunn, 1944: 477). Lieb (1988) had examined one of these, MCZ R-42186, from Boyacá department in central Colombia but, perhaps as a lapsus, did not include Boyacá in his above-cited quotation. A specimen reported as "*D. dendrophis*" (Nicéforo María, 1942: 87) from Sasaima (approximately 1,100–1,200 m, upper Río Magdalena) may also pertain to this group (or to *D. nuchale* auctorum). The three specimens I have seen from the Río Magdalena do have somewhat peculiar color patterns compared with typical *D. percarinatum* and, although their scale counts are similar to *D. percarinatum*, segmental counts by themselves often are unhelpful in distinguishing species of *Dendrophidion* (Cadle, 2012; this paper). Unfortunately, the only male among the three is a small

juvenile (217 mm SVL) with retracted hemipenes previously exposed by a somewhat mangled dissection. Some aspects of their morphology (e.g., a proportionally short spinose + apical region) seem unlike other *D. percarinatum* hemipenes I have examined but better preparations would be needed for confirmation. Study of additional specimens from this area will be needed to resolve the taxonomic status of these populations, but the available specimens are, in any case, seemingly geographically isolated from other known populations referable to *D. percarinatum* (Fig. 9).

A summary of the Colombian specimens referred to *Dendrophidion percarinatum* by Lieb (1988) and my re-assessments of their identities are as follows: MCZ R-21984, R-42185 (= *D. bivittatum*); FMNH 54949, FMNH 54958-64, FMNH 54965, LACM 36782, LACM 45443, USNM 151659 (= *D. prolixum*); and MCZ R-42186 (= *species inquirendum*). I concur with the identity of the other Colombian specimens cited by Lieb (1988) as *D. percarinatum* as redefined here: FMNH 63761, FMNH 63772–73, FMNH 78118, USNM 151658. Stafford (2003: 111) referred LACM 45443 from Chocó department to *D. vinitor* but there are no documented occurrences of that species complex in Colombia (Cadle, 2012: 206–207), and I refer LACM 45443 to *D. prolixum*.

Natural History. General overviews of the natural history of *Dendrophidion percarinatum* include Guyer and Donnelly (1990, 2005), Savage (2002: 657–658), Solórzano (2004: 234–236), and McCranie (2011: 108–111). Diet and reproductive parameters are summarized by Goldberg (2003), Stafford (2003), and Sexton and Heatwole (1965). *Dendrophidion percarinatum* is a diurnal, terrestrial to semiarboreal snake of lowland and premontane moist tropical forests. At night it has been found sleeping on low vegetation. The diet consists primarily of terrestrial leaf-litter frogs (e.g., *Pristimantis*, *Craugastor*), with a lesser component comprising lizards (*Anolis*, *Cnemidophorus*; Stafford, 2003). *Dendrophidion percarinatum* is oviparous with recorded

clutch sizes of three to six and perhaps with multiple clutches per year in the southern portion of the range (Goldberg, 2003; Stafford, 2003).

Brief field notes recorded for Panamanian specimens by Charles W. Myers include the following (observations by day except where indicated). Six specimens were on the forest floor (AMNH R-129757; KU 107647, 107651–53, 107656). Four were associated with water courses: on a riverbank, along a forest stream, in leaves of a dry stream bed, in a river (AMNH R-119376, 109643; KU 107650, 107659). One was in an open grassy situation (KU 107645), and two were sleeping at night on a palm leaf 3 ft. (~0.9 m) above a stream bank and in a *Heliconia* 5 ft. (~1.5 m) above ground (KU 107654–55). Myers' notes indicate that a light quickly awakens sleeping snakes, which "then behave as if flying snakes." One specimen encountered by day remained motionless rather than fleeing (KU 107652). Myers forced the hind legs of a large *Craugastor* (*C. fitzingeri* group) from either KU 107654 or 107655 (adults, 543 and 720 mm SVL, respectively).

Dendrophidion percarinatum is sympatric with several other species of *Dendrophidion* within its range. The range of *D. percarinatum* overlaps with *D. apharocybe* and/or *D. nuchale* auctorum from Honduras to Panama, and all three occur together at some localities (e.g., La Selva Biological Station, Costa Rica). At the Las Cruces Biological Station in southwestern Costa Rica *D. percarinatum* is sympatric with three other species—*D. crybelum, D. nuchale* auctorum, and *D. paucicarinatum*—yielding perhaps the highest species density of *Dendrophidion* anywhere. In western Colombia the distributions of *D. percarinatum, D. prolixum,* and *D. nuchale* auctorum overlap broadly, with two of the three documented sympatrically at several localities; it would be unsurprising to find the three species occurring together.

TWO NEW SPECIES FROM WESTERN COLOMBIA AND ECUADOR

Dendrophidion percarinatum as redefined here is relatively homogeneous in color pattern and hemipenial morphology from eastern Honduras to northwestern Colombia. However, in western Colombia and Ecuador are snakes similar to *D. percarinatum* in standard scutellation characters and body proportions, but they differ strongly from that species in coloration and hemipenial morphology. Lieb (1988, 1996) included these snakes in his concept of *D. percarinatum,* and his concept was followed by others (e.g., Savage, 2002; Stafford, 2003; Cadle, 2010). However, they comprise diagnosable units that I consider two distinct new species. Both new species have an exceptionally long, slender hemipenis (gracile morphology) and color patterns different from *D. percarinatum.* The taxonomic distinction of the new species is also supported by the fact that the distributions of *D. percarinatum* and the first of the new species to be described overlap in western Colombia, including the three localities of documented sympatry mentioned above. In the area of distributional overlap, specimens of *D. percarinatum* maintain the typical color pattern and hemipenial morphology expressed throughout the rest of its geographic range, whereas the sympatric new species is distinctive in both features. The situation in western Ecuador proved more confusing because not only do the two new species occur there but *D. brunneum* does as well. Preserved specimens of the three species can be a challenge to distinguish, and in fact, I was unsuccessful in allocating some specimens to any of the three with certainty.

Dendrophidion prolixum **New Species**

Figures 1D, 10–11, 12B, 13B, 14–17, 19, 42, 43A

Drymobius dendrophis. Boulenger, 1913: 1034 (specimen from Peña Lisa, Colombia; = BMNH 1913.11.12.40).
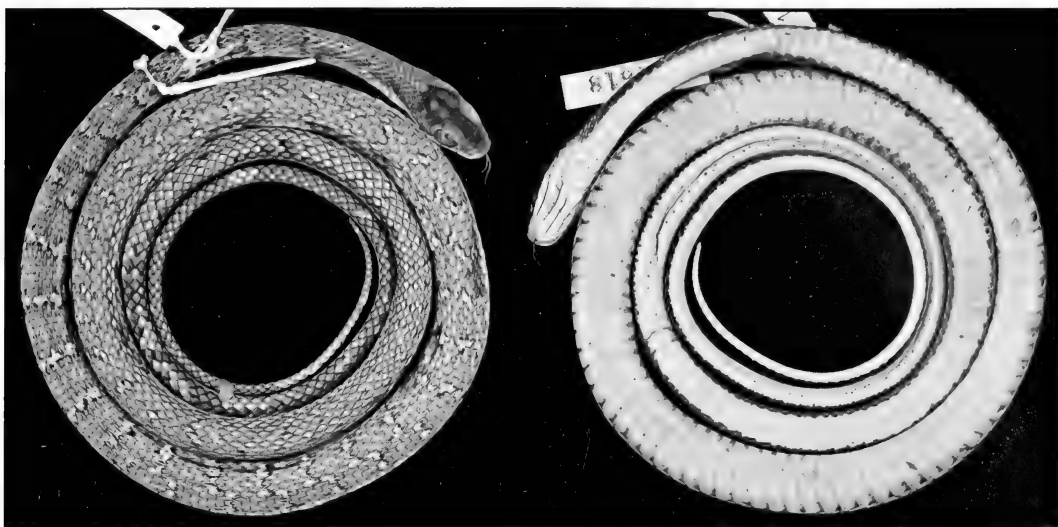
Figure 10.   Holotype of *Dendrophidion prolixum* (AMNH R-109721). Male from Quebrada Guanguí, Chocó department, Colombia.

?*Dendrophidion dendrophis* (part). Peters and Orejas-Miranda, 1970: 80 ("southern part of Central America and northern South America"). Pérez-Santos and Moreno, 1988: 134 (Pacific lowlands of Colombia).

Dendrophidion percarinatum (part). Dunn, 1944: 477 (? part). Savage and Villa, 1986: 148, 169. Lieb, 1988: 172; 1996: 636.1. Pérez-Santos and Moreno, 1991b: 138. Savage, 2002: 657–658. Stafford, 2003: 111 (BMNH 1913.11.12.40). Solórzano, 2004: 234–236. Guyer and Donnelly, 2005. McCranie and Castañeda, 2005: 8. McDiarmid and Savage, 2005: 391, 421. Cadle, 2010: 24.

Holotype (Figs. 10–11). AMNH R-109721 from Quebrada Guanguí, 0.5 km above Río Patia (upper Saija drainage), 100–200 m, Cauca department, Colombia [about 02°50′N, 77°25′W; Myers, 1991: 8]. Collected 9 February 1973 by Charles W. Myers and John W. Daly (field number C. W. Myers 11618).

The holotype is a male, presumed adult, 754 mm total length, 307 mm tail length (447 mm SVL); relative tail length 41% of total length, 67% of SVL; dorsocaudal reduction from 8 to 6 at the level of subcaudal 27; 153 ventrals, 2 preventrals, 142 subcaudals; 12 left and 11 right infralabials. An unusual temporal scale configuration: 2+3+2 on each side (Fig. 11A). Supralabial/temporal pattern G (irregular because of divisions in temporal scales). Other head scales are typical of the species (Table 1 and description below). Both hemipenes are retracted but exposed by a ventral incision in the tail base; the right hemipenis extends to the middle of subcaudal 13, the left to the middle of subcaudal 15. The retractor penis magnus is slightly divided proximally. The type retains elements of the juvenile color pattern: approximately 51 pale crossbands on the body (tending to form ocelli and somewhat indistinct posteriorly; Fig. 11B), an indistinct broken line on the suture line of dorsal rows 2 and 3 posteriorly (Fig. 11C), and a venter with only scattered small dark spots in addition to dark transverse lines indicated only at the lateral edges of the ventral scutes.

Paratypes. **Colombia:** *Cauca:* Quebrada Guanguí, 0.5 km above Río Patia (upper Saija drainage), 100–200 m, AMNH R-109722–28
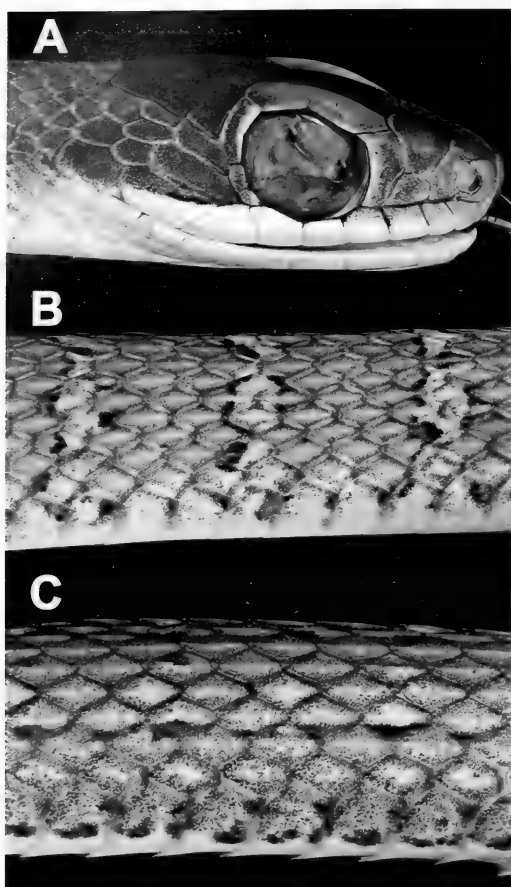
Figure 11.   Holotype of *Dendrophidion prolixum* (AMNH R-109721). (A) Head, right side. (B) Midbody pattern, lateral view. (C) Posterior lateral pattern.

(topotypes). *Chocó:* Peña Lisa, Condoto, 300 ft. [90 m], BMNH 1913.11.12.40. Playa de Oro, Río San Juan, 400 m, FMNH 54965, AMNH 108469. Quebrada Bochoramá, Loma de Encarnación on right bank, LACM 45443. Quebrada Docordó, middle Río San Juan (about 17 km airline SSW Noanamá), AMNH R-123749–51. Quebrada Pangala, lower Río San Juan (about 17 km airline NE Palestina), AMNH R-123746. Quebrada Taparal, lower Río San Juan (about 7 km airline NE Palestina), AMNH R-123744, R-123753. Upper Río Buey, 110–160 m, LACM 36782. Sierra [Serranía] de Baudó, 3,000 ft. [915 m], Pacific side, ANSP 25609. Serranía de Baudó, north slope of Alto del

Buey, 900 m, AMNH R-119801. *Risaralda:* [Between] Pueblo Rico [and] Santa Cecilia, Pacific side, 800 m, FMNH 54949, 54958–64. *Valle del Cauca:* Río Raposo, Virology Field Station near Buenaventura, USNM 151659.

Referred Specimens. **Colombia:** *Chocó:* Quebrada Pangala, lower Río San Juan (about 17 km airline NE Palestina), AMNH R-123747. *Nariño:* Riquarte [= Ricaurte], 3,900 ft. [1,189 m], Pacific side, ANSP 25608. **Ecuador:** *Esmeraldas:* Immediate environs of Cachaví, 20 m, USNM 237064. Río Cachaví, USNM 237065. *Imbabura:* Paramba, northwestern Ecuador [= Hacienda Paramba; 800–1,000 m], FMNH 4055, 4056(?) (the last two specimens not included in data summaries). The referred specimens are small juveniles except FMNH 4056 (adult female in fair condition).

Etymology. The species name is the neuter form of the Latin adjective *prolixus* meaning "stretched far out" or "long," used especially in reference to parts of the body. The reference is to the unusually long hemipenis of this species compared with most other *Dendrophidion.*

Diagnosis. Dendrophidion prolixum is characterized by (1) dorsocaudal reduction from 8 to 6 occurring anterior to subcaudal 27 (range, 8–26); (2) divided anal plate; (3) subcaudal counts >130 in males and females and adult tail length >60% of SVL; (4) subadults with narrow pale crossbands or transverse rows of ocelli separated by >3 dorsal rows on the neck (adults retain bands or become predominantly brown or green without distinct pale bands); total number of pale bands on the body fewer than 60 (range, 49–57) when they are distinct; (5) ventrals immaculate or (in some adults) with narrow transverse dark lines across the anterior border of each ventral plate; (6) in life, head reddish brown and dorsum mainly green (brownish green in juveniles); and (7) everted hemipenis of "gracile" morphology, with an exceptionally long, slender hemipenial body proximal to an expanded tip bearing spines, calyces, and other apical ornamentation (retracted hemipenis nearly always to subcaudal 10 or

greater); total number of enlarged spines on the hemipenis >60 (65–89 in four organs studied).

"Gracile" hemipenial morphology will distinguish *D. prolixum* from all other species of *Dendrophidion* except *D. graciliverpa* described herein and perhaps *D. bivittatum* (see above comments where the gracile morphology is described). *Dendrophidion bivittatum* has a different color pattern (greenish dorsum with prominent blackish longitudinal stripes), a tail <60% of SVL, and fewer than 130 subcaudals.

Dendrophidion prolixum differs from species of the *D. dendrophis* species group (*D. dendrophis, D. atlantica, D. nuchale auctorum, D. apharocybe, D. crybelum, D. vinitor*) in having a reduction in the dorsocaudal scales anterior to subcaudal 30 (posterior to subcaudal 30 in the *D. dendrophis* group except occasional females). A high number of subcaudals and divided anal plate will distinguish it from *D. apharocybe, D. crybelum,* and *D. vinitor* (<130 subcaudals and anal plate nearly always single in these species). *Dendrophidion dendrophis* and *D. nuchale* auctorum may have either single or divided anal plates, but these species have different color patterns, usually involving numerous narrow pale bands and/or ocelli (see Savage, 2002: 654–655, for discussion of *D. nuchale*), attain greater body sizes, and have different hemipenial morphologies (robust morphology and enormously enlarged spines in *D. dendrophis* and *D. nuchale*). *Dendrophidion prolixum* differs from *D. boshelli* in having 17 midbody scale rows (15 in *D. boshelli*).

Dendrophidion paucicarinatum lacks distinct pale crossbands and has a higher number of ventrals than *D. prolixum* (>175 compared with <165 in *D. prolixum*). *Dendrophidion paucicarinatum* may have either a single or divided anal plate. *Dendrophidion prolixum* differs from *D. brunneum* in color pattern (adult *D. brunneum* generally lack pale bands) and in hemipenial morphology (robust in *D. brunneum*; see Fig. 3 and Cadle, 2010).

Dendrophidion prolixum is distinguished from *D. graciliverpa* by the wide spacing of the pale dorsal bands on the neck (bands generally separated by >3 dorsal scale rows in *D. prolixum,* <3 dorsal rows in *D. graciliverpa*). Consequently, *D. prolixum* has fewer pale bands on the body when these can be discerned: 49–57 in *D. prolixum* compared with 57–87 in *D. graciliverpa*. In life *D. prolixum* has a reddish brown head and greenish body, compared with a green head and brown to gray body in *D. graciliverpa*. These two species are exceedingly similar in most characteristics (Table 1), and I discovered no consistent differences in hemipenial morphology between them in the few everted hemipenes examined when intraspecific variation is considered. Preserved specimens without discernible pale crossbands are problematic to identify, and several specimens from the borderlands of northern Ecuador and southern Colombia are of questionable referral to either *D. prolixum* or *D. graciliverpa*.

Dendrophidion prolixum has previously been confused with *D. percarinatum*, and these species cannot be distinguished by traditional scutellation features other than a few mean character differences (Table 1). These two species differ in (1) color pattern: reddish brown head with a greenish brown to green body, and venter either immaculate or with dark transverse lines (*D. prolixum*) vs. head and body primarily browns to grays, and venter immaculate (*D. percarinatum*); (2) number of pale crossbands on the body: 49–57 and separated by ≥3 dorsal scale rows on the neck (*prolixum*) vs. 71–96 and separated by <3 dorsal scale rows on the neck (*percarinatum*) (pale crossbands can be indistinct in either species, but especially adult *D. prolixum*); (3) relationship between the posterior supralabials and temporals (see Materials and Methods and Table 1): G pattern most commonly (*D. prolixum*) vs. P pattern most commonly (*D. percarinatum*); (4) hemipenial morphology: gracile (*prolixum*) vs. robust (*percarinatum*); retracted hemipenes of *D. percarinatum*

TABLE 4. COMPARISON OF PRESERVED SPECIMENS OF THREE SPECIES OF THE *PERCARINATUM* COMPLEX IN WESTERN COLOMBIA AND ECUADOR. PATTERN ELEMENTS ARE BASED ON JUVENILES WITH DISTINCT BANDING PATTERNS, WHICH ARE RETAINED ONLY IN SOME ADULTS OF EACH OF THE THREE SPECIES.

	D. percarinatum, Figures 12A, 13A	*D. prolixum,* Figures 12B, 13B	*D. graciliverpa,* Figures 12C, 13C
Supralabial/temporal pattern	usually *P*	usually *G*	usually *G*
No. of dorsal rows separating neck bands	< 3	3–4	< 3
No. of pale bands on the body	71–96	49–57	57–87
Head cap	brown	brown	dark gray
Form of the neck bands	usually bandlike	usually ocellate (rounded pale spots surrounded by dark pigment); often heavily invested with dark pigment	bandlike (usually) or ocellate
Distinctness of neck bands	usually distinct	usually distinct	often obscured by gray head cap extending onto the neck
Contact between neck bands and ventral pale coloration	pale portion of bands usually confluent with pale ventral color	pale portion of bands usually cut off from pale ventral color by two or three dorsal rows; often a distinct dark brown lower border on neck ocelli	pale portion of bands confluent or not (extension of dark gray head color often interrupts bands on lower dorsal rows)

rarely extend to subcaudal 10, whereas retracted organs of *D. prolixum* nearly always extend beyond subcaudal 10. The strong differences between *D. prolixum* and *D. percarinatum* in color pattern and hemipenial morphology are maintained in the area of western Colombia where their geographic ranges overlap, including several localities of sympatry discussed later.

Distinguishing Juvenile Preserved Specimens of the D. percarinatum *Complex.* Preserved juveniles of *Dendrophidion prolixum*, *D. percarinatum*, and *D. graciliverpa* present some challenges to identify, which is relevant not only to proper species recognition but also to discerning distributions, range overlap, and sympatry of the three species. The pattern of pale crossbands on the neck and a few other characters offer differentiating, if subtle, characters (Table 4, Figs. 12–13), although no single character will necessarily be decisive for a given specimen. These characters will also work with those adults that retain distinct bands. These characters

were instrumental in identifying the southernmost specimen of *D. percarinatum* in my sample (Figs. 12A; 13A, left) and in demonstrating sympatry between *D. percarinatum* and *D. prolixum* in western Colombia discussed later in this species account. There is also potential confusion of juvenile *D. graciliverpa* and *D. brunneum* in western Ecuador, but I have seen too few of the last species to be confident of differentiating juvenile characters; this problem is discussed in the later section on *D. brunneum*.

The two most consistent characters (Table 4) are the total number of pale crossbands on the body and their separation on the neck. These two in combination will usually easily separate *D. prolixum* (Figs. 12B, 13B) from the other two species (pale bands are distinct in juveniles of all three species, unlike in adults). *Dendrophidion percarinatum* and *D. graciliverpa* have a greater total number of bands, which are more narrowly separated on the neck. Side by side comparison of either of these with *D. prolixum* immediately shows a greater
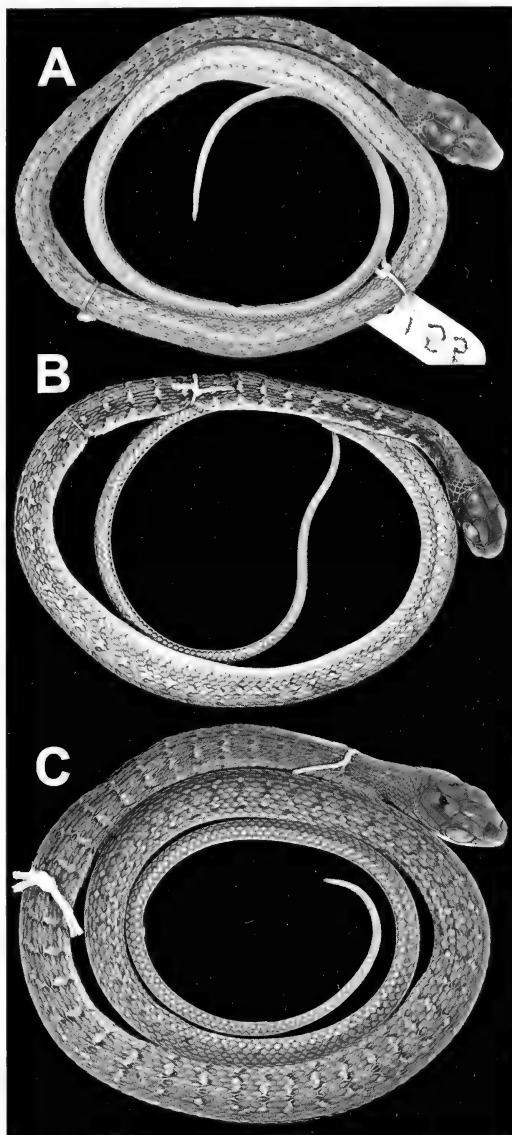
Figure 12. Juvenile specimens of (A) *Dendrophidion percarinatum* (USNM 151658, Chocó department, Colombia). (B) *D. prolixum* (USNM 237065, Esmeraldas province, Ecuador). (C) *D. graciliverpa* (KU 179501, Pichincha province, Ecuador).

band density on the neck in the first two compared with *D. prolixum* (Fig. 13).

Most of the other characters in Table 4 are subject to some intraspecific variation (supralabial/temporal pattern) or to conditions of preservation interacting with the color pattern of a given specimen. None-

theless, careful comparisons usually make it possible to identify preserved specimens confidently (coloration in life would prove diagnostic, if available). For example, in *Dendrophidion prolixum* the neck bands are distinctly ocellate, having the form of pale spots that are usually at least partly surrounded by dark pigment and are not confluent with the pale ventral color (Fig. 13B). Neck bands in *D. percarinatum* and *D. graciliverpa* are usually more band-like (narrow, relatively straight) and usually confluent with the pale ventral color. This pattern can be disrupted if the bands are disrupted on the side of the neck, as occurs with some frequency in *D. graciliverpa* (e.g., Fig. 13C, right side). In these cases the upper portions of the crossbands can appear as ocelli, but they are not generally set off by dark pigment as in *D. prolixum* (Fig. 13B). In a few specimens of *D. graciliverpa* the neck bands are distinctly more ocellate, and other characters must be used.

Clearly, preserved juveniles of *Dendrophidion percarinatum* and *D. graciliverpa* will cause the most difficulty because these two can have similar total number of bands (Table 1). Three features in combination usually permit separation: the supralabial/temporal pattern (P vs. G, subject to intraspecific variation documented in Table 1); the shading of the head cap (usually brown and similar to the rest of the dorsum in well-preserved *D. percarinatum* vs. dark gray in *D. graciliverpa*, which presumably reflects the green coloration of the head/neck in life); and the distinctness of the anterior three or four pale crossbands on the neck (distinct in *D. percarinatum* vs. obscured by dark gray [green in life] extension of the head cap coloration onto the neck in *D. graciliverpa*; compare Figs. 13A, C). In *D. graciliverpa* the dark gray extension onto the neck sometimes (seemingly mostly in smaller juveniles) occurs only on the lower dorsal scale rows. This obscures the ventral portions of the neck bands, resulting in the appearance of ocelli in this species. This potentially creates some confusion with *D. prolixum*, but
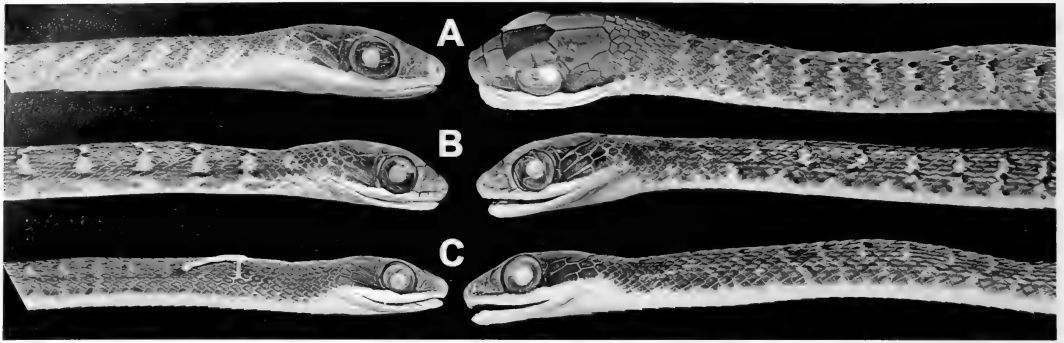
Figure 13.   Comparison of pale bands on the anterior body of juvenile specimens. Each pair (left, right) representative of one species: (A) *Dendrophidion percarinatum* (USNM 151658, 191 mm SVL and AMNH R-123748, 272 mm SVL; both Colombia). (B) *D. prolixum* (AMNH R-109725, 208 mm SVL, Colombia; USNM 237065, 210 mm SVL, Ecuador). (C) *D. graciliverpa* (KU 179501, 231 mm SVL and KU 291237, 265 mm SVL; both Ecuador).

distinct dark brown flecks or spots generally edge the ocelli in the last species.

Description (17 males, 17 females). Table 1 summarizes size, body proportions, and meristic data for *Dendrophidion prolixum*. Largest specimen (ANSP 25609) a female 675 mm SVL (total length 966+ mm, tail incomplete); the largest female with complete tail (USNM 151659) was 662 mm SVL, 1,116 mm total length. Largest male (AMNH R-123750) 650 mm SVL (1,003+ mm total length, tail incomplete); largest male with complete tail (AMNH R-123751) 642 mm SVL, 1,037 mm total length. Tail 38–40% of total length (62–67% of SVL) in males; 38–42% of total length (63–72% of SVL) in females.

Dorsal scales in 17–17–15 scale rows, the posterior reduction by fusion of rows 2+3 (N = 25) or 3+4 (N = 35) or by loss of row 3 (N = 8) at the level of ventrals 84–110 (sexual dimorphism discussed below). Ventrals 150–163 (averaging 157.4) in males, 152–164 (averaging 160.9) in females; ventrals preceded by 2 preventrals in about 70% of specimens (24% have only 1 preventral and rarely 3 preventrals were present or preventrals were absent). Anal plate divided. Subcaudals 134–150 (averaging 140.5) in males, 133–150 (averaging 142.9) in females. Preoculars 1, postoculars 2 (rarely 3), primary temporals usually 2 (rarely 1 or 3), secondary temporals 2 (rarely 3), supralabials usually 9 with 4–6 bordering the eye (rarely

10 with 4–7 bordering the eye), infralabials usually 10 (range 8–12 with high frequencies of 9 and 11). Dorsocaudal reduction from 8 to 6 occurs at subcaudals 16–26 in males, 8–24 in females. Maxillary teeth 36–42 (averaging 38), usually with 3 or 4 posterior teeth enlarged and ungrooved; rarely, only 2 or as many as 5 teeth were enlarged. Enlarged teeth are not offset and there is no diastema.

Two apical pits present on dorsal scales. Most specimens lack keels on the lower 4, 5, or 6 dorsal scale rows on the neck (occasionally lacking on higher rows); nearly all specimens lack keels only on row 1 at midbody (sometimes keels are weak on row 2 and one specimen lacked keels on row 2); on the posterior body keels are almost always present on all except dorsal row 1 (one specimen lacked keels on rows 1–2, and another had weak or partial keels on some scales in row 1). Fusions or divisions of temporal scales occurred with the following frequencies: upper or lower temporal divided vertically (4), upper temporal divided horizontally (1), upper primary + secondary temporal fused (2), upper + lower primary fused (1, partial fusion). Seventy-six percent of scorings of the supralabial/temporal pattern were G, whereas only 4.5% were the P pattern; the remaining were irregular or ambiguous patterns.

Hemipenis unilobed, with an exceptionally long hemipenial body proximal to a
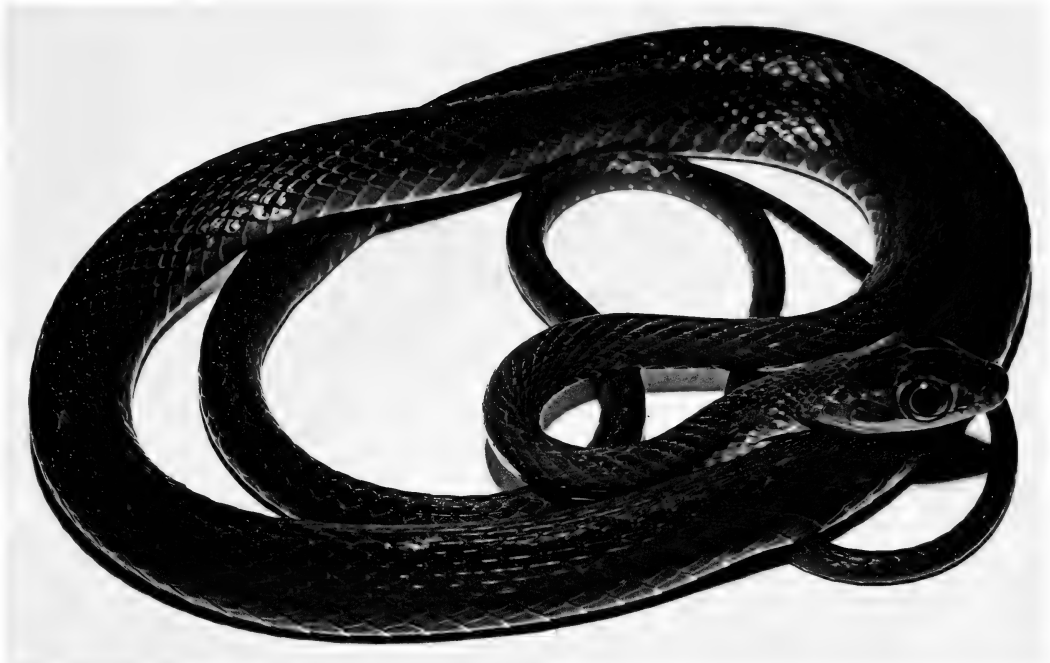
Figure 14.   *Dendrophidion prolixum* in life from the type locality (AMNH R-109726). Adult male, 628 mm SVL. From a color slide by Charles W. Myers.

somewhat bulbous apex. Overall morphology "gracile." Spinose region followed distally by 2 flounces and poorly developed calyces. Enlarged spines >60. Apex nude except for poorly developed calyxlike structures on the asulcate side and thickened tissue immediately adjacent to the tip of the sulcus spermaticus. Sulcus spermaticus simple, centrolineal, with a slightly flared tip in everted organs. Retracted hemipenis nearly always to subcaudal 10 or greater (to 15 or more).

Variation and Sexual Dimorphism. Tails are proportionally shorter in small individuals. Specimens <300 mm SVL have tail lengths 35–39% of total length, 53–64% of SVL ($N = 9$, males and females combined). No strong geographic trends were evident among the characters examined. Males and females differ significantly in ventral counts (female greater), the point of dorsocaudal reduction (male more distal), and the point of dorsal scale reduction (female more

posterior) (Table 1). The sexes do not differ in adult body size, relative tail lengths, or subcaudal counts. These are common patterns in other species of *Dendrophidion* (Cadle, 2012) and are found widely among other snakes.

Coloration in Life. The following color description for *Dendrophidion prolixum* is extracted from color notes of Charles W. Myers for specimens from western Colombia: the type locality (two juveniles, four adults), Serranía de Baudó (one juvenile), and Playa de Oro (one adult). Notes for individual specimens are presented after the summary. A color photograph of a specimen from the type locality is in Figure 14 (AMNH R-109726).

The color pattern changes ontogenetically from banded juveniles to (usually) more uniformly patterned adults (see variation below). Three juveniles have pale brown or tan crossbands (pale blue on the neck in one specimen) on a brown to grayish brown

dorsum. Adults are seemingly polymorphic in dorsal ground color (greenish to brownish or reddish brown); the largest adults for which color descriptions are available (>550 mm SVL) are green to dark green but may have a brown or reddish brown suffusion. The head of adults is reddish brown, contrasting with the general dorsal coloration; reddish brown dorsolateral and lateral stripes may be present on the anterior half of the body. The venter is white to grayish white anteriorly in juveniles and adults, and there may be a yellowish wash on the posterior venter and tail. The venter in small juveniles is immaculate, but larger individuals develop indistinct to prominent transverse grayish lines across the anterior edges of the ventral scales (superficially, the lines seem to be on the posterior edges of the scutes, but that is an illusion caused by the lines showing through the nearly-transparent posterior edge of the next anterior ventral scute).

Although Myers' notes do not indicate pale dorsal bands in individuals >447 mm SVL (see below), most preserved specimens retain some trace of bands (appearing as scattered whitish dorsal flecks or transverse rows of pale spots); one large adult female is strongly banded (see below) so retention of distinct crossbands may vary. The following notes on coloration in life from field notes of Charles W. Myers are arranged in order of increasing SVL so as to highlight the relation of color pattern to size (starting with AMNH R-109721 and following are considered adults):

AMNH R-119801 (juvenile, Serranía de Baudó, 211 mm SVL): Body grayish brown with pale blue lateral spots on neck, these turning pale brown on rest of body. Reddish brown lateral stripe. Underside of head white, turning grayish white over rest of ventral surfaces. Upper one-fifth of iris tan, lower four-fifths reddish brown. Tongue black.

AMNH R-109722–23 (juveniles, Quebrada Guanguí, 235 mm and 283 mm SVL): Tan interspaces on brown dorsum. Venter white anteriorly, grading to yellowish posteriorly. Iris tan in upper quarter, brown below. Tongue black.

AMNH R-109721 (holotype, Quebrada Guanguí; male, 447 mm SVL): Reddish brown with gray interspaces; touch of green on lower sides of neck. Underside of head and anterior venter white with some blotches of yellow on throat and supralabials, turning light yellow on posterior belly and under tail. Iris brown, tongue black.

AMNH R-109727 (Quebrada Guanguí; male, 564 mm SVL): Top and sides of head red-brown, body green. Labials and most of under-head bright yellow with only a few small white areas. Color otherwise like [AMNH R-109726, below].

AMNH R-109724 (Quebrada Guanguí; female, 594 mm SVL): Head red-brown; body overall dark green, with some dark reddish suffusions anteriorly. Supra- and infralabials bright golden yellow. Venter whitish anteriorly, turning golden yellow (like labials) under posterior belly and tail. Iris red-brown, palest in upper quarter sector. Tongue black.

AMNH R-109726 (Quebrada Guanguí; male, 628 mm SVL; Fig. 14): Green on snout, turning red-brown atop most of head, with the red color extending caudad on neck in the form of vague dorsal and lateral stripes. Supra- and infralabials bright golden yellow, genials mostly white. Venter grayish white with gray crosslines, turning light yellow under tail. Iris brown. Tongue black.

AMNH R-108469 (Playa de Oro; male, 644 mm SVL): Green above and on outer quarters of ventrals, being brightest on lower sides and ventral tips. Head deep red-brown, this color extending on body as a pair of vague dorsolateral stripes (parts of scale rows 6–8) and as a vague lateral stripe (rows 2–3). These stripes disappear at midbody, and posteriorly the dorsum acquires a slight brownish suffusion in the green. Labials and middle of venter white, turning pale yellow under tail. Iris red-brown, turning tan in upper quarter. Tongue blackish gray.

A color photograph of the head and neck of a snake from northwestern Ecuador (Ortega-Andrade et al., 2010: appendix 3, "*Dendrophidion brunneus*") may be a photograph of *Dendrophidion prolixum.*
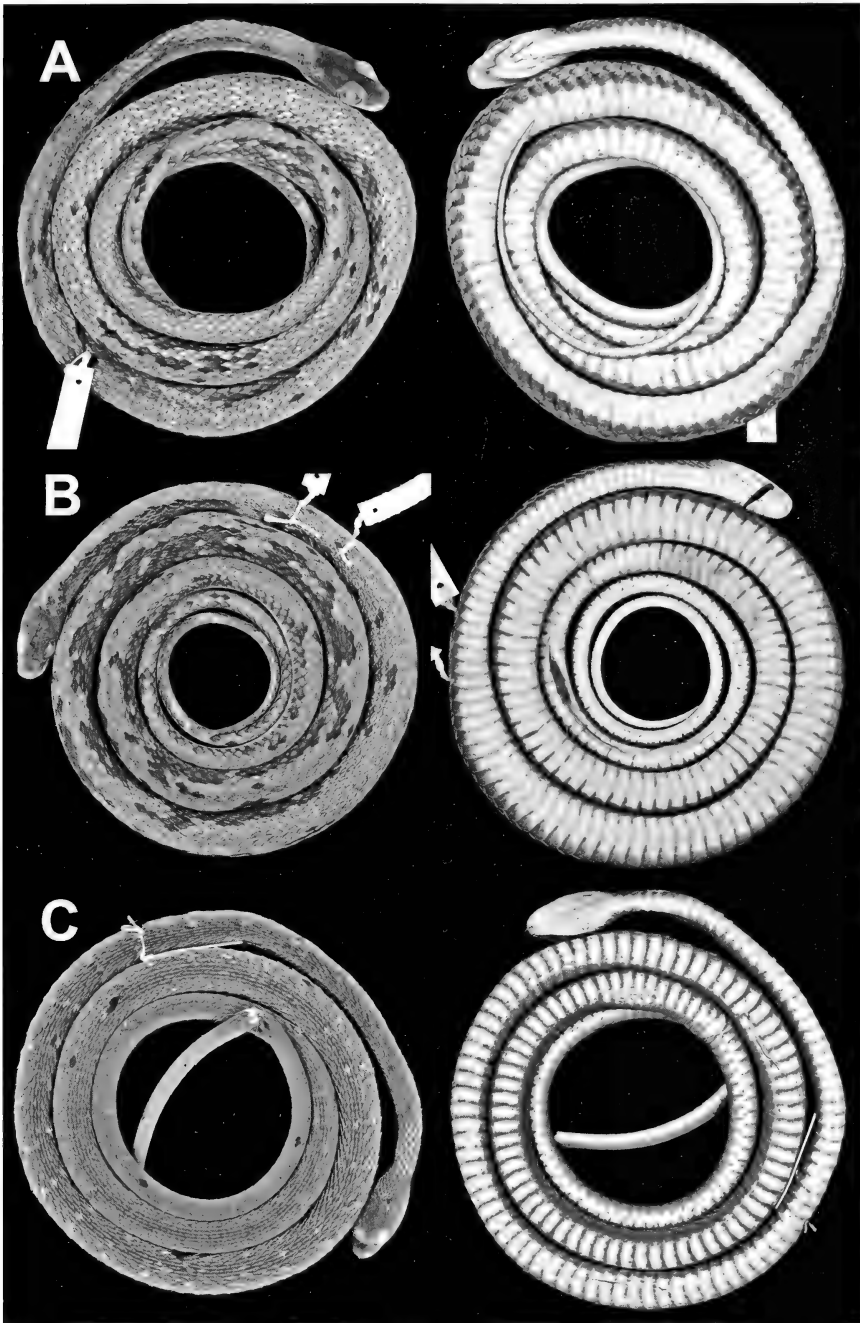
Figure 15.　*Dendrophidion prolixum* adult dorsal and ventral patterns. (A) AMNH R-123746 (532 mm SVL; Quebrada Pangala). (B) AMNH R-109727 (564 mm SVL; Quebrada Guanguí). (C) AMNH R-123753 (598 mm SVL; Quebrada Taparal).
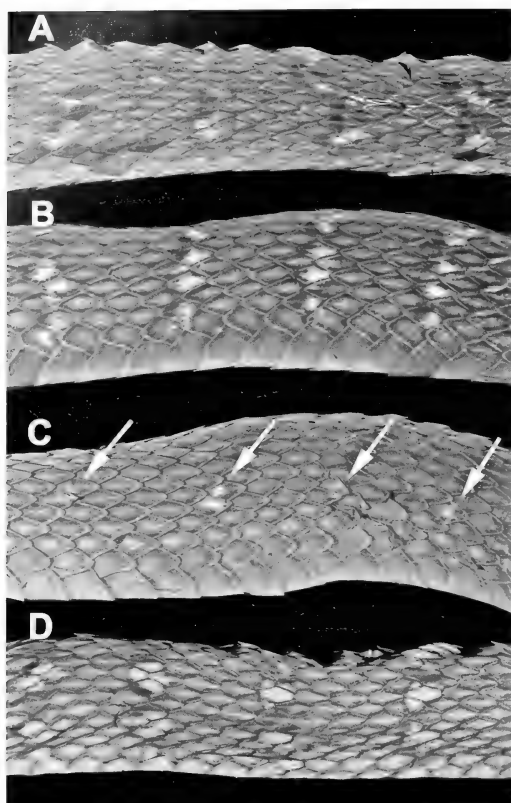
Figure 16.   Variation in expression of transverse rows of pale spots/ocelli at midbody in preserved adults of *Dendrophidion prolixum*. (A) FMNH 54960 (587 mm SVL). (B) FMNH 54958 (648 mm SVL). (C) FMNH 54964 (661 mm SVL). (D) USNM 151659 (662 mm SVL). Arrows in panel C indicate traces of ocelli reduced to small pale flecks; compare panel D, which is of similar size.
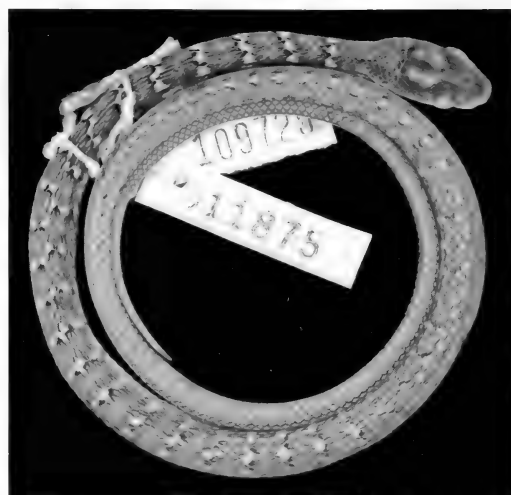
Figure 17.   *Dendrophidion prolixum* juvenile. AMNH R-109725 (Chocó department, Colombia; 208 mm SVL).

The photo shows the top of the head brown or reddish brown, extending onto neck with a narrow brownish lateral stripe on rows 2–3, a dorsolateral stripe on rows 6–7 or more; remainder of neck scales bright green; upper labials and visible portions of gular/anterior ventrals bright yellow. The color pattern is similar to several of the above-described specimens (compare especially AMNH R-109726, R-108469). This photograph potentially documents one Ecuadorian locality for *D. prolixum* (see later discussion of problematic localities).

Coloration in Preservative. Ground color of adults brown, grayish brown, or dark gray, usually with some indication of pale (cream to whitish) crossbands or transverse rows of spots (Figs. 15–16). The variation in dorsal ground colors is perhaps due to preservation differences. Pale crossbands are more prominent in smaller individuals (Fig. 17) than larger ones; crossbands in the largest specimens are sometimes so reduced that only a trace is evident (Fig. 16C); these specimens appear dark blue gray, sometimes blackish (Figs. 15B, C). The venter is immaculate in juveniles, but most adults have indistinct to prominent transverse narrow dark gray or blackish lines across the anterior edges of the ventral scutes (sometimes more continuous or prominent posteriorly than anteriorly) (Fig. 15). The whole range of color patterns in preserved specimens is seen in a series from the type locality (AMNH R-109721-28).

Distribution (Fig. 18). Lowlands and premontane foothills of western Colombia (Chocó, Risaralda, Valle del Cauca, and Nariño departments) and northwestern Ecuador (Esmeraldas province). Latitudinal range from about 6°6′N south nearly to the equator (Fig. 18). Elevational distribution from about 100 m up to 930 m in the Serranía de Baudó (Chocó department, Colombia) and 1,189 m (Ricaurte, Nariño department, Colombia). The distribution in southern Colombia and northwestern

Ecuador presents some interpretive problems taken up in the next section.

Sympatry between *Dendrophidion prolixum* and *D. percarinatum* is documented at three localities in western Colombia: two in the Río San Juan drainage (Playa de Oro and Quebrada Pangala) and another at the Río Raposo just south of Buenaventura (Fig. 9). At these localities the two species maintain their distinguishing characteristics as given in the above diagnoses and in Table 4. Documentation for these localities is provided by the following specimens: Playa de Oro (AMNH R-108468, *percarinatum*; AMNH R-108469, *prolixum*), Quebrada Pangala (AMNH R-123745 and R-123748, *percarinatum*; AMNH R-123746–47, *prolixum*), and the Río Raposo just south of Buenaventura (USNM 151658, *percarinatum*; USNM 151659, *prolixum*). Two examples are presented in Figure 19. At Playa de Oro the documenting specimens are both males with everted hemipenes (Fig. 19A), which are described and illustrated later (see Figs. 39, 42).

Interpretive Problems Associated with the Southern Portion of the Distribution of Dendrophidion prolixum. The southern portion of the distribution of *Dendrophidion prolixum* (localities 1–4 in Fig. 18) and its overlap with that of *D. graciliverpa* described later is problematic in several respects. The documentation for these localities is entirely based on small juveniles that I refer to *D. prolixum* (and one of the records is based on the identification of a photograph in the literature). The only adult from the four localities cannot with any certainty be attributed to any species. Moreover, a few adult specimens from other parts of northwestern Ecuador could be referred to either *D. prolixum* or *D. graciliverpa*. These interpretive problems are discussed in the following paragraphs, beginning with numbered localities in Figure 18 for which concrete evidence for the occurrence of *D. prolixum* exists. Reference to the above discussion on the identification of juveniles (see Diagnosis and Table 4) is pertinent here.
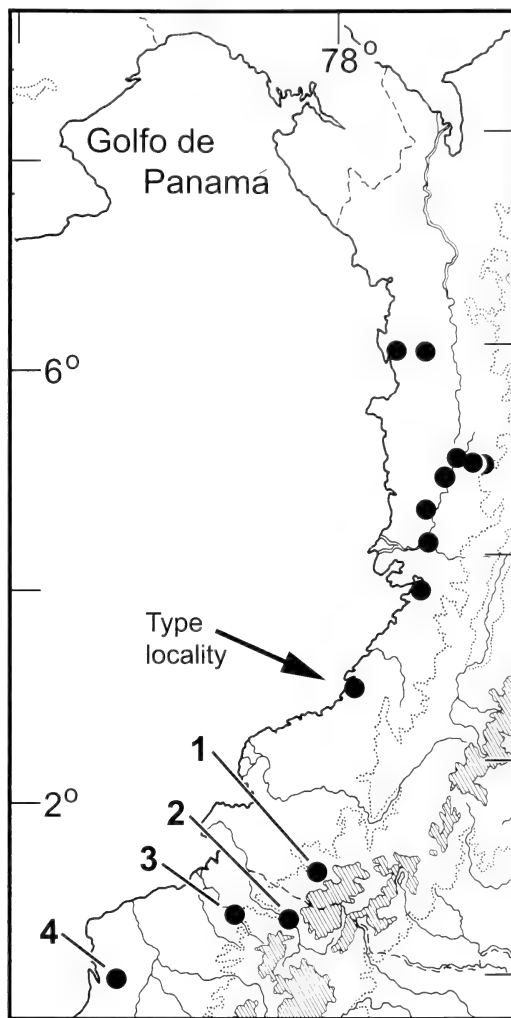
Figure 18. Distribution of *Dendrophidion prolixum*. Arrow indicates the type locality. Numbered localities are the following discussed in the text: *1,* Ricaurte (Nariño department, Colombia). *2,* Paramba (Imbabura province, Ecuador). *3,* Río Cachaví (Esmeraldas province, Ecuador). *4,* Bilsa Biological Station (Esmeraldas province, Ecuador).

Localities 1 and 3 (Fig. 18; Ricaurte, Colombia and Río Cachaví, Ecuador). These localities are documented by three juvenile specimens: ANSP 25608 (Ricaurte) and USNM 237064–65 (Río Cachaví; Fig. 12B). Diagnostic characters of the three specimens are the wide separation, distinctness, and somewhat ocellate form of the pale bands on the neck, low number of pale body bands (52, 49, and 57,
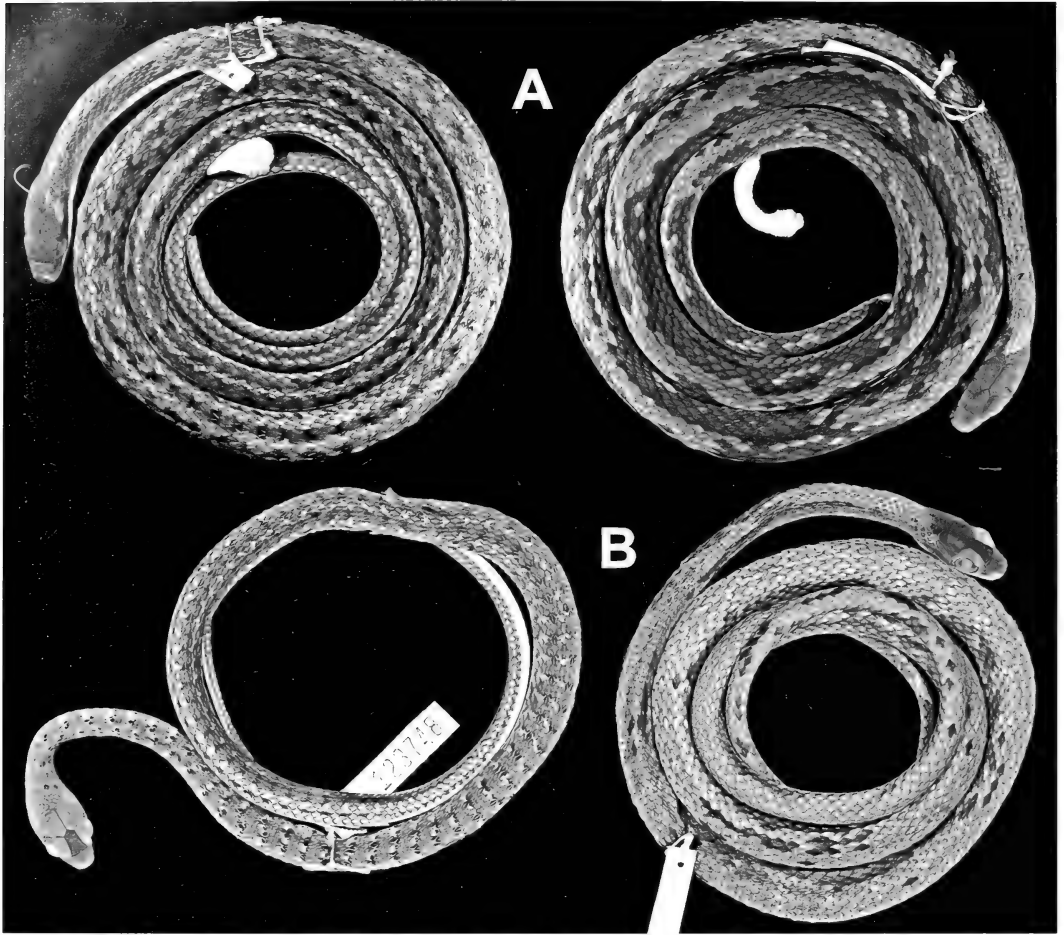
Figure 19.   Examples of sympatry between *Dendrophidion percarinatum* and *D. prolixum* in western Colombia. Specimens on the left are *D. percarinatum*; on the right are specimens of *D. prolixum* from the same localities: (A) Playa de Oro (AMNH R-108468 and AMNH R-108469, respectively); (B) Quebrada Pangala (AMNH R-123748 and AMNH R-123746, respectively). See Figure 9 for locations. Everted hemipenes of the specimens in panel A are illustrated in Figures 39A and 42, respectively.

respectively), and brownish head/neck ground color. These characters are considered diagnostic of *D. prolixum*, so the identity of these specimens is reasonably secure.

Locality 2 (Paramba, Ecuador). Two females are available from this locality (FMNH 4055–56). FMNH 4055 is a small juvenile (234 mm SVL) with an incomplete tail, 158 ventrals, a dorsocaudal reduction at subcaudal 11, and supralabial/temporal pattern G on both sides. Its scale counts and the G supralabial/temporal pattern are consistent with either *D. prolixum*, *D.*

graciliverpa, or *D. brunneum*, the three species known from the region. The supralabial/temporal pattern makes one of the first two more likely than *D. brunneum* simply based on frequency of occurrence (71.6% of *brunneum* scores were P, only 4% G). The pattern of FMNH 4055 is suggestive of *D. prolixum* (dark brown ground color with somewhat ocellate pale spots on the neck, wide spacing of the neck spots (2.5–4 dorsal rows), and 59 total bands on the body. FMNH 4056 is an adult (517 mm SVL) with 161 ventrals, 144 subcaudals, dorsocaudal reduction at subcaudal 9, a

relative tail length of 42% of total length (72% of SVL), and supralabial/temporal pattern G on both sides. The specimen is overall very dark gray, almost blackish, with no discernible dorsal pattern and an immaculate venter. All of these characters are consistent with *D. prolixum*, *D. graciliverpa*, or *D. brunneum* (with the last less likely based on the supralabial/temporal pattern). Based on FMNH 4055, I include locality 2 as a documented locality for *D. prolixum*; either of the other two species could be represented by FMNH 4056.

Locality 4 (Bilsa Biological Reserve). I have seen two juveniles from this locality, USNM 541964 and KU 291237 (Fig. 13C, right), which I refer to the new species *D. graciliverpa* based on color pattern and scutellation characteristics (Table 4). Both have the G supralabial/temporal pattern, and the retracted hemipenis of KU 291237 extends to the middle of subcaudal 10 (not examined for USNM 541964). A herpetofaunal survey report illustrates in color three species of *Dendrophidion* from Bilsa Biological Reserve (Ortega-Andrade et al., 2010: 148). One photograph is correctly identified as "*D. nuchale*" (auctorum). A second, "*D. percarinatus*," appears to be the species here described as *D. graciliverpa*. The third species, "*D. brunneus*," has a color pattern very similar to one described above for *D. prolixum*: a reddish brown head with the brown color extending onto the neck as dorsolateral and lateral stripes on a green ground color; labials, throat, and anterior ventrals yellow. Thus, I tentatively include locality 4 in the distribution of *D. prolixum*, but it needs verification. The photographs of "*D. percarinatus*" and "*D. brunneus*" in Ortega-Andrade et al. (2010) appear to be juveniles. If I have identified the photograph correctly, it would corroborate the only documented sympatry between *D. prolixum* and *D. graciliverpa*.

The fact that all of the southern records of *Dendrophidion prolixum* are based on juveniles and the lack of adults from this region is disconcerting. Moreover, several adults from other localities in western

Ecuador are without discernible pattern elements and are dark gray or brownish, similar to some adult *D. prolixum*. I refer these to *D. graciliverpa* but that is based mainly on the fact that the only specimens from the same or nearby localities are referable to that species based on color pattern characters visible in preserved specimens—certainly a less than desirable situation. Additional data on coloration in life would help resolve these problems because *D. prolixum* and *D. graciliverpa* are otherwise quite similar in characters observable on preserved specimens, including hemipenial morphology discussed later.

Natural History. The type locality of *Dendrophidion prolixum* is also the type locality of *Phyllobates terribilis* and *Colostethus lacrimosus* (Myers et al., 1978, Myers, 1991). Myers et al. (1978: 321–324, figs. 4–5) described and illustrated the area as of 9–21 February 1973, when Myers and Daly collected the topotypic series of *D. prolixum*. The following is quoted from their account (references to figures and notes omitted):

[Quebrada Guanguí is set] in rough hilly country at the western foot of a northerly inclined spur of the Cordillera Occidental. … Slopes are more often steep than gentle, and perpendicular surfaces are not uncommon. Hillside soils are gravelly in places. Drainage is by clear-water streams flowing over rock, gravel, and sand. The principal stream, a tributary of the Río Saija, is the Río Patia, which originates along the western base of Cerro Tambor. The Quebrada Guanguí is a southward flowing tributary that empties into the Río Patia at an elevation of about 90 m. above sea level. Hilltops in the immediate vicinity are about 200 m. above sea level.

The region has a decidedly tropical wet climate (*Af* in the Köppen system [Köppen, 1931]) [and] receives a yearly rainfall probably in excess of 5 m. … It seems certain that relative humidity is always very high, especially inside the forest.

There is no undisturbed forest along the larger streams, where small terraces and adjacent hillsides are either under cultivation … or in dense second growth. Inland, the native lowland rain forest is relatively undisturbed but only of moderate height, probably due to the precipitous slopes. There are occasional tall emergents that break the uniformity of the forest canopy. Most of the larger trees have buttressed roots, and tall palms with stilt roots are common. Tree-trunk moss is sparse. Small bromeliads commonly grow low on the trunks, but the bromeliad population is not dense and they rarely occur on the ground. The understory and ground vegetation of saplings and treelets, small palms, and herbaceous plants and ferns, varies from dense to moderately open. The forest tends to be most open on gravelly slopes, some of which are quite wet due to seepage. Leaf litter is sparse. (Myers et al., 1978: 321–322)

Three specimens are accompanied by notes indicating they were active by day on the forest floor (AMNH R-119801; juvenile), on a stream bank (AMNH R-109727; adult), or on the ground in a brushy part of a ridge top forest (but with large trees, shaded at ground level) (AMNH R-109726; adult).

In addition to sympatry between *Dendrophidion prolixum* and *D. percarinatum* discussed above, *D. prolixum* is broadly sympatric with *D. nuchale* auctorum throughout western Colombia; sympatry is documented at the type locality (AMNH R-109718-20) and Quebrada Docordó (CAS 119591, 119604; AMNH R-123752). The distributions of *D. prolixum* and *D. graciliverpa* seemingly overlap in northwestern Ecuador and documentation of actual sympatry is poor, but may occur at the Bilsa Biological Station (Esmeraldas province); see above discussion.

Dendrophidion graciliverpa **New Species**

Figures 1B, 1E, 2, 3, 12C, 13C, 20–26, 35B, 43B, 44–46

?*Herpetodryas dendrophis* (part). Jan 1863: 81 (Cayenne, Popayán, Guayaquil, Ecua-

dor). Jan and Sordelli, 1869: Livr. 31, pl. 3, fig. 2 (young individual from "Équateur"). The young specimen illustrated by Jan and Sordelli has a pattern and head scalation consistent with *D. graciliverpa*; the adult (their fig. 1), a blotched snake, appears to be *Drymobius rhombifer* (a conclusion reached independently by Savage and McDiarmid; personal communication from Jay M. Savage).

Drymobius dendrophis (part). Boulenger, 1894: 16 (a male from western Ecuador collected by Louis Fraser, BMNH 1860.6.16.59)

?*Dendrophidion dendrophis* (part). Pérez-Santos and Moreno, 1988: 134 (Pacific lowlands of Colombia). Pérez-Santos and Moreno, 1991b: 135 ("southern part of Central America and northern South America").

Dendrophidion percarinatum (part; western Ecuador included implicitly or explicitly as part of the distribution). Dunn, 1944: 477 (? part). Savage and Villa, 1986: 148, 169. Lieb, 1988: 172; 1996: 636.1. Almendáriz, 1991: 143. Pérez-Santos and Moreno, 1991a: 134. Savage, 2002: 657. Köhler, 2003: 200; 2008: 215. Solórzano, 2004: 234–236. Guyer and Donnelly, 2005. McCranie and Castañeda, 2005: 8. McDiarmid and Savage, 2005: 391, 421. Rojas-Runjaic and Rivero, 2008: 129. Cadle, 2010: 24.

Dendrophidion percarinatus. Ortega-Andrade et al., 2010: 148.

Holotype (Figs. 20, 21, 23, 26A). AMNH R-110584 from 3 km E Pasaje, 30 m elevation, El Oro province, Ecuador [03°20′S, 79°49′W]. Collected 11 February 1974 by Charles W. Myers and John W. Daly (field number C. W. Myers 12250).

The holotype is an adult male, 964 mm total length, 359 mm tail length (605 mm SVL); relative tail length 37% of total length, 59% of SVL; dorsocaudal reduction from 8 to 6 at the level of subcaudals 26–27; 157 ventrals, 2 preventrals, 137 subcaudals. Head scales are typical of the species
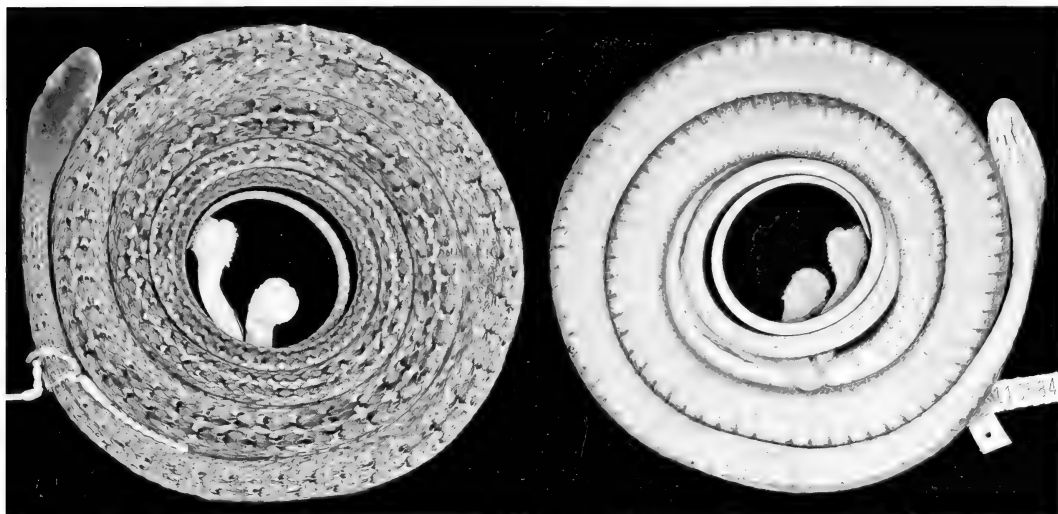
Figure 20.   Holotype of *Dendrophidion graciliverpa* (AMNH R-110584). Adult male from near Pasaje, El Oro province, Ecuador.

(Table 1 and description below) except that three postoculars are present on each side; supralabial/temporal pattern G (Fig. 21). Both hemipenes are fully everted. The right hemipenis was fully inflated for illustration and description but was not removed from the specimen; at full inflation it is about 38.6 mm in length (Fig. 44). The preserved type has pale crossbands (87 on the body) and a pale vertebral line (Fig. 26A); the venter has dense gray pigment laterally, indistinct narrow grayish lines on the anterior edges of the ventral scutes (more prominent posteriorly), and irregular small dark spots on the posterior ventrals. The head and neck are dark gray. In life the head was bright green and the dorsum brown to orangish brown but without distinct crossbands (detailed color notes below; see Fig. 23).

Paratopotypes. AMNH R-110585–86, AMNH R-119835. *Other Paratypes*: "Peru," no specific locality [probably Ecuador; see Cadle, 1989: 422–423], ANSP 5519. **Ecuador:** "western Ecuador," no other data, BMNH 1860.6.16.59.[2] [*Chimborazo*]: Chaguarapata, 2,000 ft., AMNH R-23032. *El Oro*: Hualtaco, USNM 237085. Rosa Delia Plantation, USNM 60523. *Esmeraldas*: Bilsa Biological Reserve, KU 291237. [*Guayas*]:

Guayaquil, USNM 12268. Río Pescado [about 488 m], AMNH R-23438. [*Guayas?*]: Headwaters of the Río Congo, USNM 237063. *Imbabura*: Lita, USNM 237084. *Los Ríos*: Finca Playa Grande [53 m], UIMNH 77347. Playas de Montalvo, 15 m, UMMZ 83949. [*Los Ríos*]: Centro Científico Rio Palenque, 47 km S. Santo Domingo de los Colorados on rd to Quevedo [220 m], MCR R-156328–29, R-156955. [*Loja*]: Alamor, AMNH 22232. *Pichincha*: Puerto Quito, MCZ R-166539. [*Santo Domingo de los Tsáchilas*] [ex *Pichincha*]: Canoas near Santo Domingo de Los Colorados, USNM 237067. Finca La Esperanza near Santo Domingo de los Colorados, USNM 237072. Joe Ramsey Farm, km 19 on Chone Road, 18 km W of Santo Domingo de los Colorados, USNM 237069. Meme, km 96 on road to Saloya at crossing of Río Toachi,

---

[2] I arbitrarily assigned this BMNH catalogue number to one specimen of a series of four (see footnote 3, Appendix 1, for details). By this scheme, BMNH 1860.6.16.59 is a male with an incomplete tail, and the largest specimen of the series (1,054+ mm total length, 676 mm SVL). These details should enable the identification of the correct specimen if the catalogue numbers ultimately become dissociated. The other three specimens of the series are *Dendrophidion brunneum.*

Figure 21.   Holotype of *Dendrophidion graciliverpa* (AMNH R-110584), head in lateral view.

USNM 237074–75. Mulaute, on tributary of Río Blanco. USNM 237073. Rancho Santa Teresita. km 25 on route to Chone from Santo Domingo de Los Colorados, USNM 283531–32. Río Baba, 24 km S Santo Domingo de los Colorados, UIMNH 77345, 92243. Río Baba, 19 km S and 5 km E Santo Domingo de los Colorados, UIMNH 92244. Santo Domingo de los Colorados, 550–660 m, KU 179500–01; USNM 237068. 2 km E of Santo Domingo de Los Colorados, USNM 237070. 5 km W of Santo Domingo de los Colorados, USNM 237071.

Other Referred Specimens (Ecuador). *Cotopaxi*: Las Pampas [1,750 m], MCZ R-163968–69. *Esmeraldas*: Quininde [about 100 m], USNM 237066. 41 km WSW of Quininde, Bilsa Biological Reserve, Black Trail, 300 m, USNM 541964. [*Los Ríos*]: 1 km N Buena Fe, MCZ R-156327. [*Santo Domingo de los Tsáchilas*] [ex *Pichincha*]: below Río Toachi, USNM 237076.

Etymology. The specific name is a feminine noun in apposition derived from the Latin words *gracilis* (slender or gracile) + *verpa* (penis). The name refers to the long, slender hemipenis of this species in comparison specifically to *Dendrophidion percarinatum*, with which it has been confused, but also more generally to hemipenes of most other species of *Dendrophidion*.

Diagnosis. Dendrophidion graciliverpa is characterized by (1) dorsocaudal reduction from 8 to 6 occurring anterior to subcaudal 28 (range, 7–27); (2) divided anal plate; (3) subcaudal counts ≥120 in males and females; (4) subadults with narrow pale bands (<1 dorsal scale width on the neck)

or transverse rows of ocelli; adults retain bands or become predominantly brown or green (pale bands usually separated by fewer than three dorsal scale rows on the neck; total number of pale bands on the body >55); (5) ventrals immaculate or with narrow transverse dark lines across the anterior border of each ventral plate; (6) in life, head greenish brown to green and body brownish, olive, or grayish; and (7) everted hemipenis of the "gracile" morphology, with an exceptionally long, slender hemipenial body proximal to an expanded distal portion, which bears spines, calyces, and other apical ornamentation (retracted hemipenis nearly always to subcaudal 10 or greater); total number of enlarged spines on hemipenis >80 (81, 84, and 116 in three studied organs).

"Gracile" hemipenial morphology will distinguish *D. graciliverpa* from all other species of *Dendrophidion* except *D. prolixum* described herein and perhaps *D. bivittatum* (see above comments where the gracile morphology is described). *Dendrophidion bivittatum* has a different color pattern (greenish dorsum with blackish longitudinal stripes).

Dendrophidion graciliverpa differs from species of the *D. dendrophis* species group (*D. dendrophis*, *D. atlantica*, *D. nuchale auctorum*, *D. apharocybe*, *D. crybelum*, *D. vinitor*) in having a reduction in the dorsocaudal scales anterior to subcaudal 30 (posterior to subcaudal 30 in the *D. dendrophis* group except occasional females). A divided anal plate will distinguish it from *D. apharocybe*, *D. crybelum*, and *D. vinitor* (anal plate nearly always single in these species). *Dendrophidion dendrophis* and *D. nuchale* auctorum may have either single or divided anal plates but have different color patterns (see Duellman, 1978: 236–237, 2005: pl. 175; Savage, 2002: 654, pls. 413–415), attain greater body sizes, and have different hemipenial morphologies (robust morphology and enormously enlarged spines in *D. dendrophis* and *D. nuchale*). *Dendrophidion graciliverpa* differs from *D. boshelli* in having 17 midbody scale rows (15 in *D. boshelli*).

Dendrophidion graciliverpa has previously been confused with *D. percarinatum*, and these species cannot be distinguished by traditional scutellation features other than a few mean character differences (Table 1). These two species differ in (1) color pattern: greenish head and anterior body, and venter either immaculate or with dark transverse lines (*D. graciliverpa*) vs. head and body primarily browns to grays, and venter immaculate (*D. percarinatum*); (2) hemipenial morphology: gracile (*graciliverpa*) vs. robust (*percarinatum*); retracted hemipenis nearly always to subcaudal 10 or greater (*D. graciliverpa*) vs. <10 subcaudals (*D. percarinatum*); total number of enlarged spines on the hemipenis >80 (*D. graciliverpa*) vs. fewer than 45 (*D. percarinatum*); (3) relationship between the posterior supralabials and temporals as discussed above: G pattern most commonly (*D. graciliverpa*) vs. P pattern most commonly (*D. percarinatum*). *Dendrophidion graciliverpa* has a greater number of pale bands on the body and different overall coloration than *D. prolixum* (see account for the last species and Table 4 for details).

Description (22 males, 21 females). Table 1 summarizes size, body proportions, and meristic data for *Dendrophidion graciliverpa*. Largest specimen (BMNH 1860.6.16.59) a male 676 mm SVL (1,054+ mm total length, tail incomplete; largest male with a complete tail (AMNH R-110584) 605 mm SVL (964 mm total length). Largest female (KU 179500) 663 mm SVL (922+ mm total length, tail incomplete); largest female with complete tail (USNM 237085) 631 mm SVL, 1,027 mm total length. Tail 37–42% of total length (59–72% of SVL) in males; 36–39% of total length (56–64% of SVL) in females. Dorsal scales in 17–17–15 scale rows, the posterior reduction by fusion of rows 2+3 ($N = 13$), 3+4 ($N = 34$), or loss of row 3 ($N = 7$) at the level of ventrals 78–101 (see sexual dimorphism below). Ventrals 153–163 (averaging 157.5) in males, 152–166 (averaging 160.7) in females; ventrals preceded by 2 (rarely 1 or 3) preventrals. Anal plate divided. Subcaudals 132–153

(averaging 142.3) in males, 120–143 (averaging 133.5) in females. Preoculars 1, postoculars 2 (occasionally 3), primary temporals usually 2 (rarely 3), secondary temporals 2 (rarely 1), supralabials usually 9 with 4–6 bordering the eye (rarely 8 and with other combinations bordering the eye), infralabials usually 10 (range 8–12 with high frequencies of 9 and 11). Dorsocaudal reduction from 8 to 6 occurs at subcaudals 12–27 in males, 7–19 in females. Maxillary teeth 33–44 (averaging 39), usually with the 3 or 4 posterior teeth enlarged, ungrooved, and not offset; rarely, 5 teeth were enlarged. Maxillary diastema absent.

Two apical pits present on dorsal scales. Usually the lower 5–7 dorsal rows on the neck lack keels; keels are usually lacking on the lower 2 rows at midbody (or row 1 only but with weak keels on row 2); all except the first dorsal row are keeled on the posterior body (keels sometimes weak or absent on row 2 as well). Nearly 67% of scorings for the supralabial/temporal pattern were G, and only about 3% were P (the remainder ambiguous or irregular). Fusions or divisions of temporal scales were moderately common, with the following frequencies: upper or lower primary or secondary divided vertically (5.8%), upper primary divided horizontally (1%), upper or lower primary + secondary fused (1%). One specimen had 17–19–17 dorsal scale rows. Tails are proportionally shorter in small individuals. Specimens <300 mm SVL have tail lengths 34–38% of total length, 52–62% of SVL ($N = 11$, males and females combined). No strong geographic trends were evident among the characters examined.

Hemipenis unilobed and of the gracile morphotype. Proximal portion of hemipenial body exceptionally long, slender, and ornamented with minute spines. Distal region slightly bulbous, containing a spinose region followed distally by 2 flounces and a largely nude apex. Usually an exceptionally large irregular calyx, and sometimes additional poorly developed calyces, on the asulcate side of the apex. Sulcus spermaticus simple, centrolineal, with the appearance of a terminal division in everted organs
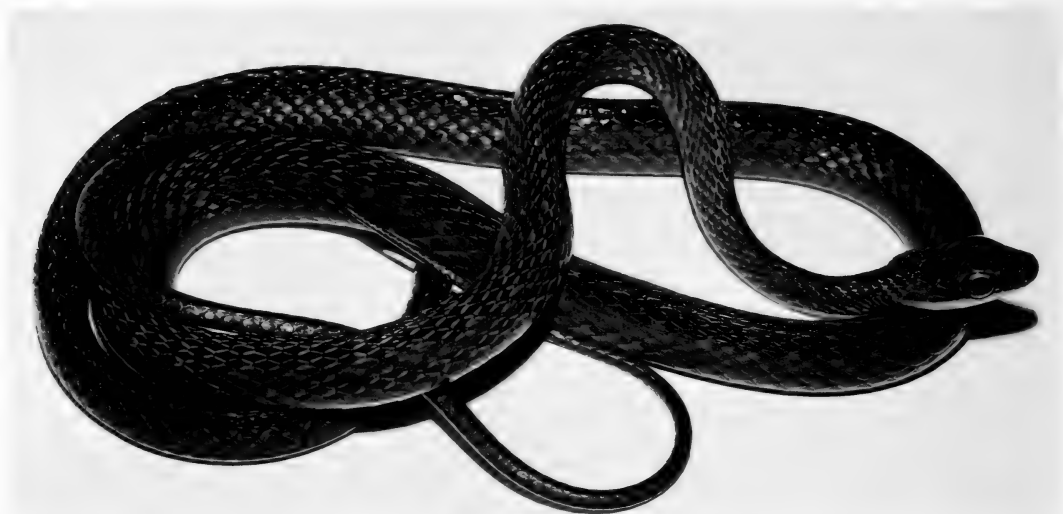
Figure 22.   Holotype of *Dendrophidion graciliverpa* in life (AMNH R-110584). Adult male, 605 mm SVL. From a color slide by Charles W. Myers.

(divergent sulcus lips separated by a triangular tissue wedge).

Sexual Dimorphism. Females average a significantly greater mean adult body size and ventral counts and a more posterior point of dorsal scale reduction than males, whereas males have a greater mean relative tail length and subcaudal counts and a more posterior point of dorsocaudal reduction than females (Table 1).

Coloration in Life. Color notes for four specimens from the type locality (field notes of Charles W. Myers for AMNH R-110584-86, R-119835) indicate that the head and neck are greenish brown in juveniles to bright green in adults. Ground color of the rest of the dorsum is brown to orangish brown or olive. Concealed anterolateral edges of the dorsal scales are bright yellow, especially on the anterior body. Supralabials yellowish white to golden yellow. Gular region white. Venter pale green to bright golden yellow.

Myers' coloration notes on individual specimens are here quoted in full:

AMNH R-110584–86 (holotype and two topotypes; Fig. 22): Head and neck greenish brown in smallest specimen [AMNH R-

110586; 409 mm SVL], bright green in [AMNH R-110584–85; 605 and 453 mm SVL, respectively]. Body color brown to orangish brown with concealed (anterolateral) scale edges bright yellow, especially on anterior body. Supralabials yellowish white (two smaller specimens) to light golden yellow (largest; holotype). Under head white; slight yellowish tinge under neck; anterior venter pale green, turning bright golden yellow under posterior body and tail. Upper one-third of iris tan, lower two-thirds dark brown. Tongue black, including tips.

AMNH R-119835 (topotype, 565 mm SVL): Head and front of neck region bright green, turning olive with grayish black markings on body. Genial plates white, but labials and entire venter bright golden yellow. Top quarter-sector of iris tan, lower three-quarters dark brown. Tongue, including tips, black.

Color notes for specimens from Pichincha province are the following:

KU 179501 (231 mm SVL; field notes of John D. Lynch): Brown above with creamy brown bars edged with black (neck and head with green wash). Lips and throat lemon yellow. Venter somewhat dirty
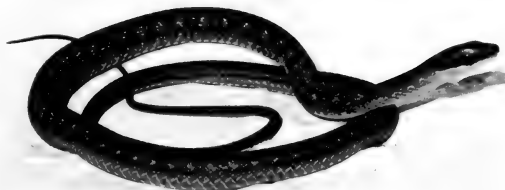
Figure 23.   *Dendrophidion graciliverpa* in life (MCZ R-156328, a juvenile, 308 mm SVL, from Pichincha province). From a color slide by Kenneth Miyata (courtesy of MCZ Department of Herpetology).

yellow. Upper edge of iris pale copper. Most of iris reddish brown.

MCZ 156328 (308 mm SVL; notes from a color slide by Kenneth Miyata reproduced here as Fig. 23): Similar to the above-described AMNH specimens in having a greenish brown head and neck, with the rest of the dorsum various shades of brown, including pale brown crossbands or dorsolateral ocelli on a medium brown ground color; on the posterior half to two-thirds of the body, a narrow dusky to dark brown lateral line along the suture line of dorsal rows 2 and 3, ending at the vent; and a dark brown line along the subcaudal/dorsocaudal border the entire length of the tail. The labials, throat, and visible portions of the anterior ventrals are pale yellow.

KU 179500 (663 mm SVL; field notes of John D. Lynch): Brown above with pea green on skin between scales. Lips, throat, and anterior venter lemon yellow. Middle one-third of venter dull gray-green with some yellow. Posterior belly and underside of tail yellow. Iris brown.

Based on these descriptions it appears that the green coloration of the head and neck may be less intense or greenish brown in smaller specimens, becoming bright green in adults, at least in El Oro province. The presence of green on the head was not mentioned for KU 179500, an adult female, but was present in a juvenile from the same locality (KU 179501) and in MCZ 156328 (Fig. 23) from a nearby locality. This may indicate some variation in the presence of anterior green coloration. Oddly, the prominent pale crossbands and vertebral line in the preserved holotype (Fig. 20) are not

evident in the live specimen (Fig. 22). Indistinct indications of crossbands can be discerned by subtle transverse alignment of dark pigment middorsally but this would not be clear except by comparison of the photos of the live and preserved specimens. In fact, Myers' notes mention no pale bands on any of the four specimens from the type locality and yet all of them have distinct pale bands in preserved specimens (Fig. 24D shows another example). This surely gives one pause in the interpretation of the considerable variation in pattern evident among the preserved specimens referred to this species. The possibility that more than one taxon is represented should be reevaluated as material with associated color notes becomes available.

A photograph of a specimen from Esmeraldas province (Ortega-Andrade et al., 2010: 148, "*Dendrophidion percarinatus*") may be *D. graciliverpa*. Its head is greenish gray anteriorly, more greenish posteriorly. Supralabials whitish. Anterior dorsal ground color pale green. The pale bands on the neck are more ocellate (invested with blackish pigment tending to form round yellow spots partly surrounded with black) than is typical in *D. graciliverpa*, but their spacing appears too close for *D. prolixum*. Anterior ventrals pale yellow with whitish patches.

The disparity in appearance between pale-banded preserved specimens of *Dendrophidion graciliverpa* compared with more uniformly colored live specimens (Figs. 20, 22) is considerable, but there is precedent in other snakes for similar alterations in color pattern due to preservation. Smith (1955) reported a situation in which transverse series of *pale* spots appeared in preserved specimens of *Thamnophis rufipunctatus* in the positions occupied by *dark* spots in life. The difference in spotting resulted in dramatically different appearances of the preserved vs. live specimens. Smith attributed the coloration differences, in part, to the differential solubility of various skin pigments in alcohol. Realization of these preservational
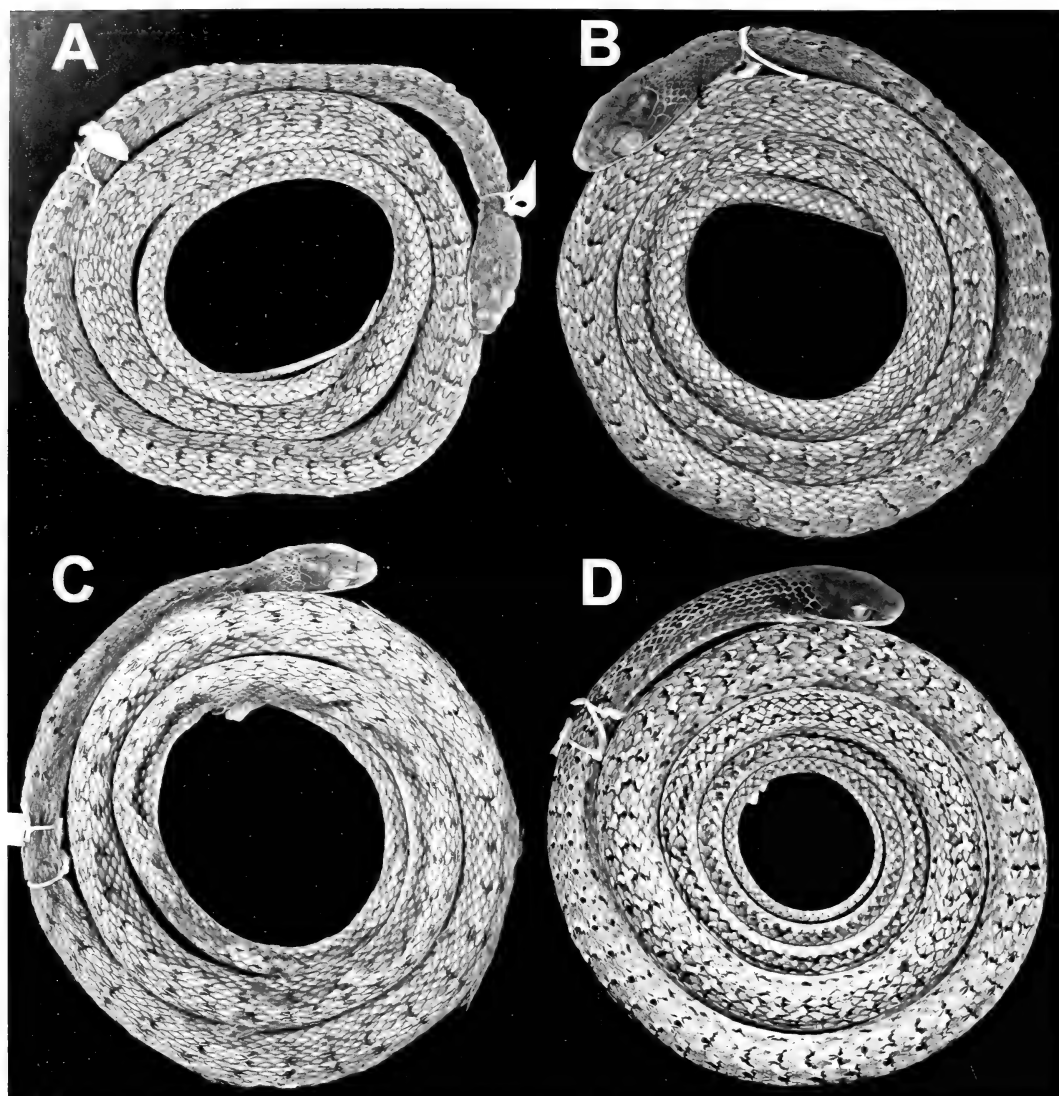
Figure 24. Representative preserved specimens of *Dendrophidion graciliverpa* with prominent bands. (A) AMNH R-23438 (Guayas province). (B) AMNH R-22232 (Loja province). (C) UIMNH 77347 (Los Ríos province). (D) AMNH R-110585 (El Oro province, topotype).

effects on color pattern helped Smith resolve some nomenclatural issues related to original descriptions of color pattern in this group of *Thamnophis*. What remains unclear is why some preserved specimens I refer to *D. graciliverpa* have prominent pale bands in preservative whereas others do not (see the next section). The differences among preserved specimens suggest some-

thing more than simple differential solubility of pigments. This will probably only be resolved when more data on coloration in life and preservative for individual specimens are available.

Coloration in Preservative. Preserved adult specimens exhibit two basic patterns, one with pale crossbands (similar to the juvenile pattern) and the other more
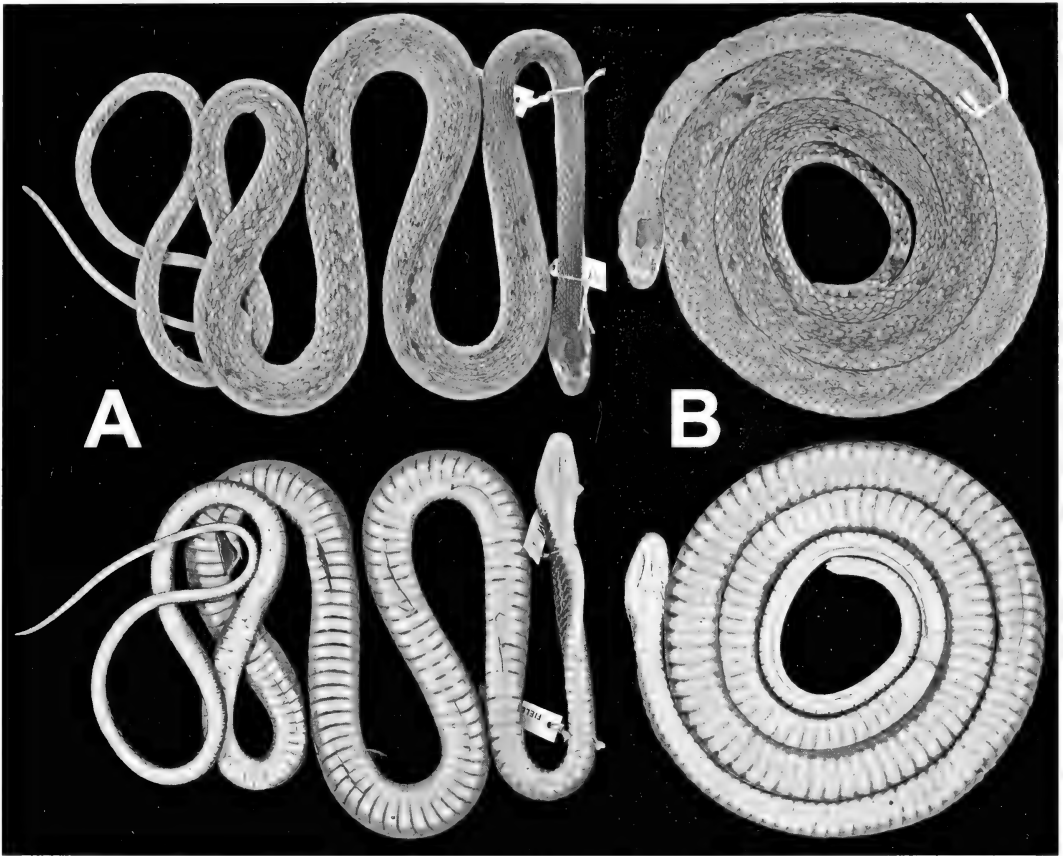
Figure 25. Representative preserved specimens of *Dendrophidion graciliverpa* without strongly banded patterns (dorsal and ventral). (A) USNM 283532. (B) KU 179500. Both specimens from Pichincha province.

unicolor or with indistinct crossbands (Figs. 24–26). The extent of gradation between these pattern forms is unclear, although there is considerable variation in the expression of distinct bands. The two forms are described separately here.

Crossbanded pattern (Figs. 24, 26A–C, F): Dorsal ground color brown, grayish brown, reddish brown, or gray. Individual scales finely peppered with blackish/dark brown, often more concentrated on posterior scale edges (keels often paler than rest of scale). Head and neck often darker (often dark gray) than remainder of dorsum. Many specimens have narrow pale crossbands (one dorsal scale or less) bordered with irregular black or dark brown flecks on anterior and posterior edges; these are

present the entire body length and usually become indistinct on the proximal portion of the tail. Crossbands often less distinct on neck of adults (more evident in juveniles overall), restricted middorsally (lower sides of neck dark gray or gray). Vertebral row often paler or of contrasting color (e.g., gray compared with brown) than adjacent dorsal rows. On the posterior one-third of the body, dorsal rows 3 and 4 or just row 3 often with pale centers or paler overall than adjacent scale rows. Venter immaculate in small juveniles. Larger individuals (some juveniles but mostly adults) have varying expression of narrow dark transverse lines across anterior edges of ventral scales (expression varies from fine peppering of dark pigment across scales to dense
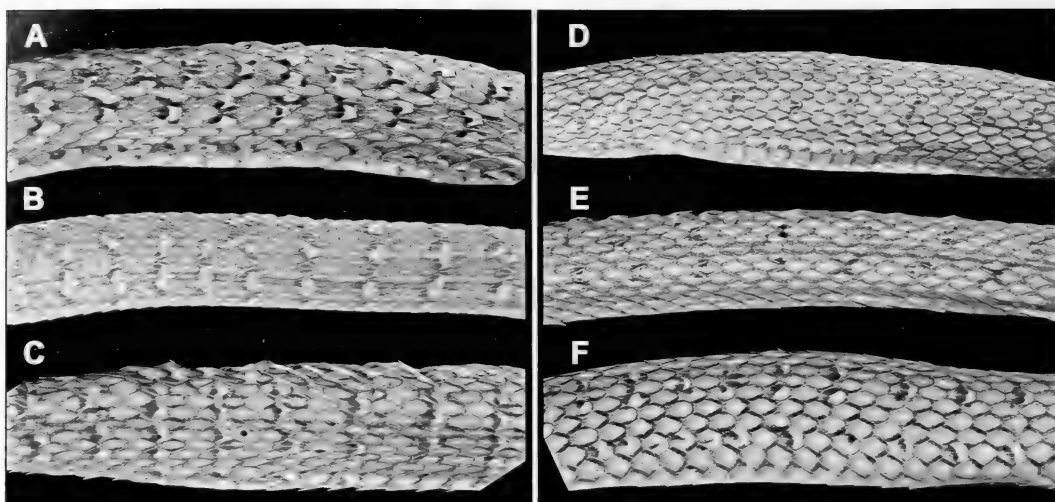
Figure 26.   Variation in dorsal patterns of preserved specimens of *Dendrophidion graciliverpa*. Dorsal views at approximately midbody except (F) (lateral view); adults except (B) (juvenile). (A) AMNH R-110584 (holotype, El Oro province). (B) KU 179501 (juvenile, Pichincha province). (C) AMNH R-23438 (Guayas province). (D) USNM 237070 (Pichincha province). (E) USNM 237085 (El Oro province). (F) AMNH R-23438 lateral view (Guayas province).

complete lines). These lines are often more distinct on posterior venter than anteriorly, where they are often incomplete across the middle of the scales. Subcaudal suture lines often bordered similarly. In addition to transverse lines, the venter may have scattered dark spots or speckling, especially posteriorly (but nowhere dense), sometimes giving the venter a "dirty" white appearance. Sometimes a poorly defined ventrolateral dark brown stripe on the anterior part of the tail at the subcaudal/caudodorsal border.

Unicolor form (Figs. 25, 26D–E): Dorsum generally gray to dark gray (sometimes more brownish with stratum corneum intact). Crossbands nowhere distinct (sometimes a middorsal indication, such as USNM 283532, in which they are indicated on posterior half of body as pale punctuations along vertebral line and dark flecking indicating the dark borders for a greater portion of the body (Fig. 25A). Dark transverse ventral lines similar to the crossbanded form, with similar variable expression in larger individuals.

Comments on Referral of Specimens. Dendrophidion graciliverpa as here con-

ceived is highly variable in the color patterns of preserved specimens. Specimens with prominent crossbands (Fig. 24) in preserved adults are mainly from the southern portion of the distribution (southern Guayas, El Oro, and Loja provinces). Preserved specimens from the north (Pichincha, Chimborazo, and Imbabura provinces) generally lack prominent crossbands in adults (indistinct indications of bands are usually present) (Fig. 25). But there are exceptions to this generalization. For example, USNM 237085, a specimen from southern Ecuador near the type locality and where nearly all other specimens have distinct pale crossbands, has only transversely oriented middorsal irregular brown spots or stipple indicating bands. Unfortunately, the extent of color variation in life is not known and pale crossbands seemingly can be enhanced upon preservation, since several specimens with color notes or photographs in life do not mention prominent pale crossbands. This is particularly well shown by photographs of the holotype in life and preserved (Figs. 20, 22, 26A). Nonetheless, a color photograph of a juvenile from the northern populations

(Fig. 23) is very similar to the life colors of the holotype. I detected no scutellation differences among northern vs. southern specimens, although scale differences often seem not to be good predictors of species limits within *Dendrophidion*.

Hemipenial morphology discussed later likewise suggests no cryptic species within my concept of *Dendrophidion graciliverpa*. However, I have examined relatively few hemipenes from different parts of the range, and some hemipenial variation seems not to correlate well with geography (see account of hemipenial morphology). The only everted organ available from northern Ecuador (USNM 237069 described and illustrated later) is virtually identical to the everted hemipenis of the holotype from southern Ecuador, despite strong differences in preserved color pattern between the two specimens. Until more thorough data are available on geographic differences in coloration, subdivision of *D. graciliverpa* is unwarranted.

There is the added complication that *Dendrophidion prolixum* also occurs in northwestern Ecuador if several juveniles are correctly referred to that taxon (see account for that species). Resolving the extent of distributional overlap and sympatry of *D. graciliverpa* and *D. prolixum* in this area will require more specimens than have been available. As suggested above, the two species seemingly occur together at the Bilsa Biological Station, but a few adult specimens without distinct patterns (dorsum uniformly dark gray or brown) could be referred to either species. The referral of these Ecuadorian specimens to *D. graciliverpa* is based to a great extent on the fact that other specimens (especially juveniles) with distinctive *graciliverpa*-like patterns have been collected at proximate localities, but no specimens with *prolixum*-like patterns are known from Ecuador except the few juveniles cited earlier. More definitive evidence is certainly desirable.

Distribution (Fig. 27). *Dendrophidion graciliverpa* occurs in the lowlands of western Ecuador from Esmeraldas and Imbabura provinces in the north to Loja province in the south. The upper elevational record, 1,750 m, is based on a juvenile male and female from Cotopaxi province (MCZ 163968–69, referred specimens). These specimens have typical *graciliverpa* banding patterns, and the retracted hemipenis of the male extends to the proximal suture of subcaudal 15 (potential confusion with *D. brunneum* is possible in this area, but gracile hemipenial morphology is decisive for identification).

Natural History. The holotype and three topotypes were collected while active in the late afternoon in dry leaf litter in a cacao plantation. AMNH R-119835 ate an *Epipedobates anthonyi* from the same site kept in a common collecting bag and later ate another from a nearby population about 1,000 m higher. Myers and Daly saw five specimens of *D. graciliverpa* during four man-hours on two visits to the type locality (one escaped after its tail broke off while pinned down under a boot). KU 179500–01 were collected by day in banana groves; the tail of the first broke during capture (John D. Lynch, field notes at KU). Despite its wide distribution in western Ecuador, virtually nothing has been reported concerning the natural history of this species. The specimens I refer to *D. graciliverpa* seemingly occupy several distinct forest types in western Ecuador (Dodson and Gentry, 1978), but detailed habitat data are needed because of microgeographic variation in the habitat mosaic of this area. The distribution of *D. graciliverpa* narrowly overlaps those of *D. nuchale* auctorum and *D. prolixum* in northwestern Ecuador and more broadly overlaps that of *D. brunneum*.

APPLICATION OF THE NAME *DENDROPHIDION BRUNNEUM* (GÜNTHER) AND NEW DATA FROM WESTERN ECUADOR

When I began work on the *Dendrophidion percarinatum* group in western Colombia and Ecuador it quickly became apparent that at least four species-group
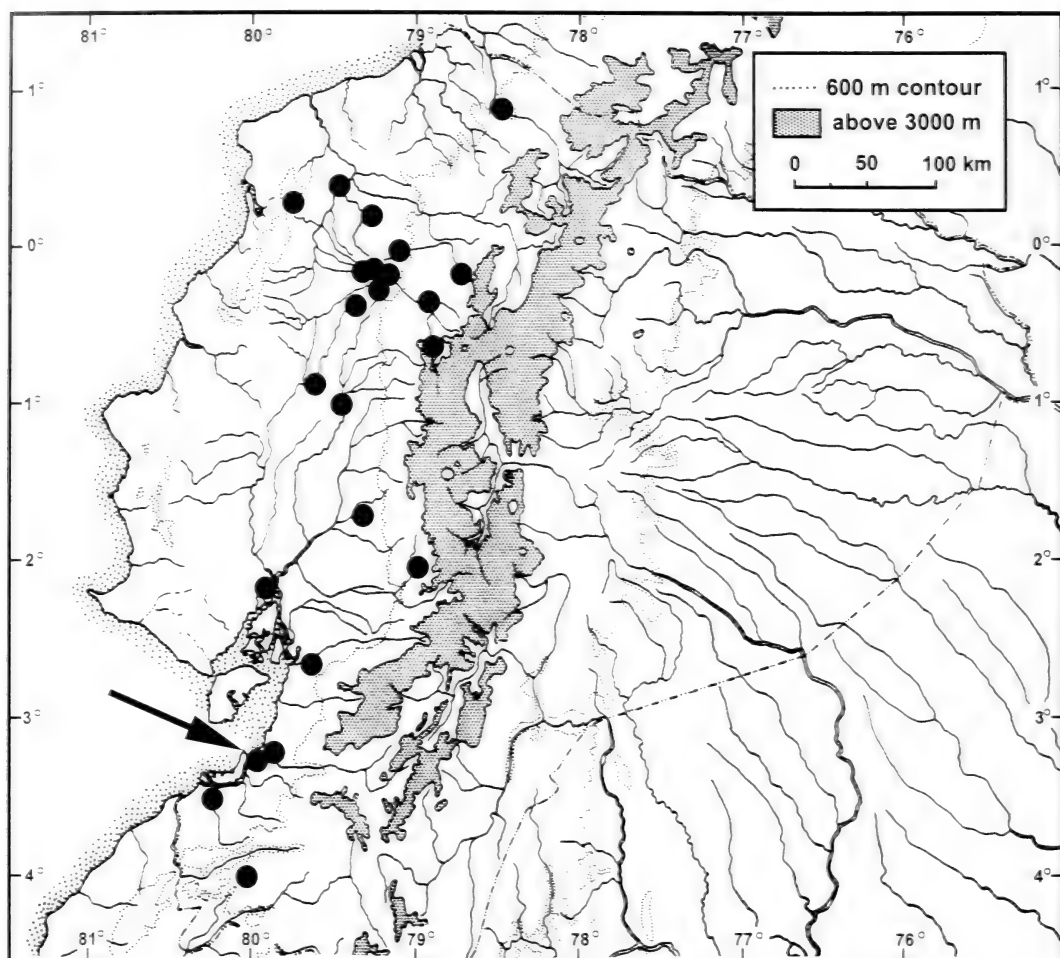
Figure 27.   Distribution of *Dendrophidion graciliverpa*. Arrow indicates the type locality.

taxa of the *percarinatum* group are present in this area (*D. nuchale* auctorum of the *dendrophis* group also occurs there, but it is easily distinguished from species of the *percarinatum* group; see Lieb, 1988; Savage, 2002). Two are the previously named taxa *D. percarinatum* (Cope), as redefined herein, and *D. brunneum* (Günther, 1858), an Ecuadorian and Peruvian species for which Lieb (1988) and Cadle (2010) summarized taxonomic and natural history data. *Dendrophidion percarinatum* and *D. brunneum* (sensu Lieb, 1988; Cadle, 2010; hereafter *D. brunneum* sensu Lieb/Cadle) have hemipenes of the "robust" morphology

characterized herein. The other two taxa in western Colombia and Ecuador are characterized by long, slender hemipenes (gracile morphotype) and aspects of coloration. These are the two new taxa described herein: *D. prolixum* and *D. graciliverpa*. All four western South American taxa of the *percarinatum* group are exceedingly similar in standard taxonomic characters (e.g., scale counts and body proportions) and are most easily distinguished by color patterns and hemipenial morphology. However, color patterns can be difficult to interpret in some preserved specimens and some specimens of all four species appear uncannily

similar. The situation is not helped by the fact that color patterns within *D. brunneum* and *D. graciliverpa* vary considerably as judged by preserved specimens. At least *D. brunneum* as presently understood is polymorphic in life colors (Cadle, 2010; data herein).

Cadle (2010) had followed Lieb (1988) in recognizing *Dendrophidion brunneum* as a species primarily of the uplands in Ecuador and Peru, with the lowland type locality (Guayaquil, Ecuador) assumed to be a shipping point for the holotype. Cadle (2010: 10–11) concluded that no lowland records of *D. brunneum* from Ecuador could be confirmed, although several from northern Peru seemed valid. That assertion is overturned by some reinterpretations and the new material uncovered in this study. Lieb (1988) had examined only three specimens of *D. brunneum* but summarized data on other specimens from the notes of James A. Peters. Cadle (2010) examined the three specimens seen by Lieb and many others of the same taxon, primarily from Peru. However, neither Cadle (2010) nor Lieb (1988) had examined the holotype of *D. brunneum* (BMNH 1946.1.12.98).

My continued study of specimens from western Ecuador (mainly labeled "*D. percarinatum*" or "*D. dendrophis*" in their respective collections) led to the realization that *D. brunneum sensu* Lieb/Cadle was much more widely distributed in western Ecuador than previously recognized. Moreover, it occurs broadly in the lowlands, where its distribution overlaps that of *D. graciliverpa*. Both species occur at Guayaquil, if the locality as a point of origin is to be believed, and have been taken at some other closely contiguous localities. Thus, two species, one with a robust hemipenis (putative *D. brunneum*) and the other with a gracile hemipenis (*D. graciliverpa*), have been confused. (*D. prolixum* seemingly occurs only in far northwestern Ecuador and seems to pose no problem concerning the name *D. brunneum*.) It was only through examination of hemipenial morphology (mainly of retracted organs, as few

everted hemipenes were available) that the species were sorted out. Preserved females, juveniles, and poorly preserved specimens of these taxa can be difficult to distinguish— scutellation is of little help, and subtle aspects of dorsal pattern sometimes provide the best clues.

The existence of two easily confused taxa in western Ecuador made it imperative to determine to which taxon—the robust or gracile hemipenis form—the name *Dendrophidion brunneum* (Günther) applies. This presented a problem inasmuch as the holotype is a female with an incomplete tail, and few coloration or pattern characters are discernible on the 150+ year old specimen. Nonetheless, a detailed consideration of the holotype suggests that Lieb (1988) and Cadle (2010) applied the name correctly to the taxon having a hemipenis of the robust morphotype. To make this case, I redescribe the holotype of *D. brunneum* and then compare it to specimens of *D. brunneum sensu* Lieb/Cadle and to *D. graciliverpa* in greater detail. I then summarize my current understanding of the apparent considerable color pattern polymorphism in *D. brunneum* and its distribution in Ecuador.

Redescription of the Holotype of Dendrophidion brunneum. The holotype of *Dendrophidion brunneum* (BMNH 1946.1.12.98; Figs. 28–29) is an adult female said to be from Guayaquil. It is in fair condition, somewhat soft, and with most of the stratum corneum missing. There is a long midventral slit in the base of the tail. Total length 867+ mm; tail length 224+ mm (with a healed cap on the stump); SVL 643 mm. Ventrals 154 (2 preventrals); 62+ subcaudals; anal plate divided; dorsocaudal reduction from 8 to 6 at subcaudal 10; Dorsals in 17–17–15 rows, the posterior reduction at ventrals 91/93 by fusion of rows 3 + 4 (left) and 2 + 3 (right); 9/9 supralabials (2–3 touching the loreal; 4–6 touching the eye); 2/2 postoculars; 2 + 2 temporals each side (upper primary temporal divided vertically on both sides); 10/10 infralabials; 34/36 maxillary teeth (left/right) with 4 or 5
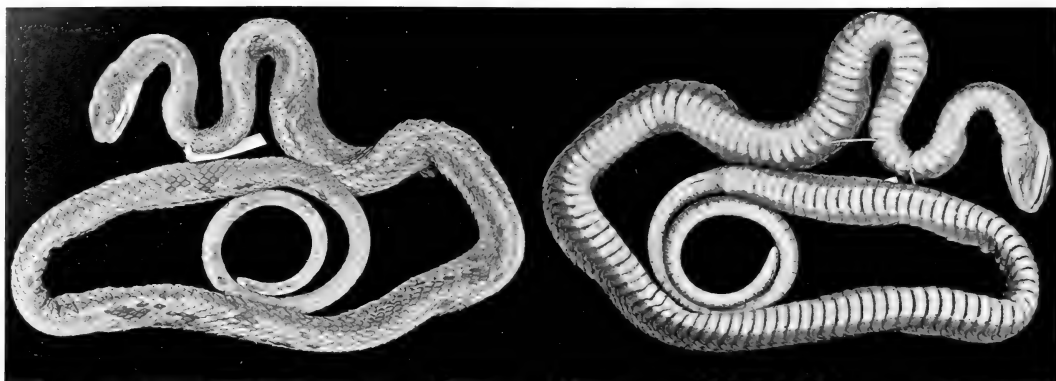
Figure 28.   Holotype of *Dendrophidion brunneum* (Günther) (BMNH 1946.1.12.98) in dorsal and ventral views.
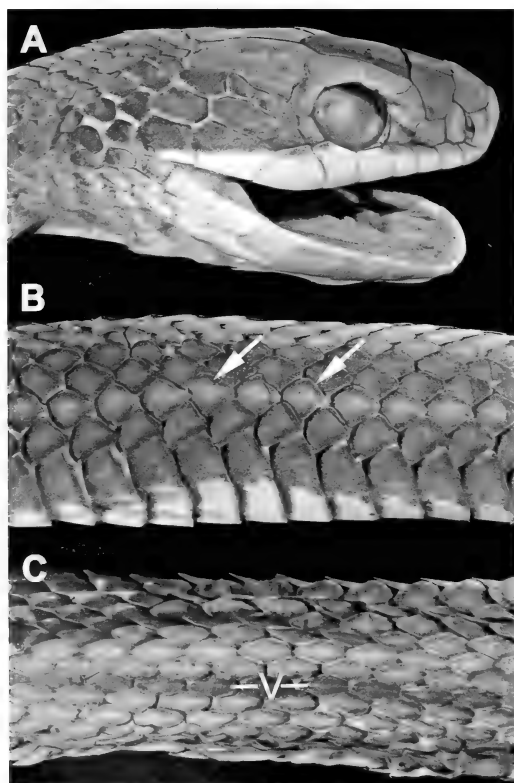

Figure 29.   Holotype of *Dendrophidion brunneum* (Günther) (BMNH 1946.1.12.98). (A) Head, right side, showing the *P* pattern of supralabial/temporal relationship (left side virtually identical). (B) Posterior body in lateral view showing subtle paling of centers of dorsal scales in row 2 (arrows). (C) Approximately midbody, middorsal view showing three pale paravertebral rows. V indicates the vertebral row.

posterior teeth enlarged, ungrooved, not offset, and without a diastema. The supralabial/temporal pattern, as described in the section on systematic characters, is the *P* pattern on both sides (Fig. 29A).

It should be noted that Günther's (1858) measurements of the holotype—"length of tail 12″; total length 39‴"—are not in modern inches, as the symbol ″ (double prime) is interpreted nowadays and as I thought before examining the specimen (Cadle, 2010: 4). Either his measurements are in error or, more likely, are in an archaic measure of inch or some other unit. I have not thoroughly investigated this detail, which seems unimportant for present purposes; the length of an inch has varied through its many centuries of use.[3] In modern inches the holotype is about 34.25 inches total length, 8.75 inches incomplete tail length. Günther (1858) did not mention the incomplete tail, although Boulenger (1894) and Parker (1938) did. Other specimens of *D. brunneum* have 4 or 5 enlarged posterior maxillary teeth like the

----

[3] In a nearly contemporaneous paper Cope (1863) also used the double prime symbol for measurements of several specimens. Myers and Cadle (1994: 25) concluded that Cope's symbol did not denote inches but perhaps represented the metric system (cm), which seemed to be the case for the holotype of *Taeniophallus poecilopogon*. However, metric units make no more sense than inches for the type of *Dendrophidion brunneum* using Günther's numbers.

Figure 30.   Maxillary dentition of *Dendrophidion brunneum*, UF 66199.

holotype, which is illustrated by another specimen (Fig. 30). The posterior teeth in *D. brunneum* are relatively more robust and not enlarged to the same extent (compared with more anterior teeth) as in some other *Dendrophidion* species (e.g., *D. apharocybe*) (Cadle, 2012: fig. 8).

The dorsum of the holotype is blue gray without stratum corneum, olive brown in patches where the stratum corneum is intact. On the posterior half of the body, scales in dorsal row 2 have somewhat pale centers (Fig. 29B). In a few places the 3 paravertebral rows appear paler compared with a darker vertebral row and lower flanks (Fig. 29C), but this is very subtle. Venter marked laterally with blue gray patches similar to the dorsum. Beginning about one-quarter of the body length behind the head are dark gray ventral lines extending across the anterior edges of each ventral scute. These are at first restricted laterally and little more than dense stippling, but by one-third the body length they are complete across the venter; they become more solid and dense posteriorly, tending to refragment a short distance anterior to the vent. Lateral subcaudal sutures lined with dark gray, and a few scattered subcaudal spots, but otherwise the subcaudals are immaculate.

Application of the Name Dendrophidion brunneum. The conclusion that Lieb (1988) and Cadle (2010) applied the name *brunneum* correctly to the robust-hemipenis taxon of western Ecuador is suggested mainly by two characters of the holotype. First, the holotype has the *P* supralabial/temporal pattern on both sides (Fig. 29A). This is by far the most prevalent pattern in *D. brunneum sensu* Lieb/Cadle; 71.6% of scorings have the *P* pattern compared with

4% with the *G* pattern ($N = 74$). In *D. graciliverpa* the *G* pattern is predominant (66.7% of scorings *G* compared with only 2.9% *P*; Table 1).

Second, the shape of the loreal in the holotype is more consistent with its shape and size in *Dendrophidion brunneum sensu* Lieb/Cadle than with *D. graciliverpa*. Cadle (2010: 4) indicated that the shape of the loreal seemed useful in distinguishing *Dendrophidion brunneum* from "*D. percarinatum*" (= *D. graciliverpa* described here): rectangular and longer than tall in *D. brunneum*, an irregular polygon as tall as or taller than long in *D. graciliverpa*. I quantified this character by measuring the loreal length (along the base at the supralabial border) and height (greatest height, usually at the posterior prefrontal suture) for a sample of *D. brunneum sensu* Lieb/Cadle and *D. graciliverpa* (both loreal scales were measured for each specimen in the sample). The results (Fig. 31) show that the subjective impression of loreal shape difference is substantially true—in *D. brunneum* the loreal scales are longer than tall, in contrast to *D. graciliverpa*, whose loreal height for a given length is nearly always greater than that of *D. brunneum*. Furthermore, loreals in *D. graciliverpa* do not attain the lengths, even in large specimens, as the loreals of *D. brunneum* (the longest measured loreal of *D. graciliverpa*, 2.34 mm, was in a specimen 658 mm SVL, just shy of the maximum recorded length of 676 mm SVL). The holotype of *D. brunneum* (asterisks indicated by arrows in Fig. 31) clearly falls in line with the specimens of *D. brunneum sensu* Lieb/Cadle.

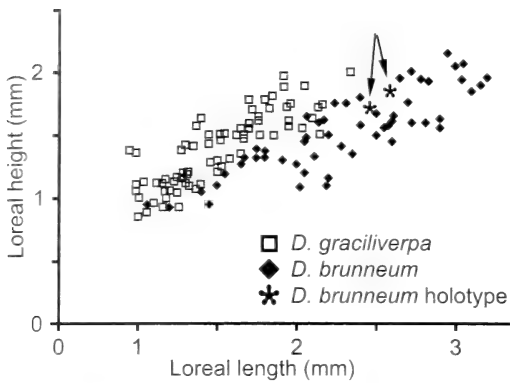Based on the supralabial/temporal pattern and the shape of the loreal, the female

Figure 31.   Bivariate plot of loreal length vs. loreal height in a sample of *Dendrophidion brunneum* and *D. graciliverpa*. The points for the holotype of *D. brunneum* (BMNH 1946.1.12.98) are shown by asterisks indicated by the arrows.

holotype of *Dendrophidion brunneum* is reliably associated with the snakes of "robust" hemipenial morphology in western Ecuador. Apart from these two characters, virtually all other characters of the holotype are consistent with either *D. brunneum* or *D. graciliverpa*. A few pattern characters are similar to other specimens referred to *D. brunneum* (e.g., pale centers on dorsal scales of row 2 and indistinct pale paravertebral rows; see Figs. 29B, 34B and Cadle, 2010: 7–8), but these are subtle and with substantial interpretation in the old holotype. Both species can have dark transverse lines on the venter, as in BMNH 1946.1.12.98 (e.g., Figs. 25, 32). Moreover, the specimens newly referred to *D. brunneum* in this paper significantly broaden my concept of color pattern variation in this species. In the following sections I address the color polymorphism and new distributional data.

Color Pattern Polymorphism in Adult Dendrophidion brunneum. Cadle (2010: 6–8) discussed polymorphism in dorsal coloration in life within a Peruvian population of *Dendrophidion brunneum*. This polymorphism involved mainly transitions between a primarily greenish to more brownish, olive, or coppery coloration, and some individual specimens showed anterior to posterior transitions in this shading.

Nonetheless, significant variation in dorsal pattern was suggested by two preserved Ecuadorian specimens with dorsolateral and lateral stripes and a Peruvian specimen that had indistinct pale anterior crossbands (Cadle, 2010: 7–8). Other specimens had dark paravertebral spots usually more prevalent on the posterior body.

The new specimens show that these color variants are more common and widespread among Ecuadorian populations. With a few notable exceptions, specimens from southern Ecuador and (especially) northern Peru appear more uniform in color pattern. The emerging picture is that *D. brunneum* (assuming only one taxon is involved) exhibits substantial color polymorphism, such as that documented for many other snake species; see Wolf and Werner (1994) for a brief review and Brodie (1990, 1992) for an elegant analysis of a case of extensive polymorphism in *Thamnophis*. Major pattern characteristics of adults are taken in turn in the following paragraphs (juvenile patterns are discussed separately below). Except for the first two color morphs, my interpretations are based entirely on preserved specimens (with the same caveats about translating preserved color patterns to life colors or vice versa mentioned in connection with *D. graciliverpa*).

Unicolor pattern (green to brown in life without distinct dark stripes, punctations, or pale crossbands; Fig. 32A): Cadle (2010) described and illustrated this color pattern in detail. The dorsum is green to brown, sometimes with yellow, bronze, or coppery highlights. All specimens from northern Peru I have seen in life, including juveniles 277–300 mm SVL, are unicolor. This is the predominant coloration of preserved specimens from both Peru and southern Ecuador, assuming that "green in life" becomes, in preserved specimens, brown with intact stratum corneum or slate blue or dark gray without stratum corneum (a common relationship in snakes). Black or dark brown flecks or spots are present in the paravertebral region of some live and preserved specimens, usually more prevalent on the
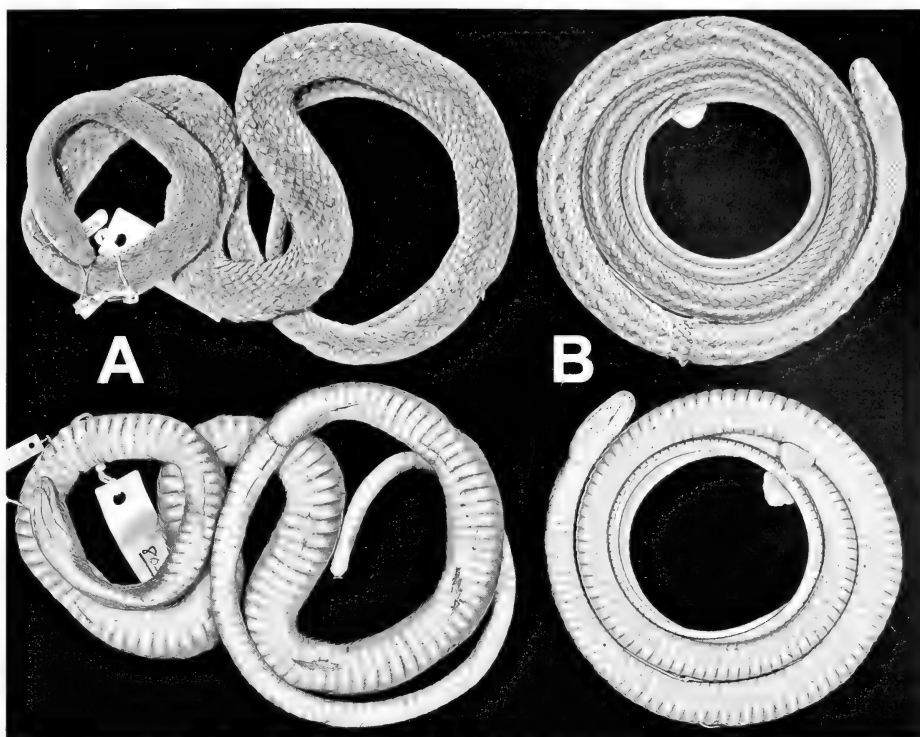
Figure 32.   Unicolor and striped color morphs of *Dendrophidion brunneum* from near Loja city in southern Ecuador (their localities are about 30–35 km apart). (A) USNM 237081. (B) KU 142802.

posterior body (Cadle, 2010: 6–7); these are comparable to similar spots in the "punctate" pattern described below but seemingly less prominent. Some specimens from central western Ecuador (e.g., UF 85105 from Los Ríos province) have nearly uniformly brownish dorsums with only hints of paravertebral spots (see punctate pattern below). Whether these are unicolor or appear more punctate in life would be interesting to know.

Striped pattern (dorsal ground color green in life, stripes dark brown to blackish; Figs. 32B, 33A): Snakes with this pattern have broad dark dorsolateral stripes (2–3 paravertebral rows wide) and a narrow dark lateral stripe on dorsal row 2, both usually more distinct on the posterior body. In life the dorsum of KU 142802 (Fig. 32B) was olive green with dark brown stripes; venter creamy white with a tinge of yellow laterally on the neck and faint blue on the anterior

margins of the ventrals; top of head olive brown, iris brown, tongue reddish brown with a black tip (field notes at KU). A color photograph perhaps of this form is in Yánez-Muñoz et al. (2009: fig. 61, labeled "*Drymoluber* sp."); this photograph shows a bright green snake (head somewhat darker green) and dark brown stripes that are less distinct on the anterior body. In preserved specimens the stripes are usually rusty reddish brown and can show less contrast with the dorsal ground color than in live specimens; in excessively darkened specimens (ground color dark gray) the rusty stripes appear paler than the background. Some striped specimens have dark paravertebral punctations on some part of the body (e.g., KU 142802, Fig. 34A) and the striped and punctate color morphs may totally grade into one another (see below); colors in life would help interpret these patterns. I suspect that older specimens (e.g., the
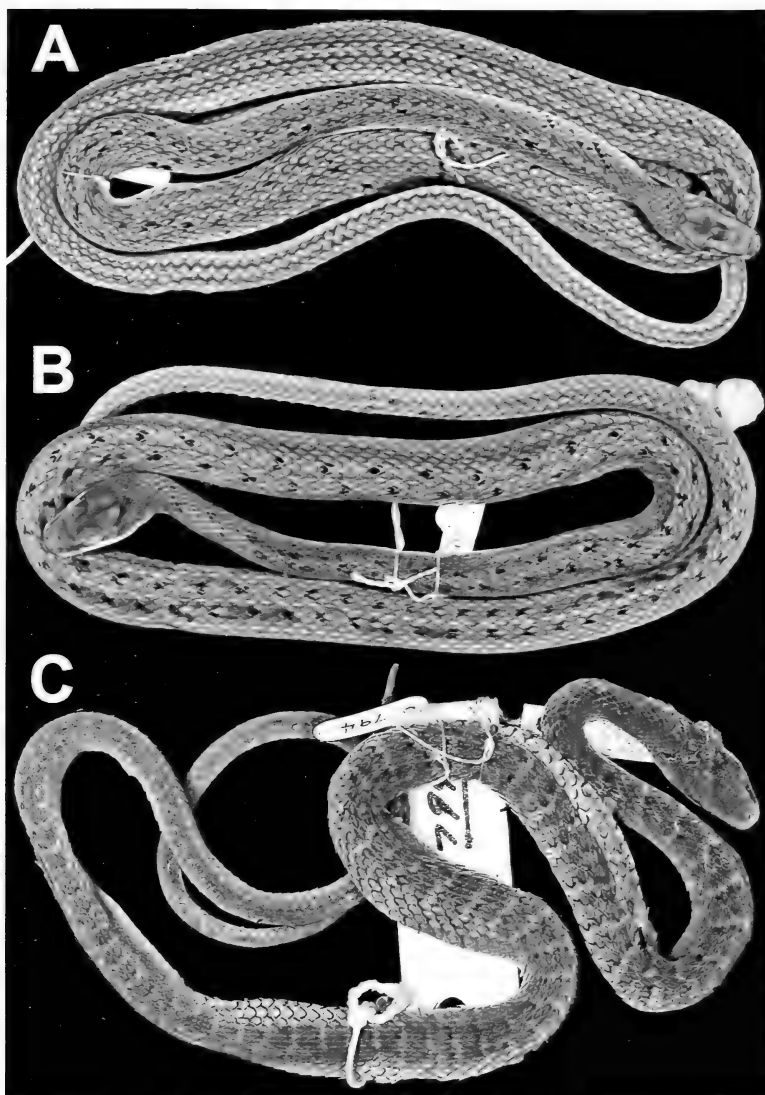
Figure 33.   Dorsal pattern polymorphism in *Dendrophidion brunneum*. (A) Striped pattern (UF 87940. (B) Punctate pattern (UF 88467). (C) Banded pattern (USNM 237079).

holotype and MCZ 8393; Figs. 29B, 34B) with pale paravertebral dorsal rows and pale dorsal row 2 on the posterior body may represent the striped morph as it ages in preservative. The striped color morph is known from montane areas in the vicinity of Loja city (KU 142802) and Azuay province (USNM 237042) and from the lowlands farther north in Guayas province (UF 87940 from Daule, Fig. 33A; USNM 237059 from Guayaquil).

Punctate pattern set within dorsolateral rusty or pale brown stripes (colors in life unknown; Figs. 33B, 34B, C): In the lowlands of Guayas province (Río Daule/ Babahoyo system) and in northern Ecuador (Imbabura province) are specimens having paravertebral stripes of varying distinctness
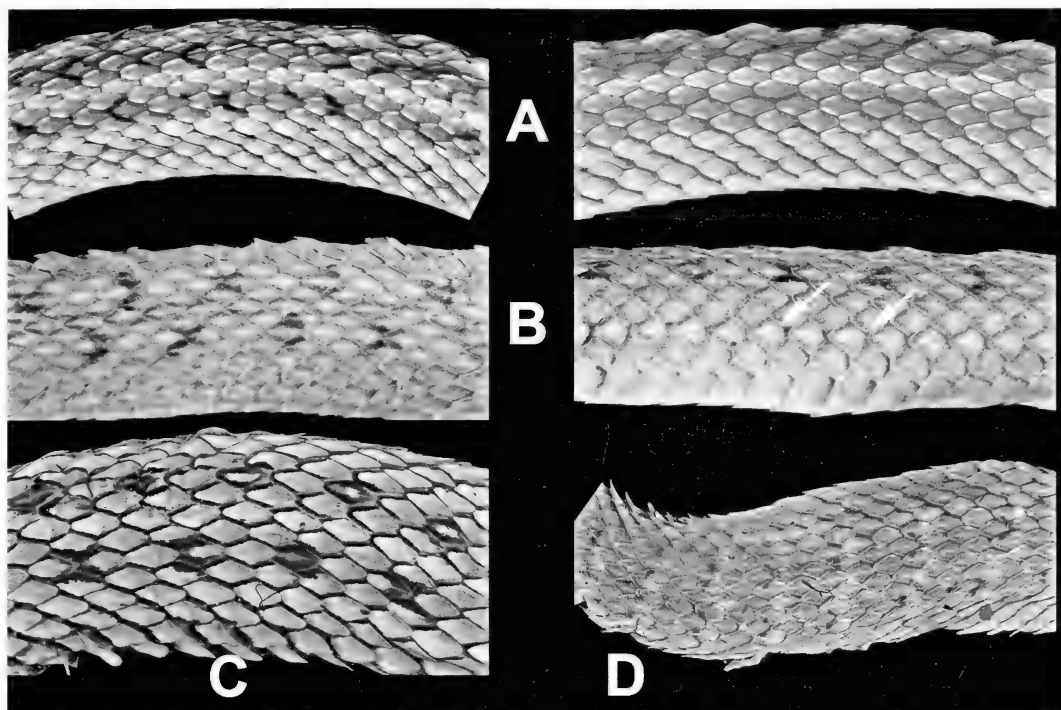
Figure 34.   Details of pattern polymorphism in *Dendrophidion brunneum*. (A) Striped pattern. KU 142802 anterior body (left) and midbody (right), dorsal perspectives. (B) Punctate pattern. MCZ R-8393 midbody in dorsal (left) and lateral (right) perspectives. Arrows in lateral perspective indicate the pale centers of dorsal scales in row 2 (compare Fig. 29B). (C) Punctate pattern. BMNH 1860.6.16.58 posterior body in dorsal perspective. (D) Banded pattern. USNM 237079 midbody in dorsal perspective.

(usually rusty red in preserved specimens) but also with extensive dark punctations within the stripes. In different specimens either the punctations or the stripes may have greater prominence, and either element can be quite indistinct. The punctations are often more distinct on one part of the body than another. Examples are UF 66199, 85105, 88466–67 (Fig. 33B); MCZ R-8393 (Fig. 34B); BMNH 1860.6.16.58 (Fig. 34C); USNM 237061 (Fig. 35A), USNM 237083. Note that the punctations are restricted to the paravertebral areas and do not cross the vertebral line to form dark transverse lines. This subtlety is often a clue in distinguishing some preserved specimens of *D. brunneum* from some confusingly similar *D. graciliverpa*. In the last species, dark borders to the pale crossbands superficially have the appearance of the paravertebral spots in *D.*

brunneum, but in *D. graciliverpa* the dark borders tend to cross the vertebral region to form a broken or more continuous middorsal transverse dark line (Fig. 35). However, this difference can be confused when the crossbands are offset, as occurs frequently in *D. graciliverpa*, or when the dark borders to the pale bands are fragmented.

Crossbanded pattern (colors in life unknown; Figs. 33C, 34D): Other than small juveniles discussed below, crossbanded specimens occur together with unicolor specimens in the highlands of Loja province and in northern Peru. Only three examples are known to me: USNM 237078–79 (567 and 328 mm SVL, male and female, respectively; presumed adult and subadult) and FMNH 232578 (adult male, 514 mm SVL; Cadle, 2010: 8). These three are from the region where the unicolor morph
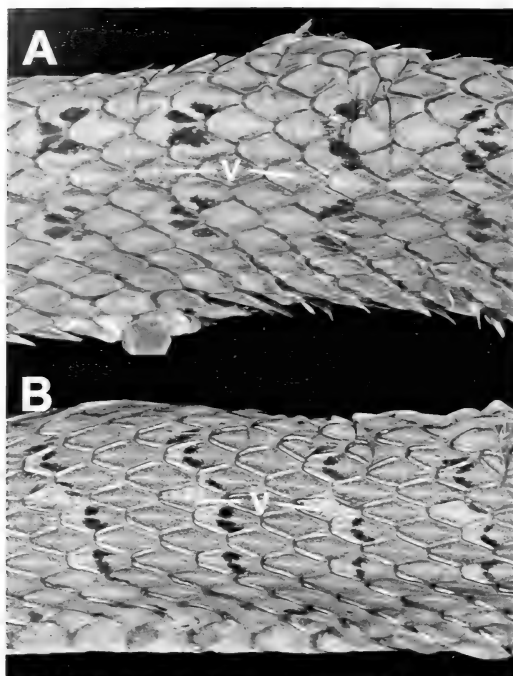
Figure 35.   Comparison of midbody pattern details of *Dendrophidion brunneum* and *D. graciliverpa*. (A) *D. brunneum*, punctate pattern (USNM 237061). (B) *D. graciliverpa* (USNM 12268). Both from Guayas province. *V* indicates the vertebral row. In *D. brunneum* the punctations are paravertebral in position and do not cross the vertebral scale row. In *D. graciliverpa* the dark borders to the pale bands form irregular lines crossing the vertebral scale row. See also Figures 24 and 26.

predominates, and unicolor specimens are known from the same localities as the three crossbanded specimens (unicolor USNM 237077, 237080–81 from the same locality as USNM 237078–79, and many unicolor specimens from the same locality as FMNH 232578; Cadle, 2010). Crossbanded specimens presumably represent individuals that retain the juvenile banded pattern to a greater size than most individuals. The bands on the juvenile (USNM 237079) are much more distinct than those on the adults (USNM 237078, FMNH 232578).

Ventral patterns in *Dendrophidion brunneum* vary from immaculate to having dense dark gray transverse lines across the anterior edges of the ventral scutes (Fig. 32). Additional dark spotting may be present, and in some specimens there is extensive expan-

sion of the lateral dark pigment common to all specimens so that only a central part of each ventral scute is relatively clear (this pattern seems rare). There seems to be little correlation of these patterns with size (most juveniles have immaculate venters but several have well developed transverse lines). Adults with relatively immaculate venters are mainly from the Río Daule/ Babahoyo system in central western Ecuador, whereas specimens from southern Ecuador and Peru usually have extensive ventral markings; this parallels the situation in juveniles (see below). But there are exceptions in both regions. For example, the holotype from central western Ecuador has a densely lined venter (Fig. 28).

Juvenile Color Patterns in Dendrophidion brunneum. Cadle (2010) referred only three juveniles (277–300 mm SVL) from northern Peru to *Dendrophidion brunneum*. These specimens had the uniformly green/brown dorsal pattern characteristic of southern populations. The absence of small juveniles attributable to *D. brunneum* was puzzling until it became clearer how to distinguish juveniles of *D. prolixum*, *D. graciliverpa*, and *D. brunneum* brought about by work on the *percarinatum* complex. Consequently, I now believe that Cadle (2010) erred in referring several small specimens from western Ecuador to "*D. percarinatum*" (= *D. graciliverpa*). These specimens are *D. brunneum* having distinctly crossbanded patterns characteristic of juveniles of most species of *Dendrophidion*.

The insight into the identity of these specimens was provided by ANSP 18122 (Chimborazo province; Figs. 36A, B), a male of 194 mm SVL having distinct pale crossbands on the anterior body (present posteriorly as well but there is a general fading on the posterior body); the posterior body has dark paravertebral punctations virtually identical to the above-described adult punctate pattern. Although I had examined the specimen for the 2010 study, I subsequently examined the internal morphology of one of its retracted hemipenes and confirmed that its morphology
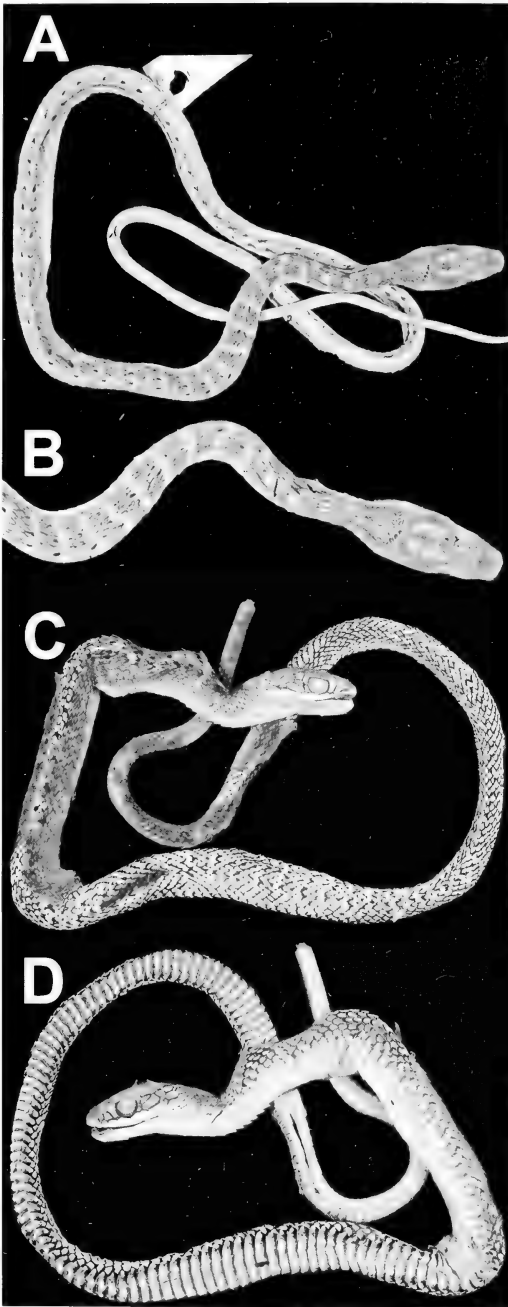
Figure 36.   Juveniles of *Dendrophidion brunneum*. (A) and (B) ANSP 18122 dorsal and anterior body detail (Chimborazo province, Ecuador). (C) and (D) BMNH 1930.10.12.22 dorsal and ventral (Loja province, Ecuador).

conforms to other retracted hemipenes of *D. brunneum* (robust morphotype and extensive apical nude area; see Fig. 3). I now believe that two females having similar patterns that I previously identified as "*D. percarinatum*" (= *D. graciliverpa*), ANSP 5709 and FMNH 16942 (317 and 284 mm SVL, respectively; Cadle, 2010: figs. 3A, C), also are juvenile *D. brunneum*.

Two other small banded juveniles that I identify as *D. brunneum* are BMNH 1930.10.12.21–22 (239 and 219 mm SVL, respectively; the first is illustrated in Figs. 36C, D). These were collected along with two adults of the unicolor pattern from the same locality (BMNH 1930.10.12.20, 1931.11.3.10). Bands on the neck extend ventrally to dorsal row 1 or to the edges of the ventrals, but on the posterior body the bands are seemingly restricted to the middorsal area (the posterior dorsum has the appearance of squarish blotches separated by pale interspaces; Fig. 36C). The pale dorsal crossbands of these two specimens are much more distinct in areas without stratum corneum than when the stratum corneum is present (compare anterior and posterior body in Fig. 36C). No typical adult *D. graciliverpa* are known from the highlands of southern Loja province (Fig. 27), whereas *D. brunneum* adults were collected at the same locality as the two juveniles. In BMNH 1930.10.12.21–22 there is the appearance of transverse dark ventral lines (Fig. 36D). In part, this is an illusion because the poor state of preservation of these specimens resulted in clearing along sutures between adjacent ventral plates; the cleared areas appear dark gray, giving the illusion of distinct transverse lines. Nonetheless, on the posterior body these specimens have somewhat heavier dark stippling along the anterior edges of the ventral plates but nowhere distinct crosslines.

The juveniles I refer to *Dendrophidion brunneum* may be distinguishable from juvenile *D. graciliverpa* in having slightly broader pale bands on the neck. In *D. graciliverpa* the neck bands are less than one dorsal scale row wide, whereas in *D.*

brunneum these bands are 1–1.5 rows wide. Larger samples would be needed to confirm whether this apparent difference holds. Similarly, the supralabial/temporal pattern can provide a clue, but this character is ambiguous in some specimens—BMNH 1930.10.12.21–22 and USNM 237079 have the *P* pattern typical of *D. brunneum*, but USNM 237080 has irregular (fragmented) temporals, and ANSP 18122 has the *G* pattern on both sides.

Covariation of Other Characters with Coloration Morphs. Given the apparent color polymorphism in *Dendrophidion brunneum* as I now conceive it, the question of how other characters covary with the patterns should be addressed, something I have not undertaken in any detail. Scutellation and other external characters of the "new" specimens are similar to my previous summary (Cadle, 2010) except that several specimens extend the lower end of the distribution of subcaudal counts: for males to 125 subcaudals from 139 (BMNH 1860.6.16.60 from "western Ecuador"), for females to 118 subcaudals from 135 (BMNH 1860.6.16.58, also "western Ecuador"). Everted hemipenes very similar to those I described earlier for the unicolor morph (Cadle, 2010) are confirmed for the striped morph (KU 142802) and for the punctate morph (UF 88467). The internal morphology of retracted hemipenes (with characteristic extensive apical nude region; Cadle, 2010; Fig. 3) was confirmed in additional specimens, and hemipenial length to verify "robust" morphology was recorded in still others (see Table 5).

Critical to thorough investigation would be more extensive knowledge of color variation in life and whether there is any geographic segregation of the color morphs, as appears to be the case for the unicolor morph. This should also help interpret patterns of specimens already on museum shelves. Of particular interest is the vicinity of Loja city in southern Ecuador where three pattern morphs occur: striped (KU 142802, which also has elements of the punctate morph; see Fig. 34A), unicolor (USNM 237077, 237080–81; BMNH 1930.10.12.20), and banded (USNM 237078–79) (Figs. 32, 33C, 34A, D). The last two color morphs occur together at La Argelia, Loja. A more detailed analysis of color variation in this region should give some insights into whether and how the color morphs intergrade. Since the possibility remains that more than one taxon still resides under the name *brunneum*, the Loja region might provide critical insights into this systematic question. The realization that four species of the *percarinatum* group occur in western Ecuador considerably advances comprehension of the systematics of *Dendrophidion* in this area but is only a first step toward full understanding.

Supplementary Notes on Hemipenial Morphology. Cadle (2010) described everted hemipenes of *Dendrophidion brunneum* in detail. Little can be added to that report, but some minor differences were noted in the hemipenes of specimens examined in this study. Just as in hemipenes of the three species described in detail in the final section of this paper, there is apparent variation in the extent of development of asulcate apical calyces and the distal flounce-like structures in *D. brunneum*. KU 142802 (Loja province) and UF 88467 (Guayas province) have everted hemipenes. In KU 142802 the fully everted, but not maximally inflated, hemipenis shows fairly well developed asulcate apical calyces that extend nearly to the center of the apex; otherwise, the extensive nude apical region is similar to organs previously described (Cadle, 2010). Spine numbers were not reported by Cadle (2010) but KU 142802 has approximately 150–160 spines on each organ. The enlarged sulcate spines are only marginally larger than other spines in the array, which is about five to six rows across on the sulcate and asulcate sides, three to four rows on the lateral sides. The tip of the sulcus spermaticus is slightly expanded in both KU 142802 and UF 88467, but without a distinct tissue ridge separating the divergent lips; the expansion is more difficult to see when the tissue is stretched upon full inflation. Two retracted organs

from Guayaquil (USNM 237059–60) show differential development of the asulcate apical calyces and the third flounce (both more fully developed in USNM 237059). Just as in the hemipenes described later herein, there may be significant variation in the development of ornamentation in *D. brunneum* but more everted hemipenes would be needed to evaluate this possibility. Retracted hemipenes of *D. brunneum* are 8–10 sub-caudals long, with most between 8 and 9 subcaudals in length; these data are present-ed in Table 5 where comparisons with the other species are made.

Distributional Notes and Sympatry of Dendrophidion brunneum *and* D. gracili-verpa. Cadle (2010) found no verifiable lowland (<1,000 m) records of *Dendrophi-dion brunneum* in Ecuador, although he considered several lowland localities from northern Peru valid. The new specimens (Appendix 1) show that this species as presently conceived is distributed widely in western Ecuador, particularly from the Río Daule/Babahoyo system and southward (Fig. 37). Contrary to what I earlier claimed (Cadle, 2010: 10), I now believe that the type locality "Guayaquil" is a valid locality for *D. brunneum* since other specimens from Guayaquil and nearby can now be documented: two juveniles reidentified above (ANSP 5709, FMNH 16942), MCZ R-8393, and USNM 237059–60. MCZ R-8393 was collected by Edward Whymper and is apparently the specimen reported by Boulenger (1882: 462; 1891: 132), who pointed out the accuracy of Whymper's localities. Cadle (2010: 11) had pondered the whereabouts of this specimen because it had disappeared from the BMNH by the time Boulenger's Catalogue appeared (Bou-lenger, 1894); for years the specimen had been identified in the MCZ as *D. dendro-phis*. Likewise, USNM 237059–60 were obtained by Gustavo Orcés-V., and there seems no reason to question the locality. Sympatry of *D. brunneum* and *D. gracili-verpa* at Guayaquil is confirmed by three males: USNM 237059–60 (*brunneum*, hemipenes to the middle of subcaudal 8

and the end of subcaudal 9, respectively) and USNM 12268 (*graciliverpa*, hemipenis to the proximal edge of subcaudal 13). In addition to length, the internal hemipenial morphol-ogy of these hemipenes was confirmed.

There is a curious gap between the two northern localities of *Dendrophidion brun-neum* (Fig. 37) and those farther south. The northern localities are represented by males so that hemipenial morphology could be confirmed (UMMZ 83706, USNM 237083). In between the two northern localities and the next one to the south, many specimens of *D. graciliverpa* have been obtained from the intensely worked region in the vicinity of Santo Domingo de los Colorados and the Río Palenque Science Center (Fig. 27). Yet, *D. brunneum* has not turned up in this area judging by specimens in U.S. collections. The reason for this gap is not obvious, but gaps seem more common in the distributions of some species of *Dendrophidion* than in other codistributed snakes (e.g., *D. clarkii* in Costa Rica and western Ecuador; J. E. Cadle and J. M. Savage, unpublished data).

HEMIPENIAL MORPHOLOGY IN THE *DENDROPHIDION PERCARINATUM* COMPLEX

The distinction between the "robust" and "gracile" hemipenial morphotypes was out-lined at the outset. In this section I describe in detail everted and retracted hemipenes of *Dendrophidion percarinatum* (robust mor-photype) and *D. prolixum* and *D. gracili-verpa* (gracile morphotype). Cadle (2012: 217–220) gave an overview of the structure of *Dendrophidion* hemipenes and terminol-ogy as applied here and detailed descrip-tions of three species in the *D. vinitor* complex. Cadle (2010) described the hemi-penis of *D. brunneum*. Hemipenes were studied in both retracted and everted conditions using methods outlined by Myers and Cadle (2003). Descriptions of everted hemipenes are based on organs that were fully everted in the field at the time of preservation. Some mineralized hemipenial structures were visualized by staining with Alizarin Red S (Cadle, 1996: 35).
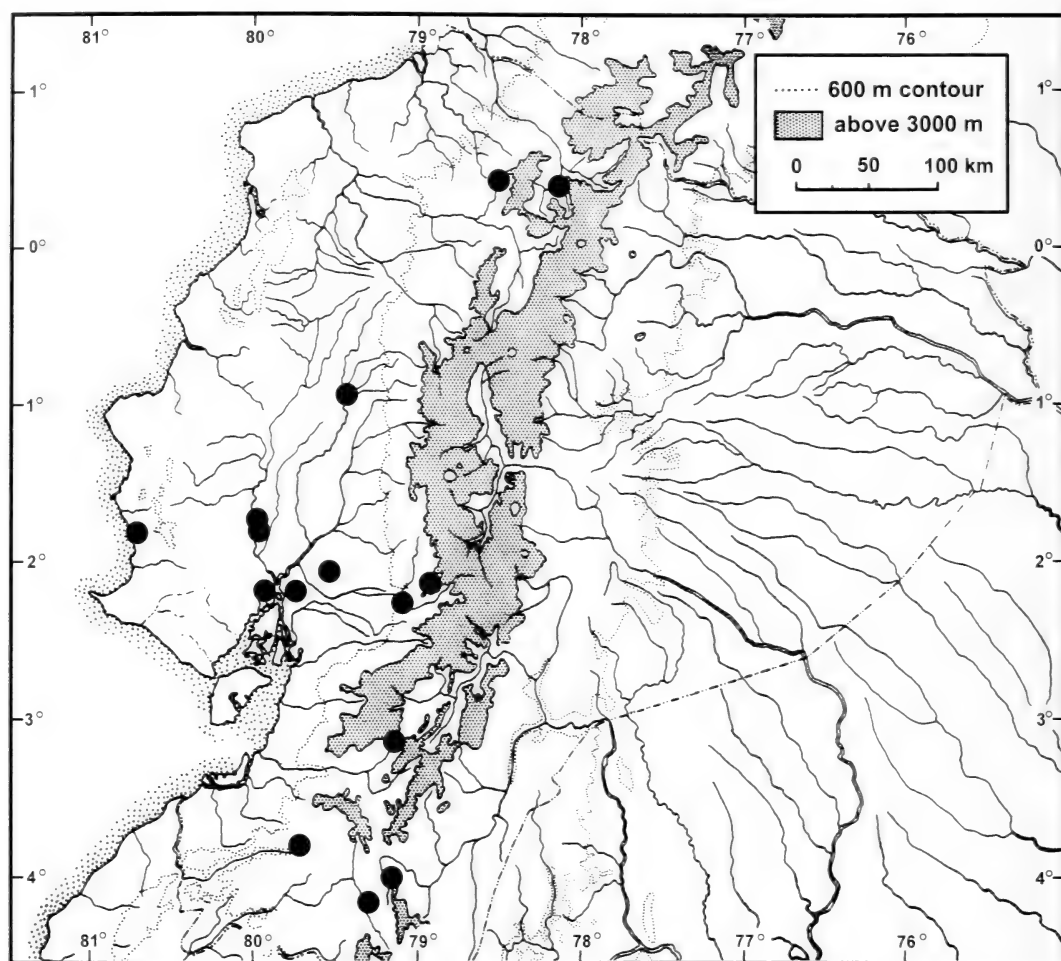
Figure 37.   Distribution of *Dendrophidion brunneum* in Ecuador based on the new material examined. Ecuadorian localities referenced by Cadle (2010) are also included.

The length of retracted hemipenes was scored as the number of subcaudals (or fraction) subtended by the organ. Most specimens for which retracted organs were examined were large enough to score fractional subcaudals converted to a number. For example, a hemipenis extending to the suture between subcaudals 7 and 8 was scored "8" (i.e., extending to the proximal suture of subcaudal 8). A hemipenis extending to the middle of subcaudal 8 was scored as "8.5." Hemipenes extending to points between the proximal suture and midpoint, or between the midpoint

and the distal suture of subcaudal 8, were scored as "8.25" and "8.75," respectively. This system clearly involves some subjectivity for pliable tissue and is more difficult for small specimens, but the resulting difficulties are ameliorated by the summary score groupings used for comparisons (Table 5). Because I was comparing specimens in some cases of a considerable size range, I was conscious of a possible relationship between snake size and retracted hemipenial length. However, there seemed to be no substantial relationship between size and hemipenial length—

TABLE 5. Length in subcaudals of retracted hemipenes of four species of the *Dendrophidion percarinatum* species group. Data for *D. percarinatum* are sorted by geographic origin. *N* = sample size.

		Length (No. of Subcaudals)					
	N	5.5–5.75	6.25–7	7.25–8	8.25–9	9.5–10	10.5
D. percarinatum							
Honduras	2		2				
Nicaragua	3			1	1	1	
Costa Rica	12		1	5	5	1	
Panama	37	2	6	11	14	3	1
Colombia	4			3	1		

		9–10	10.25–11	11.5–12	12.25–13	13.25–14	14.25–15	15.5
D. prolixum	13	3	4	1	3	1		1
D. graciliverpa	20		4	2	6	4	4	

		8	8.25–9	9.5–9.75	10.25
D. brunneum	17	2	11	3	1

juveniles had hemipenes within the range of adult hemipenial lengths as measured by subcaudals.

Dendrophidion percarinatum

Hemipenes of *Dendrophidion percarinatum* as redefined here are similar in basic structure from Honduras to Colombia (particularly when compared with the two new species described herein). Nonetheless, there is variation in virtually all aspects of hemipenial morphology, including the form of the spines and the degree to which fully formed apical calyces are developed. Despite this variation, hemipenial morphology does not suggest cryptic species within *D. percarinatum*, as was the case in the *D. vinitor* complex (Cadle, 2012). The basic structure of hemipenes of *D. percarinatum* is illustrated in Figure 38 with hemipenes from Honduras and Costa Rica. Some of the variation in structure is shown in Figures 39–40 using specimens from Costa Rica, Panama, and Colombia. However, the structural variation described is not restricted to any particular geographic region, although individual hemipenes may have unique features, as exemplified by the seemingly unique shape of UMMZ 124061 (Barro Colorado Island, Panama; Figs. 39C, 40). Sample sizes for everted hemipenes

examined are: Honduras (9), Nicaragua (1), Costa Rica (14), Panama (6), Colombia (2). The following description is a composite derived from several specimens.

Everted. Typical everted hemipenes from throughout the range of *Dendrophidion percarinatum* have a narrow, relatively short hemipenial body proximally and a bulbous distal section comprising the spinose region and apex (Fig. 38). The hemipenial body proximal to the enlarged spines comprises one half or less of the length of the organ overall; it is ornamented with minute spines in a broad band proximal to the enlarged spines. The base of the hemipenial body is nude. In adults everted hemipenes are about 25 mm or less in length.

Spines are arranged in about three loosely arranged rows all around (perhaps slightly fewer on the lateral sides). The spinose section is followed distally by two closely spaced flounces that completely encircle the organ except where interrupted by the sulcus spermaticus. The proximal flounce is broader than the distal flounce and has a more extensive fleshy base. The distal flounce forms a definitive border around the periphery of the apex. Both flounces have embedded spinules (Cadle, 2010: 19). Between the flounces are a few low, longitudinal connections, which are concen-
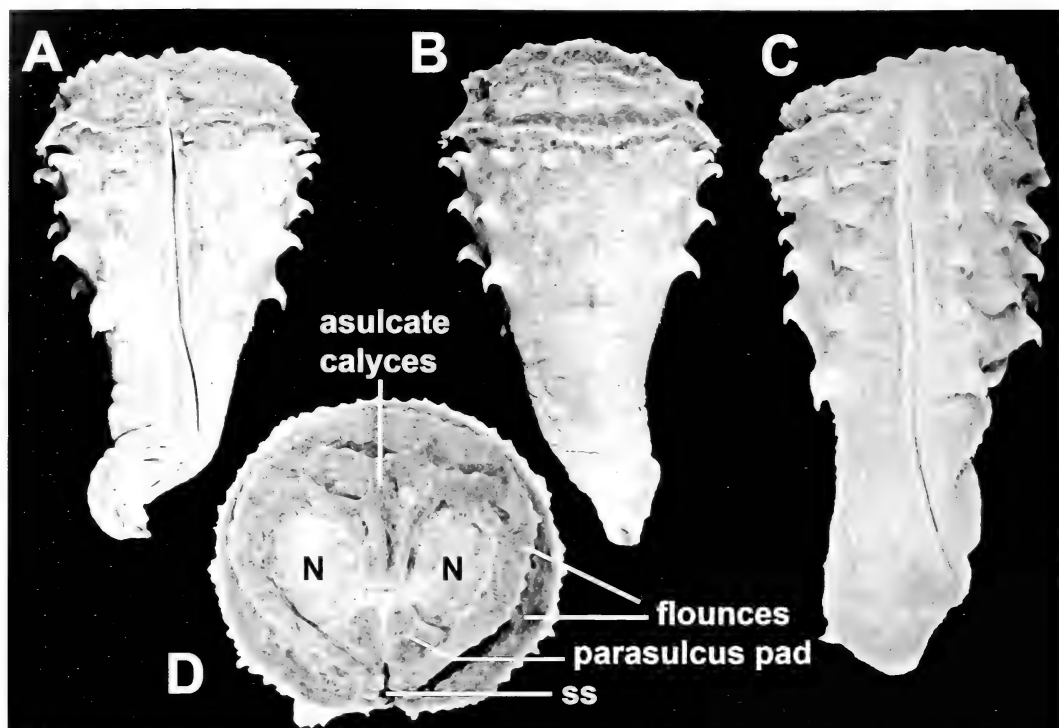
Figure 38.   Hemipenial morphology of *Dendrophidion percarinatum*. (A) and (B) Sulcate and asulcate views of USNM 559611 (Honduras). (C) Sulcate view of LSUMZ 34112 (Costa Rica). (D) Apical view of USNM 559611, sulcate edge at bottom. *Abbreviations:* N, nude patches on lateral sides of apex; ss, sulcus spermaticus.
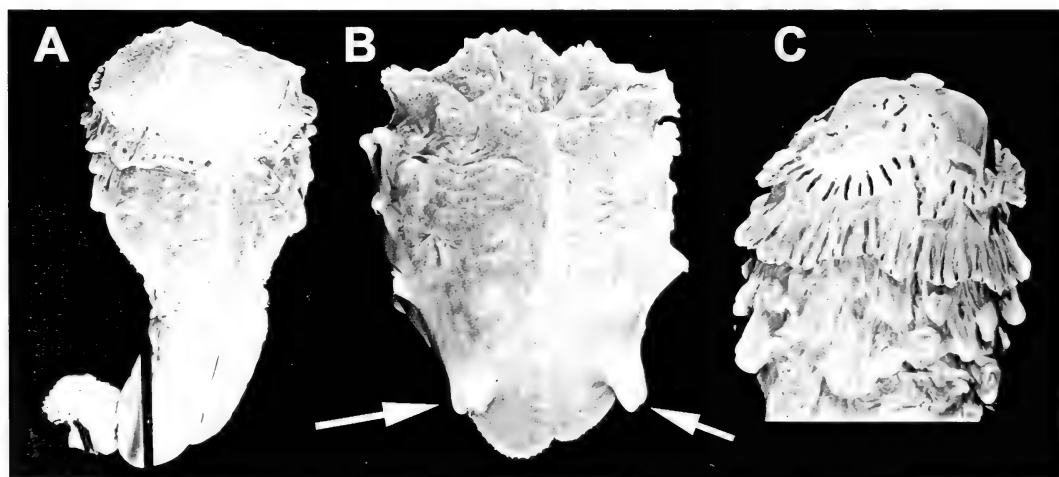

Figure 39.   Variations in hemipenial morphology of *Dendrophidion percarinatum*. (A) AMNH R-108468, sulcate view (Colombia). (B) USNM 259130, sulcate view of distal region (spines + incompletely everted apex) (Costa Rica). Arrows indicate sheathed spines. (C) UMMZ 124061, asulcate view, alizarin stained (Panama). All specimens have unusual formations of spines and/or flounces and other ornamentation compared with typical organs (Fig. 38). See text for full explanation.
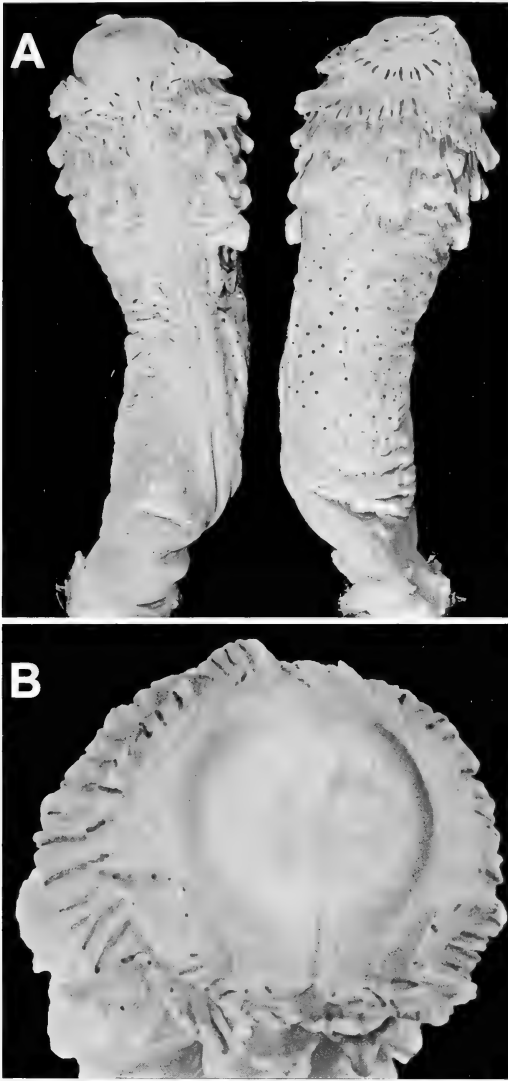
Figure 40.   Hemipenis of *Dendrophidion percarinatum* with an unusual morphology. UMMZ 124061 from Barro Colorado Island, Panama. (A) Sulcate and asulcate views. (B) Apical view, sulcate side toward the bottom. Stained with alizarin red so that embedded spinules are visible within the flounces. Apical view shows the near absence of ornamentation. See text for full explanation.

trated on the asulcate side and often incompletely connect the flounces, forming poorly developed calyces. On the asulcate side of the apex directly opposite the tip of the sulcus spermaticus are several calyces distal to the distal flounce. These calyces are within a triangular thickened expanse of

tissue that narrows distally and ends opposite the tip of the sulcus spermaticus just short of the apical center (Fig. 38D). These calyces are subject to some variation in development described below, but when fully developed, there are about three calyces adjacent to the distal flounce, several more distally, and usually a low ridge of tissue bisecting the triangular raised tissue within which the calyces sit. Peripheral to the asulcate triangular calycular tissue and structures associated with the tip of the sulcus spermaticus, the apex is nude.

The sulcus spermaticus is simple and centrolineal and ends with a slightly flared tip just short of the center of the apex; the flared tip can only be seen by parting and lifting the bulbous tissue on each side. After traversing both flounces, the sulcus spermaticus is bordered on each side by a small, roughly triangular pad of raised tissue. Within each pad is usually a single depression just distal to the distal flounce; I interpret these as rudimentary calyces (*parasulcus calyces* or *parasulcus pads* when no distinct calyx is present).

Variation in Hemipenial Morphology of Dendrophidion percarinatum. With a clear exception described below, hemipenes of *Dendrophidion percarinatum* from throughout the range are similar in form. The shape of the distal portion (spines + apical region) is sometimes more elongate, sometimes more rounded, but it is unclear how much of this variation is simply due to differences in the preservation of this pliable tissue. The length of everted hemipenes of *D. percarinatum* is 16.6–25 mm in several adults (compare *D. prolixum* and *D. graciliverpa*). There is minor variation in the number of spines in the array, as shown by these counts from everted hemipenes given as (range, mean, sample size); counts include the two enlarged sulcate spines: Honduras (31–37, 33.4, 9), Nicaragua (34, $N = 1$), Costa Rica (26–40, 32.6, 14), Panama (30–36, 31.8, 6), Colombia (30–36, 33, 2). In most hemipenes the enlarged sulcate spines at the proximal edge of the array (see Cadle,

2012: 218) are distinctly larger than any other spines, but in some organs the size distinction is much more subtle. There is much more variation in the development of apical ornamentation and in the morphology of individual spines.

Figure 38D illustrates a hemipenis with fully developed apical ornamentation (asulcate triangular raised tissue with calyces, and thick pads bordering the apical portion of the sulcus spermaticus). The asulcate calyces have well-developed walls and fully formed cuplike structure. The triangular expanse of tissue within which they sit abuts the distal flounce on the asulcate side of the apex (the distal flounce forms the proximal transverse walls of the most proximal calyces; these proximal calyces are visible at the distal tip of the organ in asulcate view, Fig. 38B). Typically, the asulcate series of calyces comprises three proximal calyces followed by two more distal and then several more irregular calyces toward the center tip of the apex. On the opposite side of the apex each of the sulcate pads has a shallow depression, which I interpret as an incompletely formed calyx; fully formed calyces within these pads were not observed in the hemipenes I examined.

Hemipenes with this fully developed morphology (Fig. 38D) are found throughout the range of *Dendrophidion percarinatum*. However, also throughout the range are hemipenes that vary in the extent to which the ornamentation is developed. In particular, substantial differences in the form of individual spines and the development of the asulcate apical calyces can result in organs that appear strongly differentiated from those with fully developed ornamentation. The strong delimitation of the apical nude areas by raised ridges observed in USNM 559611 (Fig. 38D) is attained in only a few hemipenes I examined, although these nude areas are present in all organs. I resist the temptation to state what is "normal" development in *D. percarinatum* because hemipenes with rudimentary ornamentation were common among the organs I examined.

Some of the variation is illustrated in Figures 39–40 (variation in spine morphology is discussed below). AMNH R-108468 (Fig. 39A) from Colombia shows considerable reduction of the spines to mere nubbins, as well as more subtle reductions in other ornamentation. The asulcate calyces are reduced to irregular calyxlike structures and ridges (only a single definitive asulcate calyx is present, located adjacent to the distal flounce), and its flounces are narrower and less projecting than in many other hemipenes. The only other available everted hemipenis from Colombia (AMNH R-123745) has typical spines and more definitive apical calyces. Other hemipenes show reductions similar to AMNH R-108468; when such reductions occur, the resulting structures are usually more irregular than when the full complement of ornamentation is present. Reduction in one aspect of morphology (e.g., spines) usually entails reductions in others (e.g., calyces). But there are exceptions—USNM 259130 from Costa Rica has reduced spines but unreduced apical calycular structures (Fig. 39B). The most extreme modifications were observed in a single specimen of *Dendrophidion percarinatum* from Panama, whose characteristics are described in detail.

The asulcate apical calycular area can sometimes appear as a third incomplete (noncircumferential) flounce on the asulcate edge of the apex, with a few incomplete longitudinal calycular walls. For example, AMNH R-123745 has a single small median and mostly complete calyx just distal to the circumferential flounces (proximal wall formed by the distal flounce). Distal to the median calyx is an undulating wall (incomplete flounce) centered on the asulcate side and extending about one-third of the distance around the apex. Underneath this incomplete flounce are about four low, incomplete longitudinal walls, partitioning the space between the incomplete flounce and the small median asulcate calyx.

A Most Unusual Hemipenis of Dendrophidion percarinatum. Hemipenes of UMMZ 124061 from Barro Colorado

Island, Panama, were the most peculiar organs I studied, and both are modified similarly (Fig. 40). They have an unusual overall shape (a longer proximal portion of the hemipenial body and less bulbous distal region than is typical), and nearly all aspects of their ornamentation are modified (Figs. 39C, 40). These hemipenes for a time misled me as to what the typical morphology for *Dendrophidion percarinatum* hemipenes actually was—hemipenes of UMMZ 124061 were among the first of this species I studied in detail and I entertained the idea that cryptic species were involved. Examination of other organs convinced me otherwise, and I now view the morphology of UMMZ 124061 as one extreme within a species in which variation in hemipenial morphology seems unusually great. Other specimens from BCI or the adjacent Canal Zone (e.g., CM 6869, KU 80589, UMMZ 297811) have hemipenes more typical in shape and ornamentation than UMMZ 124061, although their ornamentation varies within the limits described above. The unusual shape of UMMZ 124061 does not appear to be due to preservation artifact, which in any case, would not affect the peculiar ornamentation of this specimen.

I stained the right hemipenis of UMMZ 124061 with alizarin red to visualize mineralized structures more fully. Mineralized embedded spinules are seen in Figures 39C and 40 as dark parallel streaks within the flounces and other calycular structures. The mineralized portion of the spines is concealed by thick fleshy tissue. The narrow proximal portion of the hemipenial body has a sparse covering of minute spines on its distal half, extending farther proximally on the asulcate side than on the sulcate side (Fig. 40A; the alizarin-stained minute spines appear as tiny dark spots on the proximal portion). There are about four rows of enlarged spines adjacent to the sulcus spermaticus, narrowing to two rows on the lateral surfaces and continuing in two rows to the asulcate side. The "enlarged" sulcate spines are scarcely larger than other spines in the array. The sulcus spermaticus is

centrolineal and, after transecting the flounces, ends somewhat short of the middle of the apex. Its tip is distinctly flared and even appears somewhat divided by a low wedge of tissue separating the divergent lips.

Individual spines have a very strange structure. Each spine is enveloped by thick fleshy tissue. Close inspection shows that the tissue envelops the tip of the spine like a hood, covering the spine surface toward the apex (i.e., the distal surface) and the hooked tip. The result is that the tips of the spines are not visible except by lifting up the fleshy covering to expose them; without lifting the sheath, this area of the hemipenial body appears to be ornamented with blunt fleshy projections, as they appear in Figures 39C and 40A. The alizarin staining showed that the spines were indeed mineralized underneath and within the fleshy covering (the proximal portion of the spines extended into the fleshy sheath, even though the spine tips were free). This peculiar structure is repeated to a greater or lesser extent in many hemipenes of *Dendrophidion percarinatum* (discussed below).

Distal to the enlarged spines are two circumferential flounces similar to those on other *D. percarinatum* organs. On the asulcate side distal to the flounces is a single very large, asymmetrically positioned calyx (Fig. 39C). Two longitudinal, poorly developed calycular walls further subdivide this calyx. The distal wall of the asulcate calyx forms a sharp angle on the edge of the apex, from which a low fleshy ridge extends nearly to the middle of the apex. On the sulcate side distal to the flounces, the sulcus spermaticus is bordered on each side by a single incomplete calyx with somewhat thickened walls (the wall adjacent to the sulcus is not clearly defined). Alizarin staining showed that poorly formed embedded spinules were present at irregular intervals in both the sulcate and asulcate calyces.

Morphology of Hemipenial Spines in Dendrophidion. The peculiar structure of the spines just described for UMMZ

124061 is not an isolated case either within *D. percarinatum* or more broadly in the genus. In many *Dendrophidion* hemipenes the spines are of the typical morphology seen in most snakes. In *D. percarinatum* and other species of this species group typical spines are relatively short and strongly hooked at the tip (e.g., Fig. 38). However, in other hemipenes the spines are partially or entirely enclosed by a fleshy sheath and, in some cases, seem not only enclosed but also much reduced in size (Fig. 39A). These *sheathed* (or celate, from celatus, Latin for "hidden") spines have a blunt, fleshy appearance, but a mineralized rod within the fleshy tissue can be demonstrated by probing, by shining a strong light through the translucent tissue, or by staining with alizarin red. In some sheathed spines the mineralized portion does not project at all from the fleshy portion; in others a small point or hook protrudes through the tip (Fig. 39B, left arrow). The enveloping fleshy tissue was, in some cases such as UMMZ 124061 described above, hoodlike, whereas in others it seemed to form a more complete sheath surrounding the entire spine.

Whether spines are typical or sheathed varies intraspecifically in species of both the *Dendrophidion dendrophis* and *D. percarinatum* species groups. *Dendrophidion percarinatum* seems especially prone to this type of variation, but this could be because more everted organs have been available for this species than for any other. I detected no geographic trends in spine morphology (the variation occurs throughout the geographic range of the species). Some hemipenes I examined had a mix of sheathed and typical spines, whereas others were entirely of one type or another. In occasional specimens (e.g., USNM 259130), the spines of one hemipenis were predominantly of typical morphology, whereas the other had celate spines. Considering the entire array of spine morphologies in *Dendrophidion*, there is probably a continual gradation between the celate and typical forms.

What I refer to as celate spines may be equivalent to similar structures reported in some other snakes, for example "fleshy protuberances ... that form the swollen bases of spines" on some elapid hemipenes (Keogh, 1999: 250). Keogh (1999) scored this as a separate ornamental category than spines for Australian elapids and reported no intraspecific variation (fleshy protuberances were either present or absent for a given species). Smith (1943: 151) stated that the short spines on the hemipenis of *Elaphe taeniura* were "enclosed in a voluminous sheath." Myers (1974: 33) reported an aberrant specimen of *Rhadinella godmani* in which hemipenial spines were absent, but their locations were indicated by "enlarged tissue bases." Given the prevalence and seemingly continuous and intraspecific variation between celate and typical spines in *Dendrophidion*, it seems best to recognize celate spines as a common variant of spine morphology, rather than anomalies or an entirely different kind of hemipenial ornamentation for this group of snakes. Possibly, the variable development of spines is related to other reduced aspects of hemipenial morphology in *Dendrophidion*, such as the variable development and manifestation of calyxlike structures. Data for several snake species indicate that spines, calyces, and flounces derive from common anlagen early in development (Clark, 1944).

Retracted Hemipenes of Dendrophidion percarinatum. Retracted hemipenes of *Dendrophidion percarinatum* extend from the middle of subcaudal 5 up to the middle of subcaudal 10 (Table 5), with a clear modal length between 7 and 9 subcaudals. The retractor penis magnus has a very short proximal division. The length of retracted hemipenes observed within *D. percarinatum* (a 5-subcaudal span) is comparable to the span observed in some other snakes (e.g., *Rhadinaea decorata* [9-subcaudal span]; Myers, 1974: 75), *Dipsadoboa unicolor* and *D. weileri* (5-subcaudal spans; Rasmussen, 1993: 146), and *Tantilla* spp. (several species with 5–7-subcaudal spans; Cole and Hardy, 1981: 225–234).

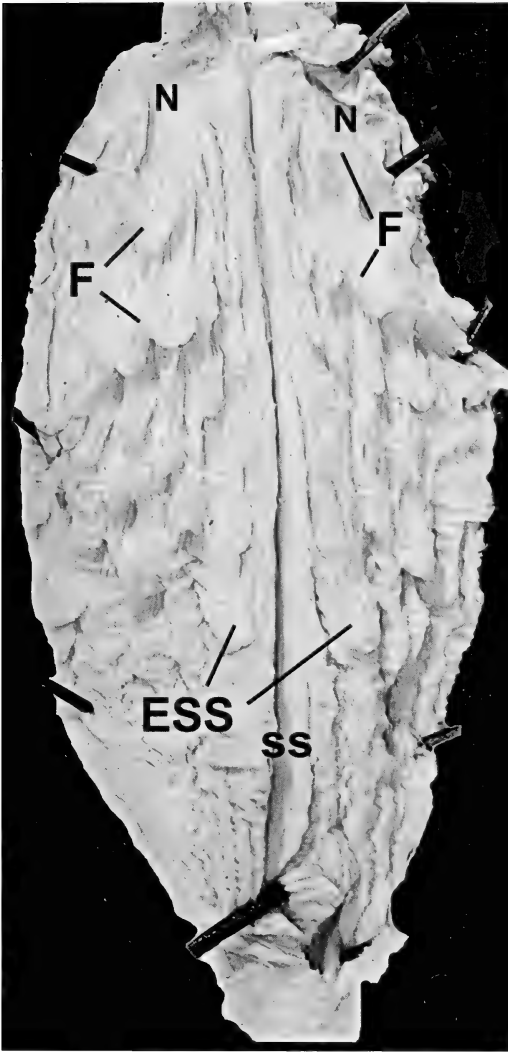The morphology of the retracted hemipenis corresponds in a straightforward

Figure 41.   Retracted hemipenis of *Dendrophidion percarinatum* (AMNH R-17374, Costa Rica). Distal toward the top. *Abbreviations:* ESS, enlarged sulcate spines; F, flounces; N, nude apical areas; ss, Sulcus spermaticus.

manner to the everted organ (Fig. 41): a proximal portion ornamented with minute spines; a spine array including a pair of spines slightly larger than others adjacent to sulcus spermaticus at the proximal edge of the array (enlarged sulcate spines); two flounces followed distally by an apex with asulcate calyxlike structures and lateral nude areas; and a simple sulcus spermaticus in its dorsolateral wall, ending with a slightly

flared tip at the distal end of the retracted organ. A few weak longitudinal connections are present between the flounces.

Dendrophidion prolixum

Everted (AMNH R-108469, Chocó department, Colombia; left hemipenis, Fig. 42). Overall morphology is the "gracile" form. Total length of organ approximately 28–30 mm. Length of the bulbous distal region from the base of the enlarged sulcate spines to the tip of the apex is 8.7 mm (30% of total length). Length from proximal flounce to tip of apex approximately 4.5 mm. The hemipenis is unilobed, somewhat clavate, and without basal pockets or lobes.

Sulcus spermaticus is centrolineal and ends just short of the center of the apex. The portion of the sulcus distal to the flounces is bordered by a thick pad of tissue on each side; no depression or other indication of rudimentary calyces were evident within these pads. The tip of the sulcus is slightly expanded and with a narrow wedge of tissue between the divergent lips, resulting in the appearance of a terminal division. The edge of the tissue bordering the short branches of the sulcus is seemingly somewhat thickened (denser white compared with adjacent wedge tissue), perhaps indicative of lip tissue. However, the wedge can be manipulated and flattened unlike in a truly divided sulcus. Each short branch of the "divided" tip is slightly expanded into a teardrop-shape at its tip.

Hemipenial body proximal to the spine array is ornamented with minute spines all around except for a nude patch comprising about the basal one-third of the organ on the left side; otherwise, the minute spines go all the way to the base of the organ and are rather densely arrayed. These minute spines are seemingly somewhat more densely arrayed toward the spine array than more basally.

The enlarged sulcate spines at the proximal edge of the spine array are about two or three times the size of others in the battery (enlarged spine on the right side
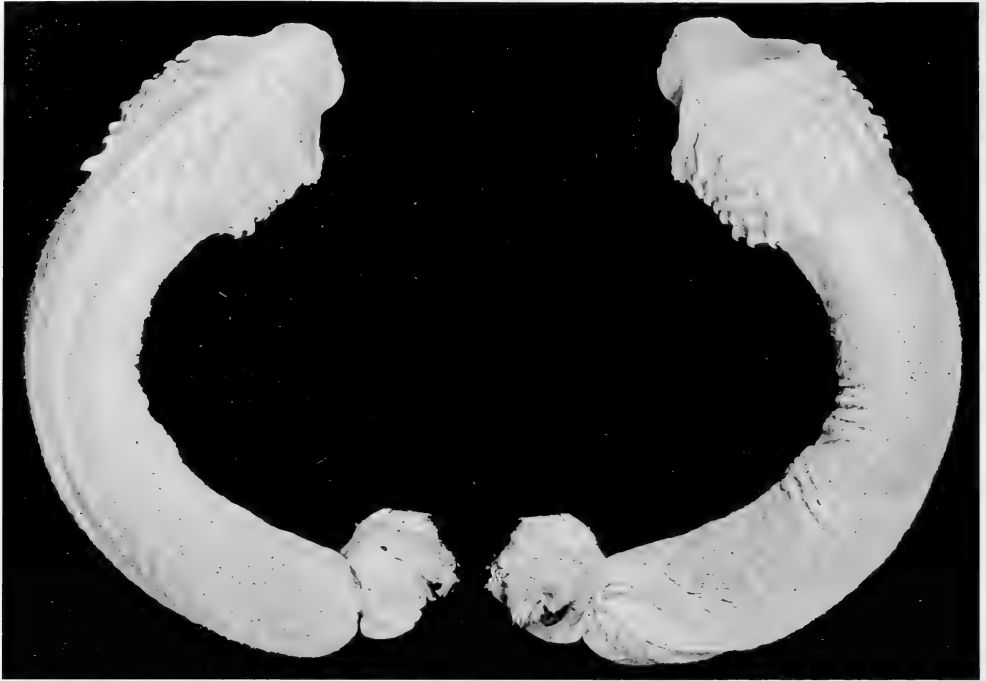
Figure 42.   Everted hemipenis of *Dendrophidion prolixum* (AMNH R-108469) in sulcate and asulcate views.

larger than the one on the left side of the sulcus). Total number of spines in the battery approximately 87+2 enlarged sulcate spines. Spines are in four to five loosely arranged rows on the sulcate and asulcate sides, three rows on the lateral sides.

Distal to the spines are a pair of circumferential flounces. The proximal flounce is broader than the distal flounce and has an outer more membranous portion and a somewhat fleshy base. The distal flounce has only a very narrow outer membranous portion; most of this flounce is fleshy. Embedded spinules are in the membranous portions of both flounces. The borders of the flounces are smooth (non-crenulate) but somewhat undulating.

On the asulcate side of the apex is a triangular pad of tissue extending toward the center of the apex from the distal flounce (point toward the apex). Within this pad is an irregular, poorly differentiated depression (rudimentary calyx) with fleshy edges. Except for this asulcate pad and

those bordering the distal portion of the sulcus spermaticus, the apex is nude. A pair of shallow dimples, probably the points of internal attachment of the retractor penis magnus, is in the center of the apex.

Retracted (FMNH 54960, Risaralda department, Colombia; Figs. 43A, C). The left hemipenis had been previously slit somewhat irregularly on its ventral/medial surface. Left and right hemipenes extend to middle of subcaudal 11. Retractor penis magnus appears proximally undivided, but there may be some separation of the muscle fibers. Sulcus spermaticus simple, but its tip is flared, and it ends at the tip of the organ. The entire portion of the sulcus distal to the flounces is bordered by a thick pad of tissue on each side; each of these contains a single, very shallow calyx.

The long proximal portion of the hemipenial body has long longitudinal folds and minute spines. On the sulcate side these spines extend nearly to the base of the organ, but toward the asulcate side a long
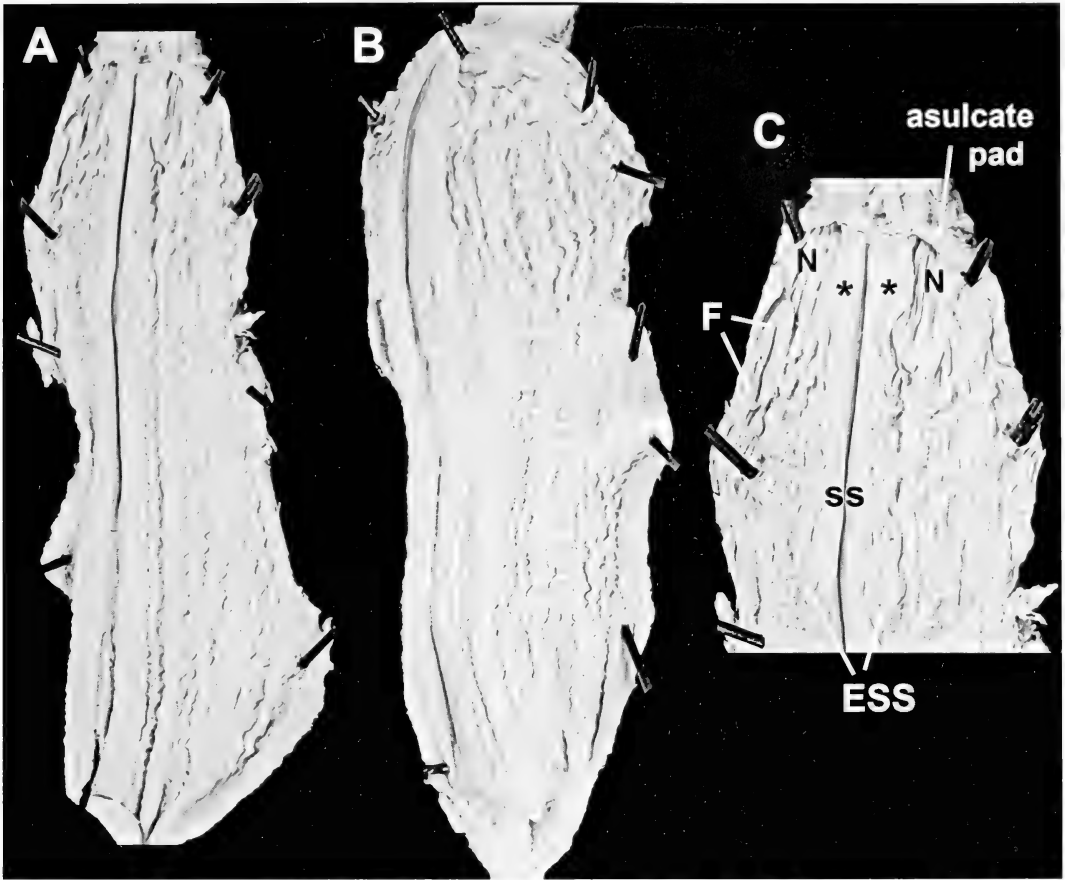
Figure 43.   Retracted hemipenes of *Dendrophidion prolixum* and *D. graciliverpa*. Distal toward the top. (A) *D. prolixum* (FMNH 54960; slit medially). (B) *D. graciliverpa* (UIMNH 77347; slit midventrally). (C) Apical region of FMNH 54960 with landmarks indicated. *Abbreviations and labels:* ESS, enlarged sulcate spines; F, flounces; N, apical nude areas; ss, sulcus spermaticus. Asterisks (*), thick pads of apical tissue bordering the distal part of the sulcus. *Asulcate pad*, thickened asulcate apical tissue bearing rudimentary calyces.

section of the organ is nude, and the minute spines are restricted to the distal third to half of the basal section. The array of enlarged spines is broader on the sulcate and asulcate sides (about four to five rows across), and narrower on the intervening sides (lateral sides of the everted organ; about three rows across). A pair of enlarged sulcate spines at the proximal edge of the array is much larger than other spines. The spines are arrayed along the longitudinal folds occupying this area of the organ.

Distal to the spine array are two flounces, which are connected at intervals with poorly developed longitudinal ridges. Each flounce

comprises a basal fleshy portion and an outer membranous portion with embedded spinules. The embedded spinules are short straight splints about the same width throughout. Distal to the flounces is a very short apex, nude except for a thick pad of tissue extending from the distal flounce to the tip of the organ and the pair of pads bordering the sulcus spermaticus. The asulcate apical pad seems to have two or more poorly developed calyces (these are difficult to probe apart).

Variation in Hemipenial Morphology. Everted hemipenes of only four specimens of *Dendrophidion prolixum* were available

(AMNH R-108469, R-123750-51, R-109726). There is little variation in morphology among these except for the asulcate apical calyx and associated structures, the calyx being more definitive in some organs than in others (similar to the variation summarized above for *D. percarinatum* and for *D. graciliverpa* described below). The "enlarged" sulcate spines are sometimes scarcely larger than other spines in array. The approximate number of spines in these organs is as follows: AMNH R-123750, 89+2 (left organ); AMNH R-109726: 65+2 (right), 70 + 2 (left); AMNH R-123751: 87+2 (right and left). The right hemipenis AMNH R-109726 had a total length of 42 mm, and the length from the enlarged sulcate spines to the tip of the apex was 7.9 mm (19% of the total length). Retracted hemipenes vary in length from nine subcaudals (one organ only) to 15.5 subcaudals (Table 5).

Dendrophidion graciliverpa

Everted (AMNH R-110584; holotype, El Oro province, Ecuador; right hemipenis) (Figs. 44–45). Total length about 39 mm. Length of apex from the proximal enlarged sulcate spine to tip of apex, 9.6 mm (distal section about 25% of the length of the organ). Maximum width of expanded apical region, 8.4 mm. Hemipenial body proximal to spines compressed laterally (i.e., broader when viewed from lateral side than when viewed from sulcate or asulcate side). Overall form of "gracile" morphology. The hemipenis is unilobed, with a gradually expanded distal section and without basal pockets or lobes. The long section of the hemipenial body proximal to the enlarged spines is ornamented with minute spines except for a nude basal patch on the right lateral and asulcate sides.

Sulcus spermaticus centrolineal, extending to the center of the apex, terminally divided with equal branches about 1.1 mm long (Fig. 45). The divergent branches are separated by a thick triangular wedge of tissue that may have distal "lip tissue"

(hence, truly divided although this would have to be verified histologically).

The enlarged spine array contains about 116+2 proximal sulcate spines about three times larger than any other spines in array. Spines in about five to six loosely arranged rows on the sulcate and asulcate sides, about three rows on each lateral side. Spines in the array somewhat larger proximally than distally. Spines followed distally by two circumferential flounces bearing embedded spinules, complete except where transected by the sulcus spermaticus; proximal flounce broader than distal one. Flounces have a thick fleshy inner portion and outer membranous portion; the spinules span the width of the membranous portion but barely enter the fleshy portions.

Entire sulcus spermaticus distal to the flounces is bordered by thick triangular pads of tissue (* in Fig. 45). These are broader adjacent to the distal flounce and each has a calyxlike depression. On the asulcate side of the apex, the distal flounce splits to form a large irregular calyx at the sulcate edge of the apical region, the *asulcate calyx* (Fig. 44B); from the distal wall of this calyx an irregular raised triangular area of tissue extends nearly to the center of the apex just opposite the tip of the sulcus spermaticus. On the apical tip lateral to the sulcus and the asulcate triangular tissue, the apex is nude, very smooth, and strongly demarcated peripherally by the distal flounce (Fig. 45).

Variation in Morphology of Everted Hemipenes. Two other everted hemipenes of *Dendrophidion graciliverpa* were studied in detail: AMNH R-119835 (topotype) and USNM 237069 (Pichincha province, Ecuador) (Fig. 46). These hemipenes are similar in basic structure to that of the holotype, but there is some variation in the shape of the apex and calyces. Some features are essentially similar to the holotype: the arrangement and relative sizes of spines, the sulcate pads distal to the flounces, the terminal division of the sulcus, the presence (but not shape) of an irregular asulcate calyx, and apical ornamentation. Basic data on the two organs are:
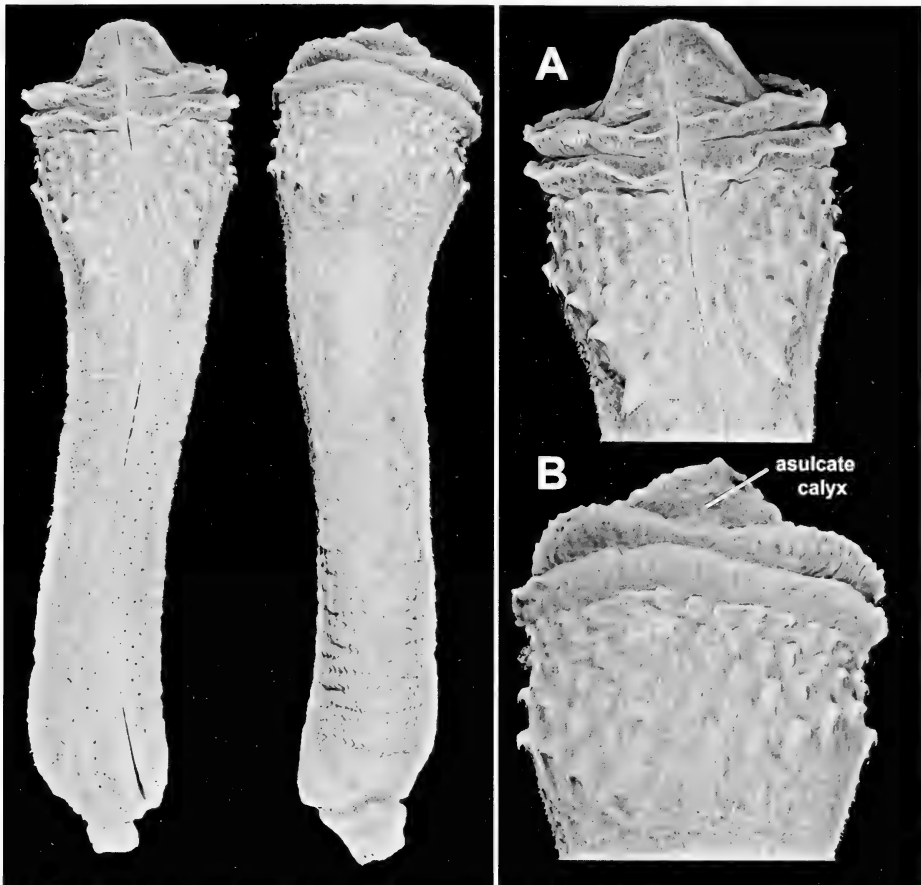
Figure 44.   Everted hemipenis of *Dendrophidion graciliverpa* (AMNH R-110584, holotype) in sulcate and asulcate views. (A) and (B) Details of apical region in sulcate and asulcate views, respectively.

USNM 237069 (Figs. 46A, C): Total length approximately 26 mm. Length of apex from the proximal enlarged sulcate spine to the tip of the apex, 7.3 mm (distal section of hemipenis 28% of the total length). Tip of the sulcus spermaticus with divergent lips but not clearly divided as in AMNH R-110584, R-119835. About 84 small spines + 2 enlarged sulcate spines. On the asulcate side of the apex is a thick triangular pad of tissue, within which is a large irregular calyx whose proximal wall is formed by the distal flounce. The large calyx has several small depressions within it (or rudimentary partitions), which makes it appear that the large calyx is formed by

fusion and obliteration of several smaller calyces.

AMNH R-119835 (Figs. 46B, D): Total length 29.4 mm. Length of narrow part of body 21 mm (measured to the base of the pair of enlarged spines at the proximal edge of the apex). Diameter of narrow part 4 × 5 mm. Length of apex from the proximal enlarged sulcate spine to tip of apex, 8 mm (distal section of hemipenis 27% of the total length). Diameter of globose part 7 × 7.5 mm. Tip of the sulcus spermaticus seemingly divided about 1 mm because a short ridge separates the divergent lips. About 81 + 2 enlarged sulcate spines. The asulcate calyx is a large oval formed by
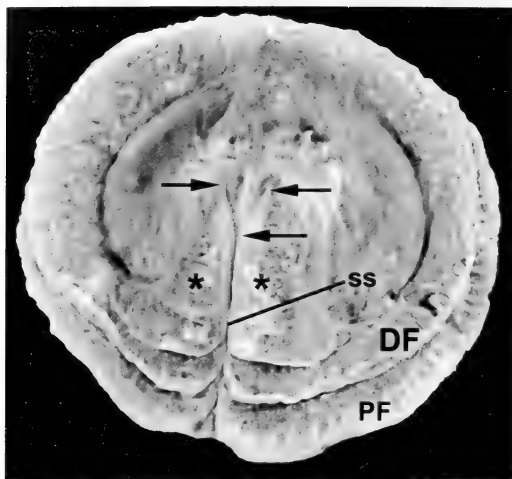
Figure 45. Apical view of the everted hemipenis of *Dendrophidion graciliverpa* (AMNH R-110584, holotype). The contrast is exaggerated so as to emphasize the divided tip of the sulcus spermaticus. *Abbreviations and labels:* Lower arrow, point of division of the sulcus spermaticus; upper arrows, tips of the branches of the divided sulcus; asterisks (*), thick pads of apical tissue bordering the distal part of the sulcus (parasulcus pads); DF, distal flounce; PF, proximal flounce; ss, sulcus spermaticus.

robust, well-defined walls created by division of the distal flounce (Fig. 46D). Within the asulcate calyx are about six pockets, seemingly formed by thinning of tissue of the hemipenial wall; these pockets are irregular in size and position, although most are nestled under the distal fleshy border of the calyx. Immediately distal to the asulcate calyx is a small, deep triangular hole surrounded by thick fleshy ridges (one of which forms part of the distal wall of the asulcate calyx); the ridges surrounding the pore fuse distally, forming a groove that extends distally and ends short of the center of the apex. This hole is presumably a rudimentary calyx.

Although all three everted organs of *Dendrophidion graciliverpa* are basically similar the shapes of their apices differ. The apex and apical ornamentation of AMNH R-110284 (holotype, El Oro province; Fig. 44) are more similar to USNM 237069 (Pichincha province; Figs. 46A, C) than they are to the topotypic specimen (AMNH R-119835; Figs. 46B, D). The apex

of the last is more rounded than in the other two hemipenes, and it has more rudimentary development of the asulcate triangular apical tissue. On the other hand, the large oval asulcate calyx of AMNH R-119835 is a very well defined structure with thick walls (Fig. 46D), whereas in the other two specimens it is a more rudimentary triangular structure without hypertrophied walls (Figs. 44B, C). The strong differences among the few everted hemipenes of *D. graciliverpa* examined suggest that considerable variation in hemipenial morphology might characterize this species, just as suggested above for *D. percarinatum*. However, based on the present small sample it is unclear that this variation is taxonomically significant. It should be noted that hemipenes depicted in Figures 44 and 46B and D are from "crossbanded" specimens of *D. graciliverpa*, whereas Figures 46A and C are from the "unicolor" pattern morph, as discussed in the section on coloration of preserved specimens.

Retracted. I examined the internal morphology of five retracted hemipenes from specimens I refer to *Dendrophidion graciliverpa* (ANSP 5519; BMNH 1860.6.16.59; UIMNH 77347; USNM 12268, 237084). All are very similar to one another and the following description is a composite account. UIMNH 77347 is illustrated in Figure 43B.

These hemipenes extended posteriorly to the suture between subcaudals 10 and 11 up to the proximal portion of subcaudal 14; when hemipenes that were examined only superficially are included, the lengths were 9–15 subcaudals (Table 5). Measured lengths in adults were 27–40.7 mm. The retractor penis magnus appeared distinctly divided in UIMNH 77347 but in other organs the separation was not so distinct. The sulcus spermaticus is simple and centrolineal (in the dorsolateral wall of the organ). It ends just short of the distal tip of the organ and has a flared tip (a couple of the specimens had a low wedge of tissue between the divergent lips but this was most likely a simple fold resulting from the packing of apical tissue in the retracted condition).
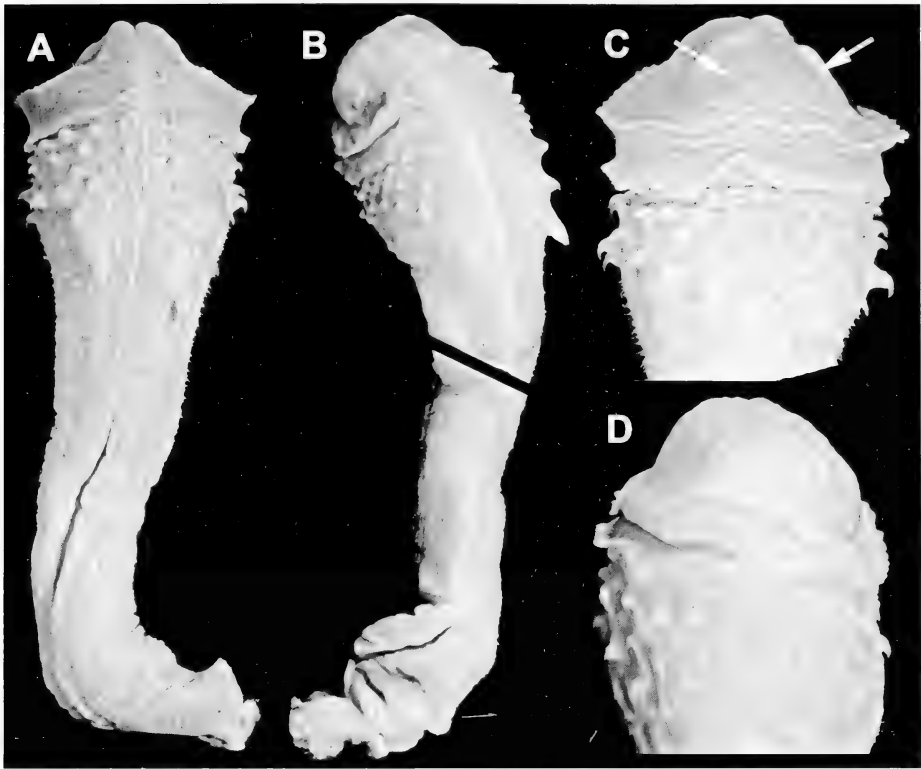
Figure 46.   Variation in hemipenial morphology of *Dendrophidion graciliverpa*. (A) USNM 237069 from Pichincha province, Ecuador (sulcate view). (B) AMNH R-119835 from El Oro province, Ecuador (topotype, sulcate view). (C) Detail of apex, USNM 237069, asulcate side. (D) Detail of apex, AMNH R-119835, asulcate side. Arrows in panel C indicate the poorly formed walls of the triangular asulcate calyx; compare panel D, in which the calyx is oval and has prominent walls. The asulcate calyx in the holotype (Fig. 44B) is more similar to that in panel C than to the topotype in panel D.

The proximal part of the hemipenis has many longitudinal ridges or folds, which are ornamented with minute spines except for the extreme base of the organ. A pair of enlarged sulcate spines is positioned at the proximal edge of the spine array, which is about three or four rows across on the sulcate and asulcate sides, slightly fewer in between. The spine array is followed distally by a pair of flounces, between which are some rudimentary longitudinal connections. Distal to the flounces on the asulcate side (ventromedial side of the in situ organ) is a single large irregular calyx, the proximal wall of which is formed by the distal flounce. From this calyx a ridge or pad of tissue extends nearly to the tip of the sulcus spermaticus on the apex. Each side of the distal portion of the sulcus spermaticus is bordered by a fleshy pad, each with a slight depression. The apex distal to the flounces is very short (about one subcaudal in length) and has thin longitudinal folds (nude tissue in the everted hemipenis), which are largely obscured by the pleats of the flounces covering it from ventral perspective.

COMPARISONS OF HEMIPENIAL MORPHOLOGY OF SPECIES IN THE *DENDROPHIDION PERCARINATUM* COMPLEX

Apart from robust vs. gracile morphology, hemipenes of the three species of the *Dendrophidion percarinatum* complex are similar in basic details: (1) proximal portion of hemipenial body ornamented at least in

part with minute spines; (2) enlarged spine array three to six rows across on the sulcate and asulcate sides and with a somewhat enlarged pair of sulcate spines at its proximal edge; (3) two circumferential flounces with embedded spinules; (4) roughly triangular asulcate apical calycular tissue that varies in morphology, but including at least one large proximal calyx bordering the distal flounce and a more or less defined ridge or other calyces extending nearly to the center of the apex; (5) a fleshy pad (sometimes with a more or less evident calyx within) bordering each side of the apical part of the sulcus spermaticus distal to the flounces; and (6) tip of the sulcus spermaticus terminally flared in everted organs, and sometimes seemingly divided by a tissue wedge in *D. prolixum* and *D. graciliverpa*. Some of these characteristics are more widely distributed within *Dendrophidion* (Cadle, 2012: 217–220). For example, two (and no more) complete circumferential flounces are characteristic of all species in the *D. percarinatum* species group, and enlarged sulcate spines are characteristic of most species of *Dendrophidion*, although details vary among species.

Dendrophidion prolixum and *D. graciliverpa* have nearly identical hemipenes and share several putatively derived hemipenial characters compared with other *Dendrophidion*, especially *D. percarinatum*. Foremost is "gracile" hemipenial morphology, which is unique among known *Dendrophidion* hemipenes, with the possible exception of *D. bivittatum* (see the introductory section on gracile and robust hemipenial morphotypes). Gracile morphology actually comprises several associated, but distinct, characteristics: the hemipenial body proximal to the enlarged spines is exceptionally long relative to the spinose + apical regions; the spinose + apical region is relatively and absolutely less bulbous than in robust hemipenes; and gracile hemipenes are longer in absolute terms than robust organs (measured length or length in subcaudals for retracted organs). Second, *D. prolixum* and *D. graciliverpa* have a large number of spines (>60 compared with ≤40 in *D. percarinatum*). Such a large number of spines is found elsewhere in *Dendrophidion* only in *D. crybelum* (Cadle, 2012: 225), *D. bivittatum* (about 65 spines in the single organ counted), *D. nuchale* auctorum (>85 in one species of the complex; Cadle and Savage, unpublished data), and *D. brunneum*, in which spines are very small and can number upward of 150. Hemipenes of *D. crybelum* and *D. brunneum* are otherwise dissimilar to *D. prolixum* and *D. graciliverpa* apart from characters common to the *D. percarinatum* species group shared by *D. brunneum*, *D. prolixum*, and *D. graciliverpa*. Third, in *D. prolixum* and *D. graciliverpa* the spines are greatly reduced in size and closely packed together (shared with *D. brunneum* and perhaps with *D. bivittatum*). Finally, in everted hemipenes of *D. prolixum* and *D. graciliverpa* the apex is strongly protruding distal to the flounces as a rounded or more angular convexity (compare Figs. 44A, 46C, D). This apical morphology may characterize *D. bivittatum* (the only everted organ examined is problematic to interpret in this regard), but it also appears rarely in *D. percarinatum*, as shown by the peculiar everted hemipenes of UMMZ 124061 (Fig. 40). These unusual and putatively derived hemipenial characters provide strong evidence that *D. prolixum* and *D. graciliverpa* are closely related within *Dendrophidion*. Further study is needed to evaluate the potential relationship of *D. bivittatum* to this pair based on several shared hemipenial characters.

Given the variability that seems to characterize hemipenes of the *Dendrophidion percarinatum* complex, I am hesitant to make much of small differences among the few available everted hemipenial preparations of *D. prolixum* and *D. graciliverpa*. The profound differences evident between two specimens of *D. graciliverpa* from the type locality (Figs. 44, 46B, D) give one pause in making too much of some differences— especially given the greater similarity of one of these (Fig. 44) to a Colombian specimen

of *D. prolixum* (Fig. 42)! Preparations differ in the shape of the apex, the prominence of the asulcate triangular apical tissue, and the shape and definitiveness of the irregular asulcate calyx and the parasulcus calyces. Because of the variability in these organs I fail to find consistent differences in hemipenial morphology between *D. prolixum* and *D. graciliverpa*. The strongly differentiated asulcate calyx of AMNH R-119835 (Fig. 46D) has no equivalent in any other hemipenis of either species. Similarly, a few other differences, including the degree of compression of the long proximal portion of the hemipenial body, the presence and size of nude areas among the minute spines, the width and morphology of the flounces, and so on cannot be ascribed taxonomic significance without additional sampling.

The Sulcus Spermaticus in the Dendrophidion percarinatum *Complex.* In the three species of the *Dendrophidion percarinatum* complex the sulcus spermaticus in retracted organs ends at the distal tip of the organ, where its lips diverge slightly as the thick parasulcus pads give way to the nude apical tissue (Figs. 41, 43C). This condition is maintained in everted hemipenes of *D. percarinatum*, in which the tip of the sulcus is entirely confluent with the nude apical area and the lateral lips of the sulcus curve sharply around the distal end of the parasulcus pads (Fig. 38D). Everted hemipenes of *Dendrophidion prolixum* and *D. graciliverpa* differ in that a narrow wedge of raised tissue occupies the space between the moderately divergent sulcus lips, resulting in the appearance of a terminal division of the sulcus (Fig. 45). With the small number of preparations of these species available, it is not clear how consistent this apparent division is or whether, in fact, medial "lip" tissue is present on the raised wedge within the divergent lateral lips. In *D. prolixum* the tissue wedge can be easily flattened with manipulation, suggesting that this morphology is not a truly divided sulcus. In two hemipenes of *D. graciliverpa* the sulcus appeared to have a short terminal division, whereas a third seemed to have only

divergent sulcus lips. This suggests that there may be some variation in the expression of this feature. Nearly complete evolutionary loss of the sulcus bifurcation may result in such variation or configurations that are not easily interpreted with respect to a more fully expressed bifurcation; see Myers (2011: 23–24) for possible routes of evolutionary loss of bifurcation of the colubrid sulcus spermaticus.

The apparent terminal division of the sulcus spermaticus in *Dendrophidion prolixum* and *D. graciliverpa* is unusual within *Dendrophidion* but not unique. *Dendrophidion dendrophis* and *D. atlantica* (Freire et al., 2010) have an unambiguously divided sulcus, with fully developed medial and lateral lip tissue along both short branches after the bifurcation. The sulcus is much more deeply forked in *D. dendrophis* than in *D. prolixum* or *D. graciliverpa*. Moreover, the fork is apparent in both the retracted and everted hemipenes in *D. dendrophis* (personal observation), as is typical for divided sulci in general and in contrast to *D. prolixum* and *D. graciliverpa*. Thus, the sulcus spermaticus in *Dendrophidion* shows a variety of conditions: truly bifurcate in *D. dendrophis* and *D. atlantica*, marginally bifurcate or not in *D. prolixum* and *D. graciliverpa*, or with an expanded tip (divergent lips) in the other species.

The terminus of the sulcus spermaticus in the *Dendrophidion percarinatum* complex shows similar ambiguity in interpretation that Myers (2011: 22–24) found in *Leptodeira*. In some species of *Leptodeira* the sulcus is "not clearly forked or divided, [and] terms such as 'simple', 'single', or 'unforked' are not adequate descriptors" of the sulcus condition (Myers, 2011: 23). The situation in the *D. percarinatum* complex is subtly different from what Myers found in *Leptodeira*. In that genus, some species have a truly simple sulcus, but more commonly a small terminal fork is present in retracted hemipenes but lost during eversion, or the terminus presents divergent lips in everted organs. In the *D. percarinatum* complex retracted hemipenes do not

exhibit a bifurcate sulcus, only an expanded sulcus tip, whereas everted organs of two species (*D. prolixum* and *D. graciliverpa*) can have an apparent terminal division to the sulcus.

CONCLUDING REMARKS

My review of two species complexes in *Dendrophidion* shows that speciation within this genus is frequently accompanied by very little differentiation in scutellation characters that typically distinguish snake species (Cadle, 2012; the present work; Table 1). Snake taxonomists rightfully use these characters because of their proven utility in studies of snake systematics, quantitative genetics, and geographic variation, not to mention the ease with which they are scored. However, *Dendrophidion* offers cautionary examples that closely related snake species may not be distinguishable by the usual scale characters. We currently have no measures of how widespread or representative this situation might be among other snakes (a few other examples are well known, e.g., some North American species of *Thamnophis*).

Subtle differences in coloration and rather more profound differences in male genital morphology accompanied speciation within the *D. vinitor* complex (Cadle, 2012), such that distinguishing these species on the basis of external characteristics is problematic (fortunately for nontaxonomists, distributions of those three species are mutually exclusive). A contrasting situation is presented by the *D. percarinatum* complex (this work). Although *D. percarinatum* is distinguished from the other two species in both color pattern characters and hemipenial morphology, *D. prolixum* and *D. graciliverpa* show differences from one another only in coloration. Their hemipenes appear identical when intraspecific variation in hemipenial characters is taken into account, and the two species are not easily distinguished on the basis of scale characters. This scenario of mosaic character evolution or disparate evolutionary rates

among characters is probably more common among snakes than is presently recognized. Close attention to subtle morphological differences among populations offers the best clues to species recognition in these cases. Many putatively widespread snake species may represent complexes of species distinguishable in only subtle ways.

The existence of cryptic species in snakes such as *Dendrophidion* has more than taxonomic interest because it bears on one of the most pressing biodiversity issues of our time: potential declines or extirpations of these snakes in much of their range. Although amphibian biologists have become well attuned to declines of Neotropical frogs and salamanders, reptile biologists have a potentially more difficult job of recognizing declines because absence can be more difficult to detect, especially for snakes (Pounds, 2000: 158–159). Nonetheless, because many tropical forest snakes (including all species of *Dendrophidion*) prey upon anurans, their populations are surely affected by amphibian declines and general environmental degradation. Cadle (2012: 208–209, 216–217) pointed out that populations of two species of the *D. vinitor* complex are probably affected to some degree by widespread amphibian declines and climate-mediated changes in rainforest leaf litter cover (Lips et al., 2006, Whitfield et al., 2007). But there are almost no quantitative or systematic measures of these effects.

Dendrophidion crybelum, known only from a very localized area in southwestern Costa Rica, has not been seen since 1987 despite resurvey of its type locality (Santos-Barrera et al., 2008; Cadle, 2012: 217). At Monteverde, Costa Rica, populations of 11 snake species, including at least one species of *Dendrophidion* (*D. paucicarinatum*), have declined since 1987, and two species are possibly locally extinct (Pounds, 2000). Similarly, *D. prolixum*, described herein, possibly has not been seen since the type series was collected in 1973 (admittedly, few collections have been made from within its known range in the intervening years). The

problem of decline and possible extinction is especially acute when unrecognized cryptic species with restricted ranges exist within what is thought to be a single widespread species, such as the *Dendrophidion* species covered here and in Cadle (2012). Loss of these species, in some cases before their formal descriptions, is cause for heightened awareness among tropical biologists of the potential collapse of populations of snake predators whose biology is intimately tied to declining prey species. Such ramifying ecosystem effects call for redoubled efforts at biodiversity documentation (including systematic studies to reveal cryptic biodiversity) and development of effective methods of ecosystem preservation and restoration.

ACKNOWLEDGMENTS

APPENDIX 1. SPECIMENS EXAMINED AND LITERATURE RECORDS OF *DENDROPHIDION PERCARINATUM* AND NEW RECORDS OF *D. BRUNNEUM* FROM ECUADOR

Museum abbreviations used throughout are the following: AMNH—American Museum of Natural History (New York). ANSP—Academy of Natural Sciences of Philadelphia. BMNH—The Natural History Museum (London). CM—Carnegie Museum (Pittsburgh). KU—University of Kansas Museum of Natural History (Lawrence). LACM—Natural History Museum of Los Angeles County (Los Angeles). MCZ—Museum of Comparative Zoology (Cambridge). MHNLS—Museo de Historia Natural La Salle (Caracas). TCWC—Texas Cooperative Wildlife Collection, Texas A and M University (College Station). UF—Florida Museum of Natural History, University of Florida (Gainesville). UIMNH—University of Illinois Museum of Natural History (Urbana). UMMZ—University of Michigan Museum of Zoology (Ann Arbor). USNM—National Museum of Natural History, Smithsonian Institution (Washington, DC). UTACV—University Texas at Arlington Collection of Vertebrates (Arlington).

Bracketed data associated with localities here and elsewhere in the text are inferences derived from sources other than original data associated with specimens as recorded in literature, museum or collectors' catalogues, or specimen labels. Countries are listed north to south Honduras to Colombia, followed by Venezuela.

Dendrophidion percarinatum

Honduras: *Atlántida:* CURLA Forestry Station, 120–500 m [15°42′N, 86°51′W fide USNM database], USNM 559613–14. Lancetilla [15°42′N, 87°26′W], MCZ R-29677. *Colón:* Los Andes [15°50′N, 85°08′W], ANSP 20817. *Gracias a Dios:* Bodega de Rio Tapalwás, 190 m [14°56′N, 84°32′W], USNM 561031, 563301. Hiltara Kiamp, 150 m [on the upper Río Warunta; 14°57′N, 84°40′W], USNM 563300, 565532. Between Hiltara Kiamp and Sachin Tingni Kiamp, 150 m [14°57′N, 84°40′], USNM 563489. Kipla Tingni Kiamp, 160 m [on the upper Río Warunta; 14°56′N, 84°40′W], USNM 565533. Oscana, 60 m [14°42′N, 84°27′W], USNM 562872–73. Rus Rus, 60 m [14°43′N, 84°27′W], USNM 559612, 561918. Sachin Tingni, 150 m [tributary of upper Río Warunta; 14°57′N, 84°40′W], USNM 563302, 563488. San San Hil Kiamp, 190 m [hill E of Río Tapalwás; 14°57′N, 84°31′W], USNM 563490, 564078. *Olancho:* Los Chorritos near Campamento, 950 m [14°33′N, 86°39′W; McCranie (2011) gives 685 m as the elevation], USNM 337504. Confluence of Río Wampú and Río Yanguay, 110 m [15°03′N, 85°08′W], USNM 321734. Quebrada El Guásimo, 140 m [tributary of Río Patuca; 14°35′N, 85°18′W], USNM 559611. Warunta Tingni Kiamp, 150 m [14°55′N, 84°41′W; McCranie, 2011: 639], USNM 561919.

Nicaragua: [*Atlántico Norte*]: Bonanza, 850 ft. [260 m; 14°02′N, 84°35′W], KU 86183. *Atlántico Norte:* Musawas, Huaspuc River [14°09′N, 84°42′W], AMNH R-75428. *Atlántico Sur:* El Recreo, 10 mi. W Rama [12°10′N, 84°19′W], LACM 74148. Seven miles above Rama, Rio Siquia [approximately 12°10′N, 84°18′W], UMMZ 79767. 10 mi. above Recero [= Recreo], Rio Siquia Mico [12°07′N, 84°26′W; see Cadle, 2012: 234], UMMZ 79764. *Boaco:* Comoapa [= Camoapa; 12°23′N, 85°31′W, about 520 m], MCZ R-9550. *Chontales:* Santo Domingo, Chontales Mines, 2,000 ft. [610 m; 12°16′N, 85°05′W], BMNH 94.10.1.18 (specimen not seen; Stafford, 2003).

Costa Rica: No additional data, AMNH R-17374, USNM 259130. *Alajuela:* Venado, 9 km N Arenal, 252 m [10°33′N, 84°45′W], LACM 148580. *Cartago:* Pavones de Turrialba [09°54′N, 83°37′W], UTACV 12898. Turrialba, 605 m [09°54′N, 83°41′W], LACM 148577, 148579. *Guanacaste:* Tilarán, 1,300 ft. [400 m; 10°28′N, 84°58′W], USNM 70663. *Heredia:* Finca La Selva, 2.4 km SE Puerto Viejo [35–137 m; 10°26′N, 83°59′W; various locations within the La Selva Biological Station], KU 305559; LACM 148558, 148560, 148583–86. *Limon:* Barra del Colorado, 4 m [10°42′N, 83°36′W], LACM 148587. Batán [10°05′N, 83°20′W], KU 30998. Vicinity of Cahuita, about 4 m [09°44′N, 82°50′W], LACM 148582. Los Diamantes [about 300 m; 10°12′N, 83°47′W; experimental station about 1 km E Guápiles], KU 30997. La Lola, 39 m [10°06′N, 83°23′W], LACM 148578. Pandora, 17 m [09°44′N, 82°58′W], LACM 148581. 2.3 km E Siquirres, 280 m [10°06′N, 83°31′W], UMMZ 137389.

Puntarenas: Boruca [09°00′N, 83°19′W], AMNH R-17366 (lectotype). Parque Nacional Carara, 1.9 rd mi. S Rio Tárcoles on Hwy 34 [09°46′N, 84°36′W], TCWC 84024, 84083. Palmar [a Taylor locality = Palmar Sur fide Jay M. Savage, personal communication], KU 31948. 15 km E Palmar Norte, N Lagarto at Quebrada Yan, 70 m [08°57′N, 83°23′W], LACM 148574. 2 km S entrada Palmar Sur, 15 m [8°58′N, 83°27′W], LACM 148592. Vicinity of Rincón de Osa [08°42′N, 83°29′W; various localities within 7.5 km W to SW of the settlement, 5–60 m elevation; see McDiarmid and Savage, 2005], ANSP 27900; KU 102505–06; LACM 114100–01, 148561–148563, 148565, 148570–73, 148575–76; LSUMZ 34112–13. Finca Las Cruces, about 6 km S San Vito de Java [approximately 1,200 m; 08°47′35″N, 82°57′30″W], LACM 114102–04, 148566. Golfito, 12 m [08°36′N, 83°09′W], LACM 148568. 0.4 km W of Motel Bella Vista, Golfito, 15 m [08°36′N, 83°09′W], LACM 148564. 6.3 km S of Pan American Hwy on Golfito Rd., 7 m [08°37′N, 83°04′W], LACM 148567. Gromaco, at juncture of Río Cotón and Río Coto Brus, 480 m [08°55′N, 93°06′W], LACM 148569. Vicinity of Río Disciplina, 80 m [08°58′N, 83°20′W], LACM 148588. San Luís River at footbridge, about 740 m [10°16′N, 84°49′W], LACM 148559. *San José:* 1.4 mi. N and 0.6 mi. NNE (by road) Bijagual; Montañas Jamaica, Parque Nacional Carara [09°43′N, 84°34′W], TCWC

83370. "Los Cusingos" [09°43′N, 84°34′W; in Quizarrá on the lower slopes of Volcán Chirripó near Santa Elena], Kohler (2008: fig. 582).

Panama: No additional data, FMNH 31214–16 (heads only). "Canal Zone," no additional data, FMNH 6118. *Bocas del Toro:* Almirante, 10 m [09°18′N, 82°24′W], KU 80224, UMMZ 142638. 1.5 mi. W Almirante, Nigua Creek, 10 m [09°17′N, 82°24′W], KU 107644. 4 km W Almirante, 10 m [09°17′N, 82°24′W], KU 107645. Hill above Miramar, 180 m [08°59′N, 82°15′W], KU107647. Torres, western Panama [09°25′N, 82°31′W], MCZ R-19343. [*Chiriquí*]: "Chiriquí," BMNH 94.5.17.8–9 (specimens not seen; Stafford, 2003).

Coclé: El Valle de Anton, 2,000 ft. [610 m; 08°37′N, 80°08′W], AMNH R-71681. *Colón:* Canal Zone, Acliote [= Achiote] Rd., 5.1 km NW Escobal Rd., N of road [approximately 09°15′N, 80°02′W], UMMZ 155740. Agua Clara, Chagres River [09°11′N, 79°41′W], ANSP 25144. Near Buena Vista on Trans-Isthmian Highway, 200 ft. [61 m; 09°16′N, 79°41′W], FMNH 154474. Canal Zone, Buena Vista Peninsula, 1.75 km NNW of Frijoles [09°10′34″N, 79°48′W], USNM 196306. Canal Zone, Camp Chagres, 120 ft [40 m; 09°21′N, 79°57′W], KU 75676. Canal Zone, Fort Randolph [09°23′N, 79°53′W], MCZ R-20552. Canal Zone, Salamanca Hydrographic Station, Río Pequení [09°20′N, 79°36′W], MCZ R-39978. Gamboa [09°07′N, 79°42′W], FMNH 154510, USNM 297811. Gatún [09°16′N, 79°55′W], FMNH 16760, USNM 54080. Canal Zone, Atlantic side, Gatún, Fort Davis, [09°17′N, 79°54′W], MCZ R-22255. Cartí Rd. [not located], USNM 266157. *Darién:* Río Tuira, Boca de Cupe, 30 m [08°03′N, 77°35′W], AMNH R-119376. Cana, 2,000 ft. [610 m; 07°47′N, 77°42′W], KU 107651, USNM 50123. [Cerro] Tacarcuna, 550 m [08°10′N, 77°18′W], KU 75677–79. Ortiga site, 8°46′ 78°00 (30 m), FMNH 170152. Along Río Canclón [= Río Canglón] near mouth of Río Chucunaque [approximately 08°20′N, 77°46′W], UMMZ 124063. Along Río Canclón [= Río Canglón] near crossing of Inter-American Highway [approximately 08°20′20″N, 77°49′50″W], UMMZ 124064. Near mouth of Río Canclón [= Río Canglón; 08°19′N, 77°46′W], UMMZ 124199. Río Tuira at Río Mono, 130 m [07°43′N, 77°33′W], KU 107652–56. Yarrssa [= Yaviza] [08°11′N, 77°41′W], UMMZ 83144. [*Herrera*]: Cerro Mangillo, 2,800 ft., Veragua [854 m; = Cerro Manglillo, 07°34′N, 80°47′W; the Manglillo Massif straddles the border between Veraguas and Herrera province; see Dunn (1943) for a brief recounting of his route], ANSP 22446. *Los Santos:* E slopes of

Cerro Hoya, 930 m [07°19′N, 80°40′W], KU 107659. *Panamá:* Canal Zone, Alhajuela [09°11′N, 79°33′W], UMMZ 76019. Altos de Majé [08°48′N, 78°31′W], AMNH R-109643. Barro Colorado Island: AMNH R-77573, 89971–72; ANSP 22560, 22878; CM S 6869, S 7711; KU 75674–75, 80589–90; MCZ R-18902; UMMZ 63762; 124061–62, 124065–66; USNM 120815. Canal Zone, Chiva Chiva [09°02′N, 79°35′W], MCZ R-24002. Cocolí [08°59′N, 79°35′50″W], USNM 193447. Canal Zone, Contractor's Hill [09°02′N, 79°39′W], CAS 98388. Canal Zone, Curundú [08°59′N, 79°33′W], KU 80255. Canal Zone, Fort Clayton [09°00′N, 79°34′W], KU 107649, 110290, MCZ R-25124. Canal Zone near Fort Clayton, [09°00′N, 79°34′W], UIMNH 41705–19. Fort Clayton, Cardenas River [09°00′N, 79°34′W], KU 110291. Gamboa or Pedro Miguel [approximately 09°03′N, 79°40′W], FMNH 154516. Canal Zone, Juan Mine [09°10′N, 79°39′W], MCZ R-26646. Canal Zone, Madden Forest, Río Pedro Miguel [09°06′N, 79°37′W], KU 107650. Canal Zone, [Madden] Forest Preserve [09°06′N, 79°37′W], AMNH R-89970. Canal Zone, Red Tank [09°00′N, 79°36′W], MCZ R-24000. Cerro Campana, 2,500 ft. [762 m; 08°41′N, 79°56′W], AMNH R-76000. Cerro Campana, 800 m [08°41′N, 79°56′W], AMNH R-129757. Cerro Jefe [09°14′N, 79°21′W], UMMZ 155732. *San Blas:* Armila, Quebrada Venado [08°40′N, 77°28′W], USNM 150139. San Ignacio de Tupile, mainland, 2.5 mi. inland, ca. 250 ft. [75 m; 09°15′N, 78°09′W], USNM 241656. *Veraguas:* Isla Gobernadora [07°33′N, 81°12′W], KU 107648.

Colombia: *Antioquia:* Medellín [06°15′N, 75°35′W], BMNH 1897.11.12.10 (questionable record; see Distribution in the *D. percarinatum* account). Urabá, Río Currulao, 50 m [08°01′N, 76°44′W], FMNH 63772–73. Urabá, Turbo [08°06′N, 76°44′W], FMNH 63761. Villa Arteaga [135 m; 07°22′N, 76°29′W], FMNH 78118, USNM 267273. *Chocó:* Quebrada Pangala, lower Río San Juan (about 17 km airline NE Palestina), 04°15′N, 77°0′W, AMNH R-123745, R-123748. Vicinity of Playa de Oro, upper Río San Juan, ca. 200 m [05°19′N, 76°24′W], AMNH R-108468. Sierra [Serranía] del Darién, Chocó, 600 ft., Pacific side [183 m], ANSP 25606. *Valle del Cauca:* Río Raposo, Virology Field Station near Buenaventura [03°43′N, 77°08′W], USNM 151658.

Venezuela: *Zulía:* Sierra de Perijá, Finca El Progreso, 840 m [10°43′13.30″N, 72°29′16.60″W], MHNLS 17932 (specimen not seen; Rojas-Runjaic and Rivero, 2008).

Dendrophidion brunneum (Ecuador only; see Cadle, 2010: 24 for other records)

Ecuador: No other data, AMNH R-18324. "Western Ecuador," BMNH 1860.6.16.58, 1860.6.16.60, 1860.6.16.67.[4] *Chimborazo:* Huigra to Río Chiguancay [02°13′S, 79°03′W], ANSP 18122. [*El Oro*]: Portovelo [610 m; 03°42′48″S, 79°36′51″W; Lynch and Duellman, 1997: 215], AMNH 18322. Zaruma [03°41′S, 79°37′W], BMNH 1894.5.29.1. *Guayas:* 5–10 km S Daule [about 01°55′S, 80°00′W], UF 87940, 88466–67. 18 km E Duran [0–50 m; about 02°14′S, 79°38′W], UF 88468. El Milagro [13 m; 02°07′S, 79°36′W], USNM 237061-62. Guayaquil [02°10′S, 79°50′W], BMNH 1946.1.12.98 (holotype); MCZ R-8393; USNM 237059. Near Guayaquil, USNM 237060. 3 km E Olan [?Olón], Crespo Hacienda, 450 ft. [137 m; Olón is on the coast at 01°48′20″S, 8045′28″W; now in the newly created province of Santa Elena], UF 66199. *Imbabura:* Ibarra [about 2,200 m; 00°21′N, 78°07′W], USNM 237083. Intag [about 1,200 m; 00°20′N, 78°32′W], UMMZ 83706. *Loja:* La Argelia, Malacatos, 2,100 m [04°14′S, 79°17′W], USNM 237077–81. *Loja:* Loja [2,200 m; 04°00′S, 79°13′W], BMNH 1930.10.12.20–22, 1931.11.3.10. Masaca (= Hacienda Masaca, near Loja) [03°53′S, 79°14′W], USNM 237082. [*Loja*]: Alamor [1,325 m; 04°02′S, 80°02′W], AMNH 22232. *Los Ríos:* Finca Playa Grande [53 m; 01°01′30″S, 79°27′39″W, 1.6 km N Quevedo; Lynch and Duellman, 1997: 216], UIMNH 77347. 20 mi. NE Quevedo [about 00°53′S, 79°17′W], UF 85105.

Dendrophidion species inquirendum

Colombia: *Boyacá:* Muzo [1,242 m; 05°32′N, 74°06′W], MCZ R-42186. *Santander:* El Centro,

---

[4] Four specimens were associated with the five BMNH catalog numbers 1860.6.16.58–60, 67–68 when specimens were received on loan. The specimens were not individually tagged with unique catalog numbers but each specimen had previously been individually identified by linen thread tied around the neck: 1, 2, or 3 threads + the smallest of the four with no thread. For purposes of reference and data collection I assigned the three with threads (1, 2, and 3, respectively) to numbers 1860.6.16.58–60, the specimen without thread to 1860.6.16.67 (−68 being therefore unused). Three of the specimens are *Dendrophidion brunneum* (1860.6.16.58, −60, −67). BMNH 1860.6.16.59 is a specimen of *D. graciliverpa* (see footnote 2).

150 m [06°55′N, 73°44′W], USNM 267241. Landazuri, 900 m [06°13′N, 73°49′W], USNM 267272.

APPENDIX 2. GAZETTEER (*DENDROPHIDION PROLIXUM* AND *D. GRACILIVERPA* LOCALITIES)

Dendrophidion prolixum (Colombia except as noted [Ecuador])

Cachaví, 20 m (Esmeraldas [Ecuador]). About 00°58′N, 78°48′W. Also known as Cachabé and San Javier de Cachabé (Paynter, 1993; Duellman and Lynch, 1997: 217).

Lita, Río Mira (Imbabura [Ecuador]). 00°50′24″N, 78°27′18″W; Duellman and Lynch, 1997: 213.

Paramba, northwestern Ecuador (Imbabura). = Hacienda Paramba. 1,067 m. 00°49′N, 78°21′W.

Peña Lisa, Condoto, 300 ft. (Chocó) 90 m; 05°04′N, 76°38′W.

Playa de Oro, Río San Juan, 400 m (Chocó) 05°19′N, 076°24′W.

[Between] Pueblo Rico [and] Santa Cecilia, Pacific side, 800 m (Risaralda). Santa Cecilia: 5°20′N, 76°08′W Pueblo Rico: 5°13′N, 76°02′W.

Quebrada Bochoramá, Loma de Encarnación on right bank (Chocó) about 51 km SE of Quibdo at approximately 5°20′N, 76°23′W, about 400 m elevation; Brame and Wake, 1972: 15.

Quebrada Docordó, middle Río San Juan about 17 km airline SSW Noanamá (Chocó). 04°33′N, 77°0′W (coordinates from AMNH database).

Quebrada Guanguí, 0.5 km above Río Patia (upper Saija drainage), 100–200 m, Cauca department, Colombia [about 02°50′N, 77°25′W; Myers, 1991: 8].

Quebrada Pangala, lower Río San Juan about 17 km airline NE Palestina (Chocó). 04°15′N, 77°00′W (coordinates from AMNH database).

Quebrada Taparal, lower Río San Juan about 7 km airline NE Palestina (Chocó). 4°12′N, 77°07′W (coordinates from AMNH database).

Quininde (Esmeraldas). 00°18′50″N, 79°27′40″W About 100 m (Duellman and Lynch, 1997: 216).

Upper Río Buey, 110–160 m (Chocó). Approximately 06°06′N, 77°05′W.

Río Cachaví (Esmeraldas [Ecuador]). 01°03′N, 78°50′W.

Río Raposo, Virology Field Station near Buenaventura (Valle del Cauca). 03°43′00″N, 77°08′00″W.

Riquarte [= Ricaurte], 3,900 ft. [1,189 m], Pacific side (Nariño). 01°13′N, 77°59′W.

Sierra [Serranía] de Baudó, 3,000 ft. [915 m], Pacific side (Chocó). Approximately 06°00′N, 077°05′W.

Serranía de Baudó, N slope of Alto del Buey, 900 m (Chocó). 06°06′N, 077°13′W.

Dendrophidion graciliverpa (Ecuador)

Alamor (Loja). 04°02′S, 80°02′W.

Bilsa Biological Reserve (Esmeraldas). 00°15′N, 79°45′W. Ortega-Andrade et al. (2010: 1) give coordinates: 00°21′33″N, 79°42′02″W; 300–750 m elevation.

Buena Fe, 1 km N of (Los Ríos). 02°16′S, 79°37′W.

Canoas near Santo Domingo De Los Colorados. (Santo Domingo de los Tsáchilas/Pichincha) Not located.

Centro Científico Río Palenque (Los Ríos). 00°35′11″S, 79°22′W, 220 m elevation. Along the road between Santo Domingo de los Colorados and Quevedo. Dodson and Gentry (1978) describe the environment and geography of the area.

Chaguarapata, 2,000 ft. (Chimborazo). Approximately 02°07′S, 78°59′W. This locality goes by several spellings in the literature (mostly ornithological): Chaguarpata (Paynter, 1993), Charguarpata (Chapman, 1926), Chahuarpata (various). The elevations given are not consistent among sources. AMNH catalogue data for AMNH R-23032 give 2,000 ft., which may be the actual elevation the specimen was collected by G. H. H. Tate. Chapman (1926: 705) gives the elevation of Charguarpata as 5,800 ft., whereas Tate's typed itinerary in the AMNH mammal department gives 2,300 ft. for the elevation. Chapman (1926: 706) states that Chaguapata is "in the forest above Cayandeled," which is a hacienda north of Bucay in the Río Chimbo basin (see Chapman, 1926: map, pl. 30).

Finca La Esperanza near Santo Domingo de los Colorados. (Santo Domingo de los Tsáchilas/Pichincha). 00°15′S, 79°09′W, 500 m; a farm just NW of Santo Domingo de los Colorados (Lynch and Duellman, 1997: 212).

Finca Playa Grande (Los Ríos). 53 m; 01°01′30″S, 79°27′39″W; near Quevedo; Lynch and Duellman, 1997: 216.

Guayaquil (Guayas). 02°10′S, 79°54′W.

Hualtaco (El Oro). 03°26′S, 80°15′W.

Joe Ramsey Farm, km 19 on Chone Road, 18 km W of Santo Domingo de los Colorados (Santo Domingo de los Tsáchilas/Pichincha). 00°14′S, 79°20′W (USNM electronic database).

Las Pampas (Cotopaxi). 1,750 m; 00°40′S, 78°50′W. Also referred to as San Francisco de las Pampas (Lynch and Duellman, 1997).

Meme, km 96 on road to Saloya at crossing of Río Toachi (Pichincha). 00°06′S, 79°08′W.

Mulaute, on tributary of Río Blanco. (Pichincha). 00°05′S, 79°09′W (USNM electronic database).

Playas De Montalvo 15 m (Los Ríos). 01°48′S, 79°20′W (Paynter, 1993). Also referred to as "Playas" (Chapman, 1926: 732; Brown, 1941: 836).

Puerto Quito (Pichincha). 00°07′N, 79°16′W.

Quininde (Esmeraldas). 00°18′50″N, 79°27′40″W, 40 m elevation (Lynch and Duellman, 1997: 216). Also known as Rosa Zarate.

Rancho Santa Teresita, km 25 on route to Chone from Santo Domingo de Los Colorados (Santo Domingo de los Tsáchilas/Pichincha). 00°15′S, 79°23′W (USNM electronic database).

Río Baba (Santo Domingo de los Tsáchilas/Pichincha). Approximately 00°25′S, 79°17′W, Lynch and Duellman, 1997: 216. Humid tropical. Southward flowing river on Pacific coastal plain; riparian rainforest along river.

Río Congo, headwaters of. USNM database places this locality in Guayas province, which is the location of the main part of the Río Congo. The "headwaters," depending on interpretation, are potentially farther north (Manabí or Los Ríos provinces).

Río Palenque Science Center. See Centro Científico Río Palenque.

Río Pescado (Guayas). About 02°41′S, 79°32′W. This is a collecting site of G. H. H. Tate, a mammalogist who participated in the AMNH ornithological expeditions in the early 1920s (Chapman, 1926). Its location seems to be of some confusion, as various published papers on insects, mammals, and frogs that Tate collected there place the locality in at least four different Ecuadorian provinces (Manabí, Guayas, Azuay, Chimborazo). I am grateful to Neil Duncan of the AMNH mammalogy department

for checking Tate's field notes and a typed summary of the trip in the department archives. He provided the details given here. Tate worked at "Río Pescado" from May 14 to June 3, 1922 (e.g., AMNH R-23438, a specimen of *Dendrophidion graciliverpa*, was collected 19 May 1922). The camp on the Río Pescado was three hours by trail east from Naranjal (02°40′22″S, 79°36′54″W) into the foothills at 1,600 ft [488 m]. The camp was located about 0.5 mi. above the junction of the Río Pescado and the Río Chacayacu and near the Guayas-Azuay provincial border.

Below Río Toachi (Santo Domingo de los Tsáchilas/Pichincha). Lat/Long from USNM database: 00°11′S, 79°11′W (USNM electronic database). Lynch and Duellman (1997: 217) for Río Toachi: 00°23′S, 78°56′W, 800 m elevation.

Rosa Delia Plantation (El Oro). 03°17′S, 79°55′W.

Santo Domingo de los Colorados, 550–660 m (Santo Domingo de los Tsáchilas/Pichincha). 00°15′S, 79°10′W.

LITERATURE CITED

ALEMÁN, G. C. 1953. Contribución al estudio de los reptiles y batracios de la Sierra de Perijá. *Memorias de la Sociedad de Ciencias Naturales de La Salle* **13**: 205–225.

ALMENDÁRIZ, A. 1991. Anfibios y reptiles. *Politécnica* **16**: 89–162.

AMARAL, A. DO. "1929" [1930]. Estudos sobre ophidios neotropicos. XVIII—Lista remissiva dos ophidios da Região Neotropica. *Memorias do Instituto Butantan* **4**: 127–128 + i–viii + 129–271.

AUTH, D. L. 1994. Checklist and bibliography of the amphibians and reptiles of Panama. *Smithsonian Herpetological Information Service* **98**: 1–59.

BOLAÑOS, F., J. M. SAVAGE, AND G. CHÁVES. 2010. Anfibios y reptiles de Costa Rica, pp. 1–19. *In* O. Breedy, R. Vargas, and F. Bolaños (eds.), *Listas Zoológicas Actualizadas UCR*. San Pedro: Museo de Zoología, Univ. de Costa Rica. [modified 18 August 2010; cited 1 January 2012]. Available from: http://museo.biologia.ucr.ac.cr.

BOULENGER, G. A. 1882. Account of the reptiles and batrachians collected by Mr. Edward Whymper in Ecuador in 1879–1880. *Annals and Magazine of Natural History* **9**: 457–467.

BOULENGER, G. A. 1891. Reptilia & Batrachia, pp. 128–136. *In* E. Whymper (ed.), *Supplementary Appendix to Travels amongst the Great Andes of the Equator*. London: John Murray.

BOULENGER, G. A. 1894. *Catalogue of the Snakes in the British Museum (Natural History)*. Vol. 2. London: British Museum (Natural History).

BOULENGER, G. A. 1913. A collection of Batrachians and reptiles made by Dr. H.G.F. Spurrell, F.Z.S., in the Choco, Colombia. *Proceedings of the Zoological Society of London* **68**: 1019–1038.

BRAME, A. H., JR., AND D. B. WAKE. 1972. New species of salamanders (genus *Bolitoglossa*) from Colombia, Ecuador, and Panama. *Contributions in Science, Natural History Museum of Los Angeles County* **219**: 1–34.

BRODIE, EDMUND, D. III. 1990. Genetics of the garter's getaway. *Natural History* **1990**: 45–51.

BRODIE, EDMUND, D. III. 1992. Correlational selection for color pattern and antipredator behavior in the garter snake *Thamnophis ordinoides*. *Evolution* **46**: 1284–1298.

BROWN, F. M. 1941. A gazetteer of entomological stations in Ecuador. *Annals of the Entomological Society of America* **34**: 809–851.

CADLE, J. E. 1989. A new species of *Coniophanes* (Serpentes: Colubridae) from northwestern Peru. *Herpetologica* **45**: 411–424.

CADLE, J. E. 1996. Systematics of snakes of the genus *Geodipsas* (Colubridae) from Madagascar, with descriptions of new species and observations on natural history. *Bulletin of the Museum of Comparative Zoology* **155**: 33–87.

CADLE, J. E. 2005. Systematics of snakes of the *Dipsas oreas* complex (Colubridae: Dipsadinae) in western Ecuador and Peru, with revalidation of *D. elegans* (Boulenger) and *D. ellipsifera* (Boulenger). *Bulletin of the Museum of Comparative Zoology* **158**: 67–136.

CADLE, J. E. 2007. The snake genus *Sibynomorphus* (Colubridae: Dipsadinae: Dipsadini) in Peru and Ecuador, with comments on the systematics of Dipsadini. *Bulletin of the Museum of Comparative Zoology* **158**: 183–284.

CADLE, J. E. 2010. Systematics, natural history, and hemipenial morphology of *Dendrophidion brunneum* (Günther), a poorly known snake from the Andes of Ecuador and Peru. *Zootaxa* **2433**: 1–24.

CADLE, J. E. 2012. Cryptic species within the *Dendrophidion vinitor* complex in Middle America (Serpentes: Colubridae). *Bulletin of the Museum of Comparative Zoology* **160**: 183–240.

CHAN, L. M., J. L. BROWN, AND A. D. YODER. 2011. Integrating statistical genetic and geospatial methods brings new power to phylogeography. *Molecular Phylogenetics and Evolution* **59**: 523–537.

CHAPMAN, F. M. 1926. The distribution of bird-life in Ecuador; a contribution to a study of the origin of Andean bird-life. *Bulletin of the American Museum of Natural History* **55**.

CLARK, H. 1944. The anatomy and embryology of the hemipenis of *Lampropeltis*, *Diadophis*, and *Thamnophis* and their value as criteria of relationship in the family Colubridae. *Proceedings of the Iowa Academy of Sciences* **51**: 411–445.

COLE, C. J. AND L. M. HARDY. 1981. Systematics of North American colubrid snakes related to *Tantilla planiceps* (Blainville). *Bulletin of the American Museum of Natural History* **171**: 199–284.

COPE, E. D. 1863. Descriptions of new American Squamata in the museum of the Smithsonian Institution, Washington. *Proceedings of the Academy of Natural Sciences of Philadelphia* **15**: 100–106.

COPE, E. D. "1893" [1894]. Second addition to the knowledge of the Batrachia and Reptilia of Costa Rica. *Proceedings of the American Philosophical Society* **31**: 333–347.

COPE, E. D. "1894" [1895]. On a collection of Batrachia and Reptilia from the island of Hainan. *Proceedings of the Academy of Natural Sciences of Philadelphia* **46**: 423–428.

COPE, E. D. 1895. The classification of the Ophidia. *Transactions of the American Philosophical Society* **18**: 186–219 + pls. 14–33.

COPE, E. D. 1900. The crocodilians, lizards, and snakes of North America. *Report of the U.S. National Museum, under the Direction of the Smithsonian Institution* **1898**: 155–1294.

DAZA, J. M., T. A. CASTOE, AND C. L. PARKINSON. 2010. Using regional comparative phylogeographic data from snake lineages to infer historical processes in Middle America. *Ecography* **33**: 343–354.

DODSON, C. H., AND A. H. GENTRY. 1978. Flora of the Rio Palenque Science Center, Los Ríos Province, Ecuador. *Selbyana* **4**: 1–628.

DUELLMAN, W. E. 1978. The biology of an equatorial herpetofauna in Amazonian Ecuador. *Miscellaneous Publications, Museum of Natural History, University of Kansas* **65**: 1–352.

DUELLMAN, W. E. 2005. *Cusco Amazónico: The Lives of Amphibians and Reptiles in an Amazonian Rainforest.* Ithaca, New York: Cornell Univ. Press.

DUNN, E. R. 1943. Zoological results of the Azuero Peninsula Panama Expedition of 1940. Part 1—A new species of *Peripatus*. *Notulae Naturae* **123**: 1–3.

DUNN, E. R. 1944. The snake genus *Dendrophidion* in Colombia. *Caldasia* **2**: 474–477.

DUNN, E. R., AND J. T. EMLEN, JR. 1932. Reptiles and amphibians from Honduras. *Proceedings of the Academy of Natural Sciences of Philadelphia* **84**: 21–32.

FAIRCHILD, G. B., AND C. O. HANDLEY, JR. 1966. Gazetteer of collecting localities in Panama, pp. 9–20 + map. *In* R. L. Wenzel and V. J. Tipton (eds.), *Ectoparasites of Panama.* Chicago: Field Museum of Natural History.

FREIRE, E. M. J., U. CARAMASCHI, AND U. GONÇALVES. 2010. A new species of *Dendrophidion* (Serpentes: Colubridae) from the Atlantic rain forest of northeastern Brazil. *Zootaxa* **2719**: 62–68.

GAIGE, H. T., N. HARTWEG, AND L. C. STUART. 1937. Notes on a collection of amphibians and reptiles from eastern Nicaragua. *Occasional Papers of the Museum of Zoology, University of Michigan* **357**: 1–18.

GOLDBERG, S. R. 2003. Reproduction in four species of *Dendrophidion* from Costa Rica (Serpentes: Colubridae). *Transactions of the Illinois State Academy of Science* **96**: 295–300.

GÜNTHER, A. 1858. *Catalogue of Colubrine Snakes in the Collection of the British Museum.* London: British Museum (Natural History).

GÜNTHER, A. 1885–1902. *Biologia Centrali-Americana, Reptilia and Batrachia* [SSAR reprint 1987]. Ithaca, New York: Society for the Study of Amphibians and Reptiles.

GUYER, C. 1994. The reptile fauna: diversity and ecology, pp. 210–216 + appendix 6. *In* McDade, L. A., K. S. Bawa, H. A. Hespenheide, and G. S. Hartshorn (eds.), *La Selva: Ecology and Natural History of a Neotropical Rainforest.* Chicago: The Univ. of Chicago Press.

GUYER, C., AND M. A. DONNELLY. 1990. Length-mass relationships among an assemblage of tropical snakes in Costa Rica. *Journal of Tropical Ecology* **6**: 65–76.

GUYER, C., AND M. A. DONNELLY. 2005. *Amphibians and Reptiles of La Selva, Costa Rica, and the Caribbean Slope: a Comprehensive Guide.* Berkeley: Univ. of California Press.

IBÁÑEZ, D. R., F. A. AROSEMENA, F. A. SOLÍS, AND C. A. JARAMILLO. "1994" [1995]. Anfibios y reptiles de la Serranía Piedras-Pacora, Parque Nacional Chagres. *Scientia (Panamá)* **9**: 17–31.

IBÁÑEZ, D. R., AND F. A. SOLÍS. "1991" [1993]. Las serpientes de Panamá: lista de especies, comentarios taxonómicos y bibliografía. *Scientia (Panamá)* **6**: 27–52.

INTERNATIONAL COMMISSION ON ZOOLOGICAL NOMENCLATURE. 1999. *International Code of Zoological Nomenclature.* 4th ed. London: International Trust for Zoological Nomenclature in association with the British Museum (Natural History).

JAN, G. 1863. *Elenco sistematico degli Ofidi descritti e disegnati per l'Iconographia Generale.* Milan: A. Lombardi.

JAN, G., AND F. SORDELLI. 1860–1881. *Iconographie générale des ophidiens.* Vols. 1–3, livrs. 1–50. Milan: Jan and Sordelli.

KEOGH, J. S. 1999. Evolutionary implications of hemipenial morphology in the terrestrial Australian elapid snakes. *Zoological Journal of the Linnean Society* **125**: 239–278.

KÖHLER, G. 2003. *Reptiles of Central America (English edition).* Offenbach, Germany: Herpeton.

KÖHLER, G. 2008. *Reptiles of Central America (2nd English edition).* Offenbach, Germany: Herpeton.

KÖPPEN, W. P. 1931. *Grundriß der Klimakunde.* Berlin: Walter de Gruyter und Co.

LANCINI, A. R. 1979. *Serpientes de Venezuela.* Caracas: Ernesto Armitano.

LAURENCIO, D., AND J. H. MALONE. 2009. The amphibians and reptiles of Parque Nacional Carara, a transitional herpetofaunal assemblage in Costa Rica. *Herpetological Conservation and Biology* **4**: 120–131.

LIEB, C. S. 1988. Systematic status of the Neotropical snakes *Dendrophidion dendrophis* and *D. nuchalis* (Colubridae). *Herpetologica* **44**: 162–175.

LIEB, C. S. 1996. *Dendrophidion percarinatum. Catalogue of American Amphibians and Reptiles* **636**: 636.1–636.2.

LIPS, K. R., F. BREM, R. BRENES, J. D. REEVE, R. A. ALFORD, J. VOYLES, C. CAREY, L. LIVO, A. P. PESSIER, AND J. P. COLLINS. 2006. Emerging infectious disease and the loss of biodiversity in a Neotropical amphibian community. *Proceedings of the National Academy of Sciences, USA* **103**: 3165–3170.

LYNCH, J. D., AND W. E. DUELLMAN. 1997. Frogs of the genus *Eleutherodactylus* (Leptodactylidae) in western Ecuador: systematics, ecology, and biogeography. *University of Kansas Museum of Natural History, Special Publications* **23**: iv + 236 + 8 pls.

McCRANIE, J. R. 2009. Amphibians and reptiles of Honduras [Internet], pp. 1–20. *In* O. Breedy, R. Vargas, and F. Bolaños (eds.), *Listas Zoológicas Actualizadas UCR*. San Pedro: Museo de Zoología, Univ. de Costa Rica [modified 12 November 2009]. Available from: http://museo.biologia.ucr.ac.cr.

McCRANIE, J. R. 2011. *Snakes of Honduras: Systematics, Distribution, and Conservation*. Ithaca, New York: Society for the Study of Amphibians and Reptiles.

McCRANIE, J. R., AND F. E. CASTAÑEDA. 2005. The herpetofauna of Parque Nacional Pico Bonito, Honduras. *Phyllomedusa* **4**: 3–16.

McCRANIE, J. R., F. E. CASTAÑEDA, AND K. E. NICHOLSON. 2002. Preliminary results of herpetofaunal survey work in the Rus Rus region, Honduras: a proposed biological reserve. *Herpetological Bulletin* **81**: 22–29.

McCRANIE, J. R., J. H. TOWNSEND, AND L. D. WILSON. 2006. *The Amphibians and Reptiles of the Honduran Mosquitia*. Malabar, Florida: Krieger Publishing Co.

McDIARMID, R. W., AND J. M. SAVAGE. 2005. The herpetofauna of the Rincón area, Península de Osa, Costa Rica, a Central American lowland evergreen forest site, pp. 366–427. *In* M. A. Donnelly, B. I. Crother, C. Guyer, M. H. Wake, and M. E. White (eds.), *Ecology and Evolution in the Tropics, a Herpetological Perspective*. Chicago: Univ. of Chicago Press.

MYERS, C. W. 1974. The systematics of *Rhadinaea* (Colubridae), a genus of New World snakes. *Bulletin of the American Museum of Natural History* **153**: 1–262.

MYERS, C. W. 1982. Blunt-headed vine snakes (*Imantodes*) in Panama, including a new species and other revisionary notes. *American Museum Novitates* **2738**: 1–50.

MYERS, C. W. 1991. Distribution of the dendrobatid frog *Colostethus chocoensis* and description of a related species occurring macrosympatrically. *American Museum Novitates* **3010**: 1–15.

MYERS, C. W. 2003. Rare snakes—five new species from eastern Panama: reviews of northern *Atractus* and southern *Geophis* (Colubridae: Dipsadinae). *American Museum Novitates* **3391**: 1–47.

MYERS, C. W. 2011. A new genus and new tribe for *Enicognathus melanauchen* Jan, 1863, a neglected South American snake (Colubridae: Xenodontinae), with taxonomic notes on some Dipsadinae. *American Museum Novitates* **3715**: 1–33.

MYERS, C. W., AND J. E. CADLE. 1994. A new genus for South American snakes related to *Rhadinaea obtusa* Cope (Colubridae) and resurrection of *Taeniophallus* Cope for the "*Rhadinaea*" brevirostris group. *American Museum Novitates* **3102**: 1–33.

MYERS, C. W., AND J. E. CADLE. 2003. On the snake hemipenis, with notes on *Psomophis* and techniques of eversion: a response to Dowling. *Herpetological Review* **34**: 295–302.

MYERS, C. W., J. W. DALY, AND B. MALKIN. 1978. A dangerously toxic new frog (*Phyllobates*) used by Emberá Indians of western Colombia, with discussion of blowgun fabrication and dart poisoning. *Bulletin of the American Museum of Natural History* **161**: 307–366.

MYERS, C. W., D. R. IBÁÑEZ, AND J. E. CADLE. 2007. On the uniquely fragmented distribution of a rare Panamanian snake, *Dipsas nicholsi* (Colubridae: Dipsadinae). *American Museum Novitates* **3554**: 1–18.

NATIONAL GEOSPATIAL-INTELLIGENCE AGENCY (NGA) [INTERNET]. Springfield (VA): NGA GEOnet Names Server (GNS) (US); 2010-2012. Available from: http://earth-info.nga.mil/gns/html/.

NICÉFORO MARÍA, H. 1942. Los ofidios de Colombia. *Revista de la Academia Colombiana de Ciencias Exactas, Físicas y Naturales* **5**: 84–101.

NICHOLSON, K.E., J. R. McCRANIE, AND G. KÖHLER. 2000. Herpetofaunal expedition to Parque Nacional Patuca: a newly established park in Honduras. *Herpetological Bulletin* **72**: 26–31.

ORTEGA-ANDRADE, H. M., J. BERMINGHAM, C. AULESTIA, AND C. PAUCAR. 2010. Herpetofauna of the Bilsa Biological Station, province of Esmeraldas, Ecuador. *Check List* **6**: 119–154.

PARKER, H. W. 1938. The vertical distribution of some reptiles and amphibians in southern Ecuador. *Annals and Magazine of Natural History* series 11, **2**: 438–450.

PAYNTER, R. A., JR., 1993. *Ornithological Gazetteer of Ecuador*. 2nd ed. Cambridge: Museum of Comparative Zoology.

PAYNTER, R. A., JR.. 1997. *Ornithological Gazetteer of Colombia*. 2nd ed. Cambridge: Museum of Comparative Zoology.

PÉREZ-SANTOS, C. 1999. *Serpientes de Panamá/Snakes of Panama*. Seville: Comité Español del Programa MaB y de la Red IberoMaB de la UNESCO.

PÉREZ-SANTOS, C., AND A. G. MORENO. 1988. *Ofidios de Colombia*. Torino: Museo Regionale di Scienze Naturali.

PÉREZ-SANTOS, C., AND A. G. MORENO. 1989. Addenda y corrigenda al libro "*Ofidios de Colombia*." *Bollettino del Museo Regionale di Scienze Naturali, Torino* **7**: 1–17.

PÉREZ-SANTOS, C., AND A. G. MORENO. 1991a. Distribución y amplitud altitudinal de las serpientes en Ecuador. *Revista Española de Herpetología* 5: 125–140.

PÉREZ-SANTOS, C., AND A. G. MORENO. 1991b. *Serpientes de Ecuador*. Torino: Museo Regionale di Scienze Naturali.

PÉREZ-SANTOS, C., A. G. MORENO, AND A. GEARHART. 1993. Checklist of the snakes of Panama. *Revista Española de Herpetología* 7: 113–122.

PETERS, J. A., AND B. OREJAS-MIRANDA. 1970. Catalogue of the Neotropical Squamata: part I. Snakes. *Bulletin of the United States National Museum* 297: 1–347.

POUNDS, J. A. 2000. Amphibians and reptiles, pp. 149–177. *In* N. M. Nadkarni and N. T. Wheelwright (eds.), *Monteverde, Ecology and Conservation of a Tropical Cloud Forest*. New York: Oxford Univ. Press.

RAND, A. S., AND C. W. MYERS. 1990. The herpetofauna of Barro Colorado Island, Panama: an ecological summary, pp. 386–409. *In* A. H. Gentry (ed.), *Four Neotropical Rainforests*. New Haven, Connecticut: Yale Univ. Press.

RASMUSSEN, J. B. 1993. A taxonomic review of the *Dipsadoboa unicolor* complex, including a phylogenetic analysis of the genus (Serpentes, Dipsadidae, Boiginae). *Steenstrupia* 19: 129–196.

ROJAS-RUNJAIC, F. J. M., AND E. E. INFANTE RIVERO. 2008. First record of the forest racer snake *Dendrophidion percarinatum* (Cope, 1893) (Serpentes: Colubridae) from Venezuela. *Caribbean Journal of Science* 44: 128–130.

ROZE, J. A. 1966. *La Taxonomía y Zoogeografía de los Ofidios en Venezuela*. Caracas: Univ. Central de Venezuela.

SANTOS-BARRERA, G., J. PACHECO, F. MENDOZA-QUIJANO, F. BOLAÑOS, G. CHÁVES, G. C. DAILY P. R. EHRLICH, AND G. CEBALLOS. 2008. Diversity, natural history and conservation of amphibians and reptiles from the San Vito region, southwestern Costa Rica. *Revista de Biología Tropical* 56: 755–778.

SAVAGE, J. M. 1973. *A preliminary handlist of the Herpetofauna of Costa Rica*. Lawrence, Kansas: American Society of Ichthyologists and Herpetologists.

SAVAGE, J. M. 1980. *A Handlist with Preliminary Keys to the Herpetofauna of Costa Rica*. Los Angeles: Allan Hancock Foundation.

SAVAGE, J. M. 2002. *The Amphibians and Reptiles of Costa Rica, a Herpetofauna between Two Continents, between Two Seas*. Chicago: The Univ. of Chicago Press.

SAVAGE, J. M., AND F. BOLAÑOS. 2009. A checklist of the amphibians and reptiles of Costa Rica: additions and nomenclatural revisions. *Zootaxa* 2005: 1–23.

SAVAGE, J. M., AND J. VILLA. 1986. *Introduction to the Herpetofauna of Costa Rica/Introducción a la Herpetofauna de Costa Rica*. Ithaca, New York: Society for the Study of Amphibians and Reptiles.

SCHMIDT, K. P. "1933" [1935]. Amphibians and reptiles collected by the Smithsonian Biological Survey of the Panama Canal Zone. *Smithsonian Miscellaneous Collections* 89: 1–20.

SCOTT, N. J., JR., J. M. SAVAGE, AND D. C. ROBINSON. 1983. Checklist of reptiles and amphibians, pp. 367–374. *In* D. H. Janzen (ed.), *Costa Rican Natural History*. Chicago: Univ. of Chicago Press.

SEXTON, O. J., AND H. HEATWOLE. 1965. Life history notes on some Panamanian snakes. *Caribbean Journal of Science* 5: 39–43.

SMITH, H. M. 1941. A new name for the Mexican snakes of the genus *Dendrophidion*. *Proceedings of the Biological Society of Washington* 54: 73–76.

SMITH, H. M. 1955. Effect of preservatives upon pattern in a Mexican garter snake. *Herpetologica* 14: 165–168.

SMITH, H. M. 1958. Handlist of the snakes of Psanama. *Herpetologica* 11: 222–224.

SMITH, H. M., AND C. GRANT. 1958. New and noteworthy snakes from Panama. *Herpetologica* 14: 207–215.

SMITH, M. A. 1943. *The Fauna of British India, Ceylon, and Burma, Including the Whole of the Indo-Chinese Sub-region. Reptilia and Amphibia*. Vol. III—*Serpentes*. London: Taylor and Francis Ltd.

SOLÓRZANO, A. 2004. *Serpientes de Costa Rica: Distribución, Taxonomía e Historia Natural/ Snakes of Costa Rica: Distribution, Taxonomy and Natural History*. Eagle Mountain, Utah: Eagle Mountain Publishing LC.

STAFFORD, P. J. 2003. Trophic ecology and reproduction in three species of Neotropical forest racer (*Dendrophidion*; Colubridae). *Herpetological Journal* 13: 101–111.

STUART, L. C. 1932. Studies on Neotropical Colubrinae. I. The taxonomic status of the genus *Drymobius* Fitzinger. *Occasional Papers of the Museum of Zoology, University of Michigan* 236: 1–16.

TAYLOR, E. H. 1951. A brief review of the snakes of Costa Rica. *University of Kansas Science Bulletin* 34, part 1: 3–188.

TAYLOR, E. H. 1954. Further studies on the serpents of Costa Rica. *University of Kansas Science Bulletin* 36, part 2: 673–801.

TEST, F. H., O. J. SEXTON, AND H. HEATWOLE. 1966. Reptiles of Rancho Grande and vicinity, Estado Aragua, Venezuela. *Miscellaneous Publications of the Museum of Zoology, University of Michigan* 128: 1–63.

VILLA, J., L. D. WILSON, AND J. D. JOHNSON. 1988. *Middle American Herpetology—A Bibliographic Checklist*. Columbia: Univ. of Missouri Press.

WHITFIELD, S. M., K. E. BELL, T. PHILIPPI, M. SASA, F. BOLAÑOS, G. CHÁVES, J. M. SAVAGE, AND M. A. DONNELLY. 2007. Amphibian and reptile declines over 35 years at La Selva, Costa Rica. *Proceedings of the National Academy of Sciences, USA* 104: 8352–8356.

WILSON, L. D., AND J. R. MEYER. 1985. *The Snakes of Honduras*. 2nd ed. Milwaukee: Milwaukee Public Museum.

WILSON, L. D., AND J. H. TOWNSEND. 2006. The herpetofauna of the rainforests of Honduras. *Caribbean Journal of Science* 42: 88–113.

WILSON, L. D., AND J. H. TOWNSEND. 2007. Biogeography and conservation of the herpetofauna of the upland pine-oak forests of Honduras. *Biota Neotropica* **7**: 131–142.

WOLF, M., AND Y. L. WERNER. 1994. The striped colour pattern and striped/non-striped polymorphism in snakes (Reptilia: Ophidia). *Biological Reviews of the Cambridge Philosophical Society* **69**: 599–610.

YÁNEZ-MUÑOZ, M., P. MEZA-RAMOS, C. C. MARTÍNEZ, AND M. REYES P. 2009. Anfibios y reptiles del sur occidente de Ecuador (version 1). *Rapid Color Guide (The Field Museum)* **237**: 1–4.

Phylogeny of the *Dactyloa* Clade of *Anolis* Lizards:
New Insights From Combining Morphological
and Molecular Data

MARÍA DEL ROSARIO CASTAÑEDA AND KEVIN DE QUEIROZ

This publication has been printed on acid-free permanent paper stock.

PHYLOGENY OF THE *DACTYLOA* CLADE OF *ANOLIS* LIZARDS: NEW INSIGHTS FROM COMBINING MORPHOLOGICAL AND MOLECULAR DATA

MARÍA DEL ROSARIO CASTAÑEDA[1,2,3] AND KEVIN DE QUEIROZ[2]

CONTENTS

NOTE ADDED IN PROOF

Shortly after our paper was accepted, Nicholson and colleagues published a phylogenetic analysis of anoles and a proposal to divide *Anolis* into eight genera (Nicholson, K. E., B. I. Crother, C. Guyer, and J. M. Savage. 2012. It is time for a new classification of anoles (Squamata: Dactyloidae). *Zootaxa* 3477: 1–108). Here, we comment briefly on their study as it pertains to the phylogeny and taxonomy of the *Dactyloa* clade.

Despite not inferring *Dactyloa* to be monophyletic in the tree used for their proposed taxonomy (i.e., the consensus tree from the combined morphological and molecular parsimony analysis; their fig. 5A, note positions of *Anolis bonairensis*, *A. chloris*, *A. peraccae*, and *A. apollinaris*), Nicholson et al. (2012) recognized *Dactyloa* as one of their eight genera without making reference to this inconsistency (although *Dactyloa* was inferred to be monophyletic in their molecular tree, fig. 4A). By contrast, our combined data set supported the monophyly of *Dactyloa* (Figs. 3, 4), and we have chosen to treat *Dactyloa* as a subclade of *Anolis* rather than as a separate genus in the interest of avoiding disruptive and unnecessary name changes.

Some of our informally named series correspond, with some differences in species composition, to the species groups proposed by Nicholson et al. (2012). We describe the differences below.

Our *latifrons* series corresponds to their *latifrons* species group, except that in the tree purportedly used for their taxonomy (fig. 5A), *A. aequatorialis* and *A. ventrimaculatus* were inferred to be part of this species

[1] Department of Biological Sciences, The George Washington University, 2023 G Street NW, Washington, DC 20052.
[2] Department of Vertebrate Zoology, National Museum of Natural History, Smithsonian Institution, MRC 162, Washington, DC 20560. Author for correspondence (mcastanedaprada@fas.harvard.edu).
[3] Address through April 2014: Museum of Comparative Zoology, Harvard University, 26 Oxford Street, Cambridge, Massachusetts 02138.

group (both species are absent from their molecular tree, fig. 4A), although their classification (appendix III) places both species in their *punctata* species group with no explanation for this inconsistency. We inferred these two species with strong support to be part of a monophyletic *aequatorialis* series that is mutually exclusive with respect to both the *latifrons* and *punctatus* series. Additionally, we have tentatively placed *A. mirus* and *A. parilis* in the *aequatorialis* series based on their previous inclusion in the traditional *aequatorialis* series (Williams, 1975; Ayala-Varela and Velasco, 2010); the tentative assignment reflects the current absence of these species from explicit phylogenetic analyses. By contrast, Nicholson et al. (2012) assigned *A. mirus* and *A. parilis*, neither of which was included in any of their analyses, to their *latifrons* species group without explanation. Finally, we placed *A. propinquus* in the *latifrons* series based on its hypothesized close relationship to *A. apollinaris* (Williams, 1988). By contrast, Nicholson et al. (2012) placed this species, which was not included in any of their phylogenetic analyses, in their *punctata* species group without explanation.

The combination of our *aequatorialis* and *punctatus* series corresponds roughly to the *punctata* species group in the classification of Nicholson et al. (2012, appendix III). We inferred these two series to be mutually exclusive clades (results further supported by molecular data alone; Castañeda and de Queiroz, 2011). Contradicting their own taxonomy, the tree of Nicholson et al. (2012, fig. 5A) supports the separation of the *aequatorialis* series, in that *A. aequatorialis*, *A. ventrimaculatus*, *A. chloris*, and *A. peraccae* are not inferred to be part of their *punctata* species group, despite being referred to that group in their classification (appendix III). Their tree does place *A. fasciatus* in their *punctata* species group, whereas our results indicate that this species is part of the *aequatorialis* series. We have treated *A. calimae* and *A. cuscoensis* as *incertae sedis* within *Dactyloa* based on conflicting results for *A. calimae* (also found by Castañeda and de Queiroz, 2011) and the inferred inclusion of *A. cuscoensis* by Poe et al. (2008) in clades not inferred in our study. By contrast, Nicholson et al. (2012) referred these two species to their *punctata* species group, although neither species was included in any of their phylogenetic analyses. Similarly, we have treated *A. laevis* and *A. phyllorhinus*, species formerly placed in the *laevis* series, as *incertae sedis* based on their current absence from explicit phylogenetic analyses (although we consider it likely that *A. phyllorhinus* belongs to the *punctatus* series). By contrast, Nicholson et al. (2012) assigned both of these species to the *punctata* species group, although neither was included in any of their phylogenetic analyses.

Our *Phenacosaurus* and our *heterodermus* series both correspond approximately to the *heterodema* species group of Nicholson et al. (2012), with the exception that they included *A. carlostoddi*, *A. bellipeniculus*, and *A. neblininus*. We consider these

three species as *incertae sedis* within *Dactyloa* based on conflicting results in our analyses for *A. carlostoddi* and *A. neblininus* and the absence from explicit phylogenetic analyses of *A. bellipeniculus*, as well as its previously inferred close relationship to *A. neblininus* (Myers and Donnelly, 1996).

Our *roquet* series corresponds approximately to their *roquet* species group. However, in the tree purportedly used for their taxonomy (their fig. 5A), their *roquet* species group is not monophyletic: *A. bonairensis* is inferred as sister to *A. occultus* outside of *Dactyloa* (*A. bonairensis* is not included in their molecular-only tree; fig. 4A). By contrast, we inferred *A. bonairensis* to be part of a monophyletic *roquet* series (Figs. 3, 4).

Our combined analyses are based on a sample of 60 of the 83 currently recognized species in the *Dactyloa* clade, 40 of which were sampled for molecular data, whereas the combined analysis of Nicholson et al. (2012) is based on a sample of 31 *Dactyloa* species, 16 of which were sampled for molecular data (three others were sampled for molecular data only). Additionally, our molecular data consists of ~4,950 base positions representing three gene regions and both mitochondrial and nuclear DNA, whereas theirs consists of ~1,500 base positions representing one of the two mitochondrial gene regions used in our study. Because our results are based on larger samples of *Dactyloa* species (for both molecular and morphological data), as well as larger samples of molecular data (with respect to both numbers of bases and numbers of gene fragments, and including both mitochondrial and nuclear genes), and because many of their taxonomic conclusions that differ from ours are either contradicted by their own results or unsubstantiated, we do not consider any of the differences between our phylogenetic results and taxonomic conclusions compared with those in the study by Nicholson et al. (2012) to warrant changes to our proposed taxonomy. In contrast to Nicholson et al. (2012), we refrain from assigning some species to series and treat some taxonomic assignments as tentative because of contradictory results or poorly supported inferences, and we present justifications for all taxonomic decisions pertaining to species not included in our analyses.

ABSTRACT.   We present a phylogenetic analysis of the *Dactyloa* clade of *Anolis* lizards, based on morphological (66 characters of external morphology and osteology) and molecular (~4,700 bases of mitochondrial and nuclear DNA) data. Our set of morphological characters includes some that exhibit continuous variation and others that exhibit polymorphism within species; we explored different coding methods for these classes of characters. We performed parsimony and Bayesian analyses on morphology-only and combined data sets. Additionally, we explicitly tested hypotheses of monophyly of: 1) *Dactyloa* including *Phenacosaurus*, 2) *Dactyloa* excluding *Phenacosaurus* (as traditionally circumscribed), 3) taxa previously ranked as series or species groups described based on

morphological characters, and 4) clades inferred from molecular data. The morphological data alone did not yield *Dactyloa* or any of the previously recognized series described based on morphological characters; only the *Phenacosaurus* clade (as delimited based on molecular data) was inferred with the morphological data, and only in the parsimony analysis. In contrast, *Dactyloa* was inferred as monophyletic with the combined data set, although topology tests failed to reject the hypothesis of non-monophyly. Additionally, five clades inferred based on molecular data (eastern, *latifrons*, *Phenacosaurus*, *roquet*, and western) were inferred with the combined data sets with variable support and including additional species for which molecular data were not available and which have geographic distributions that conform to those of the clades in which they were included. Of the previously recognized taxa based on morphological characters, only the *roquet* series, which corresponds in species composition to the *roquet* clade, was inferred with the combined data. Topology tests with the combined data set rejected the monophyly of the *aequatorialis*, *latifrons* (as traditionally circumscribed), and *punctatus* series but not that of the *tigrinus* series and *Phenacosaurus* (as traditionally circumscribed). Our phylogenetic analyses and topology tests indicate that a new taxonomy for *Dactyloa* is warranted; we therefore present a revised taxonomy based on the results our phylogenetic analyses and employing phylogenetic definitions of taxon names.

Key words: *Anolis*, Character coding, *Dactyloa*, Phylogeny, Taxonomy

INTRODUCTION

The *Anolis* clade, one of the most diverse groups of vertebrates traditionally ranked as a genus, is composed of 384 currently recognized species (Uetz, 2012). This group of lizards is primarily Neotropical in distribution. Its members are characterized (with a few exceptions) by the possession of adhesive toe pads formed by laterally expanded subdigital scales, called lamellae, that are covered by microscopic setae, and of extensible and often brightly colored throat fans, called dewlaps, that are supported by elongated second ceratobranchials and occur in males and often in females (Etheridge, 1959).

Based on Etheridge's (1959) seminal work on the phylogeny and taxonomy of anoles, two large groups, traditionally ranked as sections, were informally recognized within *Anolis* based on the absence (alpha section) or presence (beta section) of

transverse processes on the anterior autotomic caudal vertebrae. Each section was further subdivided into series and species groups based on morphological characters (Etheridge, 1959; Williams, 1976a,b). Subsequent to the morphological studies of Etheridge (1959) and Williams (1976a,b), a wide variety of data have been brought to bear on the phylogeny and taxonomy of *Anolis*, including albumin immunology (e.g., Gorman et al., 1980b, 1984; Shochat and Dessauer, 1981), allozymes (e.g., Gorman and Kim, 1976; Gorman et al., 1980a; Burnell and Hedges, 1990), behavior (e.g., Gorman, 1968), karyotypes (e.g., Gorman et al., 1968, 1983; Gorman and Stamm, 1975), and DNA sequences (e.g., Jackman et al., 1999; Schneider et al., 2001; Glor et al., 2003). Analyses of these data have provided support for the monophyly of the beta section and of several series and species groups (e.g., Creer et al., 2001; Schneider et al., 2001; Jackman et al., 2002; Nicholson, 2002). However, they have also indicated that other groups, including the alpha section, are not monophyletic. Additionally, the phylogenetic relationships within and among some groups are still disputed (e.g., Jackman et al., 1999; Nicholson, 2002; Poe, 2004).

Within the alpha section, Etheridge (1959) recognized the *latifrons* series for species with at least four postxiphisternal chevrons attached to the bony dorsal ribs and an arrow-shaped interclavicle (in which the lateral processes of the interclavicle are divergent from the proximal parts of the clavicles). Etheridge's (1959) *latifrons* series was composed of all mainland alpha *Anolis* (excluding *Phenacosaurus*; see below) along with the species in the *roquet* series from the southern Lesser Antilles, as well as *Anolis agassizi* and *A. gorgonae* from the Pacific islands of Malpelo and Gorgona, respectively. The *latifrons* series of Etheridge (1959) corresponds to the genus *Dactyloa*, one of five genera recognized by Guyer and Savage (1987 [1986]) based on a proposal to "divide" *Anolis* taxonomically. Although the recognition of those genera is

controversial (Cannatella and de Queiroz, 1989; Williams, 1989; Poe and Ibañez, 2007), some recent authors apply some of the same names to clades within *Anolis* regardless of rank and not necessarily with identical composition (e.g., Nicholson, 2002; Brandley and de Queiroz, 2004; de Queiroz and Reeder, 2008). In the present study, we use the name *Dactyloa* for the clade originating in the most recent common ancestor of the species included in the genus *Dactyloa* by Savage and Guyer (1989), which also includes the anoles formerly assigned to the genus *Phenacosaurus* according to the results of recent phylogenetic analyses (e.g., Jackman et al., 1999; Poe, 2004; Nicholson et al., 2005; Castañeda and de Queiroz, 2011). Currently, there are 83 recognized species in the *Dactyloa* clade, distributed among seven subgroups (based on morphological characters) commonly assigned to the rank of series: *aequatorialis, laevis, latifrons, punctatus, Phenacosaurus, roquet,* and *tigrinus* (see "Current Taxonomy within *Dactyloa*," below).

Three phylogenetic analyses have included more than 20% of the currently recognized *Dactyloa* species: Poe (2004) included 28 species, Nicholson et al. (2005) included 17 species (13 of which were included in Poe [2004]), and Castañeda and de Queiroz (2011) included 42 species (including 22 of 28 of Poe [2004] and 15 of 17 of Nicholson et al. [2005]). In Poe's (2004) combined analysis of allozyme, karyotype, morphological, and molecular data, *Dactyloa* (as defined in the previous paragraph, the name was not used by Poe) was inferred to be monophyletic based on the arrow shape of the interclavicle and the presence of a splenial in the mandible. However, bootstrap support for the clade (Poe, 2004, fig. 2, node 352) was less than 50% and both morphological characters supporting it are reversals to ancestral conditions. In the analyses of Nicholson et al. (2005, fig. 1) and Castañeda and de Queiroz (2011, fig. 1), based on molecular data, *Dactyloa* was inferred with moderate to strong bootstrap support (≥80%) and Bayesian posterior probabilities (≥0.90).

Of the seven subgroups described within *Dactyloa* based on morphological characters, only the *roquet* series has been consistently inferred by several phylogenetic analyses and has passed explicit statistical tests of monophyly (Jackman et al., 1999; Poe, 2004; Nicholson et al., 2005; Castañeda and de Queiroz, 2011). *Phenacosaurus*, as traditionally circumscribed, was inferred as monophyletic by Poe (2004) and Nicholson et al. (2005), although only two and three species of this group, respectively, were included in their phylogenetic analyses. In the analyses of Castañeda and de Queiroz (2011), which included six species of *Phenacosaurus*, the group was inferred as monophyletic with the exception of *A. neblininus*. The remaining subgroups have not been inferred in phylogenetic analyses or passed explicit statistical tests of monophyly, although the *laevis* series has not been tested (Poe, 2004; Nicholson et al., 2005; Castañeda and de Queiroz, 2011). In contrast to the poor support for the traditional series, Castañeda and de Queiroz (2011) inferred five strongly supported subclades within *Dactyloa*, which they recognized informally as eastern, *latifrons, Phenacosaurus, roquet,* and western clades. Although some of these clades bear the same names as species groups recognized by Williams (1976b) and series recognized by Savage and Guyer (1989), their composition is not necessarily the same.

In this study, we describe and score 66 morphological characters (external and osteological) for 60 species of *Dactyloa* and 6 outgroup species (including non-*Dactyloa* *Anolis* and non-*Anolis* Polychrotinae) to resolve the phylogenetic relationships within the *Dactyloa* clade. We analyze the morphological characters alone and in combination with ~4,720 bases of DNA sequence data presented by Castañeda and de Queiroz (2011). We perform parsimony and Bayesian analyses and examine different coding methods for continuous and polymorphic characters. We use tree topology tests to test hypotheses of monophyly of: 1) *Dactyloa* including *Phenacosaurus*, 2)

Dactyloa excluding Phenacosaurus (as traditionally circumscribed), 3) the traditionally recognized series delimited based on morphological characters (Williams, 1976b; Savage and Guyer, 1989), and 4) the clades inferred based on molecular data (Castañeda and de Queiroz, 2011). Based on the results of our analyses, we present a revised taxonomy that is consistent with the current knowledge of the phylogenetic relationships within the Dactyloa clade.

Current Taxonomy within Dactyloa

Based on morphological characters, six subgroups ranked as species groups by Williams (1976b) and as series by Savage and Guyer (1989) have been recognized within Dactyloa: aequatorialis, laevis, latifrons, punctatus, roquet, and tigrinus. In agreement with recent phylogenetic analyses (e.g., Jackman et al., 1999; Poe, 2004; Nicholson et al., 2005; Castañeda and de Queiroz, 2011), we recognize the group of species previously identified as the genus Phenacosaurus as an additional subgroup of Dactyloa. Some Dactyloa species have not been assigned to any of these subgroups; for example, Anolis agassizi, A. anchicayae, A. cuscoensis, and A. ibanezi were referred to what is here recognized as the Dactyloa clade, but with no series assignment (Etheridge, 1959; Poe et al., 2008, 2009a,b). Other species have been assigned to subgroups, but assignment was inconsistent. For example, Anolis kunayalae was described as morphologically similar to A. mirus and A. parilis, both members of the aequatorialis series, but assigned by the describing authors (Hulebak et al., 2007) to the latifrons group sensu stricto (= latifrons species group of Williams, 1976b) which is equivalent to the latifrons series of Savage and Guyer (1989); we therefore consider the series assignment of this species uncertain.

Aequatorialis series. The aequatorialis series is currently composed of 13 species: A. aequatorialis, A. anoriensis, A. antioquiae, A. eulaemus, A. fitchi, A. gemmosus, A. maculigula, A. megalopithecus, A. mirus, A. otongae, A. parilis, A. podocarpus, and A. ventrimaculatus, which are characterized by moderate to large body size (adult male snout-to-vent length [SVL] 66–101 mm), small head scales, smooth ventral scales, uniform dorsal scalation, and in some species narrow toe lamellae (Williams, 1976b; Williams and Acosta, 1996; Ayala-Varela and Torres-Carvajal, 2010; Ayala-Varela and Velasco, 2010; Velasco et al., 2010). The species in the aequatorialis series are distributed between 1,300 and 2,500 m above sea level in the Andes of Colombia (western and central cordilleras) and Ecuador (eastern and western slopes) (Williams and Duellman, 1984; Ayala-Varela and Torres-Carvajal, 2010; Velasco et al., 2010; Ayala and Castro, unpublished).

Laevis series. The laevis series, composed of A. laevis, A. phyllorhinus, and A. proboscis, is characterized by the presence of a soft, median protuberance from the snout, called a proboscis (Williams, 1976b, 1979) or nose leaf (Peters and Orces, 1956). Members of this series have a disjunct geographic distribution: A. laevis is distributed in the eastern foothills of the Peruvian Andes, A. proboscis is found at mid-elevations on the western slopes of the Ecuadorian Andes, and A. phyllorhinus is found in central Amazonia (Williams, 1979; Rodrigues et al., 2002).

Latifrons series. The latifrons series is composed of 12 species: A. apollinaris, A. casildae, A. danieli, A. fraseri, A. frenatus, A. insignis, A. latifrons, A. microtus, A. princeps, A. propinquus, A. purpurescens, and A. squamulatus, which are characterized by adult SVL > 100 mm, large dewlaps in adult males (>500 mm^2), expanded toe lamellae, small head scales, smooth to weakly keeled ventral scales, and uniform dorsal scalation (Williams, 1976b; Savage and Talbot, 1978). These species, also called the giant mainland anoles (Dunn, 1937), are distributed in the lowlands and premontane forests of Costa Rica, western Panama, Colombia (western cordillera), and Ecuador; in the northern central lowlands of Venezuela; and in the inter-Andean valleys of Colombia (Savage

and Talbot, 1978; Arosemena et al., 1991; Ayala and Castro, unpublished).

Punctatus *series.* The *punctatus* series is composed of 21 species: *A. anatoloros, A. boettgeri, A. calimae, A. caquetae, A. chloris, A. chocorum, A. deltae, A. dissimilis, A. fasciatus, A. festae, A. gorgonae, A. huilae, A. jacare, A. nigrolineatus, A. peraccae, A. philopunctatus, A. punctatus, A. santamartae, A. soinii, A. transversalis,* and *A. vaupesianus.* The characters used to diagnose this series include adult SVL < 100 mm, wide toe lamellae (compared with the narrow lamellae observed in the *aequatorialis* series), small head scales, smooth to weakly keeled ventral scales (except in *A. punctatus boulengeri,* which has strongly keeled ventrals), uniform dorsal scalation, and in some species a protuberant snout in males (Williams, 1976b, 1982). Species in the *punctatus* series are distributed in the western lowlands of Panama, Colombia, and Ecuador; the mid- to high elevations of the Andes of Colombia (including the Sierra Nevada de Santa Marta), Venezuela, and Peru (eastern slope); the Amazon region and the Orinoco delta (Williams, 1982; Rodrigues, 1988; Poe and Yañez-Miranda, 2008; Poe et al., 2008, 2009a,b; Ayala and Castro, unpublished).

Roquet *series.* The *roquet* series is composed of 9 species: *A. aeneus, A. blanquillanus, A. bonairensis, A. extremus, A. griseus, A. luciae, A. richardii, A. roquet,* and *A. trinitatis.* The monophyly of this series is supported by karyological (Gorman and Atkins, 1969), morphological (Lazell, 1972; Poe, 2004), and molecular data (cytochrome *b* sequences, Giannassi et al., 2000; ND2 sequences, Creer et al., 2001). Six morphological synapomorphies support the monophyly of this series: 1) greater sexual size dimorphism, 2) an increase in interparietal scale size relative to surrounding scales, 3) an increase in mean number of postmental scales, 4) a straight (as opposed to concave) posterior border of the mental scale, 5) supraorbital semicircles in contact, and 6) interparietal scale in contact with the supraorbital semicircles (Poe, 2004). The *roquet* series is distributed in the southern

Lesser Antilles, from Martinique south to Grenada, and on the islands of La Blanquilla, Bonaire, Tobago, and Trinidad (where *A. aeneus* and *A. trinitatis* have been introduced; Gorman and Dessauer, 1965, 1966) and Guyana (where *A. aeneus* has been introduced; Gorman and Dessauer, 1965; Gorman et al., 1971).

Tigrinus *series.* The *tigrinus* series is composed of 9 species: *A. lamari, A. menta, A. nasofrontalis, A. paravertebralis, A. pseudotigrinus, A. ruizii, A. solitarius, A. tigrinus,* and *A. umbrivagus,* and is characterized by small body size (adult male SVL = 40–60 mm), large smooth head scales, a large interparietal scale bordered by large scales and usually in contact with the supraorbital semicircles, and ventral scales smooth and larger than dorsal scales. Some species exhibit a parietal knob (a small projection of the posteriormost end of the central ridge of the Y-shaped parietal crests), externally visible in some species on the occipital area between the post-interparietal scales and nape scales (Williams, 1976b, 1992). Species in the *tigrinus* series are distributed in high elevations of the Sierra Nevada de Santa Marta (Colombia), the Andes of Colombia (eastern cordillera) and Venezuela, and the Atlantic forest of southeastern Brazil (Williams, 1992; Bernal Carlo and Roze, 2005).

Phenacosaurus. *Phenacosaurus* is composed of 11 species: *A. bellipeniculus, A. carlostoddi, A. euskalerriari, A. heterodermus, A. inderenae, A. neblininus, A. nicefori, A. orcesi, A. tetarii, A. vanzolinii,* and *A. williamsmittermeierorum.* Earlier, *Phenacosaurus* was considered a separate genus from *Anolis* (Barbour, 1920) based on the heterogeneous dorsal scalation (enlarged round flat scales surrounded by smaller scales and granules), the tail structure (probably prehensile), an elevated rim of head plates (casque), digits widely and evenly dilated (such that their sides are parallel), and a "feebly developed" dorsonuchal crest (Lazell, 1969). However, recent phylogenetic analyses (Poe, 1998, 2004; Jackman et al., 1999; Nicholson et al., 2005; Castañeda and de Queiroz, 2011)

inferred these species to be nested within the clades composed of the species assigned to both *Anolis* and *Dactyloa*; therefore, we here consider *Phenacosaurus* another subgroup of *Dactyloa*. *Phenacosaurus* species are distributed in the Andean highlands (between 1,300 and 3,000 m) of Colombia, northern Ecuador, central Peru, and western Venezuela and the isolated tepuis of southeastern Venezuela (Lazell, 1969; Myers et al., 1993; Barros et al., 1996; Myers and Donnelly, 1996; Williams et al., 1996; Poe and Yañez-Miranda, 2007).

MATERIALS AND METHODS

Taxon and Character Sampling

Morphological data were collected for 60 species of *Dactyloa*, representing the subgroups *aequatorialis*, *latifrons*, *laevis*, *Phenacosaurus*, *punctatus*, *roquet*, and *tigrinus*. *Anolis anoriensis* (a recently described species formerly considered part of *A. eulaemus*) was treated as conspecific with *A. eulaemus* given that the description of the former was published after our data analyses were performed. Six species were included as outgroups: one non-*Anolis* Polychrotinae (*Polychrus marmoratus*) and five species representing different series of non-*Dactyloa Anolis* (*Anolis bimaculatus*, *A. cuvieri*, *A. equestris*, *A. occultus*, *A. sagrei*). A total of 643 alcohol-preserved (66 species; 393 males, 250 females), 123 dry (49 species), and 10 cleared and stained (9 species) specimens were examined. Additional data were collected from radiographs of 394 specimens (60 species). External characters were scored for all 66 species, and osteological characters were scored for 63 species (14 of which were only scored from radiographs and thus lack data for all cranial characters). The largest specimens available were examined as a proxy for including adult specimens only. All specimens measured at least 70% of the maximum SVL reported in the literature for the same sex and species (Williams and Acosta, 1996; Savage, 2002). A complete list of specimens examined is given in the Supplementary Appendix 1.[1]

Sixty-six morphological characters were examined, including both continuous characters (those that can be represented by real numbers, e.g., tail length) and discrete characters (those that can only be represented by integer values, including meristic and presence/absence, e.g., number of elongated superciliary scales). This data set includes characters of external morphology and osteology that have been previously used in *Anolis* phylogenetic analyses, have been regarded as diagnostic for *Anolis* subgroups, or have been used historically for species identification (Etheridge, 1959; Williams, 1976b, 1989; de Queiroz, 1987; Etheridge and de Queiroz, 1988; Frost and Etheridge, 1989; Williams et al., 1995; Poe, 1998, 2004; Jackman et al., 1999; Brandley and de Queiroz, 2004). Given that sexual dimorphism occurs in many species of *Anolis* (e.g., Schoener, 1969; Butler et al., 2000, 2007), characters were scored for both males and females and combined only when t tests (for continuous characters) or chi-square tests (for discrete characters) revealed no significant difference between the sexes or when tests could not be performed because sample sizes were too small. When significant differences were found, only data from males were used. However, given the small number of specimens available as dry skeletons and the absence of information on sex for roughly one-third of them, data for characters examined on dry specimens were combined without evaluating whether some of the characters exhibit sexual dimorphism. To ensure character independence, we performed correlation tests between characters. To remove the effects of correlation, we estimated residuals by regressing each variable against the correlated variable; residuals were used in subsequent analyses. In cases where a character was correlated with several others (e.g., SVL, head length,

---

[1] Supplementary material referenced in this paper is available online at www.mcz.harvard.edu/Publications/.

and head width), after residual estimation between two of the variables a second correlation test was performed to ensure that the resulting residuals were not still correlated with the other characters. A list of the characters analyzed, including measurement and coding details, is given in Appendix I.

Character Coding

Continuous Characters. Continuous characters were coded using two methods: the gap-weighting method of Thiele (1993), and Torres-Carvajal's (2007) modification of Wiens (2001) modification of Thiele's method. In Thiele's (1993) method, continuous characters are coded into discrete values while retaining information about order and relative distance between states. Average values per species were standardized by calculating the natural logarithm (ln, or ln + 1 when zero average values were present) to ensure equal variances; then each standardized average value (x) was range-standardized by applying the formula $x_s = [(x - min)/(max - min)] \times (n - 1)$, where min and max are the minimum and maximum among the standardized average values, respectively, and n is the number of states used. One hundred and one states (0–100, $n = 101$) were used in the parsimony analyses (which allows capturing differences of 0.01 between states) and six states (0–5, $n = 6$) were used in the Bayesian analyses (in that 6 is the maximum number of ordered character states allowed in MrBayes v.3.1.2). Use of the term $(n - 1)$ is a modification of Thiele's (1993) equation, in which n was used incorrectly, because using n will lead to the recognition of an additional state (i.e., the total number of states is one greater than the value of the highest numbered state). Therefore, to ensure a total of 101 (or 6) states (including state "0"), $n - 1$ was used instead. Finally, the resulting values were rounded to the nearest integer and treated as states of a multistate ordered character. Wiens (2001) suggested a modification of Thiele's method

using character state (step) matrices to increase the number of character states (then limited in PAUP* v.4.0b10 to 32 states on 32-bit computers). In this method, the term n of Thiele's equation is replaced by 1,000 (the maximum cost in a step matrix in PAUP*), and the difference between range-standardized scores (x_s) determines the cost of transformation between the corresponding states in the step matrix. Given that the default cost of character state transformation in PAUP* is 1, this approach requires weighting non-continuous characters by 1,000 to maintain equal weights among characters. Torres-Carvajal (2007) suggested a modification of Wiens' approach in which the term 1,000 in Wiens' equation is replaced by 1; this practice results in step matrices containing scores between 0 and 1 (rather than 0 and 1,000) and does not involve reweighting the non-continuous characters. Step matrices, in which transformation costs between states are differences between these scores, were generated in PAUP* as described by Torres-Carvajal (2007).

Polymorphic Characters. Polymorphic characters (including presence/absence and meristic) were coded using two different approaches: the MANOB approximation (*Man*hattan distance, *ob*served frequency arrays) of the frequency parsimony method described by Berlocher and Swofford (1997), and the majority or modal condition. Berlocher and Swofford's (1997) method was originally described for allele frequency data (see also Swofford and Berlocher, 1987) but has been applied to polymorphic morphological characters (Wiens, 2000; Brandley and de Queiroz, 2004; Torres-Carvajal, 2007). Under this approach, each taxon with a unique combination of allele (character state) frequencies is assigned a different character state, and changes between states are assigned costs equal to the Manhattan distances between those states using step matrices, which are analyzed under the parsimony criterion. In the MANOB method, the reconstructed hypothetical ancestors are required to have

a state (an array of allele [character state] frequencies) from the pool of states observed in the terminal taxa. Under the alternative majority or modal method, a polymorphic species is assigned the most common state in the individuals examined. The modal coding method was used despite being outperformed by the frequency coding method (Wiens, 1995, 1998; Wiens and Servedio, 1997) to perform Bayesian analyses because, currently, the only models available for morphological characters in MrBayes do not allow unequal rates (analogous to differential parsimony costs) among states. Cases with a 50:50 distribution of states were treated as partial uncertainty; that is, from the subset of states observed in a taxon, the software assigns to the taxon the state that minimizes length on a given tree.

Comparison of Coding Methods. To compare alternative coding methods, we estimated phylogenetic information content using the g_1 statistic (Fisher, 1930; Sokal and Rohlf, 1995; Zar, 1999). The g_1 statistic measures the skewness of a distribution and has been used to test for phylogenetic signal in data sets as part of the tree length distribution skewness test (Hillis, 1991; Huelsenbeck, 1991; Hillis and Huelsenbeck, 1992). The test is based on the observation that the shape of the distribution of tree lengths (for all possible trees, or for a random subset when it is not feasible to evaluate the lengths of all possible trees) provides information about the presence of phylogenetic signal in the data (Hillis, 1991). Data sets with phylogenetic signal show a left-skewed distribution of lengths ($g_1 < 0$), which indicates that there are fewer solutions near the best solution than anywhere else in the distribution (Hillis and Huelsenbeck, 1992). We evaluated phylogenetic signal in each of our data sets by comparing the observed g_1 values against a distribution obtained from data with no phylogenetic signal. To construct the null distribution, we used Mesquite v.2.75 (Maddison and Maddison, 2011) to perform 1,000 random permutations (by shuffling

states within characters among taxa) of data sets containing only those characters coded with the method being tested. We calculated the g_1 scores for the randomized matrices by evaluating 10,000 random trees in PAUP*. Coding methods whose g_1 scores fell outside the 95% confidence interval were considered to have significant phylogenetic signal.

Besides testing for phylogenetic signal in each data set, we evaluated differences in amounts of phylogenetic signal among data sets based on different coding methods. We did this by directly comparing g_1 values as estimates of the amount of hierarchical information recorded by each coding method. Values were compared between methods for coding continuous characters (Thiele's [1993] gap-weighting method with 101 character states versus Torres-Carvajal's [2007] version of the gap-weighting method versus Thiele's [1993] gap-weighting method with 6 character states) and between methods for coding polymorphic characters (frequency arrays using Manhattan distance step matrices versus using modal conditions). The g_1 values were estimated in PAUP* from data sets containing only those characters coded with the method being tested; g_1 values for each method were estimated from 10 samples of 500,000 random trees, and differences between the g_1 values were evaluated using t tests. To further assess differences (or the lack thereof) between the different coding methods, we performed reciprocal topology tests (Larson, 1998), in which for each data set (or portion thereof), the optimal tree inferred from that data set was compared (using two-tailed Wilcoxon signed-ranks tests) with the optimal trees inferred from data sets based on alternative coding methods.

Morphological Data Sets and Phylogenetic Analyses

Based on the results of the statistical tests comparing g_1 values, we selected Torres-Carvajal's (2007) version of the gap-weight-

ing method for coding continuous characters and the frequency arrays using Manhattan distance step matrices for coding polymorphic characters. This morphology-only data set will be referred to as the Torres-freq data set (See Supplementary Appendix 2) and was used for all subsequent parsimony analyses. A second morphology-only data set was constructed with continuous characters coded using Thiele's (1993) gap-weighting method with six character states and polymorphic characters coded using the modal condition. This data set, hereafter referred to as Thiele6-mode (See Supplementary Appendix 3), was specifically constructed to fulfill the requirements of running analyses in MrBayes (a maximum of six ordered character states and only rates [analogous to costs] of 0 and 1). Both data sets include 66 species and 66 characters (33 external, 33 osteological; 20 continuous, 31 discrete polymorphic, and 15 discrete non-polymorphic; Appendix I).

Parsimony analyses were performed on the Torres-freq data set using PAUP* (Swofford, 2002) with equal costs for state transformations, except for continuous and polymorphic characters (20 and 31 characters, respectively), in which differential costs were implemented with step matrices (see Supplementary Appendix 4), and for discrete (non-continuous, non-polymorphic) multistate ordered characters, which were weighted so that the range of each character equals 1. For each data set, a heuristic search with 1,000 replicates of random stepwise addition was performed, with all additional options left on default settings. Nodal support was assessed with non-parametric bootstrap resampling (BS; Felsenstein, 1985) using 100 bootstrap pseudoreplicates and heuristic searches with 50 replicates of random stepwise addition (remaining options were left on defaults) for each bootstrap pseudoreplicate.

Bayesian analyses were performed on the Thiele6-mode data set in MrBayes (Ronquist and Huelsenbeck, 2003) using Mkv and Mkv + rate variation (rv) models for morphological data (Lewis, 2001). The Mkv model is analogous to the Jukes Cantor (JC) model of molecular sequence evolution, which assumes equal state frequencies, equal transformation rates between states, and equal rates among characters. The Mkv + rv model allows rate heterogeneity among characters using the symmetric Dirichlet (for multistate characters) and beta (for binary characters) distributions, in which one parameter determines the shape of the distribution of rates. This approach is similar to using the gamma (Γ) distribution to model rate variation among sites in molecular sequence data. Four independent runs—each with four Markov chains, a random starting tree, and default heating settings—were run for 10 million generations. Trees were sampled with a frequency of one every 1,000 generations. The first 25% of the trees were discarded as the "burn-in" phase. Stationarity in the post-burn-in sample was confirmed following the same procedures outlined in Castañeda and de Queiroz (2011). The maximum clade credibility tree (i.e., the tree with the highest product of posterior clade probabilities) was obtained using the TreeAnnotator package of BEAST v.1.6.2 (Drummond and Rambaut, 2007). Bayesian posterior clade probabilities (PP) were calculated based on the post-burn-in sample of trees for all four independent runs combined. Nodes with posterior probabilities greater than 0.95 were considered strongly supported, with the precaution that PP might overestimate clade support, especially in short internodes (Suzuki et al., 2002; Alfaro et al., 2003; Lewis et al., 2005). Bayes Factors (Kass and Raftery, 1995; Pagel and Meade, 2005) were used to compare the results obtained with the Mkv and Mkv + rv models for the morphological characters.

Combined Data Sets and Phylogenetic Analyses

The same two morphological data sets used in the morphology-only analyses were combined with the DNA sequence data (40 species of *Dactyloa* and six outgroup species) from Castañeda and de Queiroz (2011). Two

species for which DNA sequence data were available, *Anolis* sp1 and *A.* sp2, were excluded from our combined data sets because of the absence of morphological data. DNA sequence data included three gene regions: 1) the mitochondrial NADH dehydrogenase subunit II (ND2), five transfer RNAs (tRNA[Trp], tRNA[Ala], tRNA[Asn], tRNA[Cys], tRNA[Tyr]), and the origin for light strand replication (O_L, ~1,500 bases); 2) a fragment of the mitochondrial cytochrome oxidase subunit I (COI, ~650 bases), and 3) the nuclear recombination activating gene (RAG-1, ~2,800 bases). The combined data sets included 60 species of *Dactyloa*, 20 of which were missing molecular data, and 6 outgroup species (for a total of 66 species). Hereafter, the combined data sets will be referred to as CombTorres-freq and CombThiele6-mode, respectively. Parsimony analysis of the combined data set was run under the same conditions used for the morphology-only data sets. For the Bayesian analysis, the data were partitioned into morphological and molecular data. The latter were further partitioned (based on the results of Castañeda and de Queiroz [2011]) by gene region and, within each region, by codon position and tRNAs (ND2: four partitions; COI: three partitions, RAG-1: three partitions). The model of evolution for each molecular partition was selected based on the Akaike Information Criterion (AIC) as implemented in Modeltest (Posada and Crandall, 1998) v.3.7. For the morphological partition, the model of evolution was selected based on the Bayes factor scores from the morphology-only analyses (see above). Bayesian analyses were run under the same conditions used for the morphology-only analyses, except that the number of runs was increased to five and the number of generations was increased to 50 million to ensure that stationarity and convergence between chains were achieved.

Tests of Phylogenetic Hypotheses

We tested hypotheses concerning the monophyly of: 1) *Dactyloa* including *Phenacosaurus*, 2) *Dactyloa* excluding *Phenaco-saurus* (as traditionally circumscribed), 3) subgroups described based on morphological characters for which we had adequate taxon samples: *aequatorialis*, *latifrons* (as traditionally circumscribed), *Phenacosaurus* (as traditionally circumscribed), *punctatus*, *roquet*, and *tigrinus*, and 4) the clades inferred by Castañeda and de Queiroz (2011) based on molecular data: eastern, *latifrons*, *Phenacosaurus*, *roquet*, and western. Given that we obtained data for only one species of the *laevis* series, no tests were performed regarding the monophyly of that series.

Phylogenetic hypotheses were tested using parsimony-based (Templeton, 1983) and Bayesian (Larget and Simon, 1999; Huelsenbeck et al., 2001) topological tests. The data sets (morphology-only and combined) with polymorphic characters coded using Torres-Carvajal's (2007) method and continuous characters coded with frequency arrays using Manhattan distance step matrices were selected to perform the parsimony-based tests. For the Bayesian tests, the data sets (morphology-only and combined) with continuous characters coded using Thiele's (1993) method with six character states and polymorphic characters coded using the modal condition were used.

For the parsimony-based tests, optimal trees resulting from parsimony analyses of the morphology-only and combined data sets were compared with optimal trees resulting from parsimony analyses of the same data sets incorporating each hypothesis as a topological constraint (performed using the same search conditions as for the unconstrained analyses). In cases in which the hypothesis of interest (e.g., previously recognized taxa based on morphological data or clades inferred based on molecular data) was obtained in the optimal unconstrained trees, the alternative hypothesis of non-monophyly was tested. Topologies corresponding to the hypotheses of interest were constructed using MacClade (Maddison and Maddison, 2001) v.4.07 and imported into PAUP* as topological constraints. Monophyly constraints were used for the hypotheses of previously recognized

taxa based on morphological characters, because all species included in the tests had been previously assigned to a group. Backbone constraints were used for the hypotheses of clades recognized based on molecular data, because the species for which only morphological data were available had not previously been assigned to any of the clades. Wilcoxon signed-ranks (WSR) tests (Templeton, 1983) were used to determine whether the optimal unconstrained tree is significantly different from the hypothesis corresponding to the constraint (Larson, 1998) and were performed as two-tailed tests in PAUP*. In the Bayesian tests, trees contained in the 95% credible set of trees from the post-burn-in sample for each data set were loaded into PAUP* and filtered based on topological constraints corresponding to each hypothesis. Topologies that were not present within the 95% credible set of trees (i.e., those that resulted in no trees retained under a given topological constraint) were considered rejected by the test.

RESULTS

Comparisons Between Coding Methods

All the methods resulted in characters with significant phylogenetic signal (as assessed by g_1) when compared with randomly permuted data ($P < 0.001$ for all coding methods). Of the methods used to code continuous characters, Torres-Carvajal's (2007) version of the gap-weighting method resulted in the most left-skewed distributions (g_1 values most negative; $g_1 = -0.301 \pm 0.004$), indicating that this method yielded characters that contain the most phylogenetic information. The method of Thiele (1993), with 101 character states, followed ($g_1 = -0.269 \pm 0.003$), and the same method with 6 character states resulted in the least skewed distributions ($g_1 = -0.253 \pm 0.003$). Comparing the coding methods used for polymorphic characters, the frequency arrays using Manhattan distance step matrices resulted in larger negative g_1 values ($g_1 = -0.175 \pm 0.004$) than did the modal condition

method ($g_1 = -0.156 \pm 0.004$). Statistical (t) tests indicated significant differences between all coding methods for both continuous ($P < 0.001$ for all comparisons) and polymorphic ($P < 0.001$) characters in the amount of phylogenetic information recorded.

Phylogenetic Analyses

In all Bayesian analyses, the average standard deviation of split frequencies of converging chains reached values lower than 0.06, and the potential scale reduction factor (PSRF) of all runs combined reached 1.0 for most parameters. Bayes factors (BF) favored the Mkv + rv model over the Mkv model (BF = 194.46) in the analyses of morphology-only data sets, although the majority-rule consensus tree inferred using the simpler Mkv model was more resolved and contained more moderately to strongly supported nodes. With the Mkv model, 31 nodes were resolved, 14 of which had moderate (PP ≥ 0.75) to strong (PP ≥ 0.95) support (PP = 0.77–0.99; tree not shown); with the Mkv + rv model, 24 nodes were resolved, 12 of which had moderate support (PP = 0.76–0.94; tree not shown). In the Bayesian analyses of the combined data set, the five independent runs did not all converge onto the same likelihood values; instead, three runs converged onto a lower negative natural log likelihood score, and the remaining two converged onto a higher score. However, the relationships among species in the majority-rule topologies resulting from the two sets of runs were very similar, differing only in one poorly supported node. Nodal support and substitution model parameter values were also very similar, except for the rate variation among sites (alpha) and the rate multiplier (m) for several partitions. For this reason, two of the five runs were discarded, and only the three with lower negative natural log likelihood scores were used for tree estimation and hypotheses testing.

Morphology-only Data Sets. The parsimony analysis (Torres-freq data set) yielded a single fully resolved most parsimonious tree of 466.63 steps (CI = 0.22, RI = 0.53; Fig. 1). In this tree, *Dactyloa* is not inferred

to be monophyletic, and non-*Dactyloa* *Anolis* outgroup species are located in three different places (two within *Dactyloa*). These results are poorly supported (BS = 0%), and only two small, deeply nested clades in the entire tree are moderately supported (BS = 75–81%). All species previously placed in the genus *Phenacosaurus* were included in a clade (BS = 0%) that also contained *A. microtus* and *A. proboscis* (traditionally placed in the *latifrons* and *laevis* series, respectively). The *Phenacosaurus* clade, as defined in Castañeda and de Queiroz (2011), which includes all the *Phenacosaurus* species sampled in their study except *A. neblininus*, was inferred with the addition of *A. tetarii* (for which no molecular data are available) with low nodal support (BS = 44%). The Bayesian analysis (Thiele6-mode data set) under the Mkv + rv model, resulted in a fully resolved but poorly supported maximum clade credibility tree (Π PP = 1.497 $\times$ 10^{-12}; Fig. 2). *Dactyloa* was not inferred to be monophyletic, and non-*Dactyloa* *Anolis* outgroup species were located in four different places in the tree (all within *Dactyloa*). Species previously placed in the genus *Phenacosaurus*, except *A. carlostoddi* and *A. neblininus*, formed a paraphyletic group at the base of the tree. In both parsimony and Bayesian analyses, neither the series based on morphological characters nor the clades based on molecular data (except the *Phenacosaurus* clade in the parsimony analyses) were inferred.

Combined Data Sets. The parsimony analysis (CombTorres-freq data set) yielded a single fully resolved tree of 10,431.86 steps (CI = 0.30, RI = 0.43; Fig. 3). The Bayesian analysis (CombThiele6-mode data set) resulted in a fully resolved maximum clade credibility tree (Π PP = 1.449 $\times$ 10^{-8}; Fig. 4). In both analyses, *Dactyloa* was inferred to be monophyletic with low to moderate support (BS = 51%, PP = 0.81). Eleven unambiguous morphological synapomorphies support the monophyly of *Dactyloa* (Supplementary Appendix 5); however, this interpretation should be made with

caution because it is most likely the result of biased outgroup sampling. For example, three out of five outgroup species have very large body sizes (maximum male SVL > 123 mm; Williams and Acosta, 1996) compared with most *Anolis* species, and as a result, a decrease in maximum male SVL is inferred as a synapomorphy of *Dactyloa*. In the parsimony analysis, the major clades inferred by Castañeda and de Queiroz (2011)—that is, eastern, *latifrons*, *Phenacosaurus*, *roquet*, and western—were inferred with weak to strong nodal support (BS = 6–93%). Similarly, in the Bayesian analysis, all five clades were inferred with weak to strong nodal support (0.15 < PP < 0.97). For the purpose of assigning species to these clades (eastern, *latifrons*, *roquet*, *Phenacosaurus*, and western), the clades were delimited using nodes bounded by species for which molecular data were available (e.g., the eastern clade is defined as the clade originating with the last common ancestor of a particular set of species inferred from molecular data [Castañeda and de Queiroz, 2011], thus excluding species outside that node that are more closely related to the eastern clade than to any of the other four mutually exclusive clades). In both parsimony and Bayesian analyses, the same sets of additional species, for which only morphological data were available, were included in the western and *Phenacosaurus* clades. In the case of the *latifrons* and eastern clades, different sets of additional species (for which only morphological characters were available) were inferred in the parsimony and Bayesian analyses. No additional species were included in the *roquet* clade in either analysis. In the following paragraphs, the species composition of each clade is detailed, with daggers (†) indicating species lacking molecular data. The synapomorphies that support each clade, inferred based on the parsimony analysis, are given in Supplementary Appendix 5.

The western clade was inferred with weak to moderate support in the parsimony and Bayesian analyses (BS = 25%, PP = 0.82; Figs. 3, 4) and is supported by nine
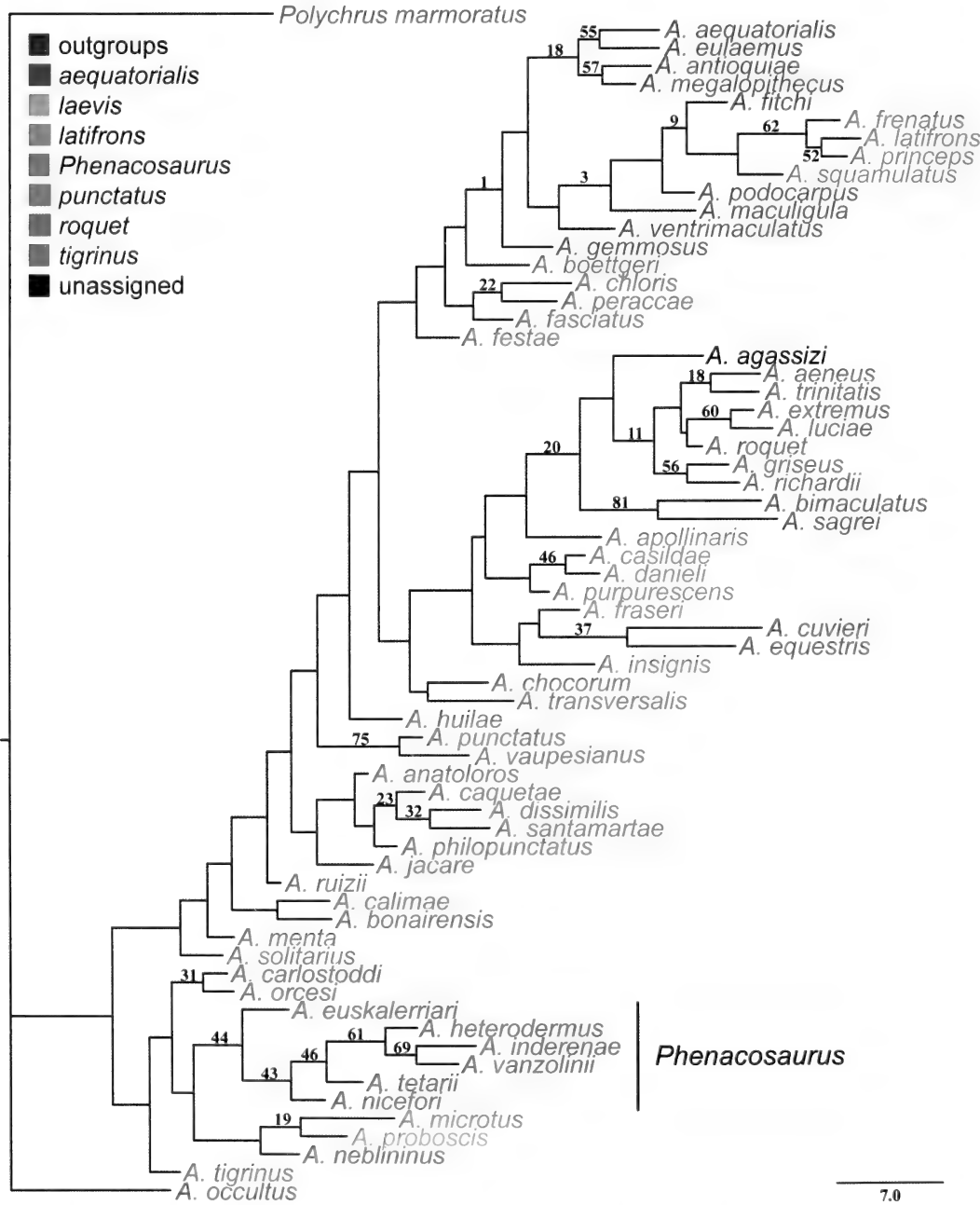
Figure 1. Most parsimonious tree inferred with the Torres-freq morphology-only data set (TL = 466.63, CI = 0.22, RI = 0.53). Bootstrap support (BS) values are shown above branches; missing values above branches indicate BS = 0%. The traditional species groups/series based on morphological characters (see text for details) are differentiated by color. One major *Dactyloa* subclade, of those described based on molecular data (see text for details), is indicated on the right.

Figure 2.   Bayesian maximum clade credibility tree inferred with the Thiele6-mode morphology-only data set using the Mkv + rv model. Bayesian posterior probabilities are shown above branches. The traditional species groups/series based on morphological characters (see text for details) are differentiated by color.

Polychrus marmoratus

outgroups
aequatorialis
laevis
latifrons
Phenacosaurus
punctatus
roquet
tigrinus
unassigned

69 — A. aequatorialis
— A. eulaemus
27 — A. antioquiae†
47 A. megalopithecus†
41 — A. gemmosus
— A. ventrimaculatus
25 — A. chloris
75 A. festae
71 A. peraccae
18 47 A. fasciatus†
A. boettgeri†
6
17 50 A. fitchi
A. squamulatus†
A. podocarpus
A. huilae
32 A. agassizi
63 A. insignis
A. microtus
26 A. apollinaris†
A. fraseri
A. chocorum
20 16 A. frenatus
80 A. latifrons†
12 42 A. princeps
92 A. casildae
A. maculigula
A. danieli
A. purpurescens†
A. philopunctatus†
A. caquetae†
A. dissimilis†
22 A. santamartae†
14 A. calimae
19 A. menta†
13 12 A. neblininus
A. solitarius†
A. ruizii†
69 A. anatoloros
24 A. jacare
30 A. carlostoddi†
19 A. orcesi†
6 A. tigrinus
77 A. punctatus
61 A. vaupesianus†
A. transversalis
99 A. aeneus
72 99 A. extremus
A. roquet
97 A. richardii
93 90 A. griseus
A. trinitatis
91 A. bonairensis
A. luciae
A. euskalerriari
87 89 A. heterodermus
76 57 A. inderenae
A. vanzolinii
58 83 A. tetarii†
A. nicefori
A. proboscis†
94 A. bimaculatus
43 A. sagrei
A. cuvieri
A. equestris
A. occultus

51

western

latifrons

eastern
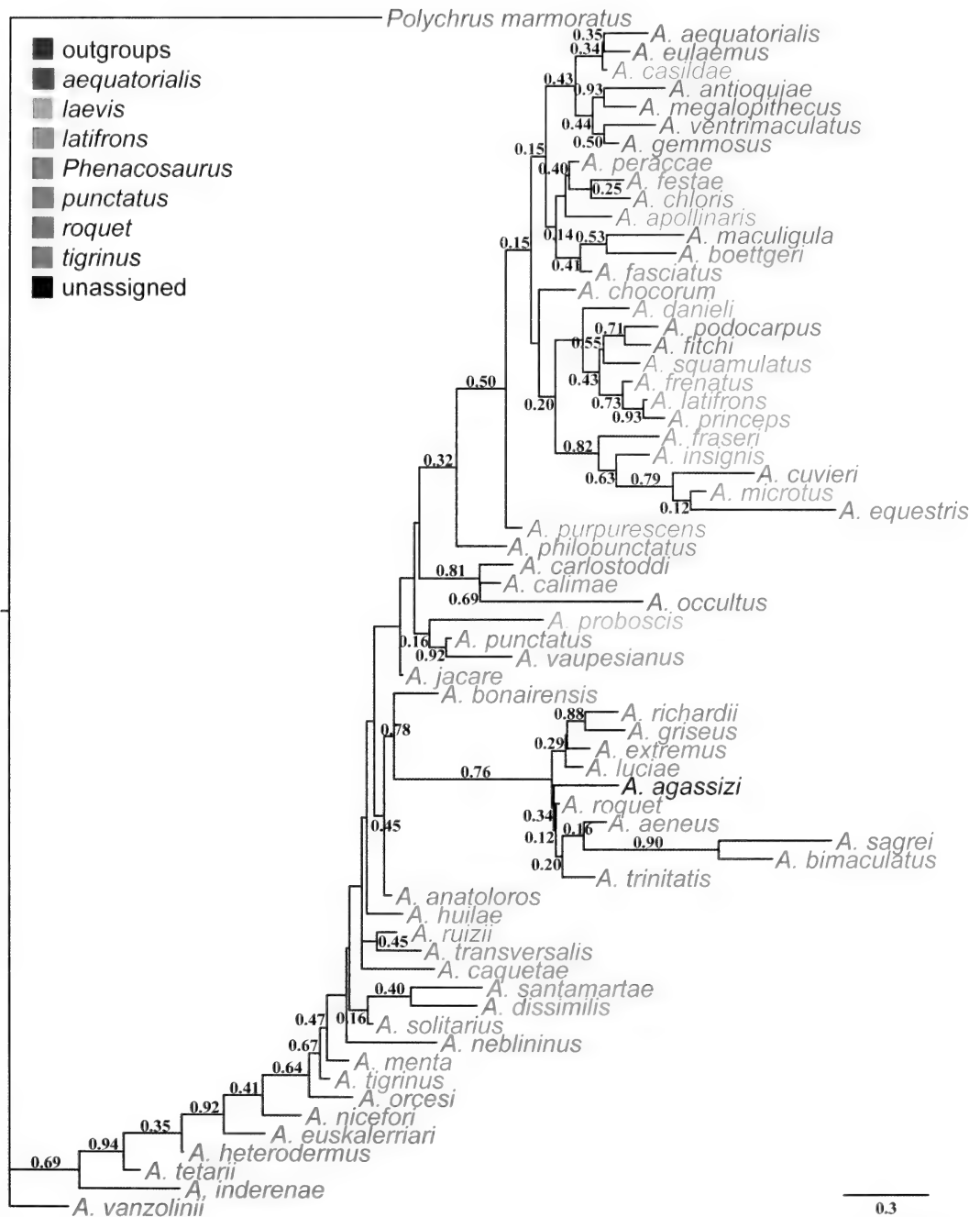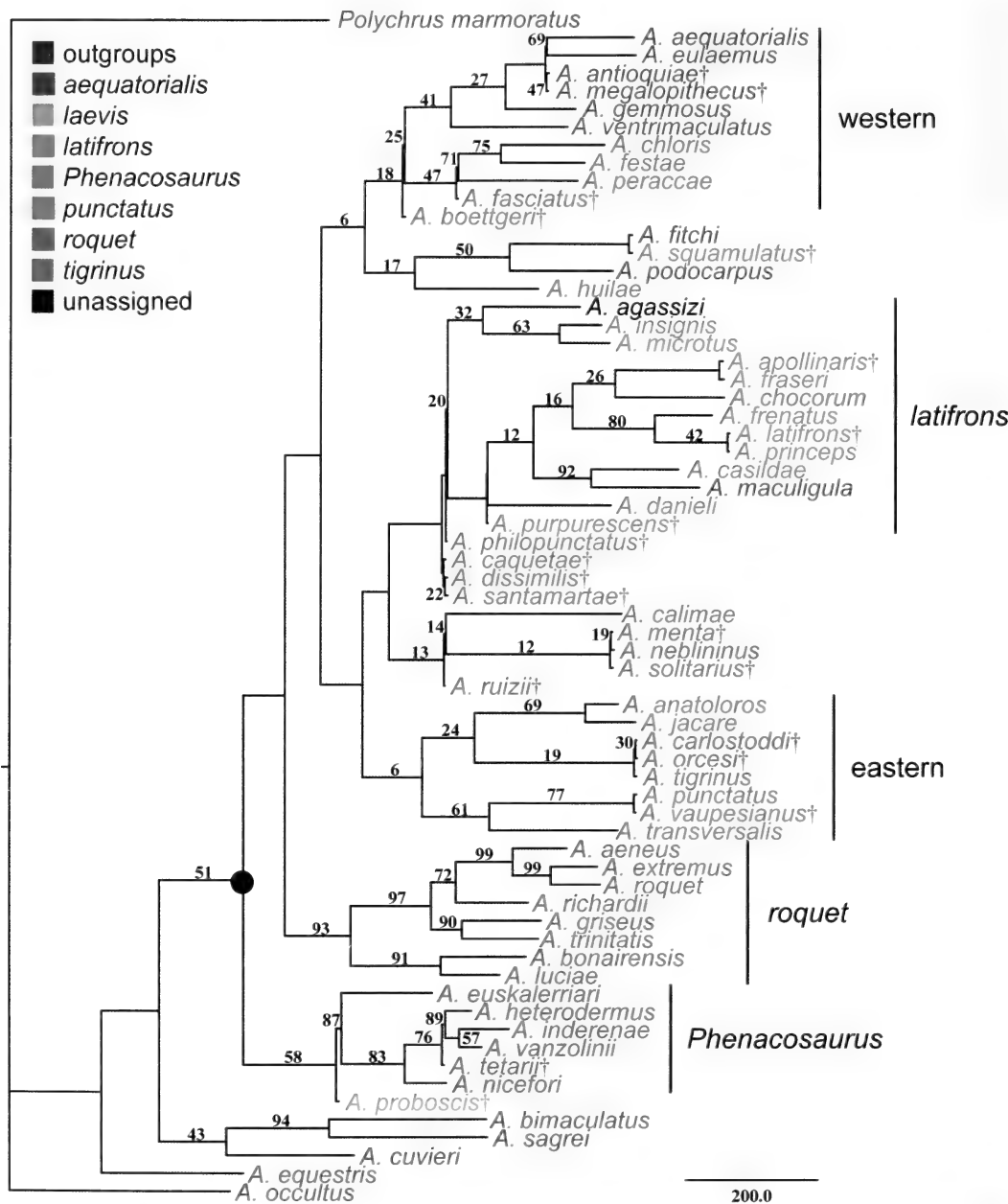
roquet

Phenacosaurus

200.0

Figure 3.   Most parsimonious tree inferred with the CombTorres-freq combined data set (TL = 10,431.86, CI = 0.30, RI = 0.43). Bootstrap support (BS) values are shown above branches; missing values above branches indicate BS = 0%. Daggers (†) following species names indicate the species for which only morphological data were available. The traditional species groups/ series based on morphological characters (see text for details) are differentiated by color. Major *Dactyloa* subclades described based on molecular data (see text for details) are indicated on the right. The *Dactyloa* clade is indicated with a black dot on the corresponding node.

morphological characters (Supplementary Appendix 5). In both analyses, this clade is composed of the same 10 species: *A. aequatorialis*, *A. antioquiae*†, *A. chloris*, *A. eulaemus*, *A. fasciatus*†, *A. festae*, *A. gemmosus*, *A. megalopithecus*†, *A. peraccae*, and *A. ventrimaculatus*. Within this clade, the topologies are largely congruent, with the exception of the position of *A. gemmosus* and the internal relationships within the clade composed of *A. chloris*, *A. fasciatus*, *A. festae*, and *A. peraccae*. Additionally, in the parsimony analysis, *A. boettgeri* is inferred with weak support as the sister group of the western clade (BS = 18%), whereas in the Bayesian analysis, the sister taxon of the western clade is the clade (*A. boettgeri*, *A. huilae*) (PP = 0.49).

The *latifrons* clade was inferred in the parsimony analysis with low nodal support (BS = 20%; Fig. 3) and is supported by five morphological characters (Supplementary Appendix 5); it is composed of 13 species: *A. agassizi*, *A. apollinaris*†, *A. casildae*, *A. chocorum*, *A. danieli*, *A. fraseri*, *A. frenatus*, *A. insignis*, *A. maculigula*, *A. microtus*, *A. latifrons*†, *A. princeps*, and *A. purpurescens*†. In the Bayesian analysis, the *latifrons* clade was inferred with low support (PP = 0.46; Fig. 4) and is composed of the same set of species as the parsimony analysis with the addition of *A. squamulatus*. Three mutually exclusive subclades were inferred by both analyses: (*A. agassizi* (*A. microtus*, *A. insignis*)) (BS = 32%, PP = 0.61), (*A. casildae*, *A. maculigula*) (BS = 92%, PP = 0.62), and (*A. frenatus* (*A. latifrons*, *A. princeps*) (BS = 80%, PP = 0.72). In both analyses, *A. philopunctatus* was inferred as the sister taxon of the *latifrons* clade.

The eastern clade was inferred in the parsimony analysis (Fig. 3) with low nodal support (BS = 6%) and is supported by seven morphological characters (Supplementary Appendix 5); it is composed of eight species: *A. anatoloros*, *A. carlostoddi*†, *A. jacare*, *A. orcesi*†, *A. punctatus*, *A. tigrinus*, *A. transversalis*, and *A. vaupesianus*†. In the Bayesian analysis (Fig. 4), the eastern clade was inferred with low nodal

support (PP = 0.15) with 11 species: *A. anatoloros*, *A. dissimilis*†, *A. jacare*, *A. menta*†, *A. punctatus*, *A. ruizii*†, *A. santamartae*†, *A. solitarius*†, *A. tigrinus*, *A. transversalis*, and *A. vaupesianus*†. Despite the differences in species composition, two subclades were inferred in both analyses (Figs. 3, 4): (*A. transversalis* (*A. punctatus*, *A. vaupesianus*)) (BS = 61%, PP = 0.71) and (*A. anatoloros*, *A. jacare*) (BS = 69%, PP = 0.94).

The *roquet* clade was inferred with strong support in both parsimony and Bayesian analyses (BS = 93%, PP = 0.97; Figs. 3, 4) and is supported by 16 morphological characters (Supplementary Appendix 5). In both analyses, this clade is composed of the same eight species: *A. aeneus*, *A. bonairensis*, *A. extremus*, *A. griseus*, *A. luciae*, *A. richardii*, *A. roquet*, and *A. trinitatis*. The topology within this clade is identical for both phylogenetic analyses, with all nodes moderately to strongly supported (BS ≥ 72%, PP ≥ 0.96).

The *Phenacosaurus* clade was inferred with moderate support in both parsimony and Bayesian analyses (BS = 87%; PP = 0.84; Figs. 3, 4) and is supported by 19 morphological characters (Supplementary Appendix 5). In both analyses, this clade is composed of the same six species, *A. euskalerriari*, *A. heterodermus*, *A. inderenae*, *A. nicefori*, *A. tetarii*†, and *A. vanzolinii*, all previously placed in the genus *Phenacosaurus*. The relationships within this clade are identical between parsimony and Bayesian analyses; however, in the parsimony analysis, *A. proboscis* is inferred as its sister group (BS = 58%), whereas in the Bayesian analysis, *A. orcesi* is inferred as its sister group with moderate support (PP = 0.87), and *A. proboscis* is the sister group to that (*A. orcesi*, *Phenacosaurus*) clade (PP = 0.43).

In both parsimony and Bayesian analyses, nine species, *A. boettgeri*†, *A. calimae*, *A. caquetae*†, *A. fitchi*, *A. huilae*, *A. neblininus*, *A. philopunctatus*†, *A. podocarpus*, and *A. proboscis*†, were not included in any of the five major clades within *Dactyloa* when those clades are treated as originating in the last
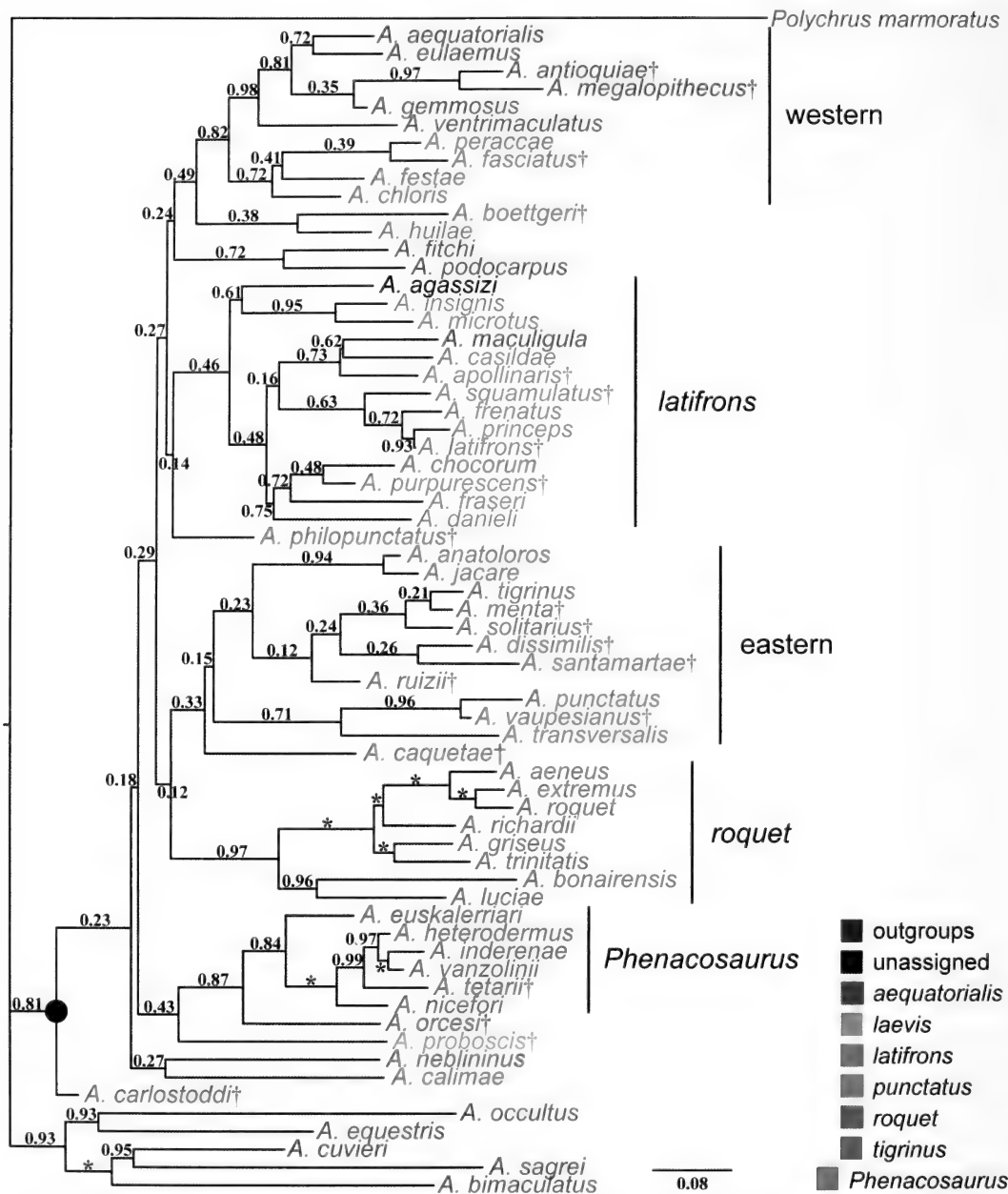
Figure 4.   Bayesian maximum clade credibility tree inferred with the CombThiele6-mode combined data set. Bayesian posterior probabilities (PP) are shown above branches; asterisks (*) indicate PP = 1.0. Daggers (†) following species names indicate the species for which only morphological data were available. The traditional species groups/series based on morphological characters (see text for details) are differentiated by color. Major *Dactyloa* subclades described based on molecular data (see text for details) are indicated on the right. The *Dactyloa* clade is indicated with a black dot on the corresponding node.

Table 1. Results of the Wilcoxon signed ranks (WSR) and Bayesian (B) tests of phylogenetic hypotheses of previously recognized taxa based on morphological characters (top) and of clades inferred based on molecular data (bottom) on the basis of morphological data only (Torres-freq, Thiele6-mode). For the Torres-freq data set, differences between tree lengths of unconstrained analyses and those constrained to correspond to each tested hypothesis (ΔTL) and WSR *P*-values are given. For the Bayesian tests of the Thiele6-mode data set, the presence (+) or absence (−) of the alternative topology in the 95% credible set of trees is shown. Significant results are indicated with an asterisk (*).

| | Dataset | | |
| | Torres-freq | | Thiele6-mode |
Test Hypothesis	ΔTL	WSR *P*-Value	B
Traditional groups			
Dactyloa	6.86	0.280	−*
Dactyloa excluding *Phenacosaurus*[a]	13.44	0.001*	−*
aequatorialis series	0.99	0.697	−*
latifrons series[b]	7.33	0.131	−*
punctatus series	9.32	0.332	−*
roquet series	0.84	0.851	+
tigrinus series	2.89	0.175	−*
Phenacosaurus[a]	2.33	0.629	−*
Groups based on molecular data			
Eastern clade	2.58	0.468	−*
latifrons clade	8.42	0.145	−*
Phenacosaurus clade	n/a[c]	n/a[c]	+
Phenacosaurus clade not monophyletic	0.44	0.827	n/a[c]
roquet clade	0.84	0.851	+
Western clade	1.05	0.969	−*

[a] As traditionally circumscribed, which includes (of the species sampled) *A. carlostoddi*, *A. euskalerriari*, *A. heterodermus*, *A. inderenae*, *A. neblininus*, *A. nicefori*, *A. orcesi*, *A. tetarii*, and *A. vanzolinii*.

[b] As traditionally circumscribed, which includes (of the species sampled) *A. apollinaris*, *A. casildae*, *A. danieli*, *A. fraseri*, *A. frenatus*, *A. insignis*, *A. latifrons*, *A. microtus*, *A. princeps*, *A. purpurescens*, and *A. squamulatus*.

[c] Not applicable: the hypothesis in question was present in the optimal (unconstrained) tree(s), so the alternative hypothesis (monophyly or non-monophyly) was tested instead.

common ancestors of the species for which molecular data were available (see above). However, *A. boettgeri*†, *A. fitchi*, *A. huilae*, and *A. podocarpus* were consistently placed closer to the western clade than to any of the four other major clades; *A. philopunctatus*† was consistently placed closer to the *latifrons* clade, and *A. proboscis*† was consistenty placed closer to *Phenacosaurus*. Additionally, the positions of *A. carlostoddi*†, *A. dissimilis*†, *A. menta*†, *A. orcesi*†, *A, ruizii*†, *A. santamartae*†, *A. solitarius*†, and *A. squamulatus*† were inconsistent (particularly relative to the five major clades) between parsimony and Bayesian analyses.

Tests of Phylogenetic Hypotheses

The WSR and Bayesian tests performed on the morphology-only data sets (Torres-freq and Thiele6-mode, respectively) yielded very different results (Table 1): the WSR test failed to reject the monophyly of *Dactyloa* and each of the subgroups previously described based on morphological characters: *aequatorialis*, *latifrons*, *punctatus*, *roquet*, *tigrinus*, and *Phenacosaurus*; in contrast, the Bayesian test rejected the monophyly of *Dactyloa* and all of the previously recognized subgroups except the *roquet* series. Of the hypotheses tested, only the monophyly of *Dactyloa* excluding *Phenacosaurus* was rejected by both the WSR and Bayesian tests. When testing the clades inferred based on molecular data (Castañeda and de Queiroz, 2011) with the morphological data, contradictory results between the parsimony and Bayesian approaches were found again (Table 1): monophyly of the eastern, *latifrons*, *roquet*, and western clades was not rejected with the

TABLE 2.   RESULTS OF THE WILCOXON SIGN RANKS (WSR) AND BAYESIAN (B) TESTS OF PHYLOGENETIC HYPOTHESES OF PREVIOUSLY RECOGNIZED TAXA BASED ON MORPHOLOGICAL CHARACTERS (TOP) AND OF CLADES INFERRED BASED ON MOLECULAR DATA (BOTTOM) ON THE BASIS OF COMBINED MORPHOLOGICAL AND MOLECULAR DATA (COMBTORRES-FREQ, COMBTHIELE6-MODE). FOR THE COMBTORRES-FREQ DATA SET, DIFFERENCES BETWEEN TREE LENGTHS OF UNCONSTRAINED ANALYSES AND THOSE CONSTRAINED TO CORRESPOND TO EACH TESTED HYPOTHESIS (ΔTL) AND WSR P-VALUES ARE GIVEN. FOR THE BAYESIAN TESTS OF THE COMBTHIELE6-MODE DATA SET, THE PRESENCE (+) OR ABSENCE (−) OF THE ALTERNATIVE TOPOLOGY IN THE 95% OF CREDIBLE SET OF TREES IS SHOWN. SIGNIFICANT RESULTS ARE INDICATED WITH AN ASTERISK (*).

	Dataset		
	CombTorres-freq		CombThiele6-mode
Test Hypothesis	ΔTL	WSR P-Value	B
Groups based on morphological data			
Dactyloa not monophyletic	1.47	0.712	+
Dactyloa excluding *Phenacosaurus*[a]	44.83	0.003*	−*
aequatorialis series	135.33	<0.001*	−*
latifrons series[b]	83.91	<0.001*	−*
punctatus series	170.43	<0.001*	−*
roquet series not monophyletic	35.09	0.016*	+
tigrinus series	4.82	0.336	+
Phenacosaurus group[a]	21.35	0.253	+
Groups based on molecular data			
Eastern clade not monophyletic	17.63	0.366	−*
latifrons clade not monophyletic	25.56	0.054	−*
Phenacosaurus clade not monophyletic	59.81	<0.001*	−*
roquet clade not monophyletic	25.11	0.077	−*
Western clade not monophyletic	9.90	0.687	−*

[a] As traditionally circumscribed, which includes (of the species sampled) *A. carlostoddi, A. euskalerriari, A. heterodermus, A. inderenae, A. neblininus, A. nicefori, A. orcesi, A. tetarii,* and *A. vanzolinii.*
[b] As traditionally circumscribed, which includes (of the species sampled) *A. apollinaris, A. casildae, A. danieli, A. fraseri, A. frenatus, A. insignis, A. latifrons, A. microtus, A. princeps, A. purpurescens,* and *A. squamulatus.*

WSR test, but it was rejected—except in the case of the *roquet* series—with the Bayesian test. The parsimony analysis indicated monophyly of the *Phenacosaurus* clade, but the WSR test failed to reject its non-monophyly; conversely, the Bayesian analysis indicated non-monophyly of the group, but the Bayesian test failed to reject its monophyly.

With the combined data sets, the WSR and Bayesian tests yielded mostly congruent results concerning taxa recognized previously on the basis of morphological characters (Table 2). The non-monophyly of *Dactyloa* (given that this hypothesis was inferred in the optimal tree) and the monophyly of the *tigrinus* series and *Phenacosaurus* were not rejected by either test. In contrast, both tests rejected the monophyly of the *aequatorialis, latifrons,* and *punctatus* series. The non-monophyly of the *roquet* series (a clade inferred in both parsimony and Bayesian optimal trees), was rejected by the WSR test, but not by the Bayesian test. The monophyly of *Dactyloa* excluding *Phenacosaurus* was rejected by both the WSR and Bayesian tests.

The clades inferred based on molecular data (Castañeda and de Queiroz, 2011) were also present in the parsimony and Bayesian optimal trees of the combined data sets; therefore, the non-monophyly of these groups was tested. Results obtained with the WSR and Bayesian tests differed in most cases (Table 2): the WSR test rejected the hypothesis of non-monophyly of the *Phenacosaurus* clade and failed to reject the non-monophyly of the eastern, *latifrons, roquet,* and western clades. In contrast, the Bayesian tests rejected the non-monophyly of all these clades.

DISCUSSION

The objectives of this study were to reconstruct the phylogeny of the *Dactyloa* clade based on morphological characters alone and in combination with molecular data, to explore different coding methods for continuous and polymorphic characters that

were part of our data set, and to test hypotheses of monophyly of previously described taxa. In the following paragraphs, we discuss the advantages and disadvantages of the different coding methods used, the phylogenetic relationships inferred, and their implications regarding previously recognized taxa. Finally, based on our findings, we propose a new taxonomy that recognizes only monophyletic taxa and in which names are defined following the rules of PhyloCode.

Differences Among Coding Methods

For continuous characters, the coding method of Torres-Carvajal (2007) resulted in characters containing the largest amount of phylogenetic signal, followed by Thiele's (1993) method using 101 character states. The main disadvantage of Torres-Carvajal's (2007) method is that it results in a significant increase of computation time compared with Thiele's (1993) method (MRC, personal observation), presumably because it uses step matrices. Although Thiele's (1993) method discretizes continuous characters, it maintains information on order and magnitude of change between states. Therefore, its implementation using 101 character states (i.e., allowing a 0.01 resolution between states) might be sufficient to approximate a continuous distribution (particularly if the values from the continuous distribution are estimated at a similar level of precision). Despite significant differences in g_1 values, reciprocal WSR tests (Larson, 1998) indicate that phylogenetic inferences between the two methods (at least for the *Dactyloa* data set) are not strongly in conflict: tests for differences between the optimal trees resulting from only continuous characters under each of the two coding methods (i.e., Thiele's [1993] gap-weighting method with 101 character states or Torres-Carvajal's [2007] step matrix modification of it) using the data sets produced by each of the coding methods were not statistically significant ($P = 0.872$ using the Thiele-coded data set; $P = 0.391$ using the Torres-coded data set). In contrast, reciprocal tests between the optimal trees

resulting from only continuous characters coded with Thiele's (1993) method using 101 states compared with using 6 states were statistically significant ($P = 0.036$ using the data set with 101 states; $P = 0.023$ using the data set with 6 states). Similarly, reciprocal tests between the optimal trees resulting from only continuous characters coded with Torres-Carvajal's method versus Thiele's (1993) method using six states were also statistically different ($P = 0.040$ using the Torres-coded data set; $P = 0.046$ using the Thiele-coded data set). These results combined with the results based on the g_1 statistic indicate that a larger number of character states significantly increases the amount of phylogenetic information recorded by Thiele's coding method. Moreover, these findings suggest that Thiele's (1993) method, when implemented using a large number of character states, may be an effective alternative to fully continuous coding methods. Despite performing more poorly according to g_1 values, it did not yield a significantly different tree according to reciprocal tests. At least in this case, the loss of information appears to be small and is compensated by lesser computational requirements.

The polymorphic characters coded as frequency arrays using Manhattan distance step matrices were found, based on g_1 values, to contain significantly more phylogenetic signal than those coded as standard binary or multistate characters and scored using modal conditions. Reciprocal tests indicate that there are significant differences between the optimal trees resulting from data sets including only polymorphic characters coded using these two methods ($P < 0.001$ using the frequency arrays–coded data set; $P < 0.001$ using the standard coding with modes data set). This result further supports previous studies on empirical (Wiens, 1995, 1998) and simulated (Wiens and Servedio, 1997) data, showing that methods that incorporate frequency information outperform, based on accuracy measurements, other methods for analyzing polymorphic characters (including scoring

modal conditions). The advantages of frequency methods include making use of more phylogenetic information and reducing the effects of sampling errors, in that the probability of being mislead by the presence or absence of states occurring at low frequencies is reduced, which is particularly important with small sample sizes (Swofford and Berlocher, 1987; Wiens, 1995; Wiens and Servedio, 1997). The main disadvantage of some of the methods incorporating frequency information is that they significantly increase the computation time required because of the use of step matrices (e.g., Wiens, 2000; MRC, personal observation).

Phylogeny of *Dactyloa*

This study presents the phylogenetic relationships of *Dactyloa* based on molecular data for 40 species and morphological data for the same 40 species and 20 additional ones (for a total of 60 species). This represents a substantial improvement upon previous studies, which included a maximum of 42 species (Castañeda and de Queiroz, 2011), 2 of which were not included in the current study (see "Materials and Methods") for molecular data only, or a maximum of 28 species (Poe, 2004) for multiple data sources. For the combined data sets, *Dactyloa* was inferred to be monophyletic, provided that it includes the *Phenacosaurus* species, in agreement with previous studies (Poe, 1998, 2004; Jackman et al., 1999; Nicholson et al., 2005; Castañeda and de Queiroz, 2011), although its monophyly was not strongly supported according to topology tests employing constraint trees (the hypothesis of non-monophyly was not rejected, though monophyly of *Dactyloa* excluding *Phenacosaurus* was rejected). Previous analyses of the entire *Anolis* clade based on combined data, with a similar set of characters and coding methods, inferred a fully resolved but poorly supported *Dactyloa* (Poe, 2004, fig. 2), although the analysis of only the morphological component of this data set did not infer *Dactyloa* (Poe, 2004, fig. 5). In contrast, previous analyses based solely on molecular data strongly supported the monophyly of *Dactyloa* (Nicholson et al., 2005; Castañeda and de Queiroz, 2011).

The considerable difference in nodal support between the combined (morphological and molecular) and molecular-only analyses could derive from intrinsic characteristics of the morphological characters. For example, the morphological characters might be highly homoplastic, introducing support for conflicting groupings within the morphological data set, or they might have low phylogenetic information content, allowing multiple placements of taxa for which only morphological data are available. Additionally, it is possible that conflicts between the phylogenetic signal of the morphological and molecular data sets result in a reduction in nodal support. In our analyses, we excluded characters commonly used in studies of morphological convergence (e.g., limb and tail length) to avoid this potential bias (but see de Queiroz [1996, 2000] and Poe [2005] for the advantages of including these characters in phylogenetic reconstruction). Trees inferred with the morphology-only data set showed a general lack of support for any particular topology (regardless of the coding method used), which suggests that the morphological data might not have sufficient phylogenetic signal to produce any strong conflict with the molecular data (and therefore strongly affect nodal support). However, reciprocal WSR topology tests comparing the tree inferred from morphological data (Fig. 1) with that inferred based on molecular data (Castañeda and de Queiroz, 2011, fig. 1A) indicated strong disagreement between the two data sets ($P \leq 0.0001$ for each case). Therefore, the difference in nodal support between the molecular and combined analyses would seem to result, in this case, from multiple placements of at least some of the species that were scored for morphological characters only, as well as the larger total number of species within the *Dactyloa* clade (so that support is distributed among a larger number of nodes).

Castañeda and de Queiroz (2011) inferred, based on molecular data, five strongly supported clades (informally named eastern, *latifrons*, *Phenacosaurus*, *roquet*, and western) with coherent geographic distributions. Based on the combined data, we inferred those same five clades with the inclusion of additional species for which only morphological data are available. In agreement with the inferred relationships of those species, in all cases, their geographic distributions lie within or on the periphery of the clades in which they were placed. The discussion that follows concerns the composition and internal relationships of the five clades and is based exclusively on the results obtained with the combined analyses. Following Castañeda and de Queiroz (2011), we also adopt (in the following discussion) delimitations of the clades based on the species for which molecular data were available.

The western clade, as delimited by Castañeda and de Queiroz (2011), included seven species (*A. aequatorialis*, *A. anoriensis*, *A. chloris*, *A. festae*, *A. gemmosus*, *A. peraccae*, and *A. ventrimaculatus*) distributed in the western and central cordilleras of Colombia, the western slopes of the Ecuadorian Andes, and the pacific lowlands of Colombia and Ecuador. In this study, the western clade was inferred to include three additional species (considering that we treated *A. anoriensis* as conspecific with *A. eulaemus*; see "Materials and Methods"): *A. antioquiae*, *A. fasciatus*, and *A. megalopithecus*, distributed in the northernmost part of the western cordillera in Colombia (*A. antioquiae* and *A. megalopithecus*) and in the Pacific lowlands of central Ecuador (*A. fasciatus*). Two primary subclades were inferred within the western clade. The first includes four species, *A. chloris*, *A. fasciatus*, *A. festae*, and *A. peraccae*, all previously placed in the *punctatus* series (Savage and Guyer, 1989) or species group (Williams, 1976b), that have a humid forest distribution below 1,000 m above sea level and small to moderate body size (max SVL = 62, 72, 55, and 52 mm, respectively [Williams and Acosta, 1996]). The second subclade

includes six species, *A. aequatorialis*, *A. antioquiae*, *A. eulaemus*, *A. gemmosus*, *A. megalopithecus*, and *A. ventrimaculatus*, all previously placed in the *aequatorialis* series (Savage and Guyer, 1989) or species group (Williams, 1976b, 1985; Williams and Duellman, 1984; Rueda Almonacid, 1989), distributed from 1,500 to 2,000 m above sea level and with moderate to large body size (max SVL = 92, 72 [MRC, personal observation], 101, 66, 81, and 80 mm, respectively [Williams and Acosta, 1996]). In both parsimony and Bayesian optimal trees (Figs. 3, 4), *Anolis boettgeri*, *A. fitchi*, *A. huilae*, and *A. podocarpus* were inferred closer to the western clade than to any of the other five major clades. Castañeda and de Queiroz (2011) also inferred this close relationship for the last three of those species based on molecular data. *Anolis boettgeri* and *A. huilae* were previously included in the *punctatus* series (Williams, 1976b; Poe et al., 2008), whereas *A. fitchi* and *A. podocarpus* were included in the *aequatorialis* series (Williams, 1976b; Ayala-Varela and Torres-Carvajal, 2010). The geographic distributions of these four species at mid to high elevations in the eastern slopes of the Andes of Colombia (*A. huilae*), Ecuador (*A. fitchi*, *A. podocarpus*), and Peru (*A. boettgeri*), do not correspond with the Pacific lowland and Colombian inter-Andean valley distribution of the western clade and suggest that a dispersal or vicariance event was associated with the branch separating the eastern and western species (i.e., the one at the base of the western clade).

The *latifrons* clade, as delimited by Castañeda and de Queiroz (2011), included 12 species (*A. agassizi*, *A. casildae*, *A. chocorum*, *A. danieli*, *A. fraseri*, *A. frenatus*, *A. insignis*, *A. maculigula*, *A. microtus*, *A. princeps*, *A. sp1*, and *A. sp2*) distributed in the Pacific lowlands of Costa Rica, Panama, Colombia (including Malpelo island), and Ecuador and in the Colombian inter-Andean valleys below 1,000 m above sea level (except *A. danieli*, which ranges from 1,700 to 2,200 m). Most of these species

were previously placed in the *latifrons* species group (Williams, 1976b) or series (Savage and Guyer, 1989), and in all except *A. chocorum*, adult males reach a SVL greater than 100 mm (large size was considered a diagnostic feature of the traditional *latifrons* series [Williams, 1976b], also called the giant mainland anoles [Dunn, 1937]). We inferred the *latifrons* clade (excluding *A.* sp1 and *A.* sp2, which were not included in this study, see "Materials and Methods"), with the inclusion of three additional species in the parsimony analysis, *A. apollinaris*, *A. latifrons*, and *A. purpurescens*, and further including *A. squamulatus* in the Bayesian analysis. All four potentially additional species were previously included in the *latifrons* series or species group (Williams, 1976b; Savage and Guyer, 1989) and have Pacific lowland (*A. latifrons* and *A. purpurescens*) or inter-Andean (*A. apollinaris*) distributions, except *A. squamulatus* (see below). In *A. apollinaris*, *A. latifrons*, and *A. squamulatus* adult male maximum SVL exceeds 100 mm (106, 133, and 122 mm, respectively; Williams and Acosta, 1996; Ugueto et al., 2009); *A. purpurescens*, which is known from a small number of specimens, appears to be smaller (max SVL = 78 mm; Williams and Acosta, 1996). In both analyses, *A. philopunctatus* is inferred as the sister group of the *latifrons* clade. However, this species was not considered as part of the *latifrons* clade based on the delimitation of the clade using species for which molecular data were available (see above). This species was previously included in the *punctatus* series and is distributed in the Brazilian Amazon, and its adult maximum SVL = 73 mm (Rodrigues, 1988). *Anolis squamulatus* was previously placed in the *latifrons* species group of Williams (1976b) and series of Savage and Guyer (1989) based on its large dewlap, small head scales, uniform dorsal scales, and large body size (max adult male SVL > 100 mm; Williams and Acosta, 1996). Although inferred as part of the *latifrons* clade in the Bayesian analysis (Fig. 4), it was not in the parsimony analysis (Fig. 3). Moreover, *A. squamulatus* is the only species, of the sampled taxa, previously placed in the *latifrons* species group or

series that was not inferred as part of the *latifrons* clade in the parsimony analysis. However, the geographic distribution of *A. squamulatus*, in the cloud forests of the northern Venezuelan Andes, does not correspond to the Pacific lowland and Colombian inter-Andean valley distribution of the *latifrons* clade or to the Pacific mid and low elevations in Colombia and Ecuador distribution of the western clade (to which it was inferred as being closer in the parsimony analysis). Instead, it corresponds more closely to the geographic distribution of the eastern clade. Either of these alternative relationships of *A. squamulatus* (within or closer to either the western or the eastern clades) would require the convergent evolution of large body size with members of the *latifrons* clade. In agreement with previous studies suggesting the close relationship between *A. frenatus*, *A. latifrons*, and *A. princeps* and including the possibility that those three taxa represent a single species (Savage and Talbot, 1978; Williams, 1988; Castañeda and de Queiroz, 2011), we inferred the clade ((*A. frenatus* (*A. latifrons*, *A. princeps*)) in both parsimony and Bayesian analyses.

The eastern clade, as delimited by Castañeda and de Queiroz (2011), included five species (*A. anatoloros*, *A. jacare*, *A. punctatus*, *A. transversalis*, and *A. tigrinus*) distributed in the northern portion of the eastern cordillera of Colombia into the Venezuelan Andes and the Amazon region. In our parsimony results, the eastern clade was inferred to include three additional species: *A. carlostoddi*, *A. orcesi*, and *A. vaupesianus*, whereas in the Bayesian analysis, it was inferred to include six additional species: *A. dissimilis*, *A. menta*, *A. ruizii*, *A. santamartae*, *A. solitarius*, and *A. vaupesianus*. All of the potential additional species have an eastern Andean and Amazonian distribution. They occur in Amazonia (*A. vaupesianus*, *A. dissimilis*), the eastern slopes of the northern Andes of Ecuador (*A. orcesi*), the eastern cordillera of Colombia (*A. ruizii*), the Sierra Nevada de Santa Marta in Colombia (*A. menta*, *A. santamartae*, *A. solitarius*), and the Chimantá tepui in

Venezuela (*A. carlostoddi*). Within the eastern clade, two subclades were inferred in both analyses: the first includes three species, *A. anatoloros*, *A. jacare*, and *A. tigrinus*, with mostly Andean, high-elevation distributions and smaller body size (max male SVL = 55–68 mm; Williams and Acosta, 1996; Ugueto et al., 2007); the second subclade includes three species, *A. punctatus*, *A. transversalis*, and *A. vaupesianus*, with Amazonian, low-elevation distributions, and larger size (max male SVL = 76–82 mm; Williams and Acosta, 1996). It is not surprising that *A. vaupesianus* (distributed in the Vaupes and Amazonas departments in Colombia and known only from the type series) was consistently inferred as the sister taxon of *A. punctatus* (with a broad Amazonian distribution). These two species were described as close relatives that differ primarily in the size and degree of keeling of the ventral scales (smaller and weakly keeled in *A. vaupesianus* versus larger and strongly keeled in *A. punctatus*), the dewlap coloration in preservative (black skin with white scales in *A. vaupesianus* versus light skin with small dark spots and purplish scales in *A. punctatus*) and the dorsal color pattern of preserved specimens (in *A. vaupesianus*, "brown, strongly blotched with darker, dorsal blotches tending to form transverse series across the back" versus an unpatterned dark dorsum in *A. punctatus*) (Williams, 1982: 8). The unique color pattern of *A. vaupesianus* is only found in one of the paratypes (UTA 6850), whereas the coloration of the other specimens in the type series is not particularly different from that of *A. punctatus* (Williams, 1982: 8–9). Given the small differences separating these two species, a more comprehensive sampling of *A. punctatus* in Colombia (currently <10 specimens are known) and the collection of additional molecular data (particularly for *A. vaupesianus*) could clarify whether these two taxa are conspecific as well as whether the characters used to distinguish them represent extremes in a continuous distribution or are based on an atypical specimen. In contrast to the likely close relationship

between *A. punctatus* and *A. vaupesianus*, the relationships of *A. carlostoddi* and *A. orcesi* (parsimony) or *A. dissimilis*, *A. menta*, *A. santamartae*, and *A. solitarius* (Bayesian) to *A. tigrinus* are less clear. The former two species were previously placed in *Phenacosaurus* and thus not considered closely related to *A. tigrinus*. In contrast, two of the latter species, *A. menta* and *A. solitarius*, were placed in the *tigrinus* series (Williams, 1976b; Ayala et al., 1984) (the other two, *A. dissimilis* and *A. santamartae*, were placed in the *punctatus* series). In both cases, the putative clade formed by all three or all six species has low support, and given the low resolving power of the morphological data set and the fact that molecular data are available for neither *A. carlostoddi* and *A. orcesi* nor *A. dissimilis*, *A. menta*, *A. santamartae*, *A. ruizii*, and *A. solitarius*, the inferred relationships are questionable.

The *roquet* clade, as delimited by Castañeda and de Queiroz (2011), included eight species (*A. aeneus*, *A. bonairensis*, *A. extremus*, *A. griseus*, *A. luciae*, *A. richardii*, *A. roquet*, and *A. trinitatis*), distributed in the southern Lesser Antilles, from Martinique to Grenada, as well as the islands of Bonaire and Tobago (with introduced populations in Trinidad and Guyana [Gorman and Dessauer, 1965, 1966; Gorman et al., 1971]). This clade corresponds to the previously described *roquet* species group or series (Underwood, 1959; Gorman and Atkins, 1967, 1969; Lazell, 1972; Williams, 1976a; Savage and Guyer, 1989; Creer et al., 2001). One additional species, *A. blanquillanus*, from the island of La Blanquilla, was previously referred to the *roquet* series (Williams, 1976a) but was not included in our analyses; however, its inclusion in the *roquet* clade is supported by allozyme data (Yang et al., 1974; Creer et al., 2001). Poe (2004) inferred the *roquet* clade (BS = 74%, fig. 2), supported by six morphological characters (see "Current Taxonomy within *Dactyloa*"); two of those, greater sexual size dimorphism and an increase in the number of postmental scales, were also inferred as synapomorphies for the clade in this study.

The *Phenacosaurus* clade, as delimited by Castañeda and de Queiroz (2011), included five species (*A. euskalerriari, A. heterodermus, A. inderenae, A. nicefori,* and *A. vanzolinii*) distributed in the Andean regions of Colombia, Ecuador, and Venezuela, all of which were previously placed in the genus *Phenacosaurus* (Lazell, 1969; Barros et al., 1996). In this study, the *Phenacosaurus* clade was inferred with the addition of *A. tetarii*, a species that was previously placed in the genus *Phenacosaurus* (Barros et al., 1996) and whose geographic distribution (Venezuelan Andes) conforms to that of the clade. Three other species that were previously referred to *Phenacosaurus*, *A. carlostoddi, A. orcesi,* and *A. neblininus,* were not inferred to be part of this clade in the parsimony analysis. However, in the Bayesian analysis, *A. orcesi* was inferred as the sister group of the *Phenacosaurus* clade with moderate support (PP = 0.87; Fig. 4). In contrast, in the parsimony analysis, *A. orcesi* was placed in the eastern clade (as was *A. carlostoddi*), although with weak support (BS = 6%, 24%, and 19%). In both parsimony and Bayesian analyses, *A. proboscis* was inferred as sister group of the *Phenacosaurus* clade (or of the *Phenacosaurs* clade plus *A. orcesi*) with weak support (BS = 58%, PP = 0.43), a relationship also inferred by Poe (2004, fig. 2). A close relationship between *A. proboscis* and species traditionally referred to *Phenacosaurus* was also inferred by Poe et al. (2009b, 2012). The geographic distributions of both species lie on the periphery of that of the *Phenacosaurus* clade: *A. orcesi* is distributed along the eastern slopes of the northern Andes of Ecuador, whereas *A. proboscis* is distributed along the western slopes of the northern Andes of Ecuador. The more deeply nested species within the *Phenacosaurus* clade (*A. heterodermus, A. inderenae, A. tetarii,* and *A. vanzolinii*) are larger in size (max male SVL=76, 98, 86, and 104 mm, respectively [Williams and Acosta, 1996]) and correspond to the *heterodermus* group of Williams et al. (1996); the two earlier diverging lineages

(*A. euskalerriari* and *A. nicefori*) are smaller in size (max male SVL = 53 and 63 mm, respectively [Williams and Acosta, 1996]). Except for *A. euskalerriari*, all of the species in the *Phenacosaurus* clade have heterogeneous dorsal scales, suggesting that this condition originated in the ancestral lineage of *A. heterodermus* and *A. nicefori* after it diverged from that of *A. euskalerriari*. *Anolis carlostoddi, A. orcesi,* and *A. neblininus,* which were previously placed in the genus *Phenacosaurus* but were not inferred in this study to be part of the *Phenacosaurus* clade (although *A. orcesi* was inferred to be closely related in the Bayesian analysis), also lack heterogeneous dorsal scales.

Seventeen species (*A. boettgeri, A. calimae, A. caquetae, A. carlostoddi, A. dissimilis, A. fitchi, A. huilae, A. menta, A. neblininus, A. orcesi, A. philopunctatus, A. podocarpus, A. proboscis, A. ruizii, A. santamartae, A. solitarius,* and *A. squamulatus*) were not consistently placed in any of the five mutually exclusive clades just discussed, either because their positions did not satisfy the criterion based on the last common ancestor of the species for which molecular data were available or because they differed across phylogenetic methods (and were commonly poorly supported). However, 6 of the 17 species (*A. boettgeri, A. fitchi, A. huilae, A. philopunctatus, A. podocarpus,* and *A. proboscis*) were each consistently placed closer to one of the five clades than to the others. For those species whose relationships differed among analyses (*A. calimae, A. caquetae, A. carlostoddi, A. dissimilis, A. menta, A. neblininus, A. orcesi, A. ruizii, A. santamartae, A. solitarius,* and *A. squamulatus*), 9 out of 11 of which currently lack molecular data (all but *A. calimae* and *A. neblininus*), more data will be necessary to clarify their relationships within *Dactyloa*.

Previously Recognized Taxa

None of the traditionally recognized subgroups of *Dactyloa* based on morphological characters (*aequatorialis, latifrons, Phenacosaurus, punctatus, roquet,* and *tigrinus*) were

inferred in the optimal trees inferred from either the morphology-only or the combined data sets except the *roquet* series in the combined analyses. The parsimony-based topology tests (WSR) using the morphology-only data set failed to reject the monophyly of *Dactyloa* or any of the previously described subgroups (Table 1); therefore, despite the morphological data not supporting any of these groups when analyzed under parsimony, it is also unable to reject any of them using parsimony-based tests. In contrast, the Bayesian tests using the morphology-only data set rejected the hypotheses of monophyly of *Dactyloa* and all traditionally recognized series except the *roquet* series. With the combined data sets and both parsimony and Bayesian tests (2), the *aequatorialis*, *latifrons*, and *punctatus* series were also strongly rejected, but the *tigrinus* series and *Phenacosaurus* were not rejected.

Contradictory evidence and absence of support for the series described based on morphological characters is consistent with previous suggestions that morphological characters used for series delimitation might show a high degree of convergence and parallelism (Williams, 1976b: 260) and that some series were described only for convenience (Williams, 1979: 10). Furthermore, traditional series delimitation did not distinguish clearly between ancestral and derived conditions, and the former are not indicative of close phylogenetic relationships. Differences between the results of WSR and Bayesian tests might reflect the conservativeness of the WSR—the requirement of a stronger signal to reject a given hypothesis (Lee, 2000)—because Bayesian tests often rejected hypotheses when WSR tests did not, but WSR tests rarely rejected hypotheses not rejected by Bayesian tests. Differences between the data sets (i.e., resulting from alternative coding methods) do not appear to be the reason for the different results between the two tests. For one thing, the Bayesian tests rejected more of the hypotheses despite using the data set (Thiele6-mode) that contained the least phylogenetic signal. For another, WSR tests

performed on the Thiele6-mode data set (the data set used for the Bayesian tests) yielded the same qualitative results as with the Torres-freq data set (results not shown).

Proposed Taxonomy

Our results indicate that a revised taxonomy for *Dactyloa* is warranted. Optimal phylogenetic trees and topology tests indicate that most of the previously recognized taxa within *Dactyloa* based on morphological characters and traditionally ranked as species groups or series are not monophyletic. Moreover, our previously published results based on molecular data (Castañeda and de Queiroz, 2011) indicate the existence of five well-supported major subclades, and the results of the combined analyses of morphological and molecular data in the present study both corroborate the monophyly and clarify the composition of those subclades. Here, we propose a revised taxonomy based on the results of our phylogenetic analyses, including names that are defined explicitly in terms of phylogenetic relationships (de Queiroz and Gauthier, 1990, 1992).

The optimal topologies obtained from the different (parsimony versus Bayesian) methods are in substantial but not complete agreement. We considered it inappropriate to select one topology over the other because each topology has advantages and disadvantages: The parsimony tree is based on a character coding method that incorporates more phylogenetic information, whereas the Bayesian tree is based on more realistic evolutionary models. Therefore, we used a consensus tree as the basis for our proposed taxonomy (Fig. 5). Specifically, we used a pruned and regrafted[2] consensus tree (Gordon, 1980; Finden and Gordon, 1985; Bryant, 2003) derived from the most parsimonious tree (Fig. 3) and the maximum clade credibility tree (Fig. 4) for the combined morphological and molecular

---

[2] The term "grafted" seems more appropriate here, given that the branch has not been grafted before; however, we use "regrafted" because it has been commonly used in the literature.
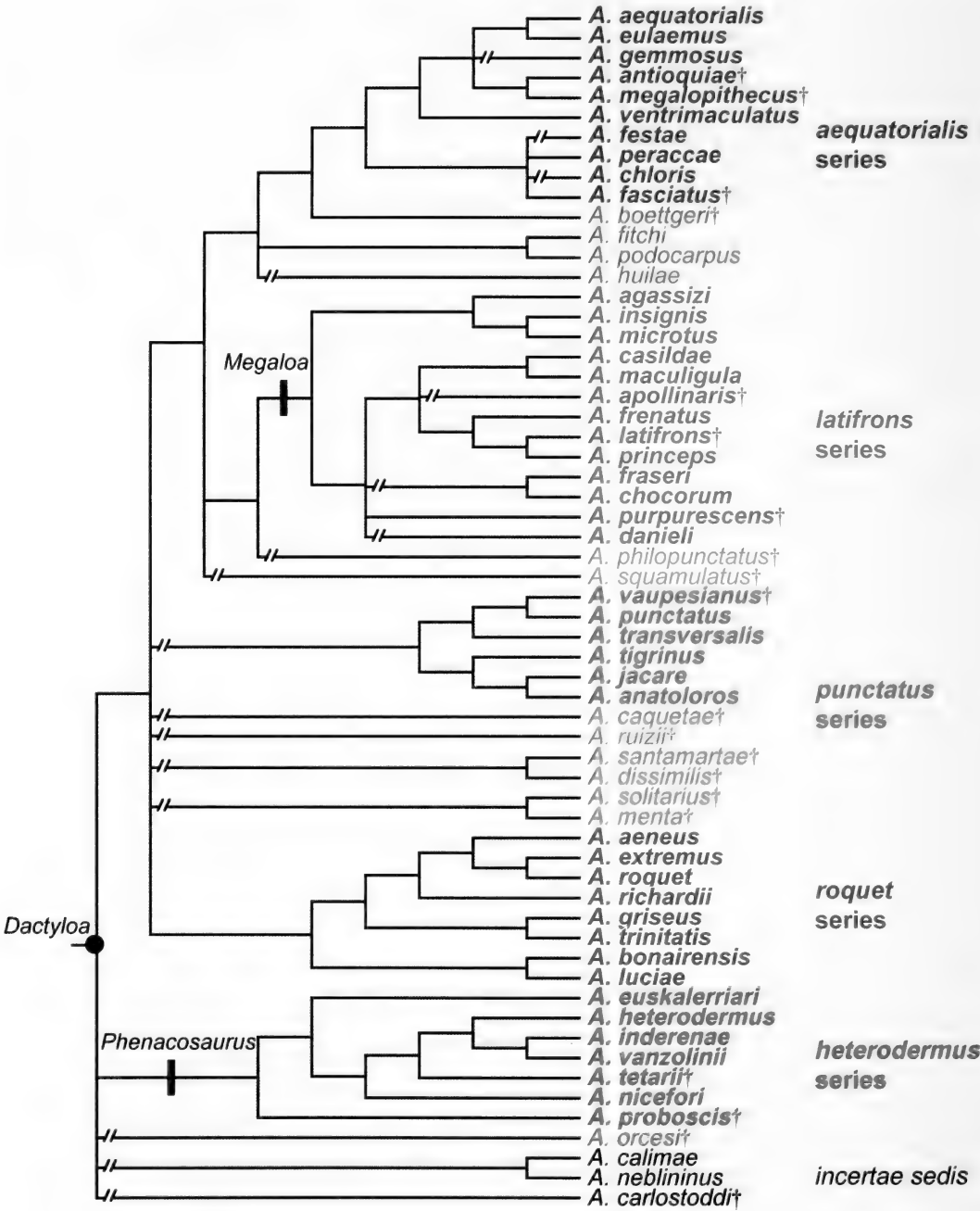
Figure 5. Pruned and regrafted consensus tree based on the most parsimonious tree (inferred with the CombTorres-freq data set; Fig. 3) and the Bayesian Maximum Clade Credibility tree (inferred with the CombThiele6-mode data set; Fig. 4) with the taxonomy proposed in this study. Daggers (†) following species names indicate the species for which only morphological data were available. Regrafted branches are indicated by a break near their bases. See text for details concerning alternative prunings and regraftings 1) within the clade composed of *A. chloris*, *A. fasciatus*, *A. festae*, and *A. peraccae*; 2) of *A. purpurescens* versus *A. danieli*; and 3) of members of the *punctatus* series. The *Dactyloa* clade is indicated with a black dot on the corresponding node. Five mutually exclusive, informally named clades ("series") within *Dactyloa* are distinguished by color, with lighter versions of the

data sets (i.e., CombTorres-freq and CombThiele6-mode matrices).

Because a few of the species (e.g., *A. carlostoddi, A. orcesi, A. squamulatus*) have very different relationships on the primary trees, the strict and semistrict consensus trees had little resolution, and we therefore originally intended to use an Adams consensus tree (for a review of consensus methods, see Swofford [1991]). However, the Adams consensus tree contained unexpected groups that we felt could not be justified on the basis of the primary trees (e.g., *A. squamulatus* closer to the western clade than to the *latifrons* clade, which is contradicted by the Bayesian tree; Fig. 4), and it turned out that the pruned and regrafted consensus tree exhibited the desired properties we had incorrectly attributed to the Adams consensus method (i.e., placement of species with conflicting relationships within the smallest possible clade in the consensus tree for which there is complete agreement concerning their higher level relationships in the primary trees).

To generate the pruned and regrafted consensus tree, we first produced agreement subtrees (also called common pruned trees; Finden and Gordon, 1985) using PAUP* with identical topologies that result from removing (pruning) the same set of taxa from the primary trees (Finden and Gordon, 1985). We obtained 12 largest agreement subtrees for the 60 *Dactyloa* species (including only one outgroup species, *Polychrus marmoratus*, to root the trees), which differed only in the inclusion of all possible combinations of two species from the clade composed of *A. festae, A. chloris, A. fasciatus,* and *A. peraccae* (six possible combinations) and the inclusion of either *A. danieli* or *A. purpurescens*. We arbitrarily selected one of the 12 largest agreement subtrees (the one including *A. fasciatus, A. peraccae,* and *A. purpurescens*)

as the base tree for the regrafting process. In the second step, we manually reattached each previously pruned species or set of species to the node representing the most recent common ancestor of its alternative placements on the primary trees. Because the position of the entire eastern clade and its possible relatives differed between the two primary trees (closer to the *latifrons* clade in the parsimony tree versus closer to the *roquet* clade in the Bayesian tree), all of those species were excluded from the largest agreement subtrees. To determine whether those species should be reattached singly or in sets, we determined the largest agreement subtree for those species (*A. anatoloros, A. caquetae, A. carlostoddi, A. dissimilis, A. jacare, A. menta, A. orcesi, A. punctatus, A. ruizii, A. santamartae, A. solitarius, A. tigrinus, A. transversalis, A. vaupesianus*), plus one representative each of the western, *latiforns, Phenacosaurus,* and *roquet* clades; we also included *Polychrus marmoratus* to root the trees. We obtained four largest agreement subtrees representing two different topologies for the set of species making up the eastern clade and its possible relatives (the other two topologies differed only in whether the representative of the western or the *roquet* clade was included). Both topologies included (*A. transversalis (A. punctatus, A. vaupesianus*)), but one included (*A. tigrinus (A. anatoloros, A. jacare*)) and *A. caquetae,* whereas the other included ((*A. dissimilis, A. santamartae*) (*A. menta, A. solitarius*)). We selected the former for grafting because those groups were consistent, after pruning, with the primary trees, whereas the latter depended on pruning the representative of the *latifrons* clade, which we intend to be a fixed point of reference (i.e., not a candidate for pruning) in this secondary analysis (given that several members of the *latifrons* clade were present in all of the primary

---

←

same hue indicating tentative assignment to the clade represented by that hue. These informally named clades have the same name as some of the groups traditionally ranked as series within *Anolis*; however, species composition is not necessarily identical. A black bar across a branch indicates an apomorphy used to define the clade name above the bar.

agreement subtrees). The resulting pruned and regrafted consensus tree (Fig. 5) serves as the basis for our taxonomy.

In all but two cases, we have selected preexisting names that have been applied traditionally to groups of species approximating, to one degree or another, the clades to which we apply them. Three of the selected names are similar in appearance to genus names; however, they are here tied to clades rather than to the rank of genus and are implicitly ranked below the genus level (given that we use the name *Anolis* in the binomina of all of the species included in the named clades). Five of the selected names combine the species name (epithet) of the first described species (e.g., "*roquet*") with the name of a rank (i.e., "series"). Because those names violate the rule stating that clade names must be single words beginning with a capital letter (ICPN, Article 17.1), they are treated here as informal names. They are nevertheless given explicit phylogenetic definitions as guides for applying the names in the context of future phylogenetic hypotheses. Despite being given explicit phylogenetic definitions, the names in question are compatible with traditional nomenclature, in that they have been defined so as to ensure that they will always refer to mutually exclusive taxa (see de Queiroz and Donoghue, 2013), as would names associated with the rank of series under traditional nomenclature. As a consequence, the "series" names are applied to clades that are more inclusive than the five clades based on the species for which molecular data were available that formed the basis of our discussion in the "Phylogeny of *Dactyloa*" section (above), though those five less inclusive clades form the cores of the "series" clades. The number of *Dactyloa* subclades named in our taxonomy exceeds five, the number of well-supported clades based on molecular data (Castañeda and de Queiroz, 2011) and corroborated in this study, because in two cases, we considered it useful to name additional clades associated with the origins of distinctive apomorphies.

Dactyloa Wagler 1830, converted clade name

Definition (branch-modified node-based): The crown clade originating in the most recent common ancestor of *Anolis punctatus* Daudin 1802 and all extant species that share a more recent common ancestor with *A. punctatus* than with *A. bimaculatus* (Sparrman 1784), *A. cuvieri* Merrem 1820, *A. equestris* Merrem 1820, *A. occultus* Williams and Rivero 1965, and *A. sagrei* Duméril and Bibron 1837. **Reference phylogeny:** Figure 5, this study (see also Poe, 2004, figs. 2–4). **Inferred composition:** *Anolis aeneus* Gray 1840, *A. aequatorialis* Werner 1894, *A. agassizi* Stejneger 1900, *A. anatoloros* Ugueto, Rivas, Barros, Sánchez-Pacheco and García-Pérez 2007, *A. anchicayae* Poe, Velasco, Miyata and Williams 2009 (inclusion based on inferred close relationship to *A. peraccae* following Poe et al., 2009b), *A. anoriensis* Velasco, Gutiérrez-Cárdenas and Quintero-Angel 2010 (inclusion based on inferred close relationship to *A. aequatorialis* following Castañeda and de Queiroz, 2011), *A. antioquiae* Williams 1985, *A. apollinaris* Boulenger 1919, *A. bellipeniculus* (Myers and Donnelly 1996) (inclusion based on inferred close relationship to *A. neblininus* following Myers and Donnelly, 1996), *A. blanquillanus* Hummelinck 1940 (inclusion based on inferred close relationship to *A. bonairensis* following Yang et al., 1974), *A. boettgeri* Boulenger 1911, *A. bonairensis* Ruthven 1923, *A. calimae* Ayala, Harris and Williams 1983, *A. caquetae* Williams 1974, *A. carlostoddi* (Williams, Praderio and Gorzula 1996), *A. casildae* Arosemena, Ibáñez, and de Sousa 1991, *A. chloris* Boulenger 1898, *A. chocorum* Williams and Duellman 1967, *A. cuscoensis* Poe, Yañez-Miranda and Lehr 2008 (inclusion based on the results of Poe et al., 2008), *A. danieli* Williams 1988, *A. deltae* Williams 1974 (inclusion based on inferred close relationship to *A. dissimilis* following Williams, 1974), *A. dissimilis* Williams 1965, *A. eulaemus* Boulenger 1908, *A. euskalerriari* (Barros, Williams, and Viloria 1996), *A.*

extremus Garman 1887, *A. fasciatus* Boulenger 1885, *A. festae* Peracca 1904, *A. fitchi* Williams and Duellman 1984, *A. fraseri* Günther 1859, *A. frenatus* Cope 1899, *A. gemmosus* O'Shaughnessy 1875, *A. gorgonae* Barbour 1905 (inclusion based on inferred close relationship to *A. andianus* [a synonym of *A. gemmosus* according to Williams and Duellman (1984)] following Barbour, 1905), *A. griseus* Garman 1887, *A. heterodermus* Duméril 1851, *A. huilae* Williams 1982, *A. ibanezi* Poe, Latella, Ryan and Schaad 2009 (inclusion based on inferred close relationship to *A. chocorum* following Poe et al., 2009a), *A. inderenae* (Rueda and Hernández-Camacho 1988), *A. insignis* Cope 1871, *A. jacare* Boulenger 1903, *A. kunayalae* Hulebak, Poe, Ibáñez and Williams 2007 (inclusion based on inferred close relationship to *A. mirus* following Hulebak et al., 2007), *A. laevis* (Cope 1876) (inclusion based on inferred close relationship to *A. proboscis* following Williams, 1979), *A. lamari* Williams 1992 (inclusion based on inferred close relationship to *A. tigrinus* following Williams, 1992), *A. latifrons* Berthold 1846, *A. luciae* Garman 1887, *A. maculigula* Williams 1984, *A. megalopithecus* Rueda Almonacid 1989, *A. menta* Ayala, Harris and Williams 1984, *A. microtus* Cope 1871, *A. mirus* Williams 1963 (inclusion based on inferred close relationship to *A. fraseri* following Williams, 1963), *A. nasofrontalis* Amaral 1933 (inclusion based on inferred close relationship to *A. tigrinus* following Amaral, 1933), *A. neblininus* (Myers, Williams and McDiarmid 1993), *A. nicefori* (Dunn 1944), *A. nigrolineatus* Williams 1965, *A. orcesi* (Lazell 1969), *A. otongae* Ayala-Varela and Velasco 2010 (inclusion based on inferred close relationship to *A. gemmosus* following Ayala-Varela and Velasco, 2010), *A. paravertebralis* Bernal Carlo and Roze 2005 (inclusion based on inferred close relationship to *A. solitarius* following Bernal Carlo and Roze, 2005), *A. parilis* Williams 1975 (inclusion based on inferred close relationship to *A. mirus* following Williams, 1975), *A. peraccae* Boulenger 1898, *A. philopunc-* *tatus* Rodrigues 1988, *A. phyllorhinus* Myers and Carvalho 1945 (inclusion based on inferred close relationship to *A. punctatus* following Myers and Carvalho, 1945), *A. podocarpus* Ayala-Varela and Torres-Carvajal 2010, *A. princeps* Boulenger 1902, *A. proboscis* Peters and Orcés 1956, *A. propinquus* Williams 1984 (inclusion based on inferred close relationship to *A. apollinaris* following Williams, 1988), *A. pseudotigrinus* Amaral 1933 (inclusion based on inferred close relationship to *A. tigrinus* following Amaral, 1933), *A. punctatus* Daudin 1802, *A. purpurescens* Cope 1899, *A. richardii* Duméril and Bibron 1837, *A. roquet* (Bonnaterre 1789), *A. ruizii* Rueda and Williams 1986, *A. santamartae* Williams 1982, *A. soinii* Poe and Yañez-Miranda 2008 (inclusion based on inferred close relationship to *A. transversalis* following Poe and Yañez-Miranda, 2008), *A. solitarius* Ruthven 1916, *A.squamulatus* Peters 1863, *A. tetarii* (Barros, Williams, and Viloria 1996), *A. tigrinus* Peters 1863, *A. transversalis* Duméril 1851, *A. trinitatis* Reinhardt and Lütken 1862, *A. umbrivagus* Bernal Carlo and Roze 2005 (inclusion based on inferred close relationship to *A. solitarius* following Bernal Carlo and Roze, 2005), *A. vanzolinii* (Williams, Orcés, Matheus, and Bleiweiss 1996), *A. vaupesianus* Williams 1982, *A. ventrimaculatus* Boulenger 1911, and *A. williamsmittermeierorum* Poe and Yañez-Miranda 2007 (inclusion based on inferred close relationship to *A. orcesi* following Poe and Yañez-Miranda, 2007). **Comments:** The name *Dactyloa* was previously used by Savage and Guyer (1989) for a taxon ranked as a genus containing all species referred to the *Dactyloa* clade in this study except those species formerly assigned to the genus *Phenacosaurus* Barbour 1920 (*A. bellipeniculus*, *A. carlostoddi*, *A. euskalerriari*, *A. heterodermus*, *A. inderenae*, *A. neblininus*, *A. nicefori*, *A. orcesi*, *A. tetarii*, *A. vanzolinii*). Here, the name *Dactyloa* is not associated with the rank of genus (it is implicitly associated with a lower rank) so that the binomina of the included species retain the prenomen (genus name) *Anolis*.

The following named clades are subclades of *Dactyloa*.

aequatorialis series Savage and Guyer 1989, informal clade name

Definition (branch-modified node-based): The crown clade originating in the most recent common ancestor of *Anolis aequatorialis* Werner 1894 and all extant species that share a more recent common ancestor with *A. aequatorialis* than with *A. latifrons* Berthold 1846, *A. punctatus* Daudin 1802, *A. roquet* (Bonnaterre 1789), and *A. heterodermus* Duméril 1851. **Reference phylogeny:** Figure 5, this study. **Inferred composition:** *Anolis aequatorialis* Werner 1894, *A. anoriensis* Velasco, Gutiérrez-Cárdenas and Quintero-Angel 2010 (see "Comments"), *A. antioquiae* Williams 1985, *A. boettgeri* Boulenger 1911 (see "Comments"), *A. chloris* Boulenger 1898, *A. eulaemus* Boulenger 1908, *A. fasciatus* Boulenger 1885, *A. festae* Peracca 1904, *A. fitchi* Williams and Duellman 1984 (see "Comments"), *A. gemmosus* O'Shaughnessy 1875, *A. huilae* Williams 1982 (see "Comments"), *A. megalopithecus* Rueda Almonacid 1989, *A. peraccae* Boulenger 1898, *A. podocarpus* Ayala-Varela and Torres-Carvajal 2010 (see "Comments"), and *A. ventrimaculatus* Boulenger 1911. Other species that may belong to the *aequatorialis* series are *A. anchicayae* Poe, Velasco, Miyata and Williams 2009, *A. mirus* Williams 1963, *A. otongae* Ayala-Varela and Velasco 2010, and *A. parilis* Williams 1975 (see "Comments"). **Comments:** Referral of *A. anoriensis* to this clade is based on the results of Castañeda and de Queiroz (2011). In the context of the reference phylogeny, six species not traditionally included in the *aequatorialis* series (e.g., Savage and Guyer, 1989) are included in the *aequatorialis* series as conceptualized here: *A. boettgeri*, *A. chloris*, *A. fasciatus*, *A. festae*, *A. huilae*, and *A. peraccae*. There is strong evidence supporting inclusion of *A. chloris*, *A. festae*, and *A. peraccae* (Castañeda and de Queiroz, 2011), and *A. fasciatus* is placed consistently in a subclade with those three

species (Figs. 3, 4). In contrast, because of inconsistent placement of *A. huilae* between analyses (Fig. 3 versus Fig. 4), because of weak support for the inclusion of both *A. boettgeri* and *A. huilae* and because molecular data are currently lacking for *A. boettgeri*, inclusion of those two species in the *aequatorialis* series should be considered tentative. Additionally, *A. maculigula*, a species included in the traditional circumscription of the *aequatorialis* series, is excluded based on strong evidence supporting its inclusion in the *latifrons* series (see below). The inclusion of *A. fitchi* and *A. podocarpus*, traditionally included in the *aequatorialis* series (Savage and Guyer, 1989), should also be considered tentative given the weak support for the relevant relationships (Figs. 3, 4). Although the parsimony analysis (Fig. 3) places *A. squamulatus* in the *aequatorialis* series, we have tentatively retained that species in the *latifrons* series based on the results of the Bayesian analysis (Fig. 4) and its large body size (see "Comments" on the *latifrons* series). The inclusion of *A. mirus*, *A. otongae*, and *A. parilis*, previously considered members of the *aequatorialis* series (Williams, 1975; Ayala-Varela and Velasco, 2010), should also be considered tentative given the current absence of these species from explicit phylogenetic analyses. *Anolis anchicayae*, inferred as closely related to *A. peraccae* in a recent phylogenetic analysis (Poe et al., 2009b), should also be considered tentatively included in the *aequatorialis* series given that in that analysis these two species were not inferred as close relatives of *A. aequatorialis*.

The *aequatorialis* series as conceptualized here corresponds approximately to the western clade of Castañeda and de Queiroz (2011). However, the *aequatorialis* series is more inclusive than the western clade of Castañeda and de Queiroz (2011) in that it appears to include *A. boettgeri*, *A. fitchi*, *A. huilae*, and *A. podocarpus* and might also include some species currently considered *incertae sedis* within *Dactyloa* or absent from explicit phylogenetic analyses if they

are found to be more closely related to *A. aequatorialis* than to *A. latifrons*, *A. punctatus*, *A. roquet*, and *A. heterodermus*. Additionally, species in the western clade of Castañeda and de Queiroz (2011) are characterized by having a cohesive western Andean geographic distribution, but *A. boettgeri*, *A. fitchi*, *A. huilae*, and *A. podocarpus*, and possibly other species in the more inclusive *aequatorialis* series, do not conform to this geographic pattern (see "Phylogeny of *Dactyloa*" above for more details about the geographic distributions of the four species mentioned).

latifrons series Gorman and Dessauer 1966, informal clade name

Definition (branch-modified node-based): The crown clade originating in the most recent common ancestor of *Anolis latifrons* Berthold 1846 and all extant species that share a more recent common ancestor with *A. latifrons* than with *Anolis aequatorialis* Werner 1894, *A. punctatus* Daudin 1802, *A. roquet* (Bonnaterre 1789), and *A. heterodermus* Duméril 1851. **Reference phylogeny:** Figure 5, this study. **Inferred composition:** *Anolis agassizi* Stejneger 1900, *A. apollinaris* Boulenger 1919, *A. casildae* Arosemena, Ibáñez, and de Sousa 1991, *A. chocorum* Williams and Duellman 1967, *A. danieli* Williams 1988, *A. fraseri* Günther 1859, *A. frenatus* Cope 1899, *A. insignis* Cope 1871, *A. kunayalae* Hulebak, Poe, Ibáñez and Williams 2007, *A. latifrons* Berthold 1846, *A. maculigula* Williams 1984, *A. microtus* Cope 1871, *A. princeps* Boulenger 1902, *A. philopunctatus* Rodrigues 1988 (see "Comments"), *A. purpurescens* Cope 1899, and *A. squamulatus* Peters 1863 (see "Comments"). Other species that may belong to the *latifrons* series are *A. ibanezi* Poe, Latella, Ryan and Schaad 2009, and *A. propinquus* Williams 1984 (see "Comments"). **Comments:** Referral of *A. kunayalae* to this clade is based on the results of Nicholson et al. (2005, fig. 1, where *A. kunayalae* corresponds to Nicholson et al.'s "New Species 1" [Hulebak et al., 2007]). In the context of the reference

phylogeny, four species not traditionally included in the *latifrons* series (e.g., Savage and Guyer, 1989) are included in the *latifrons* series as conceptualized here: *A. agassizi*, *A. chocorum*, *A. maculigula*, and *A. philopunctatus*. There is strong evidence supporting inclusion of the former three species (Castañeda and de Queiroz, 2011). In contrast, because of weak support for the relationship of *A. philopunctatus* (Figs. 3, 4) and because of a current lack of molecular data, its inclusion in the *latifrons* series should be considered tentative. Similarly, the inclusion of *A. squamulatus*, traditionally included in the *latifrons* series (e.g., Savage and Guyer, 1989) should be considered tentative given the weak and inconsistent support for the relevant relationships (Fig. 3 versus Fig. 4) and the current lack of molecular data. We have tentatively included *A. squamulatus* in the *latifrons* series, where it was placed in the Bayesian tree (Fig. 4), rather than in the *aequatorialis* series, where is was placed in the parsimony tree (Fig. 3) or in the *punctatus* series, with which it agrees best in terms of geographic distribution (see "Phylogeny of *Dactyloa*," above) because it shares the derived character of large body size with members of the *latifrons* series. *Anolis propinquus* has traditionally been considered part of the *latifrons* series (Williams, 1988); however, the inclusion of this species should be considered tentative given its current absence from explicit phylogenetic analyses. Inclusion of *Anolis ibanezi*, inferred as closely related to *A. chocorum* in a recent phylogenetic analysis (Poe et al., 2009a), should also be considered tentative given that the phylogenetic tree was not shown by Poe et al. (2009a); thus, the placement of these two species with respect to the *latifrons* series as conceptualized here is uncertain.

The first use of the name "*latifrons* series" appears to have been in Etheridge's (1959) dissertation; however, that use does not qualify as published according to the ICPN (Article 4.2). Moreover, Etheridge used the name for a more inclusive taxon

approximating the clade to which the name *Dactyloa* is applied here. The oldest published use of the name "*latifrons* series" appears to be that of Gorman and Dessauer (1966), who also used the name for the more inclusive clade. As delimited here, the *latifrons* series more closely approximates the taxon called the *laticeps* group by Cope (1899; which appears to be a lapsus because the species is elsewhere [p. 7] referred to by the correct name *A. latifrons*), the giant mainland anoles or *squamulatus-latifrons* group by Dunn (1937), the *latifrons* species group by Williams (1988), the *latifrons* series by Savage and Guyer (1989), and the *latifrons* clade of Castañeda and de Queiroz (2011). However, the *latifrons* series as conceptualized here is potentially more inclusive than the *latifrons* clade of Castañeda and de Queiroz (2011), in that it appears to include *A. philopunctatus* and might also include some species currently considered *incertae sedis* within *Dactyloa* or absent from explicit phylogenetic analyses if they are found to be more closely related to the *A. latifrons* series than to *A. aequatorialis, A. punctatus, A. roquet,* and *A. heterodermus.*

Megaloa Castañeda and de Queiroz, new clade name

Definition (apomorphy-based): The clade originating in the ancestor in which a maximum SVL > 100 mm in males, synapomorphic with that of *Anolis latifrons* Berthold 1846, originated. **Reference phylogeny:** Figure 5, this study. **Inferred composition:** *Anolis agassizi* Stejneger 1900, *A. apollinaris* Boulenger 1919, *A. casildae* Arosemena, Ibáñez, and de Sousa 1991, *A. chocorum* Williams and Duellman 1967 (see "Comments"), *A. danieli* Williams 1988, *A. fraseri* Günther 1859, *A. frenatus* Cope 1899, *A. insignis* Cope 1871, *A. latifrons* Berthold 1846, *A. maculigula* Williams 1984, *A. microtus* Cope 1871, *A. princeps* Boulenger 1902, and *A. purpurescens* Cope 1899 (see "Comments"). Another species that might belong to *Megaloa* is *A. squamulatus* Peters 1863 (see

"Comments"). **Etymology:** Derived from the Greek *Mega* (large) + *loa* (the last part of the name *Dactyloa*) in reference to the large body size of the members of this subclade of *Dactyloa*.[3] **Comments:** Two supraspecific names are based on species in this clade: *Diaphoranolis* Barbour 1923 (type species = *D. brooksi* = *Anolis insignis* according to Etheridge [1959] and Savage and Talbot [1978]) and *Mariguana* Dunn 1939 (type species = *Anolis agassizi*). These names were applied to taxa ranked as genera and separated from *Anolis* based on differences in dorsal scalation (juxtaposed pavement-like scales in *A. insignis* [Barbour, 1923], and tiny non-imbricating granules interspersed with larger, single, obtusely keeled scales in *A. agassizi* [Dunn, 1939; Etheridge, 1959]) and dewlap morphology (supposedly nonextensible in *A. insignis* [Barbour, 1923] and poorly developed in *A. agassizi* [Dunn, 1939]). Given that we are emphasizing the associations of names with clades, rather than with categorical ranks, and that neither of these names has been associated with the clade of mainland anoles with large body size (if they have been associated with clades at all, those clades are subclades of the large size clade), it is more appropriate to create a new name for this clade than to use either *Diaphoranolis* or *Mariguana* (which remain available for smaller clades including their type species). Therefore, we created a name that refers etymologically to the large size character (see "Etymology").

In the context of the reference phylogeny, *A. chocorum* and *A. purpurescens* are included in *Megaloa* despite not being known to possess the synapomorphy of the clade. In the case of *A. chocorum*, smaller size is parsimoniously interpreted as a reversal. In the case of *A. purpurescens*, the only two known male specimens have

---

[3] The component *loa* is not intended to have any other meaning beyond reference to *Dactyloa* because it contains parts of both of the Greek words on which the name *Dactyloa* is based (*daktylos*, finger + *oa*, hem, border; in reference to the toe pads).

SVLs of 74 and 78 mm and have been considered juveniles (Williams 1988; MRC, personal observation), which suggests that adults may reach a body size larger than 100 mm.

Megaloa corresponds closely to the *laticeps* group of Cope (1899; which appears to be a lapsus because the species is elsewhere [Cope, 1899: 7] referred to by the correct name, *A. latifrons*), the giant mainland anoles or *squamulatus-latifrons* group of Dunn (1937), the *latifrons* species group of Williams (1988), the *latifrons* series of Savage and Guyer (1989), and the *latifrons* clade of Castañeda and de Queiroz (2011). However, it should be noted that *Megaloa* as conceptualized here is less inclusive than the *latifrons* series as conceptualized here, in excluding species that are more closely related to *A. latifrons* than to *A. aequatorialis, A. punctatus, A. roquet,* and *A. heterodermus* but branched from the lineage leading to *A. latifrons* before large size evolved (currently, there is only one known species, *A. philopunctatus*, that is considered to belong to the *latifrons* series but not to *Megaloa* [Fig. 5]). If *A. squamulatus* (which exhibits large body size) is part of the *latifrons* series, then it is also likely part of *Megaloa*, although it might not be part of either clade (see "Comments" on the *latifrons* series).

punctatus series Guyer and Savage 1987 ("1986"), informal clade name

Definition (branch-modified node-based): The crown clade originating in the most recent common ancestor of *A. punctatus* Daudin 1802 and all extant species that share a more recent common ancestor with *A. punctatus* than with *Anolis aequatorialis* Werner 1894, *A. latifrons* Berthold 1846, *A. roquet* (Bonnaterre 1789), and *A. heterodermus* Duméril 1851. **Reference phylogeny:** Figure 5, this study. **Inferred composition:** *Anolis anatoloros* Ugueto, Rivas, Barros, Sánchez-Pacheco and García-Pérez 2007, *A. caquetae* Williams 1974 (see "Comments"), *A. dissimilis* Williams 1965 (see "Comments"), *A. jacare* Boulenger

1903, *A. menta* Ayala, Harris and Williams 1984 (see "Comments"), *A. punctatus* Daudin 1802, *A. ruizii* Rueda and Williams 1986 (see "Comments"), *A. santamartae* Williams 1982 (see "Comments"), *A. solitarius* Ruthven 1916 (see "Comments"), *A. tigrinus* Peters 1863, *A. transversalis* Duméril 1851, and *A. vaupesianus* Williams 1982. Other species that might belong to the *punctatus* series are *A. deltae* Williams 1974, *A. gorgonae* Barbour 1905, *A. lamari* Williams 1992, *A. nasofrontalis* Amaral 1933, *A. paravertebralis* Bernal Carlo and Roze 2005, *A. pseudotigrinus* Amaral 1933, *A. soinii* Poe and Yañez-Miranda 2008, and *A. umbrivagus* Bernal Carlo and Roze 2005 (see "Comments"). **Comments:** In the context of the reference phylogeny, eight species traditionally associated with the *punctatus* series are excluded (*A. boettgeri, A. chloris, A. chocorum, A. fasciatus, A. festae, A huilae, A. peraccae, A. philopunctatus*), and four species not traditionally associated with the *punctatus* series (all placed in the *tigrinus* series, see below) are included (*A. menta, A. ruizii, A. solitarius, A. tigrinus*). *Anolis tigrinus* and its previously hypothesized relatives have traditionally been included in the *tigrinus* series (e.g., Williams, 1976b, 1992; Savage and Guyer, 1989); however, strong evidence supports *A. tigrinus* as nested within the *punctatus* series (Castañeda and de Queiroz, 2011). Williams (1992) noted problems in distinguishing the *punctatus* and *tigrinus* series (referred to by him as species groups) and raised the possibility that the *tigrinus* series is an ecomorphic subgroup of the *punctatus* series (he considered members of the *tigrinus* series to be representatives of the twig ecomorph, whereas he classified at least some members of the *punctatus* series as trunk-crown anoles). Our results support this hypothesis and we therefore consider *A. tigrinus* and its relatives part of the *punctatus* series rather than a separate *tigrinus* series, although a clade containing *A. tigrinus* and all species closer to it than to *A. punctatus* could be recognized as a sub-series or a species group within the *punctatus* series.

Strong evidence also supports the inclusion of *A. chloris*, *A. fasciatus*, *A. festae*, and *A. peraccae* in the *aequatorialis* series and *A. chocorum* in the *latifrons* series (see "Comments" on the *aequatorialis* and the *latifrons* series, above) and therefore the exclusion of those species from the *punctatus* series. In contrast, because of inconsistent placement or weak support for the relevant relationships between analyses (Fig. 3 versus Fig. 4), and because of a current lack of molecular data for most of the species (all except *A. huilae*), exclusion of *A. boettgeri*, *A. huilae*, and *A. philopunctatus* from the *punctatus* series and inclusion of *A. menta*, *A. ruizii*, and *A. solitarius* in that series should be considered tentative. For similar reasons, inclusion of *A. caquetae*, *A. dissimilis*, and *A. santamartae*, all traditionally included in the *punctatus* series (Williams, 1965, 1974, 1982), should also be considered tentative. *Anolis calimae*, another species traditionally referred to the *punctatus* series (Ayala et al., 1983), was inferred as closely related to species that we tentatively refer to the *punctatus* series in the parsimony tree (Fig. 3) but not in the Bayesian tree (Fig. 4); because of this and additional contradictory results regarding the relationship between *A. calimae* and the *punctatus* series (Castañeda and de Queiroz, 2011), *A. calimae* is here considered *incertae sedis* (which does not rule out inclusion in the *punctatus* series). The long branch leading to this species and its ambiguous relationships are consistent with Williams' (1983) conclusion that this species has no evident close relatives. The geographic distribution of *A. calimae* in the central portion of the western Cordillera of Colombia between 1,300 and 1,800 m (Ayala et al., 1983) does not correspond to the eastern distribution of the *punctatus* series but instead corresponds more closely to the distribution of the *aequatorialis* or the *heterodermus* series.

Although *A. carlostoddi* and *A. orcesi* were placed in the *punctatus* series in the parsimony tree (Fig. 3), they were not placed there in the Bayesian tree (Fig. 4). We have considered *A. carlostoddi incertae sedis* within *Dactyloa* based on the deep level of disagreement concerning its placement between analyses (Figs. 3, 4), as indicated by its basal regrafted position on the pruned and regrafted consensus tree (Fig. 5). The eastern distribution of *A. carlostoddi* suggests that it may be part of the *punctatus* series, as does that of *A. neblininus*, another species that we consider *incertae sedis* but which is grouped in the parsimony tree with species that we tentatively refer to the *punctatus* series (*A. menta*, *A. solitarius*, and *A. ruizii*). By contrast, we have tentatively assigned *A. orcesi* to the *heterodermus* series (and *Phenacosaurus*) based on moderate support from the Bayesian analysis for its inclusion (Fig. 4) as well as its possession of characters of the twig ecomorph (Losos, 2009). The distribution of *A. orcesi* on the eastern slopes of the northern Andes of Ecuador is consistent with referral to the *heterodermus* series, although it is also compatible with referral to the *punctatus* series (see "Comments" section on the *heterodermus* series below). The inclusion of *A. deltae*, *A. gorgonae*, and *A. soinii*, traditionally considered members of the *punctatus* series (Williams and Duellman, 1967; Williams, 1974; Poe and Yañez-Miranda, 2008), and *A. lamari*, *A. nasofrontalis*, *A. paravertebralis*, *A. pseudotigrinus*, and *A. umbrivagus*, traditionally considered members of the *tigrinus* series (Williams, 1992; Bernal Carlo and Roze, 2005), should also be considered tentative given their current absence from explicit phylogenetic analyses.

The *punctatus* series as conceptualized here is more inclusive than the eastern clade of Castañeda and de Queiroz (2011) in that it includes species that are more closely related to *A. punctatus* than to *Anolis aequatorialis*, *A. latifrons*, *A. roquet*, and *A. heterodermus*, but that diverged before the last common ancestor of the members of the eastern clade and might also include some species currently considered *incertae sedis* within *Dactyloa* or absent from explicit phylogenetic analyses. Additionally, species in the eastern clade of Castañeda and de Queiroz (2011) are characterized by having a cohesive

eastern Andean and Amazonian geographic distribution, and it is possible that some species in the *punctatus* series do not conform to this geographic pattern. All of the species here tentatively referred to the *punctatus* series (*A. caquetae*, *A. dissimilis*, *A. menta*, *A. ruizii*, *A. santamartae*, *A. solitarius*) are outside of the eastern clade in the parsimony tree (Fig. 3), and one of them (*A. caquetae*) is outside of the eastern clade in the Bayesian tree (Fig. 4), although all have eastern geographic distributions (see "Phylogeny of *Dactyloa*" above for details).

roquet series Williams 1976a, informal clade name

Definition (branch-modified node-based): The crown clade originating in the most recent common ancestor of *Anolis roquet* (Bonnaterre 1789) and all extant species that share a more recent common ancestor with *A. roquet* than with *A. aequatorialis* Werner 1894, *A. latifrons* Berthold 1846, *A. punctatus* Daudin 1802, and *A. heterodermus* Duméril 1851. **Reference phylogeny:** Figure 5, this study. **Inferred composition:** *Anolis aeneus* Gray 1840, *A. blanquillanus* Hummelinck 1940 (see "Comments"), *A. bonairensis* Ruthven 1923, *A. extremus* Garman 1887, *A. griseus* Garman 1887, *A. luciae* Garman 1887, *A. richardii* Duméril and Bibron 1837, *A. roquet* (Bonnaterre 1789), and *A. trinitatis* Reinhardt and Lutken 1862. **Comments:** Referral of *A. blanquillanus* to this clade is based on the results of Yang et al. (1974) and Creer et al. (2001). The *roquet* series as conceptualized here corresponds exactly in known composition to the *roquet* group, species group, series, and clade of previous authors (Underwood, 1959; Gorman and Atkins, 1967, 1969; Lazell, 1972; Williams, 1976a; Savage and Guyer, 1989; Creer et al., 2001; Castañeda and de Queiroz, 2011). Nevertheless, the *roquet* series as conceptualized here is potentially more inclusive than the *roquet* clade of Castañeda and de Queiroz (2011) in that it could include some species currently considered *incertae sedis* within *Dactyloa* or absent from explicit

phylogenetic analyses if they are found to be more closely related to the *roquet* clade than to the four other mutually exclusive *Dactyloa* subclades inferred by Castañeda and de Queiroz (2011).

heterodermus series Castañeda and de Queiroz, new informal clade name

Definition (branch-modified node-based): The crown clade originating in the most recent common ancestor of *Anolis heterodermus* Duméril 1851 and all extant species that share a more recent common ancestor with *A. heterodermus* than with *Anolis aequatorialis* Werner 1894, *A. latifrons* Berthold 1846, *A. punctatus* Daudin 1802, and *A. roquet* (Bonnaterre 1789). **Reference phylogeny:** Figure 5, this study. **Inferred composition:** *Anolis euskalerriari* (Barros, Williams, and Viloria 1996), *A. heterodermus* Duméril 1851, *A. inderenae* (Rueda and Hernández-Camacho 1988), *A. nicefori* (Dunn 1944), *A. orcesi* (Lazell 1969) (see "Comments"), *A. proboscis* Peters and Orcés 1956 (see "Comments"), *A. tetarii* (Barros, Williams, and Viloria 1996), and *A. vanzolinii* (Williams, Orcés, Matheus, and Bleiweiss 1996). Another species that might belong to the *heterodermus* series is *A. williamsmittermeierorum* Poe and Yañez-Miranda 2007 (see "Comments"). **Comments:** Inclusion of *A. orcesi*, a species traditionally included in *Phenacosaurus* (Lazell, 1969), should be considered tentative given the inconsistent placement of this species between analyses (Fig. 3 versus Fig. 4) and because molecular data are currently lacking. We have included *A. orcesi* in the *heterodermus* series, where it was placed in the Bayesian tree (Fig. 4), rather than in the *punctatus* series, where it was placed in the parsimony tree (Fig. 3), because of the stronger support obtained for that relationship as well as its sharing of characters of the twig ecomorph with other species traditionally referred to *Phenacosaurus* (Losos, 2009). The geographic distribution of *A. orcesi* along the eastern slopes of the northern Ecuadorean Andes corresponds with the distribution of

the *heterodermus* series, but also with that of the *punctatus* series. *Anolis williamsmittermeierorum*, previously considered closely related to *A. orcesi* (Williams and Mittermeier, 1991; Poe and Yañez-Miranda, 2007), is tentatively referred to *Phenacosaurus* given the current absence of this species from explicit phylogenetic analyses.

Anolis proboscis, *A. laevis*, and *A. phyllorhinus* were previously placed in the *laevis* species group or series, a group characterized by the presence of a nose leaf (Williams, 1979). Here we consider the relationships of *A. laevis* and *A. phyllorhinus* to be uncertain (see "Comments" section on *Phenacosaurus* below). The geographic distribution of *A. laevis* in the eastern foothills of the Peruvian Andes does not suggest a close relationship with *A. proboscis* but is consistent with referral to the *heterodermus* series (as well as the *aequatorialis* and *punctatus* series). In contrast, the geographic distribution of *A. phyllorhinus* in central Amazonia (Williams, 1979; Rodrigues et al., 2002) suggests neither a close relationship to *A. proboscis* nor inclusion in the *heterodermus* series but instead suggests inclusion in the *punctatus* series as proposed by Rodrigues et al. (2002), Yánez-Muñoz et al. (2010), and Poe et al. (2012). If *A. laevis* and one or both other species form a clade within the *heterodermus* series, then that clade could be recognized as the *laevis* species group (see also comments on *Scytomycterus*, below). If *A. laevis* and one or both other species are closely related to members of the *punctatus* series, as has been hypothesized previously (Williams, 1965, 1979), then they should be included within the *punctatus* series (perhaps as the *laevis* species group). However, if *A. laevis* and one or both of the other species lie outside of the five clades whose names incorporate the term "series" as defined here, then it would be appropriate to include them in a separate *laevis* series (defined as the most inclusive crown clade containing *A. laevis* but not *Anolis aequatorialis*, *A. latifrons*, *A. punctatus*, *A. roquet*, and *A. heterodermus*).

Regardless of whether a separate *laevis* series is to be recognized, if *A. laevis* forms a clade with either or both *A. phyllorhinus* and *A. proboscis* that can be diagnosed by the nose-leaf synapomorphy (but see Yánez-Muñoz et al., 2010), the name *Scytomycterus* Cope 1876 (derived from the Greek *Skytos*, skin or leather, + *mykteros*, nose; type species = *A. laevis*) would be an appropriate name for that clade. However, if *A. phyllorhinus* or *A. proboscis* form a clade but are not closely related to *A. laevis*, which differs from the other two species in having only a rudimentary nose leaf (Williams, 1979), the name *Scytomycterus* is not appropriate for that clade (given that the type is *A. laevis*); therefore, if that clade is to be named, a new name would be appropriate.

The *heterodermus* series as conceptualized here corresponds closely to the *Phenacosaurus* clade of Castañeda and de Queiroz (2011) and *Phenacosaurus* as conceptualized here. However, it should be noted that the *heterodermus* series as conceptualized here is potentially more inclusive than *Phenacosaurus* as conceptualized here (see below), in that it might include some species currently considered *incertae sedis* within *Dactyloa* or absent from explicit phylogenetic analyses if they are found to be more closely related to *A. heterodermus* than to members of the other four well-supported clades but branched from the lineage leading to *A. heterodermus* before the twig morphology evolved (currently, all species assigned to the *heterodermus* series are also referred to *Phenacosaurus*).

Phenacosaurus Barbour 1920, converted clade name

Definition (apomorphy-based): The clade originating in the ancestor in which the combination of morphological characters of the twig ecomorph (long pointed snout; forelimbs, hindlimbs, and tail short in proportion to body size), synapomorphic with that in *Anolis heterodermus* Duméril 1851, originated. **Reference phylogeny:** Figure 5, this study. **Inferred composition:** *Anolis euskalerriari* (Barros, Williams, and

Viloria 1996), *A. heterodermus* Duméril 1851, *A. inderenae* (Rueda and Hernández-Camacho 1988), *A. nicefori* (Dunn 1944), *A. orcesi* (Lazell 1969) (see "Comments"), *A. proboscis* Peters and Orcés 1956 (see "Comments"), *A. tetarii* (Barros, Williams, and Viloria 1996), and *A. vanzolinii* (Williams, Orcés, Matheus, and Bleiweiss 1996). Another species that might belong to *Phenacosaurus* is *A. williamsmittermeierorum* Poe and Yañez-Miranda 2007 (see "Comments"). **Comments:** *Phenacosaurus* was originally proposed (Barbour, 1920) as the name of a genus separate from *Anolis*. However, the addition of subsequently discovered species (e.g., Dunn, 1944; Lazell, 1969; Rueda and Hernández-Camacho, 1988; Myers et al., 1993; Barros et al., 1996; Williams et al., 1996) has decreased the morphological gap between the two taxa, and several phylogenetic studies (e.g., Jackman et al., 1999; Poe, 2004; Nicholson et al., 2005; Castañeda and de Queiroz, 2011; this study) have inferred *Phenacosaurus* to be nested within *Anolis*, so that recognizing *Phenacosaurus* as a genus would render *Anolis* paraphyletic. We therefore use the name *Phenacosaurus* for a subclade of *Anolis* that is not associated with the rank of genus (it is implicitly associated with a lower rank). All species in the *Phenacosaurus* clade have been considered twig anoles (Losos, 2009), an ecomorphological category characterized by long pointed snouts, few toepad lamellae, short limbs, and short, often prehensile, tails. Because several of those characters were used in the original diagnosis of *Phenacosaurus* (Barbour, 1920), we have defined that name as referring to the clade of twig anoles that includes its type species (*A. heterodermus*).

In the context of the reference phylogeny, one species not traditionally referred to *Phenacosaurus* is included (*A. proboscis*). Molecular data are currently lacking for *A. proboscis*, but this species was consistently placed with other species referred to *Phenacosaurus* (see also Poe et al., 2009b, 2012). *Anolis proboscis* possesses the morphological features characteristic of the twig ecomorph: long pointed snout, forelimbs, hindlimbs,

and tail short in proportion to body size. Moreover, ecological data indicates *A. proboscis* should be classified as a twig anole (Losos et al., 2012; Poe et al., 2012). Two species traditionally referred to *Phenacosaurus*, *Anolis carlostoddi* and *A. neblininus*, were placed inconsistently between analyses (Fig. 3 versus Fig. 4), but in neither case were they placed within *Phenacosaurus*. Because molecular data are currently lacking for *A. carlostoddi* and because some analyses based on molecular data suggest inclusion of *A. neblininus* in *Phenacosaurus* (Castañeda and de Queiroz, 2011, fig. 2C), neither species can be confidently excluded. Both species are here considered *incertae sedis* within *Dactyloa*. Inclusion of *A. orcesi*, a species traditionally included in *Phenacosaurus* (Lazell, 1969), should be considered tentative given the inconsistent placement of this species between analyses (Fig. 3 versus Fig. 4) and because molecular data are currently lacking. We have included *A. orcesi* in *Phenacosaurus*, where it was placed in the Bayesian tree (Fig. 4), rather than in the *punctatus* series, where it was placed in the parsimony tree (Fig. 3), because of the stronger support obtained for that relationship as well as its sharing of characters of the twig ecomorph with other species traditionally referred to *Phenacosaurus* (Losos, 2009). *Anolis williamsmittermeierorum*, previously considered closely related to *A. orcesi* (Williams and Mittermeier, 1991; Poe and Yañez-Miranda, 2007), is tentatively referred to *Phenacosaurus* given the current absence of this species from explicit phylogenetic analyses. *Anolis bellipeniculus* is tentatively excluded from *Phenacosaurus* based on its previously hypothesized close relationship to *A. neblininus* (Myers and Donnelly, 1996) and is here considered to be of uncertain position within *Dactyloa* (see "Incertae sedis," below).

Williams (1979) hypothesized that *A. laevis* and *A. phyllorhinus* are closely related to *A. proboscis*, which is here included in *Phenacosaurus*; however, that relationship has been questioned by Yánez-Muñoz et al. (2010) and Poe et al. (2012), and therefore

we consider *A. laevis* and *A. phyllorhinus* to be *incertae sedis* within *Dactyloa*. Little is known about *A. laevis*, which is known only from the type specimen, now in poor condition (Williams, 1979). However, as illustrated in Williams (1979, fig. 1), this specimen does not possess a nose leaf but only a protruding rostral scale, which is questionably homologous with the ample appendages of the other species. Moreover, the geographic distribution of *A. laevis* in the eastern foothills of the Peruvian Andes does not suggest a close relationship with *A. proboscis*, and although it is consistent with referral to the *heterodermus* series, it is also consistent with referral to the *aequatorialis* and *punctatus* series. *Anolis phyllorhinus* is better known, and although it possesses a true nose leaf, which is both similar to and different from that of *A. proboscis*, the information in Williams (1979) and Rodrigues et al. (2002) suggest that *A. phyllorhinus* is a trunk-crown rather than a twig anole (e.g., green coloration, moderate snout and limb lengths, long tail, high lamella counts, relatively large perch diameters, upward flight behavior, and high degree of similarity to *A. punctatus*, which has been classified as a trunk-crown anole [Williams, 1992]). Moreover, the geographic distribution of *A. phyllorhinus* in central Amazonia (Williams, 1979; Rodrigues et al., 2002) suggests neither a close relationship to *A. proboscis* nor inclusion in the *heterodermus* series but instead suggests inclusion in the *punctatus* series. Although we think that Yánez-Muñoz et al. (2010) are likely correct in assigning *A. phyllorhinus* in the *punctatus* series, the inclusion of neither *A. phyllorhinus* nor *A. laevis* in an explicit phylogenetic analysis leads us to treat both species as *incertae sedis* within *Dactyloa*.

Phenacosaurus as conceptualized here is more inclusive than the *Phenacosaurus* clade of Castañeda and de Queiroz (2011) in that it contains species (e.g., *A. proboscis* and possibly *A. orcesi*, see below) that share the twig ecomorph synapomorphy with *A. heterodermus* but lie outside of the smallest clade containing *A. heterodermus* and *A.*

euskalerriari. *Phenacosaurus* as conceptualized here is less inclusive than the *heterodermus* series as conceptualized, in excluding species that are more closely related to *A. heterodermus* than to members of the other four clades recognized here whose names include the term "series," but branched from the lineage leading to *A. heterodermus* before the twig morphology evolved (although currently all known species referred to *Phenacosaurus* are also referred to the *heterodermus* series).

Incertae sedis

The placement of the following species could not be resolved because of lack of data or because of conflicting results between analyses, and we therefore defer assigning them to any of the above described clades until more definitive evidence is available: *A. calimae* Ayala, Harris and Williams 1983, *A. carlostoddi* (Williams, Praderio and Gorzula 1996), *A. laevis* (Cope 1876), *A. neblininus* (Myers, Williams and McDiarmid 1993), and *A. phyllorhinus* Myers and Carvalho 1945. Possible relationships of these species have been discussed under "Comments" on the *punctatus* series (*A. calimae, A. carlostoddi, and A. neblininus*), the *heterodermus* series (*A. laevis* and *A. phyllorhinus*), and *Phenacosaurus* (*A. carlostoddi, A. laevis, A. neblininus* and *A. phyllorhinus*). We also consider the position of *A. bellipeniculus* (Myers and Donnelly 1996) to be uncertain within *Dactyloa* given its hypothesized close relationship to *A. neblininus* (Myers and Donnelly, 1996) and the uncertain relationships of that species. The eastern distribution of *A. bellipeniculus* on the isolated Cerro Yaví tepui of southeastern Venezuela (Myers and Donnelly, 1996) suggests that it may be part of the *punctatus* series. Similarly, the placement of *A. cuscoensis* Poe, Yañez-Miranda and Lehr 2008 is considered unresolved, because although this species has been included in an explicit phylogenetic analysis (Poe et al., 2008), its hypothesized relationships are incongruent

with the clades recognized here. The geographic distribution of this species along the eastern slopes of the southern Peruvian Andes (Poe et al., 2008) is congruent with the distributions of the *heterodermus*, *punctatus*, and *aequatorialis* series (if extended to the south). Although many species in the *aequatorialis* series have western distributions, the earliest branching species within the clade (including *A. boettgeri*, which was considered closely related to *A. cuscoensis*) inhabit the eastern slopes of the Andes.

According to the definitions presented above, some species might not belong to any of the five clades whose names incorporate the term "series"; specifically, any species or clade that is sister to a clade composed of two or more of the five clades whose names include the term "series" would not be a member of any of those clades. If strong support were to be found for such relationships, new "series" names could be proposed for the corresponding species or clades, although such names might be judged unnecessary for "series" composed of single species. Currently, however, most known species of *Dactyloa* are at least tentatively referable to one of the five mutually exclusive "series" clades, and even those species that are the best candidates for not being members of those clades (i.e., the species that we consider *incertae sedis*) might belong to them.

ACKNOWLEDGMENTS

APPENDIX I

Morphological Character Descriptions

Description of morphological characters used in phylogenetic analyses. Ranges of species means (for continuous characters) correspond to values before data transformation and coding. Results of correlation tests (R^2 and P values) are shown.

External Characters, Examined on Alcohol-Preserved Specimens

1. Maximum male snout-to-vent length (SVL; Williams et al., 1995, character 35). Measured with a 1-mm precision ruler from the tip of the snout to the anterior lip of the cloacal opening. Continuous character. Range: 41–170 mm.
2. Ratio of maximum female SVL to maximum male SVL (Poe, 1998, character 11), both measured with a 1-mm precision ruler. This character was not correlated with SVL ($R^2 = 0.03$, $P = 0.25$). Continuous character. Range: 0.64–1.35.
3. Length of head (Poe, 2004, character 4), measured with 0.01-mm precision calipers from the tip of the snout to the anterior edge of the ear opening. This character was correlated with SVL ($R^2 = 0.94$, $P < 0.001$) and head width ($R^2 = 0.97$, $P < 0.001$). To correct for size, head length mean values were natural log transformed and regressed on natural log–transformed SVL mean values. Residuals were subsequently used. Continuous character. Range: 10.68–47.16 mm.

4.   Width of head (Poe, 2004, character 5), measured with 0.01-mm precision calipers at the widest part of the head—usually the corners of the mouth. This character was correlated with SVL ($R^2 = 0.94$, $P < 0.001$) and head length ($R^2 = 0.97$, $P < 0.001$). To correct for size, head width mean values were natural log transformed and regressed on natural log–transformed SVL mean values. Residuals were subsequently used. Continuous character. Range: 5.00–29.46 mm.

5.   Height of ear (Poe, 2004, character 6), measured between the internal borders with 0.01-mm precision calipers. This character was correlated with SVL ($R^2 = 0.58$, $P < 0.001$), head length ($R^2 = 0.46$, $P < 0.001$), and head width ($R^2 = 0.56$, $P < 0.001$). To correct for size, ear height mean values were natural log transformed and regressed on natural log–transformed SVL mean values. Residuals were subsequently used. Continuous character. Range: 0.60–4.84 mm.

6.   Interparietal scale length (modified from Poe, 2004, character 7), measured with 0.01-mm precision calipers from the anterior to posterior edges of the scale. The interparietal scale is defined as the scale overlying the parietal foramen (Peters, 1964). Located in the parietal area, this scale is typically of larger size than surrounding scales and exhibits an area of clear skin above the parietal eye. In some species, no clear skin area is observed, but a scale appears to be homologous to the interparietal based on position, shape, and size. These scales were measured as interparietals. When scale edges were not parallel to each other, the distance between the most anterior to the most posterior points on the scale were measured. This character was correlated with SVL ($R^2 = 0.07$, $P = 0.03$), head length ($R^2 = 0.09$, $P = 0.002$), and head width ($R^2 = 0.10$, $P = 0.01$). To correct for size, interparietal length mean values were natural log transformed and regressed on natural log-transformed SVL mean values. Residuals were subsequently used. Continuous character. Range: 0.55–3.86 mm.

7.   Mean number of dorsal scales in 5% of SVL (Poe, 2004, character 19). The equivalent of 5% of SVL was set on 0.01-mm precision calipers, and the number of scales contained in this length was counted three times (using the average as the final count) lateral to the dorsal midline at the level of the forelimbs. This character is an estimate of dorsal scale size. Continuous character. Range: 4.20–18.27.

8.   Mean number of ventral scales in 5% of SVL (Poe, 2004, character 20). The equivalent of 5% of SVL was set on 0.01-mm precision calipers, and the number of scales contained in this length was counted three times (using the average as final count) lateral to the ventral midline in middle and posterior areas of the body. This character is an estimate of ventral scale size. Continuous character. Range: 5.08–13.80.

9.   Mean number of scales between the second canthals (Williams et al., 1995, character 2). Minimum count between left and right second canthals, excluding canthal scales. This character was not correlated with SVL ($R^2 = 0.01$, $P = 0.38$), head length ($R^2 < 0.001$, $P = 0.93$), or head width ($R^2 = 0.003$, $P = 0.64$), thus no correction for size was applied. Continuous character. Range: 2.00–17.50.

10.   Mean number of postrostral scales (Williams et al., 1995, character 3). Postrostrals are all scales in contact with (posterior to) the rostral scale, between supralabials. This character was correlated with SVL ($R^2 = 0.08$, $P = 0.02$) and head width ($R^2 = 0.07$, $P = 0.03$), but not head length ($R^2 = 0.05$, $P = 0.06$). To correct for size, mean numbers of postrostral scales were natural log transformed and regressed on natural log–transformed SVL mean values. Residuals were subsequently used. Continuous character. Range: 2.88–8.60.

11.   Mean number of scales between supraorbital semicircles (Williams et al., 1995, character 6). Minimum count between left and right supraorbital seimicircles. This character was correlated with SVL ($R^2 = 0.20$, $P < 0.001$), head length ($R^2 = 0.16$, $P < 0.001$), and head width ($R^2 = 0.18$, $P < 0.001$). To correct for size, the mean numbers of scales between supraorbital semicircles were $\ln(x + 1)$ transformed and regressed on natural log–transformed SVL mean values. Residuals were subsequently used. The $\ln(x + 1)$ transformation was used because this character contains mean zero values. Continuous character. Range: 0–5.50.

12.   Mean number of loreal rows (Williams et al., 1995, character 10). Loreal scales cover the area between canthals, supralabials, and subocular scales. Rows were counted as the minimum number of scales, in a straight line, from the first or second canthal to the sublabial scales on the right side of the head, unless the area was damaged, and then the left side was scored. This character was correlated with SVL ($R^2 = 0.12$, $P = 0.01$), head length ($R^2 = 0.06$, $P = 0.05$), and head width ($R^2 = 0.10$, $P = 0.01$). To correct for size, mean numbers of loreal rows were natural log transformed and regressed on natural log–transformed SVL mean values. Residuals were subsequently used. Continuous character. Range: 1.00–10.20.

13.   Mean number of supralabial scales to below the center of the eye (Williams et al., 1995, character 16), counted from the rostral (not included) to the midpoint of the eye. More than half the scale had to be anterior to the center of the eye to be included in the count. This character was correlated with SVL ($R^2 = 0.12$, $P = 0.01$), head length ($R^2 = 0.15$, $P < 0.001$), and head width ($R^2 = 0.09$, $P = 0.02$). To correct for size, mean numbers of supralabial scales were natural log

transformed and regressed on natural log–transformed SVL mean values. Residuals were subsequently used. Continuous character. Range: 5.00–11.00.

14. Mean number of postmental scales (Williams et al., 1995, character 17). Postmentals are all scales in contact with (posterior to) the mental scale between the infralabials (i.e., including the anteriormost sublabial scale on left and right sides). This character was correlated with SVL ($R^2 = 0.06$, $P = 0.04$) and head width ($R^2 = 0.07$, $P = 0.03$), but not head length ($R^2 = 0.03$, $P = 0.21$). To correct for size, mean number of postmental scales were natural log transformed and regressed on natural log–transformed SVL mean values. Residuals were subsequently used. Continuous character. Range: 2.63–10.13.

15. Mean number of sublabial scales (Williams et al., 1995, character 18; Poe, 2004, character 44). Sublabial scales are abruptly enlarged scales (more than twice the size) located medial and parallel to the infralabials and posterior to the mental. This character was correlated with SVL ($R^2 = 0.13$, $P < 0.001$), head length ($R^2 = 0.07$, $P = 0.03$), and head width ($R^2 = 0.11$, $P = 0.01$). To correct for size, the mean number of sublabial scales were $\ln(x + 1)$ transformed and regressed on natural log–transformed SVL mean values. Residuals were subsequently used. The $\ln(x + 1)$ transformation was used because this character contains mean zero values. Continuous character. Range: 0–7.00.

16. Mean number of scales between the interparietal scale and the supraorbital semicircles (Williams et al., 1995, character 13; Poe, 2004, character 46). The minimum number of scales between the interparietal scale and the supraorbital semicircles was counted. This character was correlated with SVL ($R^2 = 0.11$, $P = 0.01$), head length ($R^2 = 0.07$, $P = 0.03$), and head width ($R^2 = 0.09$, $P = 0.02$). To correct for size, the mean number of scales between interparietal and supraorbital semicircles were $\ln(x + 1)$ transformed and regressed on natural log–transformed SVL mean values. Residuals were subsequently used. The $\ln(x + 1)$ transformation was used because this character contains mean zero values. Continuous character. Range: 0–7.25.

17. Number of elongated superciliary scales (Williams et al., 1995, character 8). Superciliaries are scales along the dorsal rim of the orbit, and elongation occurs toward the posterior end of the orbit. Left and right sides were scored separately. States: (0) 0, (1) 1, (2) 2, (3) 3. Polymorphic character. Ordered.

18. Number of scales between subocular and supralabial scales (Williams et al., 1995, character 15; Poe, 2004, character 28). The minimum number of scales was recorded for each specimen. States: (0) 0, (1) 1, (2) 2. Polymorphic character. Ordered.

19. Number of ventral scales posteriorly bordering one scale (modified from Poe, 2004, character 14). Middle and posterior ventral areas were examined. Ventral scales may be bordered posteriorly by two scales (0), by two and three scales (1), or by three scales (2). Polymorphic character. Ordered.

20. Shape of the base of the tail (modified from Williams et al., 1995, character 30; Poe, 2004, character 15). On each specimen, at the point where the knee would reach the tail if the leg were folded back, the height and width of the tail was measured, and then the ratio of width/height was calculated. States: (0) tail round, for ratios larger than 1; (1) tail laterally compressed, for ratios smaller than 1. Polymorphic character.

21. Toepad overlap (Williams et al., 1995, character 27; Poe, 2004, character 9). The toepad under phalanges III and IV may project distally under phalanx II (0) or not project distally (1), or the toepad may be completely absent (2). Polymorphic character. Ordered.

22. Male dewlap extension (Williams et al., 1995, character 33; Poe, 2004, character 16). On the ventral side, the posterior extension of the unfolded dewlap is examined. Four states were considered: posterior extension past the arm insertion (0), posterior extension to arm insertion (1), shorter than arm extension (2), dewlap absent (3). Polymorphic character. Ordered.

23. Female dewlap extension (Williams et al., 1995, character 34; Poe, 2004, character 17). Measurement and coding as in male dewlap extension. This character is not correlated with male dewlap extension ($R^2 = 0.210$, $P = 0.136$); therefore, it was considered a separate character. Polymorphic character. Ordered.

24. Size of scales in supraocular discs (modified from Poe, 2004, character 41). Three different states were considered: (0) scales vary continuously in size, in which a few scales are slightly larger (less than twice the size) than the others, showing gradual reduction in size; (1) one to three abruptly enlarged scales (more than twice the size) with all other scales of smaller size; and (2) all scales about equal in size. Polymorphic character. Unordered.

25. Dewlap scales (modified from Poe, 2004, character 21). The scales on the dewlap may be in rows of single scales (0); in double rows (1) or have scattered scales covering the entire dewlap (2). In some specimens, most rows were either single or double, with a few rows exhibiting the alternative condition. In such cases, the most common condition was scored for the specimen. Polymorphic character. Unordered.

26. Width of mental relative to rostral (modified from Poe, 2004, character 27). In ventral view, the mental scale may be broader than the rostral (0), the rostral scale may be broader than the mental (1), or both

scales may show the same width (2). Polymorphic character. Unordered.

27. Enlarged postanal scales in males (Williams et al., 1995, character 32). Postanal scales may be: (0) absent, (1) present, as a pair of significantly enlarged (more than four times the surrounding scales), (2) present, as a series of more than two scales slightly enlarged (less than twice the size of surrounding scales). Polymorphic character. Unordered.

28. Presence or absence of tail crest in males (Williams et al., 1995, character 31). The tail crest in males may be: (0) absent, (1) present as a series of enlarged, but not elevated, serrated scales, or (2) present as the result of enlarged neural spines. The presence of a crest is associated with sex and age of the specimen; therefore, when intraspecific variation was observed (presence and absence) the species was coded as present. However, states 1 and 2 were never observed in the same species. Unordered.

29. Heterogeneous flank scales (modified from Williams et al., 1995, character 23). Heterogeneous scales may be (0) absent, (1) very large and separated from one another by many scales of much smaller size, (2) a mosaic of scales of different sizes but not very different in size from one another, or (3) of average size surrounded by granular-minute scales. Polymorphic character. Unordered.

30. Mental scale (Poe, 2004, character 26). The mental scale may be partially divided (0), in which a longitudinal split begins from the posterior edge of the mental but does not reach the anterior edge, or completely divided (1), in which the split is complete. Polymorphic character.

31. Frontal depression (Poe, 2004, character 45). A depression around the frontal area may be absent (0), in which case the dorsal surface of the snout is flat, or present (1). Polymorphic character.

32. Presence or absence of an externally visible parietal eye (Estes et al., 1988, character 26). The parietal eye, when visible externally, is located within the interparietal scale (see character 6). States: absent (0), present (1). Polymorphic character.

33. Keeling of dorsal, ventral, supradigital and head scales (Williams et al., 1995, characters 20, 25, 29, 1; Poe 2004, character 40). Dorsal, ventral, and supradigital scales may be smooth (S) or keeled (K); head scales may in addition be rugose (R) or have pustules (P). The four apparently independent characters were combined as one after correlation was found between ventral, supradigital, and head keeling with dorsal keeling ($R^2 = 0.201, P < 0.0001; R^2 = 0.635, P < 0.0001; R^2 = 0.456, P < 0.0001$, respectively). The condition present in the majority of the scales was reported. Dorsal scale keeling was scored excluding middorsal scales because these often differ from the remaining dorsals (e.g., some species exhibit smooth dorsal scales, but a double row of keeled middorsal scales). Weakly keeled specimens were coded as keeled. Rugose refers to multiple, less pronounced keels or bent ridges (these two conditions were commonly found combined in one scale); with pustules refers to multiple granular projections scattered on the scale. States (for dorsals, ventrals, supradigitals, head scales): KKKK (0), KKKR (1), KKKS (2), KKSP (3), KSKK (4), KSKS (5), SSKR (6), SSKS (7), SSSS (8), SSSR (9). Modal condition coded. Unordered.

Osteological Characters Examined on Dry, Cleared, and Stained Specimens and/or Radiographs.

34. Shape of parietal crests (Etheridge, 1959, fig. 9; Cannatella and de Queiroz, 1989, characters 6, 7; Williams, 1989, character 7, modified from Poe, 1998, character 87). Three different states were considered: (0) trapezoid–shape: lateral borders of the crest reach the occipital crest directly (i.e., do not touch each other before occipital crest contact); (1) V-shape: lateral borders of the crest join at the point of contact with the occipital crest, and there is no extension beyond the point of contact; (2) Y-shape: lateral borders of the crest join before occipital crest contact and extend posteriorly beyond the point of contact (i.e., a unified crest extends toward or beyond the occipital). Etheridge (1959) showed that this character exhibits ontogenetic variation, from a U/trapezoid shape seen in early stages to an intermediate V-shape, to a Y-shaped crest seen in adult stages. To compensate for the absence of sex and SVL information to confirm adulthood in some specimens, the most developed state observed (following Etheridge's ontogenetic sequence) was scored for each species. Ordered.

35. Presence or absence of crenulation along lateral edges of parietal (Poe, 1998, character 88). The parietal may exhibit irregular (crenulated) or smooth lateral edges. States: absent (0), present (1). Polymorphic character.

36. Extension of the parietal roof (modified from Poe, 2004, character 59). In anoles, a parietal casque has been defined as the shelf-like posterolateral extension of the parietal roof over the supratemporal processes of the parietal. Poe (2004) coded the presence or absence of the casque, but we found variation in the length of the extension. The roof extension may be large, almost completely covering the supratemporal processes and sometimes extending beyond the posteriormost margin, or the extension could be small, leaving more of the supratemporal process uncovered and not reaching the posterior margin of the parietal. States: not extended (0; e.g., *A. chocorum*, MCZ 115732); present and small, not reaching posteriormost margin of supratemporal processes (1; e.g., *A. fitchi*, MCZ 178084); present and large, reaching or
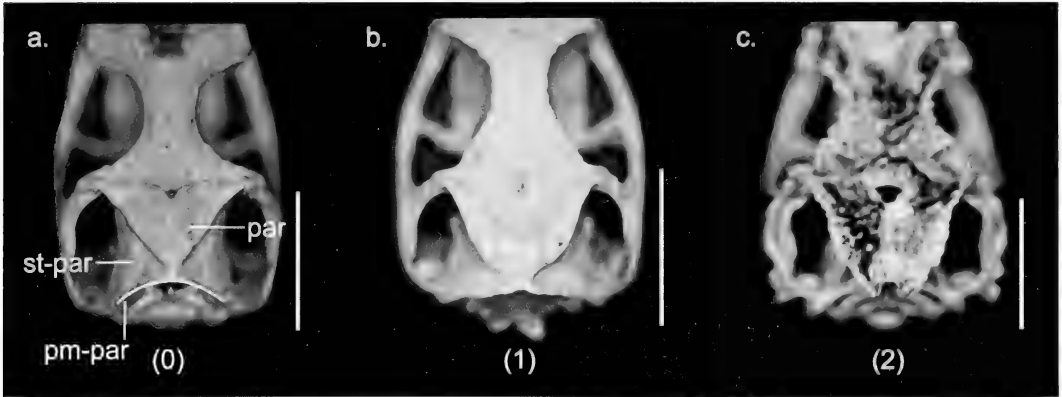
Figure 6.   Dorsal views of the skulls of three anoles illustrating differences in the extension of the parietal roof (character 36). (a) *Anolis chocorum*, MCZ 115732 (state 0); (b) *Anolis fitchi*, MCZ 178084 (state 1); (c) *Anolis heterodermus*, MCZ 110138 (state 2). Scale bar = 5 mm. Abbreviations: par, parietal; st-par, supratemporal processes of the parietal; pm-par, posterior margin of parietal.

extending beyond the posteriormost margin of supratemporal processes (2; e.g., *A. heterodermus*, MCZ 110138) (Fig. 6). The largest extension of the parietal roof observed among all individuals was scored for each species. Ordered.

37.   Parietal foramen (Etheridge, 1959; Williams, 1989, character 5). The parietal foramen may be located completely within the parietal (0) or may be at the fronto-parietal suture (1). Cases in which the foramen is located within the parietal but connected to the fronto-parietal by a suture were coded as 0. Absence of the parietal foramen was coded as ?, instead of as a third state, given that the information on the presence or absence of an externally visible parietal eye was coded as a separate character

(character 32) from alcohol-preserved specimens. Polymorphic character.

38.   Fronto-parietal suture (this study). The fronto-parietal suture may form a straight transverse line (i.e., perpendicular to the longitudinal axis of the body) (0; e.g., *A. danieli*, MCZ 164894) or it may exhibit a posteriorly convex curve in the center because of extension of the frontal bone into the parietal bone (1; e.g., *A. eulaemus*, MCZ 158390) (Fig. 7). Significant variation was observed in the latter state (from a slight to a substantial protuberance), but this variation was not quantified. Polymorphic character.

39.   Presence or absence of postfrontal (Etheridge and de Queiroz, 1988, character 6; Poe, 1998,
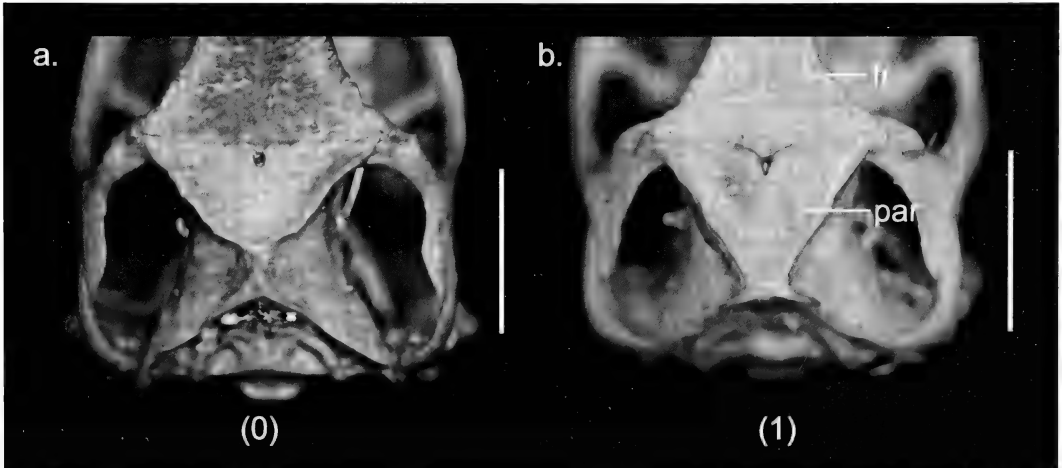

Figure 7.   Dorsal views of the skulls of two anoles illustrating differences in the fronto-parietal suture (character 38). (a) *Anolis danieli*, MCZ 164894 (state 0); (b) *Anolis eulaemus*, MCZ 158390 (state 1). Scale bar = 5 mm. Abbreviations: fr, frontal; par, parietal.

character 92; 2004, character 62). The postfrontal bone is located in the posterodorsal margin of the orbit between (or overlapping) the frontal and the postorbital. States: absent (0), present (1). Polymorphic character.

40.   Frontal (Poe, 1998, character 94; 2004, character 64). The anterior suture of the frontal may be in contact only with nasals (0), may be separated from nasals by an open gap (1), or may be in contact with both the premaxilla and nasal (2). State 1 includes cases where the gap was along the entire suture or, most commonly, in the center only, allowing partial lateral contact between frontal and nasals. Posterior extension of the premaxilla, sufficient to potentially contact the frontal (i.e., if the gap were absent), was never observed along with the open gap. Polymorphic character. Unordered.

41.   Prefrontals (Poe, 1998, character 93, fig. 4). Prefrontals may be in contact with nasals (0) or may be separated from nasals by the contact between frontal and maxilla (1). Any contact between prefrontal and nasal was scored as 0. Differences between left and right sides were observed in some specimens; therefore, each side was treated separately for frequency calculations. Polymorphic character.

42.   Posterior extension of maxilla (Poe, 1998, character 103, fig. 8). Different landmarks have been used as boundaries to quantify the posterior extension of the maxilla (e.g., Estes et al., 1988, character 27; Frost and Etheridge, 1989, character 3). Following Poe (1998), the posterior edge of the ectopterygoid was used to delimit two different states: (0) maxilla does not extend posteriorly beyond the posterior edge of ectopterygoid (including cases in which it extends to that level) or (1) maxilla extends beyond the posterior edge of ectopterygoid. Differences between left and right sides were observed in some specimens; therefore, each side was treated independently for frequency calculations. Polymorphic character.

43.   Mean number of premaxillary teeth (de Queiroz, 1987, characters 43, 44). This character was not correlated with SVL ($R^2 = 0.01$, $P = 0.46$), head length ($R^2 = 0.013$, $P = 0.39$), or head width ($R^2 = 0.009$, $P = 0.47$); thus, no correction for size was applied. Range: 6–13. Continuous character.

44.   Presence or absence of pterygoid teeth (Etheridge, 1959; Poe, 1998, character 101). Pterygoid teeth are found along the edge facing the pyriform recess, either clumped or in a single row. States: absent (0), present (1). Polymorphic character.

45.   Presence or absence of contact between jugal and squamosal (Frost and Etheridge, 1989, character 8). The jugal and squamosal bones may be in contact along the ventral edge of the temporal bar, or they may be separated by the postorbital bone. In some specimens, differences between the left and right sides were found; therefore, each side

was treated separately for frequency calculations. States: absence (0), presence (1). Polymorphic character.

46.   Shape of posteroventral corner of jugal (modified from Poe, 2004, character 69). Poe (2004) recognized two states of this character: posteroventral corner of jugal is anterior to the posterior edge of jugal (in species where the posterior edge of the jugal shows a straight or convex border) or is posterior to the posterior edge of the jugal (in species where the posterior edge of jugal shows a concave border). However, we found these two character states not to be mutually exclusive; therefore, the states were modified as follows: posterior border of the jugal concave, with a sharp (pointed) posteroventral corner (0), or posterior border straight or convex, with a rounded posteroventral corner (1). Differences between left and right sides were observed in some specimens; therefore, each side was treated independently for frequency calculations. Polymorphic character.

47.   Presence or absence of contact between parietal and epipterygoid (Poe, 1998, character 99). The epipterygoid extends from the palate toward the skull roof and may or may not reach the parietal. In some species, the most distal portion of the epipterygoid is cartilaginous and often lost during skull preparation, rendering the structure not in contact with the parietal. Cases in which the absence of contact is an artifact of preparation could not be distinguished from those in which the epipterygoid (with or without cartilaginous portion) is short enough not to be in contact with the parietal. All cases with no contact were coded as absence. No intraspecific variation was observed. States: absent (0), present (1).

48.   Supraoccipital cresting (Poe, 1998, character 105, fig. 9; 2004, character 55). The supraoccipital may show: (0) a single medial process (called *processus ascendens*; e.g., *A. heterodermus*, MCZ 110133); (1) a medial process in addition to two distinct and smaller lateral processes (not always ossified; e.g., *A. chloris*, MCZ 101290) or (2) a continuous (e.g., *A. agassizi*, MCZ 18088) or partially continuous crest (showing two lateral processes with a distinct crest between them) running along the edge of the osseus labyrinth (Fig. 8). Significant ontogenetic variation was observed within each one of the states, but a sequence linking all three states was not observed; therefore, the modal condition was scored for each species. Unordered.

49.   Contact between parietal and supraoccipital (this study). The parietal may be widely separated from the supraoccipital, leaving free space between the two on either side of the processus ascendens (0; e.g., *A. princeps*, MCZ 147444), or may be in contact (or almost in contact) with the supraoccipital, leaving no open space in between (1; e.g., *A. ventrimaculatus*, MCZ 127711) (Fig. 9). Polymorphic character.
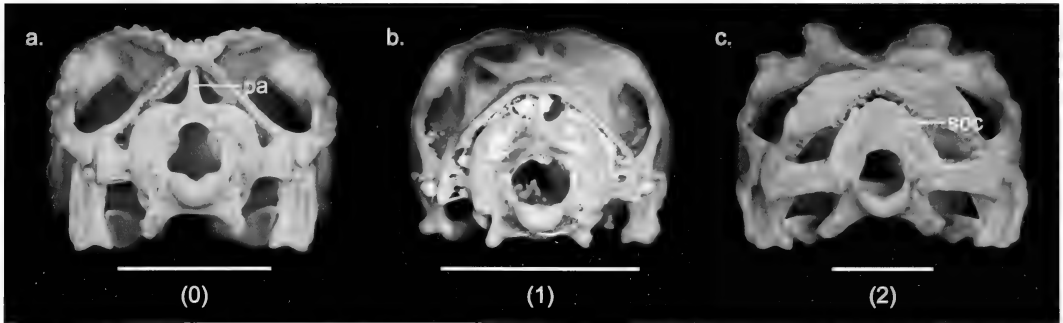
Figure 8.   Posterior views of the skulls of three anoles illustrating differences in the supraoccipital cresting (character 48). (a) *Anolis heterodermus*, MCZ 110133 (state 0); (b) *Anolis chloris*, MCZ 101290 (state 1); (c) *Anolis agassizi*, MCZ 18088 (state 2). Scale bar = 5 mm. Abbreviations: pa, processus ascendens; soc, supraoccipital.

50.   Extension of the supratemporal processes of the parietal (this study). In some species (e.g., *A. agassizi*, MCZ 27120), the supratemporal processes of the parietal extend dorsally forming a vertical flange (1); in others (e.g., *A. heterodermus*, MCZ 110133), the supratemporal processes of the parietal do not extend (0) (Fig. 10). Significant variation was observed in the height of the extension, but it was not quantified. Additionally, ontogenetic variation was observed within some species; therefore, the most developed state (i.e., supratemporal processes extended) was scored for the species if it was observed in any specimens. States: supratemporal processes of the parietal not extended (0), extended (1).

51.   Presence or absence of the quadrate lateral shelf (Poe, 1998, character 106, fig. 10). The quadrate lateral shelf is the lateral extension of the external edge of the quadrate. Ontogenetic variation was observed within some species; thus, the developed state (i.e., presence of quadrate lateral shelf) was scored for the species when observed. States: absent (0), present (1).

52.   Presence or absence of angular process of prearticular (de Queiroz, 1987, character 41, fig. 28; Poe, 1998, character 110, fig. 11). This process is located on the medial side of the retroarticular process of the prearticular and has a fin-like or rounded shape. Presence was coded as a significant extension beyond an imaginary line along the medial edge (in dorsal view) of the prearticular. Absent and rudimentary processes were coded as absent. Differences in size of the process were observed, but were not quantified. Poe (1998, 2004) called this structure angular process of the articular, but the articular is an endochondral (rather than dermal) bone that results from the ossification of the posterior end of Meckel's
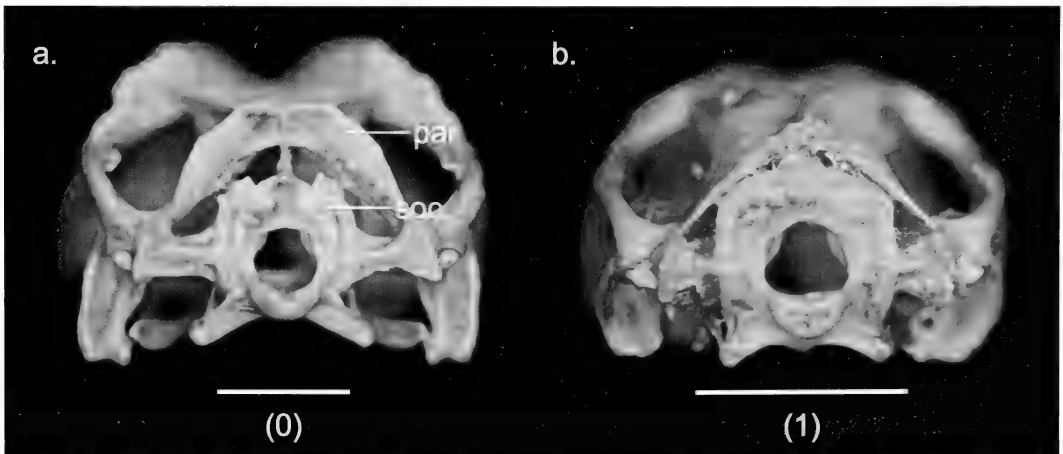

Figure 9.   Posterior views of the skulls of two anoles illustrating differences in the contact between the parietal and supraoccipital (character 49). (a) *Anolis princeps*, MCZ 147444 (state 0); (b) *A. ventrimaculatus*, MCZ 127711 (state 1). Scale bar = 5 mm. Abbreviations: par, parietal; soc, supraoccipital.
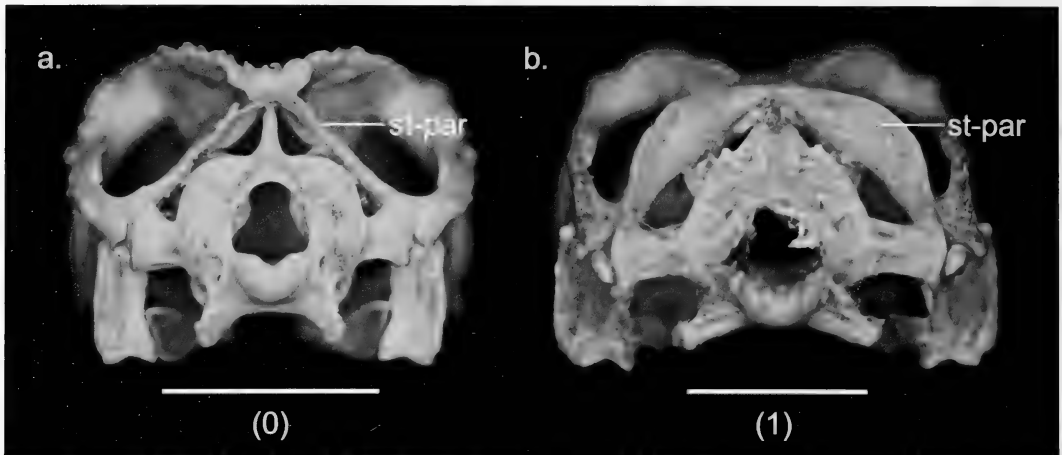
Figure 10.   Posterior views of the skulls of two anoles illustrating differences in the extension of the supratemporal processes of the parietal (character 50). (a) *Anolis heterodermus*, MCZ 110133 (state 0); (b) *Anolis agassizi*, MCZ 27120 (state 1). Scale bar = 5 mm. Abbreviations: st-par, supratemporal processes of the parietal.

cartilage and forms the articular condyle, but neither the retroarticular nor the angular process (de Queiroz, 1987). No intraspecific variation was observed. States: absent (0), present (1).

53.   Position of posteriormost tooth with respect to the combined alveolar-mylohyoid foramen (camf; modified from de Queiroz, 1987, characters 34, 35; Poe, 1998, character 109; 2004, character 81). Etheridge (1959) reported that in some iguanids (e.g., anoles) the anterior mylohyoid foramen (amf, usually located within the splenial) is united with the anterior inferior alveolar foramen (aiaf, located between the dentary and splenial), resulting in a single foramen. In the present study, the single foramen is called the combined alveolar-mylohyoid foramen (camf). Poe (1998, 2004) compared the position of the posteriormost tooth to the amf, which is the same as this character. We compared the position of the posterior edge of the posteriormost tooth to the camf, and considered three states: posteriormost tooth is anterior to camf (0), overlaps with camf (1), posteriormost tooth is posterior to camf (2). Left and right mandibles were coded separately. Polymorphic character. Unordered.

54.   Shape of the posterior suture of dentary (Poe, 1998, character 111, fig. 12). In lateral view, the suture of the dentary with the surangular may have a distinctly pronged (i.e., with two process-es) or a blunt, undifferentiated shape. No intraspecific variation was observed. States: pronged (0), blunt (1).

55.   Position of posterior suture of dentary, relative to mandibular fossa (Poe, 1998, character 112). Given the possible shape of this suture (blunt or pronged), the anteriormost aspect of the

posterior border is the point used for comparison. States: posterior border of dentary is anterior to mandibular fossa (0) or within mandibular fossa (1). Polymorphic character.

56.   Position of surangular foramen (Frost and Etheridge, 1988, character 19, fig. 3; Poe, 1998, character 115, fig. 13). The surangular foramen (on the lateral surface of the mandible; same as Poe's [2004] supra-angular foramen) may be located entirely within the surangular (0) or be partially bordered by the dentary (1). Differences between left and right sides were observed in some specimens; therefore, each side was treated separately for frequency calculations. Polymorphic character.

57.   Presence or absence of splenial bone (Etheridge, 1959; Poe, 2004, character 85). States: absent (0), present as anteromedial sliver (1), or present and large, as in *Polychrus* and other non-anole iguanids (2). No intraspecific variation was observed. Ordered.

58.   Presence or absence of angular bone (Etheridge, 1959). States: absent (0), present (1). No intraspecific variation was observed.

59.   Overlap between clavicles and lateral processes of interclavicle (modified from Etheridge, 1959). Etheridge (1959) described two different types of interclavicles in anoles: arrow-shaped (in which the lateral processes of the interclavicle are caudolat-erally directed and only medially overlapped by the clavicle) or T-shaped (in which the lateral process-es are laterally directed and broadly overlapped by the clavicle). The two components of the inter-clavicle shape, as described by Etheridge (1959), can vary independently; therefore, this character was divided into two. The first was quantified as
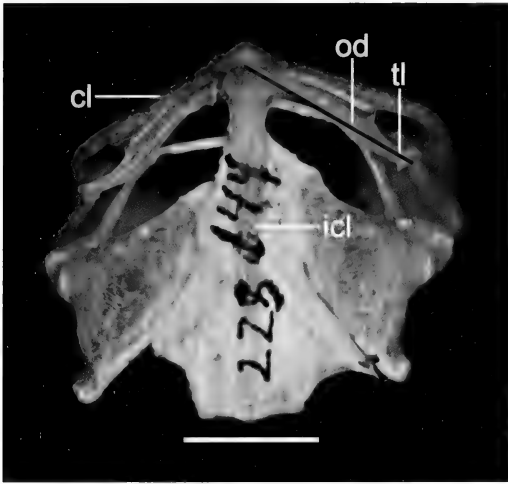
Figure 11. Ventral view of the pectoral girdle illustrating details on measurements of the overlap between clavicles and the lateral processes of the interclavicle (character 59). Scale bar = 5 mm. Abbreviations: cl, clavicle; icl, interclavicle; od, overlapped distance; tl, total length of lateral process of interclavicle.
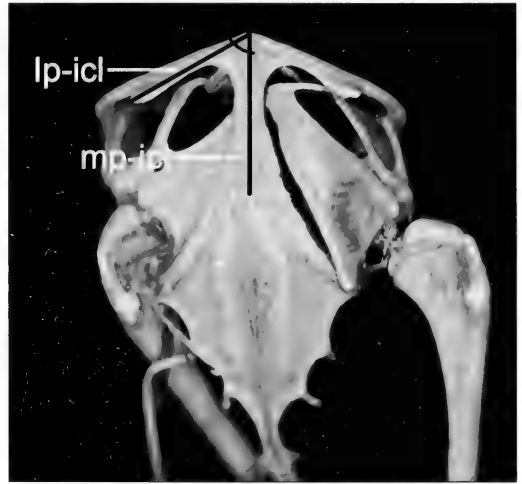

Figure 12. Ventral view of the pectoral girdle illustrating details on measurements of the angle between the median (posterior) process and the lateral process of the interclavicle (character 60). Abbreviations: lp-icl, lateral process of interclavicle; mp-icl, medial process of interclavicle.

the fraction of the length of the lateral process of the interclavicle in direct contact with (i.e., overlapped by) the clavicle. The total length of the lateral process was measured as a straight line from the midline of the interclavicle (an imaginary line along the long axis of the median [posterior] process) to the tip of the lateral process (Fig. 11). The overlapped distance was measured along the same straight line. Length measurements were made on photographs of dry or clear and stained interclavicles using the software MacMorph (Spencer and Spencer, 1993). Two measurements were made on each side (left and right sides separately) and used to calculate the average per species. Continuous character. Range: 0.36–0.96.

60. Angle between the median (posterior) process and the lateral process of the interclavicle (this is the second character derived from the arrow-shaped and T-shaped conditions of Etheridge [1959] described in the previous character). The angle was measured between the long axis of the median process and that of the lateral process (as described in the previous character; Fig. 12) on photographs of dry or cleared and stained interclavicles, using the software MacMorph (Spencer and Spencer, 1993). Two measurements were made on each side (left and right sides separately) and used to calculate the average per species. Continuous character. Range: 44.9–64.5.

61. Postxiphisternal inscriptional rib formula (Etheridge, 1959). The postxiphisternal inscriptional ribs are the cartilaginous ventral rib elements located

caudal to the xiphisternum. The first number in the formula refers to the number of such ribs attached to the (ossified) dorsal ribs; the second refers to the number of floating (unattached) postxiphisternal inscriptional ribs caudal to the attached ones. The modal condition was scored for each species. States: (0) 2:2, (1) 3:1, (2) 4:0, (3) 4:1, (4) 5:0, (5) 5:1, (6) 5:2, (7) 8:1. This character was ordered using a step matrix (modified from Jackman et al., 1999), in which the gain or loss of a rib or a connection (from attached to floating or vice versa) costs one step.

62. Number of presacral vertebrae (Etheridge, 1959). The presacral vertebrae are all vertebrate anterior to the sacrum. States: (0) 22, (1) 23, (2) 24, (3) 25, (4) 27. Polymorphic character. Ordered.

63. Number of lumbar vertebrae (Etheridge, 1959). The lumbar vertebrae are post-thoracic vertebrae (i.e., those that are not attached directly or indirectly to the sternum) that bear no ribs. States: (0) 1, (1) 2, (2) 3, (3) 4, (4) 5. Polymorphic character. Ordered.

64. Type of caudal vertebrae (Etheridge, 1959). Caudal vertebrae may be of the alpha type (0), in which the transverse processes are caudolaterally or laterally directed and present only on the most anterior vertebrae (7–15), or the beta type (1), in which transverse processes are present much farther posteriorly in the caudal sequence, where they are directed craniolaterally. No instraspecific variation was observed.

65. Caudal autotomy septa (Etheridge, 1959). Autotomy septa are observed in radiographs as unossi-

fied areas in the vertebrae anterior, posterior, or through the transverse process. The anteriormost autotomy septum usually coincides with a change in the condition of the transverse process (e.g., disappearance, change in direction, or appearance of a second pair; Etheridge, 1959). This character exhibits ontogenetic variation, as in some species, progressive fusion of the septa occurs from caudal to cranial with age (Etheridge, 1959). To account for this variation, three states were recognized: septa absent in all specimens, representing those species that do not have (at any life stage) autotomy (0), septa present in some specimens and absent in others, representing those species that progressively lose autotomy with age (1), or septa present in all specimens, representing those species that retain autotomy throughout life (provided that large individuals were examined) (2). This coding approach is strongly biased by sample size but was the best found to incorporate information on the gradual change of the character. Ordered.

66.   Mean number of caudal vertebrae bearing transverse processes (Etheridge, 1959). Transverse processes are always present on the anteriormost caudal vertebrae and progressively decrease in size posteriorly until absent. Continuous character. Range: 6.8–32.2.

LITERATURE CITED

ALFARO, M. E., S. ZOLLER, AND F. LUTZONI. 2003. Bayes or bootstrap? A simulation study comparing the performance of Bayesian Markov chain Monte Carlo sampling and bootstrapping in assessing phylogenetic confidence. *Molecular Biology and Evolution* **20:** 255–266.

AROSEMENA, F. A., R. IBAÑEZ D., AND F. DE SOUSA. 1991. Una nueva especies de *Anolis* (Squamata: Iguanidae) del grupo *latifrons* de Fortuna, Panamá. *Revista de Biología Tropical* **39:** 255–262.

AYALA, S., D. HARRIS, AND E. E. WILLIAMS. 1983. New or problematic *Anolis* from Colombia. I. *Anolis calimae,* new species, from the cloud forest of western Colombia. *Breviora* **475:** 1–11.

AYALA, S. C., AND F. CASTRO. Familia Iguanidae—II Anolinos. *In* S. C. Ayala and F. Castro (eds) *Saurios de Colombia.* Unpublished manuscript.

AYALA, S. C., D. M. HARRIS, AND E. E. WILLIAMS. 1984. *Anolis menta,* sp. n. (Sauria, Iguanidae), a new *tigrinus* group anole from the west side of the Santa Marta Mountains, Colombia. *Papéis Avulsos de Zoologia* **35:** 135–145.

AYALA-VARELA, F. P., AND O. TORRES-CARVAJAL. 2010. A new species of dactyloid anole (Iguanidae, Polychrotinae, *Anolis*) from the southeastern slopes of the Andes of Ecuador. *ZooKeys* **53:** 59–73.

AYALA-VARELA, F. P., AND J. A. VELASCO. 2010. A new species of dactyloid anole (Squamata: Iguanidae) from the western Andes of Ecuador. *Zootaxa* **2577:** 46–56.

BARBOUR, T. 1920. A note on *Xiphocercus. Proceedings of the New England Zoological Club* **7:** 61–63.

BARBOUR, T. 1923. Notes on reptiles and amphibians from Panamá. *Occasional Papers of the Museum of Zoology, University of Michigan* **129:** 1–16.

BARROS, T., E. E. WILLIAMS, AND A. VILORIA. 1996. The genus *Phenacosaurus* (Squamata: Iguania) in western Venezuela: *Phenacosaurus tetarii,* new species, *Phenacosaurus euskalerriari,* new species, and *Phenacosaurus nicefori* Dunn, 1944. *Breviora* **504:** 1–30.

BERLOCHER, S. H., AND D. L. SWOFFORD. 1997. Searching for phylogenetic trees under the frequency parsimony criterion: an approximation using generalized parsimony. *Systematic Biology* **46:** 211–215.

BERNAL CARLO, A., AND J. A. ROZE. 2005. Lizards of the genus *Anolis* (Reptilia: Polychrotidae) from Sierra Nevada de Santa Marta, Colombia, with description of two new species. *Novedades Colombianas* **8:** 9–26.

BRANDLEY, M. C., AND K. DE QUEIROZ. 2004. Phylogeny, ecomorphological evolution, and historical biogeography of the *Anolis cristatellus* group. *Herpetological Monographs* **18:** 90–126.

BRYANT, D. 2003. A classification of consensus methods for phylogenetics, pp. 1–21. *In* M. Janowitz, F. J. Lapointe, F. McMorris, B. Mirkin, and F. Roberts (eds.), *BioConsensus.* Piscataway, New Jersey: American Mathematical Society Publications–DIMACS Series in Discrete Mathematics and Theoretical Computer Science.

BURNELL, K. L., AND S. B. HEDGES. 1990. Relationships of West Indian *Anolis* (Sauria: Iguanidae): an approach using slow-evolving protein loci. *Caribbean Journal of Sciences* **26:** 7–30.

BUTLER, M. A., S. A. SAWYER, AND J. B. LOSOS. 2007. Sexual dimorphism and adaptive radiation in *Anolis* lizards. *Nature* **447:** 202–205.

BUTLER, M. A., T. W. SCHOENER, AND J. B. LOSOS. 2000. The relationship between sexual size dimorphism and habitat use in Greater Antillean *Anolis* lizards. *Evolution* **54:** 259–272.

CANNATELLA, D., AND K. DE QUEIROZ. 1989. Phylogenetic systematics of the Anoles: is a new taxonomy warranted? *Systematic Zoology* **38:** 57–69.

CASTAÑEDA, M. d. R., AND K. DE QUEIROZ. 2011. Phylogenetic relationships of the *Dactyloa* clade of *Anolis* lizards based on nuclear and mitochondrial DNA sequence data. *Molecular Phylogenetics and Evolution* **61:** 784–800.

COPE, E. D. 1899. Contributions to the herpetology of New Grenada and Argentina, with descriptions of new forms. *Philadelphia Museums Science Bulletin* **1:** 1–21.

CREER, D. A., K. DE QUEIROZ, T. R. JACKMAN, J. B. LOSOS, AND A. LARSON. 2001. Systematics of the *Anolis roquet* series of the southern Lesser Antilles. *Journal of Herpetology* **35:** 428–441.

DE QUEIROZ, K. 1987. Phylogenetic systematics of Iguanine lizards. A comparative osteological study.

University of California Publications in Zoology **118:** 1–203.

DE QUEIROZ, K. 1996. Including the characters of interest during tree reconstruction and the problems of circularity and bias in studies of character evolution. *American Naturalist* **148:** 700–708.

DE QUEIROZ, K. 2000. Logical problems associated with including and excluding characters during tree reconstruction and their implications for the study of morphological character evolution, pp. 192–212. *In* J. J. Wiens (ed.), *Phylogenetic Analysis of Morphological Data.* Washington, DC: Smithsonian Institution Press.

DE QUEIROZ, K., AND M. DONOGHUE. 2013. Phylogenetic nomenclature, hierarchical information, and testability. *Systematic Biology.* doi: 10.1093/sysbio/sys054

DE QUEIROZ, K., AND J. GAUTHIER. 1990. Phylogeny as a central principle in taxonomy: phylogenetic definitions of taxon names. *Systematic Zoology* **39:** 307–322.

DE QUEIROZ, K., AND J. GAUTHIER. 1992. Phylogenetic taxonomy. *Annual Review of Ecology and Systematics* **23:** 449–480.

DE QUEIROZ, K., AND T. REEDER. 2008. Squamata—Lizards, pp. 24–45. *In* B. I. Crother (ed.), *Scientific and Standard English Names of Amphibians and Reptiles of North America North of Mexico, with Comments Regarding Confidence in Our Understanding.* Society for the Study of Amphibians and Reptiles, *Herpetological Circular* No. 37.

DRUMMOND, A. J., AND A. RAMBAUT. 2007. BEAST: Bayesian evolutionary analysis by sampling trees. *BMC Evolutionary Biology* **7:** 214.

DUNN, E. R. 1937. The giant mainland Anoles. *Proceedings of the New England Zoological Club* **16:** 5–9.

DUNN, E. R. 1939. Zoological results of the George Vanderbilt South Pacific Expedition of 1937. Part III—The lizards of Malpelo Island, Colombia. *Notulae Naturae* **4:** 1–3.

DUNN, E. R. 1944. The lizard genus *Phenacosaurus. Caldasia* **3:** 57–62.

ESTES, R., K. DE QUEIROZ, AND J. GAUTHIER. 1988. Phylogenetic relationships within Squamata, pp. 119–281. *In* R. Estes and G. Pregill (eds.), *Phylogenetic Relationships of the Lizard Families—Essays Commemorating Charles L. Camp.* Stanford, California: Stanford Univ. Press.

ETHERIDGE, R. 1959. The relationships of the Anoles (Reptilia: Sauria: Iguanidae): an interpretation based on skeletal morphology. Ph.D. Thesis. Ann Arbor, Michigan: Univ. of Michigan.

ETHERIDGE, R., AND K. DE QUEIROZ. 1988. A phylogeny of Iguanidae, pp. 283–367. *In* R. Estes and G. Pregill (eds.), *Phylogenetic Relationships of the Lizard Families—Essays Commemorating Charles L. Camp.* Stanford, California: Stanford Univ. Press.

FELSENSTEIN, J. 1985. Confidence limits on phylogenies: an approach using the bootstrap. *Evolution* **39:** 783–791.

FINDEN, C. R., AND A. D. GORDON. 1985. Obtaining common pruned trees. *Journal of Classification* **2:** 255–276.

FISHER, R. A. 1930. The moments of the distribution for normal samples of measures of departure from normality. *Proceedings of the Royal Society* A, **130:** 16–28.

FROST, D. R., AND R. ETHERIDGE. 1989. A phylogenetic analysis and taxonomy of iguanian lizards (Reptilia: Squamata). *Miscellaneous Publications University of Kansas Natural History Museum* **81:** 1–65.

GIANNASI, N., R. S. THORPE, AND A. MALHOTRA. 2000. A phylogenetic analysis of body size evolution in the *Anolis roquet* group (Sauria: Iguanidae): character displacement or size assortment? *Molecular Ecology* **9:** 193–202.

GLOR, R. E., J. J. KOLBE, R. POWELL, A. LARSON, AND J. B. LOSOS. 2003. Phylogenetic analysis of ecological and morphological diversification in Hispaniolan trunk-ground anoles (*Anolis cybotes* group). *Evolution* **57:** 2383–2397.

GORDON, A. D. 1980. On the assessment and comparison of classifications, pp. 149–160. *In* R. Tomassone (ed.), *Analyse de Donnees et Informatique.* Le Chesnay, France: INRIA.

GORMAN, G. C. 1968. The relationships of *Anolis* of the *roquet* species group (Sauria: Iguanidae). III. Comparative study of display behavior. *Breviora* **284:** 1–31.

GORMAN, G. C., AND L. ATKINS. 1967. The relationships of *Anolis* of the *roquet* species group (Sauria: Iguanidae). II. Comparative chromosome cytology. *Systematic Zoology* **16:** 137–143.

GORMAN, G. C., AND L. ATKINS. 1969. The zoogeography of Lesser Antillean *Anolis* lizards—an analysis based upon chromosomes and lactic dehydrogenases. *Bulletin of the Museum of Comparative Zoology* **138:** 53–80.

GORMAN, G. C., D. G. BUTH, M. SOULÉ, AND S. Y. YANG. 1980a. The relationships of the *Anolis cristatellus* group: electrophoretic analysis. *Journal of Herpetology* **14:** 269–278.

GORMAN, G. C., D. G. BUTH, M. SOULÉ, AND S. Y. YANG. 1983. The relationships of the Puerto Rican *Anolis*: electrophoretic and karyotypic studies, pp. 626–642. *In* A. G. J. Rhodin and K. Miyata (eds.), *Advances in Herpetology and Evolutionary Biology.* Cambridge, Massachusetts: Museum of Comparative Zoology.

GORMAN, G. C., D. G. BUTH, AND J. S. WYLES. 1980b. *Anolis* lizards of the eastern Caribbean: a case study in evolution. III. A cladistic analysis of albumin immunological data, and the definitions of species groups. *Systematic Zoology* **29:** 143–158.

GORMAN, G. C., AND H. C. DESSAUER. 1965. Hemoglobin and transferring electrophoresis and relationships of island populations of *Anolis* lizards. *Science* **150:** 1454–1455.

GORMAN, G. C., AND H. C. DESSAUER. 1966. The relationships of *Anolis* of the *roquet* species group (Sauria: Iguanidae). I. Electrophoretic comparison

of blood proteins. *Comparative Biochemistry and Physiology* **19**: 845–853.

GORMAN, G. C., AND Y. J. KIM. 1976. *Anolis* lizards of the eastern Caribbean: a case study in evolution. II. Genetic relationships and genetic variation of the *bimaculatus* group. *Systematic Zoology* **20**: 167–185.

GORMAN, G. C., P. LICHT, H. C. DESSAUER, AND J. O. BOOS. 1971. Reproductive failure among the hybridizing *Anolis* lizards of Trinidad. *Systematic Zoology* **20**: 1–18.

GORMAN, G. C., C. S. LIEB, AND R. H. HARWOOD. 1984. The relationships of *Anolis gadovi*: albumin immunological evidence. *Caribbean Journal of Science* **20**: 145–152.

GORMAN, G. C., AND R. B. STAMM. 1975. The *Anolis* lizards of Mona, Redonda, and La Blanquilla: chromosomes, relationships, and natural history notes. *Journal of Herpetology* **9**: 197–205.

GORMAN, G. C., R. THOMAS, AND L. ATKINS. 1968. Intra- and interspecific chromosome variation in *Anolis cristatellus* and its closest relatives. *Breviora* **293**: 1–12.

GUYER, C., AND J. M. SAVAGE. 1987 [1986]. Cladistic relationships among anoles (Sauria: Iguanidae). *Systematic Zoology* **35**: 509–531.

HILLIS, D. M. 1991. Discriminating between phylogenetic signal and random noise in DNA sequences, pp. 278–294. *In* M. M. Miyamoto and J. Cracraft (eds.), *Phylogenetic Analyses of DNA Sequences.* New York: Oxford Univ. Press.

HILLIS, D. M., AND J. P. HUELSENBECK. 1992. Signal, noise and reliability in molecular phylogenetic analyses. *Journal of Heredity* **83**: 189–195.

HUELSENBECK, J. P. 1991. Tree-length distribution skewness: an indicator of phylogenetic information. *Systematic Zoology* **40**: 257–270.

HUELSENBECK, J. P., F. RONQUIST, R. NIELSEN, AND J. P. BOLLBACK. 2001. Bayesian inference of phylogeny and its impact on evolutionary biology. *Science* **294**: 2310–2314.

HULEBAK, E., S. POE. R. IBÁÑEZ, AND E. E. WILLIAMS. 2007. A striking new species of *Anolis* lizard (Squamata, Iguania) from Panama. *Phyllomedusa* **6**: 5–10.

JACKMAN, T. R., D. J. IRSCHICK, K. DE QUEIROZ, J. B. LOSOS, AND A. LARSON. 2002. Molecular phylogenetic perspective on evolution of lizards of the *Anolis grahami* series. *Journal of Experimental Zoology* **294**: 1–16.

JACKMAN, T. R., A. LARSON, K. DE QUEIROZ, AND J. B. LOSOS. 1999. Phylogenetic relationships and tempo of early diversification in *Anolis* lizards. *Systematic Biology* **48**: 254–285.

KASS, R. E., AND A. E. RAFTERY. 1995. Bayes factors. *Journal of the American Statistical Association* **90**: 773–795.

LARGET, B., AND D. L. SIMON. 1999. Markov chain Monte Carlo algorithms for the Bayesian analysis of phylogenetic trees. *Molecular Biology and Evolution* **16**: 750–759.

LARSON, A. 1998. The comparison of morphological and molecular data in phylogenetic systematics, pp. 275–296. *In* R. DeSalle and B. Schierwater (eds.), *Molecular Approaches to Ecology and Evolution.* Basel, Switzerland: Birkhäuser Verlag.

LAZELL, J. D., JR. 1969. The genus *Phenacosaurus* (Sauria: Iguanidae). *Breviora* **325**: 1–24.

LAZELL, J. D., JR. 1972. The anoles (Sauria: Iguanidae) of the Lesser Antilles. *Bulletin of the Museum of Comparative Zoology* **143**: 1–115.

LEE, M. S. Y. 2000. Tree robustness and clade significance. *Systematic Biology* **49**: 829–836.

LEWIS, P. O. 2001. A likelihood approach to estimating phylogeny from discrete morphological character data. *Systematic Biology* **50**: 913–925.

LEWIS, P. O., M. T. HOLDER, AND K. E. HOLSINGER. 2005. Polytomies and Bayesian phylogenetic inference. *Systematic Biology* **54**: 241–253.

LOSOS, J. B. 2009. *Lizards in an Evolutionary Tree: Ecology and Adaptive Radiation of Anoles.* Berkeley and Los Angeles, California: Univ. of California Press.

LOSOS, J. B., M. L. WOOLLEY, D. L. MAHLER, O. TORRES-CARVAJAL, K. E. CRANDELL, E. W. SCHAAD, A. E. NARVÁEZ, F. AYALA-VARELA, AND A. HERREL. 2012. Notes on the natural history of the little-known Ecuadorian horned anole, *Anolis proboscis.* *Breviora* **531**: 1–17.

MADDISON, D. R., AND W. P. MADDISON. 2001. *MacClade: Analysis of Phylogeny and Character Evolution.* Version 4.03. Sunderland, Massachusetts: Sinauer Associates.

MADDISON, W. P., AND D. R. MADDISON. 2011. Mesquite: A Modular System for Evolutionary Analysis. Version 2.75. Available from: http://mesquiteproject.org.

MYERS, C. W., AND M. A. DONNELLY. 1996. A new herpetofauna from Cerro Yaví, Venezuela: first results of the Robert G. Goelet American Museum—TERRAMAR expedition to the northwestern Tepuis. *American Museum Novitates* **3172**: 1–56.

MYERS, C. W., E. E. WILLIAMS, AND R. W. MCDIARMID. 1993. A new anoline lizard (*Phenacosaurus*) from the highland of Cerro de la Neblina, southern Venezuela. *American Museum Novitates* **3070**: 1–15.

NICHOLSON, K. E. 2002. Phylogenetic analysis and a test of the current infrageneric classification of *Norops* (Beta *Anolis*). *Herpetological Monographs* **16**: 93–120.

NICHOLSON, K. E., R. E. GLOR, J. J. KOLBE, A. LARSON, S. B. HEDGES, AND J. B. LOSOS. 2005. Mainland colonization by island lizards. *Journal of Biogeography* **32**: 929–938.

PAGEL, M., AND A. MEADE. 2005. Mixture models in phylogenetic inference, pp. 121–139. *In* O. Gascuel (ed.), *Mathematics of Evolution and Phylogeny.* Oxford: Oxford Univ. Press.

PETERS, J. A. 1964. *Dictionary of Herpetology: A Brief and Meaningful Definition of Words and Terms Used in Herpetology.* New York: Hafner VII.

PETERS, J. A., AND V. G. ORCES. 1956. A third leaf-nosed species of the lizard genus *Anolis* from South America. *Breviora* **62:** 1–8.

POE, S. 1998. Skull characters and the cladistic relationships of the Hispaniolan dwarf twig *Anolis*. *Herpetological Monographs* **12:** 192–236.

POE, S. 2004. Phylogeny of anoles. *Herpetological Monographs* **18:** 37–89.

POE, S. 2005. A study of the utility of convergent characters for phylogeny reconstruction: do eco-morphological characters track evolutionary history in *Anolis* lizards? *Zoology* **108:** 337–343.

POE, S., F. AYALA, I. M. LATELLA, T. L. KENNEDY, J. A. CHRISTENSEN, L. N. GRAY, N. J. BLEA, B. M. ARMIJO, AND E. W. SCHAAD. 2012. Morphology, phylogeny, and behavior of *Anolis proboscis*. *Breviora* **530:** 1–11.

POE, S., AND R. IBÁÑEZ. 2007. A new species of *Anolis* lizard from the cordillera de Talamanca of western Panama. *Journal of Herpetology* **41:** 263–270.

POE, S., I. M. LATELLA, M. J. RYAN, AND E. W. SCHAAD. 2009a. A new species of *Anolis* lizard (Squamata, Iguania) from Panama. *Phyllomedusa* **8:** 81–87.

POE, S., J. VELASCO, K. MIYATA, AND E. E. WILLIAMS. 2009b. Descriptions of two nomen nudum species of *Anolis* lizard from northwestern South America. *Breviora* **516:** 1–16.

POE, S., AND C. YAÑEZ-MIRANDA. 2007. A new species of phenacosaur *Anolis* from Peru. *Herpetologica* **63:** 219–223.

POE, S., AND C. YAÑEZ-MIRANDA. 2008. Another new species of green *Anolis* (Squamata: Iguania) from the eastern Andes of Peru. *Journal of Herpetology* **42:** 564–571.

POE, S., C. YAÑEZ-MIRANDA, AND E. LEHR. 2008. Notes on variation in *Anolis boettgeri* Boulenger 1911, assessment of the status of *Anolis albimaculatus* Henle and Ehlr 1991, and description of a new species of *Anolis* (Squamata: Iguania) similar to *Anolis boettgeri*. *Journal of Herpetology* **42:** 251–259.

POSADA, J. L., AND K. A. CRANDALL. 1998. Modeltest: testing the model of DNA substitution. Version 3.7 (June 2005). *Bioinformatics* **14:** 817–818.

RODRIGUES, M. T. 1988. A new anole of the *punctatus* group from central Amazonia (Sauria: Iguanidae). *Papéis Avulsos de Zoologia* **36:** 333–336.

RODRIGUES, M. T., V. XAVIER, G. SKUK, AND D. PAVAN. 2002. New specimens of *Anolis phyllorhinus* (Squamata, Polychrotidae): the first female of the species and of proboscid anoles. *Papéis Avulsos De Zoologia* **42:** 363–380.

RONQUIST, F., AND J. P. HUELSENBECK. 2003. MrBayes 3: Bayesian phylogenetic inference under mixed models. *Bioinformatics* **19:** 1572–1574.

RUEDA, J. V., AND J. I. HERNÁNDEZ CAMACHO. 1988. *Phenacosaurus inderenae* (Sauria: Iguanidae), nueva especie gigante, proveniente de la cordillera oriental de Colombia. *Trianea* **2:** 339–350.

RUEDA ALMONACID, J. V. 1989. Un nuevo y extraordinario saurio de color rojo (*Iguanidae: Anolis*) para la Cordillera Occidental de Colombia. *Trianea* **3:** 85–92.

SAVAGE, J. M. 2002. *The Amphibians and Reptiles of Costa Rica. Herpetofauna between Two Continents, between Two Seas.* Chicago: Univ. of Chicago Press.

SAVAGE, J. M., AND C. GUYER. 1989. Infrageneric classification and species composition of the anole genera, *Anolis, Ctenonotus, Dactyloa, Norops,* and *Semiurus* (Sauria: Iguanidae). *Amphibia-Reptilia* **10:** 105–116.

SAVAGE, J. M., AND J. J. TALBOT. 1978. The giant anoline lizards of Costa Rica and western Panama. *Copeia* **1978:** 480–492.

SCHNEIDER, C. J., J. B. LOSOS, AND K. DE QUEIROZ. 2001. Evolutionary relationships of the *Anolis bimaculatus* group from the northern Lesser Antilles. *Journal of Herpetology* **35:** 1–12.

SCHOENER, T. W. 1969. Size patterns in West Indian *Anolis* lizards: I. Size and species diversity. *Systematic Zoology* **18:** 386–401.

SHOCHAT, D., AND H. C. DESSAUER. 1981. Comparative study of albumins of *Anolis* lizards of the Caribbean islands. *Comparative Biochemistry and Physiology* **68A:** 67–73.

SOKAL, R. R., AND F. J. ROHLF. 1995. *Biometry: The Principles and Practice of Statistics in Biological Research.* 3rd ed. San Francisco: W.H. Freeman.

SPENCER, M. A., AND G. S. SPENCER. 1993. MacMorph Image Analysis Software, Version 2.1. Stony Brook, New York.

SUZUKI, Y., G. V. GLAZKO, AND M. NEI. 2002. Over-credibility of molecular phylogenies obtained by Bayesian phylogenetics. *Proceedings of the National Academy of Science* **99:** 16138–16143.

SWOFFORD, D. L. 1991. When are phylogeny estimates from molecular and morphological data incongruent? pp. 295–333. *In* M. M. Miyamoto and J. Cracraft (eds.), *Phylogenetic Analysis of DNA Sequences.* New York: Oxford Univ. Press.

SWOFFORD, D. L. 2002. PAUP*. *Phylogenetic Analysis Using Parsimony (* and Other Methods).* Version 4. Sunderland, Massachusetts: Sinauer Associates.

SWOFFORD, D. L., AND S. H. BERLOCHER. 1987. Inferring evolutionary trees from gene frequency data under the principle of maximum parsimony. *Systematic Zoology* **36:** 293–325.

TEMPLETON, A. R. 1983. Phylogenetic inference from restriction endonuclease cleavage site maps with particular reference to the evolution of humans and apes. *Evolution* **37:** 221–244.

THIELE, K. 1993. The holy grail of the perfect character: the cladistic treatment of morphometric data. *Cladistics* **9:** 275–304.

TORRES-CARVAJAL, O. 2007. Phylogeny and biogeography of a large radiation of Andean lizards (Iguania, *Stenocercus*). *Zoologica Scripta* **36:** 311–326.

UETZ, P. (ED.) [Internet]. The Reptile Database [cited 2012 Mar 10]. Available from: http://www.reptile-database.org/.

UGUETO, G. N., G. RIVAS, T. BARROS, AND E. N. SMITH. 2009. A revision of the Venezuelan anoles II: redescription of *Anolis squamulatus* Peters 1863

and *Anolis tigrinus* Peters 1863 (Reptilia: Polychrotidae). *Caribbean Journal of Science* **45**: 30–51.

UGUETO, G. N., G. RIVAS-FUENMAYOR, T. BARROS, S. J. SÁNCHEZ-PACHECO, AND J. E. GARCÍA-PÉREZ. 2007. A revision of the Venezuelan Anoles I: a new *Anolis* species from the Andes of Venezuela with the redescription of *Anolis jacare* Boulenger 1903 (Reptilia: Polychrotidae) and the clarification of the status of *Anolis nigropunctatus* Williams 1974. *Zootaxa* **1501**: 1–30.

UNDERWOOD, G. 1959. The anoles of the eastern Caribbean (Sauria, Iguanidae): revisionary notes. *Bulletin of the Museum of Comparative Zoology* **121(part III)**: 191–226.

VELASCO, J. A., P. D. A. GUTIÉRREZ-CÁRDENAS, AND A. QUINTERO-ANGEL. 2010. A new species of *Anolis* of the *aequatorialis* group (Squamata: Iguania) from the central Andes of Colombia. *Herpetological Journal* **20**: 231–236.

WIENS, J. J. 1995. Polymorphic characters in phylogenetic systematics. *Systematic Biology* **44**: 482–500.

WIENS, J. J. 1998. Testing phylogenetic methods with tree congruence: phylogenetic analysis of polymorphic morphological characters in phrynosomatid lizards. *Systematic Biology* **47**: 427–444.

WIENS, J. J. 2000. Coding morphological variation within species and higher taxa for phylogenetic analysis, pp. 115–145. *In* J. J. Wiens (ed.), *Phylogenetic Analysis of Morphological Data*. Washington, DC: Smithsonian Institution Press.

WIENS, J. J. 2001. Character analysis in morphological phylogenetics: problems and solutions. *Systematic Biology* **50**: 689–699.

WIENS, J. J., AND M. R. SERVEDIO. 1997. Accuracy of phylogenetic analysis including and excluding polymorphic characters. *Systematic Biology*, **46**: 332–345.

WILLIAMS, E. E. 1965. South American *Anolis* (Sauria, Iguanidae): two new species of the *punctatus* group. *Breviora* **233**: 1–15.

WILLIAMS, E. E. 1974. South American *Anolis*: three new species related to *Anolis nigrolineatus* and *A. dissimilis*. *Breviora* **422**: 1–15.

WILLIAMS, E. E. 1975. South American *Anolis*: *Anolis parilis*, new species, near *A. mirus* Williams. *Breviora* **434**: 1–8.

WILLIAMS, E. E. 1976a. West Indian anoles: a taxonomic and evolutionary summary. 1. Introduction and a species list. *Breviora* **440**: 1–21.

WILLIAMS, E. E. 1976b. South American anoles: the species groups. *Papéis Avulsos de Zoologia* **29**: 259–268.

WILLIAMS, E. E. 1979. South American anoles: the species groups. 2. The proboscis anoles (*Anolis laevis* group). *Breviora* **449**: 1–19.

WILLIAMS, E. E. 1982. Three new species of the *Anolis punctatus* complex from Amazonian and inter-Andean Colombia, with comments on the eastern

members of the *punctatus* species group. *Breviora* **467**: 1–38.

WILLIAMS, E. E. 1985. New or problematic *Anolis* from Colombia. IV. *Anolis antioquiae*, new species of the *Anolis eulaemus* subgroup from western Colombia. *Breviora* **482**: 1–9.

WILLIAMS, E. E. 1988. New or problematic *Anolis* from Colombia. V. *Anolis danieli*, a new species of the *latifrons* species group and a reassessment *Anolis apollinaris* Boulengeri, 1919. *Breviora* **489**: 1–25.

WILLIAMS, E. E. 1989. A critique of Guyer and Savage (1986): cladistic relationships among anoles (Sauria: Iguanidae): are the data available to reclassify anoles? pp. 434–478. *In* C. A. Woods (ed.), *Biogeography of the West Indies: Past, Present and Future*. Gainsville, Florida: Sandhill Crane Press.

WILLIAMS, E. E. 1992. New or problematic *Anolis* from Colombia. VII. *Anolis lamari*, a new anole from the cordillera oriental of Colombia, with a discussion of *tigrinus* and *punctatus* species groups boundaries. *Breviora* **495**: 1–24.

WILLIAMS, E. E., AND N. ACOSTA B. 1996. *The* Anolis *Handlist*. Version 1.0b0. Cambridge, Massachusetts: Museum of Comparative Zoology.

WILLIAMS, E. E., AND W. E. DUELLMAN. 1967. *Anolis chocorum*, a new *punctatus*-like anole from Darien, Panama (Sauria, Iguanidae). *Breviora* **256**: 1–12.

WILLIAMS, E. E., AND W. E. DUELLMAN. 1984. *Anolis fitchi*, a new species of the *Anolis aequatorialis* group from Ecuador and Colombia, pp. 257–266. *In* R. A. Siegler, L. E. Hunt, J. L. Knight, L. Malaret, and N. L. Zuschlag (eds.), *Vertebrate Ecology and Systematics—A Tribute to Henry S. Fitch*. Lawrence, Kansas: University of Kansas, Museum of Natural History Special Publication No. 10.

WILLIAMS, E. E., AND R. MITTERMEIER. 1991. A Peruvian phenacosaur (Squamata: Iguania). *Breviora* **492**: 1–16.

WILLIAMS, E. E., M. J. PRADERIO, AND S. GORZULA. 1996. A phenacosaur from Chimantá Tepui, Venezuela. *Breviora* **506**: 1–15.

WILLIAMS, E. E., H. RAND, A. S. RAND, AND R. J. O'HARA. 1995. A computer approach to the comparison and identification of species in difficult taxonomic groups. *Breviora* **502**: 1–47.

YÁNEZ-MUÑOZ, M. H., M. A. URGILÉS, M. ALTAMIRANO-BENAVIDES, AND S. R. CÁCERES. 2010. Redescripción de *Anolis proboscis* Peters & Orcés (Reptilia: Polychrotidae), con el descubrimiento de las hembras de la especie y comentarios sobre su distribución y taxonomía. *Avances* **2**: B7–B15.

YANG, S. Y., M. SOULÉ, AND G. C. GORMAN. 1974. *Anolis* lizards of the eastern Caribbean: a case study in evolution. I. Genetic relationships, phylogeny, and colonization sequence of the *roquet* group. *Systematic Zoology* **23**: 387–399.

ZAR, J. H. 1999. *Biostatistical Analysis*. 4th Ed. Upper Saddle River, New Jersey: Prentice Hall.

Species names and credits for the photographs included on the front cover

Clockwise, starting from upper right corner:
Anolis agassizi, María Margarita Womack
Anolis punctatus, Roy W. McDiarmid
Anolis aequatorialis, D. Luke Mahler
Anolis trinitatis, Kevin de Queiroz
Anolis heterodermus, Juan L. Parra